MIX DESIGN CONSIDERATIONS FOR COLD AND HALF-WARM BITUMINOUS MIXES WITH EMPHASIS ON FOAMED BITUMEN

by

Kim Jonathan Jenkins B.Sc(Eng) M.Sc(Eng) Pr.Eng

Dissertation
Submitted to the Department of Civil Engineering,
Faculty of Engineering, University of Stellenbosch
In fulfilment for the degree

Doctor of Philosophy
(Engineering)

First Promotor
Professor Ir. Martinus F.C. van de Ven
University of Stellenbosch, South Africa

Second Promotor
Professor dr.Ir. André A.A. Molenaar
Delft University of Technology, The Netherlands

Internal Examiner
Professor Frederick Hugo PhD DEng

External Examiner
Professor Alex Visser PhD

University of Stellenbosch
September 2000

DECLARATION

I the undersigned hereby declare that the work contained in this dissertation is my own original work and has not previously in its entirety or in part been submitted at any university for a degree.

SUMMARY

The use of foamed bitumen and bitumen emulsion as binders for use in road rehabilitation is gaining favour globally. High-level road facilities through to unpaved roads requiring attention are being treated with these binders due to environmental, economic and practical benefits in the use of cold bituminous mixes. In addition, static and mobile plant with the capability of performing stabilisation using bitumen-emulsion and foamed bitumen has become commercially available and widely utilised, as a result of development in recycling technology and lapse in patent rights on foam nozzles.

An understanding of the behaviour and failure mechanisms of these cold mixes, as well as sound guidelines for the mix design procedures of cold mixes, especially foamed bitumen, and design guidelines for pavements structures incorporating these materials, are lacking however. Mix designs are carried out primarily on the basis of experience and pavement designs are empirically based.

The main objective of this dissertation is to address the need for a fundamental understanding of foamed bitumen and foamed bitumen mixes, and in so doing to develop techniques for adjudicating mixes, optimising their composition and rationalising their design both as mixes and as layers in road pavements. At the same time the exploration of new applications for foamed bitumen and the possibilities for progressive related technology, is a priority.

To commence, this study includes an appraisal of most of the literature available on foamed bitumen. This is followed by a fundamental investigation of the colloidal mass of foam that is produced when small quantities of cold water are added to hot bitumen. Factors influencing the quality of the foam are identified and a Foam Index is developed for characterisation and optimisation of the foam.

The spatial composition of a cold foamed bitumen mix, including Interaction of the foam with moist mineral aggregate, is also addressed in this dissertation. In particular, the stiffening of the filler mastic using foamed bitumen as binder is analysed. Techniques of optimising the sand type and content in the mix are also developed and guidelines for desired aggregate structures for foam treatment are established.

The temperature of the mineral aggregate has been shown to have a profound influence on the behaviour and performance of a foamed bitumen mix. This has been selected as a focal area of further investigation and the research has lead to the development of a new process called "The half-warm foamed bitumen treatment process" that can produce mixes with almost the quality of hot mix asphalt with up to 40% less energy consumption.

Other processes developed in this research include the use of cold mix asphaltic blocks for construction of road pavements in developing areas. This technology enhances the use of a high labour component in road construction in an economically competitive manner. The dissertation provides details for mix design and construction of the cold mix blocks.

Finally, the study includes models for the performance prediction of foamed bitumen mixes. In particular, foamed mixes that exhibit stress-dependent behaviour have been investigated and models established on the basis of triaxial testing and accelerated pavement testing for the prediction of permanent deformation of such layers under repeated loading.

Practical applications of the research findings are summarised in Appendix F. This includes:

- methods for optimisation of the foamed bitumen properties,
- guidelines for the selection of the ideal aggregate structure for cold foamed mixes,
- procedures for carrying out cold mix design in the laboratory (including mixing, compaction and curing),
- procedures for manufacturing half-warm foamed mixes in the laboratory,
- methods for manufacturing cold mix blocks, and
- pavement design methods for road structures incorporating foamed mix layers.

Appendix G outlines statistical techniques that are relevant to the design of experiments in pavement engineering including examples of applications of these procedures. The techniques are applied selectively in the relevant chapters of the dissertation.

OPSOMMING

Die gebruik van skuim bitumen en bitumen emulsie as bindmidel in pad rehabilitasie begin groter voorkeur wêreldwyd geniet. Van hoë vlak padfasiliteite tot ongeplaveide paaie wat aandag benodig, word met hierdie binders behandel vanweë die omgewings-, ekonomiese en praktiese voordele wat hierdie koue bitumen mengsels inhou. Voorts is statiese en mobiele masjinerie wat die vermoë het om stabilisasie in die gebruik van bitumenemulsie en skuimbitumen te bewerkstellig, in die handel verkrygbaar. Dit word algemeen gebruik as 'n uitvloeisel van ontwikkelings in herwinningstegnologie en die verslapping van patenteregte op skuim sproeikoppe.

'n Leemte bestaan in die begrip van die gedrags- en swigtingsmeganismes van hierdie koue mengsels, asook goeie riglyne vir die mengselontwerp van koue mengsels en in besonder skuimbitumen, en ontwerpriglyne vir plaveisel strukture waar hierdie materiaal geinkorporeer is. Mengselontwerpe word hoofsaaklik uitgevoer op grond van ondervinding, terwyl plaveisel ontwerpe empiries gebaseer is.

Die hoofdoel van die verhandeling is om die behoefte vir 'n fundamentele begrip van skuim bitumen en skuimbitumen mengsels aan te spreek, en daardeur tegnieke te ontwikkel vir die be-oordeling van mengsels, optimsering van hul samestelling en rasionalisering van hul ontwerp vir beide mengsels en plaveisellae. Terselfdertyd is die ondersoek na nuwe toepassings van skuim bitumen en die moontlikhede van nuwe tegnologie 'n prioriteit.

As beginpunt sluit hierdie studie 'n waardeskatting van die meeste literatuur beskikbaar op skuim bitumen in. Dit word gevolg deur 'n basiese ondersoek na die kolloidale massa van skuim wat geproduseer word wanneer klein hoeveelhede koue water by warm bitumen gevoeg word. Faktore wat die gehalte van die skuim beinvloed word uitgewys en 'n Skuim Indeks is ontwikkel vir die karakterisering en optimisering van die skuim.

Die ruimtelike samestelling van 'n koue bitumen mengsel, wat die interaksie van die skuim met vogtige minerale samevoegings (aggregate) insluit, word ook aangespreek. Besondere aandag word gewy aan die verharding van die vuller mastiekgom wat gebruik word as bitumen binder. Tegnieke om die sandtipe en inhoud van die mengsel te optimiseer is ontwikkel en riglyne vir die verlangde samevoegingstrukture (aggregate strukture) vir skuimbehandeling is opgestel.

Daar is bevind dat die temperatuur van die minerale aggregaat 'n duidelike invloed op die gedrag en verrigting van 'n skuimbitumen mengsel het. Dit is gekies as 'n fokuspunt vir verdere studie en die navorsingswerk daarop het gelei tot die ontwikkeling van 'n nuwe proses wat "Die half-warm skuim bitumen behandelings proses" genoem word. Hierdie proses produseer mengsels wat byna gelykstaande is aan die gehalte van warm gemengde asfalt, maar met tot 40% minder energie verbruik.

Ander prosesse wat met dié navorsing ontwikkel is, sluit koue gemengde asfaltiese blokke in, wat gebruik word in die konstruksie van padplaveisel in ontwikkelende gebiede. Hierdie tegnologie bevorder die ekonomiese gebruik van 'n hoë

arbeidskomponent in padkonstruksie. Die studie stel besonderhede vir die mengselontwerp en konstruksie vir koue gemengde blokke voor.

Laastens sluit die studie modelle in vir die werkverrigtingsvoorspelling van skuimbitumen mengsels. Op basis van drie-assige proewe in die laboratorium en versnelde belasting van paaie is modelle ontwikkel vir skuim bitumen mengsels wat spanningsafhanklike gedrag vertoon (die sogenaamde "granulêre" groep) om die permanente deformasie in die lae as gevolg van herhaalde verkeersbelasting te voorspel.

'n Opsomming van al die praktiese toepassings van die ontwikkelings van die navorsing word in Appendix F verskaf. Dit sluit in:

- optimesering van die eienskappe van skuimbitumen,
- riglyne vir gewenste samestelling van aggregaat in skuimbitumen mengsels,
- ontwerp metodes vir koue skuimbitumen mengsels in die laboratorium (meng, verdigting en curing),
- produksie metodes vir half-warme mensels in die laboratorium,
- produksie metodes vir blokke wat met koue mengsels gemaak word, en
- plaveisel ontwerp metodes van strukture wat skuimbitumen lae inkorporeer.

Appendix G gee 'n oorsig van statistiese tegnieke wat relevant is vir die ontwerp van eksperimente, insluitend voorbeelde van toepassings van die prosedures in plaveiselingenieurswese. Die tegnieke word selektief toegepas in die relevante hoofstukke van die verhandeling.

SAMENVATTING

Het gebruik van schuimbitumen en bitumenemulsie als bindmiddel in wegenbouwmaterialen geniet wereldwijd steeds meer belangstelling. Zowel voor de rehabilitatie van bestaande, verharde, wegen als voor de opwaardering van onverharde wegen worden deze bindmiddelen, vanwege de milieutechnische, economische en uitvoeringstechnische voordelen die koudasfalt mengsels bieden ten opzichte van andere mengsels, steeds meer toegepast. De toepassing is mede mogelijk door de commerciële beschikbaarheid van moderne statische en mobiele menginstallaties en stabilisatie machines. De ontwikkelingen in de recycling technologie en het verloop van patent rechten op schuimsproeikoppen hebben hierbij een belangrijke rol gespeeld.

De kennis van de gedrags- en bezwijkmechanismes van koude mengsels is volstrekt onvoldoende en bruikbare richtlijnen voor het mengselontwerp van koude mengsels, in het bijzonder met schuimbitumen, worden node gemist. Er zijn geen ontwerprichtlijnen voor verhardingsconstructies waarin het materiaal wordt toegepast. Het mengselontwerp wordt hoofdzakelijk uitgevoerd op basis van ervaring, terwijl het verhardingsontwerp gebaseerd is op empirie.

Het hoofddoel van deze dissertatie is om aan de behoefte voor een fundamenteel begrip van schuimbitumen en schuimbitumenmengsels te voldoen, en daardoor technieken te ontwikkelen voor het beoordelen van mengsels, optimalisering van hun samenstelling en rationalisering van hun ontwerp zowel voor mengsels als voor lagen in verhardingen. Tegelijkertijd is een prioriteit het onderzoek van nieuwe toepassingen voor schuimbitumen en de mogelijkheden voor nieuwe technologie.

De dissertatie start met een overzicht en de beoordeling van de beschikbare literatuur op het gebied van schuimbitumen. Vervolgens wordt fundamenteel onderzoek beschreven, dat is gedaan naar de colloïdale massa van schuim die geproduceerd wordt wanneer een kleine hoeveelheid koud water wordt toegevoegd aan het warme bitumen. De belangrijke faktoren die de kwaliteit van het schuim beïnvloeden zijn geidentificeerd en op basis hiervan is een "Schuim Index" ontworpen om het schuim beter te kunnen karakteriseren en optimaliseren.

De ruimtelijke samenstelling van een koudasfalt mengsel wordt behandeld, met speciale aandacht voor de interactie tussen het schuim en het vochtige aggregaat. De interactie tussen vulstof en schuimbitumen in de mastiek is apart bestudeerd. Deze verschilt sterk van die bij warm asfalt mengsels. Technieken zijn ontwikkeld voor het optimaliseren van het zandtype en de samenstelling van het mengsel. Tevens zijn richtlijnen opgesteld voor de gewenste gradering van het mineraal aggregaat voor mengsels met schuimbitumen.

Uit het onderzoek blijkt dat de temperatuur van het mineraal aggregaat een belangrijke invloed heeft op de eigenschappen en de performance van een mengsel met schuimbitumen. Om die reden is de temperatuur gekozen als kernparameter voor het verder uitgevoerde onderzoek. Dat onderzoek heeft geresulteerd in de ontwikkeling van een nieuw proces, nl. "het halfwarme schuimbitumen behandelings proces". De mengsels die via dit proces geproduceerd worden hebben nagenoeg

dezelfde eigenschappen als warm asfalt mengsels, er wordt echter een besparing op het energie gebruik tot 40% bereikt.

Tijdens het onderzoek zijn ook andere producten ontwikkeld zoals asfaltstraatstenen van koude mengsels die, in analogie met betonstraatstenen, in de verhardingskonstruktie gebruikt kunnen worden. Dit is een belangrijk aspect voor ontwikkelingslanden, want deze technologie maakt het mogelijk om een hoge arbeidscomponent te combineren met een economisch concurerend produkt. In deze studie zijn de details voor het mengselontwerp en de produktie van koudasfalt straatstenen uitgewerkt.

De dissertatie eindigt met het beschrijven van modellen die gebruikt kunnen worden voor het voorspellen van de performance van verhardingslagen van mengsels gemaakt met schuimbitumen. Op basis van tri-axiaal proeven in het laboratorium en het versneld belasten van verhardingen zijn voor mengsels gemaakt met schuimbitumen die spanningsafhankelijk gedrag vertonen (de zogenaamde "granulaire" groep) modellen ontwikkeld om de blijvende vervorming in deze lagen ten gevolge van herhaalde verkeersbelasting te voorspellen.

Een samenvatting van mogelijke praktische toepassingen van ontwikkelde technologie uit dit onderzoek wordt in Appendix F gegeven. Dit sluit in:

- optimalisering van de eigenschappen van het schuimbitumen,
- richtlijnen voor de gewenste samenstelling van aggregaat in schuimbitumen mengsels,
- ontwerp methodes voor mengsels in het laboratorium (menging, verdichting, curing ens.),
- productie methodes voor half-warme mengsels in het laboratorium,
- productie methodes voor blokken die met koude mengsels gemaakt worden, en
- ontwerp methodes voor verhardingen die lagen met schuimbitumen mengsels bevatten.

Appendix G geeft een overzicht van statistische technieken die relevant zijn voor het ontwerp van experimenten met voorbeelden van toepassingen van de procedures in de wegenbouw. Verschillende technieken zijn selectief toegepast in relevante hoofdstukken van de dissertatie.

ACKNOWLEDGEMENTS

I gratefully acknowledge the following persons:

- Professor Martin van de Ven for selfless contribution of time, support and assistance, and for incisive insights and inspiration.
- Professor André Molenaar for sound advice and guidance, for facilitating a fifteen month research period at Delft University of Technology where I was appointed as Universitair Docent towards this PhD, with generous technical and financial assistance, and for kind hospitality.
- Professor Fred Hugo, Director of the Institute for Transport Technology (ITT) for support both financial and logistical and for sound advice.
- De Heer Jack de Groot for inspiration, benevolence and arrangement of the use of research facilities at van Hees contractors and Zuid Nederlandse Asfalt Centrale (ZNAC), who in turn provided kind support.
- Fellow "promovendi's" at University of Stellenbosch and Delft University of Technology for solidarity, support and stimulating interaction.
- CAPSA-Colas for kind award of a study bursary.
- SABITA for financial support in purchasing a laboratory foam plant.
- Steph Bredenhann of Entech Consultants for facilitating the cold mix block trial section at Sir Lowry's Pass Village
- Roy Derbyshire formerly of Stewart Scott and Mark Bondietti of Cape Town City Council for facilitating the cold in place recycling trials on Vanguard Drive
- Laboratory assistants Carl Weston and Jeremy Jarvis for sweat and toil and going the extra distance.
- Laboratory assistants at Delft University of Technology.
- Liezl Rabie and Delysia Baard for kind and patient support.
- My wife Kathryn and children Anton, Nicholas and Julia for steadfast love, patience, sacrifice and humour throughout.
- My mother and late father for laying the foundation.
- To the Almighty who provides the true meaning. Thine be the Glory.

CONTENTS

CHAPTER 1 : INTRODUCTION

CHAPTER 2 : LITERATURE STUDY OF FOAMED BITUMEN MIXES

CHAPTER 3 : CHARACTERISATION OF FOAMED BITUMEN

CHAPTER 4 : MIX DESIGN CONSIDERATIONS FOR COLD MIXTURES

CHAPTER 5 : HALF-WARM FOAMED BITUMEN MIXTURES

CHAPTER 6 : COLD MIX BLOCKS

CHAPTER 7 : PERFORMANCE AND MODELLING OF FOAMED BITUMEN MIXTURES

CHAPTER 8 : CONCLUSIONS AND RECOMMENDATIONS

APPENDICES

APPENDIX A : FOAMED BITUMEN CHARACTERISTICS

APPENDIX B : FILLER AND FOAMED BITUMEN MASTIC

APPENDIX C : DETAILS OF HALF-WARM FOAMED BITUMEN MIXES USED IN THE FEASIBILITY STUDY

APPENDIX D : HALF-WARM FOAMED BITUMEN MIXES DETAILED INVESTIGATION : PRODUCTION & TEST RESULTS

APPENDIX E : TRIAXIAL TESTS ON FOAMED BITUMEN MIXES

APPENDIX F : PRACTICAL GUIDELINES FOR THE DESIGN AND USE OF COLD AND HALF-WARM FOAMED BITUMEN MIXES

APPENDIX G : STATISTICAL DESIGN OF EXPERIMENTS

DEFINITION OF TERMS

TERM	DEFINITION
Anti-foamants or Anti-foaming agents or Antifoams	Foam inhibitors that prevent the manufacture of foam or destruct existing foams i.e. reduce the expansion and stability of foam
Apparent Relative Density	The ratio of the mass in air of a given volume of material (excluding the permeable voids but including the impermeable voids normal to the material) at a stated temperature, to the mass in air of an equal volume of distilled water at the same temperature
Asphalt cement	American definition of bitumen
CMA	Cold mix asphalt which is equivalent to cold bituminous mix
Coarse Aggregate	Mineral aggregate greater than 4,75mm in particle size
Cold mix or cold bituminous mix	A road building material comprising mineral aggregate that has been treated with a bituminous binder and is workable at ambient temperatures, with the ability to be placed, levelled and compacted without the addition of heat
Decay or Foam Decay	Generic term used to describe the "breaking", collapse or subsidence of foam with time
Defoamant	See anti-foamant
Expansion Ratio	Ratio of the maximum volume of foamed bitumen produced relative to the original volume of the bitumen, usually measured in a vessel of known capacity
Filler or Dust	Mineral aggregate less than 0,075mm in particle size
Fine Aggregate	Mineral aggregate less than 4,75mm in particle size
Fluff Point Moisture Content	Moisture content at which a material occupies the maximum loose volume in an uncompacted state
Foamability	The ability of foam to be produced from a given substance, with higher expansion ratios and half-lives implying improved foamability
Foamant or Foaming agent	An agent or additive that is added to bitumen or to the foamant water to encourage either expansion or stability of the foamed bitumen i.e. increase in expansion ratio or half-life or both
Foamant water	Cold or warm water that is injected into hot bitumen at pressure to create a foam. Foamant water generally equates to 1% to 4% of bitumen (m/m)
Half-life	The time taken for foamed bitumen to subside from its maximum volume to half of the maximum volume, recorded in seconds i.e. a measure of foamed bitumen's stability
Half-warm foamed mix	Mineral aggregate that has been heated to temperatures above ambient but below 100°C, with or without the addition of compaction moisture, and mixed with foamed bitumen
Mastic	Mixture of filler, bitumen and sometimes water
Mortar	Mixture of the sand fraction, filler, bitumen and sometimes water
Sand fraction	Mineral aggregate less than 2,36mm in particle size, without the filler fraction
Spray time	Period of discharge of foamed bitumen from an expansion chamber, measured in seconds

LIST OF SYMBOLS AND ABBREVIATIONS

SYMBOL	DESCRIPTION
3PB	Three point beam test that utilises two simple supports and a single line load midway between the supports. Static and dynamic tests are possible.
4PB	Four point beam test that utilises two simple supports and two line loads equally spaced between the supports. Dynamic tests are used.
α	Type I error or contractor's risk i.e. the probability of rejecting an acceptable quality lot
β	Type II error or client's risk i.e. the probability of accepting an sub-standard quality lot
COV	Coefficient of variance = σ/μ
ER_a	Actual expansion ratio of foamed bitumen with due consideration of foam decay during the spray time
ER_m	Measured expansion ratio recorded at the moment discharge into a vessel is complete i.e. at the end of the spray time
HMA	Hot mix asphalt
HW	Half-warm
K_α	standardised normal deviate, which is a function of the desired confidence level, $100(1-\alpha)$
MC	Moisture content = Mass of moisture / Dry Mass of Aggregate x 100 (%)
M_r	Resilient Modulus = for small deformations
μ	True mean of a random variable i.e. of the entire population of observations
ν	Poisson's Ratio = Radial Strain/Axial Strain
N	Number of observations or tests
R	Limit of variability = probable range of the true mean from the average at a given level of reliability
RAP	Reclaimed or Recycled Asphalt Pavement
S	Standard deviation of a sample of observations
σ	true standard deviation of the random variable (parameter) being considered i.e. of the entire population
SMA	Stone Mastic Asphalt, with a stone skeleton
STAB	Steenslag Asfalt Beton or continuously graded asphalt
$\tau_{1/2}$	Half-life of a foamed bitumen (see definition)
TU	Delft University of Technology
US	University of Stellenbosch
$\%V_{db}$	Percent of the bulk volume of the entire water, bitumen and solid aggregate components in a mastic occupied by the compacted filler
VIM	Voids in Mix = Volume of air voids in mix excluding water/ Total volume of mix including water x 100 (%)
VMA	Voids in Mineral Aggregate = Volume of Voids in Dry Aggregate/ Volume of Dry Aggregate x 100 (%)
$\bar{x}$	Mean of a sample of observations
ZOAB	Zeer Open Asfalt Beton or Porous Asphalt with a high void content

CHAPTER 1

INTRODUCTION

1. BACKGROUND

In terms of our modern civilisation, it is a fact that there are more people alive on our planet today (more than 6 billion), than have ever perished in the history of humankind. Development of the global road infrastructure is analogous to this situation with the majority of the requisite capacity of roads being presently in place. For this reason, road maintenance, rehabilitation and upgrading have become increasingly important to pavement engineers.

In particular, cold recycling of existing pavements using foamed bitumen and bitumen emulsion is gaining favour as a means of road rehabilitation for existing high-level facilities through to the upgrading of unpaved roads. This is due to environmental, economic and practical benefits in the use of cold bituminous mixes. In addition, static and mobile plant with the capability of performing stabilisation with bitumen-emulsion and foamed bitumen, has become commercially available and globally utilised, as a result of development in recycling technology and lapse in patent rights on foam nozzles. An understanding of the behaviour and failure mechanisms of these cold mixes, as well as sound guidelines for the mix design procedures of cold mixes, especially foamed bitumen, and design guidelines for pavements structures incorporating these materials, are lacking however.

The advances in mix design procedures and appurtenant equipment for hot mix asphalt have overshadowed developments in cold-mix design. Initiatives such as SHRP Superpave (1994) in the United States of America, as well as research produced at LCPC in France, to cite but two examples, have opened up new avenues in the hot mix asphalt design approach. Contemporary research undertaken on cold mixes has been limited, by comparison. The volumetric considerations, mode of failure and critical mechanical properties that influence the performance of these materials require clarification for reliable and cost-effective pavement layers to be manufactured. These are areas that require more definition through research in order to provide pavement engineers with the tools to make judicious decisions.

At the same time, scope exists for the development of new or improved technologies for the treatment of road construction materials. The mineral aggregates and associated binders and modifiers used in the roads industry at present, occur in sufficient quantities to satisfy the current demands albeit with diminishing resources. Alternative hardware materials are unlikely to be found in sufficient quantities for road pavements to replace existing materials and the objective of these new or improved technologies should therefore be focussed on utilising the currently available materials in a more efficient and cost-effective manner. In addition, consideration of the environment through sustainable development of roads is of paramount importance. This is applicable to both new construction and road rehabilitation works, with the latter placing emphasis on recycling as

focal point in future technologies. The potential for developments in cold bituminous mixes in the field of recycling is substantial and requires exploration.

In addition to the ubiquitous opportunities for advances in technology, Southern Africa in particular, has a need for developing technologies in road construction that provide employment opportunities for local inhabitants in developing areas. Programmes have been established in this region for increases in the labour component of infrastructural development contracts. Labour intensive construction requires technical soundness and economical competitiveness for these initiatives to be successful. Cold bituminous mixes are materials with the potential for utilisation in labour intensive construction and in the process providing good quality services. These materials have not been fully exploited in this field and scope exists for the development of new construction processes that extract more benefits from the foamed bitumen and emulsion stabilised mixes.

Against this backdrop of opportunity and challenge, a research dissertation into cold bituminous mixes has been structured. This Chapter introduces foamed bitumen treatment and explores some of the differences between foamed bitumen, bitumen emulsion and conventional hot mix asphalt highlighting the advantages and disadvantages of each. In addition the chapter provides the background of mix design procedures for bituminous mixes in the road engineering industry and their purpose, with emphasis on the foamed bitumen mixes. Finally and most importantly, the objectives of the research dissertation are detailed.

1.1 What is foamed bitumen?

A foaming mass of bitumen can be produced through the injection of small quantities of cold moleculised water (typically 2% by mass), as a fine mist, into hot penetration grade bitumen in an expansion chamber. In the foamed state, which is a temporary state of low viscosity, bitumen can be added to and mixed with mineral aggregates at ambient temperatures and at in situ moisture contents. The foamed bitumen process is analogous to a baker beating an egg, which is viscous, into foam of low viscosity before mixing it with flour. The beaten egg increases in volume, which is necessary in order to evenly distribute it amongst the flour and produce a mix of acceptable quality and consistency.

During the mixing process, foamed bitumen is selective in its dispersion throughout the mineral aggregate by showing preference to adhesion to the finer particles i.e. fine sand and smaller. The moisture in the mix prior to the addition of the foam assists in the dispersion of the binder during mixing. As the foamed bitumen collapses during mixing, only a limited number of bitumen beads are attached to the larger aggregate particles resulting in partial coating.

2. BENEFITS OF FOAMED BITUMEN STABILISATION

2.1 Advantages and Disadvantages of Foamed Bitumen

For any product to have a sustainable demand it must have certain qualities which make it advantageous over other products. Some of the ***advantages*** of foamed bitumen cold-mix over other cold mixes and Hot Mix Asphalt HMA (SAT, 1998) include :

- *reduced atmospheric pollution*, with little or no hydrocarbon emissions from foamed bitumen (and also from bitumen-emulsions),
- *conservation of heat (energy)*, the binders can be applied to cold damp aggregates, generally without the aggregate requiring preheating, which consumes significantly higher energy than heating the bitumen,
- *conservation of non-renewable energy resources and reduction of health risks*, in the case of emulsions and foamed bitumen, the binders do not require a petroleum solvent to reduce the viscosity for mixing (compared with cold mixes produced using cut-back bitumens) which create volatile emissions during evaporation into the atmosphere,
- *suitability of aggregate types*, the variety of parent rock types with which the foamed bitumen binder is compatible, is greater than for bitumen-emulsion mixes,
- *lower optimum binder contents*, due to the fact that foamed bitumen only partially coats the large particles, the bitumen is more effectively used in the mortar of the mix and the binder contents of foam mixes are generally lower than HMA,
- *less plant ageing of binder*, due to lower aggregate temperatures the binder experiences less hardening during the foamed bitumen mixing process than with HMA,
- *less compaction-moisture problems with foam*, where the materials that require recycling have high field moisture contents, foamed bitumen stabilisation results in less increase in fluid content than emulsions, enabling easier compaction; in addition, compaction can be carried out immediately with foam, with minimal need for aeration,
- *applicable material types*, both marginal and recycled materials can be used to produce cold mixes of varying qualities i.e. good quality crushed aggregate is not a necessity and locally available material can often be used, decreasing haul distances and other costs,
- *no wastage*, high proportions of marginal and recycled materials in a foamed mix results in less impact on the environment due to elimination of wastage of non-renewable resources,
- *early strength characteristics,* after compaction foamed bitumen mixes have sufficient strength to be trafficked immediately without detrimental effects, provided the traffic volumes are not too high; this is considerably more difficult with emulsion treated materials, which require a longer curing period (but is not as effective as HMA),
- *ability to be stockpiled*, foamed bitumen mixes may be produced in bulk and stockpiled close to the point of application, to be placed and compacted at a later stage, providing flexibility in mix manufacture techniques; binder run-off and leaching problems, as experienced with rainfall on some emulsion mixes, are dramatically reduced with foamed bitumen mixes, and

- *user friendliness of material*, where problems are encountered with level control or compaction, foamed mix layers can be reworked. This also enables hand-work to be successfully carried out e.g. labour intensive construction

However, there are also ***disadvantages*** in the use of foamed bitumen mixes that should be taken cognisance of:

- *level of skill required*, the mix design and manufacture process for foamed bitumen mixes requires an advanced level of experience in order to produce a satisfactory quality product,
- *mix design procedures* are not as well formulated for cold mixes as for HMA making the process of acquiring experience in mix production and specification difficult,
- *anti-foamants* added to some bitumens in the refining process preclude their suitability for use in foamed bitumen without the addition of foamants, which adds to the cost of the binder,
- *pavement design procedures*, no transfer functions have been developed for the design of foamed bitumen layers in a pavement, making accurate design of the entire pavement structure difficult, and
- *cost-benefits difficult to prove*, without reliable long term pavement performance predictions, the life-cycle cost benefit is difficult to ascertain. For this reason many clients are not often prepared to take the risk of using a less well researched product.

2.2 Comparison of foamed bitumen with other bituminous binders

In order to highlight some of the differences between foamed bitumen and other bituminous binders, Table 1 - 1 has been developed. It compares the materials and the manufacture and construction processes for mixes utilising the different binders.

Table 1 - 1. Summary of comparative manufacture and construction processes for different bituminous binders.

FACTOR	***BITUMEN EMULSION***	***FOAMED BITUMEN***	***HOTMIX BITUMEN***
Aggregate types applicable	• Crushed rock • Gravel • Recycled (RAP)	• Crushed rock • Gravel • Recycled (RAP) • Marginal (sands) • Contaminated materials	• Crushed rock • Some RAP
Bitumen temperature during mixing	50°C – 70°C	170°C – 200°C	140°C – 180°C
Aggregate temperature during mixing	• Ambient (cold) • Warm (49°C – 85°C) • Warm (104°C – 127°C)	• Ambient (cold) • Half-warm ? (40°C – 99°C)	• Hot (140°C – 200°C)
Moisture content during mixing	OMC + 1% – Emulsion content	Fluff Point* i.e. 65% - 85% of OMC	Dry
Type of coating of aggregate	"painting" or coating of coarse particles and cohesion of mix with fines mortar	Partial coating of large aggregate with "spot welding" of mix with fines mortar	Coating of large aggregate with controlled film thickness
Construction and compaction temperature	Ambient	Ambient Or 40°C - 95°C for Half-warm mixes	140°C – 160°C
Rate of initial strength gain	Slow	Medium	Fast
Modification potential of binder	√	?	√
Important parameters of binder	• Emulsion type (anionic, cationic..) • Solids content • Breaking time • Curing	• Half-life • Expansion Ratio • "Foamability" • Penetration • Softening Point	• Penetration • Softening point • PI • Viscosity

*see Definition of Terms

3. THE NEED FOR MIX DESIGN CRITERIA

3.1 Purpose

In the civil engineering industry, the production of materials to be utilised for infrastructural development requires both strategy and control. These materials are often a combination of numerous ingredients that are formulated, combined and processed to provide a composite product for a specific purpose or application. In order to produce construction materials with the necessary quality and consistency to fulfil their intended function, adequate procedures need to be established to assist in identifying optimal formulation, blending and production. This process is the mix design procedure. It is particularly pertinent to road pavement materials where the ingredients are predominantly natural and variable, and the area of the application influences their availability, suitability and the behaviour of the composite material.

Optimisation of the mix design of materials takes place not only in terms of volumetrics and compaction characteristics, but also requires the consideration of engineering properties of the mix, durability and long term performance. At the same time, economic considerations remain paramount in the selection of mix designs. For bituminous mixes, the binder has a significant influence on the cost of the overall material.

Of all of the aspects to mix design, performance is one of the most difficult to address. This is due to a number of factors including:

- the diversity of ways in which the performance of a material may be measured e.g. durability, resistance to fatigue etc,
- difficulties in identifying the mode of failure of the material and mechanisms contributing to this failure,
- the variety of mix properties and intrinsic material properties that can influence performance e.g. gradation of mineral aggregate, hardness of aggregate, binder content etc,
- the variety of external factors that have an influence on performance e.g. climate, loading speed, magnitude, configuration etc. and their variability,
- the difficulties in simulating long term effects in a manner that is not mutually exclusive for different mix properties,
- the time and cost involved in modelling long term behaviour of materials through research.

Notwithstanding these difficulties, performance requires careful consideration in the mix design of engineering materials. In particular, any material needs to be characterised in terms of its basic components, critical parameters and performance requirements. Figure 1 - 1 provides a conceptualisation of a holistic approach to mix design of materials for road pavements. This is particularly pertinent to new materials undergoing research and development.

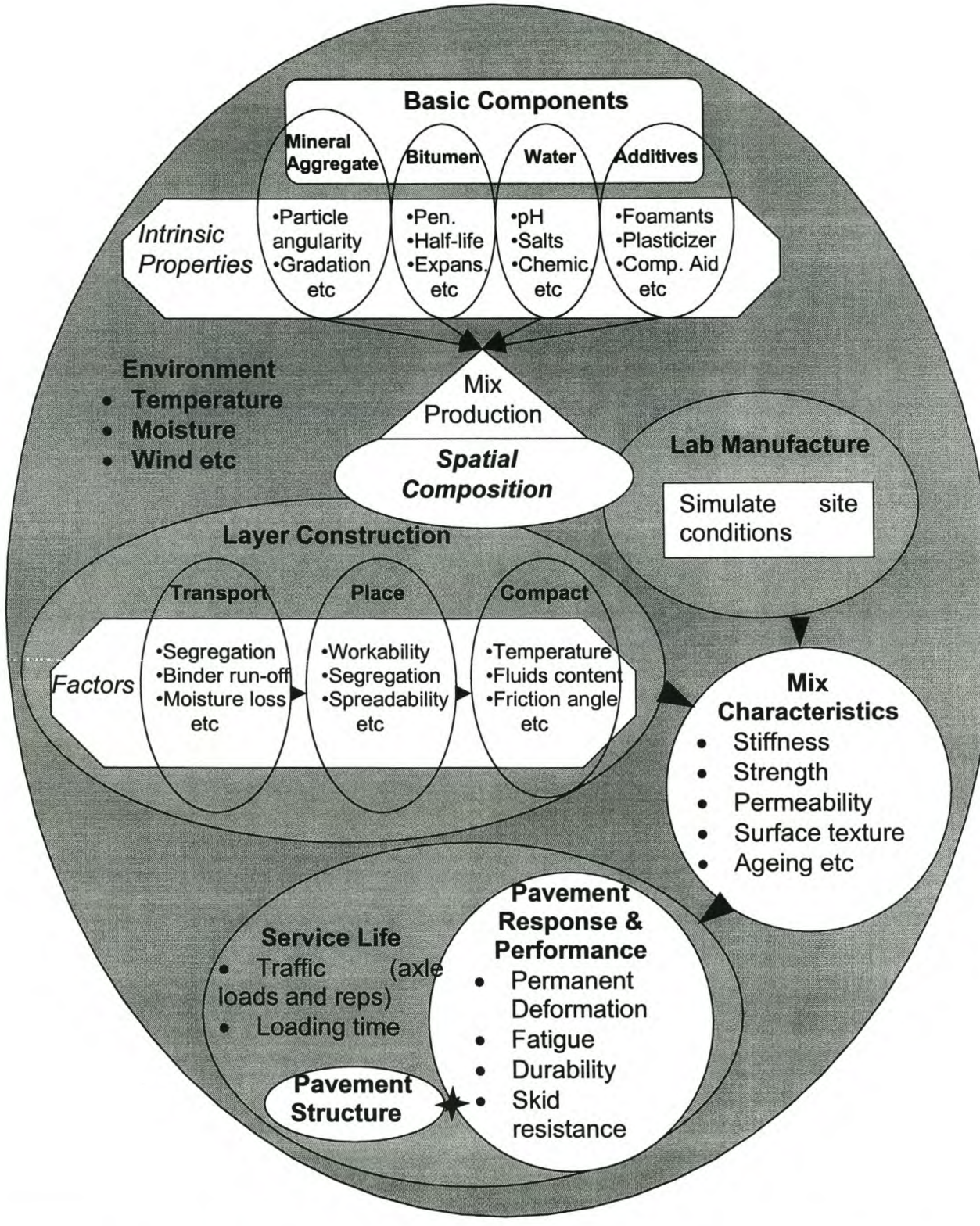

Figure 1 - 1. Conceptual framework for mix design of foamed bitumen materials

3.2 Mix Design of Cold Mixes, particularly Foamed Bitumen

The current selection criteria for the optimal mix components of bituminous materials differ significantly from one country to another. This is applicable to both hot mix asphalt and cold mixes. It should be noted that no standard mix design procedure for foamed bitumen could be found in any country and the methodologies presently applied are based on different mix formulations and interpretations. Various modes of failure have been considered important including permanent deformation, fatigue and shear, which will be elaborated upon in Chapter 2. This has led to the evaluation of the properties of foamed bitumen mixes during the laboratory designs using a variety of tests such as the Indirect Tensile Strength (ITS) Test, the Unconfined Compressive Strength (UCS) Test, the Stability from the Marshall Test as well as many others. The relevance of these tests and the failure mechanisms require critical review in a rational approach to the design of cold mixes.

A conceptual framework for a cold mix design procedure relative to hot-mix asphalt (HMA) design, assists in highlighting some of the focus areas that are required for the design of foamed bitumen mixes and at the same time underlines intrinsic differences between the two material types. Figure 1 - 2 provides a simplified flowchart for asphaltic mix design, for both hot and cold mixes. This also serves as a frame of reference for reviewing the current literature on foamed bitumen as it provides perspective on the characteristics and function of the mix.

It is apparent from Figure 1 - 2 that, although some of the aspects of the mix design process such as material selection, are shared by cold mixes and hot mixes, some fundamental differences in the composition and preparation of these mixes occur. In particular, the binder characteristics differ markedly between hot and cold mix asphalt. In addition, the inclusion of the water phase into cold mixes introduces a more complicated volumetric composition. These and many other factors require consideration in the development of improved mix design procedures for cold bituminous mixes.

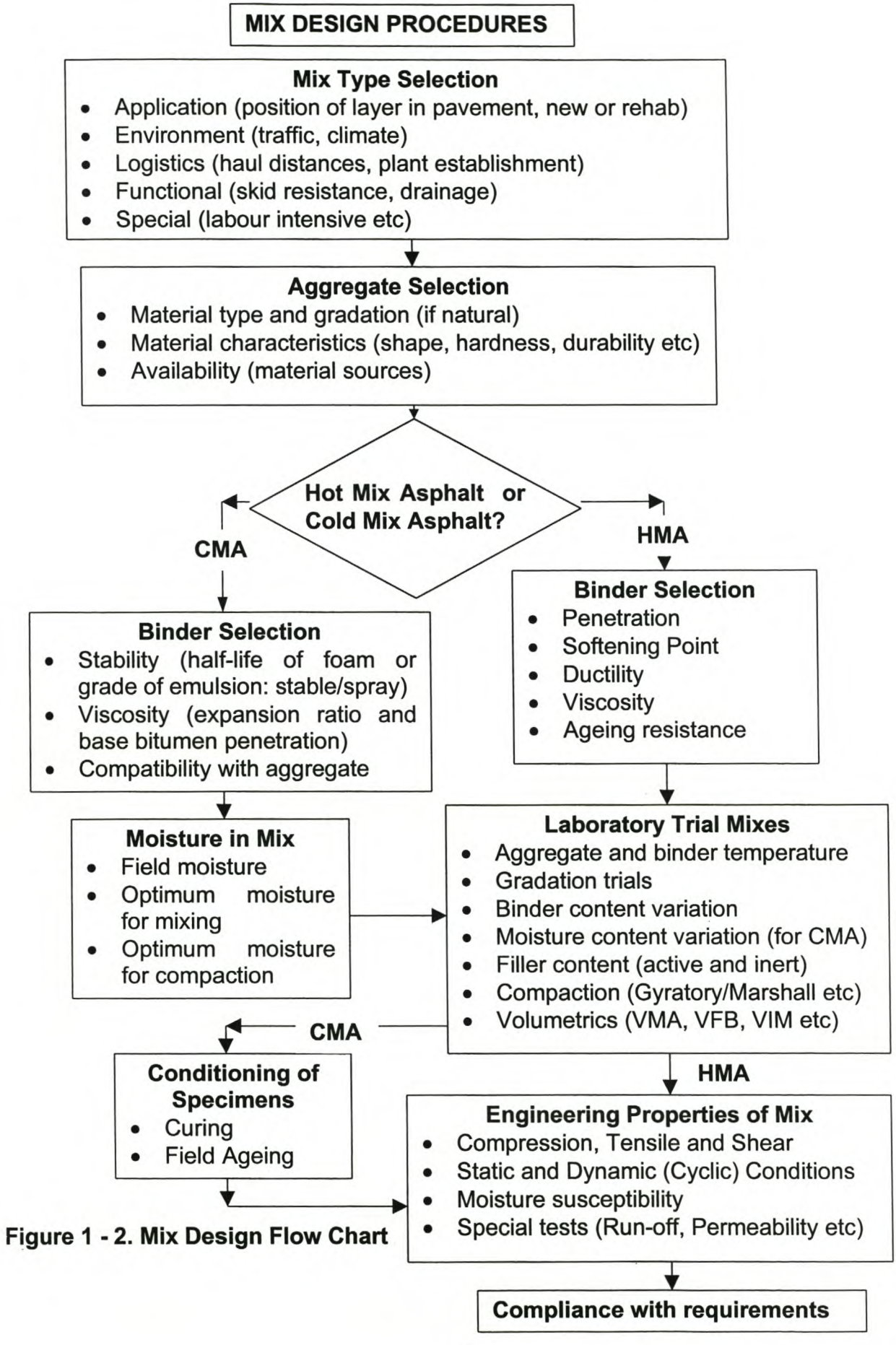

Figure 1 - 2. Mix Design Flow Chart

4. OBJECTIVES OF DISSERTATION

Motivation for carrying out research carries with it objectives that are intended to be fulfilled through the work. In a broader perspective, the aims invariably include requirements set by sponsors of the work. But these require refinement into specific objectives of the research.

The primary objective of the study is to address the need for a fundamental understanding of foamed bitumen and foamed bitumen mixes as pavement engineering materials, and in so doing to develop techniques for adjudicating mixes, optimising their composition and rationalising their design both as mixes and as layers in road pavements. At the same time the exploration of new applications for foamed bitumen and the possibilities for progressive related technology, is a priority. In order to strive to achieve this main objective, several sub-objectives have been identified each with appurtenant activities, as detailed below:

- *Development of a fundamental understanding of mechanisms governing the behaviour of foamed bitumen, apart from the mineral aggregate*. Current understanding of foamed bitumen behaviour is limited and based on empirical relations. Reasons for change in the characteristics of the foam with adjustment in bitumen type, bitumen temperature and application rate of foamant water, for example, are neither understood nor documented. As such, optimisation of the foam properties is not possible. The identification of relevant factors that influence foam behaviour and the development of models that utilise these factors to effectively optimise the foamed bitumen for cold mix production, is an objective therefore. If possible, such models should be structured so as to be suitable for implementation by industry. This objective is addressed in Chapter 3.

- *Improvement of understanding of behaviour of cold mixes, and in particular foamed bitumen mixes in terms of spatial composition including the establishment of models.* At present only rudimentary methods of monitoring mineral aggregate suitability for treatment with foamed bitumen are documented. Fundamental reasoning for the suitability of certain spatial compositions for foamed bitumen treatment with identification of pertinent factors as mix design criteria requires development therefore. In particular, interaction of foamed bitumen and the filler fraction and the influence of moisture on the mix characteristics require clarity. To this end, an objective of the research is the recognition of these factors (at least the most important ones) and the establishment of well-founded boundaries within which these factors should be approached for mix design purposes. Chapter 4 focuses on the aims of this mix design objective.

- *Investigation of possibilities for new technologies that could improve the quality of foamed mixes.* Foamed bitumen mixes have historically been approached solely as cold mixes for use below the base layer in moderately to heavily trafficked roads. In particular, influences of the aggregate temperature during the manufacture of foamed mix have been ignored. An objective of the research is to identify the degree to which this factor and others, influence the behaviour and performance of the mix and to

develop workable methods of improving mix quality through effective manipulation of such variables. The implications of mix modification require verification through measured performance relative to mixes of known characteristics, which is addressed in Chapter 5.

- *Development of possible cold mix technologies that lend themselves to labour intensive construction.* In terms of the requirements of the CAPSA-Colas bursary held by the candidate, the development of technologies that include bituminous materials eminently suited to labour intensive construction in developing countries, forms an objective of the research. In particular, bituminous blocks that can be cost-effectively produced and constructed for road pavements in developing areas are needed. Relevant mix design criteria and manufacture and construction methods of such blocks become the focus of this objective, outlined in Chapter 6.

- *Identification of the mechanisms that influence the performance of foamed bitumen mixes and development of models suited for relevant pavement design.* Division of cold foamed mixes into representative groupings with similar behavioural characteristics followed by the selection of pertinent performance criteria for mix and pavement design is an objective of the research. Mechanisms that influence performance should preferably be measurable through mix design and utilised in pavement design incorporating the relevant foamed mix material. Exhaustive failure mechanisms of foamed mixes are not an objective; one highly relevant mechanism is sufficient. Chapter 7 aims to fulfil this objective.

5. REFERENCES

SAT (Society for Asphalt Tehnology), 1998. **Bituminous Materials on Site (BMOS) Course**. Module 6 Notes prepared by K.J. Jenkins and Q. Smith. Peninsula Technikon, Cape Town, South Africa.

SHRP (Strategic Highway Research Program), 1994 . **Superior Performing Asphalt Pavements (Superpave) : The Product of the SHRP Asphalt Research Program**, National Research Council, Washington DC 1994.

CHAPTER 2

LITERATURE STUDY OF FOAMED BITUMEN MIXES

1. INTRODUCTION

1.1 Brief history of Foamed Bitumen

More than forty years ago Dr Ladis Csanyi at the Bituminous Research Laboratory of the Engineering Experiment Station, Iowa State University successfully injected steam into bitumen to create a foaming mass (Csanyi, 1957 and 1959). Csanyi's invention was inspired by the abundance of ungraded marginal loess materials in his state of Iowa, and a shortage of good quality aggregate. Initially, he began experimenting with the "impact process" patented by a Swiss, Albert Sommer, whereby the binder is introduced into a mixer in atomised form and aggregate is passed through the cloud of atomised bitumen (Csanyi, 1956). It was natural progression that led to the development of a system where the binder is foamed *before* it makes contact with the mineral aggregate.

Dr Csanyi discovered that, during its metastable life, the foamed bitumen could be mixed with a variety of soils to improve their properties and produce a road building material. Since then the foamed bitumen process experienced only limited application on a global scale, primarily due to the exclusive rights of the patent holders on the foam nozzles.

Dr Csanyi did attempt water as a foaming agent (as well as air, gases and other foaming agents), in addition to steam but opted to use the latter because

"*the use of steam proved to be the simplest, most effective and efficient*" (Csanyi, 1959).

The assistant, Mr R Nady (Lee, 1981) of Professor Csanyi provides an additional reason for the latter's selection of steam as a foamant. Nady states that, in the early days the asphalt plants had a steam jetty to keep bitumen warm and to keep the pipe jacketing on the piping system and the pugmills warm, making steam readily available.

In 1968 Mobil of Australia acquired the patent rights for the Csanyi process, the nozzle of which is shown in the Figure 2 - 1. Within two years Mobil had modified the process by replacing the steam with 1% to 2% cold water that is combined with the hot bitumen in a suitably designed expansion chamber to produce the foam, which is discharged under pressure (Lee, 1981). A patent for the expansion chamber/nozzle system was granted to Mobil in Australia in 1971 and was extended to at least 14 countries. This lead to trials of the foamed bitumen process being carried out in some 16 countries in the 1970's.

By 1982, Australia alone had placed some 2,9 million m^2 of foamed bitumen mixtures, generally as a base or sub-base layer. South Africa, New Zealand, Japan, Germany etc

had all laid lesser coverage of foamed materials by 1982; whilst by the same date, the USA had produced hundreds of kilometres of surface layer mixtures with foamed bitumen.

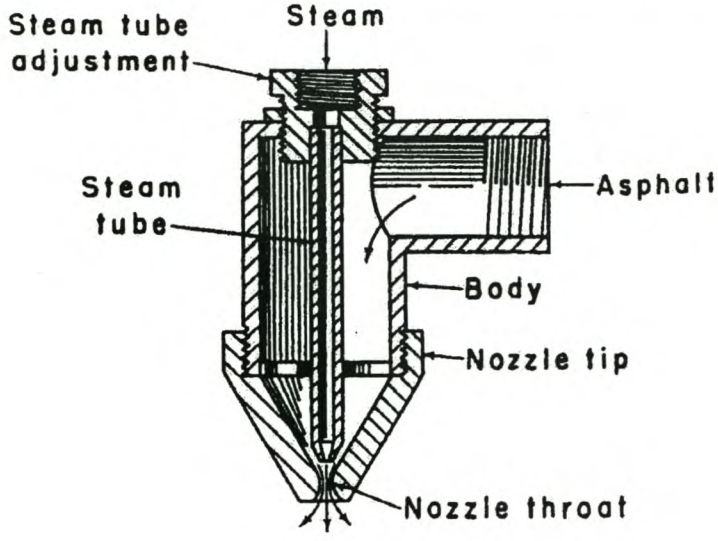

Figure 2 - 1. Original Spray Nozzle for Foamed Bitumen Process (Csanyi, 1957)
(Csanyi's asphalt is bitumen)

With the lapse of the patent rights in the 1990's, interest in the process has burgeoned, with various foamed bitumen mixers being commercially available for purchase. Both static mixers and mobile "in situ recyclers" have been developed incorporating the foamed bitumen process. A wide variety of static plant mixers are utilised to blend foaming bitumen with mineral aggregate, including:

- Twin-shaft pugmill type mixers,
- Free-fall vertical shaft mixers,
- Drum mixers, and
- Laboratory agitators or mixers.

Pavement layers that have been produced using these mixers have been the focus of research. The publications are reviewed in the literature study.

2. HISTORICAL MIX DESIGN CONSIDERATIONS

2.1 Introduction

The history of foamed bitumen, as detailed in Section 1.1, dates back to 1957 when Prof Ladis Csanyi first injected steam into bitumen to create a temporary colloidal mass that could be mixed with damp mineral aggregates at ambient temperatures. Since that time, literature has been published on a variety of different materials treated with foamed bitumen using a variety of foaming plants in various climates. Much of the literature emanates from Australia where Mobil Oil held the patent rights on the foaming expansion chamber/nozzle system, after acquiring the rights from Prof Csanyi and modifying the system to use cold foamant water instead of steam. Other countries noted for their involvement in foamed bitumen prior to the 1990's include the USA, the UK, Canada, Norway and South Africa.

As the use of foamed bitumen has expanded to a diversity of countries, so the selection criteria for the optimum mix components has varied, based on different formulations and interpretations of the product. The mix design procedures for foamed mixes have not been formalised due mainly to limited application and often secretive approaches to the process by operators. This has resulted in an absence of fundamental guidelines for the use of the product, stifling further development of the process.

The available literature on foamed bitumen requires review in order to gain perspective on the evolution of the mix design approach over the decades to current thinking. The lack of standard mix design procedures has resulted in wide speculation regarding various modes of failure of the material including permanent deformation, fatigue and shear. This has led to the evaluation of the properties of foamed bitumen mixes during the laboratory designs using a variety of tests, including amongst others the Indirect Tensile Strength (ITS) Test, the Unconfined Compressive Strength (UCS) Test, the Stability from the Marshall Test and many others.

The conceptual framework for a cold-mix design procedure relative to hot-mix asphalt (HMA) design provided in Chapter 1, assists in highlighting some of the focus areas when working with foamed bitumen mixes and at the same time underlines intrinsic differences between the two material types. This is used as a frame of reference for the literature review on foamed bitumen as it provides perspective on the characteristics and function of the mix.

2.2 Bitumen requirements

The foam characteristics of bitumen i.e. the expansion ratio and half-life, see "Definition of Terms", are influenced by a variety of factors and can vary significantly. Variations in the foam characteristics, in turn, have a bearing on the performance of the foamed bitumen mix. Changes in the expansion ratio, for example, result in variation in the viscosity of the binder at time of mixing, which influences the dispersion of the binder in the mix. Variations in the half-life have a bearing on the time available for mixing before the foam collapses to its original state.

2.2.1 Foamability

In the analysis of variables that influence the "foamability" of bitumen, Brennen *et al.* (1983) identified three factors viz,

- The amount of foam produced,
- The amount of water in the foam, and
- The foaming temperature of the bitumen.

Although these three factors are important, they do not completely explain the fluctuations in foamability of bitumen. The amount of foam produced is a function of the time of discharge of the foam and the bitumen pressure in the foam system. The influence of these factors is explored further in Chapter 3, see Figure 3-2. Brennen *et al.* produced curves characterising foamed bitumen with water application rate as the independent variable and the added influence of temperature variation, see Figure 2 - 2. An increase in bitumen temperature generally resulted in an increase in expansion ratio but a decrease in half-life. The same trend was noted for an increase in foamant water application.

Ruckel *et al.* (1982) established a proposed testing procedure for foamed bitumen characterisation. This includes 6 variables in the sensitivity analysis to establish the desired conditions for foam production, including bitumen temperatures of 163°C and 177°C, and foamant water application rates of 1,5%, 2% and 2,5% by mass of the bitumen. Ruckel *et al.* suggest that each new batch should be tested and that duplicate tests should be carried out until repeatability is established. This approach is commendable, but for reasons provided in this research, is inadequate as it ignores a number of factors that are highly relevant to the analysis process, such as the temperature of the vessel into which the foam is discharged, the time of spraying the foam etc.

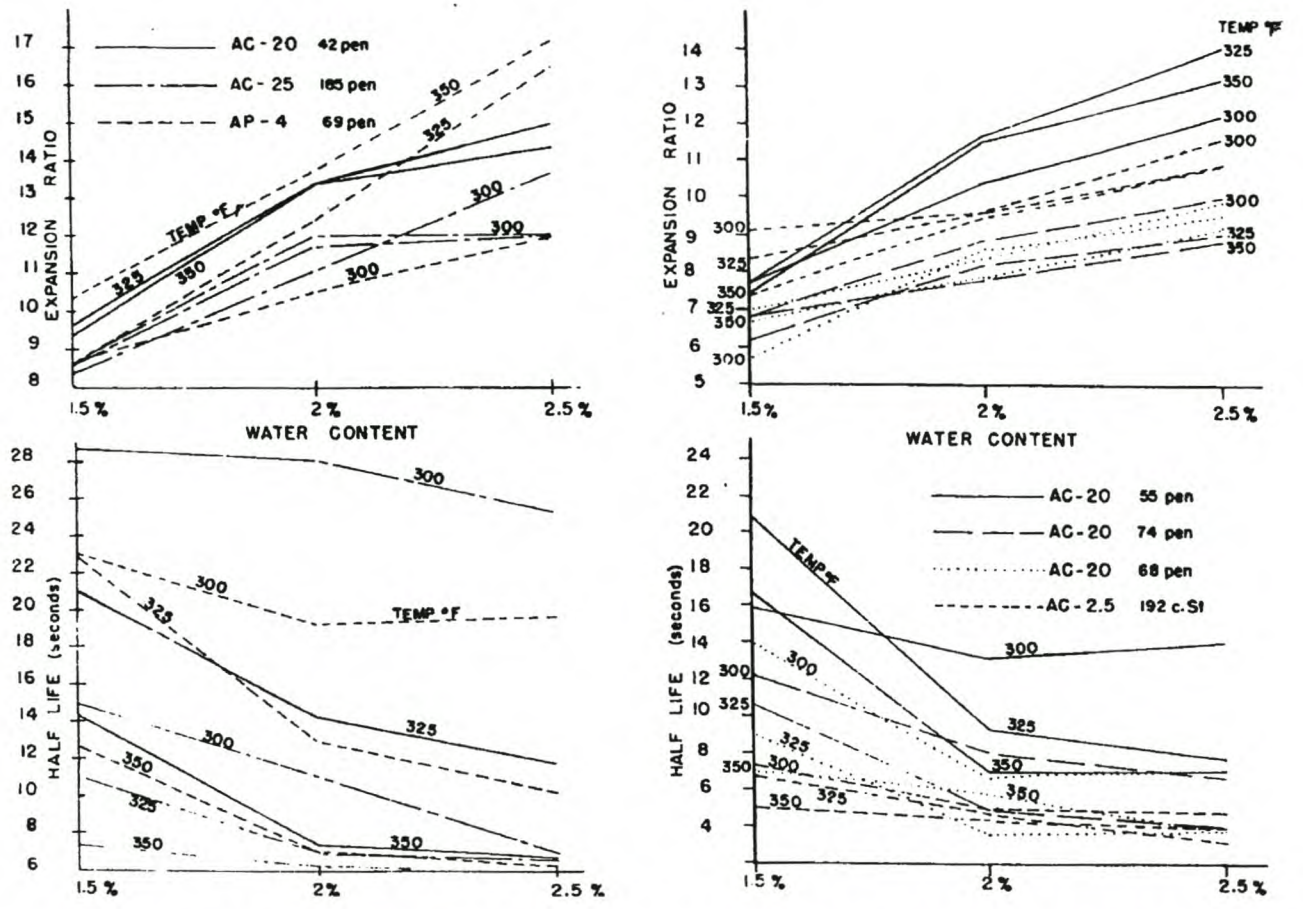

Figure 2 - 2. Expansion Ratio and Half-life Relationships for Foamed Bitumen Produced from Different Penetration Grades (Brennen *et al.*, 1983)

The foam characteristics have been shown by Bowering and Martin (1976) to influence cohesion, stability and unconfined compressive strength. By increasing the expansion ratio of the foam from 3:1 to 15:1, all three of these properties and in particular the cohesion, are increased for a sandy loam stabilised with foamed bitumen. In order to ensure that the quality of a foam mix is maintained, given the variation in foam properties, guidelines have been provided for the foam characteristics in some countries. Notably, Ruckel *et al.* (1983) and Acott and Myburgh (1983) recommended limits of 8 to 15 for the foam (expansion) ratio and 20 seconds (minimum) for half-life for tests in a 1 gallon container, whilst the CSIR (1998) recommends an expansion ration of at least 10:1 and a half-life of at least 12 seconds.

Maccarrone *et al.* (1994) investigated the influence of additives or "foamants" that extend the half-life of a foamed bitumen. With the addition of 0.5% to 0.75% foamant, the expansion ratio of the bitumen was maintained at between 8:1 and 15:1 whilst the half-life increased to in excess of 40 seconds. Such additives are useful where bitumens have been treated with silicone defoamants or anti-foamants and do not produce the desirable characteristics. There can be, however, significant financial implications by including an additive in a foaming process.

Lee (1981) studied the effects of half-life and foam (expansion) ratio on Marshall properties of foamed-mixes. The expansion ratio utilised ranged from 5 to 20 and the half-life from 11 to 136 seconds. The study revealed no significant trends in the mixes in terms of Marshall Stability and Immersion Stability relative to the foam characteristics. The properties of the mix selected for analysis are not considered entirely appropriate, however, as tensile strength would have been preferred. In addition, the temperature of the aggregate was not taken into consideration in the experiment, which could have influenced the results.

2.2.2 Bitumen properties

Several researchers have investigated the influences of the penetration grade on the foaming characteristics of bitumen in the past. Initially, Csanyi (1957) stated that:

> *"An asphalt cement having a penetration of 85 to 100, when foamed will have a penetration of over 300 at the same temperature, for some time after it has foamed. Chemical constituent tests indicate that the asphalt has not changed even though its consistency and viscosity have changed."* And *"The foam remains soft even at temperatures at which the parent asphalt cement has stiffened materially."*

Csanyi found it possible using his foaming apparatus, to produce two different types of foam, namely "discrete foam" and "concentrated foam" which comprised separate individual small bubbles and agglomerations of bubbles respectively.

Brennen *et al.* (1983) and Lee (1981) did not show conclusive correlation between penetration grade and foam characteristics. Brennen *et al.* state that:

> *"The results indicate that viscosity alone is not sufficient to explain the variations in expansion ratio and half-life".*

Abel (1978) produced more conclusive results with the finding that bitumens of lower viscosity foamed more readily than those of higher viscosity, providing foams with higher expansion ratios and half-lives; but that the higher viscosity bitumens produced an improved coating of aggregate. With the exception of Ruckel *et al.* (1983) and the CSIR (1998) however, no cognisance was taken of the vessel into which foam was discharged and measured. Even then, critical properties such as vessel temperature, time of foam discharge etc were ignored by Ruckel *et al.* As shown in Chapter 3, all of these factors have a significant bearing on the foam properties.

In addition to penetration and viscosity of the bitumen, the Penetration Index (PI) can also influence the foam characteristics. This was not considered in previous research carried out in this field and is therefore explored further in Chapter 3.

2.3 Aggregate properties

Since the inception of the use of foamed bitumen, a wide range of materials has been successfully treated for use in road construction. Aggregates of sound and marginal quality, from both virgin and recycled sources have been utilised in the process.

As a result of the ubiquitous nature of suitable aggregates for foam treatment, research initiatives have generally focussed on specific types of materials. Acott (1979 and 1980) for example, concentrated his research on sands stabilised with foamed bitumen, including aeolian sand, river sand, mine sand and blends of these materials. The shear properties of the materials were analysed using the Hveem Resistance Value in the laboratory and the Vane Shear Strength in the field. Most of these materials were found to be suitable as a base layer for moderately trafficked roads with low wheel loads and fast moving vehicles.

2.3.1 Aggregate gradation

From their experience with the foamed bitumen process using different material types, Mobil Oil established guidelines for suitable gradations of aggregates that may be utilised for foam stabilisation (Akeroyd and Hicks, 1988). Figure 2 - 3 defines the envelopes for different levels of suitability of materials for use in the foam process, as developed by Mobil.

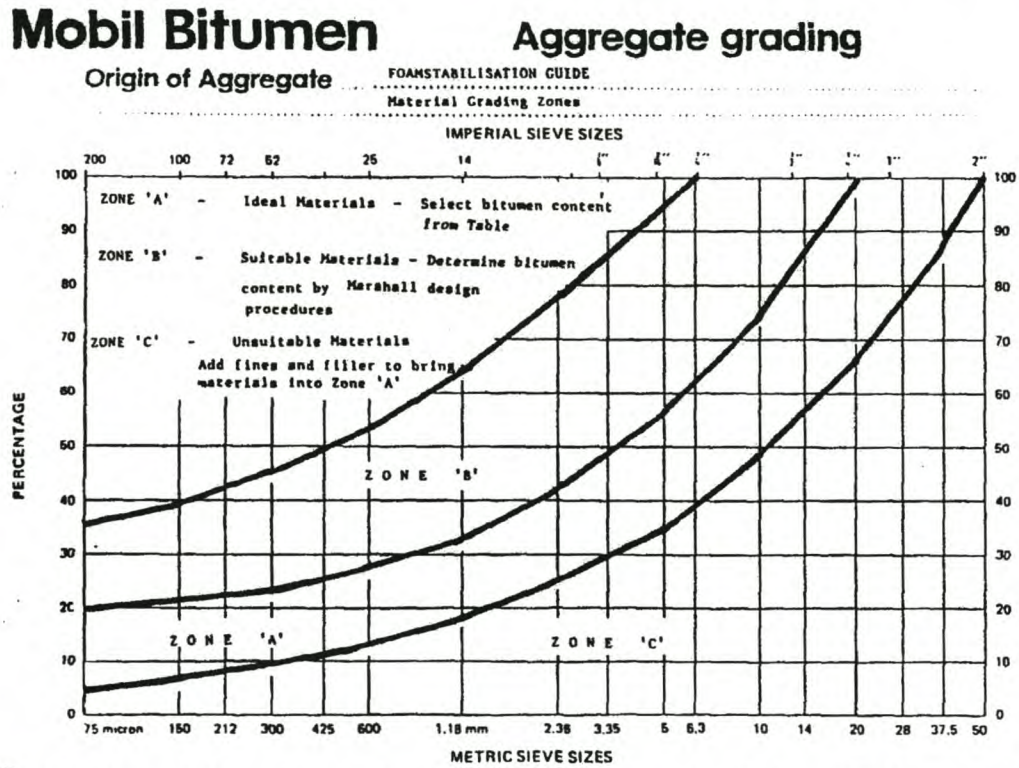

Figure 2 - 3. Ranking of suitability of aggregates for foamed bitumen stabilisation by grading envelopes.

According to Figure 2 - 3, not only has the suitability of aggregate been defined by Mobil, but guidelines have also been provided for the design binder content for the ideally graded

material in Zone A. Grading alone, however, is inadequate in completely defining the foamed bitumen mix design and additional material properties are required to provide a more accurate mix design. Even in the two-phase system of Hot Mix Asphalt (HMA) with mineral aggregate and binder, laboratory testing is carried out in order to refine the mix design and include volumetric considerations.

Grading has also been utilised as a property to not only classify the suitability of a material, but also to provide an indication of the optimum binder content using foamed bitumen. Using this approach Bowering and Martin (1976) and later Ruckel *et al.* (1982) established a table ranking the various materials for use in foamed bitumen mixes. The soil types, as given in Table 2 - 1, have been substituted for the Unified Soil Classifications used in the original guidelines.

Table 2 - 1. Ranking of suitability of materials for foam treatment (after Ruckel *et al.*, 1982)

Soil type	Suitability for Foamed Mix	Optimum Bitumen Content (% m/m)	Comments
Well graded gravel, little or no fines	Good	2.0 – 2.5	Permeable (improve with crushed fraction)
Well graded gravel + some clayey silt	Good	2.0 – 4.0	Permeable (improve with crushed fraction)
Well graded gravel + sandy silt	Good	2.0 – 4.0	Permeable (improve with crushed fraction)
Poorly graded gravel + sandy clay	Good	2.5 – 3.0	Low permeab. (improve with crushed fraction)
Clayey gravel	Poor	4.0 – 6.0	Improve with lime
Well graded sand	Fair	4.0 – 5.0	Needs filler
Well graded silty sand	Good	2.5 – 4.0	
Poorly graded silty sand	Poor	3.0 – 4.5	Use lower pen bitumen, add filler
Poorly graded sand	Fair	2.5 – 5.0	Needs filler
Silty sand	Good	2.5 – 4.5	
Slightly clayey, silty sand	Good	4.0	
Clayey sand	Poor	4.0 – 6.0	Needs small % lime
	Good	3.0 – 4.0	After lime modification

2.3.2 Filler content

According to literature, the factor emanating from the grading that has the highest impact on the optimum binder content of a foam mix, is the filler content. The fraction of mineral aggregate smaller than 0,075mm has been shown by various researchers to have a bearing on the behaviour of a foamed mix. For this reason, Ruckel *et al.* (1982) established a guide for the recommended design bitumen content for different aggregate gradings based on the filler content, as shown in Table 2 - 2 below.

Table 2 - 2. Guidelines for Design Bitumen Content as a Function of Filler Content Targeted for Foamed Mix (after Ruckel *et al.*, 1982)

Passing 4,75 mm sieve (%)	Passing 0,075 mm sieve (%)	Foamed bitumen content (% m/m dry aggregate)
< 50	3.0 – 5.0	3.0
	5.0 – 7.5	3.5
	7.5 – 10.0	4.0
	>10.0	4.5
> 50	3.0 – 5.0	3.5
	5.0 – 7.5	4.0
	7.5 – 10.0	4.5
	>10.0	5.0

Unfortunately Table 2 - 2 provides very broad guidelines and the properties of filler materials, which can vary significantly, have not been accounted for. The Rigden voids of different fillers and "Bitumengetal" i.e. moisture content at which the filler becomes plastic, for example, are properties that are used to define fillers, and their bearing on foamed mixes requires further investigation. At the same time, one of the pertinent features of the table is the excessively high filler:binder ratios in comparison with HMA. The generally recommended f/b (m/m) for foamed bitumen mixes is apparently well in excess of 0.9. This is investigated further in Chapter 4.

2.3.3 Plasticity

Reference has been made in the literature on foamed bitumen and bitumen emulsion to the influence of plasticity on mix performance. Indirectly, this is addressed in Table 2 - 1 with the materials having higher clay contents being less suited to foam treatment or requiring modification. Bowering and Martin (1976) confirmed that high plasticity clayey gravels respond poorly to the foamed bitumen treatment process unless modified before the addition of binder.

Lee (1981) from his research with foamed mixes, states that a limited percentage of plastic fines is acceptable, but lime pre-treatment may be advisable and economic if the Plasticity Index PI > 8%. Lancaster *et al.* (1994) suggested a maximum PI limit of 12% before lime modification is necessary. In addition, Lancaster *et al.* states that cementitious additives should be limited to 2% by mass of the aggregate, to minimise the potential of shrinkage cracking in the foam treated layer.

2.3.4 Material Type

The types of material suitable for treatment using the foamed bitumen process have been referred to in literature by gradation and properties rather than by parent material type. For example, Ruckel *et al.* (1983) list suitable materials for foam treatment as crushed stone, rock, gravel, sand, silty sand, sandy gravel, slag, reclaimed aggregate, ore tailings and others. Most of these materials have been investigated by other researchers, with Acott

(1979) investigating sands, Lee (1981) investigating recycled materials and Dijkink (1992) investigating slag residue and ashes from zinc production, to name but a few.

No reference could be found in the literature, however, where specific rock types that are unsuitable for foamed bitumen treatment have been identified. This indicates a low dependency of the foam process on the particle charge of basic or acidic rocks, unlike the emulsion process where rock type influences the selection and performance of bitumen emulsions as binder. Aggregate types that experience moisture susceptibility in the form of stripping e.g. "glassy" granite in hot mixes, however, can encounter the same problems with a foamed bitumen binder, from experience of the author.

2.4 Fluid considerations

2.4.1 Foamed bitumen content

The influence of foamed bitumen content on different mix properties has been the point of focus of many researchers investigating foamed bitumen mixes. Not only is it important to optimise the binder content in a foamed mix from an economic perspective, but it is imperative that the critical engineering properties for suitable performance, are selected for the optimisation.

Shackel *et al.* (1974) carried out a series of triaxial tests on Sydney crushed breccia. For these materials it was shown that an increase in the binder content resulted in an increase in the number of load repetitions in the dynamic triaxial test, to achieve 2% axial strain. Bowering and Martin (1976) studied the influence of binder content in terms of Hveem Resistance, Relative Stability, Cohesion and Unconfined Compressive Strength (UCS) of foamed mixes manufactured from a variety of materials. These properties, which represent a variety of performance characteristics (including permanent deformation and fatigue), were found to increase to a maximum followed by a decline, for increasing binder content. Models for the relation of these properties to performance are not included in the literature.

Brennen *et al.* (1983) investigated the influence of the binder content of a foamed mix on the moisture sensitivity of the mix. For RAP mixes, it was concluded that, the higher the binder content of the mix, the lower the level of moisture absorption of the specimen during vacuum saturation. A benefit in increasing the binder content can therefore be expected in some cases in terms of a reduced moisture susceptibility of foamed mixes.

2.4.2 Moisture content of foamed bitumen mix

From the inception of foamed mixes, the moisture in the mineral aggregate prior to the addition of foamed bitumen has been considered vitally important in terms of a carrier for the binder during **mixing**, a **compaction** agent and a promoter of **shelf-life**. The inclusion of the water phase into the asphaltic mix is the primary factor that sets foamed bitumen apart from conventional HMA. The father of foamed bitumen, Csanyi (1960) wrote that :

> *"The water added to aggregate during mixing softens the clayey materials or heavy soil fractions so that the agglomerations are broken up and uniformly distributed throughout the mix. The water also separates the fine particles and*

suspends them in a liquid medium, making channels of moisture through which the foamed asphalt may penetrate to coat all the mineral particles. The quantity of water is not critical, but sufficient water must be in the mix to make a satisfactory mixture. Excess moisture is undesirable because it makes the mix too soupy and may reduce coating of the aggregates. The proper quantity of water for any mix may be readily determined by a few trial batches."

The observations of Csanyi highlight the multi-functional nature of the moisture in the mix i.e. it is necessary for particle suspension, binder dispersion, workability, compaction etc. The optimisation of the moisture content is exclusive to the particular function. Bowering (1970) and Brennen *et al.* (1983) verified this with research efforts focussed on investigating the effects of varying the moisture in the aggregate prior to **mixing** with foamed bitumen. The "fluff point" concept was introduced as a result, which is defined as the moisture content at which the material occupies the maximum loose volume. The fluff point was proposed as the ideal moisture content of a particular material for blending with foamed bitumen. Brennen *et al.* also considered the amount of moisture critical because:

- too little moisture impedes dispersion of the foam, workability and compaction of the mix, and
- too much moisture increases the curing time and reduces the density and strength of the compacted mix.

Lee (1981) established that the optimum mixing moisture content varies with gradation of the aggregate and in particular the size of the fraction smaller than 0,075mm. He recommends that 65% to 85% of the optimum moisture content as established using standard AASHTO compaction, should be used for the mixing moisture content during foam stabilisation. Lee stresses that this moisture content is a very important design factor in the construction of foamed mixes. He states that the addition of moisture to a foamed mix after stabilisation with foamed bitumen is of no benefit. Figure 2 - 4 provides a representation of the influence of mixing moisture content on the Marshall stability of a foamed mix. Provided that the specimens were all tested at the same moisture content and density (which is uncertain), Lee's work underlines the importance of mixing moisture on the behaviour of a foamed mix.

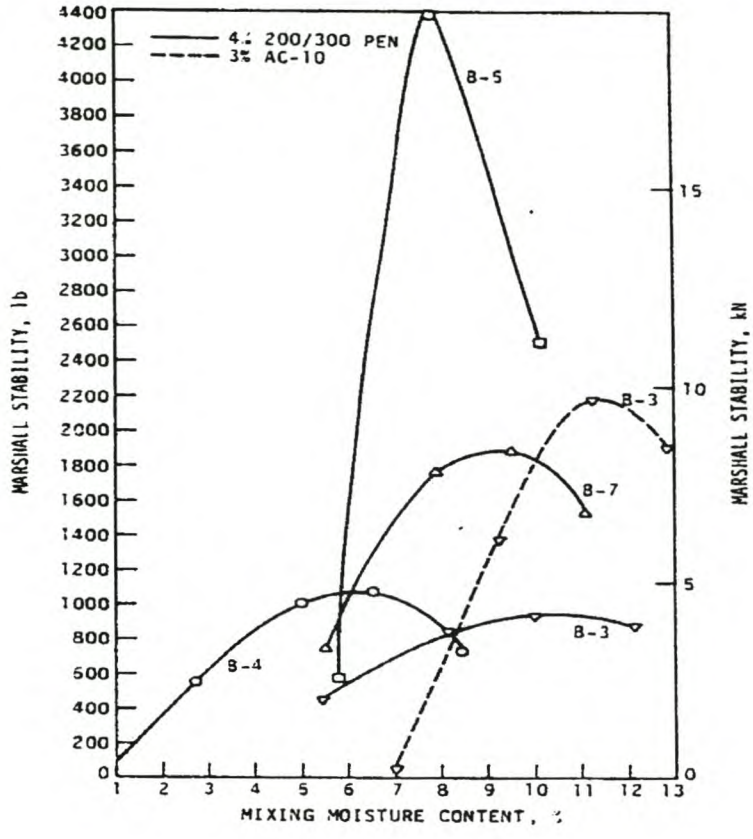

Figure 2 - 4. Influence of Mixing Moisture Content on Marshall Stability for Foamed RAP Mixes B-3 to B-7 with Different Gradations(Lee, 1981)

Ruckel *et al.* (1983) suggest that a sensitivity analysis be carried out for the mixing moisture content during the mix design for foamed bitumen stabilisation using 50%, 65% and 80% of OMC of the natural material. Overnight storage of the material after mixing is suggested to allow continued dispersion of the binder. This is in general agreement with Lee's recommendations except for the storage requirement (which would only be applicable if it simulated the actual construction process).

Some researchers consider the fluff point moisture content to be too low for mixing. For this reason Little *et al.* (1983) supplemented their mixes with moisture to obtain improved dispersion of the foam. They counteracted this increase by drying out the laboratory mix with stirring and aerating for 20 minutes, to achieve optimum moisture content (OMC) for compaction. Sakr and Manke (1985) carried out numerous tests on a variety of sands and discovered that the pre-moulding moisture content (MMC) for a foamed mix is a function of the OMC of the aggregate, the percentage of the filler fraction < 0,075mm (PF) and the bitumen content (BC). The function that was established, with R^2=0.977 is shown in Equation 2 - 1. All variables are input as percentage of the dry mass of the aggregate.

$$MMC = 8,92 + 1,48OMC + 0,40PF - 0,39BC \qquad \textbf{Equation 2 - 1}$$

The approach to reclaimed asphalt materials (RAP) has deviated from that of virgin mixes. Both Roberts *et al.* (1984) and Engelbrecht *et al.* (1985) investigated the foam treatment of RAP in a dry state i.e. without the addition of moisture. Roberts *et al.* showed that the tensile strength of the foamed mixes decreases significantly if the specimens are exposed to moisture prior to testing, but that the same order of decrease is experienced if wet RAP material is foam-mixed. Both research teams show that an optimum moisture content for **compaction** of the mix is evident (approximately 1% in this case), which is low compared to that of virgin aggregates. This was shown to have a bearing on both Hveem Stability's and Tensile Strengths.

Acott (1979) studied the influence of the compaction moisture content on the Hveem Resistance (Rt) value. Although the results shown graphically in Figure 2 - 5, indicate a decline in resistance value with increase in compaction moisture content, it is not possible to discern from the information whether this is due to the effect of moisture on compaction or the effect on mixing i.e. the distribution of the binder.

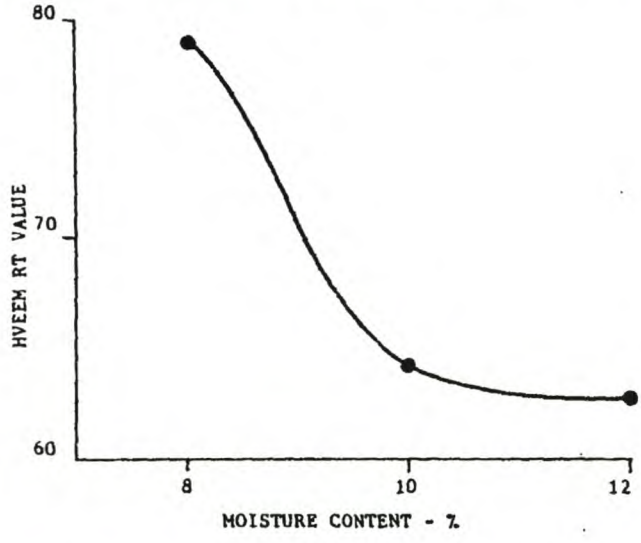

Figure 2 - 5. Influence of Compaction Moisture Content on Hveem Rt value, for a mine sand with 4% foamed bitumen (Acott, 1979).

Most researchers treat the moisture content for compaction independently to the bitumen content for foamed mixes. However, Humberto Castedo Franco and Wood (1982) state that the total fluid content (% moisture + % bitumen) provides the best compactive conditions near the soil's optimum moisture content as determined by the ASTM D 698. This approach of combining the fluids in the mix to analyse the fluid-density relationship has been adopted in the South African approach to bitumen emulsion mix design (SABITA, 1993) for mixes with low binder contents.

Moisture in a foamed mix after compaction is a third consideration concerning moisture, and is directly influenced by the curing of the mix. Shackel *et al.* (1974) investigated foam stabilised breccia in the triaxial test and found that, regardless of the bitumen content, an increase in the degree of saturation (Sr) results in an increase in permanent deformation at

the commencement of repeated loading. This is of significance to foamed mixes opened to traffic before adequate curing has been allowed to take place.

2.5 Mixing methods

In 1956 Csanyi propounded a "Mortar Theory" that suggests that individual coating of aggregate particles is desirable, rather than the bitumen permeating the entire mass forming a semi-solid-plastic cement holding the aggregates in place. This would allow the stability of the mix to be carried by the particles with the highest strength. Csanyi's philosophy was to enable marginal materials with large particles of weak crushing strength to be effectively stabilised for use in road pavements. The distribution of the binder in the mix, which in part depends on the mixing method, is the key to success of Csanyi's objective.

Csanyi (1957) further explains the importance of mixing in the foam process by describing a single bubble of bitumen bursting and coating an aggregate particle. Csanyi says:

> *"...when the bubble bursts the surface tension spreads the thin film of binder forcibly and rapidly over the surface of the aggregate. The modified surface tension of the binder when in the form of a bubble also provides natural forces that induce a high adhesion between binder and aggregate particle."*

According to literature, research conducted in a laboratory is primarily carried out with mixes that are prepared in scaled foaming plants and Hobart ® type mixers. The foamed bitumen is most often applied directly from the laboratory foam plant to the aggregate as it is being agitated in the mixer. Where the half-life of the foam exceeds 60 seconds (which usually requires the addition of a foamant), it becomes possible to manufacture the foam and dispense it into a container before blending it into the mix; but this approach is seldom used.

Eggers *et al.* (1990) state that it is imperative to utilise a laboratory mixer that emulates the mixing that takes place on site. The rotary mixing motion of the blenders used in the laboratory are neither ideal for restricting particle segregation nor from for the purpose of simulating site manufacture. The methods of site manufacture, including twin-shaft pugmills, drum-mixers, free-fall mixers and milling-drum mixers all provide sufficient volume in the mixing chamber and energy of agitation to ensure that the mineral aggregate is airborne when it makes contact with the foam. Blender type laboratory mixers do not emulate this, and the implications of these differences on the mix behaviour require consideration.

Ruckel *et al.* (1983) suggest that the mineral aggregate for a mix be divided into two fractions with 4,75mm being the cut-off, when mixes are prepared using the Hobart N50 Mixer. The fraction < 4,75mm is first mixed with the foamed bitumen, followed by blending of the coarse fraction by hand for 30 seconds. This procedure relies on the partial coating of the large particles for its efficacy. No deleterious effects have been noted using this procedure and Ruckel *et al.* state that if the mix darkens appreciably in comparison with the

colour of the moistened natural aggregate, the mixing time should be shortened. Over-mixing was noted to cause drying out and balling of a mix. These researchers also state that, after curing a layer of the mix at 110°C for 20 minutes, the mix should have darkened and be free of bitumen speckles > 1,6mm diameter. Practically all bitumen should (partially) coat the aggregate smaller than 9,5 mm with little or no coating of the aggregate larger than 9,5mm.

The method of Ruckel, which has it's origins with the Swede, K.G. Ohlson (the KGO Method), was taken a step further by Maccarrone (1994) when the two aggregate fractions were treated differently. The coarse (> 4,75mm) fraction was treated with bitumen emulsion and the fine fraction with (<4,75mm) was treated with foamed bitumen, to provide a composite mix that resembles HMA with complete coating.

2.6 Temperature considerations

The temperature of foamed bitumen mixes may influence the behaviour of the material at three different stages, namely mixing, compaction and in service (or after compaction).

Besides the recognition of the temperature of the bitumen on the foam characteristics, the temperature of the mix components during mixing has only received the attention of Bowering and Martin (1976) and Humberto Castedo Franco and Wood (1982). The work of Bowering and Martin is based on observations during research and leads to a generalised statement that, depending on aggregate type, the minimum mixing temperature of the aggregate is 13°C to 23°C, below which "poor" quality mixes will result. Humberto Castedo Franco and Wood (1982) who investigated the influence of aggregate temperature within a range of ambient temperatures (10°C, 22°C and 38°C), revealed an improvement in Hveem Stability, see Figure 2 - 6.

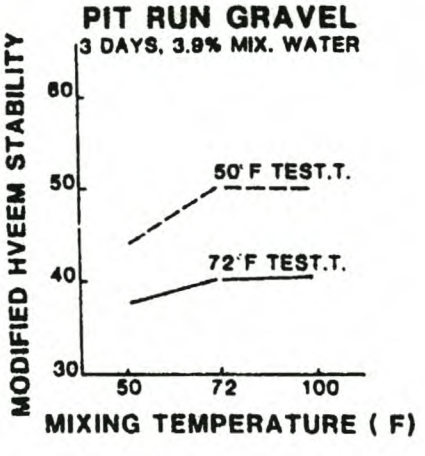

Figure 2 - 6. Influence of aggregate mixing temperature on Hveem S-value (Humberto Castedo Franco and Wood, 1982)

Humberto Castedo Franco and Wood's work does not, however, provide for the heating of aggregate to temperatures of greater than ambient but below 100°C i.e. to investigate the benefit that this might have on the mix. Unfortunately, the neglecting of aggregate temperature at the time of mixing has probably convoluted some of the research findings. The process of heating the aggregate to between 49°C and 85°C prior to mixing, has been used for the production of emulsified asphalt warm mixes in the emulsion industry (Asphalt Institute, 1992), but scope for "Half-warm foamed mixes" is still to be realised. The CSIR (1998) speculate that the heating of aggregates will increase binder dispersion within the foamed mix and aid in the coating of the large particles; but this remains unsubstantiated.

Although foamed bitumen mixes are generally regarded as cold-mixes and as such placed and compacted at ambient temperatures, the advantages of heating the cold foamed mix prior to compaction has been investigated. Numerous researchers have identified the possible benefit in this addition of heat. Bowering and Martin (1976) heated foamed surfacing mixes to 110°C for curing and compaction purposes, and compared mix properties to the same mix compacted at 23°C. The heating of the surface course mixes resulted in improved densities and significantly increased cohesion values, but resulted in variable Marshall Stability. Roberts *et al.* (1984) produced similar findings when they researched recycled aggregates, achieving substantially higher densities and engineering properties including tensile strength and stability.

Buschkuhl *et al.* (1990) studied the stabilisation of incinerator slag using foamed bitumen. Due to some marginal stabilities obtained for the mix, they investigated the benefit of increasing mix temperature to 60°C before compaction, which resulted in 25% to 158% increase in the stability values. Eggers *et al.* (1990) experimented with the same slag as Buschkuhl *et al.* (1990) and included additives called tensides in the moisture of the slag prior to mixing in an attempt to improve compactibility and hence Marshall Stability. An optimum tenside content was established that yielded maximum Marshall Stability. A post-mix heating temperature of 115°C was then used prior to compaction, which increased the stability values by a further 100%.

Engelbrecht *et al.* (1985) heated RAP mixtures to a post-mixing pre-compaction temperature of 160°C. Their findings concur with those of other researchers, with the achievement of higher densities and improved strengths. Unfortunately, the practical and cost implications of double-handling the foamed-mix material once it is already in stockpile in order to heat the mix, tends to negate the benefits of improved compaction and mix performance.

Investigation into the dependence of the engineering properties of a foamed mix on testing temperature has been reported in numerous publications. In particular, a significant decline in the Resilient Modulus (M_r) has been noted as the temperature of the compacted specimen increases, which is typical of visco-elastic materials e.g. HMA. Little *et al.* (1983) suggest that the temperature susceptibility of a mix could be used as a criterion for the selection of potential materials for use in foam stabilisation. A temperature sensitivity analysis using 0°C, 23°C and 50°C for the repeated load (cyclic) Indirect Tensile Test (ITT) at 10 Hz was recommended. No limits have been specified by Little *et al.* for the rate of reduction in M_r in the given temperature range. Although there is some merit in such an

approach, one pitfall is the use of a test in the indirect tensile mode at high temperatures. Not only will the aggregate skeleton predominantly influence the mix at the higher temperatures (with the binder in a viscous state), but also the sample will creep during testing due to the high compressive stresses at the loading plates on a cylindrical specimen. This creep disturbs the specimen, reducing the accuracy and repeatability of the test, which already does not provide desirable reliability.

In relation to HMA, foamed mixes do not necessarily display more temperature susceptibility. Bissada (1987) found that foamed sand mixes cured in the air at 23°C have higher M_r values than hot-mix sand asphalt, both tested at temperatures of above 30°C. The phenomenon which causes this shift is explored further in Chapter 4. Differences in binder distribution within the sand mix, for the two different processes, as well as ageing of the bitumen droplets in the foamed mix with high surface area, are considered from the findings of Chapter 4 to contribute to these differences.

2.7 Compaction

The distribution of binder within a foamed mix differs from that of HMA and the inclusion of the water phase sets these two mixes apart, in so doing introducing differences in compactibility. A laboratory compaction technique that not only achieves the void content expected in the field, but also emulates the particle orientation after rolling, is sought from the laboratory compaction technique.

Various compaction methods have been utilised in laboratory mix design and research of foamed mixes besides the standard Marshall compaction, as summarised in Table 2 - 3.

It should be noted that the number of cycles recommended by Maccarrone *et al.* (1994) were done so before the major adjustment in the Superpave Approach was recommended for lower levels of traffic by Brown and Mallick (1998). The values cited in the table are likely to require major adjustment too. In addition, the gyratory angle and ram pressure recommended by Maccarrone are consistent with the Australian approach to gyratory compaction and are not unique to foamed mixes.

The influence of compaction level and technique is significant. Brennen *et al.* (1983) researched recycled materials and reports that the gyratory compactor produces foamed specimens with double the Marshall Stability of those specimens compacted with 75 blows of Marshall. They also state that 75 blows of Marshall compaction is insufficient to simulate field compaction of foamed mixes. In addition, they showed that the maximum stability and stiffness and minimum flow coincided at the same binder content for the gyratory compaction but not for the Marshall compaction.

Table 2 - 3. Summary of Laboratory Compaction Techniques used for Foamed Mix Design

Compaction Method	Settings/ Temperature	Remarks	Reference
Kneading Compactor	Ambient temp.	-	Shackel (1974)
Kneading Compactor	Ambient temp.	-	Bowering & Martin (1976)
Gyratory Compactor	Angle=1° Ram pressure=1,38 MPa	Opt Bitumen Content = f(Degree of comp)	Tia and Wood (1982)
Texas Gyratory Compactor	25°C	-	Little *et al.* (1983)
Gyratory	20 revs with Ram pressure=1,38 MPa	12% higher density than 75 blows Marshall	Brennen *et al.* (1983)
Gyratory Compactor	150 cycles, Angle=2° Ram pressure=0,24 MPa for 100mmϕ 150 cycles, Angle=3° Ram pressure=0,54 MPa for 150mmϕ	-	Maccarrone *et al.* (1994)
PCG (French Gyratory Compactor)	200 cycles at French standard settings	LCPC carousel : PCG 200 gyrat. ≡ 85% Solid density	Brosseaud *et al.*, (1997)

Lewis *et al.* (1995) relate the compaction of foamed mix in the field with Bulk Relative Density as determined using Marshall compaction in the laboratory. A reduction of 3% in air voids from laboratory to field was noted for a specific mix, verifying the findings of Brennen *et al.* (1983).

Besides the influence of the degree of compaction on the optimum binder content, as reported by Tia and Wood (1982), they also found that the Hveem Stability value was not as sensitive to changes in the binder content when a lower compactive effort was applied.

The work of Brosseaud *et al.* (1997) is probably the most promising, considering it uses a modern compaction implement i.e. the Gyratory Compactor which best simulates field compaction, and relates laboratory compaction to field compaction for several foamed mixes.

It is apparent from the literature, however, that the ideal laboratory compaction technique for the mix design of foamed bitumen mixes is not yet patently verified. Both the volumetrics and the engineering properties of the mix require consideration in the selection of an appropriate compaction technique and more reliable links between laboratory and field compaction are required.

2.8 Curing considerations

Curing of cold bituminous mixes, whether emulsion or foam, is the process whereby the mixed and compacted material discharges water through evaporation, particle charge repulsion or pore-pressure induced flow paths. The reduction in moisture content leads to the increase in strength of the mix (both tensile and compressive). Bowering (1970) stated that laboratory specimens only develop full strength after a large percentage of the mixing moisture has been lost. It is difficult, however, to ascertain the type and level of laboratory curing required to simulate field curing for a given material in a specific environment. Table 2 - 4 summarises different curing methods adopted by various researchers and targeted equivalent field compaction levels.

Table 2 - 4. Different Curing Methods utilised for Foamed Mixes

Curing Method	Equivalent Field Cure	Reference
3 days @ 60°C + 3 days @ 24°C	Unspecified	Bowering (1970)
3 days @ 60°C	Construction period + early field life	Bowering and Martin (1976)
3 days @ 60°C	Between 23 and 200 days from Vane Shear Tests	Acott (1980)
1 day in mould	Short term	Ruckel *et al.* (1982)
1 day in mould +1 day at 40°C	Between 7 and 14 days (Intermediate)	Ruckel *et al.* (1982)
1 day in mould +3 days at 40°C	30 days (Long term)	Ruckel *et al.* (1982)
1 day @ 38°C	7 days	Asphalt Institute
10 days in air + 50 hours @ 60°C	Unspecified	Van Wijk and Wood (1983)
3 days @ ambient temp. + 4 days vacuum dessicat.	Unspecified	Little *et al.* (1983)
3 days @ 23°C	Unspecified	Roberts *et al.* (1984)
3 days @ 60°C	Unspecified	Lancaster *et al.* (1994)
3 days @ 60°C	1 year	Maccarrone *et al.* (1994)

Note: 1.Specimens are cured in an unsealed state in the oven, unless otherwise stated.
2.Brennen *et al.* (1981) developed the procedure to first cure the foamed specimens in the mould for 24 hours during the most fragile period.
3. Vacuum desiccation methods are in line with the Asphalt Institute design procedure (PCD-1) and require further investigation.

The findings of Acott (1980) with the objective of relating laboratory cure (as shown in Table 2 - 4) to field cure, in terms of vane shear strength for foamed sand, are shown in Figure 2 - 7. Temperature variations, precipitation and evaporation cause the variability that is noted. The figure does not include values for the strength.

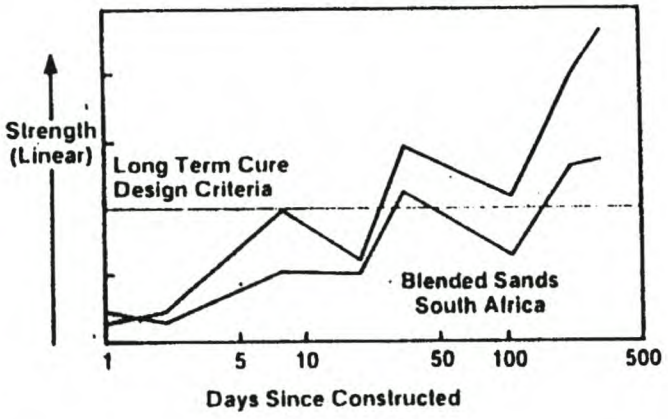

Figure 2 - 7. Rate of Gain of Field Strength (Vane Shear) of Foamed Sand Mixes (Acott, 1980)

Ruckel *et al.* (1982) state that, from the findings of other researchers, where foamed mix pavements exhibit premature distress (usually rutting or ravelling), it tends to occur in days rather than in weeks or months after construction. Clarke (1976) affirmed this when he found that foamed mixes tend to improve with age, traffic and temperatures as all these factors contribute to the removal of moisture from the mix. The ultimate strength that a road develops does play a role in pavement performance, but the strength after an early or intermediate cure represents the most critical time period. Emphasis should therefore be placed on simulating this field cure period when adjudicating mixes in the laboratory. Lee (1981) recommends that, as a result of the effect of curing on the strength development of foamed mixes, their mix design should be locally based, using information obtained from trial sections. One of the practical methods to improve the early strength of foamed mixes is to place the material in low stockpiles after mixing. According to Engelbrecht *et al.* (1985) this encourages moisture loss prior to compaction, but allowing sufficient fluids to remain to achieve acceptable compaction.

Various studies have been carried out that included experimentation with the curing temperature and moisture, to investigate the influence of these factors on the behaviour of the mix. Lee (1981) showed that both the curing temperature and the presence or absence of a mould during curing, affect the moisture content of the specimen, and the latter has a significant influence on the Marshall Stability values. This was verified by Clarke (1976) when it was shown that, for a range of curing temperatures (20°C to 60°C) the primary factor affecting the results was the moisture content to which the specimens had been cured. Ruckel at al (1982) reaffirmed this by reporting on work at the Asphalt Institute in the USA where moisture was identified as the primary factor influencing mix behaviour.

Regarding the temperature at which curing is carried out, Bowering and Martin (1976) experimented with temperatures of 23°C to 60°C, but found temperature to have *"little or no effect"*. Roberts *et al.* (1984) however, found a significant increase in tensile strength as curing temperature was increased from 23°C to 60°C. Temperature of curing cannot be ruled out as unimportant to mix preparation as temperature and moisture are dependent variables with temperature influencing the rate of moisture loss. The moisture contents of the mixes that are oven cured in an unsealed state are generally between 0% and 1,5% and always less than 4%, which is seldom representative of field conditions. In addition, the influences of curing temperature on changes in the binder condition have not been analysed in the literature, which is infelicitous considering the high surface area of the binder and higher void contents in foamed mixes.

The curing period of foamed mixes has been analysed in both laboratory and field conditions. Bowering (1970) found that the curing of laboratory specimens at 60°C results in equilibrium moisture being achieved in 3 days. Acott states that a foamed bitumen stabilised sand can increase in strength for a period of up to 3 years in the field (Lee,1981).

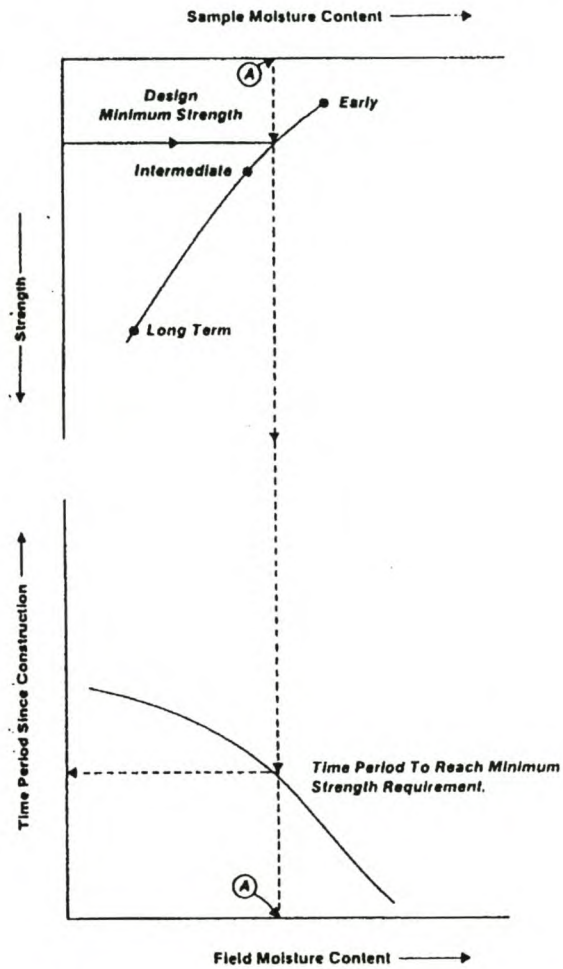

Figure 2 - 8. Determination of Curing Time required to achieve a Minimum Strength (Ruckel *et al.* , 1982)

Maccarrone (1994) showed that active fillers have a marked effect on the curing rate of cold-mixes. Addition of 2% cement works flues dust results in 80% of the oven dry modulus being achieved in one day at room temperature (which would take more than 30 days at room temperature without active filler, depending on the mix).

The challenge is to select the appropriate cure conditions in the laboratory, ensuring adequate shear strength in early life and selecting the correct stiffness for the structural design life. In addition, compaction due to traffic requires consideration. Ruckel *et al.* (1982) attempted to establish a curing procedure by which the curing time can be back-calculated, as shown in Figure 2 - 8. Although this procedure may have some merit, it requires additional testing and would only be applicable to mix designs for important routes, where early strength is essential.

2.9 Evaluation of Rheological Properties of Foamed Mix

Laboratory testing in conjunction with accelerated pavement testing of foamed mixes at Laboratoire central des Ponts et Chaussées (LCPC) provides valuable information on these mixes in relation to hot-mix asphalt and emulsion mixes (Brosseaud *et al.*, 1997). Included in the findings is a Master Curve of a fine graded (maximum size of 14mm) and a medium graded (maximum size of 20mm) foamed bitumen mix normalised to 10°C. Figure 2 - 9 reveals that the coarse foamed bitumen mix has consistent shift in complex modulus for a wide range of frequencies, being stiffer than the finer mix. More importantly, the research shows that the stiffness of foamed mixes is less frequency dependent than the reference (equivalent) asphalt mix. This could prove advantageous for rut resistance at higher temperatures and lower frequencies, as well as for resistance to fatigue in converse conditions.

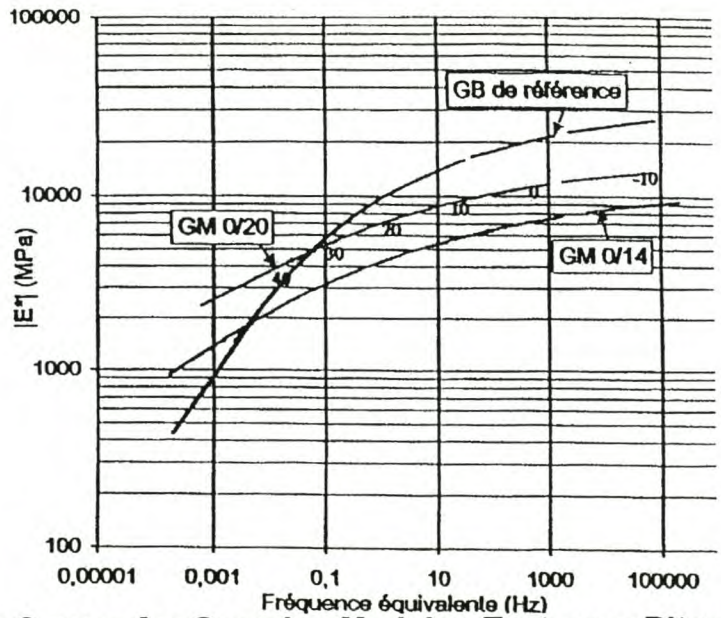

Figure 2 - 9. Master Curves for Complex Modulus Test on a Bitumen Treated Base (GB) and Foam Treated Base (GM) normalised to 10°C (Brosseaud *et al.*, 1997)

In addition, the research from LCPC provides a Black Diagram for both the finer foamed mix (GM 0/14) and the reference asphalt mix, see Figure 2 - 10. This plot once again indicates significant differences between the asphalt material and the foamed treated material. The substantially lower phase angle for the foamed mix illustrates a markedly smaller viscous component than the asphalt base, at similar binder contents (3,5% and 4% respectively) and different binder types (70/100 and 50/70 respectively). It is notable that the asphalt mixes' substantially harder binder does not have as much influence on the phase angle as the type of dispersion of binder in the mix.

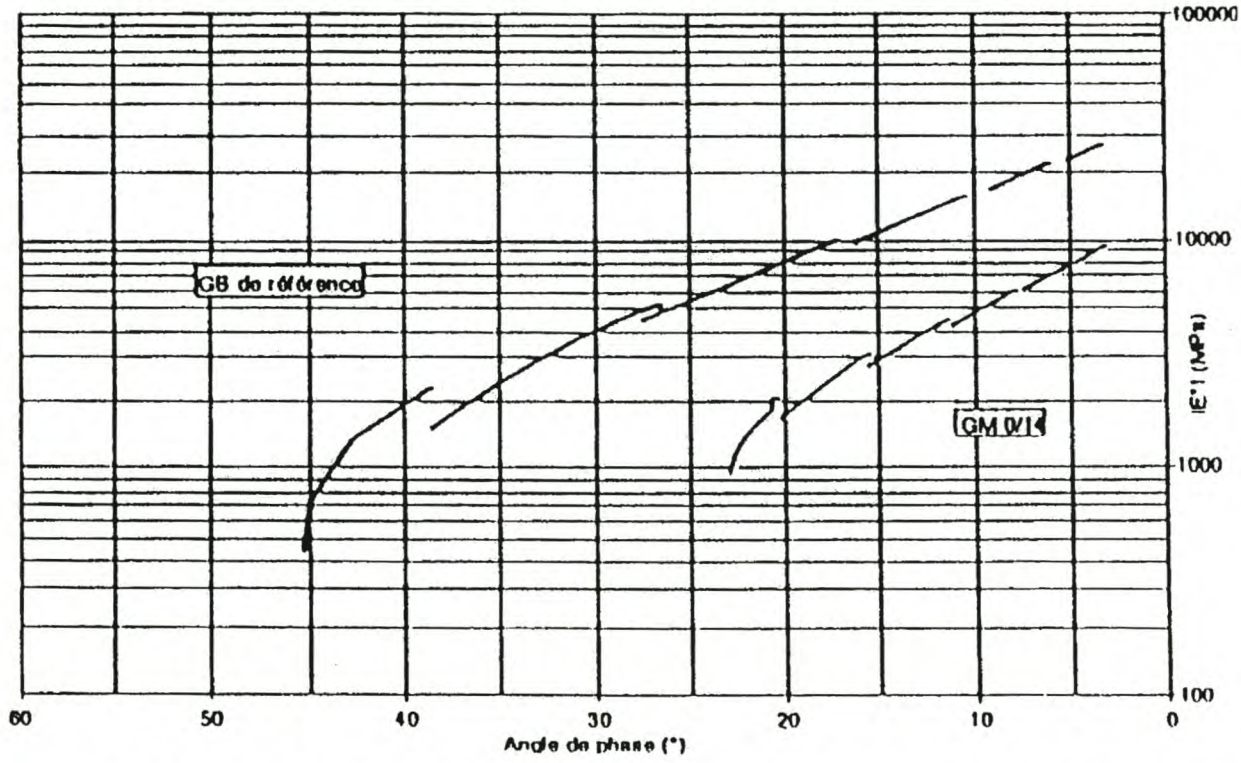

Figure 2 - 10. Black Diagram for Complex Modulus of Bitumen Treated Base (GB) and Foamed Mix (GM) relative to Phase Angle (Brosseaud *et al.*, 1997)

2.10 Evaluation of Engineering Properties

The literature on foamed bitumen mixes spans several decades and as a result numerous tests have been utilised to characterise the properties of the mix. The testing procedures of HMA have undergone major transformation in the 1990's with a shift away from the Marshall Mix Design to more fundamental tests such as Resilient Modulus, Dynamic Creep, Triaxial Creep etc. In addition, SHRP Superpave commissioned an initiative of immense proportions and as a result has introduced a menagerie of new procedures including the use of the Gyratory Compactor. Understandably, this has had a bearing on the mix design methods used for cold-mixes and many of the new techniques have been

applied in foamed bitumen mix design. The limit values of the various tests to foamed mixes are, however, uncertain, as the mechanisms of failure are as yet not clearly defined.

In order to provide an overview of the types of tests utilised for foamed bitumen research and the performance properties that are identified for measurement, Table 2 - 5 has been established. It should be noted that certain tests can provide an indication of several performance properties.

Table 2 - 5. Historical Test Methods for Foamed Mixes and their Function

PERFORMANCE PROPERTY	MIX (ENGINEERING) PROPERTY	TEST
Workability	Cohesion	Vane Shear
Fracture resistance	Tensile strength & fracture energy	Indirect Tensile Strength ITS
	Cohesion	Hveem Cohesiometer
Fatigue Resistance	Tensile strain & stiffness	Long Term Pavement Performance LTPP
Permanent Deformation Resistance	Plastic deformation	Static Creep, Dynamic Creep Triaxial
	Shear strength	Hveem Cohesiometer
		Vane Shear
	Stability	Marshall Stability
		Hveem Resistance
Load Spreading and Stress Distribution	Resilient Modulus M_r or stiffness	Indirect Tensile Test ITT (Dyn)
		Dynamic or Static Triaxial
Moisture Susceptibility	Retained strength, stability or stiffness after moisture exposure	Marshall Stability
		Indirect Tensile Strength ITS
		Indirect Tensile Test ITT (Dyn)
		Triaxial
Crushing Resistance	Compressive strength	Unconfined Compressive Strength UCS

2.10.1 Fatigue

Foamed bitumen mixes of relatively high binder content (>3,5%) are considered to behave in a manner similar to HMA. For this reason the mixes are expected to have a defined fatigue life, exhibiting cracking as a form of distress. Little *et al.* (1983) found substantially lower fatigue lives for foam than for HMA and high quality emulsion mixes, but binder contents were not compared in the study. Controlled stress beam tests were utilised in this research. Lancaster (1994) reports on TRL research in England where the fatigue performance of foamed mix was found to be comparable to dense graded asphalt; but more research was recommended.

The function describing the tensile strength of a mix i.e. tensile strength master curve, is considered to be a primary factor influencing the fatigue performance of the material. For this reason the Indirect Tensile Strength (ITS) Test is used as an engineering property that

can be used to predict performance. Maccarrone (1994) recommended that the foamed mix specimens should have a minimum ITS value of 200kPa (dry) and 100 kPa (soaked) after curing, for good performance, when tested at 25°C and 0.87mm/sec. This is applicable to bases with horizontal tensile stresses, however, and is therefore dependent on the pavement structure. The tensile strength is not a deterministic value and varies according to curing condition. Engelbrecht *et al.* (1985) found that the higher the curing temperature the lower the residual moisture content of a specimen and the higher tensile strength.

Roberts *et al.* (1984) investigated the tensile strength of RAP materials with various binders for cold bituminous mixes. They concluded that the tensile strength created by foamed bitumen binder is superior to that created by cut-back or emulsion mixes. This was shown to be true for a range of binder contents. Acott and Myburgh (1982) however, found the tensile strength of foamed mixes to be notably lower than that of hot mixes, for a range of sand materials. Foamed mixes yielded tensile strengths ranging between 105 kPa and 518 kPa whilst the equivalent hot mixes yielded values generally greater than 500 kPa.

2.10.2 Resistance to Permanent Deformation

2.10.2.1 Shear Strength

Measurement of the shear components of foamed mixes is one of the methods used for analysing the engineering properties of the mix. A variety of tests have been adopted for this purpose. Bowering and Martin (1976) used the Hveem Cohesiometer to evaluate the cohesion value at 60°C before and after three days exposure to water. Cohesion proved to be a property that revealed certain benefits of foam treatment not otherwise discernible using Marshall and CBR tests.

Acott and Myburgh (1982) utilised a vane shear test in a CBR mould to evaluate cohesion. Triaxial tests carried out on similar specimens showed an increase in cohesion from 31 kPa to 110 kPa with the addition of 3% foamed bitumen. Following this research testing on trial sections with foamed sands, a minimum vane shear value of 155 kPa was established for control testing and recommended for similar base layers.

Joubert *et al.* (1989) also conducted research on foam treated sands and noted an increase in shear strength and stiffness with time. From their research they concluded that, as it takes some two years to develop significant strength, a foamed treated sand layer will rut and will not decrease the deflections under load during this time period. The mix designs of the sand materials and the levels of traffic should be considered before this generalised statement is to be accepted.

2.10.2.2 Stability

As with hot mix asphalt, the stability of foamed mixes has historically been used as a measure of shear and deformation resistance. Again, different methods of measuring stability have been utilised. Bowering and Martin (1976) and Little *et al.* (1983) used the Modified Relative Stability at 60°C to analyse resistance to shear failure.

Acott and Myburgh (1982) utilised the Hveem Rt value tests for a variety of sands treated with foamed bitumen, with additional long-term pavement performance tests of trial sections over a period of 5 years. Using this research, they established a minimum Rt value = 65 and a Dynamic Cone Penetrometer (DCP) DN_{max} = 13,5 mm/blow. Humberto Castedo Franco and Wood (1982) found that the Hveem Stability value for a pit run gravel is dependent on the mixing temperature of the aggregate. The Hveem Stability exhibited an increasing trend with increasing aggregate temperature during mixing.

Brennen (1983) carried out Marshall Stability tests on RAP materials stabilised with 0,5% to 1% foamed bitumen. Extremely high stability values were recorded. Lee (1981) also used Marshall Stability tests on foamed mixes and found these, in general, to be significantly higher than the equivalent hot mix asphalt.

2.10.2.3 Dynamic Testing

After full scale accelerated pavement testing and wheel tracking tests, the most preferred method of testing rutting potential is the triaxial test. Shackel *et al.* (1974) carried out numerous triaxial tests on Sydney breccia in Australia treated with foamed bitumen. These tests were run in the static and dynamic mode and a good correlation was found between these two modes in terms of permanent deformation.

Shackel *et al.* also established that resistance to permanent deformation is a function of the binder content and the degree of saturation (% voids filled with water by volume) of a foam treated material. The ratio of the axial strain to the peak axial strain ($\varepsilon_{axial}/\varepsilon_{peak\ axial}$) decreases with increasing binder content and degree of saturation. In addition, these researchers found that the rate of accumulation of axial strain is a function of the binder content. The relationship follows an inverted parabola with a minimum point at a given binder content, and increasing rates of deformation at either side of this minimum.

2.10.3 Compressive strength (Crushing)

The Unconfined Compressive Strength (UCS) Test has been considered to be more appropriate for foamed treated materials than conventional hot mix asphalt by the CSIR (1998). Foamed mixes are adjudged to be more "brittle, bound" materials than HMA and crushing therefore stated as being a representative failure mechanism.

Bowering (1970) established guidelines for foamed asphalt bases underlying thin surfacing layers, including 700 kPa for a 3 day cured specimen at 60°C and 500 kPa for a specimen treated with a 4 day soak. This work was extended by Bowering and Martin (1976) by stating that the UCS for foamed mixes at ambient temperature is commonly found in the range of 1,8 MPa to 5,4 MPa.

Semmelink (1991) found that the UCS of a sand and calcrete dust mixture treated with 5% foamed bitumen was dependent on the percentage filler in the mix when tested at 25°C in accordance with (NITRR, 1986). An increase in UCS relative to the percentage passing the 0,075mm sieve was noted, as shown in Figure 2 - 11.

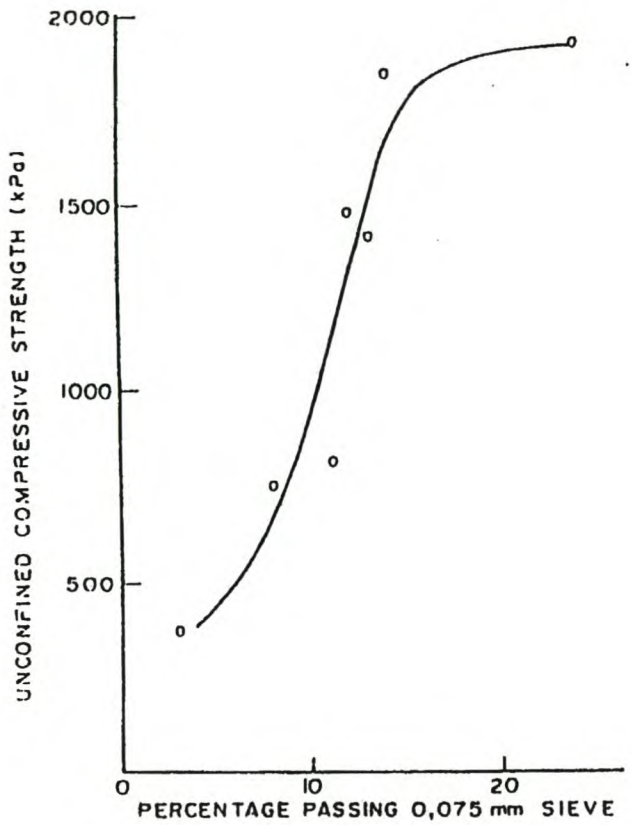

Figure 2 - 11. UCS of a foam treated sand + calrete dust versus filler fraction (%<0,075mm) (Semmelink, 1991)

2.10.4 Stiffness

Foamed mixes incorporate a binder that is visco-elastic by nature and as such the behaviour of these materials can be expected to be dependent on temperature and frequency (loading time). This is particularly important for the dynamic testing of Resilient Modulus M_r although it also has a bearing on tensile and compressive strength, fatigue life etc. In addition to the influences of the binder, other factors influencing the dynamic stiffness (M_r) of foamed mixes have been identified through research.

Shackel *et al.* (1974), through triaxial testing of foamed treated breccia, found that M_r is maximised at a degree of saturation of approximately 60% for a binder content of 4%. In addition, the M_r was found to increase under load repetitions for mixes with both 85/100 and 180/210 penetration foamed bitumen at both 5% and 6% binder content. Shackel's work showed that 10 000 load repetitions in the triaxial test, the foamed breccia's optimum M_r was a function of not only degree of saturation, but also binder content and penetration. Lower penetration binders provide higher mix stiffness, and higher binder contents also provide higher stiffness (within a certain envelope).

The findings of Shackel *et al.* formed the basis of Lancaster *et al.*'s (1994) approach to foamed mix design, which included the optimisation of the binder content in terms of the peak M_r. Lancaster *et al.* proposed that this approach be adopted for both dry cure and

soaked (24 hours at 60°C) repeated load indirect tensile modulus tests on foamed specimens. Maccarrone *et al.* (1994) also propose the approach of Lancaster *et al.* for efficiency, rather than triaxial testing. The research of Maccarrone *et al.* provides a relationship between filler content and mix stiffness, showing that an increase in filler content from 5% to 15% results in an increase in Resilient Modulus of 17%.

Humberto Castedo Franco and Wood (1982) also found that an optimum binder content yielding a peak M_r is prevalent. The binder content at the peak was found to be independent of curing time for the specimen. The value of the maximum M_r was, however, found to be dependent on the curing time. This research also confirmed the visco-elastic nature of foamed mixes by showing the temperature dependency of specimen stiffness (which is also typical of HMA, as countless researchers have shown).

Acott and Myburgh (1982) investigated numerous foam treated sands, through laboratory work and the construction of several trial sections. They found that the initial radius of curvature analysed from deflection measurements was low, indicating low early stiffness in the foam treated base layer. They therefore suggest that the M_r of a mix be determined over short, medium and long-term cure conditions; in this way the minimum stiffness required to limit the tensile strain in the surfacing to an acceptable level, can be related to the minimum desirable curing period. Tia and Wood (1982) state that M_r increases significantly in the first seven days of curing at ambient temperatures followed by a levelling off (for RAP mixes). The first week is the period that most moisture is lost.

2.10.5 Moisture susceptibility

Due to the following reasons, moisture susceptibility of foamed mixes is an important consideration:

- The binder in foamed bitumen mixes does not completely coat the larger particles of aggregate,
- binder contents utilised in the mix are generally lower than the equivalent HMA,
- the mineral aggregate is moist at the time of mixing which reduces adhesion, and
- the air void content of the mix is usually relatively high.

Lee (1981) found that the Immersion Marshall Stability values after 24 hours of soaking at 60°C for most foamed mixes were low. Lee commented that:

> *"While this test may be unrealistically severe for evaluation of stabilised foam mixes, the results do suggest the need to evaluate water susceptibility of foam mixes".*

Little *et al.* (1983) used a vacuum saturation test to determine moisture susceptibility in terms of the Resilient Modulus of a mix. This test follows the procedure later stipulated in the Asphalt Institute Manual (1992). Specimens are vacuum saturated at 100mm of Mercury for 1 hour followed by release of the vacuum and further saturation for 1 hour (with measurement of the mass of water absorbed). Using this technique, siliceous gravels and sands that were foam stabilised were found to be very moisture susceptible.

Ruckel *et al.* (1983) used the same vacuum saturation technique at 23°C in water. They state that this technique simulates the effects of prolonged exposure to sub-surface moisture such as extended heavy rainfall in the road i.e. a very harsh condition. The test results obtained, yielded absolute measures of sensitivities of mixtures to moisture. Ruckel *et al.* recommend that the test is only applied to specimens that have already been cured using the equivalent intermediate or long-term simulation.

Van Wijk and Wood (1983) used the vacuum saturation to study the moisture-exposure effects of foamed mixes in terms of Marshall Stability tests. This procedure was found to highlight the moisture susceptibility of both RAP and virgin mixes. Hotte (1995) compared the percentage of Retained Marshall Stability for 1 hour of vacuum soaking with 4 days of soaking at atmospheric conditions and found the Retained Stability to be 6,4% higher on average for the six materials tested. This provides an indication of the severity of conditioning using vacuum saturation.

Other methods of analysing moisture susceptibility include a wet cycle as part of the curing procedure. Roberts *et al.* (1984) used a wet curing cycle of 3 days at 24°C and found that the strength declined by 50% of that achieved by the dry cured specimens. A higher binder content was found to ameliorate the effects of moisture on the tensile strength.

Some effective ways of reducing the moisture susceptibility of foamed mixes include the addition of active fillers such as lime and cement (Humberto Castedo Franco and Wood, 1982) and (Maccarrone, 1994), and the application of anti-stripping agents to the bitumen. Results of the improvement of moisture resistance of foamed mix with anti-stripping agents e.g. amines, are not well documented however.

2.11 Pavement Design Considerations

2.11.1 Deflections

The measurement of surface deflections of a pavement under a load application on the surfacing layer, is a method of analysing the interaction of the different layers in the entire pavement structure. Through a back-analysis technique this can provide useful information on the effective stiffness of various layers in the pavement.

Bowering and Martin (1976) found that the deflections measured using a Benkelman Beam on a pavement incorporating a foam-treated layer, are similar to those of other types of pavement. The extremely slow rate of loading of this test requires consideration in comparing results however. Van Wijk and Wood (1983) provided more incisive results showing that trial sections incorporating the stabilisation of in situ materials with foamed bitumen, experienced an increase in average initial deflection relative to the original pavement. However, after some 250 days the deflections returned to the magnitude originally measured with the pavement still increasing in stiffness. To some extent these findings were verified by Lancaster *et al.* (1994), who reported that the deflections and radii of curvature only reduced marginally after in situ stabilisation with foamed bitumen, even after four months of curing. The publications on deflection measurements do not, however,

provide substantial comparisons between identical structures incorporating foamed and unbound layers i.e. reference test sections, and therefore only provide very limited information for use in the development of models for pavement analysis.

2.11.2 Layer thickness design

Up until the research at LCPC's Carousel in France (Goacolou *et al.*, 1997), only limited long-term pavement performance (LTPP) analysis of foam treated layers had been carried out, and is to be found in the literature. Guidelines for the design of pavements incorporating foam treated layers prior to 1997 have therefore relied upon observations, experience and engineering judgement, as well as repeated load laboratory testing. This literature, although included for completeness and discussed below, is rather dated and of limited applicability.

Bowering and Martin (1976) established a relative thickness coefficient of 1,5 for materials after foam treatment, relative to the equivalent granular base layer. The relative thickness coefficient of asphalt base to the relevant foamed mix is also 1,5. In summary, the equivalent structural strength for asphalt : foamed mix : granular base is defined by the following layer thickness ratio 1 : 1,5 : 2,25. This is analogous to ratios in structural numbers. The use of equivalency ratios is very dangerous, however, as the parameter upon which it is equivalency is based, should be pertinent to the mode of failure of the material and layer. Variation in temperature, stress distribution and ratios, binder content, compaction, curing etc can result in a change in mode of failure thus nullify the relevance of the equivalency ratio.

According to Little *et al.* (1983), there are three criteria that influence the potential of a foamed mix layer to function adequately as a structural base or full-depth layer, namely:

- Distribution of vertical stresses i.e. protection of the sub-grade,
- Resistance to permanent deformation and shear failure, and
- Fatigue life characteristics i.e. resistance to cracking under load repetitions.

Higher modular ratios distribute the stresses over the underlying layers more evenly, but at the same time this creates higher shear stresses in the upper layer. The foam treated material must be able to resist these shear stresses in order to avoid distress. Little *et al.* developed thickness equivalency ratios based on a vertical subgrade strain criterion. This was established using a multi-layer linear elastic program and modelling ε_v against results of the AASHO road test.

Tia and Wood (1983) developed structural coefficients for RAP treated with foamed bitumen. These coefficients were developed for different ranges of stiffness, to assist in the pavement design process. Lancaster *et al.* (1994) on the other hand suggest that a foamed bitumen treated layer should be analysed as a bound material, using linear-elastic methods, with the M_r value obtained from the Indirect Tensile Test. Values for M_r ranged from 2000MPa to 6000MPa soaked and 5000MPa to 10000MPa in a dry state (unsoaked).

Other methods of pavement design for foamed materials include:

- The TRRL design curve for use in the absence of other data (Ackeroyd, 1989), see Figure 2 - 12 below.
- The equivalent layer thickness catelogue (Wirtgen, 1998).
- The CSIR (1998) preliminary pavement design guidelines based on UCS, DCP and FWD (Falling Weight Deflectometer) tests on several trial sections. The design method based on the work at LCPC's Carousel (Goacolou *et al.*, 1997).

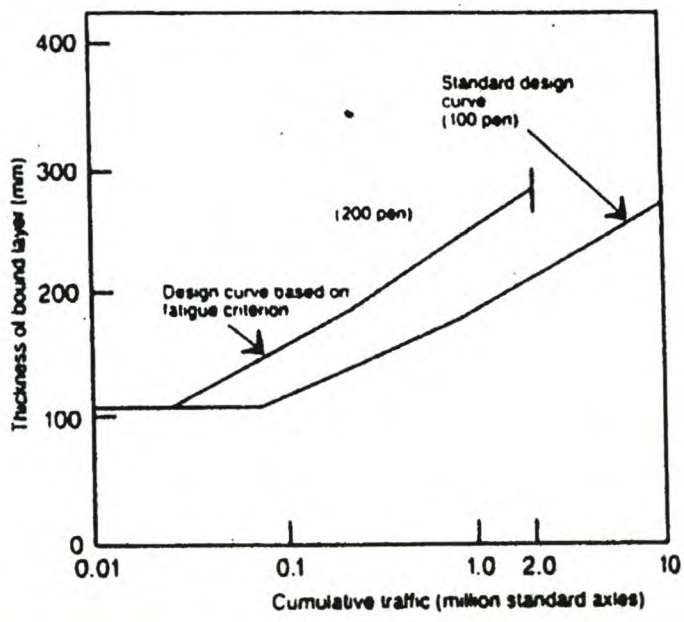

Figure 2 - 12. Interim design curve for foamed bitumen (200 pen) road based, after TRRL (Ackeroyd, 1989).

More recently, accelerated pavement testing (APT) at LCPC's Carousel in France (Brosseaud *et al.*, 1997 and Goacolou *et al.*, 1997) provided a more comprehensive approach to pavement design using foamed bitumen treated materials. Four test sections were tested simultaneously, three with different overlays on a cracked asphalt pavement viz, 10cm foam-treated overlay (GM), 10cm emulsion treated overlay (GE) and 8cm reference asphalt overlay (GB). These top layers did not comprise typical surfacing mixes. The fourth pavement included a new sandwich structure (SN) with 10cm foamed mix placed between 2x6cm low penetration (10/20) asphalt layers on an existing pavement. The trial sections were constructed, consolidated with about 90 000 repetitions of 9-ton axles and allowed to cure for 9 months before testing commenced. Axle repetitions were applied using 13-ton to 17-ton axles at 68 km/h and normalised to a 13-ton standard axle using an exponent 5 in the power law. A triangular distribution of lateral wander of 1m was applied and a total of 4,2 x 10^6 equivalent 13 ton axles were used to traffic the sections. Measurements of the pavement under wheel loads were made using the Benkelmann Beam and strain gauges in the layers. Parallel fatigue testing was carried out in the laboratory using the trapezoidal beam configuration.

Fatigue and rutting models have been established using the results of field and laboratory testing. Rutting observations on the trial sections revealed that the foam treated surfacing and the equivalent HMA have a factor two higher resistance to rutting than the emulsion treated layer, see Figure 2 - 13. In order to produce models, field deflection data was back-analysed using linear elastic analysis. Initially, the subgrade stiffness was determined and from this an existing base stiffness was chosen as three times the subgrade stiffness. The existing surfacing stiffness was, in turn, selected as three times the base stiffness. Using these values, the effective stiffness of the new layers was determined from deflection bowl results. These "elastic modulus" values at 23°C were 10000 MPa for hot-mix (grave bitume or GB), 4500 MPa for foamed mix (Grave Mousse® or GM), and 2500 MPa for emulsion mix (grave emulsion or GE). This approach ignores any stress dependency of the cold mix materials and over-simplifies the resilient modulus into one value per layer.

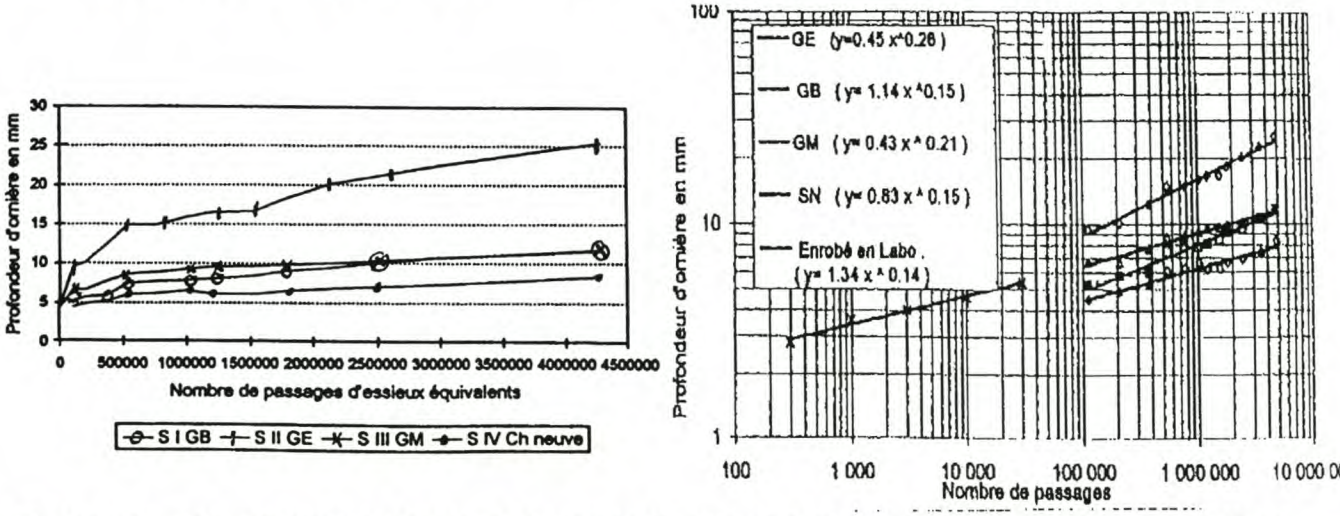

Figure 2 - 13. Rutting Curves for Asphalt, Emulsion and Foamed Bitumen Mixes, Actual left and Modelled right (Goacolou *et al.*, 1997)

The fatigue properties of the materials tested at LCPC have been analysed in the laboratory and the field. The APT enabled modelling of the crack development at the surface, where the equivalent materials were located. These curves followed Gauss-Logarithmic functions with coefficients to describe their standard deviation, see Figure 2 - 14. The $N_{50\%}$ values i.e. number of equivalent 13 ton axle repetitions to cause 50% surface cracking (etendue fissurée) from the figure, were associated with the horizontal tensile deformations determined from linear elastic analysis of the relevant pavements with interpreted layer stiffness. In this way the horizontal tensile deformation values relating to a service life of 10^6 axle repetitions of 13 tons were defined. Weaknesses in this approach include the use of only extent and ignoring the degree of cracking (which is particularly relevant to cold mix top layers), and the use of linear elastic properties for pavement analysis of cold mixes that can be stress dependent. The research showed foamed bitumen surfacing to produce smaller cracks with higher frequency of occurrence than the reference asphalt surfacing material, which produced wider cracks. This should be incorporated in the model, but has been omitted from it. In addition, the foamed surfacing layer cracks earlier than the emulsion layer, but then stabilises whilst the emulsion treated

surfacing continues to deteriorate, see Figure 2 - 14, but this has been neglected in the approximations using smoothed functions.

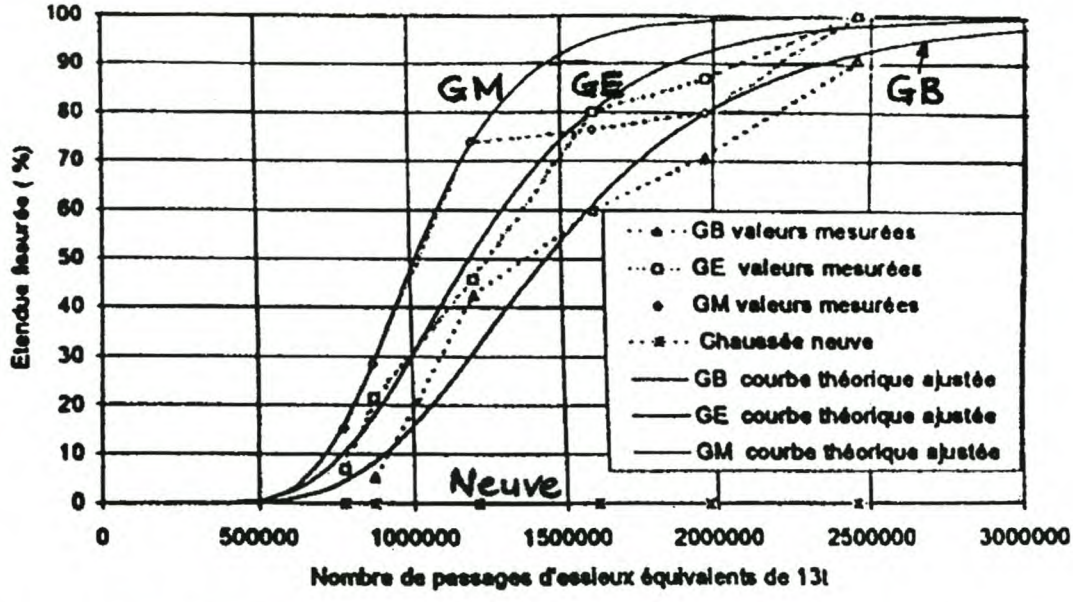

Figure 2 - 14. Modelling of the Evolution of Surface Cracking (Goacolou *et al.*,1997)

The interpretation of LCPC's results goes further to include an analysis of the shift factors for fatigue from laboratory to field results. The APT tests on the carousel were compared with laboratory fatigue results to establish a shift factor for foamed bitumen. Extensive research in France (LCPC, 1997) has led to the development of guidelines for such shift factors for hot mix asphalt and this is used as a basis for the analysis of the foamed mix shift factor. The determination of the working strain $\varepsilon_{t,ad}$ at the base of a bituminous layer is defined as:

$$\varepsilon_{t,ad} = \varepsilon\ (NE, \theta_{eq}, f)\ k_r\ .\ k_C\ .\ k_s \qquad \textbf{Equation 2 – 2}$$

Where,

ε (NE, θ_{eq}, f) = strain for which failure in bending is obtained in the laboratory,
NE = number of cycles for 50% probability of failure,
θ_{eq} = equivalent temperature,
f = equivalent frequency characteristic of the stresses imposed on the layer,
k_r = coefficient to account risk regarding layer thickness and fatigue test standard deviations,
k_C = coefficient to account for shifts in a computational model in relation to behaviour observed in actual pavements, and
k_s = coefficient to account for lack of uniformity of a soft subgrade layer.

The premise for the development of a k_c coefficient for the foamed bitumen (GM) or k_C^{GM}, is that the ratio of k_C for foamed bitumen to hot-mix i.e. GM:GB is equivalent to the ratio of k_M (the coefficient of carousel i.e. manege(M) results) for GM:GB. This implies that the

relative behaviour observed for GM and GB in the carousel during the experiment will be the same as the behaviour of these two materials in a real pavement structure, and is expressed by the following equation:

$$\frac{k_C^{GM}}{k_C^{GB}} = \frac{k_M^{GM}}{k_M^{GB}} \qquad \textbf{Equation 2 - 3}$$

This would appear to be a reasonable assumption. At the same time, LCPC states that k_M for a particular asphaltic material is a function of the working strain ratio for carousel/laboratory or:

$$k_M = \frac{\varepsilon_{6M}}{\varepsilon_{6L}} \qquad \textbf{Equation 2 - 4}$$

Where,

Superscript ^{6} = 10^6 standard axle repetitions at which equivalency is valid
Subscript $_M$ = manege (carousel)
Subscript $_L$ = laboratory

Developing Equation 2 - 4 for the two materials GM and GB yields:

$$\frac{k_M^{GM}}{k_M^{GB}} = \frac{\varepsilon_{6M}^{GM}}{\varepsilon_{6L}^{GM}} \times \frac{\varepsilon_{6L}^{GB}}{\varepsilon_{6M}^{GB}} \qquad \textbf{Equation 2 - 5}$$

The results of the research on GM and GB in the laboratory and carousel were normalised to 20°C and 25 Hz and values were obtained for Equation 2 - 5 to yield:

$$\frac{k_M^{GM}}{k_M^{GB}} = \frac{97}{105} \times \frac{166}{120} = 1.28 \qquad \textbf{Equation 2 - 6}$$

From extensive previous research in HMA by LCPC (1997) , the value of k_C is known i.e. k_C^{GB} = 1.3. Substitution of this value in Equation 2 - 3 yields a shift factor for the foamed bitumen:

$$k_C^{GM} = \frac{k_M^{GM}}{k_M^{GB}} x k_C^{GB} = 1.28 x 1.3 = 1.66 \qquad \textbf{Equation 2 - 7}$$

Earlier fatigue testing in roads trafficked with channelled wheel loads by LCPC showed that strain controlled fatigue tests provided results that were strongly dependent on the origin of the bitumen, where the same bitumen penetration grades were tested. According to LCPC, the shift factor should therefore be associated with a horizontal tensile strain ε of 80 to 90 microstrain. In this case the shift factor k_C should be 1.20 for GM and 0.93 for GB. However, the stiffness of the GB layers used in the modelling of the carousel results are

empirically based in this first estimation, so LCPC suggest that the shift factor should be selected as a value between these two extremes for the foamed bitumen, namely k_C^{GM} = 1.30. This is the same as the value for hot mix asphalt. It should be noted that this research is applicable to cold foamed bitumen mixes and is a first step towards linking laboratory and field research.

3. SUMMARY

During the forty years that the foamed bitumen process has been in existence, it has been applied to a variety of materials in diversely contrasting climates. The mix design procedures and testing methods adopted for foam testing have evolved along with the developments in HMA, although cold bituminous mixes have not achieved the same impetus as their hot counterpart. Notwithstanding this, the knowledge gained from research initiatives has provided an insight into this unique material creating a platform from which new developments may be launched. This section provides a summary of the comprehensive literature review incorporated in this chapter.

In general, ordinary penetration grade bitumens may be utilised for foamed bitumen stabilisation. The softer grades with penetrations between 80 and 250 are preferred in foamed bitumen production as blockages in expansion chambers and spray nozzles can be practically eliminated. In addition, the use of soft bitumen is possible as these bitumens provide improved foam characteristics without adversely affecting the deformation resistance of the mix. It is apparent that the prediction of the foam characteristics of bitumen from its chemical composition or crude source is not reliable practise, and physical foam tests are required.

The influence of foam characteristics on the performance of the foamed bitumen mix has not been definitively proven through research, but minimum limits have been set to ensure acceptable quality of the mix. This includes minimum values of 8 to10 (times) for the expansion ratio and 12 to 20 seconds for the half-life. The temperature of the bitumen, amount of foamant water added and amount of foam produced, have been shown to influence the foam characteristics. In addition, the application of foaming agents to the bitumen or water, can extend the half-life of the bitumen by an order of magnitude.

Guidelines have been provided for the suitability of aggregate for treatment with foamed bitumen. In particular Mobil Oil established a ranking of materials according to grading for their suitability for foam treatment. The ideal materials have a continuous grading with between 5% and 20% passing the 75 micron sieve. Materials that fall outside the ideal grading envelope, whether too coarse or too fine, can be rectified through the addition of the deficient fractions. The pitfalls of using mineral aggregate that is very finely graded is obvious, but the shortcomings of gap graded or open graded aggregates are not discussed in detail in the literature. It is discernible from the findings of research, however, that the partial coating phenomenon of foamed bitumen contributes to the unsuitability of gap graded materials, as this would discourage binder distribution throughout the mix.

The filler fraction is particularly important, as its percentage will influence the optimum foam bitumen content of the mix. In addition, plastic filler causing the natural aggregate to have a Plasticity Index in excess of between 8 and 12%, necessitates pre-treatment i.e. modification with active filler before foam stabilisation.

The binder content of foamed mixes contributes to numerous performance characteristics including permanent deformation, fatigue and moisture susceptibility. Resistance to rutting and fatigue, as analysed using certain engineering properties of a foamed mix, has been found to follow a parabolic-type convex curve with an optimum.

Moisture in the mineral aggregate at the time of mixing with foamed bitumen has been found to fulfil an important role. Sufficient water is required to encourage dispersion of the binder during mixing and create workability and compactibility, but too much water increases the curing time and reduces the density and strength of the mix. Moisture contents of 70% to 85% of the optimum moisture content, as determined using Modified AASHTO compaction, are generally the ideal mixing moisture contents to be utilised. It is advisable to utilise too much water rather than too little, as a mix can always be allowed to dry out before compaction, but the addition of water after mixing is not beneficial to the mix properties.

The method of mixing the binder with the mineral aggregate is particularly important with foamed bitumen mixes, as only a finite mixing time is available before the foam collapses and returns to a highly viscous state, with no affinity for coating large particles. A high energy of mixing is required as over-mixing in terms of time, can create balling of the mix. Particularly for laboratory Hobart® -type mixers, the splitting of the aggregate into two fractions at the 4,75mm sieve and mixing them separately with foamed bitumen, can be advantageous. This creates opportunities for the use of emulsions in combination with foamed bitumen i.e. the emulsion can be used to coat the large particles and the foamed bitumen can be used for the finer fraction.

Temperature considerations for foamed mixes have been surprisingly limited in previous research. In particular, the mixing temperature of the aggregate has only been considered for the purpose of establishing a minimum limit. (Bowering and Martin, 1976) recommended a minimum aggregate mixing temperature of between 13°C and 23°C. Research into the effects of aggregate temperature on mix integrity has focussed more on the range of ambient temperatures that can be experienced i.e. 10°C to 38°C. Unfortunately, the neglecting of aggregate temperature at the time of mixing has probably convoluted some of the research findings. Besides a speculative mention of possible benefits of increased aggregate temperatures without any substantiation, no work has been published on half-warm foamed mixes where the aggregates have been mixed at 40°C to 95°C. This provides immense opportunities for research to establish the true benefits of heating the aggregates.

The heating of foamed mixes after mixing and pre-compaction to temperatures of between 60°C and 115°C has shown significant benefits in terms of increase in density and strength

of the mix. This procedure remains impractical for application in a full-scale plant due to double-handling costs and requires economic evaluation before implementation.

Research into compaction methods in the laboratory that are both relevant and representative of field compaction is not prevalent in literature. The Marshall compaction method with 75 blows either side has been found to be inadequate. Sound guidelines for the use of gyratory compaction have not yet been established.

The curing considerations of foamed mixes are paramount to the potential success of the material in terms of performance. Although foamed mixes exhibit a faster rate of strength gain than bitumen emulsion stabilised mixes, it is in the early period of repeated loading that the majority of the permanent deformation takes place in a foamed layer. The temperature of the layer in the field and especially the loss of moisture with time are the most important factors influencing curing and hence strength gain.

A wide variety of tests have been utilised to analyse the engineering properties of foamed bitumen mixes. Using these tests it has been established that foamed mixes generally have improved stability and resistance to permanent deformation than the equivalent hot mixes. Comparative compressive strength values are variable depending on the mode of testing and temperature. However, fatigue resistance, tensile strength and moisture susceptibility is poorer, in some cases, for foamed mixes than HMA. In addition, the stiffness and potential for permanent deformation of foamed mixes are both predominantly dependent on the moisture content of the material. For this reason, it is important to cure a foamed layer sufficiently before opening to traffic otherwise load-spreading and rut-resistance functions of the base layer will not be fulfilled.

The literature does not provide a clearly defined explanation of the mode of failure of foam stabilised materials. Some researchers describe this material to be more "brittle, bound" than HMA and therefore consider crushing to be a representative failure mechanism. It should be noted that the failure is largely dependent on the quality of aggregate utilised and the binder content of the mix. The vast majority of research into foamed mixes has been focussed on marginal and recycled materials such as sand, gravel and RAP, with little emphasis on good quality virgin aggregates. The natural marginal materials in particular are characterised by below average bearing capacities and this has a strong bearing on crushing and shear type failure in the mix at relatively low binder contents.

Very few references have been found with information on accelerated testing of foamed bitumen mixes. Performance testing under repeated loading has mainly taken the form of Long-term Pavement Performance LTPP analyses of trial sections. Although details of various trial sections are provided, conclusions drawn from LTPP remain undocumented. Recent accelerated pavement testing at LCPC in France provides the only current fundamental pavement design procedures for foamed bitumen mixes. This research has also provided a first step towards linking laboratory and field research on foamed bitumen. Guidelines in other literature, based on structural ratios with comparative materials, are highly empirical tools for pavement designs incorporating foam treated materials.

The literature study highlights several focus areas for consideration in research into foamed bitumen. These factors, as detailed below, are considered relevant to the mix design of foamed bitumen materials and therefore selected as subjects of focus for this dissertation:

- *Foam characteristics:* Current understanding of the physics of foamed bitumen is under-developed and without sufficient fundamental explanation of the mechanics of foamed bitumen production. This has lead to characterisation techniques that are incomplete and that do not facilitate optimisation of the foam for use in mix production. A better understanding of foam as produced using a variety of binders is required and new or improved techniques for characterisation and optimisation of the foam require development.
- *Mineral Aggregate:* Only very rudimentary guidelines exist for the selection of mineral aggregates i.e. filler, sand and coarse fraction, for treatment with foamed bitumen, or the prediction of the behaviour of mixes comprising given aggregates. In particular, filler-binder interaction, the influence of blending of sand fractions and overall skeletal considerations for foamed mixes require further investigation with the development of more fundamentally based guidelines.
- *Moisture:* The moisture in a foamed mix is known to influence binder dispersion, binder-filler interaction, workability, compaction, shelf-life and therefore mix properties. However, techniques to design for the fluids within foamed mixes are limited and require development particularly in terms of mixing, compaction and curing.
- *Aggregate Temperature:* One of the most dominant factors that influences the behaviour of a cold foamed mix is the aggregate temperature during mixing. This factor has been ignored to a large degree in foamed mix design considerations and production in the past, even though substantial variations in ambient temperatures are possible. Therefore, it is necessary to research the implications in variation in the aggregate temperature during production so that it may be accounted for in mix design and any possible benefits in nominally increasing these temperatures can be exploited.
- *Performance:* The behavioural characteristics and mode of failure of foamed mixes remains enigmatic and unexplained in literature. For laboratory mix design procedures to be linked to field behaviour, performance models require development. Such models should be tested for selected mixes in the field through accelerated testing where possible.

4. REFERENCES

Abel F. and Hines C., 1978. **Base Stabilization with Foamed Asphalt**. Colorado Department of Highways, Denver, Interim Report. Pp 17

Acott S.M.,1979. **Sand Stabilisation using Foamed Bitumen**. *3rd Conference on Asphalt Pavements for Southern Africa. Durban*. Pp 155-172

Acott S.M.,1980. **The stabilisation of a sand by foamed bitumen – A laboratory and field performance study**. Dissertation for Master of Science in Engineering. University of Natal.

Acott S.M. and Myburgh P.A., 1982. **Design and Performance Study of Sand Bases Treated with Foamed Asphalt**. *Transportation Research Record 898*. Pp 290-296

Akeroyd F.M.L. and Hicks B.J., 1988. **Foamed bitumen road recycling**. *Highways*, January. London. Pp 42-45

Akeroyd F.M.L., 1989. **Advances in Foamed Bitumen Technology**. *5th Conference on Asphalt Pavements for Southern Africa*. Swaziland. Pp VIII-1 to VIII-4

Anderson D.A., 1987. **Guidelines on the Use of Baghouse Fines**. National Asphalt Pavement Association, Information Series 101-11/87, Maryland.

Asphalt Institute, 1992. **A Basic Asphalt Emulsion Manual**. Manual Series No 19, Second Edition. Lexington, USA. Pp 87

Asphalt Institute, 1993. **Mix Design Methods for Asphalt Concrete and other Hot Mix Types**. Manual Series No. 2 (MS-2), Sixth Edition. Lexington, USA. Pp 81-82

Bissada A.F., 1987.**Structural Response of Foamed-Asphalt-Sand Mixtures in Hot Environments**. *Transportation Research Record 1115*. Pp 134-149

Bitufoam, 1996. **Foamed bitumen**. Marketing brochure. South Africa.

Bowering R.H., 1970. **Upgrading Marginal Road Building Materials with Foamed Asphalt**. *Highway Enigineering in Australia*. Mobil Oil of Australia, Melbourne South.

Bowering R.H. and Martin C.L., 1976. **Foamed Bitumen Production and Application of Mixtures Evaluation and Performance of Pavements**. Proceedings, *Association of Asphalt Paving Technologists Volume 45*. New Orleans, Louisiana. Pp 453-477

Brennen M., Tia M., Altschaefl A. and Wood L.E., 1983. **Laboratory Investigation of the Use of Foamed Bitumen for Recycled Bituminous Pavements**. *Transportation Research Record 911*. Pp 80-87

Brosseaud Y., Gramsammer J-C., Kerzreho J-P., Goacolou H. and Le Bourlot F., 1997. **Expérimentation (premiére partie) de la Grave-Mousse ® sur le manége de fatigue**. *RGRA No 752 (Revue Géneralé des Routes et des Aerodromes)*, Juin. Pp 61 - 70

Brown E.R. and Mallick R.B., 1998. **An Evaluation of N_{design} Superpave Gyratory Factor**. *Association of Asphalt Paving Technologists AAPT*. Session II. USA. Pp 1-33

Buschkühl G., Gapski J. and Gründel R., 1990. **Bituminöse Tragschichten aus Müllverbrennungssasche und Schaumbitumen**. Diplomarbeit, Fachbereich Bauingenieurswesen, Fachhochschule Hamburg. Germany.

Clarke A.R., 1976. **Foamed Asphalt of Crushed Rock Pavements**. Report 76.3. Mobil Oil of Australia, Melbourne South

Cooley L.A., Stroup-Gardiner M., Brown E.R., Hanson D.I. and Fletcher M.O., 1998. **Characterisation of Asphalt-Filler Mortars with Superpave Binder Tests**. *Annual Meeting of Association of Asphalt Paving Technologists*, Boston.

Csanyi L.H., 1956. **Mortar Theory for Use of Ungraded Aggregates in Bituminous Mixes**. *Highway Research Board Bulletin No. 109*. Pp 1-49

Csanyi L.H., 1957. **Foamed Asphalt in Bituminous Paving Mixes**. *Highway Research Board Bulletin Volume 10 No. 160*. Pp 108-122

Csanyi L.H., 1959. **Foamed Asphalt**. *American Road Builders Association (ARBA) Technical Bulletin, Volume 240.* Pp 3-14

Csanyi L.H., 1960. **Bituminous Mixes Prepared with Foamed Asphalt**. *Iowa Engineering Experiment Station Bulletin No 189*, Iowa State University.

Dijkink H., 1992. **Immobilisation of Slag Material by Foam Bitumen**. R&E Consult. The Netherlands.

CSIR Transportek, 1998. **Foamed Asphalt, Mix Design**. Website http:\\foamasph.csir.co.za:81/chap4.htm

Eggers C., Holzhausen M. and Bartels J., 1990. **Bituminöse Tragschichten aus Müllverbrennungssasche und Schaumbitumen under besonderer Berücksichtigung von unterschiedlichen Tensiden**. Diplomarbeit, Fachbereich Bauingenieurswesen, Fachhochschule Hamburg. Germany.

Emery S.J., 1985. **Prediction of Moisture Content for use in Pavement Design**. PhD Dissertation. University of Witwatersrand, Johannesburg.

Engelbrecht J.C., Roberts F.L. and Kennedy T.W., 1985. **Cold Recycled Mixtures, with emphasis on the Curing of Foamed Specimens – A Laboratory Study**. *Annual Transportation Convention, S350 Volume T1*. Pretoria, South Africa.

FHWA Federal Highway Administration, 1994. **Superpave Asphalt Mixture Design and Analysis**. Strategic Highway Research Programme, USA.

Goacolou H., Le Bourlot F., Brosseaud Y., Gramsammer J-C., and Kerzreho J-P., 1997. **Expérimentation (premiére partie) de la Grave-Mousse ® sur le manége de fatigue**. *RGRA No 752 (Revue Géneralé des Routes et des Aerodromes)*, Septembre. Pp 61 - 70

Hotte P., 1995. **Six Years of Recycling with Foam Bitumen**. *Proceedings ARRA*. San Diego, USA.

Humberto Castedo Franco L. and Wood L.E., 1982. **Stabilization with Foamed Asphalt of Aggregates Commonly used in Low-Volume Roads**. *Transportation Research Record 898*. Pp 297-302

Jenkins K.J., Hugo F., van de Ven M.F.C. and O'Connell J., 1997. **Bitumen Emulsion Stabilised Paving Blocks – Development of Labour Intensive Manufacture and Construction Techniques**. *Second World Congress on Emulsion, Ref 4.1b-257*. Bordeaux, France

Jenkins K.J., van de Ven M.F.C., Ebels L.J. and Bredenhann S.J., 1999. **Possibilities for Cold Mix Bituminous Paving Blocks**. *Conference on Asphalt Pavements for Southern Africa, CAPSA 1999*. Victoria Falls, Zimbabwe.

Joubert G., Poolman S. and Strauss P.J., 1989. **Foamed Bitumen Stabilised Sand as an Alternative to Gravel Bases for Low Volume Roads**. *5th Conference on Asphalt Pavements for Southern Africa*. Swaziland. Pp VIII-21 to VIII-25

Khandal P.S., 1981. **Evaluation of Baghouse Fines in Bituminous Paving Mixtures**. Journal, *Association of Asphalt Paving Technologists. Vol 50*. Pp 150-210

Lancaster J., McArthur L. and Warwick R., 1994. **VICROADS Experience with Fosmed Bitumen Stabilisation**. *Proceedings 17th ARRB Conference Part 3*. Australia. Pp 193-211

LCPC (Laboratoire Central des Ponts et Chaussée) and SETRA (Service d'Études Techniques des Routes et Autoroutes), 1997. **French Design Manual for Pavement Structures : Guide Technique.** LCPC and SETRA, France.

Lee D.Y., 1981. **Treating Marginal Aggregates and Soils with Foamed Asphalt**. *Association of Asphalt Paving Technologists Volume 50*. Pp 211-250

Lewis A.J.N.L., Barron M.G. and Rutland G.P., 1995. **Foamed Bitumen – Recent Experience in South Africa**. *International Road Federation (IRF) Regional Conference, VolumeII*. Johannesburg, South Africa. Pp 1-12

Little D.N., Button J.W. and Epps J.A., 1983. **Structural Properties of Laboratory Mixtures Containing Foamed Asphalt and Marginal Aggregates**. *Transportation Research Record 911*. Pp 104-113

Maccarrone S., 1994. **Cold Asphalt as an Alternative to Hotmix**. *9th AAPA International Asphalt Conference. Australia*. Pp 19-24

Maccarrone S., Holleran G., Leonard D.J. and Hey S., 1994. **Pavement Recycling using Foamed Bitumen**. *Proceedings 17th ARRb Conference Part 3*. Australia. Pp 349-365

National Institute for Transport and Road Research NITRR, 1986. **Technical Methods for Highways TMH1**, Pretoria

Rigden P.J., 1947. **The use of Fillers in Bituminous Road Surfacings - A study of Filler-binder Systems in Relation to Filler Characteristics**. J.Soc Che Ind 66, pp 299.

Roberts F.L., Engelbrecht J.C. and KennedyT.W, 1984. **Evaluation of Recycled Mixtures using Foamed Bitumen**. *Transportation Research Record 968*. Pp 78-85

Ruckel P.J., Acott S.M. and Bowering R.H., 1983. **Foamed-Asphalt Paving Mixtures: Preparation of Design Mixes and Treatment of Test Specimens**. *Transportation Research Record 911*. Pp 88-95

SABITA, 1993. **GEMS – The Design and Use of Granular Emulsion Mixes**, Manual 14, Cape Town

Sakr H.A. and Manke P.G., 1985. **Innovations in Oklahoma Foamix Design Procedures**. *Transprtation Research Record 1034*. Pp 26-34

Semmelink C.J., 1991. **The effect of material properties on the compactibility of some untreated road building materials**. PhD Dissertation, University of Pretoria. South Africa.

Shackel B., Makiuchi K. and Derbyshire J.R., 1974. **The Response of Foamed Bitumen Stabilised Soil to Repeated Triaxial Loading**. *7th ARRB Conference. Volume 7 Part7*. Australia. Pp 74-89

Shell Bitumen, 1990. **Shell Bitumen Handbook**. Shell Bitumen U.K.

Tia M. and Wood L.E., 1982. **Use of Asphalt Emulsion and Foamed Asphalt in Cold-Recycled Asphalt Paving Mixtures**. *Transportation Research Record 898*. Pp 315-322

Van Wijk A. and Wood L.E., 1983. **Use of Foamed Asphalt in Recycling of an Asphalt Pavement**. *Transportation Research Record 911*. Pp96-103

VBW Vereniging voor Bitumineuze Werking, 1992. **Asfalt Onderzoek**. Handleiding. Proef 1.3, Netherlands. Pp 16-21

Wirtgen, 1998. **Wirtgen Cold Recycling Manual**. Windhagen, Germany.

Witczak M.W., 1972. **Design of Full-depth Asphalt Airfield Pavements**. RR 72-2. The Asphalt Institute, College Park.

CHAPTER 3

CHARACTERISATION OF FOAMED BITUMEN

1. INTRODUCTION

Foamed bitumen can be produced through the injection of small quantities of cold moleculised water, as a fine mist, into hot penetration grade bitumen in an expansion chamber. In this manner, bitumen can be mixed whilst it is foaming (in a temporary state of low viscosity) with mineral aggregates at ambient temperatures and at in situ moisture contents. The production process of foamed bitumen is illustrated in Figure 3 - 1.

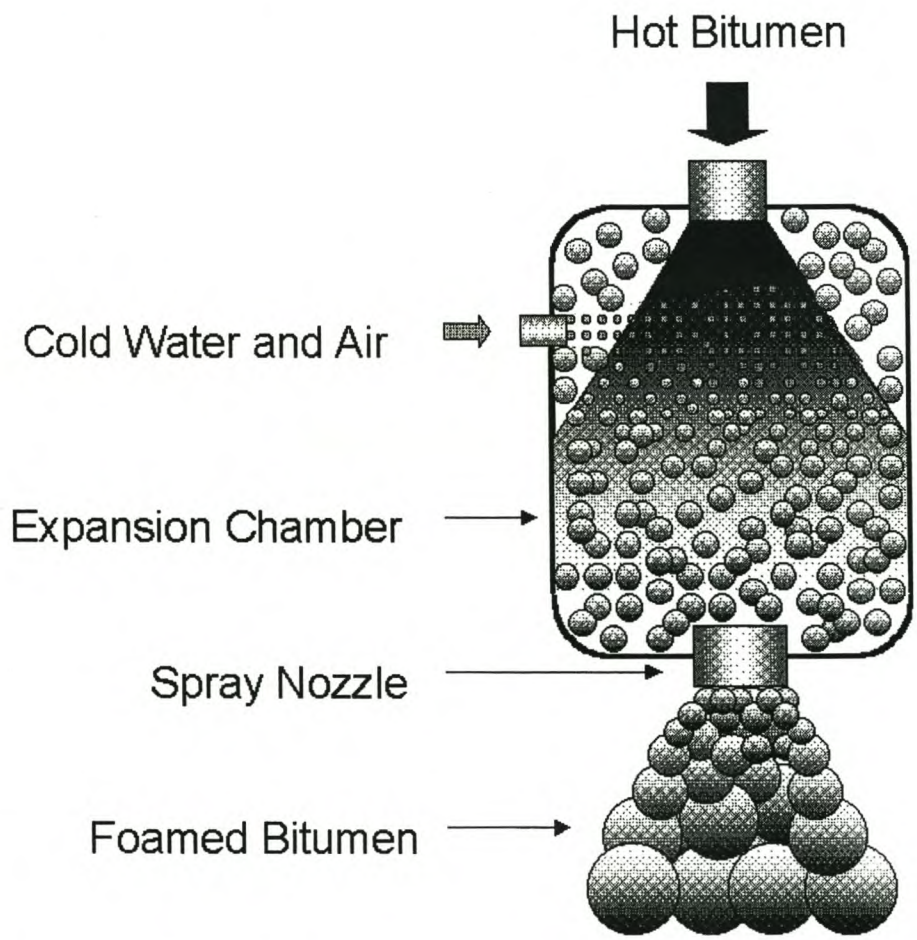

Figure 3 - 1. Production of Foamed Bitumen in an Expansion Chamber

The foamed bitumen process is analogous to the baking process where egg, which is viscous, is beaten into foam of low viscosity before mixing it with flour, as discussed in Chapter 1. The same principle applies to bitumen and mineral aggregate in order to produce a mix of acceptable quality and consistency for use in road construction.

As with most pavement engineering processes, a degree of variability is inherent to foamed bitumen stabilisation. In particular, the quality of the foam produced can vary markedly for different bitumens and different foaming apparatuses. This in turn, can influence the performance of a mix. In order to control the quality of the foamed bitumen and consequently the foam stabilised mix, the correct characteristics of the foam require analysis and monitoring.

At present, the properties of the foam are characterised by means of the expansion ratio and the half-life values. These values are calculated as follows:

- Expansion Ratio = Maximum volume of foamed bitumen/Original volume of bitumen
- Half-life = Time measured in seconds for the foamed bitumen to subside from the maximum volume to half of the maximum volume

Laboratory analysis of a given bitumen, heated and foamed into a vessel with a determined application rate of foamant water, currently requires only two points to be recorded viz. the measured maximum Expansion Ratio (ER_m) and the Half-life ($\tau_{1/2}$). By varying the application rate of the foamant water, a plot such as Figure 3 - 2 may be obtained. From such a plot, the present foam characterisation system provides for selection of an application rate of foamant water. This selection process is reliant on judgement of the trade-off between ER_m and $\tau_{1/2}$ as optimisation is not possible from such a plot. In addition, standard specifications for ER_m and $\tau_{1/2}$ are non-existent, although recommended values of ER_m > 10x and $\tau_{1/2}$>12 seconds have been recorded in literature in South Africa (CSIR, 1998), for example.

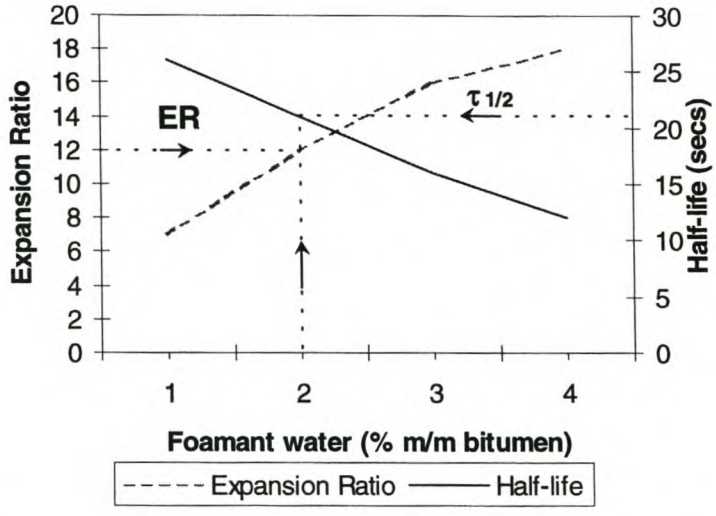

Figure 3 - 2. Foam characteristics for typical Penetration Grade Bitumen

After an intensive study of foaming characteristics, it has become evident that these two parameters and the manner in which they are currently determined are insufficient for adequate characterisation of foam properties. The two parameters merely define two points during the foam dissipation process. The remainder of the curve outlining the collapse of the foam with time (defined as "foam decay" in this dissertation), see Figure 3 - 3, is ignored in the present recommendations for foamed bitumen characteristics. Improved or additional parameters that take account of the decay curve are necessary for more complete characterisation of the foam and the prediction of performance of foamed bitumen in mixing and coating applications. In addition, tools that facilitate optimisation of the foam require development. This chapter includes the research into foamed bitumen characterisation outlining a new protocol that has been established for the standardisation of investigation and testing of the foamability of bitumen.

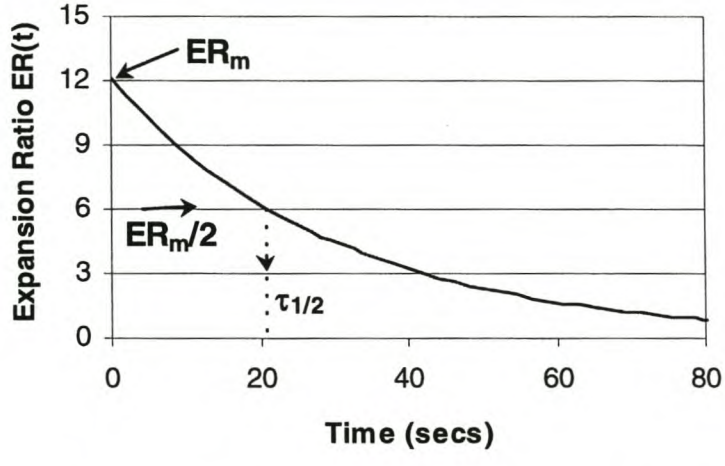

Figure 3 - 3. Foam decay curve for selected bitumen with 2% foamant water

Due to availability of resources, research has been restricted to the use of the Wirtgen WLB 10 ® laboratory foaming plant. Other custom made plants are utilised for foamed bitumen production on a laboratory scale, but have not been used in this investigation.

2. BACKGROUND

The fundamentals of the foaming process require consideration before the factors influencing the characteristics of foamed bitumen can be analysed. The laws governing the behaviour of the bitumen during foaming are primarily physical although chemistry does also play a role. Due to the physical nature of the foam, the manner in which the bitumen temperature influences the foaming characteristics pertains essentially to conservation of energy.

The process of foamed bitumen production, with the interaction of cold water droplets and hot bitumen, can be described physically. The moment that a cold water droplet (at ambient temperature) makes contact with the bitumen at 170 to 180°C, the following chain of events is postulated to occur:

- The bitumen exchanges energy with the surface of the water droplet. In this way heat is transferred to the water droplet, increasing its surface temperature and reducing the temperature of the bitumen around the droplet.
- As soon as the water droplet reaches a temperature of 100°C, the energy transferred from the bitumen exceeds the latent heat of steam, resulting in evaporation of the surface water. This results in a further reduction in temperature of the bitumen surrounding the droplet.
- The water evaporating from the droplet generates steam, which results in explosive expansion. Steam bubbles, under pressure, are forced into the continuous phase of bitumen in the expansion chamber of the foaming system. In this way a bubble is formed which encapsulates the steam under pressure. The steam could include the remainder of any unevaporated water from the droplet (if the water droplet is sufficiently large). The bubble is held intact by the surface tension of the slightly cooler bitumen film around the bubble.
- During the explosive expansion the surface tension of the bitumen film counteracts the pressure of the steam and the bubble expands with ever-diminishing pressure until a state of equilibrium is reached. Alternatively, the elongation of the bitumen for the given (short) loading time may be exceeded and the bubble will burst.
- For larger water droplets, the formation of a steam insulation layer around the remaining water droplet within the bitumen bubble will limit the generation of additional steam.
- Due to the low thermal conductive properties of bitumen and water, the bubble can remain stable for a period of time, usually measurable in seconds.

This process occurs for a multitude of bitumen bubbles that live contemporary metastable lives, providing foamed bitumen. As the colloidal mass cools at ambient temperature, the steam in the bubbles condenses causing the bubbles to collapse and the foam to "decay" or "break".

Sebba (1987) and Schramm (1994) classify foams into two distinct groups:

- Kugelschaum or wet foam or gas emulsion, comprises well separated spherical bubbles in the liquid i.e. a type air in liquid emulsion with liquid lamellae on the same scale or larger than the bubble sizes, and
- Polyederschaum or polyhedral foam, consisting of non-spherical bubbles separated by surfactant-stabilised, thin liquid films called lamellae.

Although foamed bitumen is not definitively a member of either of these classes, it would classify in bubble-form, but not in terms of chemistry, into the polyederschaum group, see Figure 3 - 4.

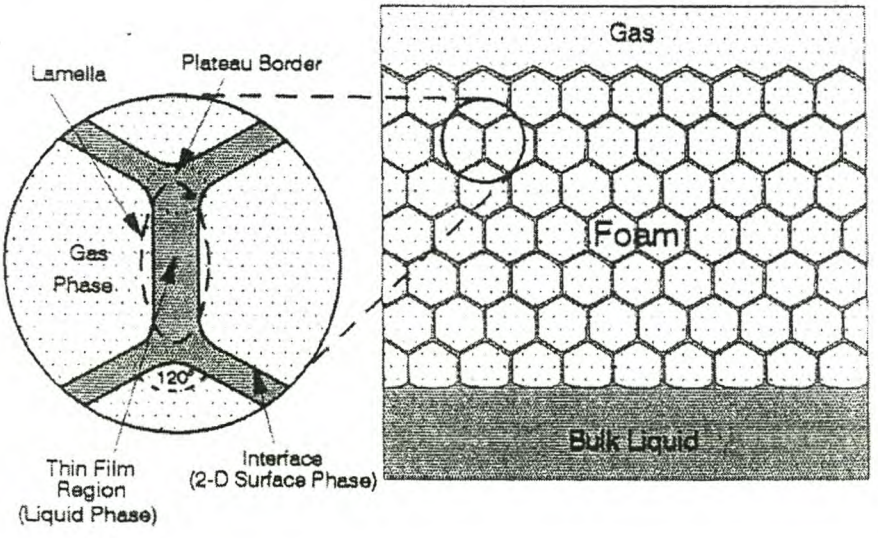

Figure 3 - 4. Generalised Foam with Non-Spherical Bubbles (Schramm, 1994)

3. THE PHYSICS OF FOAM

The physics of foamed bitumen requires exploration in order to identify some of the pertinent factors influencing foam characteristics.

3.1 Conservation of Energy

Energy, predominantly in the form of heat, is probably the dominant physical factor that influences the physics of foamed bitumen. Extending the background work of Acott (1980) and considering the production of foamed bitumen in a laboratory environment, the equilibrium temperature of the system can be calculated.

If foamed bitumen is discharged into a mild steel vessel in the laboratory for the purpose of measuring its characteristics, heat is transferred from the bitumen at temperature T_b to the vessel at temperature T_v and water at temperature T_w. In the process of foaming in a Wirtgen laboratory plant, the temperature of the surface of the water droplets (foamant water) rises to over 100°C when contact is made with the hot bitumen in the expansion chamber, converting the surface water to steam. The phase change occurs almost instantaneously, and generates pressure in the expansion chamber, which forces the foamed bitumen to be discharged from the spray nozzle.

If the equilibrium state of the system is considered only in terms of heat transfer i.e. ignoring work required to overcome the surface tension of the bitumen, and all of the foamant water is converted to steam, the conservation of energy equation is given as:

$$Q_w + Q_v = Q_b \qquad \textbf{Equation 3 - 1}$$

Equation 3 - 1 indicates that the energy gained by the water and the vessel is equal to the energy lost by the bitumen. This energy may be expressed in terms of the specific heat capacity of the various components in the system and in this manner a theoretical equilibrium temperature T can be determined.

Example 3.1

Consider a typical example of testing foam characteristics in a laboratory, where 500g of bitumen at 180°C is foamed into a vessel of mass 1500g and temperature 28°C, with the addition of 2,5% of water (m/m of bitumen) at 15°C. The heat gained by the water (Q_w) will comprise:

- the energy required to increase the water temperature from ambient to boiling point,
- the latent heat of steam, and
- heat required to increase the steam temperature to T (°C).

$$Q_w = M_w x S_w x(100-15) + M_s x L_s + M_s x S_s x(T-100) \qquad \textbf{Equation 3 - 2}$$

Where,

M_w = mass of water = 2,5x500/100 = 12,5g
M_s = mass of steam = M_w = 12,5g
S_w = specific heat of water = 1,0 cal/g
S_s = specific heat of steam = 0,5 cal/g
L_s = latent heat of steam = 539,4 cal/g

The heat gained by the vessel (Q_v) does not include phase changes and may be defined as :

$$Q_v = M_v x S_v x(T-28) \qquad \textbf{Equation 3 - 3}$$

Where,

M_v = mass of vessel = 1500g

S_v = specific heat of vessel = 0,112 cal/g

The heat lost by the bitumen (Q_b) may be defined as :

$$Q_b = M_b x S_b x (180-T) \qquad \textbf{Equation 3 - 4}$$

Where,

M_b = mass of bitumen = 500g
S_v = specific heat of bitumen = 0,5 cal/g

Substituting Equation 3 - 2 to Equation 3 - 4 in Equation 3 - 1 and solving provides:
T = 100,2°C

Using this procedure, a sensitivity analysis of the equilibrium temperature based on the temperatures of the main components may be established, see Table 3 - 1 (for 500g of bitumen foamed with 2,5% foamant water into a vessel of mass 1500g).

Table 3 - 1. Theoretical Equilibrium Temperature T (°C) for Foamed Bitumen System in Example 3.1

	Bitumen Temperature T_b			
Vessel Temp T_v	**150°C**	**160°C**	**170°C**	**180°C**
10°C	75.4	81.3	87.2	93.1
28°C	82.6	88.4	94.3	100.2
50°C	91.3	97.2	103.1	108.9
100°C	111.1	117.0	122.9	128.7

It is obvious from the range of theoretical equilibrium temperatures in Table 3 - 1 and the fact that foam stability is dependent on the steam temperature, that T_v and T_b require consideration in the determination of foam characteristics. The fact that some of the equilibrium temperatures are below 100°C which would cause steam to condense (at standard pressure) does not preclude the possibility of foam production, as time is required for thermal conductivity before the theoretical equilibrium temperature may be achieved.

The information in Table 3 - 1 can be utilised, with Avogadro's principle, to characterise the foam. In 1811 Avogadro stated that "*Equal volumes of all gases at the same temperature and pressure contain the same number of molecules*". The acceptance of the molecular nature of elements provided credibility to Avogadro's theory only after his lifetime. Contemporaries such as Dalton dispelled Avogadro's theory based on the dictum that an atom could not be split. According to Dalton the splitting of atoms was necessary since one volume oxygen combines with two volumes of hydrogen to give two volumes of steam, thus dividing an atom of oxygen between two molecules of water. Fortunately, acceptance of molecular theory corrected Dalton's misinterpretations and it is now known that there is a constant of $6,024x10^6$ molecules of water in one mole of steam (Avogadro's number).

Avogadro's theory and the Boyle-Charles-Gay-Lussac Law should be applied to the foam system. This law (Hutchinson, 1959) is given in Equation 3 - 5:

$$P \times V = n \times R \times T \qquad \textbf{Equation 3 - 5}$$

Where,

P = Pressure in Atmospheres (atm)
V = Volume in litres (l)
n = Number of moles = mass/atomic mass of compound
R = Universal Constant = 22.414/273.16 (atm.l/mole. Kelvin)
T = Temperature (Kelvin)

Using Equation 3 - 5 for the previous example of foam production, the volume of steam produced by the 12,5g of water may be calculated. At standard pressure i.e. 1 atmosphere, and a temperature of 100°C (=373.16 Kelvin), the volume of steam produced is:

$$V = \frac{12.5\text{g}}{(1.01*2+16)\text{g/mol}} * \frac{22.414\text{atm.l/mol}}{273.16\,\text{deg Kelvin}} * (100+273.16)\,\text{deg Kelvin} * 1\text{atm}$$

= 21.2 litres

The theoretical volume of 21.2 litres of foamed bitumen equates to an expansion ratio of 21.2/0.5 = 42.4, which is at least double the normally measured expansion ratio. This highlights two important scenarios for the production of foam, at least one of which needs to be true :

1. Not all of the steam is utilised for expansion of the foam. The reason for this is either :
   - Steam is lost during the foaming of bitumen i.e. it escapes. This can be observed in many cases.
   - Not all of the water is utilised to generate steam i.e. a small water droplet remains insulated by steam in the bitumen bubble, as described before.
2. The pressure inside the foam bubbles is greater than atmospheric pressure. This will be explored further at a later stage.

3.2 The foamed bitumen bubble

In order to analyse the mechanical interaction of the steam and bitumen, a bubble in isolation should be considered before the complex colloidal system can be understood. Figure 3 - 5 illustrates the changing parameters in an expanding bubble.

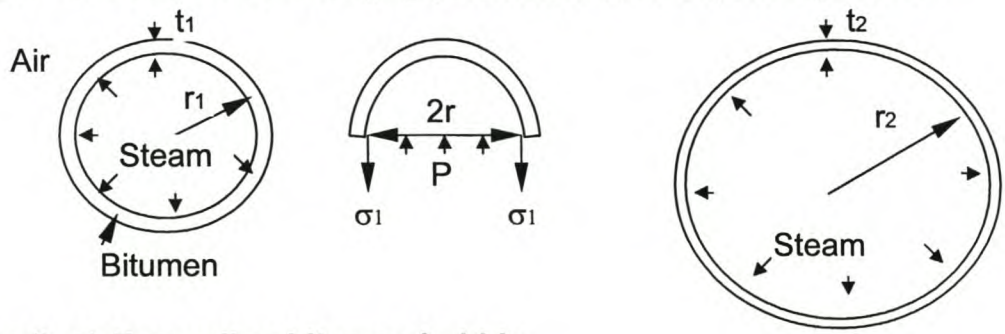

Figure 3 - 5. Expanding bitumen bubble

From the physics of a sphere it is known that :

$$\sigma_1 = \frac{P_1.r_1}{2.t_1}$$ **Equation 3 - 6**

Similarly, for the expanded bubble, the tensile stress in the bitumen is :

$$\sigma_2 = \frac{P_2.r_2}{2.t_2}$$ **Equation 3 - 7**

At the same time the corollary of the Boyle-Charles-Gay-Lussac or Universal Gas Law must also be satisfied:

$$\frac{P_1.V_1}{T_1} = \frac{P_2.V_2}{T_2}$$ **Equation 3 - 8**

Using Equation 3 - 8 and the assumption that no heat loss from the bubble has occurred i.e. $T_1=T_2$, the following can be derived :

$$P_2 = \frac{P_1.V_1}{V_2} = \frac{P_1.\frac{4}{3}\pi.r_1^3}{\frac{4}{3}\pi.r_2^3} = P_1.(\frac{r_1}{r_2})^3$$ **Equation 3 - 9**

Assuming no volume change in the bitumen during expansion of the bubble, the following is true :

$$4\pi r_1^2.t_1 = 4\pi r_2^2.t_2$$ (Surface area x thickness)

$$t_2 = t_1(\frac{r_1}{r_2})^2$$ **Equation 3 - 10**

Substituting Equation 3 - 9 and Equation 3 - 10 in Equation 3 - 7 yields :

$$\sigma_2 = \frac{r_2.P_1}{2.t_2}(\frac{r_1}{r_2})^3 = \frac{r_2.P_1.(\frac{r_1}{r_2})^3}{2.t_1.(\frac{r_1}{r_2})^2} = \frac{P_1.r_1}{2.t_1} = \sigma_1$$ **Equation 3 - 11**

Therefore the tensile stress in the bitumen remains constant during expansion of the bubble. Other phenomena that limit the expansion of the individual bubbles and ultimately the foam mass require exploration to explain the behaviour of the foam.

3.2.1 *Free Surface Energy Considerations*

Schramm (1994) observes that energy needs to be added to a system in order to achieve dispersion of a continuous phase. At the same time Acott (1980) states that the free energy of the bitumen film forming the bubble needs to remain positive for stable foam to exist with the separate phases of steam, bitumen and air. If this were not the case, then any mechanical or thermal fluctuations would expand the surface region continuously, leading to dispersion of the phases. Owing to the high interfacial area (and surface free energy) all foams are unstable in a thermodynamic sense. Surface free energy is the work required to expand the surface area and is measured in erg/cm^2, where 1erg = 10^{-7} Joules. The value of the surface tension that has been researched for penetration-grade bitumen is given in Table 3 - 2.

Table 3 - 2. Surface Tension of Bitumen (Lubbers,1985)

Temperature (°C)	Surface Tension (erg/cm^2)
25	33
100	29
150	26

Considering once again a single spherical bubble of bitumen of radius r, filled with steam, the total area producing surface tension is:

$$A = 4\pi r^2(\text{inside}) + 4\pi r^2(\text{outside}) = 8\pi r^2 \qquad \textbf{Equation 3 - 12}$$

Where the film thickness<<r

The unit change in surface area is given by:

$$\frac{dA}{dr} = 16\pi r \qquad \textbf{Equation 3 - 13}$$

Now, the free surface energy (G_b) of the foam bubble is the product of the energy per unit area or surface tension (γ) and the surface area (A).

$$G_b = \gamma.A = \gamma.8\pi r^2 \qquad \textbf{Equation 3 - 14}$$

The surface energy required to increase the radius of a bubble from r_1 to r_2 (see Figure 3 - 5) is given by:

$$\Delta G_b = \gamma.8\pi(r_2^2 - r_1^2) \qquad \textbf{Equation 3 - 15}$$

Now the energy lost by the steam is considered. This is calculated from the integral of the force on the film (F_r) over the distance it has been expanded (r_2-r_1). In order to calculate the

force on the bitumen film, the pressure in the bubble (P_r) at radius r is substituted for in accordance with Equation 3 - 9, as follows:

$$F_r = P_r.A_r = P_1.(\frac{V_1}{V_r}).A_r = P_1.(\frac{r_1^3}{r^3}).4\pi r^2 = P_1.4\pi.\frac{r_1^3}{r} \qquad \textbf{Equation 3 - 16}$$

The integration of the force over the new bubble radius yields the energy lost by the steam, as follows:

$$\Delta G_s = \int_{r_1}^{r_2} F_r.r.dr = \int_{r_1}^{r_2} P_1.4\pi(\frac{r_1^3}{r}).r.dr = \int_{r_1}^{r_2} P_1.4\pi r_1^3.dr = P_1.4\pi r_1^3(r_2 - r_1) \qquad \textbf{Equation 3 - 17}$$

For equilibrium, the energy lost by the steam (Equation 3 - 17) must equal the energy gained by the bitumen (Equation 3 - 15).

$$\Delta G_b = \Delta G_s$$

$$\gamma.8\pi(r_2^2 - r_1^2) = P_1.r_1^3.4\pi(r_2 - r_1)$$

$$\gamma.2(r_2 + r_1)(r_2 - r_1) = P_1.r_1^3(r_2 - r_1)$$

$$r_2 = \frac{P_1.r_1^3 - 2\gamma r_1}{2\gamma} \qquad \textbf{Equation 3 - 18}$$

The radius to which an individual bitumen bubble filled with steam will be expanded can therefore be approximated from the surface tension of the bitumen and the steam pressure inside the bubble. This approach ignores the effects of the colloidal mass, however.

Example 3.2:

Consider a foamed bubble at a radius of r_1=5mm which will expand to a radius of r_2=10mm before equilibrium is reached. What initial pressure P_1 was required to create this expansion and what was the final pressure P_2?

$$10^{-2} = \frac{P_1(5.10^{-3})^3 - 2*27{,}5.10^{-7+4}*5.10^{-3}}{2*27{,}5.10^{-7+4}}$$

$$P_1 = 6640\text{Pa}$$

$$P_2 = P_1.(\frac{V_1}{V_2}) = 6640*(\frac{5}{10})^3 = 830\text{Pa}$$

Using the Boyle-Charles-Gay-Lussac Law given in Equation 3 - 5, a water droplet of size 0.170mm would be required to establish an equilibrium pressure of 0.830 kPa in a bubble of 10mm radius. If all the foamant water experiences a phase change, then a foamed

system which moleculises the water particles to a maximum size of 170 μm would produce a superior quality foam.

3.2.2 *Elongation at break criteria*

Heukelom and Wijga (1973) established a relationship between elongation at break and the stiffness modulus at break of bitumens with different penetration indices. Using this relationship, an indication of the elongation of the bitumen film of a foamed bubble that is produced at an explosive breaking time, can be estimated. The following typical values have been utilised for foamed bitumen:

- Breaking time = 0.001 seconds (practically instantaneous)
- Temperature above $T_{r\&b}$ = 100 – 44 = 56°C
- Penetration Index = -0.5

From the Nomograph of Heukelom the elongation at break will be 100x. This implies that a water droplet of 0.1mm radius and circumference 0.628mm, which is encapsulated in bitumen as it is entirely vaporised, will expand to 62.8mm circumference before breaking i.e. a bubble radius of 10mm. This concurs with observations that have shown bubble radii of 10 to 15mm to be the critical radii at which breaking occurs for the foam in the frontier. The corollary is that water droplet sizes of approximately 100 to 150μm create the critical foamed bubbles which break, which agrees with the free surface energy considerations.

In addition to the over-simplified case of individual bubbles, consideration of the entire colloidal mass is also required. At the interfaces between the dispersed phase and the dispersion medium, characteristic surface properties such as adsorption and electric double layer can have a significant influence on the physical properties of the system as a whole. Shaw (1980) states that:

> *"the material within the molecular layer or so of the interface which exerts by far the greatest influence on particle-particle and particle-dispersion medium interactions"*

In the case of foamed bitumen, the material referred to is bitumen, but electrical double layers are not responsible for stability of the foam. Factors such as thermodynamics and possibly drainage are considered to be the dominant influences. Drainage in a colloidal mass of foamed bitumen refers to the gravitational flow of bitumen down the laminar part of the films to the plateau borders i.e. the line of intersection of films. In this way the plateau border thickens and the laminar films can rupture due to thinning. Two factors are likely to cause drainage of foamed bitumen:

- Van der Waal's forces favour thinning, and
- Capillary pressure, due to lower pressures at the plateau border that have curved rather than laminar surfaces, affects the equilibrium thickness, encouraging thinning.

However, drainage is considered to be a minor factor in the collapse of foamed bitumen due to the viscosity of the bitumen and time frame considered. The most important of these factors influencing the collapse or breaking of foam are discussed in Section 4.

4. FOAMED BITUMEN DECAY

Having established some of the factors influencing the behaviour of foam bitumen, the pertinent parameters for characterisation can be developed. The collapse of foamed bitumen with time, which is generically referred to as "decay", is considered to hold the key.

4.1 Factors influencing foamed bitumen decay

Schramm (1994) lists a number of factors influencing the stability of foam, namely:

- gravity drainage,
- capillary suction,
- surface drainage,
- viscosity (bulk and surface),
- electric-double layer repulsion,
- dispersion force attraction, and
- steric repulsion.

Some of these factors are irrelevant to foamed bitumen, which differs from the types (soapy or emulsion foams) found in the petrochemical industry. Instead, several causes for the breaking down of foamed bitumen bubbles with time are noted as:

- *Reduction in the temperature of the steam due to contact of the bitumen films with ambient air (and vessel) at lower temperature.* This occurs mainly with the bubbles at the frontier of the colloid mass. If the rate of temperature of the steam reduces, so the pressure in the foam bubbles diminishes according to the relation given in Equation 3 - 8. The pressure would reduce proportionately to the temperature if the surface tension of the bitumen film were negligibly small. But, where the surface tension is significant and the rate of temperature and pressure reduction exceeds the recovery rate of the bitumen film, the bubble will collapse. Larger bubbles, although possessing theoretically the same surface tension as their smaller counterparts, have a greater surface exposed surface area and will experience more rapid decrease in temperature. This faster "unloading" time will result in stiffer bitumen behaviour and less chance of recovery. The bigger bubbles will therefore collapse first!
- *Exceedance of the elongation limit of the bitumen film.* Where the water droplet initiating the formation of the foamed bitumen bubble is too large, the steam pressure inside the bubble could extend the bitumen film beyond its ductile limit, resulting in failure. Again, the bigger bubbles will fail first and steam will escape. If a small water droplet was still present in the bubble, it could generate a further bubble but less energy is available for this process as the bitumen temperature reduces.
- *Polydiverse colloidal mass.* It is apparent from literature (Adamson,1990) that a bubble pattern in which the septums of the bubbles meet at 120° will provide the most

mechanically stable configuration. The inverse of this theory is also true i.e. foams of a polydiverse nature, with a variety of bubble sizes, will be metastable with bubbles riding over each other until an equilibrium is reached. This activity can apply reactions within the colloid mass without equilibrium.

4.2 Modelling of foamed bitumen decay

Isotope decay equations are suitable for modelling of foamed bitumen "decay". Hutchinson (1959) maintains that:

> "*There is nothing notable or extraordinary about a radio-isotope until the moment of decay, and it only achieves a kind of posthumous fame. Only after it has decayed are we aware that it had previously existed as a metastable entity*".

This is partially true for foamed bitumen, although the chemistry and physics of the two processes differ significantly. Only after the foam has collapsed and is effectively dispersed in a mix, is it important.

Hutchinson also maintains that:

> "*For all practical purposes, at a time ten half-lives from the starting point, the amount of isotope remaining is so small as to be negligible".*

This statement is applicable to foamed bitumen decay too, as the half-life of the foam provides an indication of the window of time available for mixing of the bitumen with cold and damp aggregate, before mixing will no longer be effectively possible. The characteristics of the foam during its first half-life are by far the most important for foamed bitumen, with decreasing significance.

There is a difference between radio-active decay and foamed bitumen decay, in that the original matter tends to zero as time tends to infinity with the former and by definition tends to a value of one with the latter, see Figure 3 - 6. For mathematical efficiency, it is expedient to use the isotope decay model for foamed bitumen however. A simple solution to the dilemma would be to redefine the expansion ratio as the volume of foam excluding the original volume of bitumen divided by the volume of bitumen i.e. an expansion ratio of zero means that no expansion has occurred in the bitumen. This would result in foam decay tending to zero with time. Although this is applicable for mathematical correctness, for the reason given above i.e. reduced importance of the decay curve at an extended time measurement, and for mathematical reasons that become apparent in the analysis that follows in this chapter, it is not necessary. The models that are developed can and should, therefore, be applied to current foam measurement techniques without a paradigm shift in the approach of industry.

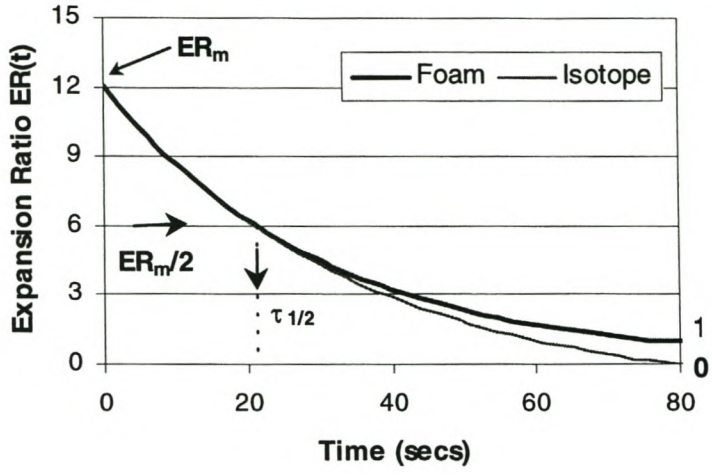

Figure 3 - 6. Foamed Bitumen Decay versus Isotope Decay with Time

The rate at which an isotope decays (Hutchinson, 1959) is given by:

$$-\frac{dx}{dt} = k.x \qquad \textbf{Equation 3 - 19}$$

Where,

x = concentration of isotope (negative sign indicates decrease)
t = time

Integration of Equation 3 - 19 with respect to time gives:

$$\ln(x) = -kt + \text{constant} \qquad \textbf{Equation 3 - 20}$$

Now set the initial value, at time zero x = a. It follows that:

$$\ln(\frac{x}{a}) = -kt$$

$$x = a.e^{-kt} \qquad \textbf{Equation 3 - 21}$$

At one half life t = $\tau_{1/2}$ and x = a/2 so :

$$\ln 2 = k.\tau_{1/2}$$

$$k = \frac{\ln 2}{\tau_{1/2}} \qquad \textbf{Equation 3 - 22}$$

Equation 3 - 21 and Equation 3 - 22 can now be applied for foamed bitumen decay, with provision for the different parameters. The new expression becomes:

$$V_t = V_{max}.e^{-kt}$$

Equation 3 - 23

Where,

$k = \ln 2/\tau_{1/2}$
$\tau_{1/2}$ = half-life (seconds)
$V_{max} = ER_m * V_b$
ER_m = Expansion Ratio (measured maximum)
V_b = Volume of bitumen = $SR * t_s/SG_b$
SR = spray rate of foamed bitumen (g/sec)
t_s = time of spraying (sec)
SG_b = specific gravity of bitumen at a given temperature (g/cm^3)
t = time after t_s for measuring volume of foam (sec)

Provision should also be made for the decay of the foam during spraying but before the volume of bitumen is measured. This is one of the omissions of the currently used techniques for foamed bitumen characteristic measurement and has an especially significant influence on bitumens with a low half-life, see Appendix A. The phenomenon of foamed decay during spraying is illustrated by considering the lifecycle of foamed bitumen produced in a laboratory vessel. Figure 3 - 7 exhibits the volume of bitumen and resultant foam superimposed on the same time scale for an example of foam characteristic measurement.

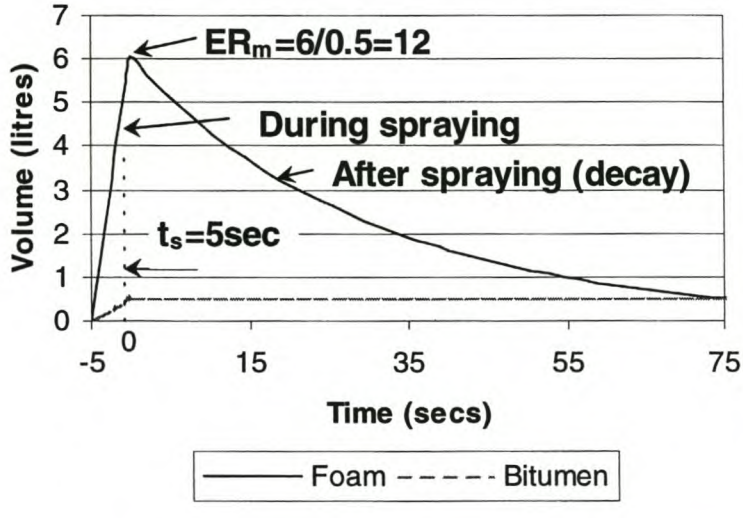

Figure 3 - 7. Lifecycle of Foamed Bitumen with a Measured Expansion Ratio of 12

It is apparent that some time is required to discharge the bitumen in the form of foam from the apparatus. In most cases, the bitumen has been decaying for up to 5 seconds (or more) before the expansion ratio (ER_m) is measured i.e. the maximum expansion ratio measured is not the actual maximum expansion ratio of the foam or $ER_m \neq ER_a$. This needs to be accounted for theoretically, as outlined in the following procedure.

In order to characterise the foam adequately the decay should be analysed separately for the two different phases of its life-span i.e. during spraying and after spraying.

4.2.1 Case 1 : Decay During Spraying ($0<t<t_s$)

The analysis of a system that is expanding and decaying simultaneously is complex and is therefore best modelled with the use of an adequate number of discrete time intervals. Consider a system where the time of spraying t_s is subdivided into x time intervals. Figure 3 - 8 provides an example of a system with x=10.

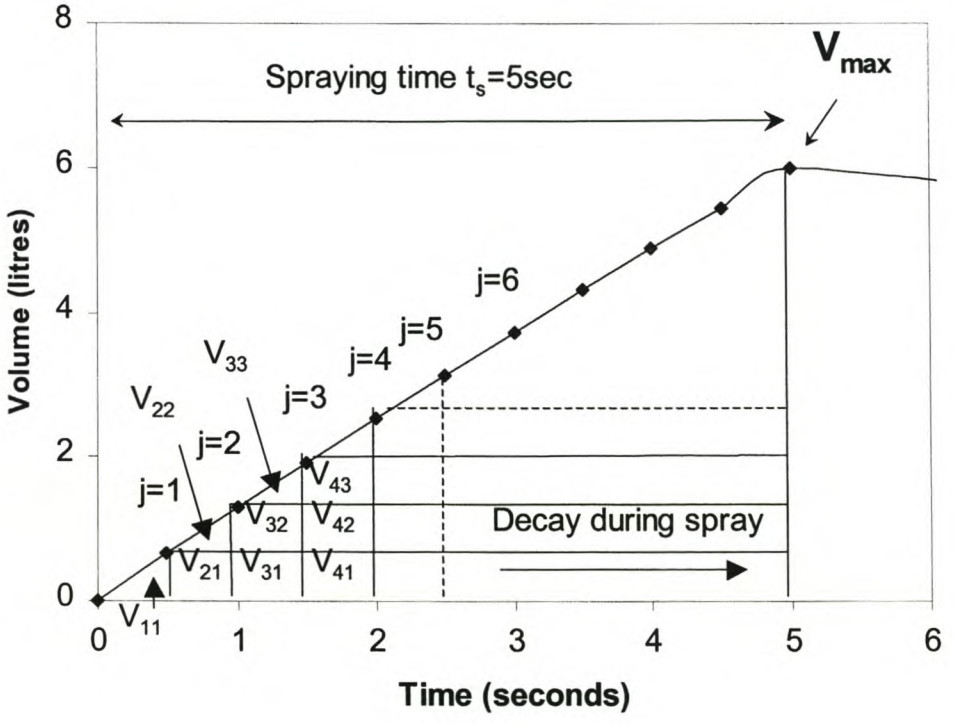

Figure 3 - 8. Analysis System for Foamed Bitumen Decay during Spraying

The decay of the bitumen can then be analysed in the individual intervals as follows:

V_{ij} = Volume of bitumen sprayed until time increment j and decayed to time increment i, where i and j are the increment numbers

$$V_{11} = \frac{x * SR}{SG_b} * ER_a * e^{\frac{-\ln 2 * x}{\tau 1/2 \ 2}}$$ **Equation 3 - 24**

For j>i

$$V_{1j} = V_{11} * e^{\frac{-\ln 2}{\tau_{1/2}} * x} \qquad \textbf{Equation 3 - 25}$$

For i>1 and j>1

$$V_{ij} = V_{i-1,j-1} * e^{\frac{-\ln 2}{\tau_{1/2}} * x} \qquad \textbf{Equation 3 - 26}$$

The cumulative volume of foam (V_{cj}) at time increment j will be the sum of the individual increments of foam volume, each decayed for it's respective time period as given below:

$$V_{cj} = \sum_{i=0}^{j} V_{ij} \qquad \textbf{Equation 3 - 27}$$

The volume obtained from Equation 3 - 27 is then utilised to calculate the "measured expansion ratio" ER_j at time increment j :

$$ER_j = \frac{V_{cj}}{\frac{SR}{SG_b} * j * x} = \frac{V_{cj}.SG_b}{SR.j.x} \qquad \textbf{Equation 3 - 28}$$

In addition, the cumulative volume of the foamed bitumen (V_{cts}) at the termination of spraying (t_s) can be determined applying Equation 3 - 27 over the period of spray.

$$V_{cts} = \sum_{i=0}^{ts/x} V_{c,ts/x} \qquad \textbf{Equation 3 - 29}$$

Using this information, the measured maximum expansion ratio ER_m at termination of spraying can be determined e.g. in the laboratory or from a known sample time at the plant.

$$ER_m = \frac{V_{cts}.SG_b}{SR.t_s} \qquad \textbf{Equation 3 - 30}$$

In this way, the actual maximum expansion ratio ER_a required to yield the measured maximum expansion ratio ER_m in the laboratory can be back-calculated. It is not possible to measure the actual expansion ratio, for practical reasons; only to back-calculate it.

Table 3 - 3. Relationship of Expansion Ratio actual vs measured

		ER_a				
Spray time	**ER_m**	**$\tau_{1/2}$=2 (secs)**	**$\tau_{1/2}$=5 (secs)**	**$\tau_{1/2}$=15 (secs)**	**$\tau_{1/2}$=30 (secs)**	**$\tau_{1/2}$=60 (secs)**
1 sec	5	6.02	5.39	5.13	5.06	5.03
	15	18.05	16.17	15.38	15.19	15.10
	25	30.05	26.95	25.64	25.32	25.15
5 secs	5	11.50	7.20	5.66	5.30	5.20
	15	34.40	21.48	16.98	16.00	15.50
	25	57.20	35.80	28.30	26.60	25.80
10 secs	5	21.34	9.88	6.38	5.66	5.33
	15	63.98	29.64	19.14	16.98	15.97
	25	106.63	49.39	31.89	28.30	26.61

Table 3 - 3 provides a sensitivity analysis of ER_a versus ER_m for different half-lives and spraying times, using the back-calculation theory provided. Using the mathematical relationship between ER_a and ER_m , a graphical relationship between these two factors has been established, see Figure 3 - 9, where t_s is the time of spraying of the foamed bitumen, $\tau_{1/2}$ is the half-life and c is a correction factor. It is apparent from this figure that for longer spraying times and shorter half-lives, it is imperative that the actual expansion ratio ER_a is back-calculated in order to prevent significant errors.

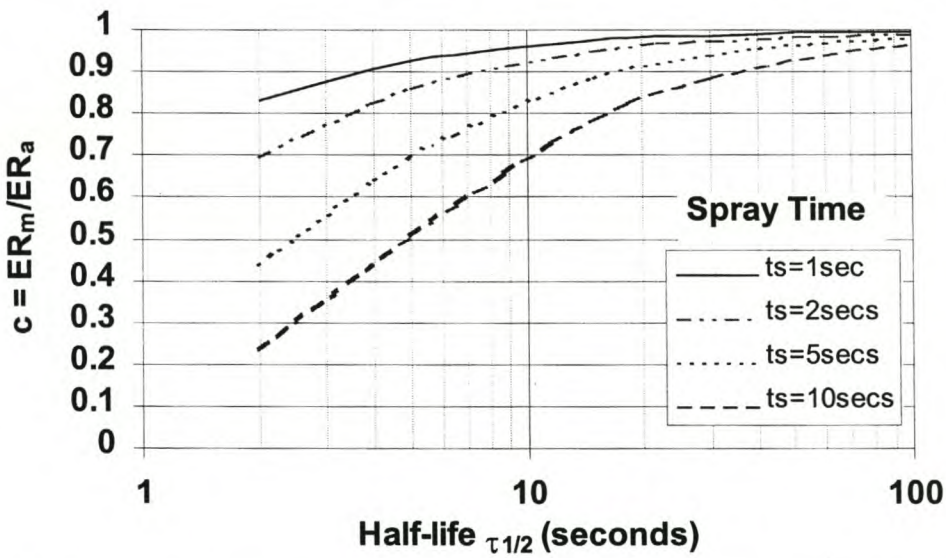

Figure 3 - 9. Relationship between Actual and Measured Maximum Expansion Ratio

4.2.2 Case 2 : Decay After Spraying ($t>t_s$)

4.2.2.1 Asymptotic Decay of Penetration Grade Bitumen

In the laboratory, following the discharge of the bitumen into the vessel, the foam often undergoes an asymptotic reduction in expansion with time. Provided that the foam is

produced under conditions that are not too far from ideal, isotope decay is most prevalent. For this reason, modelling of the decay commences with asymptotic decay. For conventional bitumens (penetration grade bitumens without additives) foamed using the Wirtgen WLB 10 Laboratory Plant ®, this foam decay can be adequately modelled using the following function :

$$V(t) = V_{cts} * e^{\frac{-\ln 2}{\tau_{1/2}} * (t - t_s)}$$ **Equation 3 - 31**

In the interests of keeping the relationship as simple as possible, this equation can be normalised in terms of time after t_s by assigning a value of t for the term $t-t_s$ in Equation 3 - 31 i.e. time t is measured from zero at the end of spraying foam (t_s). The relation for the expansion ratio with respect to time then becomes:

$$ER(t) = \frac{V_{ct}.SG_b}{SR.t_s} * e^{\frac{-\ln 2}{\tau_{1/2}} * t}$$

$$ER(t) = ER_m.e^{\frac{-\ln 2}{\tau_{1/2}} * t}$$ **Equation 3 - 32**

Where,

ER_m = Maximum Measured Expansion Ratio (immediately after discharge)

Using Equation 3 - 32, in conjunction with expansion derived from Equation 3 - 24 to Equation 3 - 30, a theoretical plot of the expansion that would be measured from the time that foam discharge commences can be plotted, see Figure 3 - 10. This example is for a bitumen with ER_m=15 and $\tau_{1/2}$=20secs.

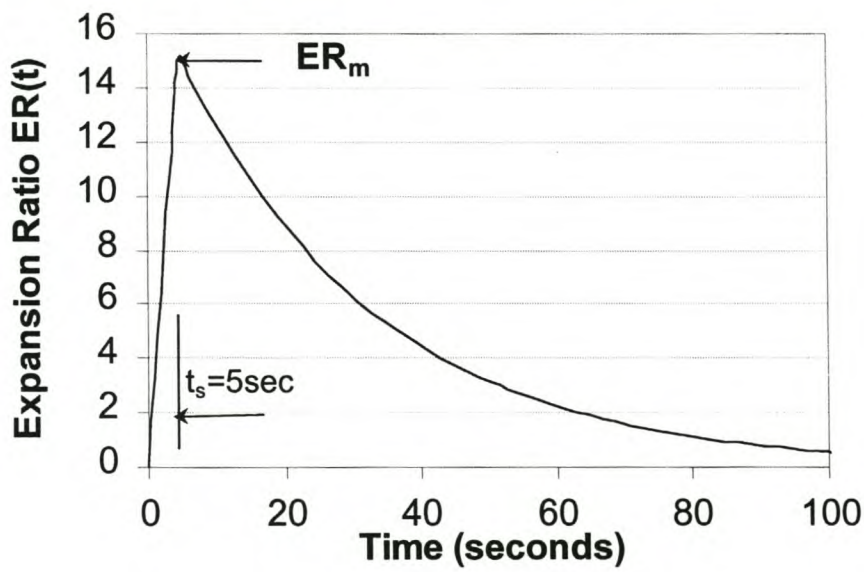

Figure 3 - 10. Theoretical Foamed Bitumen Expansion and Decay Curve (not normalised with respect to time)

The asymptotic theoretical foamed bitumen decay curve can be superimposed upon actual test data to verify the applicability of this relationship. This is illustrated for an actual foamed bitumen with ER_m=10.5 and $\tau_{1/2}$=13 seconds in Figure 3 - 11. The correlation coefficient of R^2 = 0.927 obtained, is a typical value for unmodified bitumens (without foamants or additives), but is dependent on repeated measurements for statistical reliability, and the application of standard testing procedures. In addition, adjustments to the nozzle configuration e.g. jet apertures and expansion chamber capacity, can influence the decay curve shape. The statistical sampling of foamed bitumen properties is addressed later in this chapter.

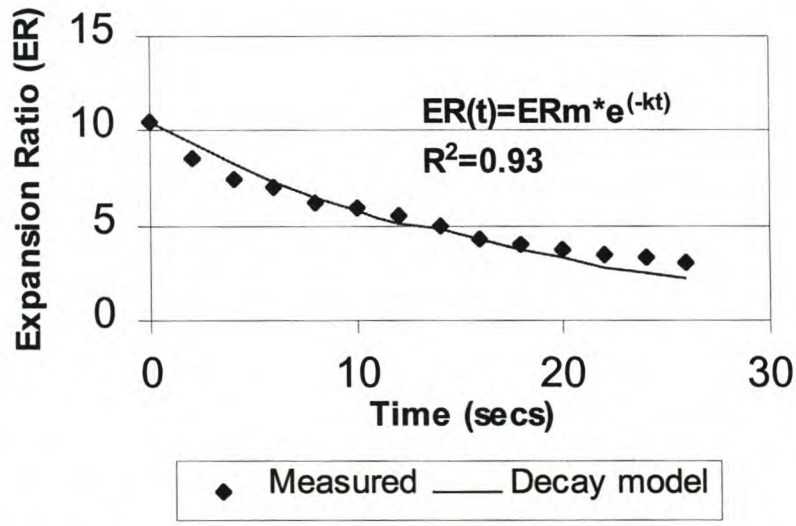

Figure 3 - 11. Theoretical Foam Bitumen Decay versus Actual Measured Values

4.2.2.2 Foam Index as a Measure of "Foamability" for Asymptotic Decay

A foam characteristic that takes account of the combined effect of the expansion and stability of foamed bitumen, is desirable to adjudge a foam's adequacy for being mixed and dispersed in a mineral aggregate. Expansion ratio and half-life, as currently applied by pavement engineers, are merely two points on the curve. The parameters are dependent variables, as can be seen in Figure 3 - 2 and, as such, should not be specified independently.

The area under the decay curve within specific limits, provides an integrated measure of the expansion and stability of foam and is therefore an important parameter for analysing foam. This area, defined as the Foam Index (FI), is developed in this dissertation for the purpose of characterising and optimising foam. It also provides an indication of the energy stored by the foam with respect to time.

Before the Foam Index can be further developed, the required limits on the decay curve require identification. The viscosity of the foam with time is the fundamental property

influencing these limits but has not been investigated in previous research. The intention of expanding bitumen into foam is to reduce its viscosity to enable mixing with mineral aggregate. The change of viscosity with expansion of the foamed bitumen is a difficult property to analyse considering the metastable nature of the foam, however. A hand-held viscometer provides a sufficiently accurate measure of viscosity for this purpose. By immersing the spindle of the viscometer in decaying foam, a trend of change in viscosity could be established. In this way, foams for a variety of bitumens and additives could be compared, see Figure 3 - 12.

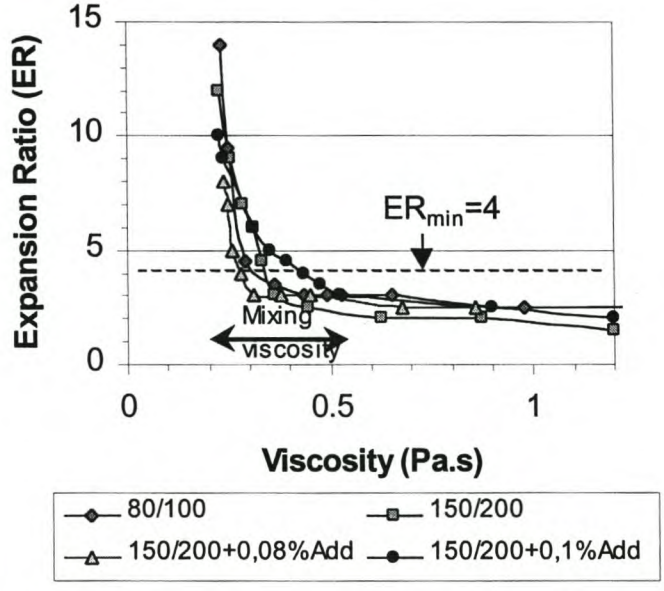

Figure 3 - 12. Relationship between viscosity and expansion ratio for foamed bitumen

Research at Shell Bitumen (1990) into hot-mix asphalt has shown that the bitumen viscosity should be between 0.2 and 0.55 Pa.s for adequate mixing and coating of the mineral aggregate. From Figure 3 - 12, the expansion ratio of the foam should be at least 4 for adequate mixing of all foamed bitumen. This value of 4 is utilised as the minimum value for calculating the area under the curve (Foam Index value), as shown in Figure 3 - 13. Such an analysis does not take cognisance of the fact that, during the mixing process, the aggregate will curtail the steady foam decay by drastically reducing the foam temperature upon contact. This phenomenon is, however, taken into consideration in the establishment of a recommended lower limit for FI.

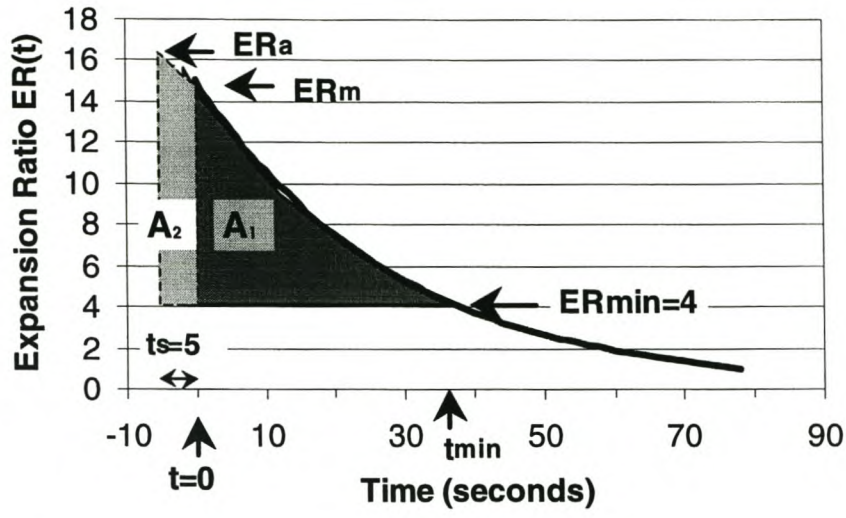

Figure 3 - 13. The Foam Index (FI) for characterising the "foamability" of bitumen for a given foamant water application rate, where FI = A1+A2

The characterisation of the foam in terms of viscosity is developed in order to obtain an empirical parameter that is an appropriate performance index of the foams' suitability for mixing and dispersion in the mineral aggregate, at the same time utilising relevant knowledge in the field of HMA.

Figure 3 - 13 provides the basis for the establishment of an equation for the calculation of the Foam Index.

$$ER_{min} = ER_m * e^{\frac{-\ln 2}{\tau_{1/2}} * t_{min}}$$

$$\ln ER_{min} = \ln ER_m - \frac{t_{min}}{\tau_{1/2}} . \ln 2$$

$$t_{min} = \frac{-\tau_{1/2}}{\ln 2} . \ln\left(\frac{ER_{min}}{ER_m}\right) \qquad \textbf{Equation 3 - 33}$$

For a given type of bitumen the Measured Maximum Expansion Ratio (ER_m) and the Half-life ($\tau_{1/2}$) can be measured in a laboratory and ER_{min}=4, therefore t_{min} can be calculated.

$$A_1 = \int_0^{t_{min}} ER_m * e^{\frac{-\ln 2}{\tau_{1/2}} * t} .dt - ER_{min}.t_{min}$$

$$= \frac{-ER_m.\tau_{1/2}}{\ln 2}\left(e^{\frac{-\ln 2}{\tau_{1/2}} * t} \right)\Bigg|_0^{t_{min}} - ER_{min}.t_{min}$$

$$= \frac{-ER_m.\tau_{1/2}}{\ln 2}\left(e^{\frac{-\ln 2}{\tau_{1/2}} * t_{min}} - 1 \right) - ER_{min}.t_{min} \qquad \textbf{Equation 3 - 34}$$

Now substituting Equation 3 - 33 in Equation 3 - 34:

$$A_1 = \frac{-ER_m.\tau_{1/2}}{\ln 2}\left(e^{\ln(\frac{ER_{min}}{ER_m})} - 1 \right) - ER_{min}\left(\frac{-\tau_{1/2}}{\ln 2}.\ln\left(\frac{ER_{min}}{ER_m} \right) \right)$$

$$= \frac{-\tau_{1/2}}{\ln 2}\left(ER_{min} - ER_m - ER_{min}.\ln\left(\frac{ER_{min}}{ER_m} \right) \right) \qquad \textbf{Equation 3 - 35}$$

Up to this point in the calculations, no correction has been made for the actual maximum expansion ratio ER_a in relation to the measured maximum expansion ratio ER_m (refer Figure 3 - 9). This should be done by including the value of A_2 from Figure 3 - 13 using $ER_a=ER_m/c$. So, using Equation 3 - 35 and a value of $E_{min}=4$ as established from viscosity tests, the Foam Index should be calculated using:

$$FI = A_1 + A_2$$

$$= \frac{-\tau_{1/2}}{\ln 2}\left(4 - ER_m - 4\ln\left(\frac{4}{ER_m} \right) \right) + \left(\frac{ER_a + ER_m}{2} \right) * t_s$$

$$= \frac{-\tau_{1/2}}{\ln 2}\left(4 - ER_m - 4\ln\left(\frac{4}{ER_m} \right) \right) + \left(\frac{1+c}{2c} \right) * ER_m * t_s \qquad \textbf{Equation 3 - 36}$$

Example 3.3:

Bitumen X is tested in the laboratory and the following foaming properties were measured (with asymptotic decay),

t_s = 5 seconds
ER_m = 15
$\tau_{1/2}$ = 10 seconds

From Figure 3 - 9, $c = ER_m/ER_a = 0.83$
From Equation 3 - 36, FI = 165.1 seconds

Currently recommended values for foamed bitumen properties (CSIR, 1998), are individually set in the "old" approach at:

ER_m (min) = 10 and

$\tau_{1/2}$ (min) = 12 seconds

From Figure 3 - 9, $c = ER_m/ER_a = 0.86$
From Equation 3 - 36, FI = 94.5 seconds

The new approach using the Foam Index does not result in the bitumen X being discarded because $\tau_{1/2}$ = 10 seconds (which is less than the value of 12 seconds recommended) whilst the expansion ratio is superior to the recommended values. The Foam Index of bitumen X is higher than the standard bitumen, indicating a better foaming performance than the standard bitumen i.e. a higher FI bitumen means that the more energy is stored in the foam during the mixing viscosity range than a lower FI bitumen. The Foam Index therefore provides a method of analysing the composite influence of expansion ratio and half-life, rather than attempting to analyse two dependent variables independently. This is applicable for ranking and selection of bitumen types, deciding on suitability of foam and optimisation of such foam.

4.2.2.3 Foam Index for Non-Asymptotic Foam Decay

Not all bitumen possesses the desired foaming characteristics for use in the foam process. The minimum expansion ratio and half-life (or a minimum FI) is not always achievable. The reasons for the poor foamability is not always clear; bitumen composition is complex and anti-foamants may be added during the refining process. Schramm (1994) mentions three types of anti-foamants:

1. Nonpolar oil with very low solubility in the aqueous phase (silicone oils).
2. Hydrophobic solid particles, typically hydrophobic amorphous silica or hydrophobic polymers.
3. Mixture of insoluble oil and hydrophobic particles.

It is especially the silicone oils that play a role in inhibiting foamed bitumen production. Drops of the almost insoluble silicone oil locate themselves in the film surface of a foam bubble, forming a lens. As the film thins with bubble expansion, so the lens forms an oil bridge. The bridge is unstable because the capillary forces dewet the film from the bridge causing the film to rupture. This causes metastable foam to become unstable.

The addition of appropriate foamants into the bitumen or foamant water can improve the foaming characteristics significantly, usually by extending the half-life. Where foamants have been used in bitumen the nature of the foam is altered and as a result, the actual decay may deviate from the decay curve model (which uses asymptotic decay). Examples of such foamed bitumen are provided in Figure 3 - 19.

The same principle applies where the configuration of the foam production plant varies significantly from that of the Wirtgen WLB10. The decay curve model can become inapplicable to foam produced in unorthodox plant or under non-optimal conditions. In

particular, the following aspects of the foaming apparatus influence the foam characteristics:

- aperture of the bitumen supply inlet,
- aperture of the spray nozzle, and
- capacity of the expansion chamber.

In order to establish whether the asymptotic decay model is applicable and to calculate the correct Foam Index, cognisance needs to be taken of the types of decay curves that are produced by different types of foamed bitumen, therefore. Extensive investigation has been carried out at G. van Hees en zonen bv. in the Netherlands and at the University of Stellenbosch as part of this research project. This particular investigation was focussed on the foam characteristics of various types of bitumen with variation in factors such as temperature, foamant water content, air pressure and additive content. Selected results are included in Appendix A, which in combination with the rest allow the foam decay to be distilled into six typical behavioural curves for foam, see Figure 3 - 14. Certain properties of the foam are related to each curve type.

Rapid Expansion: Asymptotic Decay (RE:AD) Foam

- Applicable to many penetration-grade bitumen types that are foamable.
- Foam has been produced at optimal or near optimal conditions in terms of temperature, foamant water content and expansion chamber configuration.
- No additional expansion is noted after a discharge time of 5 seconds into a pre-warmed vessel.
- Bubble sizes are small and polydiverse (evenly distributed in size) in the foam.

Rapid Expansion: Linear Decay (RE:LD) Foam

- Usually applicable foam of a bitumen with a foamant (additive).
- No additional expansion is noted after a 5 second discharge time into a pre-warmed vessel.
- Extended half-lives, in excess of 30 seconds, usually prevalent.
- Very fine bubbles with a single size distribution and practically no large bubbles (ϕ>5mm).

Rapid Expansion: Rapid Decay (RE:RD)

- Indicative of bitumen that is foamable but not recommended for use in foamed mixes.
- Rapid decay often results from incorrect foamant water application or bitumen temperature that is too low.
- Half-life values are very low (<12 seconds)

Slow Expansion: Gradual Decay (SE:GD) Foam

- The sign of bitumen that is eminently suited to being foamed.
- Usually applicable to softer grades of bitumen (> 150 penetration) or bitumen with a foamant.
- Very fine bubbles with a single size distribution and practically no large bubbles (ϕ>5mm).

- Foamant water content is close to optimum.
- Extended half-lives, often in excess of 30 seconds, are prevalent.
- Gradual decay can be quasi-linear, asymptotic or stepped (with small steps).

Plateau Expansion: Rapid Decay (PE:RD) Foam

- Indicative of bitumen not ideal for use in foamed mixes.
- Expansion can be moderate (15 to 25) or low (<15).
- Precipitous decay after the plateau usually results from an excessive proportion of large foam bubbles (ϕ>10mm) in the foam that burst rapidly and almost simultaneously with energy loss.
- Foamant water application rate of above optimum can be an influencing factor.

Plateau Expansion: Stepped Decay (PE:SD) Foam

- PE:SD together with RE:AD, make up the vast majority of foams from unmodified bitumen.
- Position of collapse point depends on the distribution of bubble sizes in the foam.
- Amount of subsidence after collapse point influences the measured half-life significantly (see graph).
- After precipitous collapse, the decay can be gradual, without a second plateau.

Low Expansion (LE) Foam (no graph required)

- Usually due to the presence of anti-foamants such as silicone oils in the bitumen.
- In some cases the bitumen can be improved and made useable through the application of foamants.

It is apparent from the PD:SD curves in Figure 3 - 13 that the half-life measurement can be sensitive to small changes in the decay curve shape. Not only are such curves prevalent in reality, but their non-uniform behaviour is not currently modelled. The Foam Index, however, by definition takes account of such irregularities, thus avoiding anomalies in half-life measurement.

Although six basic decay curves have been distilled from the results, combination of these forms may also be possible. For example, Figure A –2 in Appendix A provides data for Rapid Expansion: Stepped Decay RE:SD behaviour, which is a combination of two of the previous models.

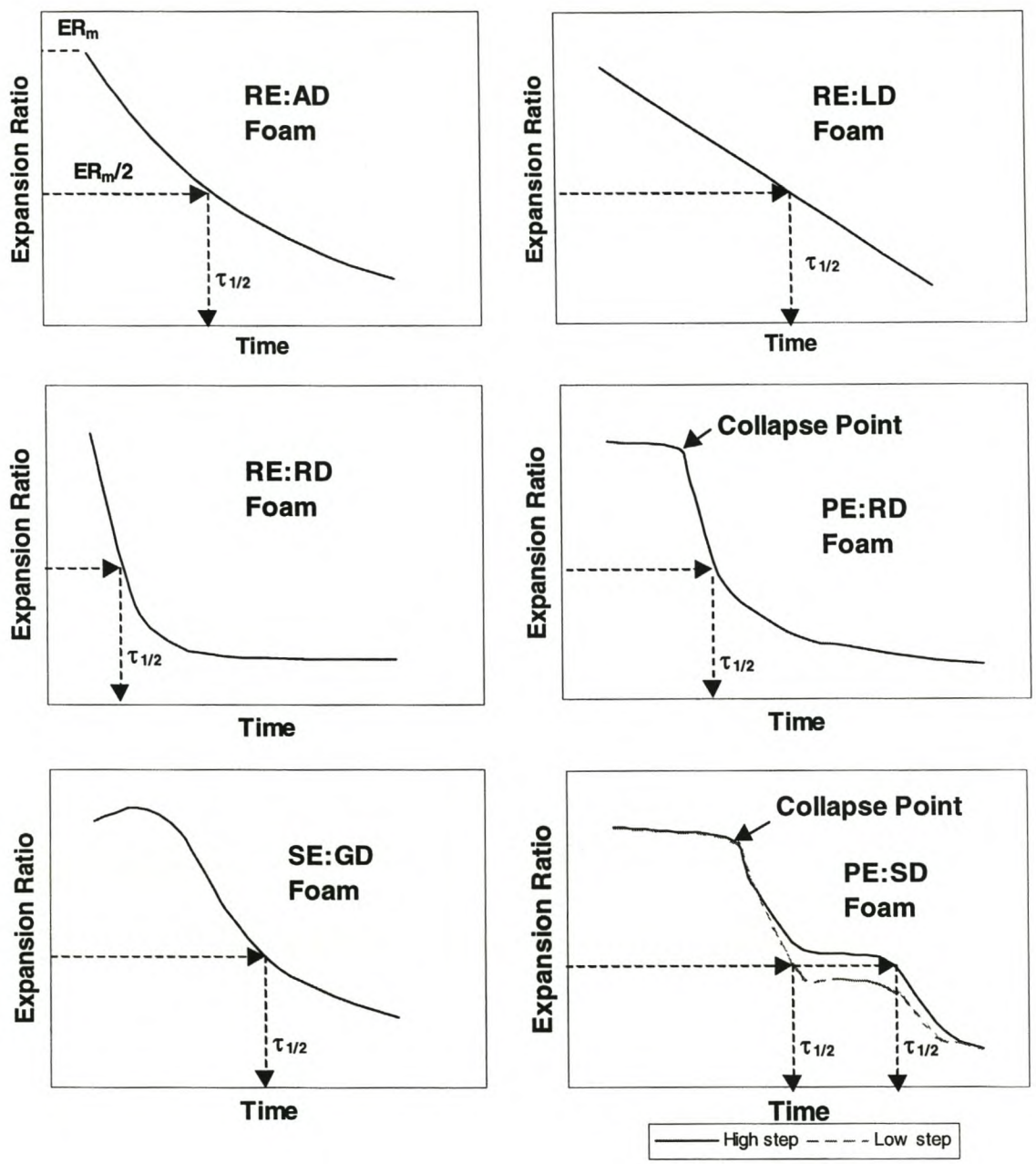

Figure 3 - 14. Six Most Prevalent Decay Curves for Foamed Bitumen

For every case of foam decay that deviates from the asymptotic decay curve model, a manual calculation of the Foam Index needs to be performed. The principle remains that the Foam Index is a function of the area under the decay curve. However, a new procedure should be followed for the calculation:

1. Measurement and plotting of the maximum ER_m and decaying expansion ratio ER of the given bitumen with time, using the standard foam testing procedures. This is done in steps which are the lesser of :

- graduations of less than 3 for expansion ratio, and
- time intervals of less than 10 seconds.

2. Step 1 is repeated at least three times.
3. In order to account for different spraying (discharge) times used in testing foam under laboratory conditions, see Appendix A, the decay curve is extrapolated back over the duration of the spraying period, see Figure 3 - 15.
4. Calculation of A_1 = the area under the decay curve between point ($t=0, ER_m$) and (t_{min}, ER_{min}) above the $ER_{min}=4$ line using an area by co-ordinates or similar routine.
5. Calculation of A_2 from time $t=-t_s$ to $t=0$ and above the $ER_{min}=4$ line using area by co-ordinates. Alternatively, if the first part of the decay curve , up to $\tau_{1/2}$ is asymptotic, the following equation can be used:

$$A_2 = \left(\frac{1+c}{2c}\right) * ER_m * t_s \qquad \textbf{Equation 3 - 37}$$

5. Calculation of the Foam Index FI = $A_1 + A_2$.

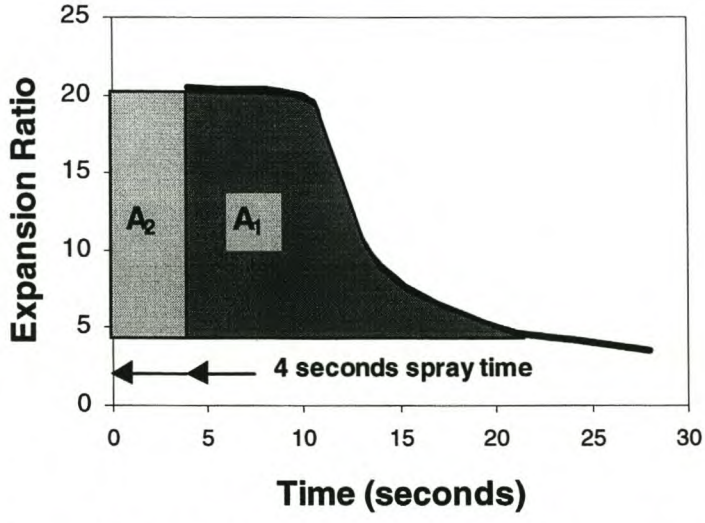

Figure 3 - 15. Foam Decay Function for PE:RD Foam at a Given Foamant Water Application Rate

This procedure of calculating FI is useful for the optimisation of the application rate of an additive to bitumen. The FI can be calculated for a range of application rates and the optimum additive content is then selected using a curve plotted from the results, see Figure 3 - 16. The figure provides the average of three tests for each point.

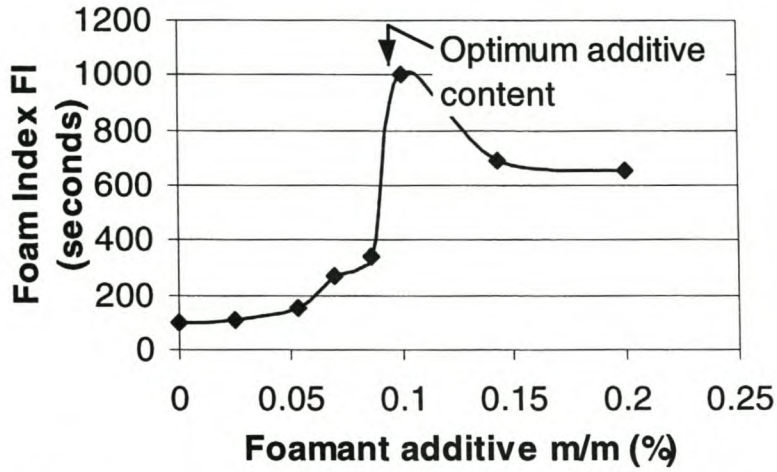

Figure 3 - 16. Influence of foamant additive content (m/m bitumen) on Foam Index (for Calref 150/200 with 2,2% foamant water)

In the same manner, the Foam Index can be utilised to determine the optimum foamant water content for specific bitumen (with or without additive). This is carried out through a sensitivity analysis of foamant water application rates. The decay curve of the foamed bitumen is recorded and the FI obtained for each application rate, see Figure 3 - 17. This is essentially a graph combining the individual components of expansion ratio and half-life shown in Figure 3 - 2. A smoothed function for the FI is obtained by applying best-fit functions to ER and $\tau_{1/2}$ on the axes of a Figure 3 - 2 type plot for the three repeat tests.

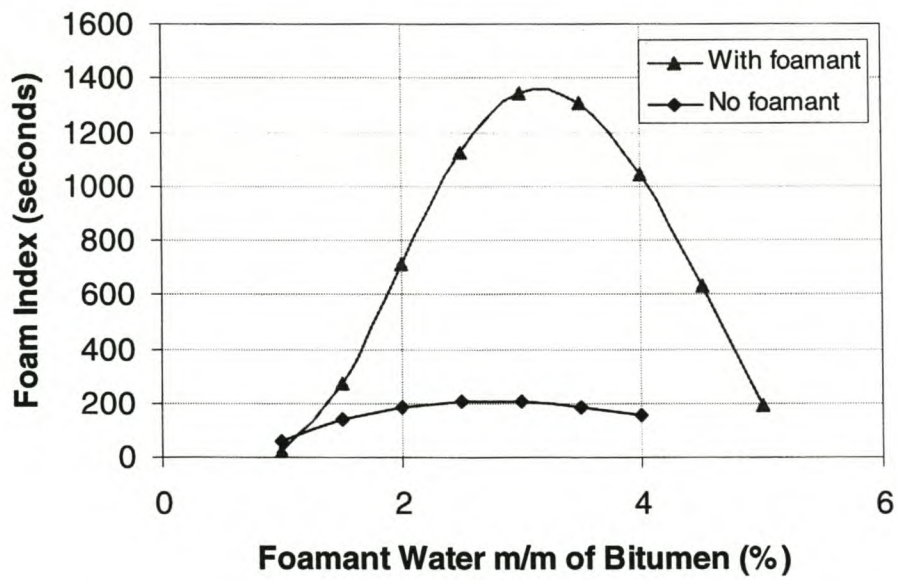

Figure 3 - 17. Optimisation of Foamed Bitumen Characteristics using the Foamed Index for Calref 150/200 Bitumen with and without Additive (Foamant M).

The optimal range of foamant water contents is in the same order for the specific bitumen tested with and without an additive. This does not necessarily hold true for all bitumen and additives. The figure, which includes three tests for each point, also shows the potential

improvements in the Foam Index of the Calref 150/200 with a specific foamant additive, in terms of the drastic increase in FI.

As shown in Figure 3 - 17, the form of FI vs water content curve does not necessarily yield a definitive optimum point, but rather a range of foamant water contents to produce optimal foamed bitumen characteristics. The most likely reason for this is:

- the lower water contents do not convert to sufficient volume of steam to produce the requisite expansion of the bitumen foam, whereas
- the higher water contents result in more steam being generated than the bitumen bubbles can accommodate, causing steam to escape and a loss of energy.

A margin between these scenarios exists for a given bitumen, which will produce optimal stored energy in the foamed bitumen and a relatively constant Foam Index. This phenomenon is graphically illustrated in Figure 3 - 18.

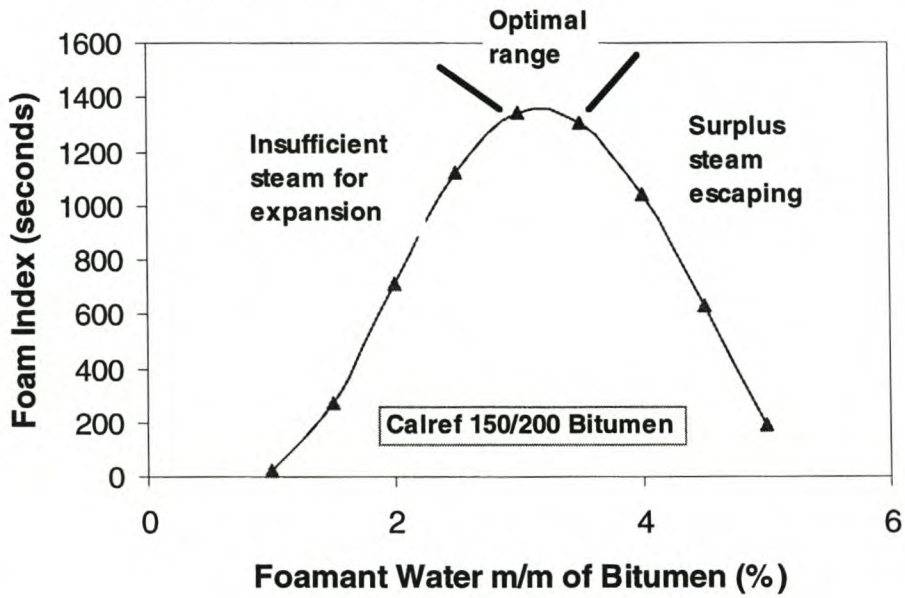

Figure 3 - 18. Generalised Approach for Optimisation of Foamant Water Application in Foamed Bitumen (in this case with Foamant)

In the same manner, the FI can be used to establish the comparable efficacy of an additive (foamant) on the foam characteristics of two different bitumens. For this purpose Nynas bitumen refined in the Netherlands and selected for favourable foam characteristics may be compared with a typical South African bitumen (Calref). Figure 3 - 19 provides the foamed bitumen decay curves (average of three tests) for Nynas bitumen with the same additive as used with the Calref bitumen.

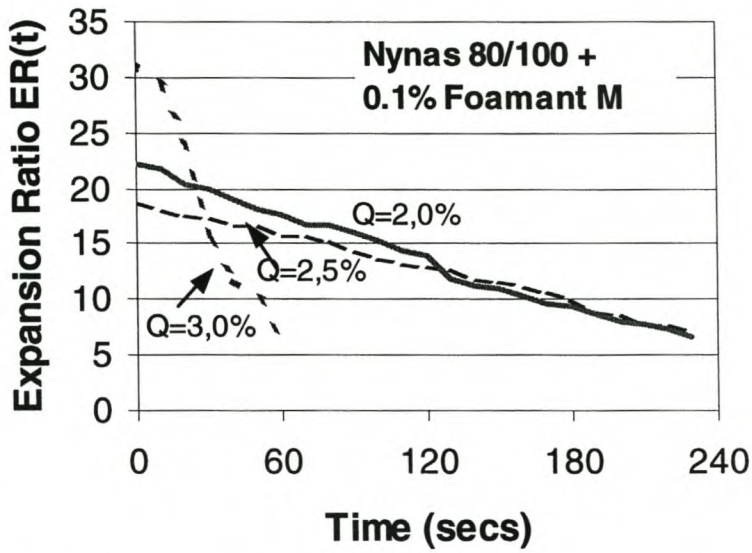

Figure 3 - 19. Foamed Bitumen Decay Curves for Belgian Bitumen with Foamant, where Q = Foamant water content m/m bitumen (%)

It is evident from Figure 3 - 19 that the decay curves for the Nynas foam are not asymptotic but rather approaching linearity at the two foamant water application rates in the optimal range. This is an example of a case for application of the modified FI calculation procedure.

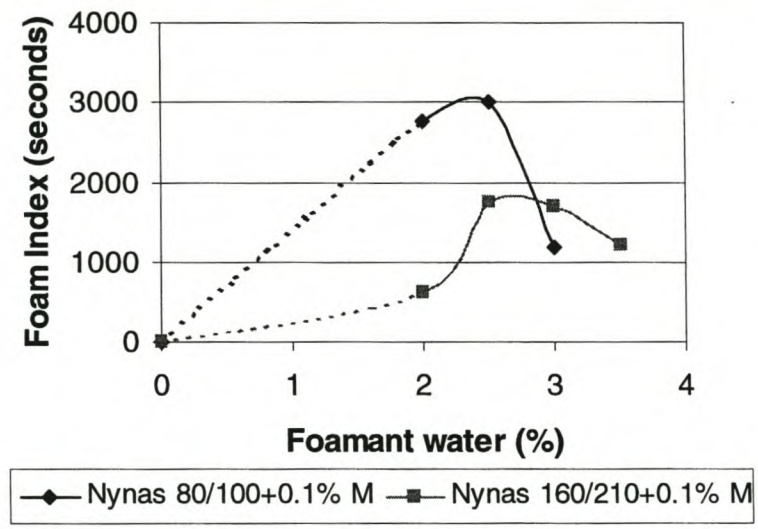

Figure 3 - 20. Influence of Foamant Water Content on Foam Index for Belgian Bitumen with Foamant M

The foam indices shown in Figure 3 - 20, indicate that the Foam Index provides the optimal range of foamant water application bitumen treated with a foamant too. It is also evident from these figures that the expansion ratio for such bitumen can be boosted to in excess of

ER_m = 30 by increasing the water application rate (from the optimum of 2,5% to 3%) at the expense of the Foam Index. This may be useful for specialist applications of foamed bitumen such as encapsulation of contaminants e.g. tars, or where fine coating of particles is required in a mixture.

Comparison of the results of the Calref and Nynas bitumen (Figure 3 - 16 to Figure 3 - 20) raises the following issues:

- There is a marked difference in foaming characteristics between the two bitumen types. The same foamant additive was utilised and it boosted the FI for both bitumens. However, the Nynas 80/100 bitumen had intrinsically better foam qualities that could not be met by the Calref 150/200, hence Nynas' three-fold higher foam index.
- The foamant has a significant contribution in the correction of the measured expansion ratio ER_m. By extending the half-life of the foamed bitumen, the foamant has the simultaneous effect of correcting ER_m so that it approaches the actual expansion ratio ER_a. This is evident in Table 3 - 4, Figure 3 - 21 and Figure 3 - 22. The correction factor c approaches unity as the Half-life increases, see Figure 3 - 9. The improvement in half-life by adding foamant "M" in this case is pronounced due to the extremely low initial values.

Table 3 - 4. Influence of Foamant "M" on Nynas 160/210 Bitumen

Foamant water	Foamant "M" (%)	ER_m	ER_a	C (ER_m/ER_a)	$\tau_{1/2}$ (secs)	FI
1	0.0	8.3	9.7	0.86	11.7	68
1.5	0.0	12.7	19.4	0.65	4.2	105
2	0.0	13.3	21.4	0.62	3.7	111
3	0.0	18.7	29.1	0.64	4.0	169
2.0	0.1	18.7	19.6	0.95	41.7	611
2.5	0.1	24.5	25.1	0.98	84.3	1740
3	0.1	30.9	31.9	0.97	57.3	1702
3.5	0.1	36.7	39.1	0.94	29.7	1211

Although a comparison of the measured expansion ratios (ER_m) for the Nynas 160/210 with and without additive "M" appear to show an increase in expansion of the foam as with the addition of "M", the actual expansion ratio (ER_a) indicates that this is not the case. Figure 3 - 22 shows a convergence of the decay curves with and without foamant, at the ER_a line. It is apparent from this figure and Figure 3 - 21 that the foamant additive has a negligible influence on the *Actual* Expansion Ratio ER_a of bitumen. Applying the current standard technique of measuring ER_m for foamed bitumen would not detect this as the ER_m values show marked improvement with inclusion of the additive whereas the influence of increase in $\tau_{1/2}$ is being measured. The effects of an additive can only be ascertained if the desired effects are clearly known and parameters and procedures are available to measure these effects. In this case, an increase in expansion may be sought; however, an increase in half-life is achieved.

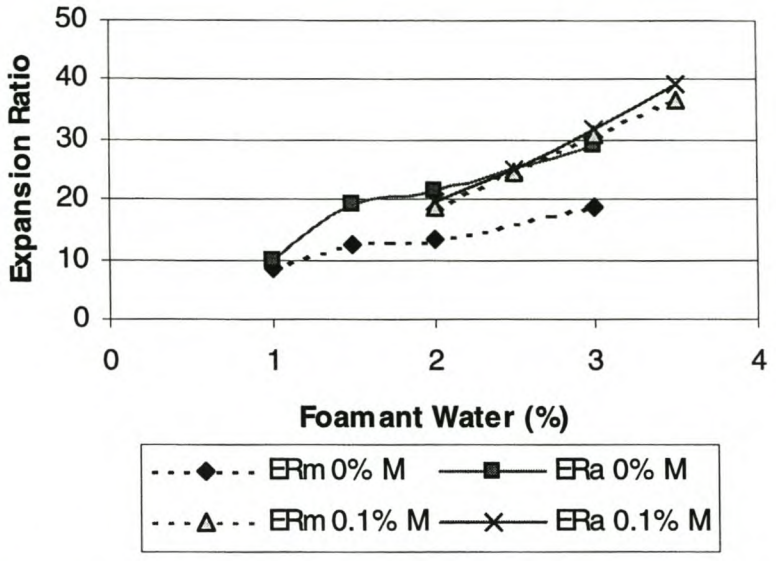

Figure 3 - 21. The Influence of Foamant Water on ER for Nynas 160/210 Bitumen with and without Foamant "M".

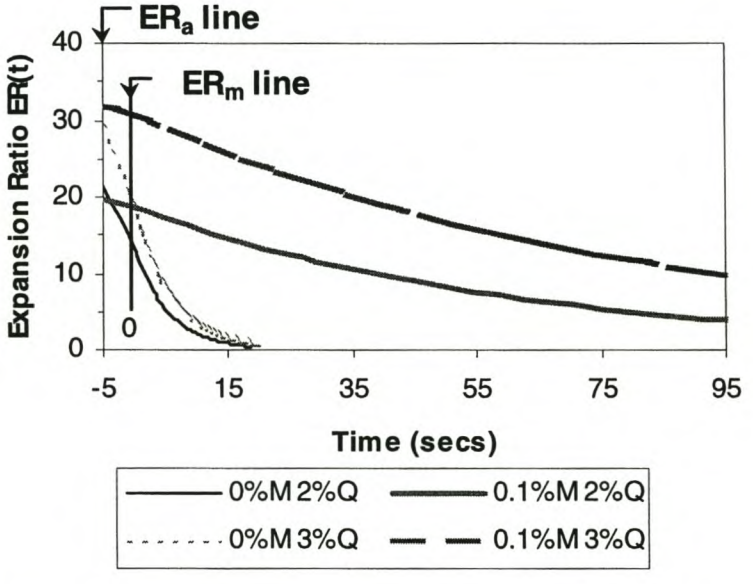

Figure 3 - 22. Decay Curves for Nynas 160/210 Bitumen with and without Foamant "M" at different Foamant Water Application Rates (Q)

4.2.3 Modified foamant water

It has been shown in Section 3.2.1 that the droplet sizes of the moleculised foamant water have a significant influence on the characteristics of the foamed bitumen. The mist of foamant water produced in the process is not only apparatus dependent, but also water quality dependent. In addition, additives can be added to not only the bitumen but also to the water to influence the characteristics of the foam.

For this reason, application of a super-plasticizer in the foamant water to reduce the surface tension of the water can influence the foam characteristics. The correct application rate of super-plasticizer results in finer water droplets being produced during moleculisation of the water and therefore a greater number of smaller droplets being injected into the expansion chamber.

A limited investigation into the use of the super-plasticizer yielded increases of approximately 60% in the expansion ratio of the foamed bitumen and a minor extension of half-life. The particular plasticizer investigated negated the effects of another additive "M" applied to the bitumen, which was intended to increase the half-life. Cognisance needs to be taken of the interaction between additives and foamants for different types of bitumen and influences cannot be considered in isolation.

4.3 Foam Index for Application to Different Mix Types

Foamed bitumen with asymptotic decay will experience a proportionate increase in the FI as $\tau_{1/2}$ increases, see Equation 3 - 36. This influence can be substantial when the increase in $\tau_{1/2}$ is large, which is the case for some foam types that have been treated with additives. However, it is not only the foam index that should be considered, but also the specific application of the foam e.g. for cold-mix or encapsulation etc. (Jenkins *et al.*, 2000). Although it is possible to moderate $\tau_{1/2}$ mathematically, this may be confusing for practitioners and it is more important to consider the Expansion Ratio and Half-life in conjunction with the Foam Index. The Foam Index has not been developed for to replace ER and $\tau_{1/2}$, but rather to enhance them.

Considering the type of mix that is to be treated with foamed bitumen, different requirements are expected from the foam, see Table 3 - 5. Encapsulation of contaminants, for example, requires a high expansion from the foam to improve coating whereas surfacing dressings require high stability (half-life) from the foam.

Table 3 - 5. Desired Values for Foam Characteristics depending on Mix Type for Application, based on Asymptotic Decay Foam

Foamed Bitumen Mix Type	Desired Minimum Values		
	ER_a	$\tau_{½}$	Foam Index
Surface Dressing	10	30	131
Cold Mix	15	15	164
RAP & Half-warm	17	13	180
Encapsulation	25	10	257

The limiting values for ER_a and $\tau_{½}$ have the effect of providing slightly higher optimum foamant water application rates for foam intended for encapsulation mixes (thus encouraging higher expansion) and lower optimum values for surface dressing type mixes (thus ensuring longer half-lives).

Using the desired Foam Indices from Table 3 - 5, a contour of equivalent Foam Index can be established, see Figure 3 - 23. In addition, absolute cut-off values for ER_a and $\tau_{½}$ require inclusion, depending on the particular process. In this way, a guideline for acceptable foams applied by industry can be established, as illustrated graphically in the figure. These functions are applicable for foam with asymptotic decay. For non-asymptotic decay foam, the same Foam Indices are recommended for all applications of foamed mixes. These can be calculated manually and checked against the relevant figure. Cold mixes produced with aggregates at ambient temperatures significantly higher than 15ºC, could be allowed a reduction in the minimum Foam Index.

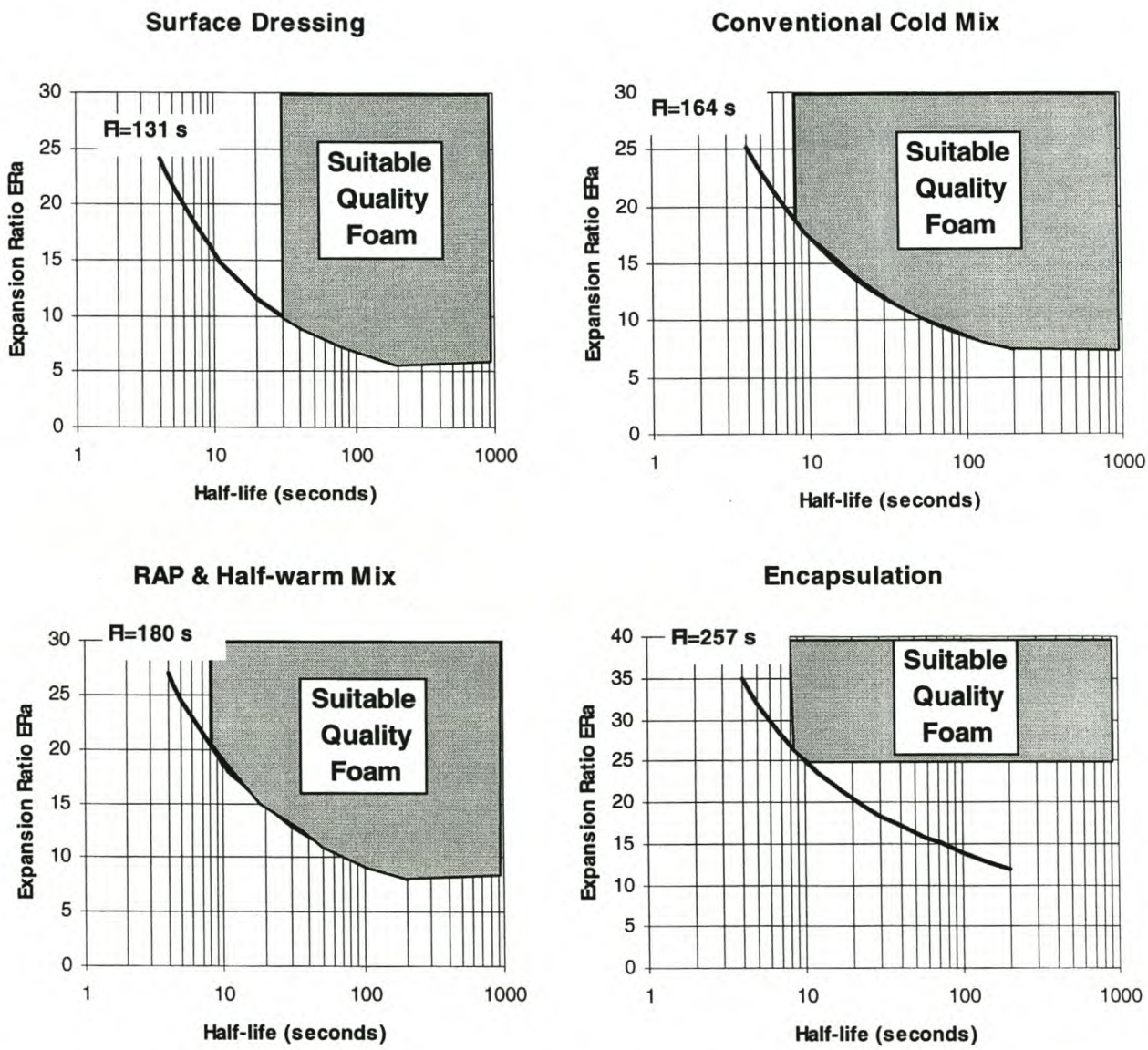

Figure 3 - 23. Interaction of Expansion Ratio and Half-life to Provide Acceptable Quality Foamed Bitumen for Different Applications in Mix Production (Half-warm Aggregate Temperature > 65ºC; other mixes Aggregate Temperature > 15ºC)

5. THE INFLUENCE OF BITUMEN TYPE AND COMPOSITION

Pavement engineers have been aware of the differences in the foaming properties of different types of bitumen for several decades. Acott (1985) stated that:

> " *the crude type and/or method of bitumen manufacture also affects the foam characteristics."*

Relationships between bitumen composition and foam characteristics are as yet undeveloped, however. With due cognisance given to the mechanisms influencing foam behaviour, as outlined in this chapter, a number of bitumen properties may be identified to contribute to the foam characteristics, including:

- Viscosity versus temperature relationships
- Ratio of Maltenes / Asphaltenes
- Composition of the bitumen
    - Saturates (parafines en naftenes) \
    - Aromatics > Maltenes
    - Resins /
    - Asphaltenes

The above properties are determined by both the origin of the bitumen and the refining and manufacture processes. However, additives such as silicone anti-foamants used in the refining process are very difficult to monitor or to identify compositionally and will more likely result in differences in the foam characteristics than the source of the bitumen will. Kendall *et al.* (1999) state:

> *"Bitumen in Australia is produced in "lube oil" refineries where the addition of 0.5% silicone doubles the throughput of bitumen. ...currently investigating practicalities of eliminating silicones from the process"*

From the limited literature available on foam characteristics, it is apparent that, where different grades of bitumen have originated from the same refining process, the softer bitumen has marginally lower surface energy (at the same temperature). Consequently, the steam pressure required to overcome the surface energy in the colloidal mass of bitumen will be less for softer grades of bitumen, yielding higher expansion ratios. Brennen *et al.* (1983) states that:

> *"...viscosity alone is not sufficient to explain the variations in expansion ratio and half-time"*

This statement emphasises the intrinsic complexity likely to enfold any correlation between bitumen properties and foamed bitumen characteristics. Considering the Penetration Index of bitumen and the "Elongation at break" criteria for foamed bitumen, theory indicates that,

two types of bitumen with the same PI should have equivalent half-lives. Figure 3 - 20 includes two types of bitumen with the same PI but different Penetrations (with an additive). Although the softer penetration bitumen would be expected to yield a higher Foam Index due to higher expansion and the same stability, this is not the case. Conversely, a higher PI value would yield a lower elongation at break and hence a lower FI.

Experimentation with foamed bitumen has shown that the presence of parafines in the bitumen can positively influence the foam characteristics. These waxy fluxes can be added to harder penetration bitumens in order to meet softer penetration specifications. Further investigation into the influence of parafines has yielded the results provided in Table 3 - 6. Not only is the Foam Index of bitumen higher, but visual observations indicate an improvement in foam quality in terms of finer bubbles.

Table 3 - 6. Average Foam Characteristics for Different Bitumen Composition

Bitumen source / Properties	Calref 150/200 with low parafine content	Sapref 150/200 with low parafine content	Calref 150/200 with higher parafine content
ER_m	19	18	19
$\tau_{1/2}$ (seconds)	14	26	39
Foam Index	279	393	596

6. STATISTICAL RELIABILITY OF FOAMED BITUMEN

Due to significant differences in foam characteristics recorded during repeat measurements, statistical analysis of the results requires consideration. For this purpose, the partial derivative equation is employed to obtain the standard deviation of the Foam Index value. Utilising Equation 3 - 36 and typical foamed bitumen characteristics viz,

$ER_m = 25$ x $\quad S_{ERm} = 1,22$

$\tau_{1/2} = 15$ seconds $\quad S_{\tau 1/2} = 1,31$

$t_s = 5$ seconds $\quad S_{ts} = 0,05$

the standard deviation of the Foam Index may be derived.

$$S_{FI}^2 = \left(\frac{\partial FI}{\partial \tau_{1/2}}\right)^2 S_{\tau 1/2}^2 + \left(\frac{\partial FI}{\partial ER_m}\right)^2 S_{ERm}^2 + \left(\frac{\partial FI}{\partial t_s}\right)^2 S_{ts}^2$$

$$= \left(-\frac{1}{\ln 2}\left(4 - ER_m - 4\ln\left(\frac{4}{ER_m}\right)\right)\right)^2 (S_{\tau_{1/2}})^2 + \left(\frac{\tau_{1/2}}{\ln 2} - \frac{4\ln 4}{ER_m^2} + \left(\frac{1+c}{2c}\right) * t_s\right)^2 (S_{ER_m})^2$$

$$+ \left(\left(\frac{1+c}{2c}\right) * ER_m\right)^2 (S_{t_s})^2$$

$$= 1749{,}5$$

$$S_{FI} = 41{,}8 \text{seconds}$$

Calculating the value of the Foam Index for this example yields FI = 429,1 seconds. The coefficient of variance of the Foam Index for typical foam characterisation is:

COV_{FI} = 41,8/429,1 = 9,7%

Although the COV of 9,7% may seem high, if all of the systematic errors of the factors influencing the foam characteristics are accounted for, this value is realistic. For example, the bitumen temperature in the kettle has a thermal gradient of up to 15ºC between the sides and the centre, as measured with an infrared gauge. Other factors such as foamant water application rate can vary by up to 10% from one spray time to the next as a result of bitumen impeding water outlet in the expansion chamber, see Figure 3 - 1.

The number of repeat measurements required for characterisation of foamed bitumen requires consideration. Using Figure G –1 of Appendix G, the coefficient of variance of 10% and number of observations of 3, yield a R = 5% deviation from the mean value for a significance level of 80% for the Foam Index. The probable range of the true mean will increase to R = 12% for one observation or foam characterisation measurement, which is unacceptably high.

7. CONCLUSIONS

7.1 Factors Influencing Foam Characteristics

In the investigation of foamed bitumen, many factors have been identified as having an influence on the quality and characteristics of the foam. These factors are listed, with an indication of *general* positive(↑) or negative(↓) effects on the foam:

Bitumen
- Bitumen type
- Bitumen temperature during foaming, higher temperature (↑)
- Bitumen spray rate, longer rate (↓)
- Additives (foamants and anti-foamants) (↑)

Foamant Water
- Application rate of foamant water, too high or low (↓)
- Foamant water composition
- Water temperature during foaming, higher temperature (↑)
- Quantity of air used for moleculising water, correct amount (↑)
- Additives (foamants) (↑)

Equipment and Settings
- Bitumen pressure, optimise (↑)
- Water pressure, optimise (↑)
- Air pressure for moleculising water, optimise (↑)
- Air temperature, higher temperature (↑)
- Temperature of vessel for capturing foam, higher temperature (↑)
- Relative humidity, higher humidity (↑)
- Expansion chamber and spray nozzle configuration

Due to the almost exhaustive nature of this list and the interdependent nature of some of the factors, only those that have been noted to have a significant influence on the foaming process have been selected for investigation. This selection was based on literature, experience and preliminary investigation into the factors.

7.2 Modelling of Foam Decay

- The currently used expansion ratio (ER_m) and half-life ($\tau_{1/2}$) characteristics, although useful, are incomplete parameters for describing the attributes of foamed bitumen. In order to improve the existing system rather than to replace it, a correction factor has been established for ER_m in order to convert it into a more useful parameter ER_a (the actual expansion ratio). This may be done taking account of half-life and the spray time of the foam in the laboratory.

- The ER_a is an intrinsic measure of bitumen's ability to expand during foaming at a fixed application of foamant water. Many foamants that are added to bitumen will increase ER_m and $\tau_{1/2}$, without changing ER_a. The ER_a remains the true measure of foam expansion.

7.3 The Foam Index

- Current practise does not provide the tools for optimisation of the foaming qualities of bitumen. A new characteristic has been developed in this research; the "Foam Index" (FI) is a useful tool for optimising the application rate of both the foamant water and proposed additives, for a given bitumen and foaming system. The Foam Index is a measure of the area under the decay curve i.e. the change in expansion ratio with time, which reflects the combined effect of the viscosity (ER) and stability ($\tau_{1/2}$) with time. This is a measure of the stored energy in the foam for a specific bitumen foamed at a known temperature with foamant water at a determined application rate.
- The FI may be determined using a standard decay equation for bitumen without foamants and exhibiting asymptotic decay. Where foamants are utilised or other factors result in the decay not being asymptotic, a plot of the decay curve and manual calculation may be utilised to obtain the Foam Index.
- Research into the viscosity of various types of bitumen during foaming has shown that the expansion ratio ER_m should be a minimum of 4 in order to ensure that the foamed bitumen is at a sufficiently low viscosity to allow mixing.
- The Foam Index can be utilised as a tool for the optimisation of the foamant water application rate to produce the most desirable properties in the foam.
- Although the environment and life-cycle of foamed bitumen for laboratory measurements and plant mixing differ significantly, the ER_a and FI obtained in the laboratory are important parameters for the comparison of different bitumen for a specific task. These characteristics can provide the basis for the selection of the appropriate bitumen. The Foam Index is not intended to replace the ER and $\tau_{1/2}$ but rather to enhance these factors.
- The required Foam Index for bitumen is dependent on the purpose for which the foam is to be used. To this end a contour of FI can be used in conjunction with absolute expansion ratio and half-life values for selection of suitable bitumen for a specific appilcation (at a specified minimum aggregate mixing temperature).

7.4 Bitumen Composition

- As with the performance properties of penetration grade bitumen used for asphalt production, the composition of the bitumen does not provide a reliable measure for prediction of performance properties of foamed bitumen. Although bitumen composition can provide indicators, physical tests are still required to more accurately and reliably determine the foamability of bitumen.

7.5 Foam Testing Procedure

- The temperature and specific heat of the vessel into which bitumen is foamed, as well as the bitumen temperature, have a significant influence on the results. To this end,

either a vessel temperature and mass should be specified for testing or at least two trials should be carried out in a vessel to achieve equilibrium temperature, before quality control tests commence. In addition, a sensitivity analysis of FI and ER_a needs to be carried out for different bitumen temperatures.

- Due to the inherent variability of the measurement of foamed bitumen characteristics, a total of at least 3 tests should be carried out for each laboratory trial, in order to obtain an acceptable level of statistical reliability for the results.

8. REFERENCES

Acott S.M.,1980. **The stabilisation of a sand by foamed bitumen – A laboratory and field performance study**. Dissertation for Master of Science in Engineering. University of Natal.

Adamson A.W., 1990. **Physical Chemistry of Surfaces**. Fifth Edition. Wiley and Sons. New York.

Bitufoam, 1996. **Foamed bitumen**. Marketing brochure. South Africa.

Brennen M., Tia M., Altschaefl A. and Wood L.E., 1883. **Laboratory Investigation of the use of Foamed Bitumen for Recycled Bituminous Pavements**. Transportation Research Record 911. Pp 80-87.

CSIR Transportek, 1998. **Foamed Asphalt, Mix Design**. Website http:\\foamasph.csir.co.za:81/chap4.htm

Heukelom W. and Wijga P.W.O. 1973. **Bitumen testing**. The Koninklijke/Shell Laboratorium, Amsterdam

Hutchinson E., 1959. **Chemistry, The Elements and their Reactions**. WB Saunders Company, Philadelphia and London

Jenkins K.J., Molenaar A.A.A, de Groot J.L.A. and van de Ven M.F.C., 2000. **Optimisation and Application of Foamed Bitumen in Road Building.** *Wegbouwkundige Werkdagen 2000. Deel 1.* Doorwerth, Netherlands.

Kendall M., Baker B., Evans P. and Ramanujam J., 1999. **Foamed Bitumen Stabilisation**. *Southern Region Symposium*, Australia.

Lubbers H.E.,1985. **Bitumen in de Weg- en Waterbouw**. Nederlands Adviesbureau voor Bitumentoepassinggen NABIT, In Dutch.

Schramm L.L., 1994. **Foams : Fundamentals and Applications in the Pertroleum Industry**. Advances in Chemistry Series 242, American Chemical Society. Washington DC.

Sebba F., 1987. **Foams and Biliquid Foams - Aphrons**. John Wiley & Sons. Chichester, England.

Shaw D.J., 1986. **Introduction to Colloid and Surface Chemistry**. Third Edition. Butterworths. London.

Shell Bitumen, 1990. **Shell Bitumen Handbook**. Shell Bitumen U.K.

CHAPTER 4

MIX DESIGN CONSIDERATIONS FOR COLD MIXTURES

1. BACKGROUND

The global increase in use of foamed bitumen mixes in road construction and rehabilitation has created a need for sound guidelines to be established for the laboratory mix design procedures. Current procedures are under-developed and insufficiently documented. At the same time, the mechanisms that influence the behaviour of bituminous mixes with an additional phase i.e. water, are inadequately explained. This chapter explores some of the unique features of cold mixtures, in particular foamed bitumen, with an analysis of how these aspects should be accounted for in a laboratory mix design. The main areas of focus are the spatial composition of the mixtures, filler/bitumen/water interaction in the mastic, ageing and curing influences and the impact of aggregate temperature on binder dispersion in the mix.

Sound guidelines for the mix design procedures of cold bituminous mixes, especially foamed bitumen, are lacking. Guidelines such as the GEMS Manual (SABITA, 1993) for granular emulsion mixes, are considered good departure points for bitumen emulsion mix design based on engineering properties of granular mixes, but scope for improvement in the methodology is apparent.

This chapter is focused on the characterisation of cold mixes in terms of volumetric properties, mechanical properties and fundamental performance parameters. This has included the investigation of a variety of good quality and marginal materials, using commercially available bitumen emulsions, a laboratory foaming plant and other specialist equipment.

2. SPATIAL COMPOSITION

The central role of spatial composition in the compositional design and performance of pavement materials is illustrated in Figure 1 – 1. Van de Ven (1998) formulated a more detailed spatial approach to asphalt by relating this material to others. In materials science the "spatial approach" is the study of the 3-dimensional volumetric structure of a material or it's surface, at micro-, meso- and macro-level in order to develop spatial models that can be used to explain material behaviour and assist in the prediction of performance. Clearly, this approach is of paramount importance to the mix design of cold bituminous mixes and should be considered at all of the phases of the material life i.e. production, transportation, compaction etc, see Figure 1 – 1.

Based on spatial considerations, the volumetric properties of cold mixes require fresh investigation. The approaches utilised to analyse the spatial composition of HMA i.e. particle angularity, Rigden voids, gradation, binder properties etc. can sometimes be adapted to research the composition of cold bituminous mixes. These adaptations, however, need to take cognisance of the specific aspects peculiar to cold mixes e.g. the aqueous phase and changes resulting from curing.

In particular, the filler fraction and the sand fraction of cold mixes require special attention in spatial considerations. Due to the unique nature of the dispersion of the binder in particularly foamed mixes, the fine fractions are the key to the material behaviour. In addition, the manner in which these fractions combine with the larger aggregate also requires consideration.

2.1 Filler, Bitumen and Water Interaction In The Mastic

2.1.1 Background

It is widely accepted that the mixture of filler and bitumen in an asphalt mix i.e. the mastic, is an important component that binds the larger particles together. Researchers in the past have developed relationships to describe the stiffening potential of filler/bitumen mastics for HMA, characterised by penetration, ductility, viscosity and softening point temperatures. Superpave (FHWA,1994) uses the term "dust-to-asphalt" ratio and specifies a range of between 0.6:1 and 1.2:1 (by mass of bitumen) to limit the stiffening effect of fillers (<0.075mm) on bitumen binders. But this ignores the intrinsic properties of the filler, which has its own unique gradation.

Rigden (1947) developed a test to measure the void content of dry, compacted filler that was later modified by Anderson (1987). This void content was theorised by Rigden to be the minimum volume available in the filler to hold the "fixed bitumen" and any excess bitumen in the mastic would then be "free bitumen". The free bitumen was considered as the binder available to lubricate the filler-bitumen mixture.

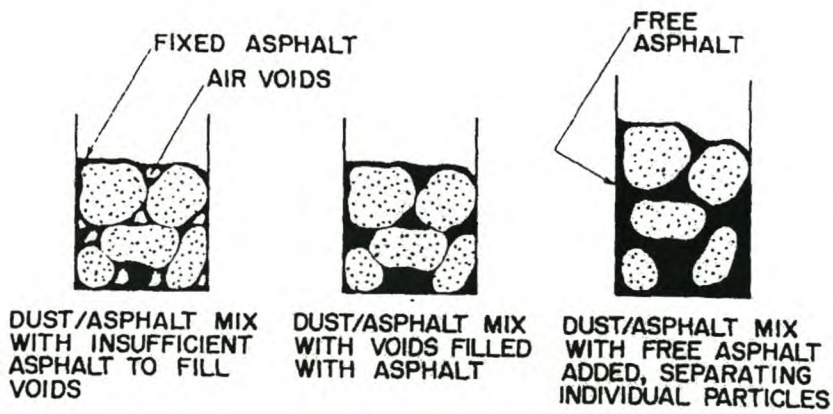

Figure 4 - 1. Concept of fixed and free binder for filler-bitumen interaction (Anderson, 1987)

The stiffening potential of the mastic has been shown by Anderson (1987), Khandal (1981) and Cooley et al (1998) to relate to the voids determined using the Rigden test. For a given filler/binder ratio, the higher the filler void percentage (and percent bulk volume of the filler), the lower the percentage free bitumen and the higher the stiffening effect of the mastic i.e. a greater change in the Ring and Ball softening point.

From the research on bitumen mastics, Anderson with his modified Rigden voids test, advocated that limiting the percentage bulk volume (bulk volume of filler including compacted voids/volume of filler + binder) to below 55% would yield stiffening ratios of less than 10 to 15. The stiffening ratio is the proportional increase in viscosity of mastic (with filler) relative to the original bitumen viscosity as measured with the Brookfield Viscometer. Similarly, Khandal suggested limiting the stiffening ratio to 11 and the increase in softening point to 11.5 °C. He showed a transition in mastic stiffening to occur at 60% bulk volume. From this, Cooley concluded that the percent bulk volume for HMA filler should be between 55 and 60%. In agreement with Khandal, Francken (OCW, 1947) uses an acceptable range of 12°C to 16°C change in softening point when the filler is added to the bitumen, for the design of asphalt mixtures. The change in softening point is, in turn, related to a filler-binder ratio. The relevance of these mix design mechanisms for HMA requires investigation for CMA.

The filler component in cold mixes, particularly that of foamed bitumen, is extremely important. During its metastable life, foamed bitumen is mixed with cold moist mineral aggregate which is being agitated in a mixer. The colloidal mass collapses very quickly during mixing, with the erupted bitumen providing globules at low viscosity that favour the particles with the highest surface-to-mass ratio i.e. the finest fraction. In this chapter the term "foamed mastic" has been used with reference to the mixture of foamed bitumen, filler and water.

The importance of the foamed mastic has been identified by researchers and for this reason, values for the filler/binder ratio of foamed bitumen stabilised mixes have been recommended. Ruckel *et al.* (1983) provide recommended binder contents for different filler fractions and mix types (sand or gravel), see Table 2 - 2. The filler/binder ratios suggested by Ruckel *et al.* range between 1:1 and 2.5:1 for gravel to 1.2:1 and 2.2:1 for sand. As with Superpave specifications for HMA (FHWA,1994) however, no account is taken of the different filler types, their gradations and voids.

In order to establish a level of reliability for the behaviour of foamed bitumen fillers, the stiffening of mastics with water and foamed bitumen requires investigation using a variety of fillers. In particular, the effect of the water phase is of interest, as this gives the foamed mastic a totally different volumetric composition.

Cooley (1998) established a composition and phase diagram of the filler mastic for combinations of filler and penetration grade bitumen. In this diagram Cooley introduces the concept of "Percent bulk volume" which is a measure of the ratio of filler volume (including voids) to the total volume of bitumen and filler (excluding voids). As the percent bulk

volume increases, so the bitumen in the mastic is located more in the filler voids thus reducing the volume of free bitumen. This is illustrated in the sketch on the left in Figure 4 - 1. The approach of Cooley has been extended to include the water phase in a foamed bitumen mastic, see Figure 4 - 2. For the purpose of calculation of the percent bulk volume, the water phase is not displaced from the voids in the filler, as the water is present in the filler before the foamed bitumen is added.

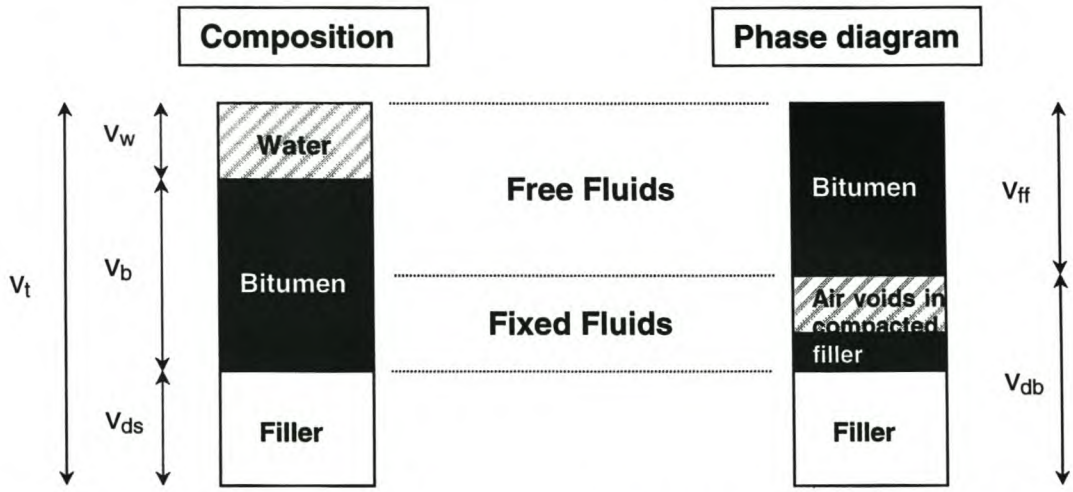

V_t = Total Volume
V_b = Volume of bitumen
V_{ds} = Volume of dust particles
V_{ff} = Volume of free fluids
V_{db} = Bulk volume of compacted dust

$\%V_{dv}$ = Perc. Voids in Compacted Dust
$= (V_{db}-V_{ds})/V_{db}$ x100
$\%V_{db}$ = Perc. Bulk Volume of Dust
$= V_{db}/(V_b+V_{ds})$ x 100
$\%V_{ff}$ = Perc. Free Fluids
$= (V_t-V_{db})/V_t$ x 100

Figure 4 - 2. Volumetrics of voids in filler/bitumen mastic for foamed bitumen
Note : V_w does not influence the value of V_{db}

2.1.2 Preparation of the foamed mastic and testing

A variety of fillers, representative of those typically used in cold mixes, have been selected for the testing programme. This included slightly plastic fillers sieved out from natural weathered gravel through to good quality crushed fillers. A 0,075mm sieve is the ceiling size for the filler fraction. The filler types are summarised in Table 4 - 1.

Table 4 - 1. Filler types for Foamed Mastic Analysis

Sample Name for Filler	Source
G1-Hornfels	Crushed Hornfels (fresh rock)
G2-Hornfels	Slightly weathered crushed Hornfels
Cyclone dust	Asphalt aggregate (Hornfels)
Calcrete	Weathered gravel Calcrete
Granite	Weathered gravel Granite
Ferricrete	Natural Ferricrete gravel

The test procedure of Anderson (1987) enables the voids in representative samples of filler to be established. This procedure utilises a mould with 12,5mm internal diameter and 100g drop-weight to compact the dust. The compacted voids in the filler may be calculated from the volumetrics of the sample. It is necessary to establish the specific gravity of the dust for the calculation of percent bulk volume. This is carried out by modifying Method B15 (CSIR, 1986) for the Apparent Relative Density test, using toluene instead of distilled water.

In order to determine a typical moisture content for the filler, at which all filler-mastics are at equivalent viscosities, the dust samples require testing by means of the "Bitumengetal" test (VBW,1992). This test determines the moisture content of dust at which an aluminium needle with a leading surface area of 50 mm^2, penetrates 50-70 dmm into the dust/water slurry i.e. it is a type of liquid limit measure for a given viscosity of the dust slurry. In the Netherlands, this test has been utilised to characterise the filler quality in addition to the Rigden voids test. The results of the "Percent Bulk Volume" and the "Bitumengetal" are given in Table 4 - 2.

Table 4 - 2. Properties of Fillers selected for Foam Mastic Manufacture

Filler Type (Parent rock)	G1 Hornfels	Cyclone Dust	G2 Hornfels	Calcrete	Granite	Ferri-crete
Voids V_{dv} (%)	43.6	44.3	41.3	49.0	46.7	44.3
Bitumengetal (% m/m)	36.5	37.6	39.2	34.2	54.4	38.2

The quality of the fillers can be adjudicated according to the limits specified in Table 4 - 3. It is evident from the results that the classification system is not consistent for both requirements. This difference can be reconciled through the observation that the voids and the surface area of mineral aggregate are not necessarily proportional, as they are dependent on different features of the spatial composition and gradation.

Table 4 - 3. Classification of Fillers (after VBW, 1992)

Filler Classification	Very Weak		Weak		Strong	
	Min	Max	Min	Max	Min	Max
Voids V_{dv} (%)	29	36	36	44	44	-
Bitumengetal	28	38	40	50	54	60

The "Bitumengetal" is a useful parameter for the preparation of fillers for foam testing. In order to have the filler fraction representative of that same fraction in a mix that is stabilised with foamed bitumen, the filler needs to be moist before foam is added to it in the laboratory. The "Bitumengetal" of that filler is not only a parameter for producing a filler-slurry of consistent viscosity for foam stabilisation, but also provides a typical moisture content for the filler fraction within a mix that is near optimum moisture content.

Example 4 – 1. Filler Moisture Content

A continuously graded mix with 7% < 0.075mm and a moisture content of 7.5% is to be treated with foamed bitumen. The moisture content of the filler alone needs to be identified for separate representative mastic to be manufactured. Utilising the particle surface area criteria of the Asphalt Institute (1993) as shown in Table 4 - 4 i.e. surface area factors for the relative aggregate fractions, and assuming a uniform film thickness of water for all particles, the moisture content of the filler fraction may be calculated. The proportional surface area and mass of filler to mix is utilised to this end.

Filler moisture content = (surface area of filler/surface area of aggregate) x moisture content x (100 / % passing of 0,075mm)
= (2,29/6,18)*7,5*(100/7) = 39.7%

This value approximates that of the "Bitumengetal" indicating that the latter could be used as a representative value for the moisture in the filler for continuously graded mineral aggregate close to optimum moisture content.

Table 4 - 4. Calculation of Surface Area for a Typical Continuously Graded Mix after (Asphalt Institute, 1993)

Sieve Size (mm)	% Passing	Surface Area Factor(m^2/kg)	Surface Area (m^2/kg)
37.5	100		
19	100		
9.5	72	0.41	0.41
4.75	53	0.41	0.2173
2.36	38	0.82	0.3116
1.18	27	1.64	0.4428
0.6	20	2.87	0.574
0.3	13.5	6.14	0.8289
0.15	9	12.29	1.1061
0.075	7	32.77	2.2939
		Total	**6.1846**

2.1.3 Characterisation of Foamed Bitumen/Filler Mastic by Change in Softening Point Temperature

Cooley *et al.*(1998) developed a unique relationship between the change in Softening Point Temperature and the Percentage Bulk Volume of the filler/bitumen in the HMA mastic. Equation 4 - 1 provides the change in Ring and Ball Softening Point (°C) relative to the Percent Bulk Volume, as defined by Cooley *et al.*

$$\Delta T_{r\&b} = 1.499e^{0.0418*(\%V_b)}$$ **Equation 4 - 1**

This relationship was further extended by Cooley *et al.* to other measures of the stiffening of the mastic relative to the Percentage Bulk Volume such as Stiffening Ratio and G*/Sin(δ) as defined in Superpave™ (FHWA,1994), all of which provide good correlation coefficients.

The Percentage Bulk Volume ($\%V_{db}$) for foamed bitumen mastic, as defined in Figure 4 - 2, is considered applicable as the primary factor influencing the stiffening of foamed mix mastics too. For this reason a standard test procedure has been established for Ring and Ball testing on foamed bitumen-filler mastics. This procedure, which has been followed throughout, is detailed in Appendix B.

Firstly, the influence of bitumen type should be accounted for. In the overall factorial design, the influence of bitumen has been investigated as a partial factorial, including two grades of bitumen i.e. 80/100 and 150/200 and three types of filler viz. G1-Hornfels, Ferricrete and Granite filler. The G1-Hornfels filler results are presented in Figure 4 - 3 as these provided the highest degree of repeatability. At least one repeat test has been performed for each data point with additional tests where the repeatability guidelines (see Appendix B) have not been complied with.

With allowance for a nominal amount of variability, Figure 4 - 3 illustrates that use of a parameter such as the change in softening point is self-normalising. Every bitumen has its own softening point (without any filler) and if this value is used as a benchmark, the increase in stiffness through addition of the filler, measured through change in softening point temperature, is a unique function. In addition, providing that two different types of bitumen have similar ageing characteristics, curing at moderate temperatures e.g. 40°C will not have a differential influence on the stiffening of the foamed mastics for the two bitumen types. The curing effects of foamed mixes are addressed in more detail elsewhere in this chapter.

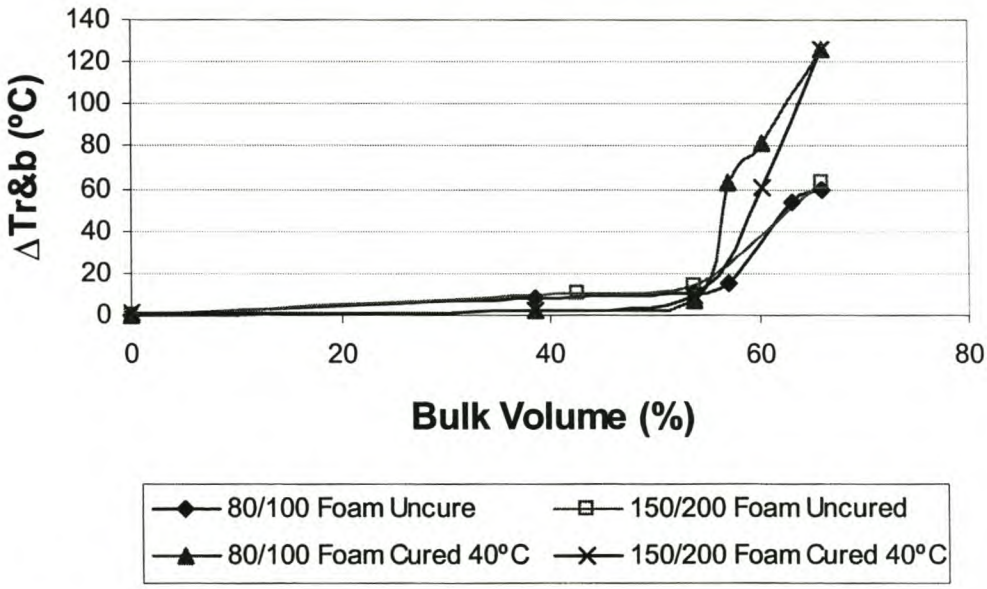

Figure 4 - 3. Change in Softening Point for Crushed Hornfels Filler/Foamed Bitumen Mastic relative to Compacted Bulk Volume for two Bitumen Grades

Investigation into the mastics produced by foamed bitumen and the full range of different filler types commenced with 150/200 penetration-grade bitumen. Figure 4 - 4 provides the relationship between the Percentage Bulk Volume ($\%V_{db}$) and the change in Softening Point Temperature for a composite plot of all six filler types listed in Table 4 - 1. Further to the findings of Cooley *et al.* the $\%V_{db}$ is once again shown to be a unique factor in the measurement of the stiffening of the mastic in the mix; in this case for a foamed mastic mix.

The feature of particular importance in Figure 4 - 4 is the $\%V_{db}$ value at which significant stiffening occurs. Compared with HMA mastic, foamed bitumen mastic stiffens at a lower $\%V_{db}$ value and it stiffens more rapidly, even though the equation for bulk volume includes only the bitumen and filler in both cases (ignoring the water). The addition of the water phase to the filler, which increases the total fluids content does not soften the mastic but rather stiffens it. This phenomenon has profound implications for the behaviour and performance of foamed mixes. In addition to the fact that the foamed mastic stiffens at lower binder contents, literature indicates that foamed bitumen mixes are generally manufactured at lower binder contents i.e. where the filler:binder ratio (m/m) > 0.9 see Table 2 - 2. This translates to bulk volume values V_{db} > 50% indicating that the mixes will have very stiff mastic and can be expected to provide remarkable resistance to permanent deformation.

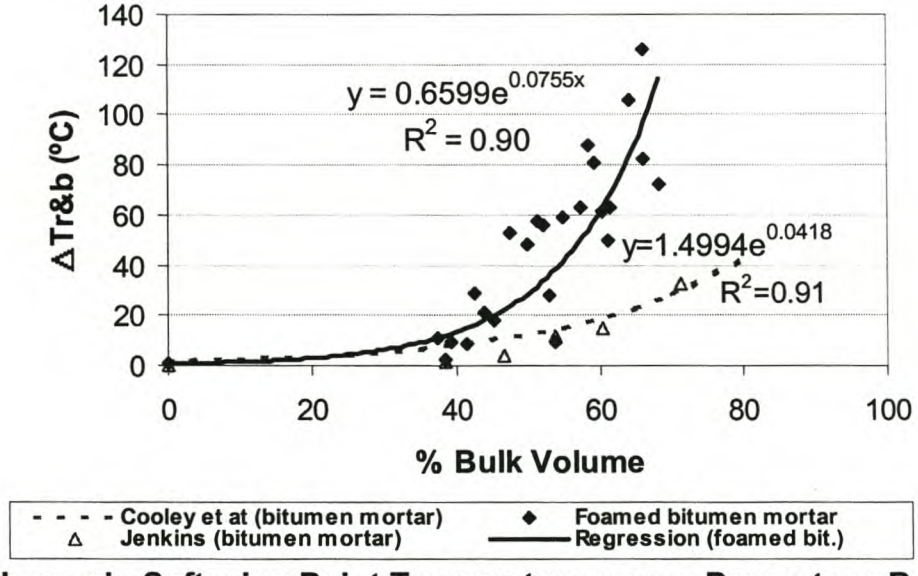

Figure 4 - 4. Change in Softening Point Temperature versus Percentage Bulk Volume of Compacted Filler for Six Filler Types with Foamed 150/200 Bitumen cured at 40°C.

Considering that the relationship expressed in Figure 4 - 3 is unique, the data plotted in Figure 4 - 4 may be extended to include other bitumen types i.e. different grades and source refineries, to yield a composite generalised equation. The additional data is plotted in Figure 4 - 5 relative to Cooley *et al.*'s relationship for HMA mastic. It is apparent that the relationship between mastic stiffening and the $\%V_{db}$ value of the filler for foamed mastic provides similar correlation as for HMA mastic. With acceptable variability, the relationship can model a variety of fillers and binders for foamed mixes.

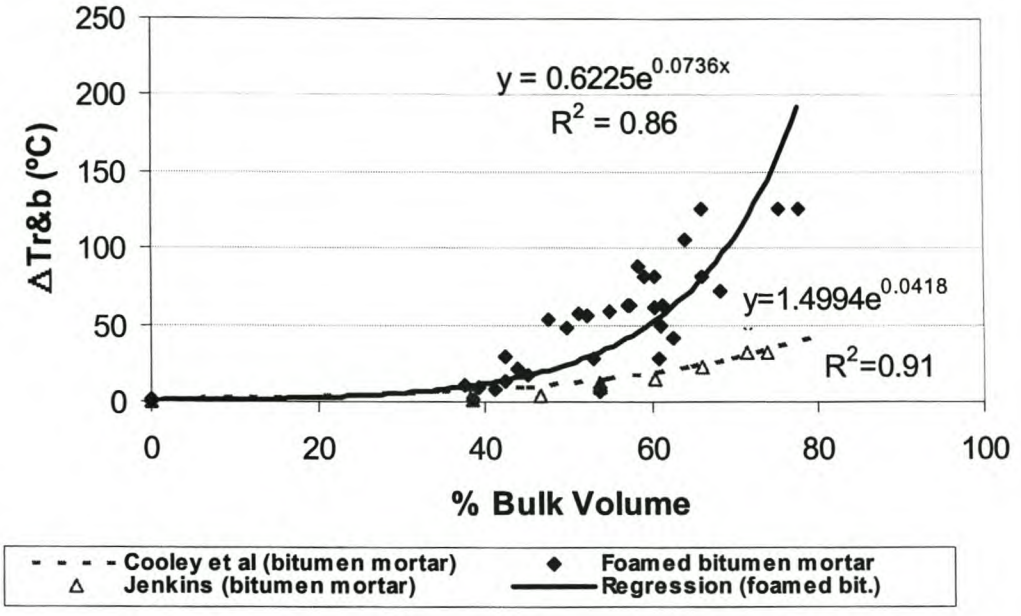

Figure 4 - 5. Change in Softening Point versus Percent Bulk Volume for a Variety of Filler Types and Foamed Bitumen Types, Cured at 40°C

The generalised Equation 4 - 2 for foamed bitumen mastics, which has a correlation coefficient R^2=0.859, has slightly poorer correlation than Cooley's work. This is probably due to the more variables such as the water phase and curing technique, as well as possible compression of the mastic during insertion into the softening point rings.

$$\Delta T_{r\&b} = 0.6225e^{0.0736x(\%Vdb)} \qquad \textbf{Equation 4 - 2}$$

The proposed limit of 60% > V_{db} > 55% for HMA is inapplicable to foamed bitumen mastics. If the same stiffening is required for HMA and foamed mastics, then the bulk volume should be limited to V_{db} < 50% for a preferable foamed mastic to be created. This, however, translates to a filler/binder ratio K= f/b of between 0.85 and 1 (m/m) for different filler types. Foamed mixes with 8% filler (< 0.075mm) for example, would require at least 8% bitumen to produce this desired ratio, which is both impractical and does not comply with the guidelines of Table 2 – 2.

The role of the moisture in the filler is an integral part of the stiffening of the foamed mastic. This becomes apparent when a comparison is made between fillers that have been treated with foamed bitumen in dry and moist conditions. Figure 4 - 6 illustrates that, without the moisture in the filler before treatment with foamed bitumen, foamed mastic behaves in a very similar manner to HMA mastic. The process of foaming the bitumen is not in itself the cause for the behavioural change of the mastic, but rather the moisture content during mixing. The foam is however necessary to enable dispersion of the binder throughout the filler. In this analysis, "wet filler" is used to describe the filler from a mix at optimum moisture content. This moisture is not to be confused with the foamant moisture (2% to 4% by mass of the bitumen), most of which evaporates during mixing.

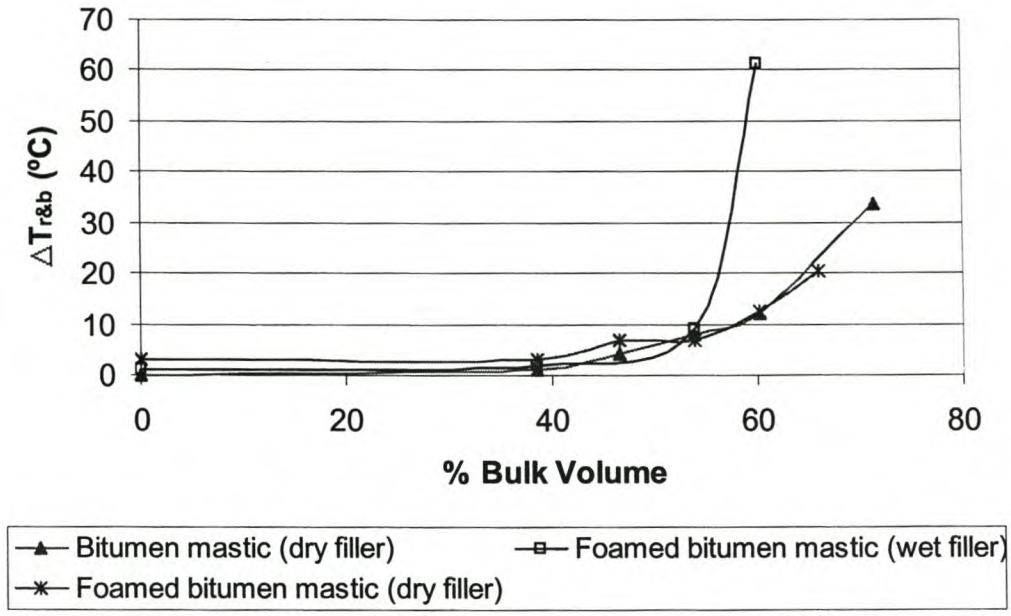

Figure 4 - 6. Influence of Moisture on Change in Softening Point of Foamed Mastic

The mastic of emulsion mixes can also be modelled in terms of stiffness using the Ring and Ball Test. Following precisely the same procedure used for the foamed mastics (including the Bitumengetal moisture content), a comparison may be made between the two different types of cold mix mastics. In the case of the emulsion, the residual binder i.e. 60% of the emulsion mass, is utilised in the $\%V_{db}$ calculation. The results plotted in Figure 4 - 7 show quicker initial stiffening of the emulsion mastic, even compared with foamed mastic, but relatively constant mastic stiffness for Bulk Volumes above 40%. It would appear that the $\%V_{db}$ is a unique property in expressing the stiffening effect of the emulsion mastic from the data obtained, but that further investigation is required. In particular, the influence of moulding moisture content and lower filler contents ($0\% < V_{db} < 20\%$) would need attention. This is not, however, a focus area of this dissertation.

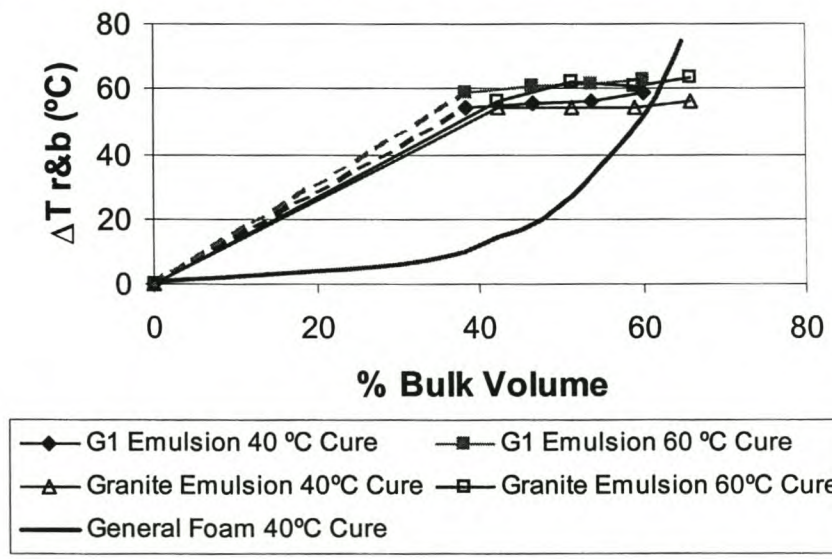

Figure 4 - 7. Stiffening effect of Mastic for Stable Grade 60 Anionic Emulsion with Two Filler Types relative to Equivalent Foamed Mastic

2.1.4 *Structure of foamed bitumen mastic*

The cause of the stiffening of the foamed bitumen mastic has not been documented in the past. The water in foamed bitumen mixes has an enigmatic effect of transforming these mixtures into pavement materials that can be stockpiled, placed and compacted at a later stage at ambient temperatures. The investigation of foamed mastics in isolation assists in clarifying the mechanisms that promote these characteristics.

During the manufacture of the foamed mastics very little of the moisture in the filler (present before mixing) is lost whilst mixing with foamed bitumen. Monitoring of the mass of the foam-stabilised mastic allows the moisture loss in the filler to be related to:

- mixing and aeration of the filler, which causes approximately 1% loss, and
- the mastic temperature exceeding that which overcomes the latent heat of steam, which causes approximately 13% loss of the original mass of moisture in the filler, see Figure 4 - 8.

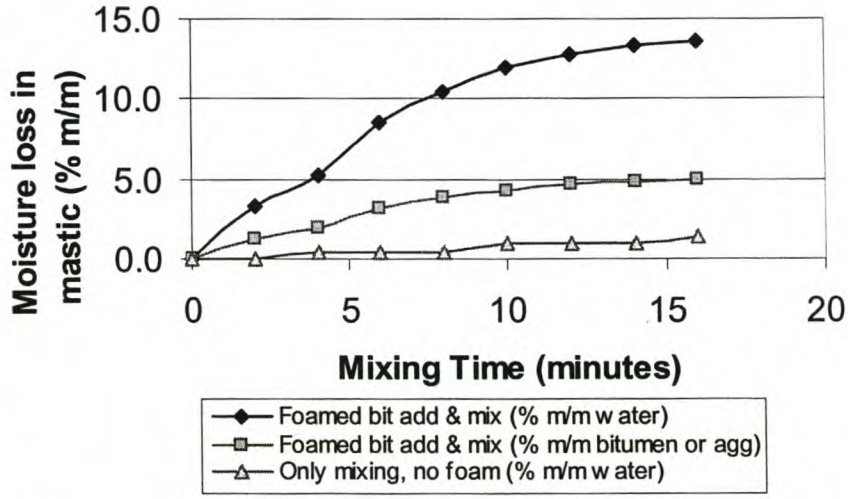

Figure 4 - 8. Moisture loss from Filler at 27°C during Mixing with Foamed Bitumen with K = f/b = 1 (m/m)

Cognisance also needs to be taken of additional losses of moisture from the mastic during curing and ageing. These losses are peculiar to the laboratory treatment process as part of the simulation of on-site and in-service effects. Unsealed curing entails the addition of the foamed mastic to the rings of the Softening Point test apparatus and placement on a tray in a draft oven for the duration indicated in Figure 4 - 9, see also Appendix B. The figure also shows the simulation of ageing that is carried out in the same manner in an oven at a raised temperature, in this case 163°C (in accordance with procedures outlined in Section 5). The sensitivity of the moisture loss to the filler:binder ratio is notable and requires consideration in the behaviour of foamed mastic.

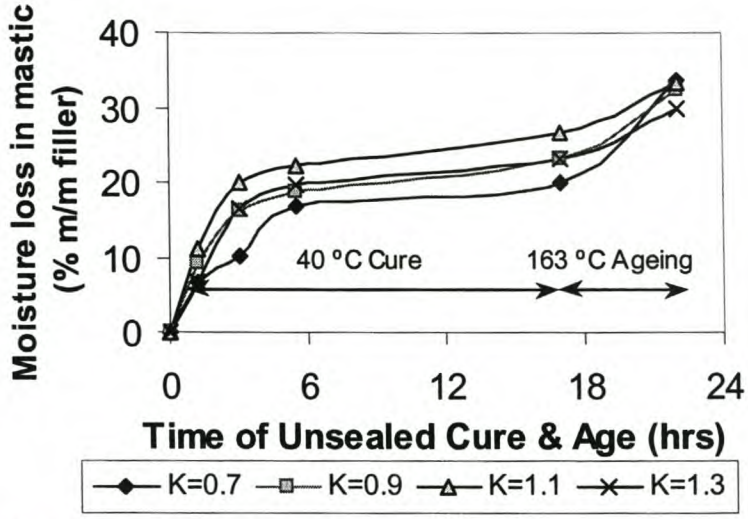

Figure 4 - 9. Moisture Loss from Foamed Bitumen Mastic with Unsealed Curing and Ageing for Different Filler:Binder (K) Ratios for a Mix at OMC

The change in the moisture regime of a laboratory manufactured foam mastic cannot be directly extrapolated to an entire foamed mixture, as the filler fraction is only a small component of the mix and receives a higher relative energy contribution from the foam when treated separately. The trend does however provide an indication of fraction of moisture that is readily available for extraction from the mastic and the fraction that requires more heat.

The remainder of the water within the mastic after foamed bitumen is applied and mixed, is not evident to the naked eye. However, upon compression of the foamed mastic, free water becomes evident at the surface, which is reabsorbed when the pressure is released. The structure of the foamed mastic, including the dispersion of the binder throughout the filler cannot be identical to HMA mastic, to enable this to occur. Electron microscopy provides a useful tool for the observation of the mastic structure.

Samples of foamed mastic for investigation under the electron microscope require vacuum drying, freezing in liquid nitrogen and prizing open to view the mastic structure. Comparison of the selected scans, reveal the pertinent findings of the differences in mastic structure between the HMA and foamed bitumen mastics. The HMA mastic in Plate 4 - 1 is a continuum of bitumen embedded with filler particles (with a few striations resulting from smear of the sample). The foamed bitumen mastic in Plate 4 - 2 comprises larger filler particles (>30μm) encapsulated with bitumen, inter-connected by threads of bitumen. It is apparent that the clay sized filler particles (< 2μm) locate themselves in the bitumen film over the larger particles as well as the threads. The voids in the mastic are significantly higher for foamed mixes than HMA, where they are virtually non-existent for HMA mastic with free bitumen. The voids in the foamed mastic between the threads of bitumen observed through microscopy, see Plate 4 - 3, would normally be filled with water, had this not been vacuum extracted. In fact, the water provides the medium for distribution of the foamed bitumen in this "thread and knot" or dog-bone configuration during mixing.

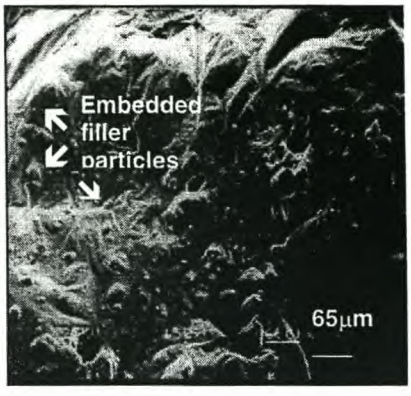

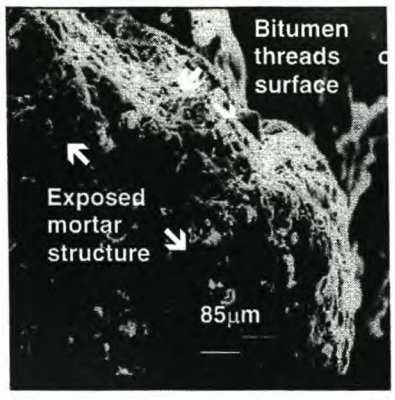

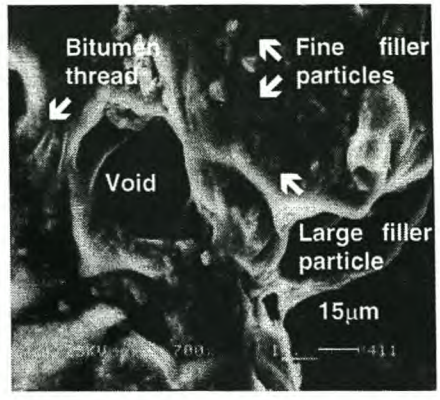

Plate 4 - 1. Conventional HMA bitumen mastic (150xmagnification) with filler dust embedded in continuum of bitumen	Plate 4 - 2. Foamed bitumen mastic (115xmagnification) with threadlike fabric of bitumen needles on sample surface	Plate 4 - 3. Foamed bitumen mastic (700xmagnification) with threads of bitumen mastic between larger particles & voids between

The implications of this structure of the foamed mastic are far-reaching in terms of both behavioural and performance characteristics of cold mixes. Some of these factors include:

- The water held within the foamed bitumen mastic assists in explaining the shelf-life characteristics of foamed mixes. Water provides the lubrication for compaction at ambient temperatures and can be released during consolidation under compaction.
- Drying out of a foam mix in stockpile i.e. prior to compaction, exposes the high surface area of bitumen "threads and knots" to oxidation, which is likely to make the mix more susceptible to ageing. This is explored further in this chapter.
- The displacement of moisture from the filler mastic that will occur during compaction, which is an irreversible process, explains the loss in shelf-life of foamed mixes after compaction. Provided that a foamed mix is kept in stockpile without significant compaction or drying out, moisture will be retained in the mastic and workability will be sustained. Compaction not only displaces moisture, but also forces more contact between bitumen particles and mineral aggregate particles.
- Curing of a foam mix after compaction is important in order to further displace water and establish an improved moisture-regime within the mix. However, the hydrophobic nature of bitumen assists in relatively rapid strength gain for foamed mixes as opposed to emulsion mixes, which have surfactants present.
- The high surface area of bitumen in the foamed mastic structure creates a high surface energy and flow can occur in the mastic once that energy is exceeded through external forces. This goes to explain the shift in stiffness from HMA mastics to foamed mastics observed in Figure 4 - 5. Due to the continuum of bitumen in the HMA mastic, the surface area of the bitumen is notably less as is the appurtenant surface free energy.

- The trend of increasing surface free energy in foamed mixes has also been noted indirectly through other research. Figure 2 – 8 provides a Master-curve of Complex Modulus for foamed mix relative to the equivalent HMA. The higher complex modulus of the foamed mix (GM in the figure) at lower frequencies (and probably higher temperatures too) is most likely primarily due to the stiffening effect of the foam mastic. The stiffer foamed mastic provides more constant complex modulus, regardless of the loading frequency. In addition, the lower phase angle of the foamed mix, illustrated in the Black Diagram in Figure 2 – 9, shows the viscous component of the mix to be relatively constant and significantly smaller than for HMA. This indicates a more constant behaviour of foamed mix due to its structure of binder dispersion throughout the aggregate, a phenomenon that would be caused by bitumen dispersed in small droplets rather than a continuum.
- The disadvantage of the dispersed structure of bitumen is, however, its potential increase in ageing susceptibility.
- The distribution of the foamed bitumen in a mix will depend on a variety of factors including moisture content of the mix, bitumen content, aggregate temperature, filler characteristics, foam characteristics and mixing techniques. These factors therefore, will each have an indirect bearing on the behaviour and performance of the mix.

The aforementioned influences of the foamed mastic structure require consideration in the mix design and manufacture of foam mixes. For this reason, some of the relevant factors are further investigated in this chapter.

2.2 Sand Fraction in Spatial Composition

The relevance of the procedure used by Ruckel *et al.* (1983) to split aggregate into the fine and coarse fractions i.e. divided at 4,75mm, for laboratory mixing with foamed bitumen, becomes apparent when considering the binder dispersion in such a mix. Ruckel *et al.* also state that the bitumen specks should be less than 1,6mm in diameter in cured foam mix. This provides a qualitative indication that substantial particle coating does not extend beyond the sand fraction in foamed mixes. It is the natural selection of the filler and sand fraction by the foamed bitumen that renders these fractions especially important in the spatial composition of the entire mix.

Dispersion of the binder in the mix and aggregate coating are two of the critical issues that are peculiar to foamed bitumen mixes. The mortar, which is the all-important matrix that harbours the bitumen exclusively, warrants separate investigation. This mortar includes:

- the sand fraction i.e. particles that pass through a 2,36mm sieve and are retained on a 0,075mm sieve,
- the filler fraction < 0,075mm,
- the foamed bitumen binder, and
- moulding moisture in the mineral aggregate.

The spatial composition of the foamed mortar is considered in more detail in this section. This compositional analysis includes the dispersion of the foamed binder in the sand fraction as well as packing considerations and volumetrics for sand and filler. Particle coating and the appurtenant factors are investigated in more detail in Chapter 5.

2.2.1 Dispersion of Foamed Bitumen in the Sand Fraction

During the application of hot foamed bitumen to cold, moist, mineral aggregate that is being agitated, the foam's meta-stable life is curtailed. As described in Chapter 3, the bitumen bubbles collapse leaving a structure of binder that is dispersed throughout the aggregate. This dispersion is dependent on a number of factors, including amongst others:

- *Foamed bitumen characteristics*: The viscosity (Expansion Ratio) and stability (Half-life) of the foamed bitumen influence the manner in which the binder is distributed in the mix,
- *Composition of Sand and Mortar Fractions*: Due to the foam bitumen's affinity for the finer mineral aggregate particles, the binder has a greater concentration in the fine aggregate fraction of the mix. Gap-graded foam mixes can experience balling where the bitumen does not bond with or coat the larger particles at all.
- *Mixing technique*: A variety of mixing techniques exist for the manufacture of foamed mixes, including twin-shaft pugmills, in situ recyclers and free-fall mixers, each of which has a different mixing energy and duration. Considering the short life of the foamed bitumen, measurable in seconds, the type of mixer directly influences the characteristics of the mix.
- *Aggregate moisture content before mixing*: Literature has shown that the moisture in the mix is the medium for the distribution of the foamed binder, see Section 2.4.2 of Chapter 2.
- *Aggregate temperature*: The temperature of the aggregate before mixing has an overwhelming influence on the equilibrium mix temperature. The transfer of heat from the foam at just over 100°C to the aggregate at less than 30°C will influence the rate of collapse of the foam i.e. the rate of viscosity increase of the binder during mixing. This is explored further in Section 4 of this chapter for cold mixes and Chapter 5 for half-warm foamed mixes (above ambient temperature).

This section aims to address the former two factors i.e. foamed characteristics and composition of the sand fraction.

The identification of the structure of the dispersed binder in terms of droplet size using, for example, sieve analysis is not possible once mixing has taken place for practical reasons. And yet, mixing itself is an intrinsic operation necessary for the creation of unique binder dispersion. Physical observation using a stereomicroscope provides an appropriate solution.

Inspection of foamed mixes under a microscope, both the complete mixture as well as finer fractions on their own, enables the distribution of the binder in the mineral aggregate to be

observed more efficiently. Where thin threads have been drawn from a bitumen droplet during the mixing process, these are ignored in the size measurement process. A summary of typical bitumen droplet sizes obtained in the mixes, is provided in Table 4 - 5.

Table 4 - 5. Typical Distribution of Bitumen Droplet Sizes from Foam Dispersed using Laboratory Mixing in Mineral Aggregate at 25°C with Differing Expansion Ratios and Foam Indices, from Microscopic Analysis

Droplet Diameter (mm)	Percentage Passing given Droplet Size	
	Acceptable Foam (ER=15 and FI=239)	Sub-standard Foam (ER<5 and FI=20)
2,36	100	100
1,18	100	90
0,6	95	80
0,3	80	25
0,15	30	5
0,075	5	<1

A distinct shift in droplet sizes occurs for different quality foamed bitumen. These droplet sizes will have a bearing on behavioural characteristics of a foamed mix, in terms of surface free energy, tensile strength, ageing and other properties. Figure 4 - 10 provides a graphical representation of the bitumen droplet sizes, illustrating the distinct difference between foam with a typical expansion ratio of 15, and sub-standard foam (ER_m<5).

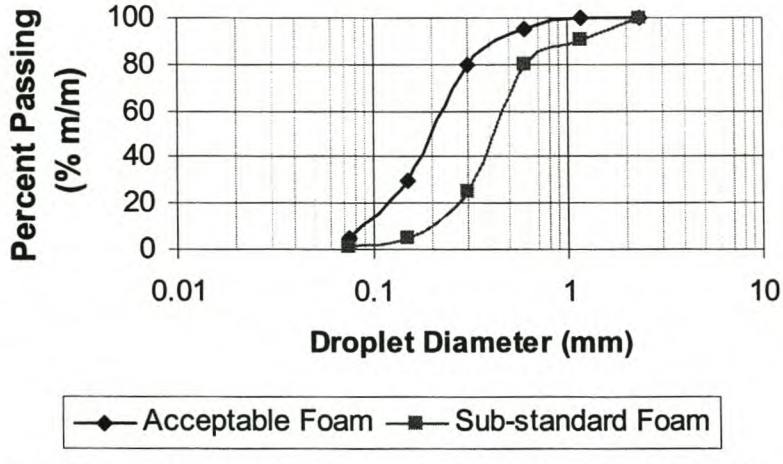

Figure 4 - 10. Typical Distribution of Bitumen Droplet Sizes for a Mixture with Different Quality Foam, Mixed in the Laboratory (see Table 4 – 4)

It is notable from Figure 4 - 10 that the bitumen spots of 1,6mm diameter that Ruckel *et al.* (1983) identified as the critical maximum droplet size in a foamed mix through observations with the naked eye, forms the upper end of the scale of droplet sizes. Distinction between the acceptable from the sub-standard foam is more accurately observed through a droplet size distribution below this diameter.

The Asphalt Institute (1993) procedure for the calculation of the surface area of aggregate particles, see Table 4 - 4, can be extended to an application with bitumen droplets. Utilising this procedure and the gradation of foamed bitumen droplets provided in Table 4 - 5, the surface area of the binder of a foamed mix can be estimated. This calculation yields 14,60 m^2/kg for the acceptable quality foam and 6,91 m^2/kg for the sub-standard foam. Utilising the value for surface free energy provided by Lubbers (1985) of 33 erg/cm^2 for bitumen at 25ºC, an increase in energy of 4,82 x 10^6 erg/kg or 0,482 Joule/kg of binder has been added to the good quality foamed mix.

The change in potential energy of the mix through the introduction of bitumen droplets is not the relevant factor influencing foamed mix behaviour, but rather the surface area that will require increase through extension under loading. Bahia *et al.* (1998) showed that, based on computer simulations and finite element analysis, and dependent on the aggregate gradation, that the bitumen binder can be subjected to strain levels 10 times higher than the bulk strain to which the mixture is subject. As a result of this, large strain testing is recommended for accurate assessment of the role of binders in mixture performance. The extent of the strains in the binder is particularly relevant to foamed mixes with droplets of significantly higher surface area.

In order to estimate the influence of variations in surface area of the bitumen droplets, a typical mix can be considered. A continuously graded asphalt mixture with 4% air voids graded between 2,36mm and 0,15mm will have a binder surface area of approximately 0,11 m^2/kg of mix whereas the equivalent foamed mix will have approximately 1,50 m^2/kg (m/m of mix) of exposed bitumen surface. This order of magnitude difference in the surface areas of the two different mix types will contribute significantly to the surface free energy required to extend the binders during strain under loading. This phenomenon will influence the potential for ageing of the foamed mix and will also have a bearing on the phase angle for foamed mix compared with HMA. The Black Diagram in Figure 2 – 9 shows that such shifts in phase angle are prevalent in foamed mixes.

2.2.2 *Packing of the Sand Fraction and its Optimisation*

Various methods exist for the optimisation of the packing of mineral aggregate. Following the pioneering work of Fuller and Thomson (1907) on gradation for maximum density, Furnas (1928) developed a model for the prediction of voids in binary systems which forms the basis for current software programmes such as PRADO (Francken and Vanelstraete, 1993) to predict the Voids in Mineral Aggregate (VMA).

Nijboer (1943) utilised a log-log gradation chart with a straight line of slope 0,45 defining the percentage passing versus sieve size, to achieve minimum VMA. Nijboer's work was extended by Duriez (1950) and Goode and Lufsey (1962) to develop a generalised equation for the maximum density gradation, see Equation 4 - 3 and Equation 4 - 4.

$$P = 100\left(\frac{S}{M}\right)^{0.45} \qquad \textbf{Equation 4 - 3}$$

$$\log B = 2 - 0.45 \log M$$ **Equation 4 - 4**

where:

P = percentage passing the particular sieve;
S = size of sieve opening for the particular sieve in microns;
M = maximum size of aggregate in microns; and
B = intercept on percentage passing axis at 1 micron (log 0) on the sieve-opening axis.

Cooper *et al.* (1985) showed through research that the maximum deformation resistance for asphalt base layers requires the minimum VMA, which is achieved when 30 to 40% of aggregate in a specific gradation passes through the 0,6mm sieve, see Figure 4 - 11.

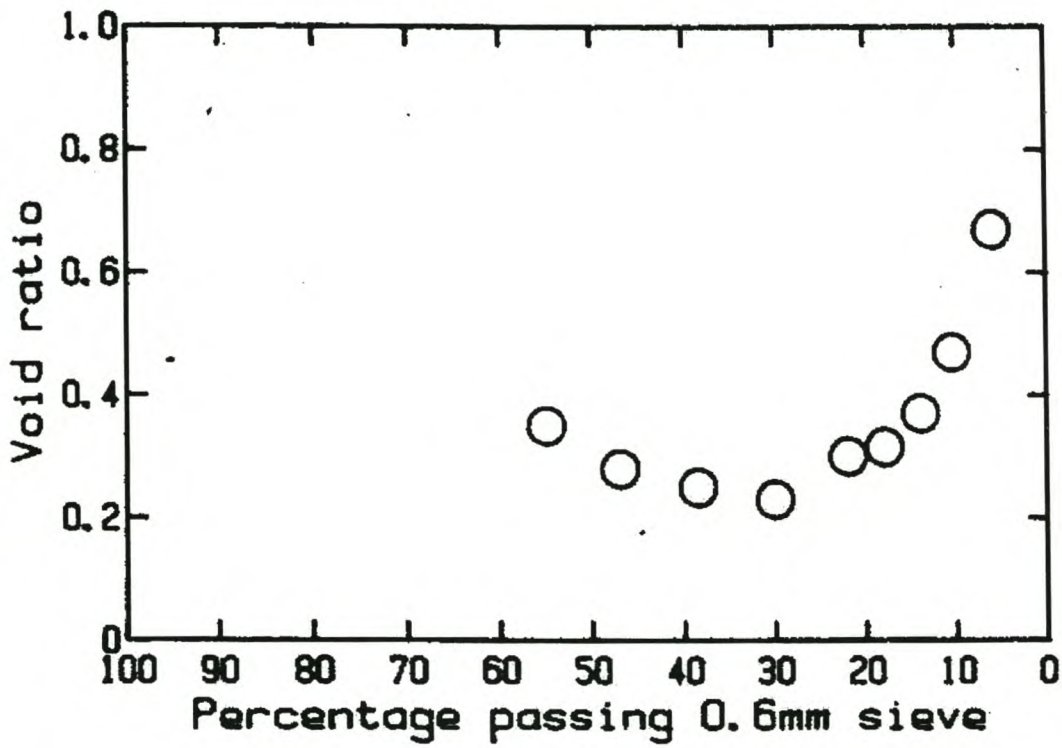

Figure 4 - 11. Variation in Void Ratio with Percentage Passing 0,6mm Sieve for Different Mixes (Cooper *et al.*, 1985)

In addition, Cooper *et al.* (1991) developed a unique gradation relationship for minimum VMA with an allowance for variation of filler content, see Equation 4 - 5. It is apparent that this relationship is based on the work of Nijboer. The Cooper relationship is useful as it provides flexibility with the filler content of a mixture, which is not possible with Equation 4 - 3.

$$P = \frac{(100 - F)(d^n - 0.075^n)}{(D^n - 0.075^n)} + F$$ **Equation 4 - 5**

where:

P = percentage by mass passing a sieve of size d (mm)
D = maximum aggregate size (mm)
F = percentage filler content
n = variable dependent on aggregate packing characteristics

Further to Furnas' work, Hudson and Davis (1965) also developed a binary system for the calculation of the void ratio from aggregate gradation. This arithmetic method for calculating VMA uses sequential combination of aggregates for sieves with a size ratio of 2. Hudson and Davis found a ratio of 1,37 between adjacent sieve sizes to provide the lowest VMA. This technique may be used to compare the VMAs for gradations obtained from the various models, see Table 4 - 6. In the table an exponent of 0,45 is used for Nijboer and Cooper *et al.* whilst 0,5 is used for Fuller. The ratio of 1,37 from Hudson and Davies does not provide the lowest VMA for an equivalent maximum size gradation. In addition, the grading requirement for the 0,6mm sieve suggested by Cooper *et al.* is not verified in the gradations obtained.

Table 4 - 6. Gradations for Minimum VMA using different Models, with VMA calculated using Hudson and Davies (1965)

Sieve Size	Percentage Passing (%)							
(mm)	Nijboer	Fuller	Cooper et al			Hudson & Davies		
0.075	8.29	6.28	5	6.28	9	5	6.28	9
0.15	11.32	8.89	8.14	9.38	12.01	6.85	8.60	12.33
0.3	15.46	12.57	12.43	13.61	16.12	9.38	11.79	16.89
0.6	21.12	17.77	18.30	19.40	21.74	12.86	16.15	23.14
1.18	28.64	24.92	26.08	27.07	29.19	17.61	22.12	31.70
2.36	39.12	35.24	36.94	37.79	39.59	24.13	30.31	43.44
4.75	53.59	50.00	51.93	52.57	53.95	33.06	41.52	59.51
9.5	73.20	70.71	72.24	72.62	73.41	45.29	56.89	81.52
19	100.00	100.00	100.00	100.00	100.00	62.05	77.93	100.00
38						85.01	100.00	
76						100.00		
VMA =	**22.76**	**22.96**	**23.29**	**22.87**	**22.74**	**22.77**	**22.77**	**23.04**

In hot-mix asphalt design there has been a movement away from minimum VMA due to a trend of decrease in optimum binder content as compaction energy increases, see Figure 4 - 12. This results in the instability of some densely graded HMA mixtures during traffic compaction. Superpave (FHWA, 1994) introduced the restricted zone to curb, amongst other things, the instability of bases in the longer term. Although this may hold true for HMA, it is not necessarily applicable to foamed mixes. The voids created by moisture migration during curing ensures that cold foamed mixes with continuous gradations having low VMAs will not be overfilled with binder and thus remain stable.

In addition, due to the size of the foamed bitumen droplets, their dispersion in the mix causing substantial coating, is restricted to the sand fraction and smaller. For this reason, gap-graded mixes and stone skeleton–type mixes do not successfully combine with foamed bitumen. For acceptable binder dispersion, sand- or filler-skeleton gradations are necessary.

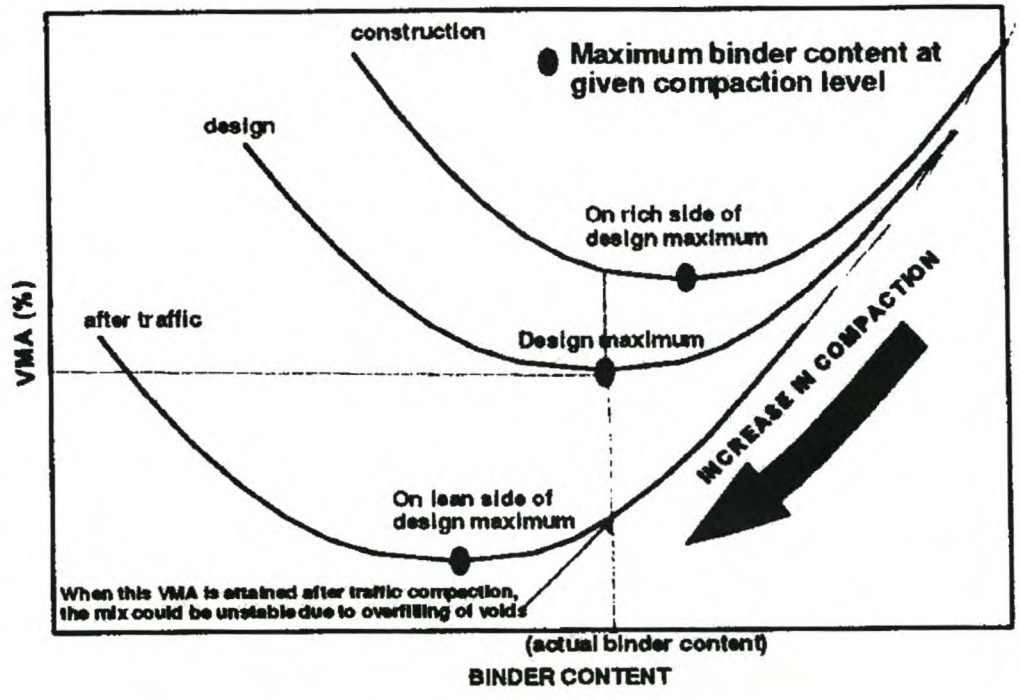

Figure 4 - 12. Influence of Compaction Energy on Optimum Binder Content (Verhaeghe *et al.*, 1995)

Although the vast majority of foamed mixes are produced using in situ or marginal materials, in many cases scope exits for improvements to the gradations and hence the volumetric composition. Optimisation of gradation can be achieved through the blending of different material types. To this end, some of the blending methods outlined in this section may be used in determining which combination of blends provides the most suitable spatial composition. However, verification of their applicability is necessary first.

The PRADO software developed by the Belgian Road Research Centre (Francken and Vanelstraete, 1993) for the formulation of the composition of dense bituminous mixes with less than 10% air voids, makes provision for the blending of different aggregates including sand fractions. The fundamental principle employed in the programme algorithm is the division of a mix into three basic constituents i.e. stones, sand and filler. The algorithm utilises a similar methodology to that of Furnas (1928) for the prediction of voids in binary

mixes. The PRADO model uses the relationship between the concentration of coarse particle components and the ratio of particle sizes to obtain the specific voids in the fine and coarse fractions, see Figure 4 - 13. The specific voids of a binary mix i.e. the ratio between the volume of the voids and that of the solids, lie in a triangle AMC, in which A and C provide the specific voids of the original components.

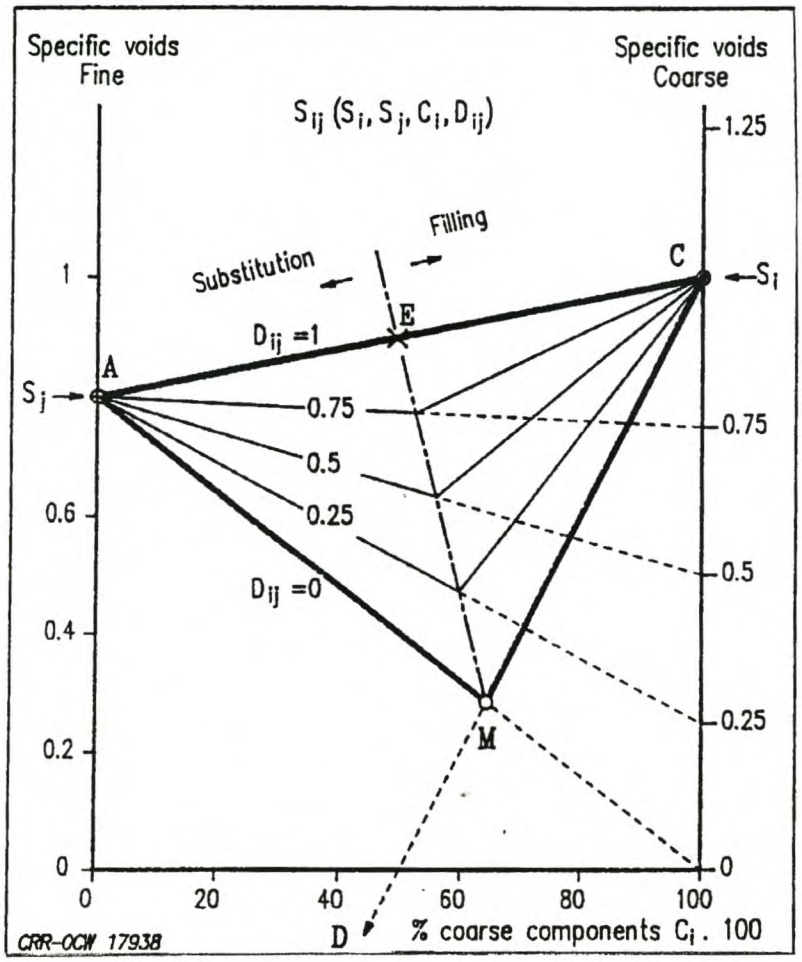

Figure 4 - 13. Example of Specific Voids of a Binary Mix of Aggregates (Francken *et al.*, 1993)

The lines in Figure 4 - 13 define two antagonistic mechanisms governing the packing of two aggregate fractions viz.

- *Substitution,* which is the replacement of space occupied by the coarse fraction due to an increase in the concentration of the fine fraction i.e. the coarse aggregate voids are overfilled with fine aggregate, and
- *Filling,* which is an increase in occupation of the voids of the coarse aggregate by the fine fraction, as the latter increases in concentration.

The mechanisms of substitution and filling are depicted graphically in Figure 4 - 14 and Figure 4 - 15. These mechanisms are paramount to foamed bitumen mixtures where the binder does not coat the larger particles, and the principles can be extended from binary mixes to entire gradations. In order to enable sufficient binder dispersion throughout a mix, the fraction that "carries" the bitumen droplets needs to provide a continuous phase in the granular structure of the mix skeleton.

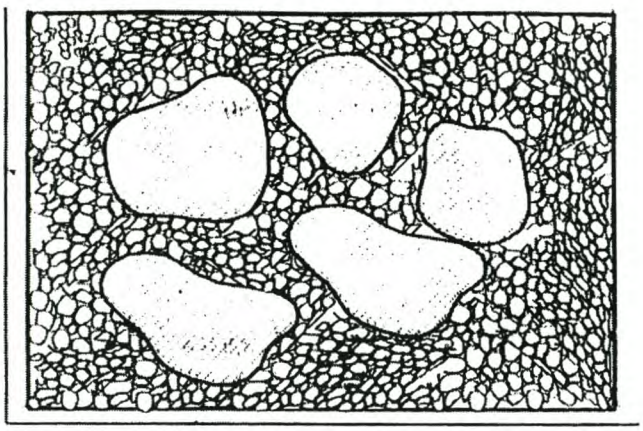

Figure 4 - 14. Substitution mechanism in a Binary Packing System

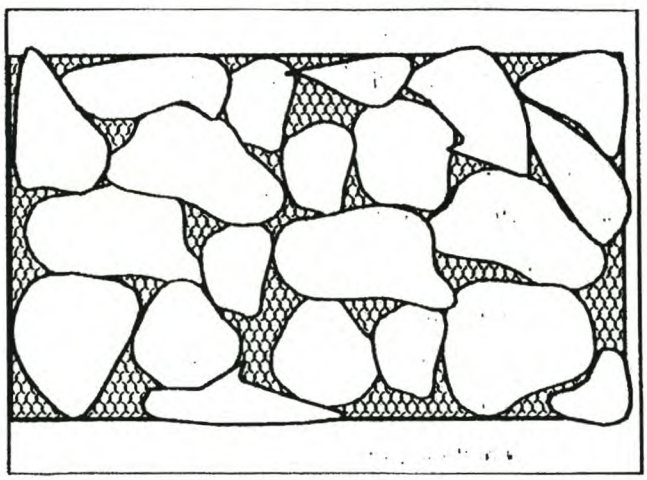

Figure 4 - 15. Filling mechanism in a Binary Packing System

The systematic combination of a series of binary mixes to describe the voids in the entire gradation, as employed by PRADO requires specific voids for each of the particle fractions. These voids have been analysed for typical European aggregates with both rounded and angular shapes, but have not been verified for South African aggregate types. Initial analysis of voids using a loose volume for the coarse aggregate and an Engelsmann Stampvolumeter ® for the sand fraction has been carried out. The use of the Engelsmann apparatus follows the procedures recommended by Goos *et al.* (1996), using 200g of sample, a stamper and 50 000 blows, however. A brief outline of this procedure is provided in Appendix B.

The analysis of typical mineral aggregate (Hornfels) used for asphalt manufacture has been carried out and is reported in Table 4 - 7. The voids in the stone fraction of the Hornfels show some agreement with PRADO's voids, but the sand fraction differs significantly. The number of blows used in the Engelsmann apparatus greatly exceeds the 4 000 blows recommended by Verbert (1979) to equate it to compaction of 50 blows per side for an asphalt mix by a Marshall hammer. This partially explains the shift in results, however considerably more verification testing is required to establish confidence limits for the correlation. This testing forms part of a separate study and does not fall under the auspices of this dissertation.

Table 4 - 7. Comparison of Voids in Individual Aggregate Fractions for a Crushed Hornfels and European Angular Aggregates in PRADO

Measured		PRADO (angular)	
Sieve Size (mm)	Voids (%)	Sieve Size (mm)	Voids (%)
<0.075	Rigden voids	< 0.0625	Rigden Voids
0.075< <0.15	47.3	0.0625< < 0.125	50
0.15< <0.3	47.5	0.125< <0.25	49
0.3< <0.6	46.2	0.25< <0.5	48
0.6< <1.18	49.7	0.5< <1	51
1.18< <2.36	49.6	1< <2	51
2.36< <4.75	50	2< <4	50
4.75< <9.5	51.7	4< < 8	50
9.5< <19	50.4	8< <16	52

As a sensitivity analysis the PRADO programme has been utilised together with the Hudson and Davis (1965) method for a combination of fine gravel material and natural aeolian sand. The results of the two models are compared with the actual VMAs obtained from tests on the material blends using the Engelsmann apparatus, see Example 4 - 2.

Example 4 – 2. Blends of Sand and Gravel for a Foamed Mix.

A wind-blown sand was blended with a fine-grained natural quartzitic gravel in different proportions to provide the most suitable blend for a foamed mix. The gradations of the two materials are given in Figure 4 - 16.

The two components are blended in different proportions and the VMA of the composite mineral-aggregate passing through the 2,36mm sieve is determined using three procedures. The number of blows of the Engelsmann apparatus was 10 000 with the inclusion of the stamper weight.

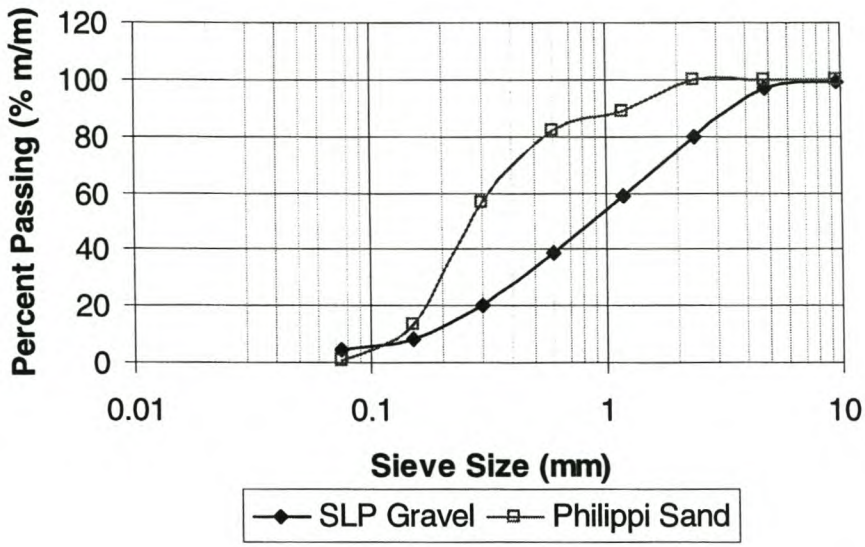

Figure 4 - 16. Gradations for two Materials (Sir Lowry's Pass SLP Gravel and Philippi Sand) to be Blended for a Foamed Mix

Although PRADO and the Engelsmann test yield similar minimum VMA points, significant variability is noted in the individual VMA data points, even when several repeat tests are carried out. This is a relevant finding considering that identical mixes have been analysed through the two calculation procedures and the measurement procedure with the Engelsmann apparatus.

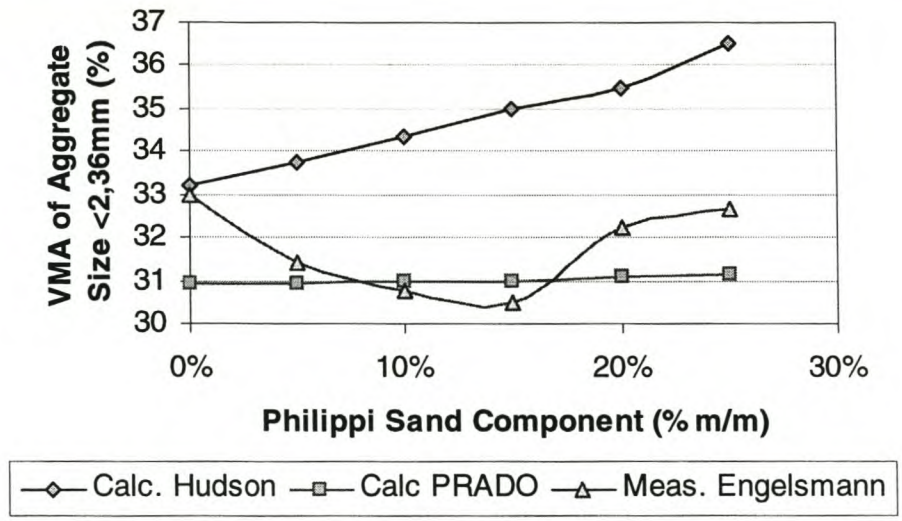

Figure 4 - 17. Voids in Mineral Aggregate for Blends of SLP Gravel and Philippi Sand determined using Different Methods

Current models such as PRADO are not yet suitably calibrated for the determination of absolute volumetric mix characteristics. However, an initial indication of optimum blend ratios can be obtained using PRADO. The use of the Engelsmann device remains a useful tool for determining the VMA for a sand and filler fraction and optimising blends.

The significance of minimum VMA in the sand fraction is apparent when the influence of the spatial composition of this fraction on the mechanical properties of the mix are considered. Blending of the mineral aggregates in a 100:0 and 90:10 ratio of SLP Gravel and Philippi sand and mixing with emulsion and foamed bitumen binders provides a comparison of the effect of the change in VMA on the tensile strength of the mix. In this case the tensile strength has been measured using the Indirect Tensile Strength (ITS) test. This comprises monotonic splitting of a 100mm diameter specimen at 25°C in the Indirect Tensile mode at a constant deformation rate of 50,4 mm/minute. Although the tensile strength derived from the ITS is not absolute for a given material, it provides a comparative measure for different mixes.

In the application of the cold mixes using this mineral aggregate, refer Chapter 6, both foamed bitumen binder and bitumen emulsion binder was utilised. It is evident from Figure 4 - 18 that the tensile strength of a foamed mixture is significantly more dependent on the VMA in the sand fraction than the emulsion mixture (both mixtures treated with medium term cure) . This highlights the importance of correct gradation of the sand fraction within the entire gradation of mineral aggregate that is treated with foamed bitumen.

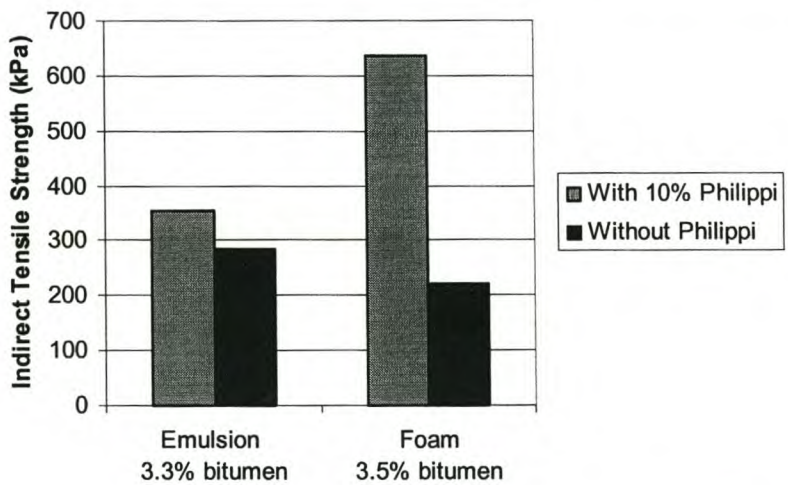

Figure 4 - 18. Indirect Tensile Strength for Fine Gravel with High VMA_{sand} (no Philippi Sand) and Low VMA_{sand} (10% Philippi Sand) when Stabilised with Emulsion or Foamed Bitumen

The dispersion of the binder within the sand fraction and other fractions of mineral aggregate is illustrated through the series of sketches provided in Figure 4 - 19. During the mixing process, the bitumen droplets coat the filler particles, then the fine particles, making agglomerations of loosely packed mortar that adheres to the larger particles.

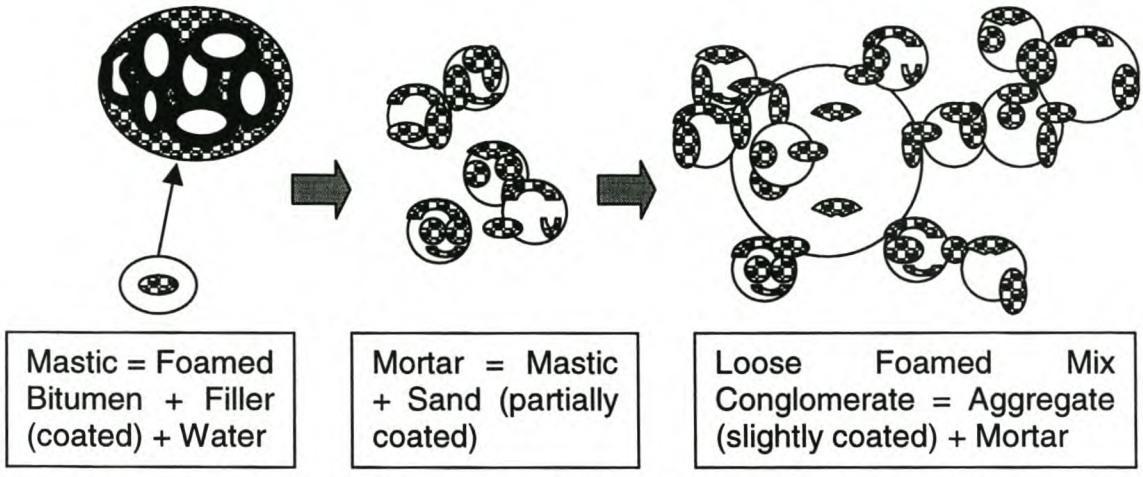

Figure 4 - 19. Dispersion of Foamed Bitumen through Aggregate during Mixing from Microscopic Observations

It is apparent from these illustrations, which are based on observations using a microscope, that adhesion of the bitumen to the aggregate is incomplete after mixing and will be influenced significantly by the compaction of the mix. The sand fraction plays an important role in distributing the mastic throughout the mix before compaction. For the compaction to effectively compress the bitumen or mastic droplets between sand grains and encourage further adhesion between grain and binder or adhesion between mastic droplets, the voids in the grain sizes need to be overfilled with mastic. Ridgeway and Tarbuck (1968) and Fedors and Landel (1979) independently state that the maximum size (or diameter) ratio of spheres that can be accommodated in the interstitial void of a particular fraction that is cubically packed, is approximately 0,4. If a gap in the sand fraction gradation exists that creates voids large enough to be under-filled by mastic, the binder adhesion to particles during mixing will not be improved through mechanical compaction forces and the mix will be more susceptible to moisture, amongst other factors. This phenomenon of compaction assisted binder dispersion and adhesion for continuously graded sands is illustrated in Figure 4 - 20.

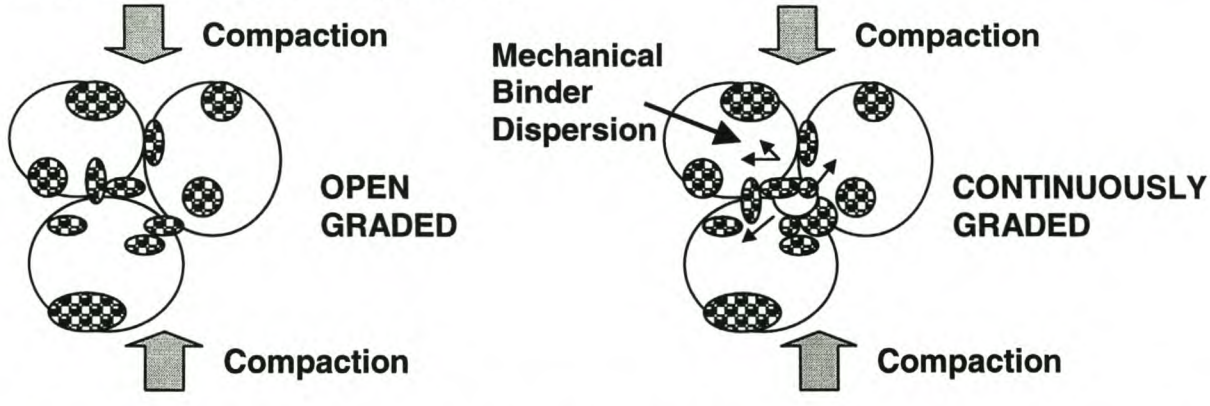

Figure 4 - 20. Compaction of Open or Gap Graded Sand versus Continuously Graded Sand for Foamed Bitumen Mixes

For a gap in the sand fraction to exist, not only does the size ratio criteria need to be satisfied, but according to Lees (1970) the ratio of particle numbers to be accommodated. The critical ratio of occupation criteria (or size ratio) cannot be considered in isolation as the number of particles per void requires consideration. According to Lees, counts of particles for two different mixes with minimum VMA have shown that 4 to 10 times as many smaller granules are present than larger particles. Statistically, it requires at least four times as many particles of the smaller size to provide sufficient probability for "all" the voids to receive a minimum of one occupant particle, due to the fact that some voids will remain empty whilst others will be overfilled with smaller particles.

Using the work of Lees (1970) in conjunction with a simple model that allows for the ratio of the number of particles to be calculated, the suitability of a sand fraction in terms of gradation, for treatment with foamed bitumen can be assessed. The mathematical model uses spherical particle shapes to obtain the ratio of number of particles of two different sizes. Based on volumetrics, a relationship of $(r_1/r_2)^3$ is used to define the ratio of the number of particles. In this way, potentially under-filled voids in sand fraction can be identified using a volumetric grading curve for the mineral aggregate.

Where the mass of large particles retained on a specific sieve is 15,6 times greater than the mass of particles retained on a sieve 0,4 times the size, under-filled voids are likely. Where the mass of large particles retained on a specific sieve is one quarter of this ratio i.e. approximately 4 or less times greater than the mass of particles retained on a sieve 0,4 times the size, a significantly high probability exists that all voids will be filled.

The procedure is outlined below:

1. Obtain a volumetric gradation curve for the mineral aggregate to be treated with foamed bitumen i.e. a gradation by mass converted using the specific gravity of the different fractions.
2. Combine this gradation, with the gradation of foamed bitumen given in Figure 4 - 10 to obtain a composite mix grading by volume, using the expected binder content and the specific gravity of the binder and aggregate.
3. Identify any point(s) of inflection (concave) in the sand fraction of the composite gradation curve and approximate the entry and exit curves to each point using linear gradations.
4. Determine the particle size 2,5 times and 0,4 times the inflection point particle size and check whether a linear approximation of gradation is applicable between the inflection point and these points.
5. Determine the corresponding percentages passing these sieve sizes i.e. $P_{2,5x}$,P_x and $P_{0,4x}$
6. Calculate the ratio of gradients of the two gradation lines and check that this value is less than 4 for suitability, see Equation 4 - 6. If this parameter is not satisfied, the gradation should be adjusted through supplementation or alternative means to tend towards the minimum VMA gradation, see Table 4 - 6.

$$\text{Gradient ratio} = (P_{2,5x} - P_x)/(P_x - P_{0,4x}) < 4 \qquad \textbf{Equation 4 - 6}$$

For foamed bitumen treated aggregates, which are substantially reliant on mechanical forces for binder adhesion and the generation of effective tensile bonds, this gradation check is not only applicable to the sand fraction but also to the entire mix.

Example 4 – 3. Analysis of Suitability of Gradation of a Sand for Foamed Bitumen Treatment

The sand fraction of a Dolerite gravel, with Specific Gravity = 2,65 is considered for use in a foamed mix. Its suitability is analysed in terms of gradation using 4% foamed bitumen as the binder content and the above procedure. Figure 4 - 21 provides a graphical solution of the composite gradation with a volumetric combination of aggregate and bitumen droplets. Using Equation 4 - 6, the ratio of gradients can be calculated as:

Gradient ratio = (29-11)/(11-7) = 4.5 which is greater than 4.0 . This indicates that the ratio of slopes of the two linear portions of the gradations exceeds 4.0 and requires adjustment.

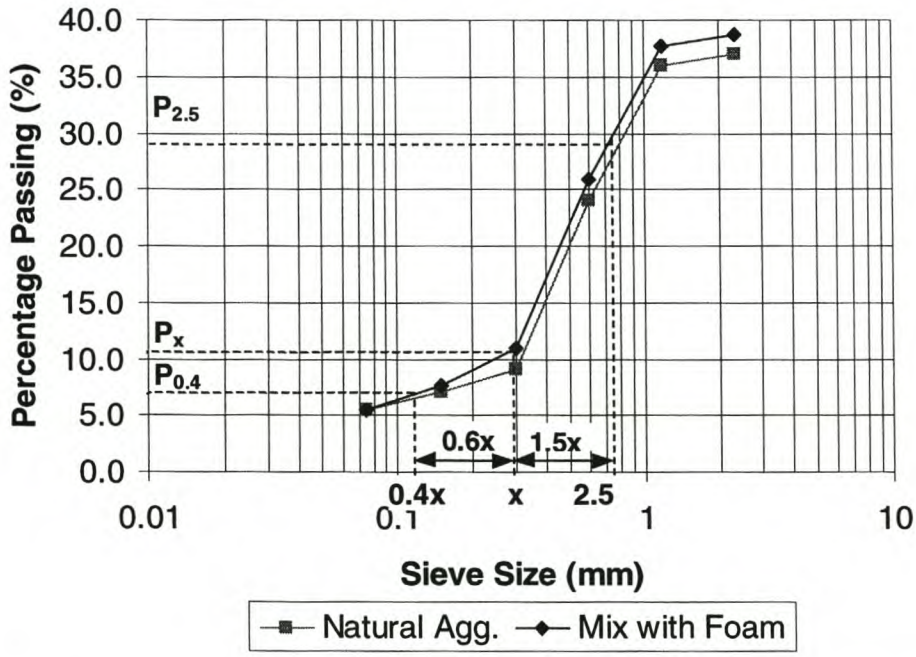

Figure 4 - 21. Gradation of Sand Portion of Dolerite Gravel, before and after addition of 4% Foamed Bitumen

The benefits of improvement in foamed mix properties can be assessed using simple mechanical tests. Utilisation of a blend of 10% of fine aeolian sand with the Dolerite gravel lifts the inflection point to provide a gradient ratio close to 1 and overfilling of the voids in the sand fraction. The inclusion of the sand in the foamed mix of 4,4% binder content (150/200 Pen bitumen) influences the mechanical properties, as outlined in Table 4 - 8. These results are given for laboratory prepared mixes that were compacted using the standard Marshall procedure and 75 blows per side of the specimen. Although these

mechanical properties may not be linked directly to performance, they provide a comparative measure of the influence of gradation on the behaviour of a foamed mix.

Table 4 - 8. Influence of Gradation Correction on Mechanical Properties of a Foamed Mix

TEST TYPE	Dolerite Gravel (with under-filled voids in sand)	Dolerite gravel with 10% aeolian sand (overfilled voids)
Dry Marshall Stability (kN)	9.1	20.4
Wet Marshall Stability (kN)	5.6	14.2
Resilient Modulus (MPa)	607	2862

Note :

- Dry Marshall Stability Tests carried out 50,4 mm/sec displacement rate and 25°C for specimens cured at 60°C for 3 days.
- Wet Marshall Stability carried out after under the same conditions as Dry Stability, after pre-treatment underwater at 25°C in a vacuum of 35mm of Hg for 1 hour and soaked for an additional hour, surface dried and tested.
- Resilient Modulus Tests carried out at 25°C in the Indirect Tensile mode at 10 Hz.

2.3 Composition of Entire Skeletal Structure

The dispersion of foamed binder in the mineral aggregate is influenced significantly by the filler fraction and the fine sand fraction. The composition and proportions of these two fractions have been shown to significantly influence characteristics of a foamed bitumen mix. This does not allow for the coarse aggregate or indeed the entire skeletal structure of mineral aggregate to be ignored.

Behavioural tendencies of foamed mixes in terms of resilient response to loading, particularly at binder contents lower than 3,5% closely resemble granular material behaviour. This trend, which is explored further in Chapter 7, is influenced by the entire skeletal structure and in particular, the coarse aggregate fraction, and account should be taken of this.

Akeroyd and Hicks (1988) have shown the importance of the gradation of the entire aggregate structure, see Figure 2 – 2. But this is insufficient to provide comprehensive guidelines for aggregate selection for foamed mixtures. Observation of different gradations that have been mixed with foamed bitumen shows that, as the coarse aggregate content increases, a point is reached where segregation of the binder dispersion occurs. This segregation, which is evident even at low binder contents, exhibits a tendency of the binder to resist adherence to the coarse aggregate, leaving only the fine aggregate enriched by bitumen with a distinct divide between the two fractions. This phenomenon may be explained mechanically i.e. mixes with insufficient "carrier fraction" (sand + filler) for the foamed bitumen droplets will result in agglomerations of binder in lumps of mortar in a dispersed phase. This mortar will partially fill the voids in the coarse aggregate fraction in stone skeleton mixes.

The phenomenon of segregation of binder dispersion, as well as the considerations of the sand and filler fractions that have been discussed previously in this chapter, can be summarised in the Francken and Vanelstraete (1993) "magic triangle". Figure 4 - 22 gives a ranking of suitability levels of different aggregate structures in terms of the combination of coarse aggregate, sand and filler fractions. In this case the 2,36mm and 0,075mm sieves are used to define the boundaries between the aggregate sizes.

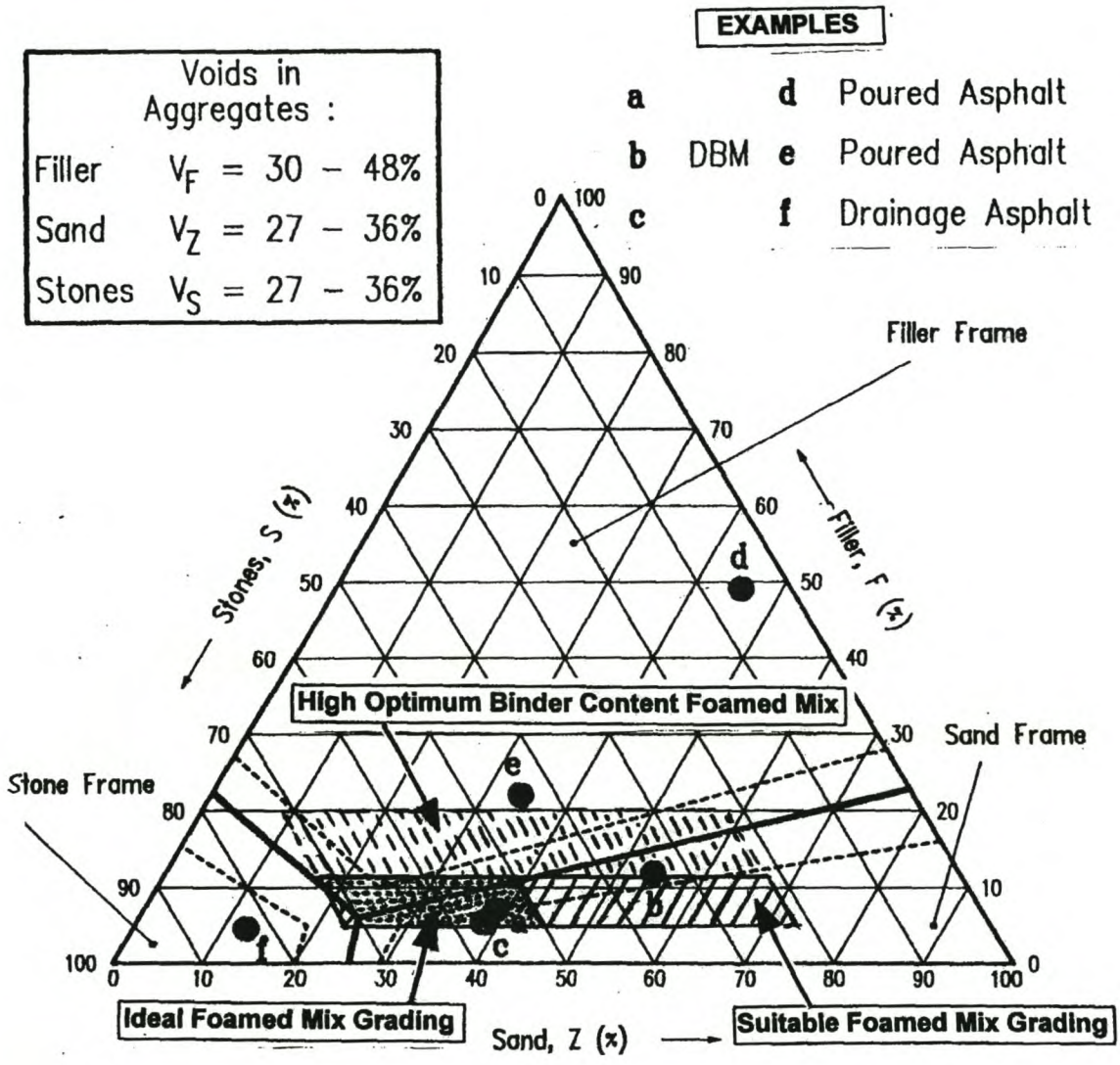

Figure 4 - 22. Suitability of Aggregate Gradations for Treatment with Foamed Bitumen, utilising the "Magic Triangle"

2.4 Moisture and Mixing Technique

2.4.1 Function of Moisture during different Phases of Foamed Mix Application

The moisture in a foamed bitumen mixture performs a multi-functional role, as outlined in Section 2.4.2 of Chapter 2. The functions of the moisture include:

- *Separation and suspension* of the fine particles to allow channels through which the foamed bitumen droplets can pass to access the particles during mixing.
- *Carrier*: to transport and disperse the bitumen droplets during mixing.
- *Lubricant*: to provide workability of the foamed mix at ambient temperatures.
- *Compaction aid*: to reduce the angle of internal friction during compaction of the foamed mix.

The influence of the moisture in the aggregate before stabilisation with foamed bitumen is highlighted when filler, in a variety of moisture conditions, is treated with bitumen. This has been illustrated in Figure 4 - 6 where little disparity is noticed between dry filler that has been treated with foamed bitumen and conventional bitumen. Differences in the behaviour of the mastic become apparent when moisture is introduced to the mastic. These differences can be expected to influence the overall behaviour of the foamed mixture.

The function of the water in the aggregate may also be viewed in terms of absorption and adsorption processes during the application of the foamed bitumen. Van der Walt *et al.* (1999) postulate that the binder adheres to the surface of the aggregate during mixing, whilst at an elevated temperature and is "sucked" into the pores of the aggregate during curing. This is claimed to apply to water-saturated bitumen, which is produced in a similar process to foamed bitumen. The conjectured penetration of water saturated bitumen into the pores of the aggregate is used as an explanation of the bond of the bitumen to the cold, damp aggregate.

The moisture content of the mineral aggregate to be treated with foamed bitumen requires optimisation at the different stages of application of the mixture. These optimum points are not acquiescent and different optimum values require consideration, as detailed below:

- *Mixing moisture content:* The "fluff point" moisture content (Bowering, 1970) has been shown to be ideal for providing optimum mixing. This is the moisture content at which the maximum bulk volume of loose mineral aggregate is obtained.
- *Workability moisture content:* The fluff point moisture content has also been shown to provide adequate workability for foamed bitumen mixes. Marginal moisture loss after mixing does not adversely affect the workability of the mix.
- *Compaction moisture content:* The moisture content that, in combination with the foamed bitumen binder, yields the optimum fluids content for the achievement of maximum dry density for the specific compaction method.
- *Field moisture content:* During the curing process of a foamed mix, excess moisture egresses from the mix during and after compaction. The field moisture content

influences the performance of a foamed mix under traffic. According to Shackel *et al* (1974) the lower the degree of saturation (Sr) of the foamed mix, the greater the resistance to permanent deformation.

The different moisture contents required at the given stages of foamed mix production and construction, underline the importance of moisture considerations during the manufacture of such mixes under laboratory conditions. In order to both simulate field characteristics and optimise the properties of the mix, moisture contents require monitoring and control in the laboratory. Each of the stages mentioned above requires optimisation for a representative mix to be produced and specimens to be manufactured for laboratory testing. Although this does not pose a problem for the first three phases, simulation of the field moisture content is a challenging aspect of mix design. Curing of laboratory specimens, which removes excess moisture after compaction and readjusts the distribution of the moisture within the material, can be utilised to replicate field moisture contents and binder condition after a certain period under traffic. This aspect is discussed further in Section 3 of Chapter 4.

In terms of compaction of foamed mixes, utilisation of the optimum moisture content determined from dry density considerations (with Modified AASHTO or Modified Proctor compaction) can be used as a guideline for the optimum fluids content. This is more accurate for some aggregates than for others, as seen in Table 4 - 9. It is also apparent that the shift between Optimum Moisture Content (OMC) and Optimum Fluids Content (OFC) is not consistently in one direction. The total fluid content concept (SABITA, 1993), which considers bitumen in cold mix to act as in a manner similar to the moisture in terms of particle lubrication for compaction, is not entirely applicable to foamed mixes therefore. Cognisance of this behaviour is required for mix design purposes.

Table 4 - 9. Optimum Water and Fluids Contents for Various Aggregates

Material Type	OMC from Mod. AASHTO (%)	Maximum Dry Density (kg/m^3)	Binder Content (%)	OFC from Mod.AASHTO (%)	Foamed-mix Dry Density (kg/m^3)
Cont.graded crushed Hornfels	6,7	2258	2	6,0	2271
Cont. graded crushed Quartzite	7,0	2181	2	5,5	2207
Crushed Brick & Concrete (22:78)	12,0	1853	2	12,9	1850
Sandy Gravel	7,0	2030	3,5	7,5	2103
Sandy Gravel	7,0	2030	4,5	8,5	2099
Ferricrete Gravel	8,0	2165	3,2	7,5	2181
Cinder Gravel	19,3	1568	1,5	19,3*	1518
Cinder Gravel	19,3	1568	3,25	19,3*	1557
Cinder Gravel	19,3	1568	4,5	19,3*	1584

Note: * signifies a selected value rather than optimized value

The determination of a desired fluid regime for compaction is further complicated by influences of the method of compaction. The mixed granulate (crushed concrete and brick)

included in Table 4 - 9 was further analysed in a gyratory compactor at 10.5%, 12.5% and 14.5% fluids content. A range of only 3 kg/m^3 in the dry density after 75 gyrations was obtained for the three different fluid contents, indicating a less defined OFC for this material when gyratory compaction is adopted. This is considered to represent field compaction more accurately and is therefore the preferred method of laboratory compaction for foamed mixes.

In order to consider the fluids regime throughout the foamed-mix production process, a flow chart of activities should be followed under laboratory conditions, see Figure 4 - 23. In this way, different interactions between a specific mineral aggregate and the foamed bitumen can be taken into account during the mix design process. The procedure makes use of the approach of Humberto Castedo Franco and Wood (1983) to treat the foamed bitumen as a lubricant in the mix during mixing and compaction, thus reducing the amount of moisture required. The fluids content (FC) is therefore the sum of moisture content (MC) and bitumen content (BC) or FC=MC+BC.

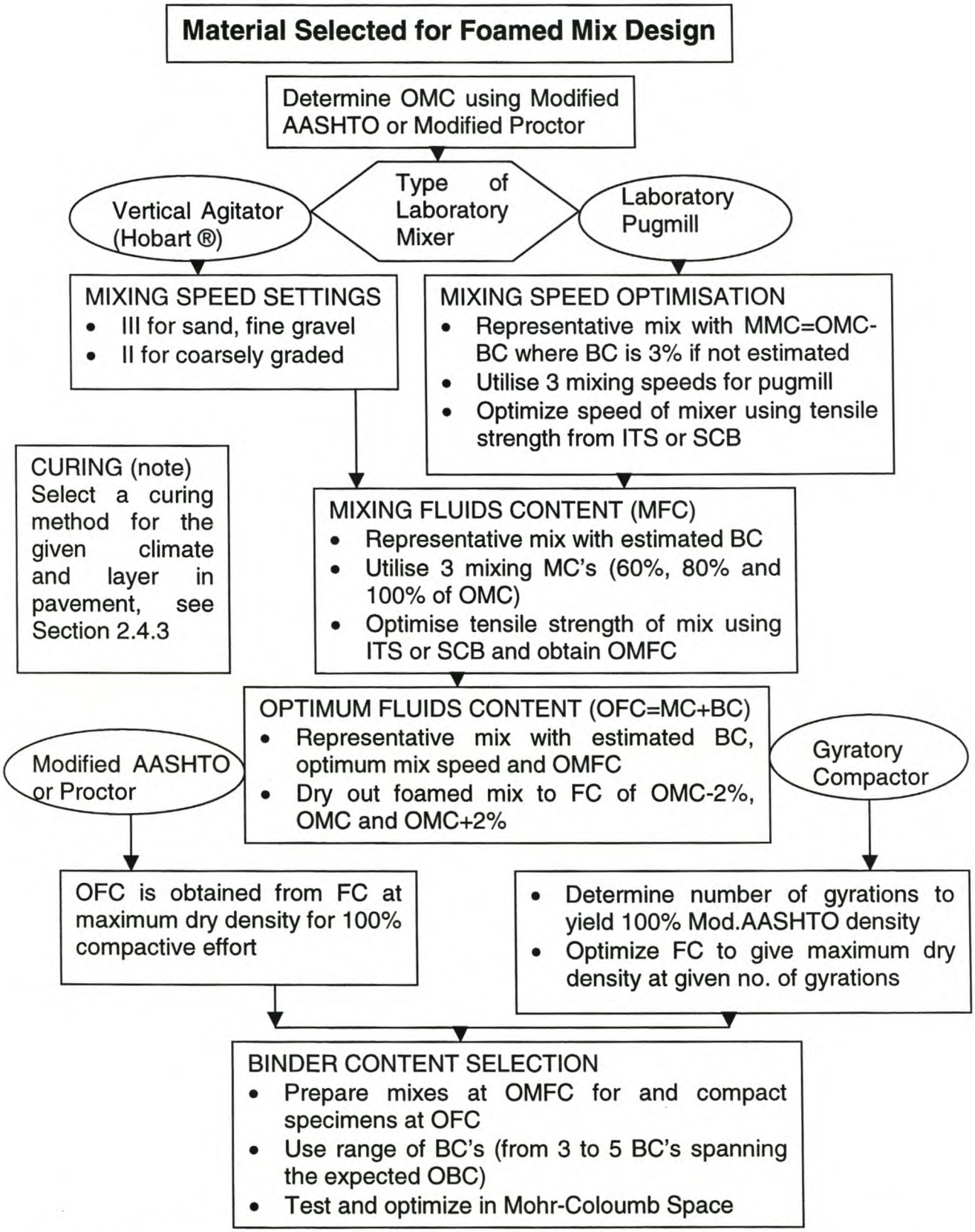

Figure 4 - 23. Comprehensive Laboratory Foamed Mix Preparation Procedure

Although the moisture in the foamed mix assists compaction, during curing and moisture loss, the volume occupied by the moisture will be replaced with air. The fluid component of the foamed mix volumetrics in the early stages of the mixture's life is therefore dynamic and can vary significantly. This moisture regime may be illustrated by considering the voids in the mineral aggregate (VMA) relative to the fluid content of a foamed mixture for a given level of compaction. At a given fluid content, optimal packing of the mineral aggregate may be achieved, see Figure 4 - 24. The volume of water V_{water} in the mineral aggregate is selected to provide the optimal packing at the required binder content. The volume of binder V_{binder} at the mix design stage is usually a trial binder-content as part of a sensitivity analysis.

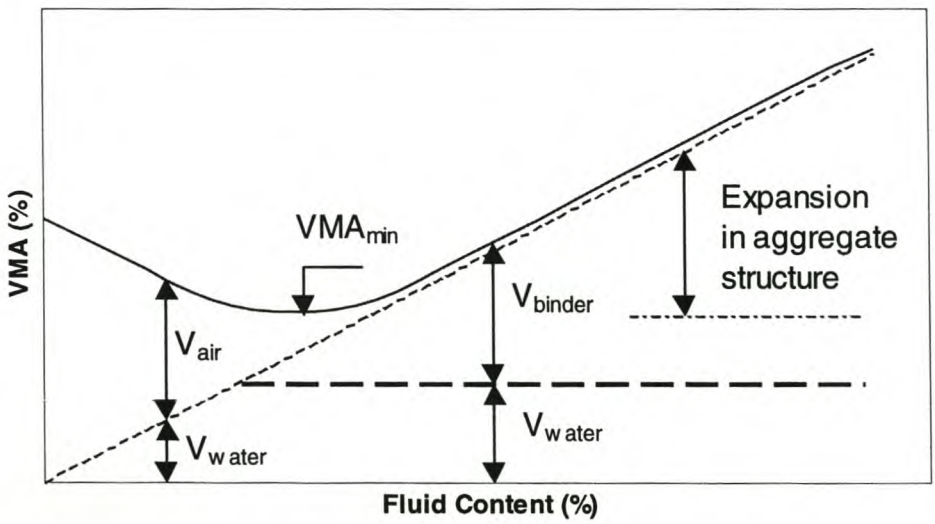

Figure 4 - 24. Volumetric Composition of a Cold Mix illustrating the influence of Fluid Content on Voids in Mineral Aggregate (VMA) for a specific Level of Compaction and limited Water Content below Optimum Moisture Content

Following compaction of a foamed mix layer and opening to traffic, the VMA will vary under the influence of traffic compaction. At the same time, the moisture content of the mix will change due to curing effects. These influences are illustrated in Figure 4 - 25 where the voids in the mineral aggregate as expressed in terms of the volume of air, binder and water is represented with respect to time. Although the rate of change in VMA in the figure is constant, in practice cyclic influences can be expected. In addition, an equilibrium moisture content will not be absolute and will vary seasonally depending on the climate. It is however, complicated to attempt to simulate these climatic effects, which are difficult to predict and combine them with soil properties that are variable. A long-term average of the equilibrium moisture content provides a preferable moisture regime at which mechanical testing can be carried out for the mix design, see Section 2.4.2.

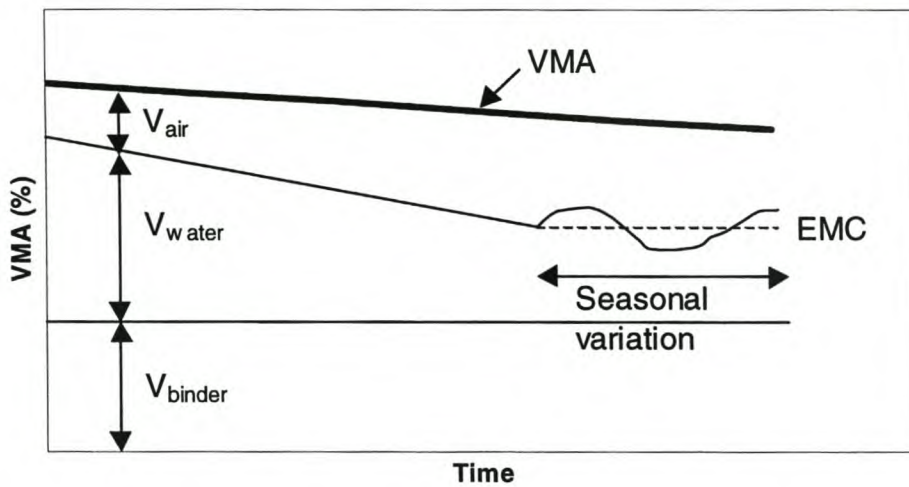

Figure 4 - 25. Variation in Composition of the VMA of a Foamed Bitumen Mix under Traffic

Where,

VMA = voids in the mineral aggregate (%)
V_{air} = volumteric composition of air in the mixture (%)
V_{water} = volumteric composition of water in the mixture (%)
V_{binder} = volumteric composition of binder in the mixture (%)
EMC = long term average equilibrium moisture content (%)

The importance of sound compaction and adequate curing can be graphically visualized in the Figure. The given conditions are preferable, where the gradient of the VMA line is shallower than the moisture loss line up to EMC. In this case a suitable design life for the road pavement layer can be realized, with air voids remaining sufficiently high (above 2%). Converse conditions can occur where compaction moisture contents of the foam treated layer are high and unfavourable conditions for curing occur i.e. months where precipitation exceeds evaporation. In such a case, the slope of the VMA line may exceed the slope of the moisture loss line resulting in loss in bearing capacity of the material through "zero air void" conditions.

2.4.2 Mixing Technique

Moisture in foamed bitumen mixes cannot be analysed in isolation of the mixing technique. As outlined in Chapters 1 and 2, various mixing techniques are utilised in the laboratory and on site to distribute moisture and foamed bitumen throughout the mineral aggregate during mix production. Free-fall mixers. in-place recyclers, pugmills and drum-mixers, and blenders constitute some of these.

In order to highlight the importance of mixing as a consideration in laboratory mix design, a limited investigation into the influence of mixing technique was carried out (Efrem, 2000).

Continuously graded cinder material was treated with foamed bitumen using a Hobart ® mixer and a PTI Pugmill ® Mixer. The different mixes were all manufactured at room temperature (20ºC) with the same mixing moisture content. Compaction of specimens was carried out using 80 revolutions of a gyratory compactor in a 150mm diameter mould followed by three days of curing at 50ºC at constant moisture conditions. The Uniaxial Compressive Strength (UCS) Tests included three results for each foamed bitumen content and the results are plotted in Figure 4 - 26. Notwithstanding minor deviations in the density of the specimens, an increase of almost 30% in the unconfined compressive strength is evident for equivalent foamed mixes with only variation of the mixing technique. Although the investigation is limited, it highlights the importance of selection of a mixing technique in the laboratory that simulates plant mixing. It is not the objective of this dissertation to investigate this phenomenon further, but more research is necessary considering that more than 90% of laboratory mixers utilise the stir-action of the blender-type Hobart mixer in the mix design of foamed mixes.

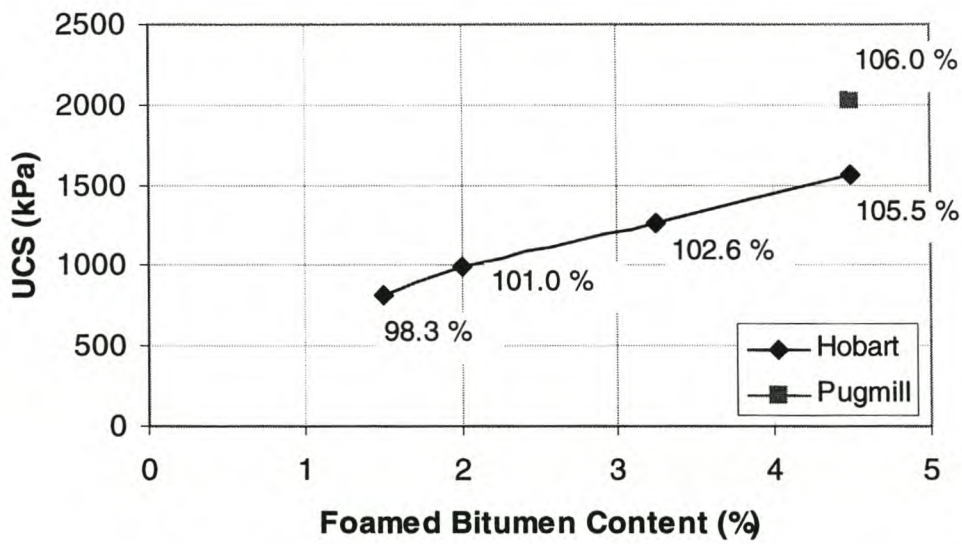

Figure 4 - 26. Influence of Mixing Technique of Foamed Bitumen Treated Cinder on Unconfined Compressive Strength (UCS) for Average of Three Repeat Tests, with Relative Modified Proctor Density Provided

2.4.3 Curing of Foamed Bitumen Mixes

It is imperative that the laboratory mix which is used for determination of the engineering properties as part of the mix design, is representative of the cold-mix placed in the field. For this reason a method of curing is required that has the same effect of a layer compacted and left in service in the road for a given period, in terms of both changes in moisture distribution and stiffening or strength gain of the mix. Some of the factors that influence curing in the road include:

- the air temperature and relative humidity on site,
- rainfall data for the area,

- the depth of the layer and the temperature of the layer,
- the air permeability of the compacted mix, and
- the drainage conditions at the boundary of the layer, including depth to the water-table.

The ultimate strength that a road develops influences the pavement performance, but the strength after an early or intermediate cure represents the most critical time period. Ruckel *et al.* (1983) state that, where foamed mix pavements exhibit premature distress, it tends to occur in days rather than weeks or months after construction. This observation underlines the importance of adequate curing for the development of a sufficient strength in a foamed mix. The correct laboratory curing technique for mix design purposes to simulate field conditions is imperative therefore.

Where the influences of early trafficking require investigation for the mix design, then short term curing of specimens is considered pertinent. For this purpose the method proposed by Ruckel *et al.* will suffice i.e. 1 day in the mould at ambient temperature.

Considering the importance of the mastic in foamed bitumen cold-mix, varying curing conditions and their influence on the mastic stiffness have been investigated. It is not practical to attempt to simulate all of the above-mentioned conditions for consideration in a mix design, so the salient features require identification.

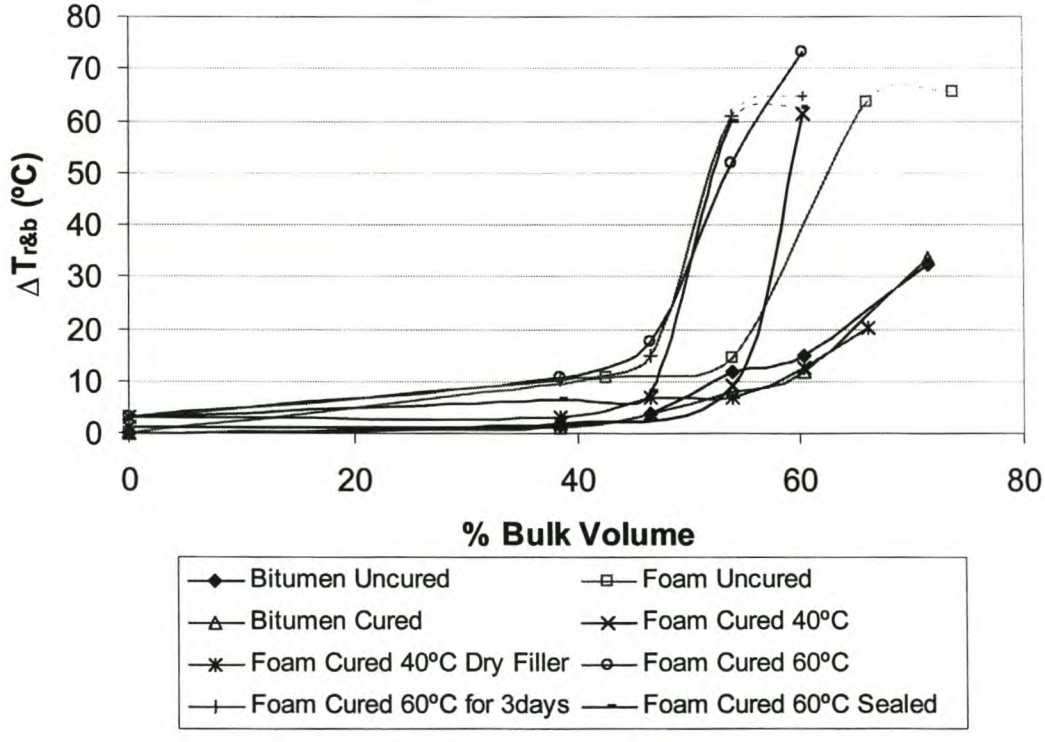

Figure 4 - 27. Change in Ring and Ball Temperature for a Foamed and Conventional Mastic using 150/200 Penetration Bitumen and Hornfels Filler, with different Curing Techniques.

Note:

- In the figure, all foamed mastics utilise moist filler unless otherwise stated.
- All conventional mastics use dry filler.
- Sealed means curing in sealed container without loss of moisture.
- All curing periods are 24 hours (constant mass) in the test rings at the stated temperatures, unless otherwise stated.

Several important issues regarding curing of foamed mixes are highlighted in Figure 4 - 27. These include:

- The importance of the moisture in the filler before mixing with foamed bitumen is evident. Where foamed bitumen is added to dry filler, the stiffness of the mastic closely resembles that of a conventional HMA mastic, also described in the work of Cooley *et al.* (1998).
- Curing at 40 °C has very little influence on ageing the bitumen and the stiffening of HMA mastic, where the surface area of bitumen is limited due to the continuum of binder.
- The difference between no cure, curing at 40 °C and 60 °C is evident by the leftward shift of the change on softening point curve. The higher air temperature at low relative humidity causes greater drying out of the mix and stiffening of the mastic. In addition, temperatures of 60 °C, which are close to the softening point of some bitumen types, also influence binder dispersion. Sealing of the mastic to limit drying out of the mastic does not effectively counteract the influence of higher curing temperature.

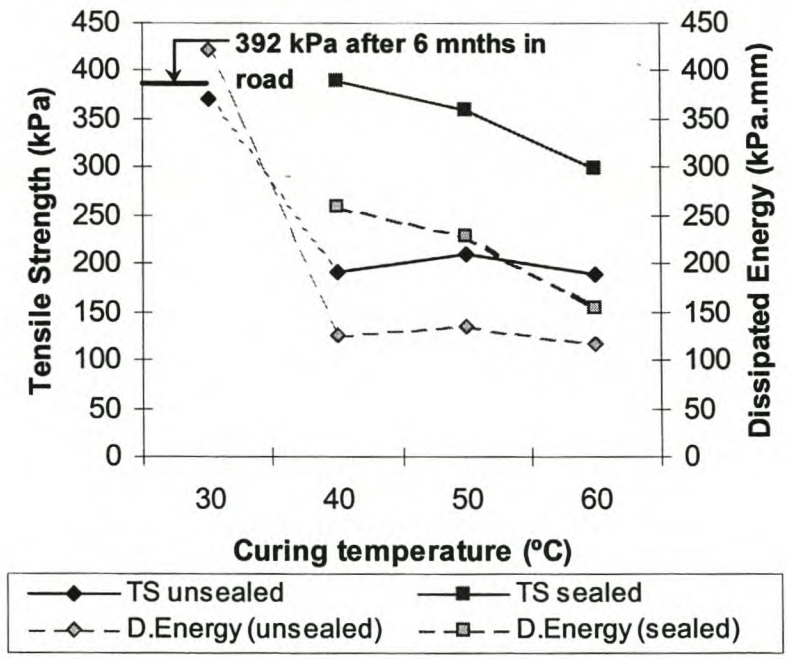

Figure 4 - 28. Influence of Laboratory Curing Temperature on Tensile Strength of Foamed Mix for Blocks (80% Reliability for 3 repeat tests on blocks)

Note: Test temperature = 25°C with TS = Tensile Strength and D. Energy = Dissipated Energy
Standard deviations range from 11kPa to 20 kPa for the Tensile Strength at different curing Temperaures

The influence of curing on the filler-bitumen mastic requires extension to the entire bituminous cold-mix. The results obtained from a trial section using cold-mix blocks in the Western Cape (Jenkins *et al.*, 1997) provide a reference for curing of the same mix at different temperatures in the laboratory, see Figure 4 - 28 and Figure 4 - 29. The foamed bitumen mix has been cured in both sealed and unsealed conditions in a draft oven and the emulsion mix unsealed.

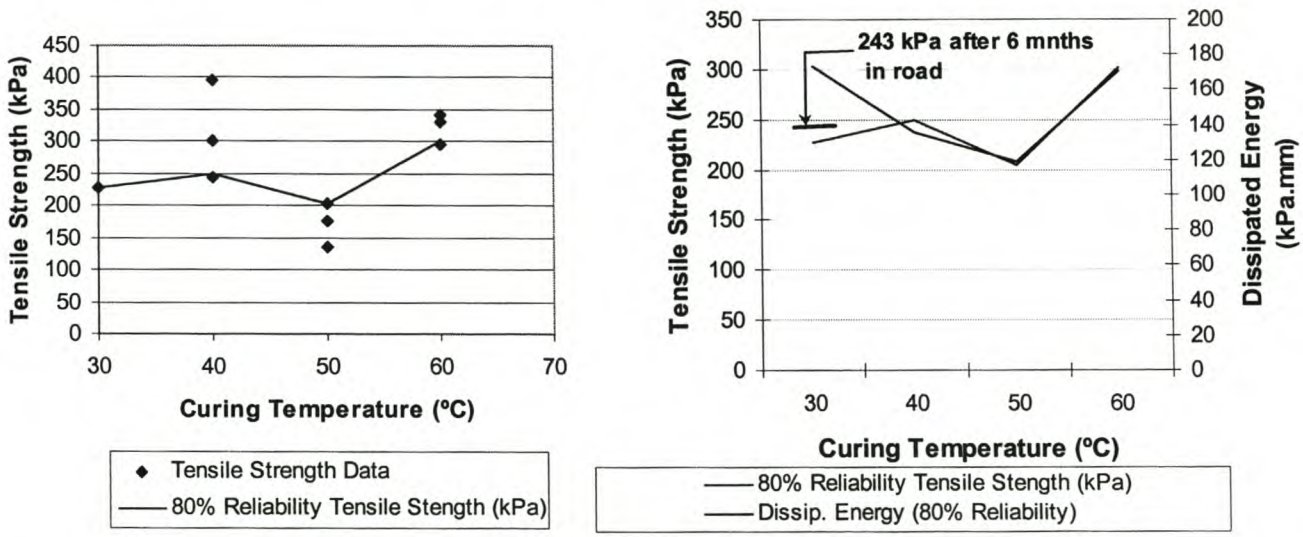

Figure 4 - 29. Influence of Laboratory Curing Temperature on Tensile Strength of Emulsion Mix for Blocks (80% Reliability for 3 repeat tests on blocks)

Note: Standard Deviations range from 24kPa to 76kPa for the Tensile Strength at different curing Temperatures

It is evident that higher curing temperatures and stiffness of mastic do not necessarily provide a greater tensile strength in the mix. In addition, with the foamed bitumen mixes it is imperative not to desiccate the laboratory specimens so that representative tensile strengths for field conditions may be obtained. Researchers of foamed bitumen, including Roberts *et al.* (1984) and Ruckel *et al.* (1983) have shown that the moisture contents of mixes that have been oven cured in an unsealed state are generally between 0% and 0,5%, which is seldom representative of field conditions.

In carrying out displacement controlled tensile tests on blocks, it is possible to obtain a load versus displacement function. The area under such a curve is a measure of the energy dissipated by the material during tensile failure. The true behaviour and appurtenant benefits in the use of visco-elastic materials such as bitumen in mixes can only be accounted for when displacement is considered in specimen analysis and not solely maximum strength. Calculation of the dissipated energy function of cold mixes for the blocks under investigation, yield the same trend as tensile strength versus curing temperature, see Figure 4 - 28 and Figure 4 - 29. Strain levels at failure would not, therefore be significantly affected by curing temperatures for cold bituminous mixes.

The mechanism for failure of cold bituminous mixes will not always be tensile, however. Shear failure and yielding in compression, as observed with granular materials in the Mohr-Coloumb stress domain, can contribute to permanent deformation. The influence of curing temperature on compressive strength of foamed bitumen stabilised mixes also requires consideration. The tests comprise Unconfined Compressive Strength (UCS) of foamed mix cured in the laboratory at different temperatures, carried out on 100mmx100mm samples at 25°C with a displacement rate of 50,8 mm/minute.

The UCS test results reaffirm the dependence of the crushing strength of cold mix on curing temperature. Specimens sealed during curing at all temperatures but 60 °C yield higher crushing strength values than the specimens allowed to dry out, with the former more closely approximating the UCS values from long term cure values in the road.

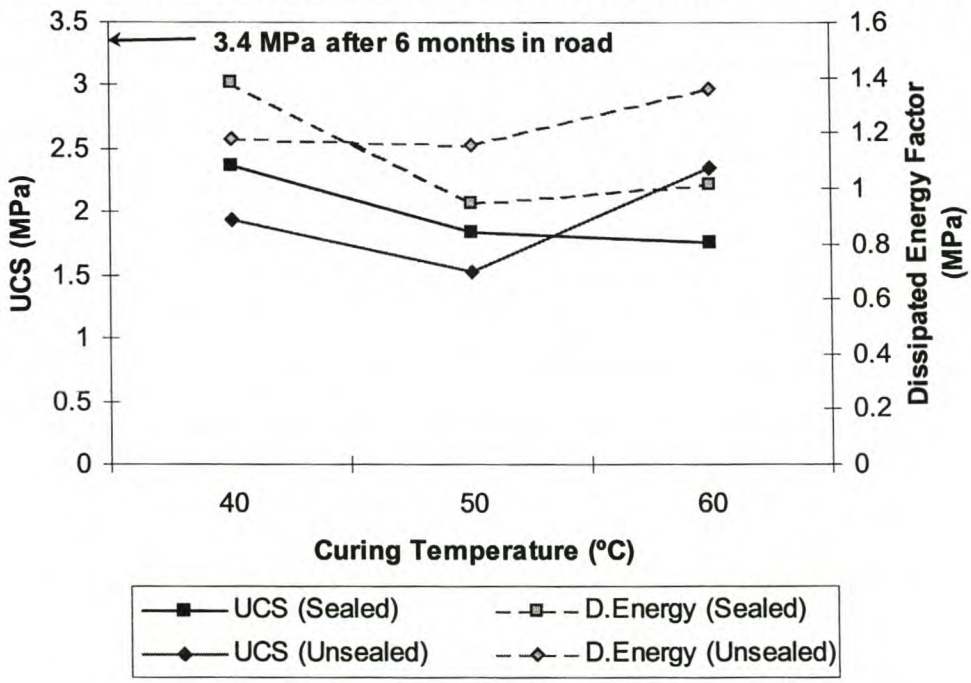

Figure 4 - 30. Unconfined Compressive Strength of a Foamed Bitumen Mix as a Function of Curing Temperature for Sealed and Unsealed Specimens in a Draft Oven (80% Reliability for at least three repeats)

Notwithstanding the variability of results for both the tensile strength tests and the UCS tests, the relative humidity during curing has a greater influence than the temperature during curing. This concurs with the findings of Lee (1981) who studied the effects of curing on Marshall Stability of foamed mixes and concluded that both temperature and moisture content have an influence, but that the latter is the dominating factor.

It is therefore important to take account of both of these factors during curing of cold mix specimens manufactured under laboratory conditions. Monitoring the temperature of curing is possible through the selection of the correct oven temperature. Adaptation of the work of Witczak (1972) to calculate the temperature in asphalt layers dependent on depth and

Mean Monthly Air Temperature, facilitates the selection of curing temperature. Witczak's work is extended in Figure 4 - 31 to provide the Material Temperature with 90% reliability (upper limit) which provides a reliable indication of curing temperature (for 72 hours in a sealed container) for foamed bitumen mixes, after comparison with site data.

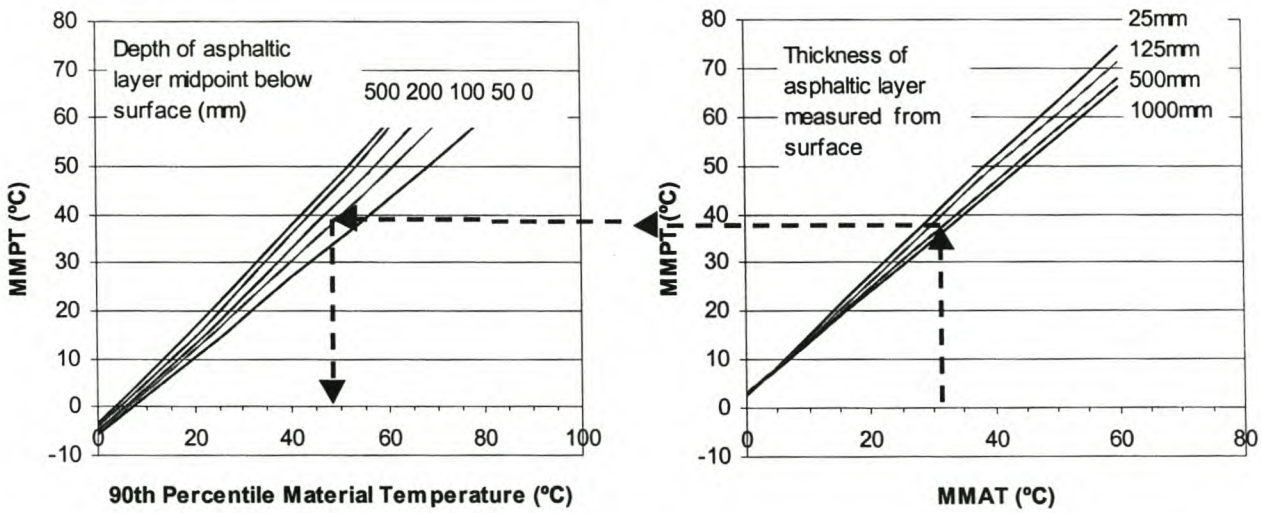

Figure 4 - 31. Nomograph for Mean Monthly Air Temperature (MMAT) related to Mean Monthly Pavement Temperature (MMPT) and 90% Reliable Upper Limit Material Temperature (after Witczak,1972)

The example given in the figure is for a 150mm thick foamed bitumen base layer with a thin surfacing which is to be placed in a region with a Mean Monthly Air Temperature of 30 °C. This material should be cured at 46 °C for 72 hours. The 90% reliable limit value is higher than the mean i.e. the upper limit, as curing is affected by extremes and only a few days of higher temperatures will accelerate the curing.

The Superpave™ approach for pavement temperature analysis (FHWA,1994) has not been selected as it uses a 7 day maximum annual temperature for surfacing mixes for binder selection, which is not as pertinent to curing of cold-mixes.

The curing procedure proposed above is applicable to the medium term cure of the foam treated layer i.e. 6 months to a year after construction, and should be carried out after specimens have spent 24 hours in the mould. The procedure for curing specimens to predict short term performance (7 to 14 days) should follow the recommendations of Ruckel *et al.* (1983) i.e. 24 hours in the mould and 24 hours at 40°C in the oven.

Fluid content considerations for the curing of foamed bitumen specimens in laboratory, as stated by Lee (1981), is of paramount importance in mix design. One possible approach to controlling the moisture content of a specimen is through the use of air-drying after compaction, to the anticipated equilibrium moisture content for the equivalent layer in the

particular region of application. In order to do this, the equilibrium moisture content of the material needs to be known.

One method developed for moisture content prediction of foamed materials uses the ratio of Equilibrium to Optimum Moisture Content (E/OMC) for the relevant layer, as reported by Emery (1985). This is a simplistic procedure as it ignores other factors that influence equilibrium moisture content (EMC) as described by Emery, but is considered satisfactory for simulating field conditions for road building materials. The mean values of the E/OMC ratio are reported in Table 4 - 10. The method has been developed for granular materials and requires adaptation for use on foamed mixes.

Table 4 - 10. Equilibrium to Optimum Moisture Content Ratios (E/OMC) for Granular Road Building Materials, Mean (after Emery,1985)

Climatic Area	Subgrade	Subbase	Base
Arid	0.71	0.7	0.53
W.Cape (Mediterranean)	0.75	0.78	0.63
Gauteng (Im<0)	0.94	(0.8)	(0.65)
Cape (Southern)	0.98	0.83	0.57
Gauteng (Im>=0)	0.96	(0.81)	(0.65)
KwaZulu Natal	1.05	(0.89)	(0.72)

Note : () denotes recommended values for use in cold mix curing, in the absence of available data. Im = Thornthwaite's Moisture Index.

Analysis of the equilibrium field moisture contents for five different roads in South Africa provides data for an uncomplicated method of calculating the curing moisture content to be established. Adjustment for the inclusion of foamed bitumen in the material requires that the fluid content be considered (moisture content MC and binder content BC) for prediction of EMC, in place of only the moisture content (for granular materials). Equation 4 - 7 provides the relationship between EMC and material properties for foamed bitumen mixes.

$$\text{Curing Moisture Content} = \text{Predicted EMC} = (OMC - BC)*(E/OMC) \qquad \textbf{Equation 4 - 7}$$

The data for five roads with different foamed mixes in different regions, measured between 6 months and 2 years after construction, provides the basis for Equation 4 - 7. This data is detailed in Table 4 - 11 and graphically represented in Figure 4 - 32.

Table 4 - 11. Fluid Considerations for Foamed Bitumen Layers in Place

REGION	CAPE	KWA-ZULU NATAL			
MATERIAL TYPE	Gravelly sand	Weathered Granite	Aeolian Sand	Weathered Granite	Weathered Sandstone
ROAD	Sir Lowry's Village	P504	P466	P423	P423
OMC (%)	7.0	8.3	16.3	8.9	8.8
BC (%)	3.6	4.3	4.5	3.1	3.1
E/OMC	0.63	0.72	0.72	0.72	0.72
(OMC-BC) x (E/OMC) (%)	2.14	2.88	8.57	4.18	4.10
FMC (%)	0.6	6.2	5.0	8.2	7.5
DIFF (%)	+1.54	-3.32	+3.57	-4.02	-3.40

Note : FMC = Field Moisture Content and DIFF = difference

The degree of variability noted around the line of equality is not excessive for foamed mixes given that factors such as seasonal variation and depth to a phreatic-surface have been ignored in the interest of simplicity. The necessity to take account of the hydrophobic nature of bitumen is evident from the shift in predicted equilibrium moisture closer to the line of equality where Equation 4 - 7 is used rather than the method of Emery intended for granular materials.

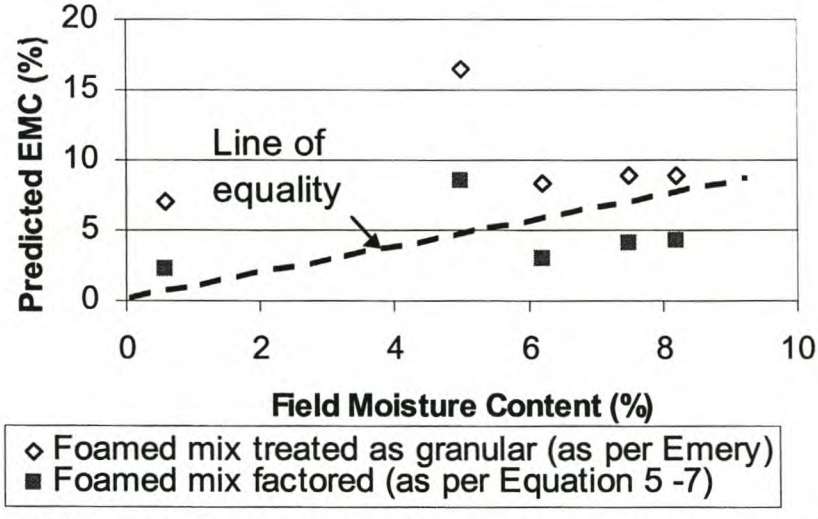

Figure 4 - 32. Relationship between Predicted and Actual Moisture in Foamed Mixes used in Five Roads in Different Areas of South Africa.

Using the predicted EMC from Equation 4 - 7, foamed bitumen specimens can be air-dried to a known moisture content after compaction. The curing of specimens in a sealed container no more than 10% larger than the sample in volume, at a temperature obtained from Figure 4 - 31, accounts for the climate in the field and adequately conditions a laboratory specimen. A period of 72 hours provides sufficient time as this allows the moisture regime in the specimen to stabilize. In this way, foamed bitumen specimens that are adequately representative of the same materials in the road can be prepared.

3. INFLUENCE OF AGGREGATE TEMPERATURE AND FOAM CHARACTERISTICS ON COLD MIX PROPERTIES

As outlined in Section 2.2.1, foamed bitumen mixes are produced with a greater number of variables that influence the binder distribution than hot mix asphalt. One such factor is the influence of variations in ambient temperature. By definition, cold mixes are manufactured at ambient temperatures. Possible variations in diurnal, seasonal and regional temperatures are significant and the actual ambient temperature where a foamed mix is manufactured, requires consideration. A second factor that can influence the mix properties is the characteristics of the foamed bitumen. The mechanical implications of changes in foam characteristics have been outlined in Section 2.2.1 but the effect that the change in binder distribution has on the entire mix remains unexplored.

The interaction of foamed bitumen and a steel vessel has been outlined in Chapter 3 in terms of conservation of heat. The temperature of the vessel influences the foamed bitumen temperature and behaviour significantly. These energy considerations can be extended for foamed bitumen mixed with cold aggregate. Utilising the conservation of energy principle with the foam and the inclusion of aggregate with a specific heat capacity of 0,201 cal/g.°C in a ratio of 96:4:4,8 by mass with foamed bitumen and water, an equilibrium temperature for the mix is obtained. The addition of 4% of binder to aggregate at ambient temperature does not increase the overall mix temperature significantly, see Figure 4 - 33. The influence of the equilibrium temperature of the foamed mix on its properties requires attention, particularly in terms of binder distribution.

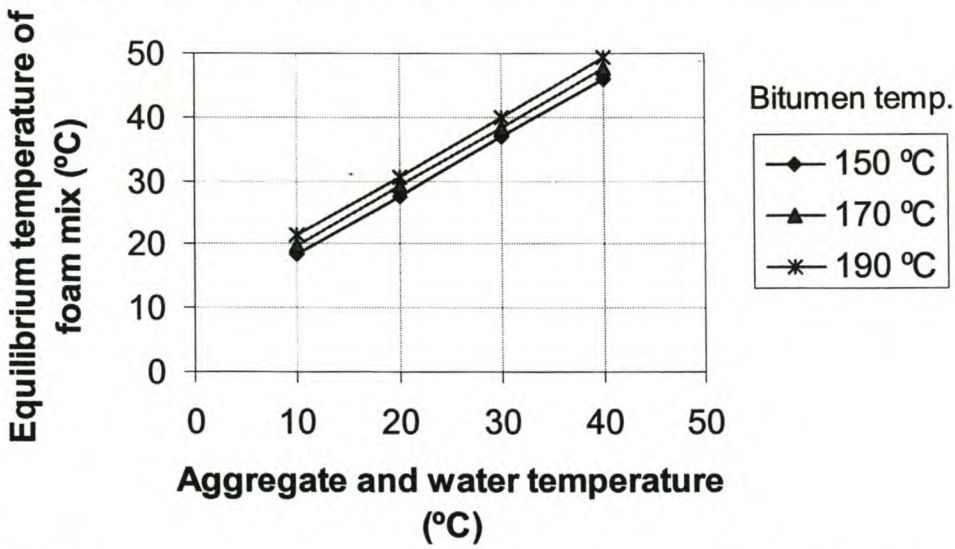

Figure 4 - 33. Equilibrium Temperature of Foamed Mix with 5% Water, 4% Foamed Bitumen (m/m of total mix) and 2,5% Foamant Water (m/m of bitumen), calculated using specific heat considerations, ignoring surface energy and air temperature considerations.

The rate of transfer heat from the foamed bitumen to the aggregate during mixing, can be estimated through the use of the coefficient of thermal conductivity of bitumen (γ = 0,17 Joule/m.s.Kelvin). This value is 10 to 20 times lower than that of Limestone and Granite

respectively. Bitumen bubbles with a plausible film thickness of 0,01mm making contact with mineral aggregate will enable 189 Joules of energy to be transferred from the bitumen at 110°C to aggregate at 20°C in 1 second. This would enable one gram of bitumen to experience a reduction in temperature of 90°C! The high surface area of contact and the thin films of bitumen in the foam mass, permit rapid transfer of heat to the aggregate, therefore. Foamed bitumen will soon increase in viscosity to levels that will prevent particle coating with cool aggregate. The corollary of this deduction is that aggregate temperature significantly influences binder distribution.

Verification of the influence of aggregate temperature and the foamed bitumen characteristics on the performance parameters of the foam mix has been investigated in this study using a gravelly sand material. The material was mixed with bitumen having different foaming characteristics, see Table 4 - 12, as determined with a Wirtgen Laboratory Foam Plant WLB 10®.

Table 4 - 12. Foamed Bitumen Characteristics before mixing

Bitumen type	Expansion Ratio	Half-life (seconds)
150/200	14	16
150/200 + foamant	14	90

Utilising the half-life as a variable for bitumen properties, the foamed binder was applied to the mineral aggregate for three temperatures that cover a spectrum of ambient temperatures of aggregate in different climates, namely 13°C, 21°C and 33°C. Compaction of specimens was carried out using a Gyratory Compactor followed by curing of specimens in a draft oven at 40°C for 72 hours in sealed containers (to maintain equivalent fluid contents for all mixes and eliminate spurious influences on stiffness).

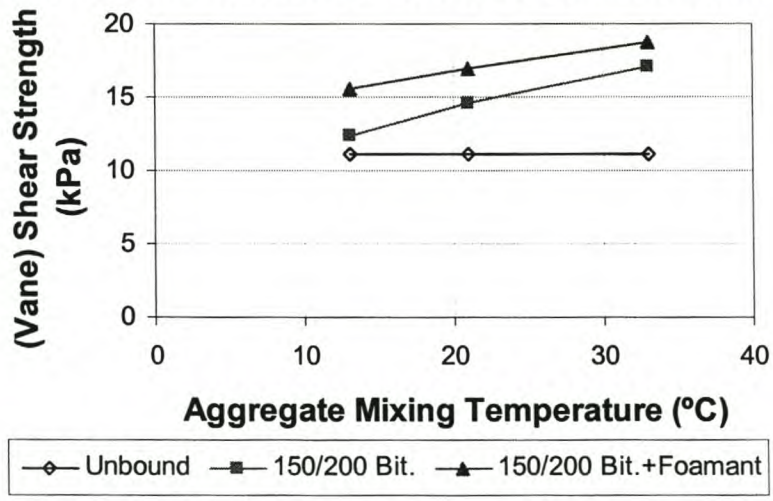

Figure 4 - 34. Influence of Aggregate Temperature on Vane Shear Strength of Foamed Mix for Different Bitumen, and Unbound (measured in mould)

The shear vane test provides a measure of the cohesion and workability of the mix. With the test carried out on lightly compacted mix (3 blows of Marshall Hammer) only marginal confinement results and the shear strength approximates the cohesion value of the

material. The most conspicuous differences between the mixes manufactured with foamed bitumen of short and extended half-life, are evident at lower aggregate temperatures, see Figure 4 - 34. The ordinary foam collapses rapidly into bitumen droplets that are less continuous in the colder mix i.e. very few threadlike strands of bitumen. The convergence of the two curves in the figure suggests that at an aggregate temperature exists (approximately 50°C in this case) where the influence of the foamant on cohesion in the mix will be neutralised. Conversely, at an aggregate temperature of 10°C the benefits of stabilising the mix with foamed bitumen, in terms of increasing cohesion and hence shear strength, approach redundancy.

Tensile strength of a granular material is related to cohesion for given stress conditions in the Mohr-Coloumb space. At the same time, tensile strength is utilized as parameter for empirical assessment of crack-resistance mix of bitumen bound mix. For this reason it is important for foamed mixes and was determined together with dynamic stiffness in the same investigation. The Semi-Circular Bending (SCB) Test (van de Ven *et al.*, 1997) carried out at 25°C, was utilised for the comparison of tensile strength and stiffness of the different mixes. Specimens were prepared in a gyratory compactor using 600kPa, 1,25° angle of gyration and 46 revolutions.

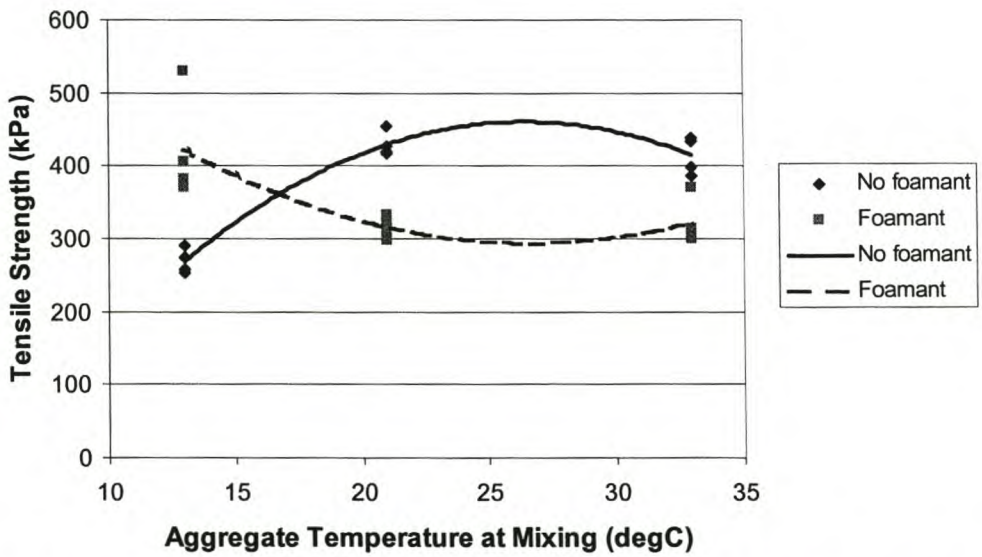

Figure 4 - 35. Influence of Aggregate Temperature on 80% Reliable Tensile Strength and Stiffness of Foam Mix measured using Semi-Circular Bending Tests

A degree of dependence between tensile strength and aggregate mixing temperature is evident for foamed mixes. With allowance for variability, an ubiquitous feature of static splitting tests, the tensile strength from the SCB test to some degree concurs with the trend in mix cohesion. The stiffness of foamed mix measured using SCB tests follows a similar trend to the tensile strength (Jenkins *et al.*, 1999a). The benefits in an extended half-life of the foamed bitumen for lower aggregate temperature i.e. generally less than 17°C, are evident. Improved stability of the foam and hence better dispersion of the binder after contact with relatively cold aggregate is the most likely cause for this. For aggregate

temperatures above 17°C, the benefit of the foamant is generally negated and can be counter-productive. Although conventional mechanical bitumen indicators such as penetration and ductility remain unchanged with the addition of this additive, other forms of chemical alteration of the bitumen properties such as adhesion, cannot be ignored.

4. MOISTURE SUSCEPTIBILITY

Due to the partially coated nature of the aggregate in foamed bitumen mixes, susceptibility of pavement layers constructed using these materials to stripping and loss of strength resulting from exposure to moisture, is an important consideration. One method of simulating moisture exposure is that recommended by the Aphalt Institute Manual (1992) where specimens are cured (medium or long term) and then exposed to moisture at 25°C for an hour under a vacuum of 100mm of Mercury. The vacuum is released and saturation continues for a further hour before testing. Tests are carried out on specimens that have been exposed to vacuum saturation as well as those that have not and the results compared.

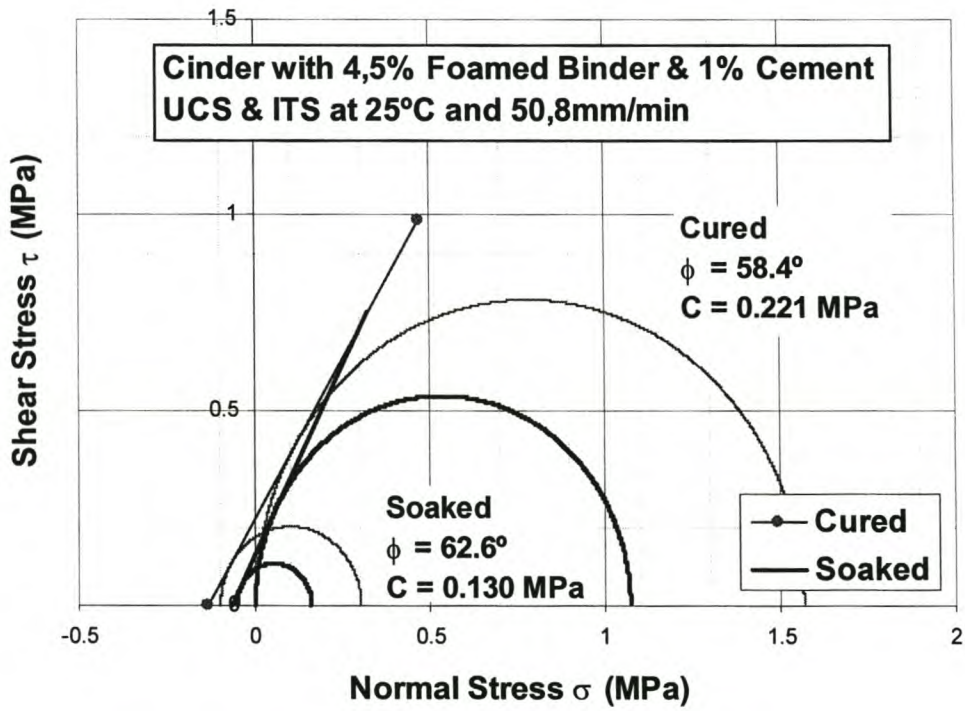

Figure 4 - 36. Combination of UCS and ITS tests on Foamed Cinder in Cured and Soaked State providing Mohr-Coloumb Failure Envelope (Average of Three Repeats)

The moisture exposure is considered to be harsh (Ruckel *et al.*, 1983) as it simulates extreme conditions in the road, but nevertheless provides a significant measure of relative moisture susceptibility, especially for cold foamed mixes, as discussed in Chapter 2. Indirect Tensile Strength (ITS) tests and Unconfined Compressive Strength (UCS) tests

have been carried out on materials using the Asphalt Institute technique and the results analysed in the Mohr-Coloumb stress state, refer (Efrem, 2000) and (Saleh, 2000). Figure 4 - 36 and Figure 4 - 37 provide the respective analyses.

As is to be expected, very little change in the friction angle of the materials occurs after saturation, whilst the most notable effects occur in reducing the bonds of the binder within the aggregate structure. The cohesion value of the mix can be reduced significantly through exposure to moisture after curing. The implications of the shift in the failure envelope after soaking is dealt in Chapter 7 in terms of the performance of a cold foamed mix layer. In this chapter the rutting potential of a foamed mix is modelled on the basis of shear properties from Mohr-Coloumb stress analysis. This is a more holistic approach to moisture susceptibility in foamed mixes, rather than previous methodologies that utilise dry:soaked ratios of Marshall or ITS tests, without taking cognisance of the stress state or performance conditions of the applicable mix.

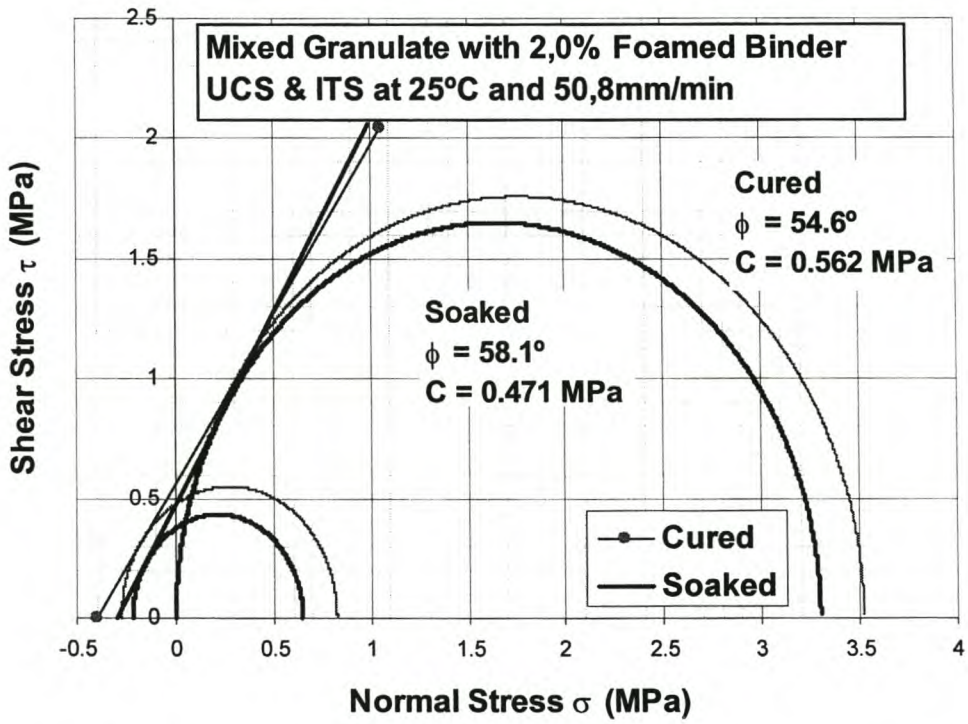

Figure 4 - 37. Combination of UCS and ITS Tests on Foamed Mixed Granulate in Cured and Soaked State providing Mohr-Coloumb Failure Envelopes (Average of Three Repeat Test for Each)

For the purpose of most efficient measurement of effects of moisture, tests that create higher tensile stresses and relatively low compressive stresses, are desirable. The Semi-Circular Bending Test (SCB) is such a test (Molenaar and Molenaar, 2000) with a favourable stress distribution, especially where non-linearity of material behaviour is taken account of, and should therefore be considered for potential measurement of moisture susceptibility of cold foamed mixes.

5. AGEING

Due to the high surface area of bitumen in foamed mixes as a result of the thread like structure, these materials can be susceptible to premature ageing. If a mix is not adequately compacted or sealed at the surface, or if allowed to dry out, oxidation can occur. The consequence would be increase in the hardness of the binder and a brittle mix that fails prematurely.

The ageing tendency of these mixes is illustrated in Figure 4 - 38, which shows the shift in stiffness of the foamed bitumen mastic as a result of 5 hours of ageing at 163°C in a draft oven, relative to cured and uncured mastic. This ageing procedure uses the ASTM (1979) D 1754-97 Standard Test Method for Effects of Heat and Air on Asphaltic Materials (Thin-film oven test) as a guide, which approximates plant ageing at 150°C for hot mix asphalt. The increase in the softening point change in excess of 20°C highlights the need to minimize the exposure of foamed bitumen mixes to ageing through surface sealing and other similar measures. More research is necessary to understand the full implication of this ageing on the performance of the mix under traffic.

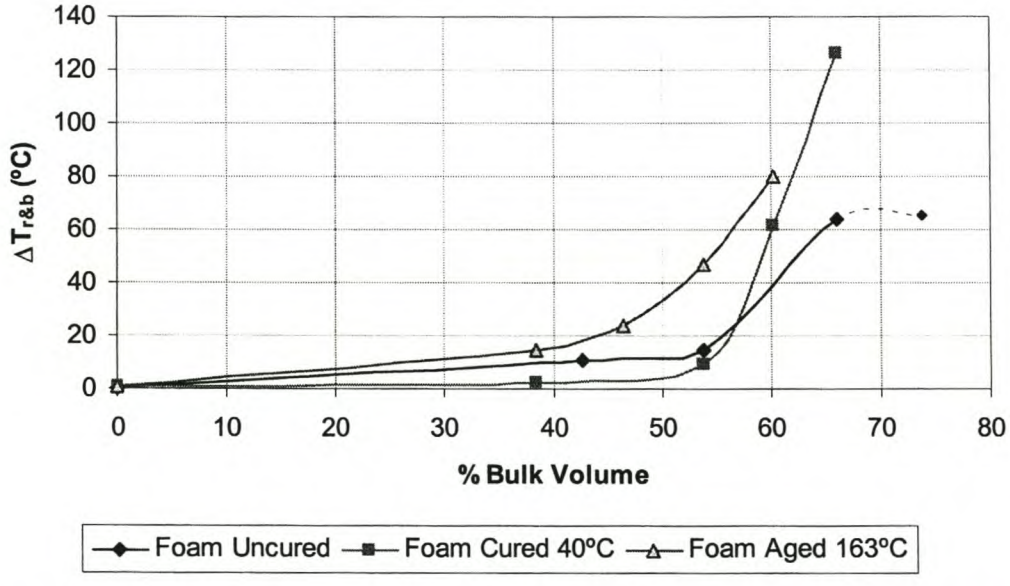

Figure 4 - 38. Change in Softening Point of Foamed Bitumen Mastic as a function of Bulk Volume for Hornfels dust and 150/200 Calref Bitumen.

6. CONCLUSIONS

There are many factors that require consideration in the mix design of mineral aggregate that has been treated with foamed bitumen. The inclusion of an additional phase in the form of water and a binder that has variable characteristics during mixing, sets these mixes apart from hot mix asphalt, necessitating special consideration. Investigation into the mechanisms by which the behaviour of cold mixes with foamed bitumen can be characterised, provide conclusions in various aspects of foamed bitumen mix design.

6.1 Foamed bitumen – filler interaction

- As with hot mix asphalt, the relationship between the "Percent Bulk Volume" of the filler and "Change in Softening Point" of the mastic is unique for foamed bitumen mixes. The proposed limits of restricting the percentage bulk volume to between 60% and 55% for HMA are inapplicable to foamed bitumen mixes, however. Where a foamed mix uses a fixed material gradation, and a proposed binder content has been established using mix properties such as tensile and compressive strength, the stiffening of foamed bitumen mastic should be calculated for the given parameters. In this way the behaviour of the overall mix can be established i.e. a mastic at greater than 45% bulk volume will produce a foamed mix with more "brittle" response than the equivalent HMA. Where the mineral aggregate composition for a foamed mix can be altered, the "Percentage Bulk Volume" can be used to achieve the desired mix characteristics.
- The presence of moisture in the mineral aggregate, and especially within the filler fraction, is the primary factor influencing the behavioural differences between the foamed bitumen and hot mix mastic. With the omission of the moisture i.e. dry mixing with foamed bitumen, the mastic produced is significantly similar to that of hot mix. This holds true for filler mixed in isolation with foamed bitumen, excluding influences that the remainder of the aggregate structure may have on the mastic.
- The filler and bitumen component of foamed bitumen mixes provides a sponge-like mastic with pores that hold the moisture in the entire mix. The water held in the mix provides the lubrication for compaction at ambient temperatures and can be released during consolidation under stresses from a compactor.
- The dispersion and structure of the binder in foamed bitumen mixes i.e. a web-like matrix of bitumen threads and droplets, results in increased surface energy of the bitumen relative to HMA. This leads to a higher complex modulus of foamed mixes at lower temperatures relative to the equivalent hot mix. The increased surface area leads to a greater susceptibility to ageing of the binder, however.

6.2 Sand fraction

- The "Voids in the mineral aggregate" (VMA) for the sand fraction is a relevant parameter for the consideration in the optimisation of an aggregate's suitability for treatment with foamed bitumen as a cold mix. Cold mixes manufactured using foamed bitumen are predominantly produced with sand skeleton aggregate structures and are partially reliant on mechanical forces during compaction to ensure satisfactory

dispersion and adhesion of the binder. A reduction in the VMA of the sand fraction can result in improvements in the tensile strength and the obvious reduction in permeability with the appurtenant advantages regarding moisture susceptibility.

- Vibratory compaction of the sand faction (<2,36 mm) to determine the VMA of this fraction using the Engelsmann apparatus provides an effective technique to optimise blends of different mineral aggregates. The ratio of combinations of different materials is that which provides a minimum VMA for the sand fraction.

6.3 Spatial Composition of Stone, Sand and Filler

- The suitability of an entire aggregate structure for treatment with foamed bitumen can be described in terms of particle size distribution using the Francken triangle. In order to achieve sufficient "carrier fraction" for the binder i.e. sand and filler, boundaries in stone, sand and filler fraction may be used to describe the preferred aggregate composition. Sand skeleton aggregate structures provide the most suitable mixes for foamed bitumen.

6.4 Moisture and Mixing

- Moisture plays a vital role in the behaviour of foamed mixtures. The moisture content requires optimisation in terms of mixing, workability, compaction, curing and performance. Rather than attempting to establish a generalised function for different materials, which is unreliable, a flow chart procedure has been established for the comprehensive determination of the optimal fluids regime for a foamed mix at the various stages of production.
- The mixing technique utilised to agitate the aggregate during the application of foamed bitumen has a significant influence on the mix properties. It is therefore essential to select a mixing method for mix design purposes that is representative of the full-scale foamed mix production plant to be utilised. If this is not possible, parallel testing is required to ascertain the differences in mix properties that may arise.
- Present curing procedures of foamed bitumen mixes manufactured in the laboratory do not take cognisance of either the moisture content of the mix or the climatic effects. An alternative procedure is proposed for curing, which uses the mean monthly air temperature of the region in which the mix is to be used to obtain the curing temperature, which is then applied for 72 hours in a draft oven.
- The moisture content that should be aimed for during curing can be approximated using a relationship between the optimum moisture content of the material, the binder content, the position of the layer and the environment or climate (calibrated for South Africa).

6.5 Temperature of Aggregate

- The aggregate temperature at time of mixing with foamed bitumen has a dominant effect on the distribution of the binder within the mix. Ambient temperature of regions of foamed bitumen application can vary considerably and cognisance should be taken of aggregate temperature in the preparation of laboratory mixes with due consideration being given to the expected mixing temperature on site.

- The benefits of increased ambient temperature include improved binder distribution and higher tensile strength values for the mix. Warming the aggregates before mixing with foamed bitumen may extend these benefits, a process discussed further in Chapter 5.
- Additives that improve the stability of foamed bitumen are advantageous for mixes where aggregate temperatures are low i.e. less than 17°C. In such cases, the additive serves to improve dispersion of the binder in the mix, in so doing improving the cohesion in the mix.

6.6 Moisture Susceptibility

- Due to the dispersed nature of the binder in a foamed mix i.e. the bitumen is in a non-continuous state with partial coating of aggregate, compacted mixes can be prone to early distress due to moisture damage. The procedure of testing for moisture susceptibility by means of vacuum saturation of specimens of proposed mixes is valid in providing insight into this phenomenon. The effect of moisture ingress, loss of binder cohesion to the aggregate can be analysed through the shift of the Mohr failure envelope before and after moisture exposure.
- Although the influences of moisture of cold foamed mixes is best interpreted through analysis of the Mohr-Coloumb failure envelope, the Semi-Circular Bending Test, which causes predominantly tensile stresses in the failure zone of a specimen, provides a more efficient method of monitoring this phenomenon.

7. REFERENCES

Akeroyd F.M.L. and Hicks B.J., 1988. **Foamed bitumen road recycling**. *Highways*, January. London. Pp 42-45

Anderson D.A., 1987. **Guidelines on the Use of Baghouse Fines**. National Asphalt Pavement Association, Information Series 101-11/87, Maryland.

Asphalt Institute, 1993. **Mix Design Methods for Asphalt Concrete and other Hot Mix Types**. Manual Series No. 2 (MS-2), Sixth Edition. Lexington, USA. Pp 81-82

ASTM, 1979. **Annual book of ASTM Standards**. American Society for Testing and Materials, Philadelphia. Pp107-110

Bahia H.U., Zhai H., Bonnetti K. and Kose S., 1998. **Non-linear Visco-elastic and Fatigue Properties of Asphalt Binders**. *Association of Asphalt Paving Technologists*. Pp 1 - 24

Bowering R.H., 1970. **Upgrading Marginal Road Building Materials with Foamed Asphalt**. *Highway Enigineering in Australia*. Mobil Oil of Australia, Melbourne South.

Cooley L.A., Stroup-Gardiner M., Brown E.R., Hanson D.I. and Fletcher M.O., 1998. **Characterisation of Asphalt-Filler Mortars with Superpave Binder Tests**. *Annual Meeting of Association of Asphalt Paving Technologists*, Boston.

Cooper K.E., Brown S.F. and Pooley G.R., 1985. **The design of aggregate gradings for asphalt basecourses**, *Proceedings of Association of Asphalt Paving Technologists*, Vol.54

Cooper K.E., Brown S.F., Preston J.N. and Akeroyd F.M.L., 1991. **Development of a practical method for design of hot-mix asphalt**, *Transportation Research Record 1317*, Transportation Research Board, Washington, D.C.

CSIR, 1986. **Technical Methods for Highways. TMH 1. Standard Methods of Testing Road Construction Materials**. National Institute for Transport and Road Research, Pretoria. Pp 147-149

Duriez, 1950. **Traité des matériaux de construction**, DUNOD, Paris.

Efrem G.E., 2000. **Stabilization of Cinder with Foamed Bitumen and Cement and its use as (Sub) Base for Roads**. Master of Science in Engineering Thesis. IHE University, Delft, Netherands.

Emery S.J., 1985. **Prediction of Moisture Content for use in Pavement Design**. PhD Dissertation. University of Witwatersrand, Johannesburg.

Fedors R.F. and Landel R.F., 1979. **An Empirical Method of Estimating the Void Fraction in Mixtures of Uniform Particles of Different Size**. *Powder Technology,* 23 (1979). Elsevier Sequola S.A. Lausanne. Pp 225-231

FHWA Federal Highway Administration, 1994. **Superpave Asphalt Mixture Design and Analysis**. Strategic Highway Research Programme, USA.

Francken L. and Vanelstraete A., 1993. **New developments in analytical asphalt mix design**, *Proceedings of the Eurobitume conference*, Stockholm

Fuller W.B. and Thompson S.E., 1907. **The laws of proportioning concrete**, Trans. ASCE, Vol. 59

Furnas C.C., 1928. **Relations between specific volume, voids and size composition in systems of broken solids of mixed sizes**, US Bureau of Mines, Report of Investigations, 2894

Goode J.F. and Lufsey L.A., 1962. **A new graphical chart for evaluating aggregate gradations**, *Proceedings of Association of Asphalt Paving Technologists, Vol. 31*

Goos D., Houtepen A. and Landa P., 1996**. Volumetric Composition Control during design and production of asphalt mixes**. Volumetric evaluation of mixes tested for the Dutch Heavy Duty Asphalt Pavement working group. *Eurobitume Congress*, Straatsburg

Hudson S.B. and Davis R.L., 1965. **Relationship of aggregate voidage to gradation**, *Proceedings of Association of Asphalt Paving Technologists*, Vol. 34

Humberto Castedo Franco L. and Wood L.E., 1982. **Stabilization with Foamed Asphalt of Aggregates Commonly used in Low-Volume Roads**. *Transportation Research Record 898*. Pp 297-302

Jenkins K.J., Hugo F., van de Ven M.F.C. and O'Connell J., 1997. **Bitumen Emulsion Stabilised Paving Blocks – Development of Labour Intensive Manufacture and Construction Techniques**. *Second World Congress on Emulsion, Ref 4.1b-257*. Bordeaux, France

Jenkins K.J. and van de Ven M.F.C., 1999a. **Mix Design Considerations for Foamed Bitumen Mixes**. *Conference on Asphalt Pavements for Southern Africa, CAPSA 1999*. Victoria Falls,Zimbabwe.

Jenkins K.J., van de Ven M.F.C., Ebels L.J. and Bredenhann S.J., 1999b. **Possibilities for Cold Mix Bituminous Paving Blocks**. *Conference on Asphalt Pavements for Southern Africa, CAPSA 1999*. Victoria Falls, Zimbabwe.

Khandal P.S., 1981. **Evaluation of Baghouse Fines in Bituminous Paving Mixtures**. *Journal, Association of Asphalt Paving Technologists*. Vol 50. Pp 150-210

Lee D.Y., 1981. **Treating Marginal Aggregates and Soils with Foamed Asphalt**. *Association of Asphalt Paving Technologists Volume 50*. Pp 211-250

Lees G., 1970. **The Rational design of aggregate gradings for dense asphaltic compositions,** *Proceedings of the Association of Asphalt Technologists*. Pp 60-99

Lubbers H.E.,1985. **Bitumen in de Weg- en Waterbouw**. Nederlands Adviesbureau voor Bitumentoepassinggen NABIT, In Dutch.

Molenaar J.M.M. and Molenaar A.A.A., 2000. **Fracture Toughness of Asphalt in the Semi-Circular Bend-Test**. *Wegboukundige Werkdagen 2000*. Doorwerth, Netherlands. Pp 163 - 177

Nijboer L.W., 1943. **Plasticity as a factor in the design of dense bituminous road carpets**, Amsterdam Laboratory of the N.V. DeBataafsche Petroleum Maatschappij (Royal Dutch Shell Group), Published by Elsevier Publishing Company, Inc

OCW (Opzoekingscentrum voor de Wegenbouw), 1947. **Handleiding voor de formulering van dichte bitumineuze mengsels**. Aanbeveling OCW – A61/87. Brussel.

Rigden P.J., 1947. **The use of Fillers in Bituminous Road Surfacings - A study of Filler-binder Systems in Relation to Filler Characteristics**. J.Soc Che Ind 66, pp 299.

Ridgeway K. and Tarbuck K.J., 1968. **Particulate Mixture Bulk Densities**. *Chemical and Process Engineering Journal* (2968). Pp 103-105

Roberts F.L., Engelbrecht J.C. and KennedyT.W, 1984. **Evaluation of Recycled Mixtures using Foamed Bitumen**. *Transportation Research Record 968*. Pp 78-85

Ruckel P.J., Acott S.M. and Bowering R.H., 1983. **Foamed-Asphalt Paving Mixtures: Preparation of Design Mixes and Treatment of Test Specimens**. *Transportation Research Record 911*. Pp 88-95

SABITA, 1993. **GEMS – The Design and Use of Granular Emulsion Mixes**, Manual 14, Cape Town

Saleh, A.H., 2000. **The Use of Mix Granulates Stabilized with Foamed Bitumen as Road Building Materials**. Master of Science in Engineering Thesis. IHE University, Delft, Netherands

Shackel B., Makiuchi K. and Derbyshire J.R., 1974. **The Response of Foamed Bitumen Stabilised Soil to Repeated Triaxial Loading**. *7th ARRB Conference. Volume 7 Part7*. Australia. Pp 74-89

Shashidhar N. and Romero P., 1998. **Factors Affecting the Stiffening Potential of Mineral Fillers**. *Transportation Research Record No. 1638*, Transportation Research Board, Pp 94 - 100

van de Ven, M.F.C., de Fortier Smit A. and Krans. R.L., 1997. **Possibilities of a Semi-Circular Bending Test**. *Eighth International Conference on Asphalt Pavements*, Seattle Washington

van de Ven M.F.C., 1998. **Spatial approach in hot mix asphalt design, just a buzz word?** *Sabita Digest*, Cape Town

van der Walt N., Botha P., Semmelink C., Engelbrecht F. and Salminen N., 1999. **The use of Foamed Bitumen in Full-depth In-place Recycling of Pavement Layers Illustrating the Basic Concept of Water Saturation in the Foam Process**. *Conference on Asphalt Pavements for Southern Africa, CAPSA 1999*. Victoria Falls,Zimbabwe

Verbert P., 1979. **Invloed van de Vullingsgraad op de Weerstand tot het vervorming van Asfaltmengsels**. Bituminfo 37/1979, Esso, Belgium

Verhaeghe B.M.J.A., van de Ven M.F.C., Grobler J.E. and Smit A. de F., 1995. **State-of-the-art review on volume-based asphalt mix design & provisional guidelines**, Volumetric design of asphalt, Phase 1, Report DPVT C-319-1F, Sabita, Cape Town

VBW Vereniging voor Bitumineuze Werking, 1992. **Asfalt Onderzoek**. Handleiding. Proef 1.3, Netherlands. Pp 16-21

Witczak M.W., 1972. **Design of Full-depth Asphalt Airfield Pavements**. RR 72-2. The Asphalt Institute, College Park.

CHAPTER 5

HALF-WARM FOAMED BITUMEN MIXTURES

1. BACKGROUND

Foamed bitumen has been in existence for more than forty years and has been successfully applied to aggregates at ambient temperatures in order to produce bituminous cold-mix, but no effort has been made to explore the benefits of heating the mineral aggregate before foam stabilisation. The "half-warm" process for foamed bitumen is aimed at improving the quality of foamed mixes and the benefit of the bitumen in the mix, through heating the aggregate above ambient temperature but below the temperatures required for hot mix production.

For many years pavement engineers have been aware of the influence of aggregate temperature on the performance of foamed bitumen mixes. However, the approach to aggregate temperature has generally been to establish a minimum critical temperature at which foamed bitumen treatment can be carried out without any detrimental effects to dispersion of the binder within the mix. Bowering and Martin (1976) refer to a "critical temperature" with a minimum of between 13°C and 23°C for the aggregate before foam treatment, depending on the aggregate type, below which mixes of poor quality are obtained. No mention is made of the influence of temperatures in excess of 23°C, mainly because these temperatures are not achievable using conventional cold in-place recycling and plant cold-mix techniques. Van Wijk and Wood (1983) merely specify a minimum temperature of 10°C for the aggregate during foam processing.

The primary improvement that is expected from the heating of aggregates before foamed bitumen treatment, is particle coating or binder dispersion. The coating of the mineral aggregate particles of an asphaltic mix has an influence on the performance of the mix. Improving the distribution of binder within a bituminous mix can increase the durability, resistance to water damage and consistency of the mix. This is the reason for certain specifications including a minimum film thickness of binder on the aggregate for HMA, for example. Particle coating is especially significant for foamed mixes where the droplets of bitumen provide the tensile strength in the mix. If these droplets are more evenly distributed, this could create a more continuous network or web of binder, which could increase the fatigue resistance of the mix.

This chapter covers research into "half-warm" foamed bitumen mixes that have been produced by heating the aggregate above ambient temperature but below 100°C before mixing. The research includes an initial feasibility study undertaken at University of Stellenbosch for ZNAC Contractors in Breda, Netherlands (Molenaar *et al.*, 1999) and (Jenkins *et al.*, 1999) followed by a second phase investigation carried out at Delft University of Technology into specific pavement materials (Jenkins *et al.*, 2000).

2. CONSIDERATIONS FOR HALF-WARM FOAMED MIXES

Comparisons between the characteristics of cold foamed bitumen mixes and hot mix asphalt provide a frame of reference for a perspective on half-warm foamed mixes. The half-warm mixes can be expected to fall within a transitional zone between cold and hot mix, thus adopting some of the characteristics of each whilst possibly losing others.

2.1 Energy Considerations

The production of conventional hot mix asphalt (HMA) uses a large proportion of the energy consumption for the evaporation of the aggregate's field moisture before mixing. The conversion of water into steam requires the latent heat of steam to be overcome, shown as the step in Stage 2 of Figure 5 - 1, which is a 500 times higher energy demand than the specific heat required by water per degree Celsius temperature change. The energy jump has been calculated using standard heat and thermo-dynamic considerations, as outlined in Chapter 3 Section 3.1, and is influenced most significantly by the moisture content of the mineral aggregate. In practise, the energy demands for heating of aggregates are some 10 to 20% higher than those given in Figure 5 - 1, due to the losses through radiation etc. that have been ignored in this simplified approach.

The advantages of remaining in the sub-boiling temperatures i.e. working entirely within Stage 1 of aggregate heating process, are apparent. Half-warm mixes, which are intended to remain entirely within Stage 1, will therefore enjoy the energy benefits illustrated in the step of the line in Figure 5 - 1 during Stage 2.

The increase of aggregate temperature in excess of 100°C to include "Warmed Foamed Bitumen Mixes" has not been considered in the research of half-warm mixes for a number of reasons:

- energy consumption benefits become redundant,
- moisture losses from the aggregate during mixing can reduce compactibility, and
- total loss of moisture from the mix making it a semi-hotmix with the potential benefits of cold mixes characteristics such as rut resistance being lost, especially where soft binders (penetration>80) are utilised.

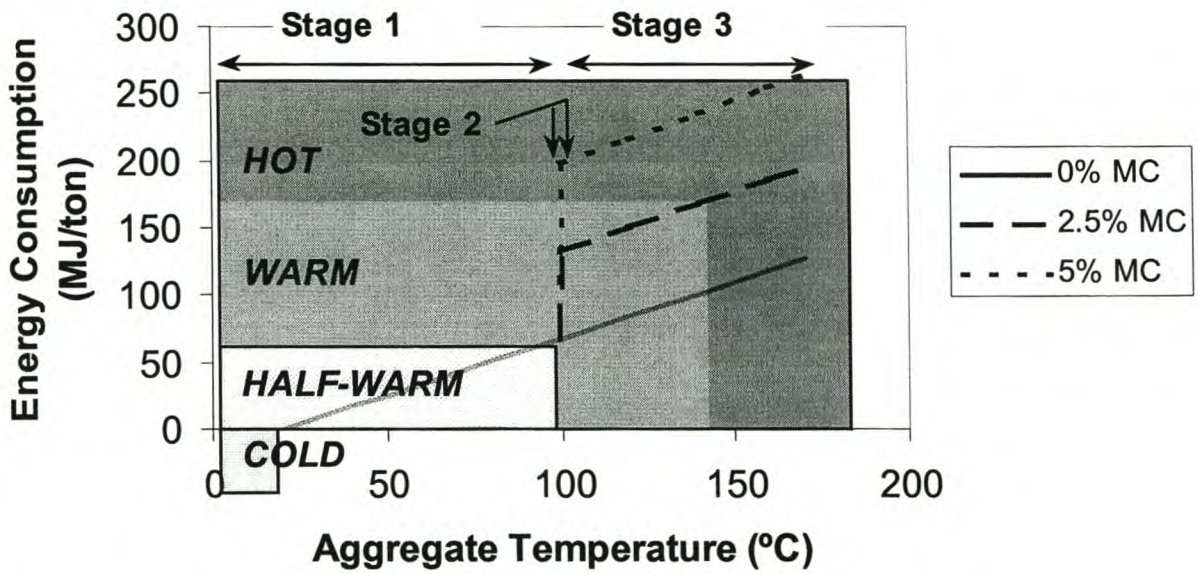

Figure 5 - 1. Classification of Asphaltic Mixes in terms of Aggregate Mixing Temperature and appurtenant Energy Consumption for Heating, Reference Material of 20°C and varying Moisture Content (MC)

The given reasons for maintaining aggregate temperatures of below 100°C in half-warm foamed mixes do not preclude the possibility of warm foamed mixes, with aggregate temperatures >100°C, being feasible for use in road pavements. For resource economy and research efficiency, however, the mixes with highest potential advantage require consideration. The term halfwarm® has become a registered product in the Benelux region for foamed mixes subsequent to this research.

2.2 Particle Coating

The influence of the aggregate temperature at the time of mixing, on the equilibrium temperature of the mix, is significant. Section 3 of Chapter 4 shows that the addition of foamed bitumen will only increase the temperature of a cold mix by some 7°C to 10°C for typical binder contents and that the original temperature of the aggregate has the dominant effect. For cold mixes, the temperature gradient between the aggregate and the foamed bitumen will significantly influence the rate of collapse of the foam. This occurs even though bitumen has relatively poor thermal conductivity properties because, in a foamed state, the surface area of bitumen that makes contact with the aggregate is high and the film thickness of bubbles is extremely thin, making the rate of heat transfer rapid.

The rate of collapse of the foam and hence the rate of viscosity increase of the binder during mixing, will therefore be rapid. Conversely, if the aggregate is at 90°C (after preheating), the equilibrium temperature of the mix will be marginally lower than 100°C.

The bitumen will therefore have a lower viscosity for a longer period during mixing, encouraging particle coating and binder dispersion in the mix.

The rate of heat transfer from the foamed bitumen to the aggregate can be estimated through the use of the coefficient of thermal conductivity of bitumen (γ = 0,17 Joule/m.s.Kelvin), which is 10 to 20 times lower than that of Limestone and Granite respectively. Considering that bitumen bubbles make contact with mineral aggregate, with a plausible film thickness of 0,01mm, implies that 189 Joules of energy can be transferred from the bitumen at 110°C to aggregate at 20°C in 1 second. This would enable one gram of bitumen to experience a reduction in temperature of 90°C. The high surface area of contact and the thin films of bitumen in the foam mass, permit rapid transfer of heat to the aggregate, therefore.

Considering energy transfer and the physics of foamed bitumen mixes, it is reasonable to expect that the concentration of the bitumen in the fine sand and silt fractions of cold foamed mix will change for half-warm mixes. Little or no coating of particles larger than 9,5mm occurs in cold foamed mix (Ruckel *et al.*, 1982), but this will change for half-warm mix. Particle coating is the most obvious manner in which cold and half-warm foamed mixes can be expected to differ.

By simplifying the individual particles into spherical shapes, the relationship between surface area and volume can be established. The relationship of the volume of a sphere to its radius is $V = \frac{4}{3}\pi r^3$ and area of a spherical particle is $A = 4\pi r^2$. As the size of a mineral aggregate particle (or radius) increases, therefore, the volume increases at a rate r/3 faster than the surface area. The corollary is that the mass : surface area ratio increases at the same rate, where particles have the same specific gravity. This is of relevance for mixtures of foamed bitumen and mineral aggregate, especially where the foamed bitumen has a temperature of 105°C to 120°C and the aggregate of some 10°C to 35°C. As the particles of mineral aggregate make contact with the foamed bitumen they acquire heat from the foam bubbles. Three possible scenarios have been identified for the metastable foamed bitumen:

1. If the particle penetrates the foam bubble, it may be burst mechanically leaving bitumen droplets either attached to or separate from the particle.
2. If a large particle makes contact with a foam bubble, high energy transfer will occur, reducing the steam pressure in the bubble causing it to collapse and reducing the temperature and hence increasing the viscosity of the bitumen, causing less coating of the particle surface as mixing continues.
3. If a small particle makes contact with the foam bubble, less heat is transferred, leaving the bubble either intact or deflated, but allowing the bitumen to retain more heat and hence remain at a lower viscosity. This allows the bitumen to displace the water around the particle and encourage coating on the relatively smaller surface area as mixing continues (before equilibrium temperature of the entire mix is reached).

A critical particle size will therefore occur in a specific mix, where complete coating is no longer possible. Ruckel *et al* (1982), from empirical observations and without the foregoing explanation, state that this critical diameter is that of fine sand for foamed-mix at ambient temperature. This critical diameter is not fixed, however, as it is related to the type and temperature of the aggregate, amongst other factors.

In addition to these scenarios, the number of particles of various sizes plays a role. The ratio of the number of particles of different sizes (radius r_1 and r_2) having the same mass is $r_1^3:r_2^3$. This indicates that during the mixing process, the probability of contact of a particle of a given radius with its own foamed bitumen bubble(s) will be inversely proportional to the third power of the radius of the particle. The necessity of including sufficient proportions of the fraction <0,075mm in the mix, which has been widely published in literature, becomes apparent. The filler fraction has an extremely high probability of particle contact with foam bubbles and will prevent the bitumen droplets from cohering to one another instead of the droplets adhering to the mineral aggregate.

In the context of the above, simplified physics of foamed bitumen mixing and distribution, the influences of heating the aggregate before mixing become apparent. As aggregate is heated, so the energy transfer from foamed bitumen to an aggregate particle during mixing will be reduced allowing the bitumen to remain at a lower viscosity and to completely or partially coat larger particles. Hence, the critical particle size that is completely coated may be increased, in theory.

3. APPRAISAL OF HALF-WARM APPLICABILITY TO VARIETY OF MIXES

3.1 Factors Selected for Consideration

As a feasibility study, the factors that could influence the behaviour of half-warm foamed mixes require investigation. These primarily include the following:

- Aggregate type and gradation.
- Aggregate temperature (at mixing and compaction).
- Associated factors e.g. the moisture content of the mix at the various stages of the production process.

A wide variety of materials require selection for the investigation, to assist in identifying possible boundaries between suitable and unsuitable aggregates. The different material types, gradations and aggregate temperatures selected, are shown in Table 5 - 1. The effects of these factors are measured in terms of the changes in mix properties, including particle coating, mix volumetrics and engineering properties. More detailed records of material properties are provided in Appendix C.

Table 5 - 1. Overview of Half-warm Foamed Mix Feasibility Study

MIX TYPES	FACTORS VARIED DURING EXPERIMENT	TESTS OR MEASURED EFFECTS
Continuously graded virgin materials	Parent material	Visual observation
Semi-gap graded virgin materials	Bitumen grade and binder content	Workability/Spreadability
RAP and RAP+virgin	Foam characteristics	Gyratory compaction
SMA	Mixing method and time	Volumetric properties
ZOAB (Porous Asphalt)	Mixing Temperature 30°C to 95°C	Selected ITS and SCB Tests
Gravel	Compaction Temperature 20°C to 70°C	
Sands	Mixing Moisture Content	
	Compaction Moisture Content	

3.2 Laboratory Manufacture of Half-warm Mixes using Hobart Mixer

The procedures for making half-warm foamed mixes in the laboratory require pursuance of several objectives:

- To simulate the possible manufacture of these mixes in a plant.
- To investigate possible benefits of modifications to standard asphalt mix manufacturing procedures.
- To attempt to optimise the benefits of heating the aggregates without inefficiencies.

These objectives are not mutually inclusive and variations to the standard procedures are therefore required. The deviations from the standards are outlined in Appendix C with a summary of activities given in Figure 5 - 2, showing the mixing process utilised for half-warm foamed mixes in the laboratory.

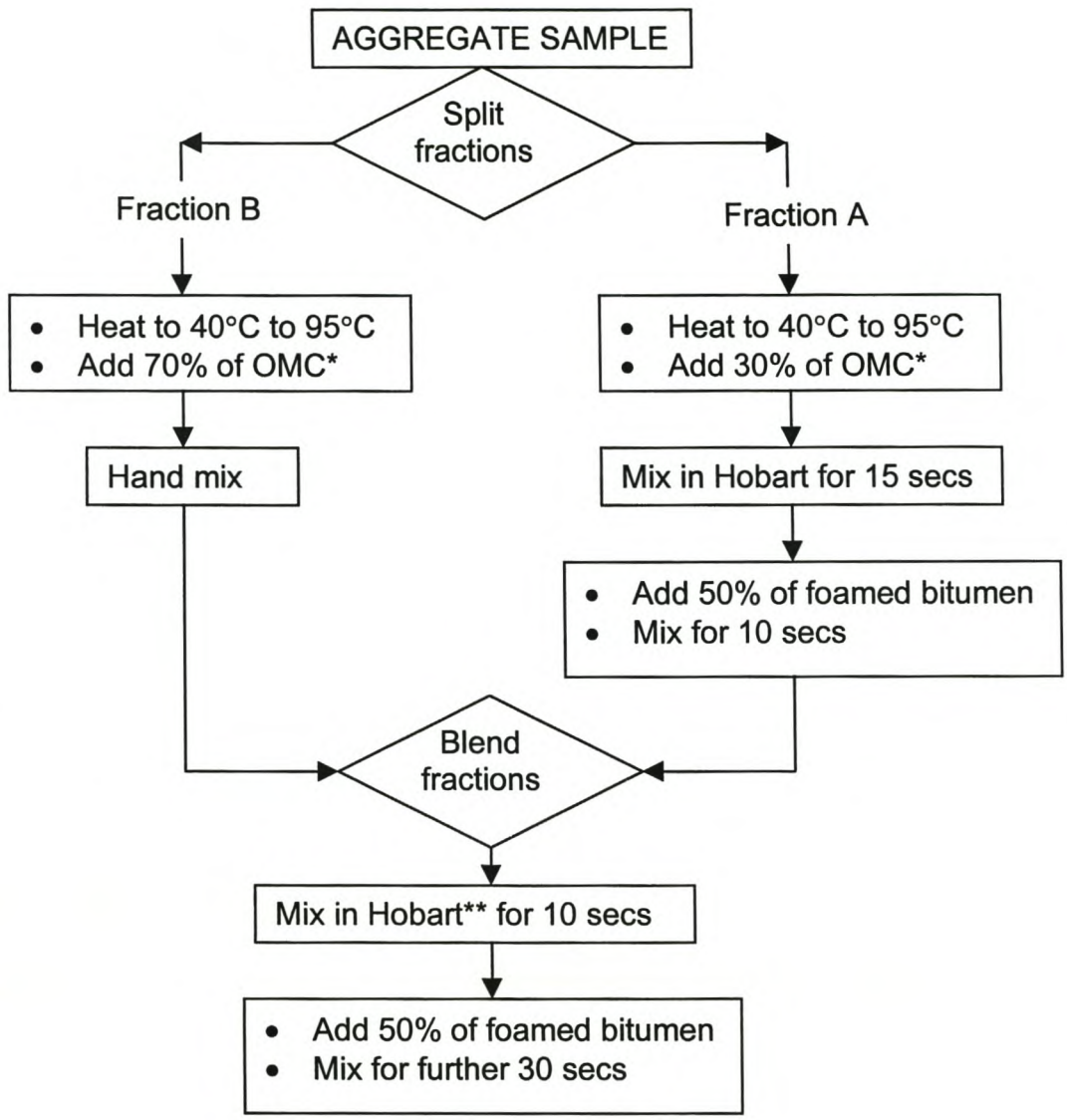

Figure 5 - 2. Flow chart for laboratory mixing of Half-warm Foamed Mixes

* The percentage of optimum moisture content added to the mix may change depending on aggregate temperature, but the 70:30 ratio should be maintained.

** Hobart Mixer ® is a blender type mixer

The initial estimates for proportioning of the moisture in the mix between the two aggregate fractions were carried out using surface area calculations (Asphalt Institute, 1993). The equation that is applicable for the calculation of total surface area is given below:

$$A = (41 + 0.41*a + 0.82*b + 1.64*c + 2.87*d + 6.14*e + 12.29*f + 32.77*g)/100$$

Equation 5 - 1

Where,

A = surface area of entire grading in m^2/kg
a = percentage passing 4,75 mm sieve
b = percentage passing 2,36 mm sieve
c = percentage passing 1,18 mm sieve
d = percentage passing 0,60 mm sieve
e = percentage passing 0,30 mm sieve
f = percentage passing 0,15 mm sieve
g = percentage passing 0,075 mm sieve

The ratio of the surface areas for two aggregate fractions is used to proportion the moisture for a continuously graded mix between the two fractions i.e. Aggregate Fraction A and Fraction B. Such proportioning is necessary when two fractions are blended separately with foamed bitumen. This approach results in a distribution of 1:10,5 for $Moisture_A$:$Moisture_B$ (the ratio that the moisture is to be divided between the two fractions). In practise, the use of the small proportion of moisture in the large aggregate during application of the half-warm process, provides poor coating of the large particles with foamed bitumen, primarily due to excessive loss of moisture from the large aggregate during mixing. Experimentation with different amounts of moisture assisted in identifying a ratio of 3:7 as being more suitable, regardless of gradation. The same principle applies to the proportions of binder applied to each fraction where a ratio of 1:1 is acceptable. The disproportionately high binder added to the large aggregate encourages coating. Table 5 - 2 provides a summary of the recommended mixing ratios.

Table 5 - 2. Mixing ratios for Half-warm mixes in Hobart ® Mixer

FRACTION	A	B
Mixing Moisture	3	7
Foamed bitumen	1	1

In addition, the splitting of aggregate into two fractions, which follows the K.G. Ohlson (KGO) method of mixing asphalt, has been found to improve binder distribution during laboratory mixing, but is not necessarily intended for application in pugmill type mixing.

3.3 Moisture Regime

In Chapter 4 the importance of moisture in a foamed mixture with regard to both the dispersion of the foamed bitumen, as well as the shelf-life, compaction and properties of the mix, has been outlined. In the case of the half-warm mix, the raised equilibrium temperature has the effect of exciting some water molecules to such a degree that moisture is rapidly lost from the mix, making this an important aspect to monitor. Not only does the raised temperature of the aggregate influence the viscosity of the foam as it subsides, but the moisture regime too.

The moisture regime in half-warm foamed bitumen mixes has been monitored at various stages in the laboratory production process, see Appendix C. Using the data from seven different mixes, at an average of four different temperatures each, a relationship has been established for the loss in moisture during half-warm foamed bitumen treatment. This relationship is outlined in Equation 5 - 2.

$$MC_f = 0.640*MC_I - 0.0232*T_a - 0.093*BC + 2.978 \qquad \textbf{Equation 5 - 2}$$

Where,

MC_f = Final moisture content immediately after mixing (%)
MC_I = Initial moisture content immediately before mixing (%)
T_a = Temperature of Aggregate (°C)
BC = Binder content of foamed bitumen (% m/m of aggregate)

The coefficient of correlation ($R^2 = 0.60$) for this relationship is acceptable for its purpose, albeit low, considering that through intentional simplification, certain factors such as aggregate type, absorption, mixing methodology etc, have been ignored. It provides a useful estimation of the moisture loss that needs to be compensated for, when using the half-warm process in the laboratory with a vertical-agitator or blender type mixer. For the relationship to remain valid, the bitumen should be below 190°C, the mixing time should not exceed 20 seconds (in the laboratory) and the aggregate temperature should range between 45°C and 98°C.

The selection of a mixing moisture content of 65% to 85% of optimum moisture content for the various mixes, in accordance with the "fluff point" or minimum bulk density for mixing, which is a cold mix design approach outlined in Chapter 2, is insufficient therefore. Up to 2.5% of moisture will be lost during mixing with aggregate at 90°C. An adjustment to this initial moisture content is required using Equation 5 - 2 in order to ensure adequate mixing. The actual moisture content after mixing should also be monitored in order to make adjustments for more accurate results. If not accounted for, the moisture deficit can have detrimental consequences in terms of particle coating, balling within the mix and compaction.

Visual assessment confirms that half-warm foamed mixes may be produced with either cold or heated water added to the heated aggregate as mixing moisture. Heating of the water improves binder dispersion and particle coating.

3.4 Particle Coating

The theory of foamed mix physics explored in Section 2.2 requires verification through a sensitivity analysis of a number of mixes with regard to aggregate temperature. Aggregate temperatures ranging between 30°C and 90°C are applicable for this purpose (Molenaar *et al.*, 1999) as this covers plausible temperatures above typical ambient temperatures.

The changes in binder distribution with different aggregate temperatures at mixing for a continuously graded Hornfels material with a maximum particle size of 26,5mm have been

observed. The findings are applicable to semi-gap graded materials too, see Appendix C. Improvements in distribution of the binder were assessed visually and quantitative measurements made by dividing the mixed aggregate into three binder coating categories:

1. *Practically uncoated particles*, with less than 20% binder coverage.
2. *Partially coated particles*, with 21% to 99% coverage, and
3. *Completely coated particles*, with 100% coverage.

The selection of these categories is based on typical ranges of coating that occur with foamed bitumen treatment. Very few particles are observed with no coating whatsoever, as lumps of mortar and mastic adhere to larger aggregate even if pure binder does not coat these larger particles.

Repeat tests with different aggregate temperatures lead to the relationship graphically illustrated in Figure 5 - 3. The influences of aggregate temperature on particle coating are applicable to semi-gap graded materials too, as well as continuously graded natural gravel and sand materials. Significant darkening of the mix is visually apparent as the mixing temperature of the aggregate is increased. This is not the case, however, for Stone Mastic Asphalt and Porous Asphalt mixes mixed in a Hobart Mixer®. These mixes show some improvement in particle coating but stripping of the binder from the larger aggregate occurs during prolonged mixing.

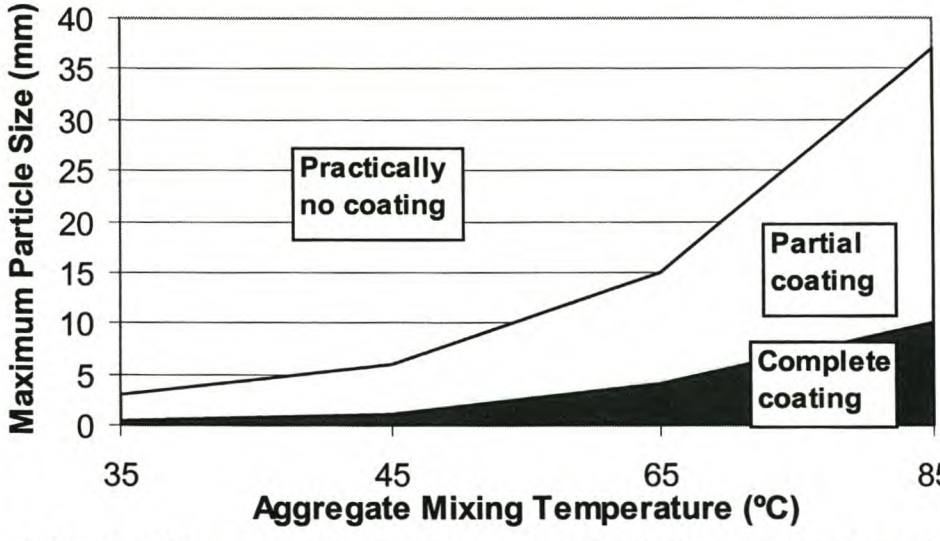

Figure 5 - 3. Effect of Aggregate Temperature on Particle Coating for a Continuously Graded Hornfels mixed with Foamed Bitumen

Half-warm foam treatment of reclaimed asphalt pavement (RAP) materials can be carried out in two fundamentally different approaches i.e. with the addition of at least 4% filler, as well as water or without these additions. Visually, these two approaches provide markedly different mixes. The first approach produces a mix resembling cold mix, with some natural colour of the aggregate still apparent and dull coloured binder, but improved aggregate coating. The second method, particularly at temperatures in excess of 85°C, produces a

mix that closely resembles HMA i.e. completely coated, even though the RAP itself may have had stone colouring due to some fractured faces before mixing.

In addition to coating influences, the inclusion of water in the recycled material before mixing has a bearing on the shelf-life of the mix. The water and filler assist in providing a workable mix at ambient temperature i.e. the same attributes of a cold mix, whereas the half-warm RAP mix without filler or water, particularly when heated to 87°C, requires placement and compaction at a minimum temperature of 65°C. The differences in the two approaches are summarised in Table 5 - 3.

Table 5 - 3. Characteristics of Half-warm Foamed Mixes with Recycled Asphalt

RAP supplements	Filler + Water	None
Particle Coating with bitumen	Partial	Complete
Shelf-life	Good	Very poor

3.5 Workability of Half-warm Mixes

Although no limits have been established for the cohesion of half-warm mixes for mix design purposes, this parameter provides a measure of workability of a mix. The cohesion of foamed bitumen stabilized sand has been investigated using a vane shear device (Acott, 1980) with particular reference to situ measurements. The properties measured using this device are relevant to workability, as cohesionless material can experience segregation whilst a mix with high cohesion will be difficult to spread and can shear during placement.

The influence of half-warm mixing with foamed bitumen on the cohesion of the material is apparent for the two mixes shown in Figure 5 - 4 (each point on the graph is an average of three tests). In order to maintain a standard consistency, three blows of the Marshall hammer were applied to each foamed mix followed by testing of the material in a 100mm diameter mould at 50°C.

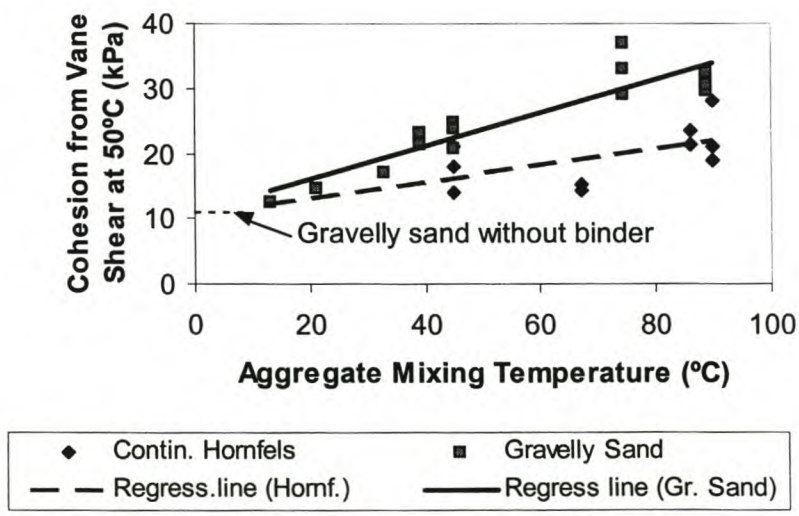

Figure 5 - 4. Influence of Mixing Temperature on Cohesion for Half-warm Foamed Bitumen Mix

The trend in the cohesion relative to the aggregate mixing temperature matches the expected behaviour considering the nature of the materials. The improvement in cohesion and hence shear strength of a foamed mix with increasing mix temperature, is more apparent for a fine grained material where the binder has more influence than aggregate interlock than for the coarse grained material. Increased cohesion could result from improved continuity of the binder in the mix where aggregate temperatures are higher; the aggregate interlock is not temperature dependent and will remain constant. Even within a range of ambient mixing temperatures (10°C to 45°C), the materials exhibit a notable increase in cohesion, a phenomenon discussed in Section 3 of Chapter 4.

The implications of the trends in cohesion measurements on the predicted workability of the half-warm foam treated materials are less significant than the possible improvements in mix performance. Not only will increased cohesion result in a raised limit for the shear envelope of the material in question, but improved continuity of the binder in the mix could substantially improve the tensile strength of the mix. This is the premise for the additional investigation of half-warm mixes, covered in the latter half of this Chapter.

3.6 Compaction

Previous research has consistently yielded the conclusion that an increase in the density of foamed bituminous mixes results in an improvement in various engineering properties of the material. In particular, the stability and stiffness of these mixes have been shown to increase with higher levels of compaction. In addition, it has been shown by Eggers *et al.* (1990) that increasing the compaction temperature of foamed mix increases the density of the mix and consequently the material properties are improved.

The findings of Eggers *et al.* have been found to be applicable to half-warm foamed mixes too. Continuously graded Hornfels mixed at 90°C with foamed bitumen has been shown to yield a decrease in air voids of some 2% with an increase in the compaction temperature of 42°C, see Table 5 - 4. The binder contents of these mixes are provided in Appendix C. The air void content is calculated in the absence of moisture.

Table 5 - 4. Compaction Characteristics of Half-warm Mixes in Gyratory Compactor

Grading	Gyrations	Half-warm Foamed Mix Properties					
Continuous	147	Mixing Temp (°C)	45	67	86	90	Comp Temp 28°C
		Voids (%)	5.0	5.8	5.1	5.0	
Continuous	147	Comp. Temp (°C)	34	39	52	76	Mixing Temp 89 to 97°C
		Voids (%)	6.5	6.1	5.5	4.7	
Semi-gap	147	Mixing Temp (°C)	45	55	70	85	Comp. Temp 28°C
		Voids (%)	7.0	6.4	5.8	5.8	

The sensitivity analysis of selected mineral aggregates with varying mixing temperatures, summarized in Table 5 - 4, provides insight into the effects of the half-warm process on compaction. The gyratory compactor utilised in this investigation is suitable for the analysis of mixes at different levels of compaction. Dependent on the type of material and anticipated levels of traffic usually encountered by such a material, the relevant number of gyrations may be selected (using the HMA requirements as a guide). In this case the selection included 147 gyrations for continuous and semi-gap graded, 75 gyrations for gravel, 60 gyrations for ZOAB and SMA and 46 gyrations for sandy gravel. Compaction at equivalent ambient temperature is necessary as a reference i.e. 28°C in this case. A repeat test is required for statistical reliability. The standard Superpave settings of 1,25° angle of gyration, 600 kPa ram pressure and 30 revolutions per minute were applied during gyratory compaction. Besides slight variation in the compaction moisture content, the aggregate temperature at mixing was the only variable in this aspect of the experiment.

The summary provided in Table 5 - 4 of the results described in Appendix C, shows that aggregate temperature during mixing influences the air voids achieved for that mix at a specific compactive effort. The general trend shows decreasing void contents for continuously and semi-gap graded foamed mixes produced at higher aggregate temperatures, although the fluid content of these mixes cannot be accurately controlled in the laboratory during compaction. This fluid content will also have a bearing on the compaction of the mix.

4. DETAILED INVESTIGATION OF CONTINUOUSLY GRADED HALF-WARM MIX (STAB)

Initial investigation of selected mechanical properties of half-warm mixes comprised mainly Indirect Tensile Strength (ITS) Tests and Semi-Circular Bending (SCB) Tests to obtain a measure of the tensile strength foamed mixes produced at different aggregate temperatures (Molenaar *et al.*, 1999). The pertinent results of these tests are detailed graphically in Appendix C. Notwithstanding significant variability in results, which is inherent to the ITS test, refer Appendix G, trends of increasing tensile strength with increasing aggregate mixing temperature are apparent. These trends are applicable to half-warm foamed mixes using natural sand and gravel, as well as semi-gap and continuously graded crushed mineral aggregate.

The trend of tensile strength and particle coating, especially with regard to the continuously graded mix with both virgin and recycled aggregate (RAP), forms the basis of mix selection for further detailed investigation of half-warm mixtures. The second phase investigation that is detailed in this section comprises aggregates utilised in the Netherlands in contrast to the South African aggregates used in the foregoing research.

4.1 Mix Composition

The continuously graded mix utilised for more detailed investigation of the half-warm foam process was selected in terms of the requirements of the RAW Specifications (CROW, 1995) for "Steenslagasfalfbeton" (STAB) or asphalt concrete. The same components and gradations were selected for all of the mixes used in the investigation. For purposes of

analysing the influences of the half-warm process on the behaviour of the mix, the equivalent mixtures with identical mineral aggregates, using both the cold foamed mix process and the hot mix process, were also tested as reference mixes. In addition, a mix comprising 50% virgin aggregate and 50% RAP, the blend of which had the same composite gradation, was also investigated. The components of the virgin mixes are detailed in Table 5 - 5.

Table 5 - 5. Components and Gradation of STAB Mix

Component	Source	Fraction of mix (% m/m)	Sieve Opening (mm)	Cumulative percent passing m/m (%)
Filler (<0,063mm)	Wigras 40K	5,4	22,4	100
	Parent filler	1,3	16	99,1
Sand	Riversand 0/2	37,8	11,2	89,32
Stone	Granite 8/16	35,3	8	75,26
	Moreane 4/8	20,2	5,6	61,68
			2	46,28
			0,063	8,04

A graphical representation of the gradation of the STAB mix shows the comparability to a Fuller gradation for the equivalent 0/16 aggregate (with n=0.45). As a reference, Figure 5 - 5 provides the appurtenant gradations relative to the zones of material suitability recommended by Ruckel *et al.* (1982) for cold foamed mix, where:

- Zone A : Most suitable aggregate for cold foamed mix
- Zone B : Less suitable aggregate for cold foamed mix
- Zone C : Unsuitable aggregate for cold foamed mix

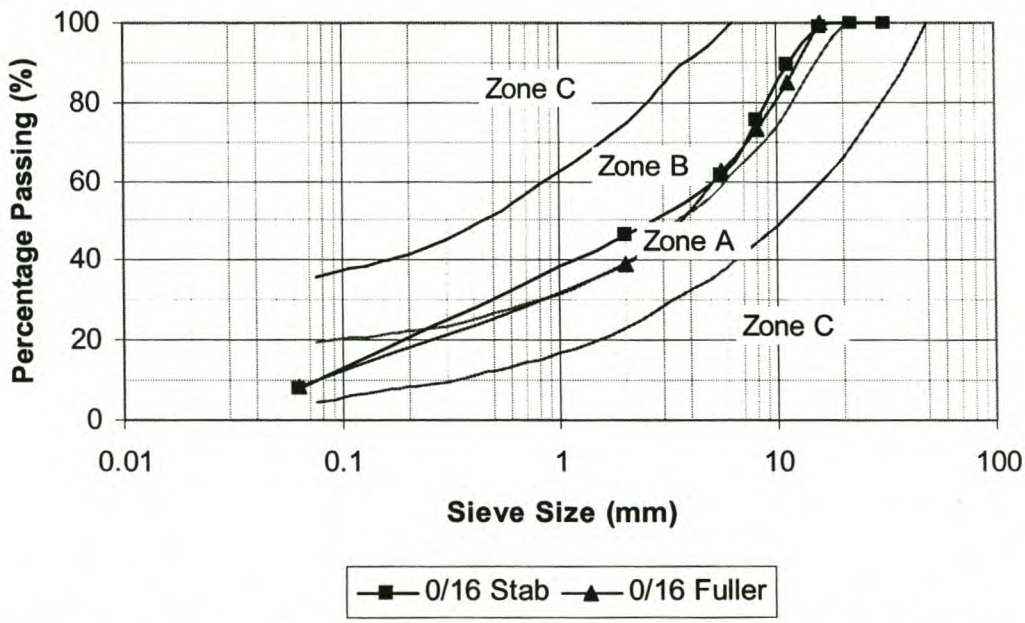

Figure 5 - 5. Gradation Curve for STAB Mix and Fuller relative to Zone Suitability Limits, after Ruckel *et al.* (1982)

The bitumen utilised as binder for the STAB was selected on the basis of foaming properties. A higher penetration bitumen is necessary for use in the half-warm stab mix manufactured using RAP than that utilised in the STAB mixes incorporating virgin aggregates, see Table 5 - 6, in order to obtain equivalent composite binder penetrations for all mixes. The penetration of the recovered binder of the RAP averaging approximately 10, makes it necessary to add considerably softer bitumen than 200 penetration bitumen to approach 80 penetration. Using the approach of "Proef 56.0" of RAW (CROW, 1995) see Equation 5 - 3, a composite penetration of 36 is obtained, but this requires complete blending of old and new bitumen, an unlikely scenario for half-warm mixes.

$$A \times \log (Pen_1) + B \times \log (Pen_2) = (A+B) \times \log (Pen_{blend}) \qquad \textbf{Equation 5 - 3}$$

Where,

A = proportion of old bitumen by mass
B = proportion of new bitumen by mass, with A+B = 1
Pen_1 = Penetration of old bitumen (dmm)
Pen_2 = Penetration of new bitumen (dmm)
Pen_{blend} = Penetration of blended bitumen (dmm)

Table 5 - 6. Bitumen and Foam Properties

Mix Type	Bitumen	$T_{r\&b}$ (°C)	Pen (dmm)	PI	Expansion Ratio	Half-Life (secs)	Foam Index
Cold, HW and HMA STAB	Elf B80E	46,5	84	-0.843	20,5	10	138
HW STAB with RAP	Elf B200E	38,5	176	-1.273	18	12	124

The selection of a binder content based on mix design experience with this mix with achievement of desirable mix properties, was 4,5% m/m of aggregate. For reference purposes this binder content forms the basis for the production of all mixes in the investigation, with the exception of one Half-warm RAP+STAB mix where the binder content was increased to improve mix properties.

4.2 Mix Production and Specimen Manufacture

4.2.1 Half-warm mix production procedure

The initial investigation into the feasibility of half-warm foamed bitumen mixes has highlighted the importance of the control of moisture content and temperature of the aggregate before mixing, see Section 3. In addition, through analysis of the mechanisms for binder dispersion in these mixes, it becomes clear that the method of mixing is an important contributing factor to the characteristics of the mix. Although the use of a twin-shaft pugmill mixer in the laboratory as opposed to a Hobart ® mixer for half-warm foamed mix production is advantageous for improved simulation of in-plant production, adjustments to the mix manufacture procedure become necessary.

The selection of a pugmill mixer necessitates reinvestigation of an optimal mixing procedure. For this purpose, a sensitivity analysis of relevant factors is required, taking account of moisture content before mixing, temperature at mixing, fractionation of mix and staged mixing, duration of mixing, compaction temperature and compactive effort i.e. number of gyrations in gyratory compactor. In the analysis of these factors, the objective played an important role i.e. to produce an asphaltic mix with the best overall properties without exceeding a 100ºC limit for aggregate temperature at mixing. The basis of this objective is optimal energy conservation through preclusion of the necessity for drying.
Visual observation of half-warm foamed mix production provided the criterion for optimisation of the factors in the sensitivity analysis. Improvement in binder dispersion within the mix through adjustments and alterations in the mixing procedure is readily apparent to the naked eye. Selected compactability tests of mixes emanating from the sensitivity analysis verified the visual observations with improved dispersion providing reduction in air voids in the mix. These trials lead to the mixing procedure provided in Appendix D. This method includes important monitoring activities such as checking mix temperature (using an infra-red gauge) and moisture content at various stages of half-warm mix production.

4.2.2 Gyratory Compaction

The SHRP Superpave initiative (FHWA,1994) has further developed the technique of gyratory compaction of asphaltic mixtures in the laboratory for both mix analysis and specimen preparation. The principle of gyratory compaction is based on subjection of an asphaltic mix to compressive and shearing forces similar in nature to those encountered under a roller during layer compaction in the field. The gyratory compaction technique is further considered to simulate additional compaction of the material during trafficking of the material. In the former objective, the Superpave Gyratory Compactor (SGC) is considered successful and therefore preferred to alternative methods such as impact compaction (such as Marshall). The latter objective of relating gyratory compaction to traffic compaction has not been completely verified and correlation, therefore, remains unreliable.

Standard Superpave Gyratory Compactors work to a specified angle of gyration of 1,25º under a compressive pressure of 600 kPa with compaction occurring at 30 gyrations per minute. In addition, the SGC's provide the facility for measurement of specimen height for each gyration. Given mix properties such as Maximum Theoretical Relative Density and the mass of mix in the compaction mould, the air voids can be monitored during compaction.

For the purpose of foamed mix production, the advantages of gyratory compaction remain valid. The guidelines of FHWA (1994) provide a useful means of determination of number of gyrations required to achieve compaction (N_{des}) equivalent to field compaction during construction. For this purpose N_{des}=80 was selected for the HMA STAB mix utilising the standard gyratory settings of the Pine Gyratory Compactor®. The voids obtained for the HMA STAB namely V_a (average) =3,2% provided the target voids for the equivalent foamed mixes both cold and half-warm. In order to achieve the same level of compaction,

an initial analysis was carried out with each mix compacted to 150 gyrations. Using these results, the number of gyrations to achieve 3,2% voids could be determined and utilised.

Following compactability analysis of each mix with the gyratory compactor, the number of gyrations for equivalent air voids could be determined. Table 5 - 7 provides the selected number of gyrations for each mix.

Table 5 - 7. Selection of Compaction Levels for Gyratory Compactor

MIX	HMA STAB	HW STAB	HW RAP+STAB (50:50)		CM STAB
Binder Content (%)	4.5	4.5	4.5	5.0	4.5
Gyrations (N_{des} for 3,2% voids)	80	80	80	80	250

4.2.3 Reduction of Edge Effects of Test Specimens

The influence of large aggregate particles seated against the annulus of a mould on reduction of mix homogeneity is well documented. Van de Ven *et al.* (1997) for example, recommend a procedure for taking account of this effect for stone mastic asphalt specimens. For test specimens, however, it is preferable to eliminate or reduce this affect. For this purpose 150mm diameter specimens have been compacted in the gyratory compactor followed by vertical coring out of 100mm diameter specimens from the centre of the cylindrical specimen. The maximum particle size to diameter ratio was 1:5,6 for the cores.

The benefits of such a procedure are measurable from the trends in density resulting from the coring. Comparisons made between the original 150mm diameter specimens and the cores of 100mm are given in Table 5 - 8. Reduction of the edge effects results in 0.01% to 0.30% increase in the bulk density. This procedure allows more accurate simulation of behaviour of the materials in the road pavement where edge effects are not prevalent within a layer.

Table 5 - 8. Density Comparison between Gyratory Specimens Before and After Coring, Average Values

	Bulk Relative Density (kg/m^3) (Standard Deviation)				
Mix Type	**HMA STAB**	**HW STAB**	**HW STAB+RAP (Low BC)**	**HW STAB+ RAP (high BC)**	**CM STAB**
150 mm specimen	2398.9 (12.0)	2386.2 (21.8)	2401.7 (6.8)	2387.9 (11.7)	-
100 mm core	2404.4 (13.0)	2386.4 (16.8)	2409.0 (5.8)	2388.8 (8.1)	2257.4 (10.3)
Difference (%)	+ 0.23	+ 0.01	+ 0.30	+ 0.04	-

4.2.4 Properties of Equivalent Mixes during Production

During the production of the equivalent hot, half-warm and cold mixes, the desired properties are not precisely achievable. For this reason monitoring of the relevant properties for the different mixes is required. Table 5 - 9 provides a summary of the average values achieved for the various mixes with their appurtenant variability.

Table 5 - 9. Mix Properties during Production of Hot, Half-warm and Cold Mix STAB; Mean Value (Standard Deviation)

Property	HMA STAB	HW STAB	HW RAP+STAB (50:50)		CM STAB
Mixing temp. (°C)	157,9 (13,3)	101,5 (2,5)	100,2 (3,9)	101,4 (3,6)	19,5 (0)
Mixing moisture (%)	-	3,0	3,0	3,0	3,0
Target binder (%)	4,5	4,5	4,5 (5,32 in RAP)	5,0	4,5
Actual binder (%)	4,57 (0,21)	4,98 (0,50)	4,80 (0.15)	5.38 (0.20)	5.02 (0.05)
Moisture after mix (%)	-	0,63	0,90	0,91	3,0
Compaction temp (°C)	147,2 (13,4)	89,1 (6,7)	86,7 (7,1)	86,3 (4,2)	31,4 (1,9)
Void content (%)	3,2 (0,5)	4,0 (0,7)	2,8 (0,2)	4,0 (0,3)	8,9 (0,4)

It is apparent from Table 5 - 9 that utilisation of optimum fluids and higher compaction energy for Cold Mix STAB i.e. a substantial increase in the number of gyrations, is insufficient to obtain the equivalent voids in the mix. It is not possible to achieve the same level of compaction for a cold mix as is obtained for a half-warm mix.

4.3 Experimental Design and Test Procedures

The initial phase of the detailed investigation was aimed at characterising the half-warm foamed bitumen mixes relative to the equivalent hot mix and cold foamed mix by means of static tests. These tests include compression tests and shear tests at a range of different temperatures and loading speeds. A complete factorial experimental design is not possible for such an investigation, so a partial factorial design is required, see Table 5 - 10. The properties measured using these tests also provides the information necessary as input parameters for three-dimensional finite element models for modelling asphaltic materials (Erkens and Poot, 1998). This facilitates possible simulation of the behaviour of such layers in a pavement once the model is sufficiently developed.

In general, tests were restricted to three repeats per set of factors; however, where the repeatability was inadequate, additional tests were carried out. The sensitivity analysis was so selected to enable development of functions for compressive and shear strength with respect to temperature and loading rate. Test temperatures of between 8°C and 40°C were

selected with the exception of the shear test where a maximum of 25°C was achievable in the test set-up.

Table 5 - 10. Experimental Design for Static Compression and Shear Tests

Displacement Rate		5mm/m	25,4 mm/minute				50,8 mm/minute			
Temperature of Test (°C)		13	8	13	25	40	8	13	25	40
Unconfined Compression Strength UCS			3A 3C 3D	4A 3D	3A 3C 3D	3C	3A 3RB 3HB 3C 3D	4A 3C 3D	3A 3RB 3HB 3C 3D	4A 3RB 3HB 3C 2D
Leutner Shear Test (normal stress)	0 MPa	3A 3HB 3C 3D	3A 3D	3A 3HB 3C 3D	3A 3D		3A 3C 3D	3A 3RB 3HB 3C 3D	3A 3RB 3HB 3C 3D	
	0,55 MPa			3A 3C 3D				3A 3C 3D		
	1,15 MPa	3HB	3A 3D	3A 3HB 3C 3D	3A 3D		3A 3C 3D	3A 3RB 3HB 3C 3D	3A 3RB 3HB 3C 3D	

Legend:
3A = 3 repeat tests for Mix A
A = Mix A Half-warm Foamed STAB
RB = Mix B Half-warm RAP + STAB at representative binder content
HB = Mix B Half-warm RAP + STAB at 0,5% higher binder content
C = Mix C Cold Foamed STAB
D = Mix D Hot-mix STAB

4.3.1 Unconfined Compressive Strength (UCS) Test Set-up

The Unconfined Compressive Strength Test is a test where uniaxial compression is applied to a cylindrical specimen at its extremities by means of end plates. Due to the loading rate and temperature dependent nature of bituminous materials, test conditions need to be selected to cover a range of these parameters. The tests were performed in the displacement-controlled mode with a continuous axial deformation rate.

The compression test set-up comprises a three-dimensional space frame in which an hydraulic MTS actuator is mounted, refer to Erkens and Poot (1998). During the test, the axial deformation and the applied force are registered via the displacement transducer

(LVDT) in the MTS loading jack and the load cell respectively. This excludes measurements of radial deformation and accurate initial axial deformation as undertaken by Erkens and Poot. The temperature of the top and bottom loading plates in the climate chamber are monitored during the test by means of thermo-couples.

The friction reduction system developed by Erkens and Poot (1998) was implemented during the testing of the foamed mixes. This is necessary to reduce the significant convoluting effect of friction between the end plates and the asphalt specimen that causes a reduction in radial deformation and over-estimation of the compressive strength of specimens that have a height to diameter ratio of less than $^{2}/_{1}$. The glycerine soap and foil that is applied to either end of the asphalt specimen has been shown to successfully reduce the friction sufficiently for specimens with height over diameter ratios of less than $^{1}/_{1}$ (Erkens and Poot, 2000). The $^{130}/_{100}$ ratios for half-warm specimens used in the investigation are thus satisfied using this technique.

The work of Erkens and Poot (1998) has shown that the force and displacement signals at the beginning of a uniaxial compression test do not immediately follow a constant rate of increase. A correction for this initial transitional period can be made through additional measurements with a short-range LVDT. In the absence of such an implement in the half-warm research, correction of the origin of the force-displacement relationship needs to be made through a lateral shift in the curve to ensure that the linear-elastic portion of the line passes through the origin, see Figure 5 - 6.

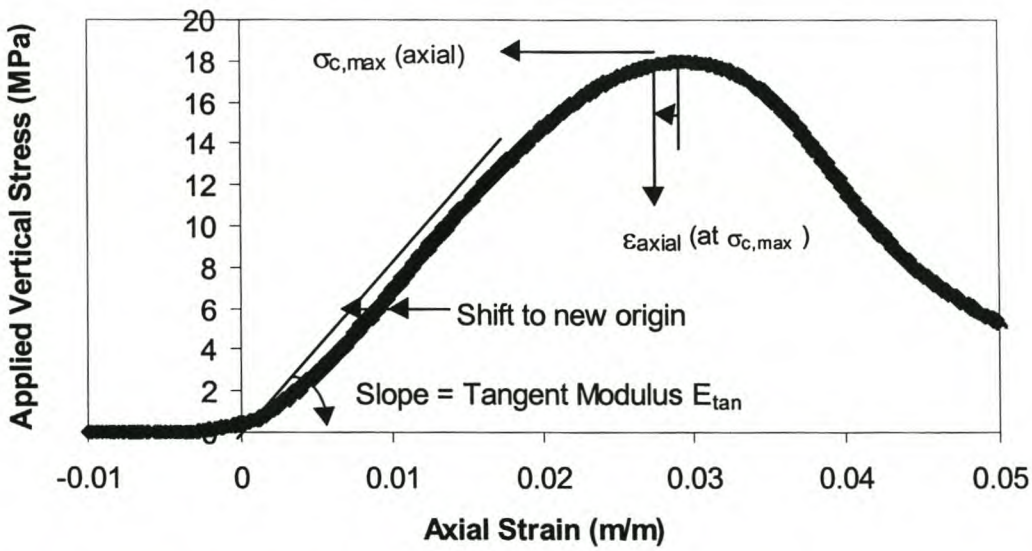

Figure 5 - 6. Typical Uniaxial Compression Test Result with Pertinent Parameters

The dissipated energy of such as test can be estimated by the area under the stress-strain curve of the results. This is relevant for comparison of materials as it is a measure of the different capacities of the equivalent mixes to dissipate the energy under given test conditions. By definition, the dissipated energy has been calculated up to the optimum point on the graph, see Figure 5 - 6 using the relationship developed in Equation 5 - 4, using units of MPa. The maximum axial stress (σ_{max}) is first corrected for displacement rate

actually measured where this deviates from the desired value, using a linear relationship between σ_{max} and displacement rate, then the dissipated energy factor is calculated. The given relationship uses approximation of two linear relationships for the curve to the optimum point. Results that do not exhibit predominantly linear behaviour to the peak, should not be analysed with such a relationship. The results of this investigation were found to be suited for application of this equation, however.

$$DissipatedEnergyFactor_{comp} = \frac{0.5 * \sigma_{max}^2}{E_{tan}} + \left(\varepsilon_{axial} - \frac{\sigma_{max}}{E_{tan}} \right) * \sigma_{max} \qquad \textbf{Equation 5 - 4}$$

The post-peak failure curve could not be measured in its entirety due to dimensional constraints in the test set-up. The area under this curve provides a measure of the toughness of a material and is also sometimes considered in dissipated energy and crack growth resistance considerations.

4.3.2 Unconfined Compressive Test Results

The axial forces and deformations applied to the specimens in the unconfined compression tests are transformed into stresses and strains using the overall geometry of the specimens i.e. cylinders, on average 130mm high and 100mm diameter. From these results the apparent compressive strength $\sigma_{c,max}$ could be determined and analysed as a function of temperature and displacement rate.

Graphical analysis of the stress-strain relationships for different materials, as typically shown in Figure 5 - 7, reveals that uniform curves with an initial linear relationship followed by smooth peak and drop-off, are obtainable from unconfined compression tests. This facilitates accurate determination of mix properties as comprehensively recorded in Appendix D.

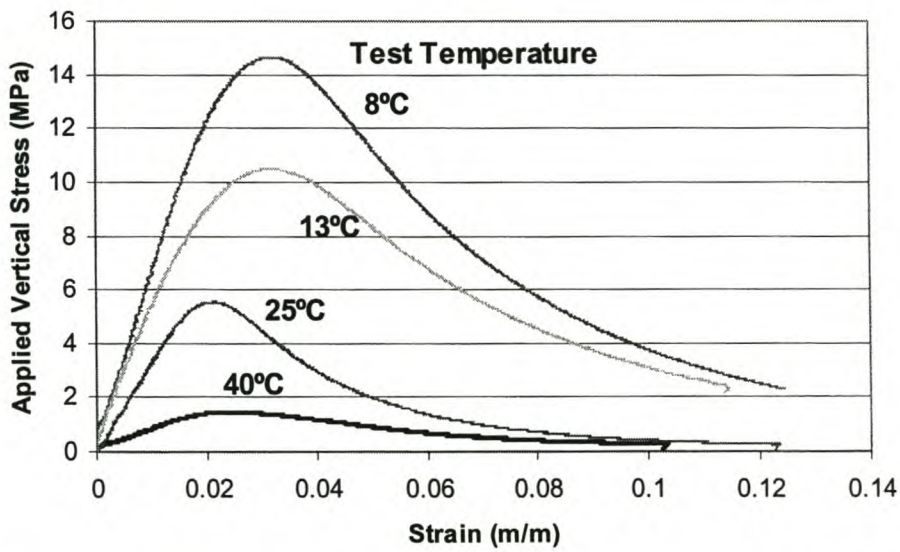

Figure 5 - 7. Typical Results of Uniaxial Stress versus Axial Strain for Half-warm Foamed STAB at Constant Displacement Rate of 50,8 mm/minute

Accurate mix preparation and precisely controlled test conditions assist in the limitation of the variability in the results of the uniaxial compression tests. This is achievable through reduction of systematic errors in particular. The values of the Coefficient of Variation for the three repeat tests summarized in Table 5 - 11, indicate that for conventional mixes such as the hot-mix STAB, highly repeatable mix properties can be measured.

Table 5 - 11. Coefficient of Variation (%) for Unconfined Compression Tests for 3 Repeats at 50,8 mm/min Displacement Rate

Test Temp (°C)	HMA STAB	HW STAB	HW RAP+STAB	CM STAB
8	4.7	4.5	12.1	11.5
13	3.0	31.7		5.0
25	7.3	23.2	13.6	2.5
40	1.0	10.6	8.1	4.5
Average	4.0	17.5	11.3	5.8

The limitation of systematic errors in the determination of mix properties, assists in more accurate assessment of the influence of various factors in mix production using different techniques. Assigning a value of one to each significant factor that influences a mix composition through variability during production and considering the aggregate influence as common to all equivalent mixes, the following simplified result is obtained:

- Hot-mix has one factor i.e. the binder with its variability,
- Cold mix has two factors i.e. the binder and moisture, and
- Half-warm mix has three factors i.e. the binder, moisture and aggregate temperature (a factor excluded from hot-mix, where the profound influence on particle coating is not evident).

In the interests of simplicity, all factors are assigned an equal weight, which is not necessarily a true reflection of practice. Analysis on the influence of mix production factors on the overall mix variability can be summarized in terms of the Coefficient of Variation (COV) of the UCS value, see Figure 5 - 8. This is a graphical illustration of the typical results obtainable from partial derivative analysis for combination of variability, see Appendix G. From such an approach it is known that the overall variability is dependent on the variability of the individual contributory factors.

The relevance of Figure 5 - 8 is that the variability of half-warm mixes is significantly higher than both cold and hot mix, and that the influence of aggregate temperature is the additional factor that requires the attention in terms of quality control, to minimize this variability. This is particularly pertinent for dependent variables such as temperature, moisture content, viscosity and compaction.

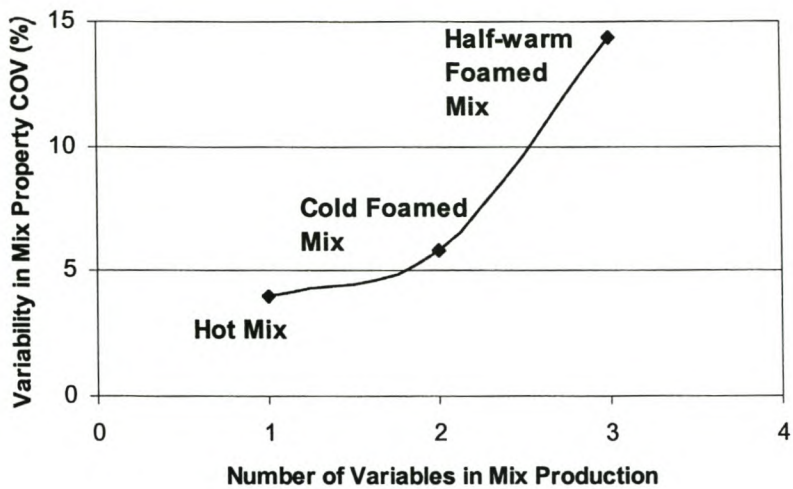

Figure 5 - 8. Influence of Number of Variables in Mix Production on Consequent Coefficient of Variation of the Mix, based on UCS

Through the use of curves fitted through the data points of compression tests at various test temperatures for a given loading rate, functions may be generated for the appurtenant relationships. These curves, given in Figure 5 - 9, show the behavioural differences between the equivalent mixes manufactured using different processes. In terms of compressive strength, the improvements created by warming of the aggregate from cold foamed mix to half-warm foamed mix become evident with compressive properties of the mix increasing to the levels of HMA. At the same time, sensitivity to rate of loading or in this case displacement rate, increases with increasing aggregate temperature at mixing.

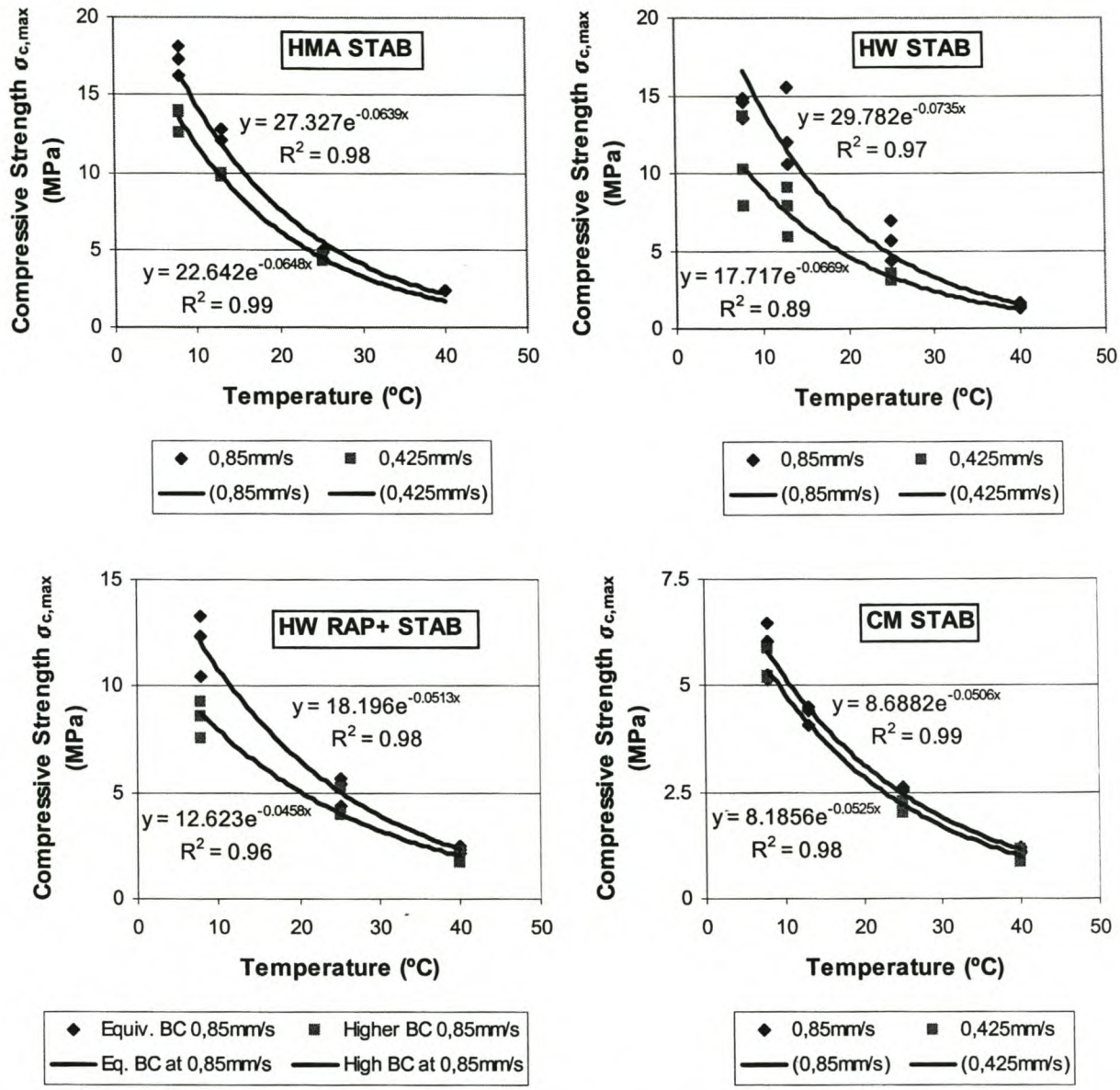

Figure 5 - 9. Compression Strength $\sigma_{c,max}$ for Four Equivalent Asphaltic Mixes relative to Test Temperature and Displacement Rate

The dependence of compressive strength to the rate of loading is not, however, significant when analysed graphically, see Figure 5 - 10. Evidence of major differences in the slope of the linear relationship are absent from the plot, for tests at a specific temperature. Although this is true for static testing, the same conclusion cannot be drawn for dynamic testing, as outlined later in this chapter.

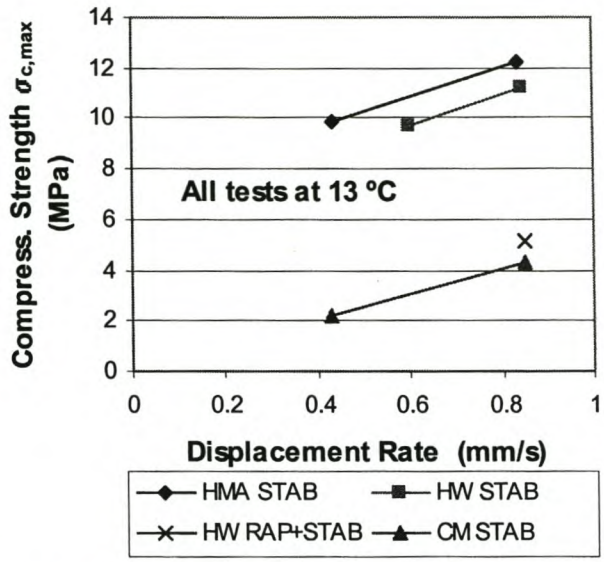

Figure 5 - 10. Maximum Compressive Strength as a Function of Displacement Rate

Analysis of dissipated energy for each mix at different test temperatures requires a value for the tangent modulus E_{tan} as well as the strain at $\sigma_{c,\,max}$. Although the latter does not provide strong trends with respect to test temperature for the four mixes, the E_{tan} value does, see Figure 5 - 11. As with the compressive strength, the tangent modulus values of half-warm mixes lies between that of the equivalent cold foamed mix and hot asphaltic mix.

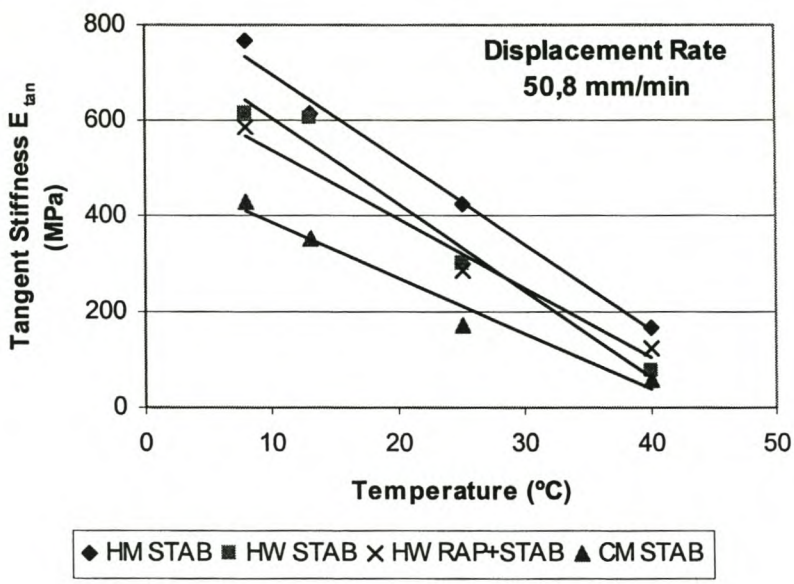

Figure 5 - 11. Average Values for Tangent Modulus (E_{tan}) from UCS Tests relative to Test Temperature

Combination of the values obtained for $\sigma_{c,\,max}$, ε_{axial} at $\sigma_{c,\,max}$ and E_{tan} in a single term which provides a measure of the fracture energy during testing is important, as such a composite term is relevant for performance estimation. Using Equation 5 - 4 to calculate this "Dissipated Energy Factor" facilitates comparison of the dissipated energy for the different mixes, see Figure 5 - 12.

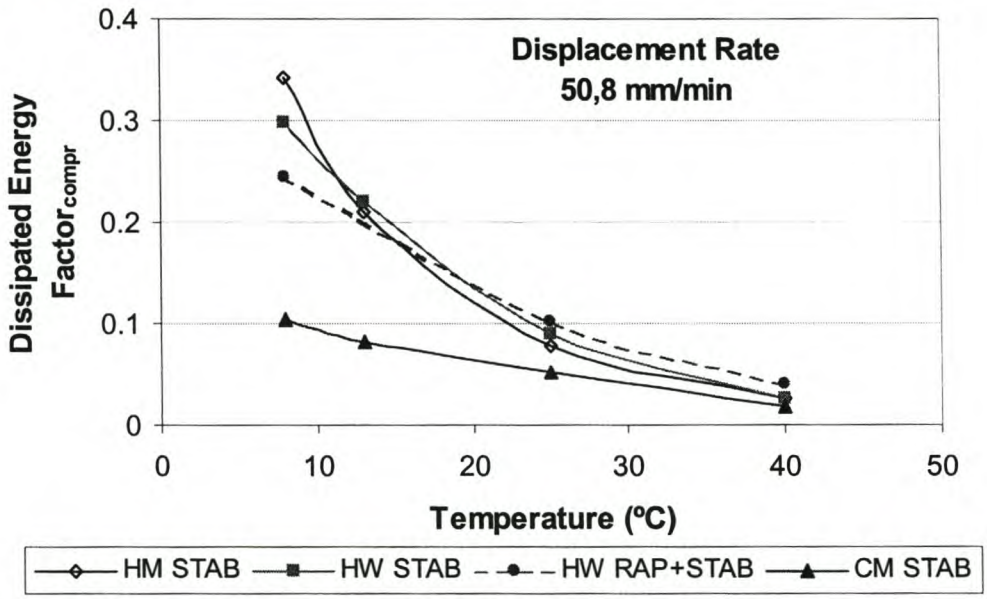

Figure 5 - 12. Dissipated Energy Factor for Equivalent Asphaltic Mixes from Unconfined Compressive Tests

Brosseaud *et al.* (1997) observed that the behaviour of cold foamed mixes shows lower sensitivity to rate of loading and test temperature than HMA, see Chapter 2. This trend is also prevalent in Figure 5 - 12. Due to this phenomenon, less change in the fracture characteristics occurs with increase in test temperature. The half-warm foamed mixes also benefit from this phenomenon, although not as significantly as the cold mix, sufficiently nevertheless to enable better dissipated energy characteristics at higher temperatures to become notable.

4.3.3 Leutner Shear Test Set-up

Shear properties of asphalt mixes, if measured in conditions with limited compressive stresses present, provide a measure of the cohesion of the mix, which is an important property to be included in Mohr-Coloumb analysis. The shear test set-up used in the investigation of the hot, half-warm and cold mixes is based on the apparatus of Leutner (1979) that was developed for testing asphalt cores.

The general configuration of the modified Leutner test is shown in Figure 5 - 13. Shearing forces are applied over the diameter of the specimen strategically positioned under circumferential loading plates. de Bondt and Scarpas (1993 and 1994) developed this apparatus to test bonding in asphalt inter-layers. In the case of de Bondt and Scarpas' work, the apparatus obtains the maximum shear force at the layer interface within the

specimen. Confining pressure is applied using an air-bellow system with a pressure gauge as control mechanism and load cell as measurement system. A set screw provides restraint at the other end of the specimen. The vertically applied load (shear force) and displacement are measured using a load cell and vertical displacement transducer (LVDT), see also Figure 5 - 14. As with the uniaxial compression test, the shear test is carried out under displacement controlled conditions.

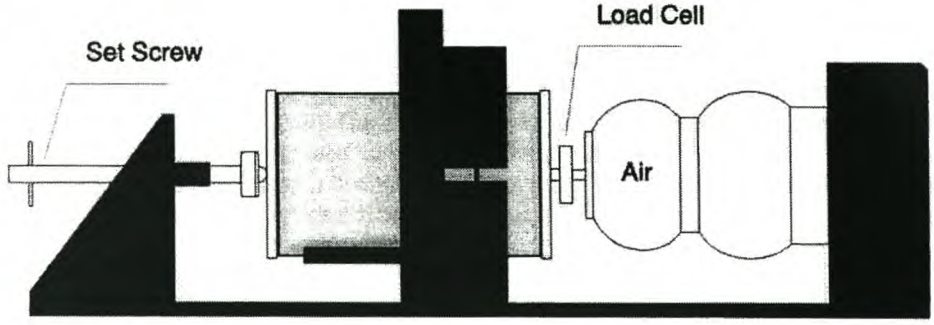

Figure 5 - 13. General Configuration of Leutner Test (de Bondt and Scarpas, 1993)

In order to obtain the desired conditions for testing of homogenous asphaltic specimens, certain parameters require careful control. For this reason, temperature control at the loading plates of the test apparatus was introduced via circulation of water through the loading head of the Leutner apparatus as a thermo-regulator, see Figure 5 - 14. This assists in maintaining the sample temperature during the test, after it has been removed from the climate chamber.

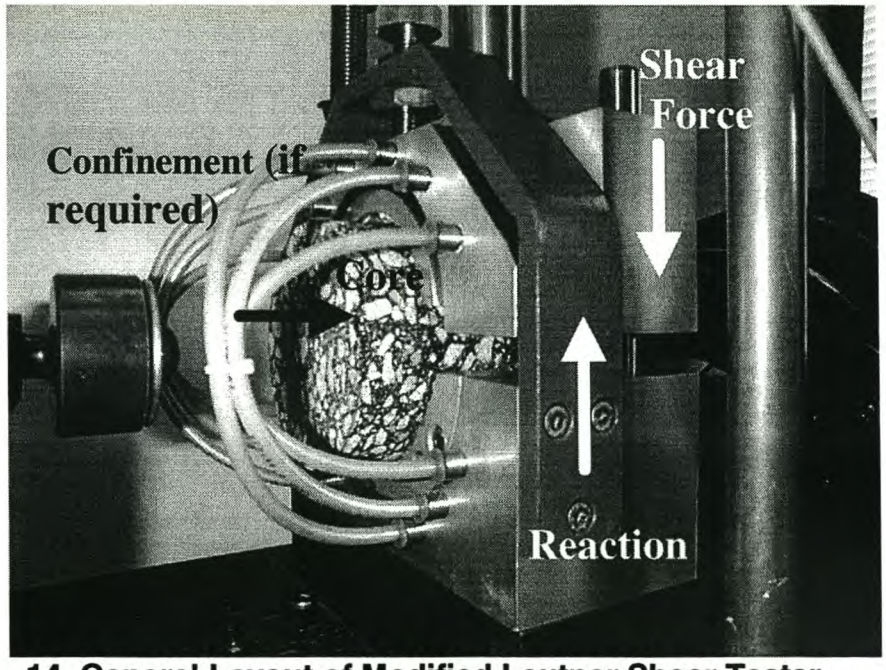

Figure 5 - 14. General Layout of Modified Leutner Shear Tester

Using homogenous specimens, such as in the investigation of half-warm foamed mixes, creates dilatant behaviour within the shear zone of the material, a factor not dominant when testing bonding between layers i.e. the usual application of the Leutner test. The dilatancy creates a more complex shear distribution than that obtained by de Bondt and Scarpas (1993 and 1994). Their finite element analyses of the stress distribution within the Leutner shear test shows that the test configuration does not provide a simple shear stress distribution across the specimen diameter, see Figure 5 - 15. Some bending and tensile stresses are introduced into the specimen due to the geometry of the apparatus and positioning of loading plates, particularly for materials with high stiffness i.e. greater than 5000 MPa.

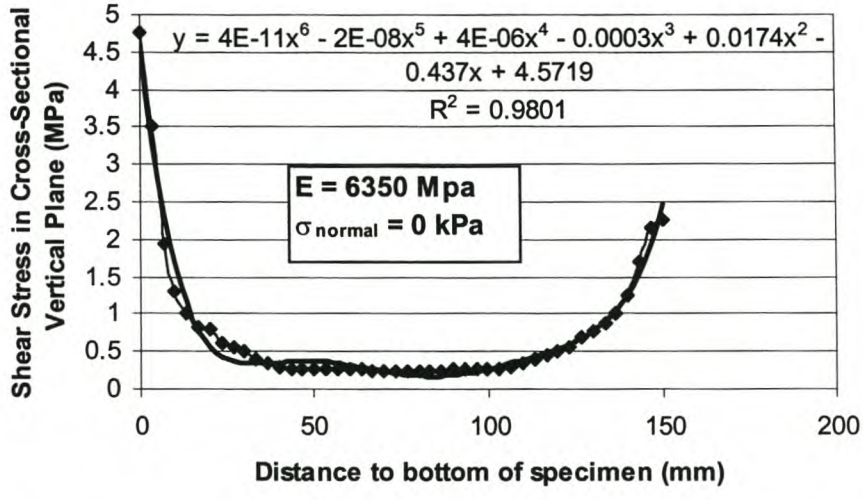

Figure 5 - 15. Shear Stress Distribution in Leutner Test after (de Bondt and Scarpas, 1993)

In the absence of a more suitable shear test, the Leutner Shear Test has been utilised along with an average shear stress value determined over the cross-section area of the specimen. At the same time, in order to minimize edge-effects of friction between the specimen and loading plates, de-bonding glycerine-soap and plastic foil were used on the specimen circumference, in the same manner as for the uniaxial compression tests on half-warm mixes.

The composition and volumetrics of specimens manufactured for the Leutner Tests are detailed in Table 5 - 9, which is also applicable to the uniaxial compression tests. The specimens were selected in a stratified-random manner from the same batches for both of these tests, so as to distribute the variability in air voids evenly between test types and conditions. This is possible when the density of each specimen has been determined.

4.3.4 Leutner Shear Test Results

The vertical forces applied to the specimens in the Leutner Shear Test across the cross-sectional area of the 100mm diameter cylinders are transposed into shear stresses using

the actual geometry of the specimens and an average stress value. From these results the maximum shear strength τ_{max} can be determined and analysed as a function of temperature and displacement rate. As with the uniaxial compression test, the Leutner test results require graphical inspection for the determination of the relevant material parameters, see Figure 5 - 16. A typical plot of results after shifting of the origin to coincide with the source of the linear portion of the output is provided in this figure.

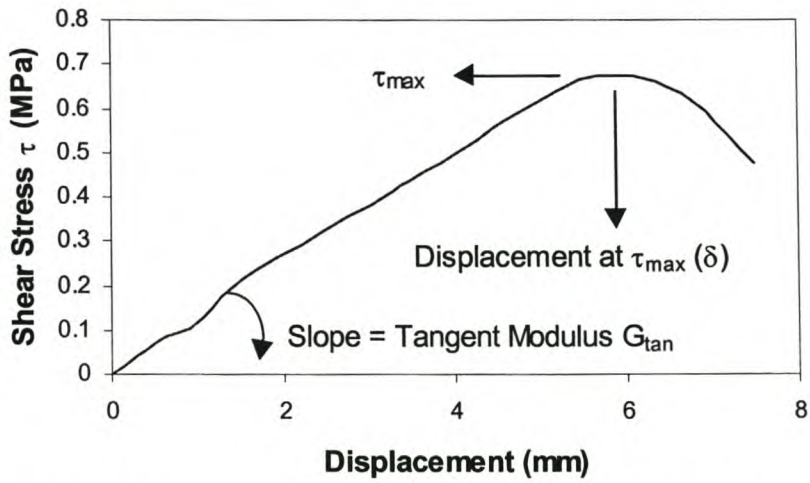

Figure 5 - 16. Typical Leutner Test Result showing Pertinent Parameters

The dissipated energy of such a shear test can be estimated by the area under the stress-strain curve. As with the UCS test, this calculated factor is relevant for comparison of materials as it is a measure of the different capacities of equivalent mixtures to dissipate energy under given test conditions. By definition, the dissipated energy has been calculated up to the optimum point on the graph using an approximation of two linear functions i.e. a line from the origin with slope G_{tan} intersected by a horizontal line tangential to the peak, see Equation 5 - 5. All parameters are measured in MPa except for the displacement δ which has units of millimetres. The shear strain is obtained through division of δ by 1,5mm , the distance between the loading plates in the Leutner device.

$$DissipateEnergyFactor_{shear} = \left(0.5 * \frac{\tau_{max}^2}{G_{tan}}\right) + \left(\frac{\delta}{1.5} - \frac{\tau_{max}}{G_{tan}}\right) * \tau_{max} \qquad \textbf{Equation 5 - 5}$$

4.3.5 Leutner Shear Test Results

Graphical analysis of the shear stress versus strain relationships for different materials tested in the Leutner apparatus yields results as illustrated in Figure 5 - 17. Parabolic curves with distinct peaks and relatively low residual post-peak shear strengths are apparent. A significant shift in the displacement at maximum shear stress with change in test temperature, is apparent from the figure.

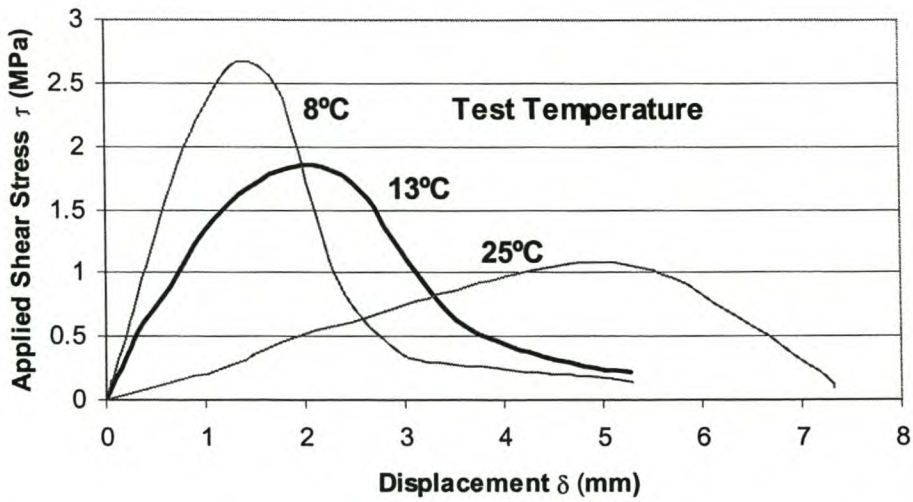

Figure 5 - 17. Typical Results of Leutner Shear Stress versus Displacement for Half-warm Foamed STAB at a Constant Displacement Rate of 50,8 mm/minute and 0 kPa Applied Normal Stress

The variability noted in the Leutner Shear Test confirms the trend in higher variability of half-warm mixes that has been observed with UCS tests. Table 5 - 12 shows substantially higher variability in the half-warm mixes, both with virgin and recycled aggregates, compared with the equivalent hot mix asphalt and cold mix.

Table 5 - 12. Coefficient of Variation (%) for Leutner Shear Tests for 3 Repeats at 50,8 mm/minute Displacement Rate and 0 kPa Confining Pressure

Test Temp (°C)	HMA STAB	HW STAB	HW RAP+STAB	CM STAB
8	11.1	4.6	-	11.0
13	9.5	28.2	28.1	3.3
25	4.8	31.0	18.9	9.8
Average	8.5	21.3	23.5	8.0

In terms of temperature and applied normal pressure, the failure envelopes can be obtained from Leutner tests for different mixes at a specific displacement rate, see Figure 5 - 18. In particular, reduced influence of test temperatures on the shear strength of half-warm STAB relative to hot-mix STAB is evident between 8°C and 13°C. In overview, differences in the failure envelopes for the four equivalent mixes arise from increased cohesion, with limited change in the friction angle. This once again highlights benefits in warming the aggregates before mixing with foamed bitumen, indicating that improved binder dispersion creates more cohesion within the mix, see HW STAB result in comparison with CM STAB.

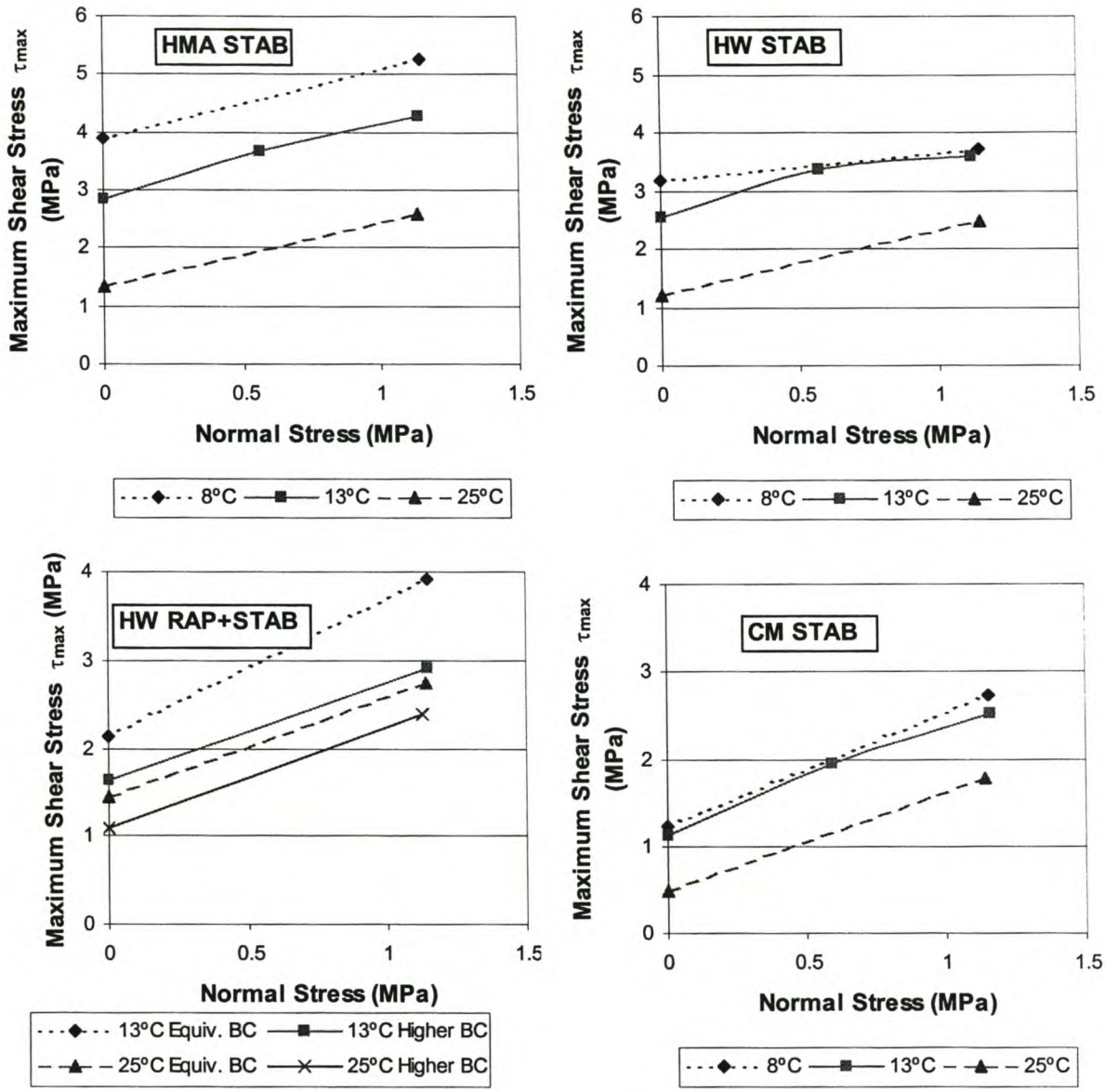

Figure 5 - 18. Failure Envelope from Leutner Shear Tests for Four Equivalent Asphaltic Mixes tested at 50,8 mm/min Displacement Rate

Summary of the average shear strength results as a function of the test temperature, see Figure 5 - 19, reveals that, as with compressive strength, the shear strength of these half-warm foamed mixes declines less rapidly with increasing temperature than the equivalent HMA. Although the shear strength of HW Stab is notably lower than that of HMA Stab at low temperature, the margin narrows as the test temperature increases to 25°C. This holds potential benefits for the half-warm foam treatment process in the production of mixes less susceptible to permanent deformation at high in-service temperatures, although the relevant dynamic tests are required to verify this.

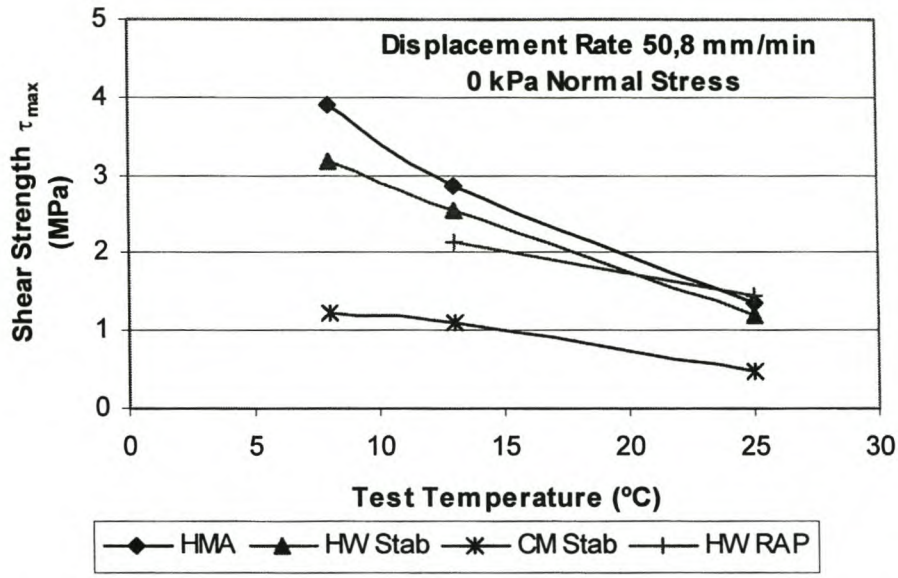

Figure 5 - 19. Shear Strength as a Function of Test Temperature for Four Asphaltic Mixes with Equivalent Compositions

As in the case of compressive strength of the mixes, no significant dependence of shear strength to the rate of displacement is notable from the results, see Appendix D. The need for large displacements during testing does not provide sufficient sensitivity to enable differentiation between the four mixes in terms of displacement rate. Dynamic testing, as covered later in this chapter, is suited for this purpose.

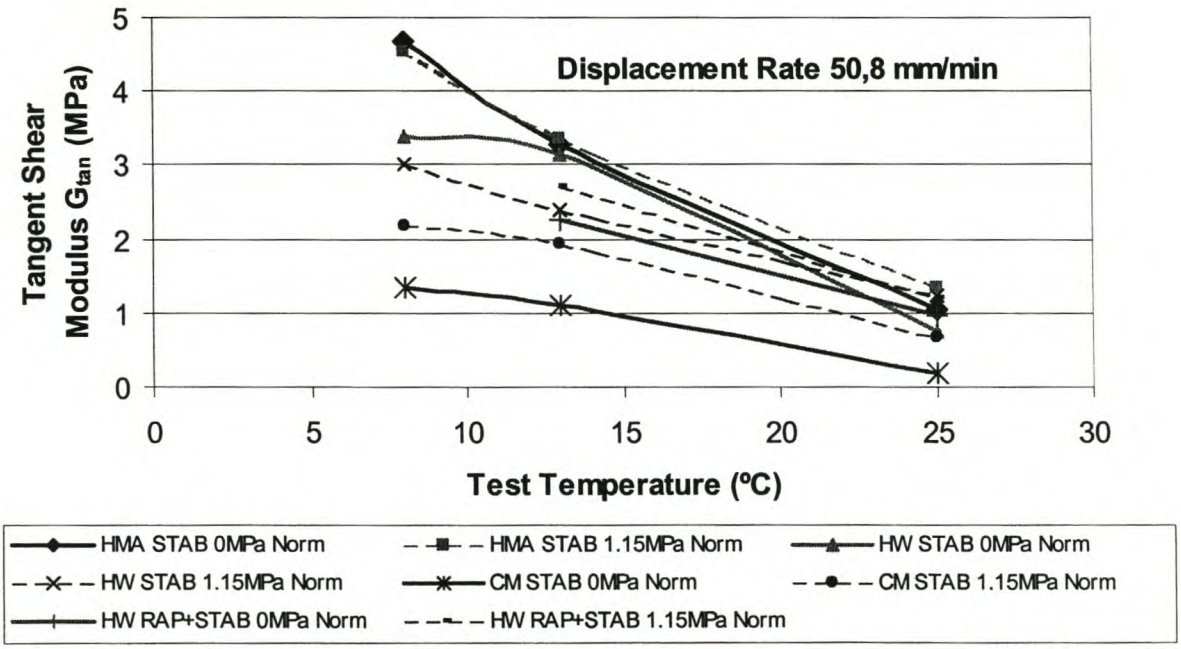

Figure 5 - 20. Static Shear Modulus from Leutner Tests for Four Asphaltic Mixes with Equivalent Composition, as a Function of Test Temperature and Normal Pressure

The slope of the shear stress function i.e. the static shear modulus or G_{tan}, as with the ultimate shear strength, provides a distinct relationship with respect to test temperature. As with τ_{max} , the G_{tan}value of half-warm foamed mixes shows less variation with decreasing temperature than the equivalent hot mix, see Figure 5 - 20.

Combination of the values obtained for τ_{max}, δ and G_{tan} in a single term which represents a measure of the fracture energy encountered during a shear test, provides a composite term that is of more relevance for performance estimation than the individual parameters. Using Equation 5 - 5 to calculate this "Dissipated Energy Factor" in shear facilitates comparison of the fracture energy for the different mixes with equivalent composition. Through consideration of the composite effect of the relevant parameters, a ranking of the mixes is obtained as shown in Figure 5 - 21. This provides insight into potential advantages of half-warm mixes within a range of realistic service temperatures.

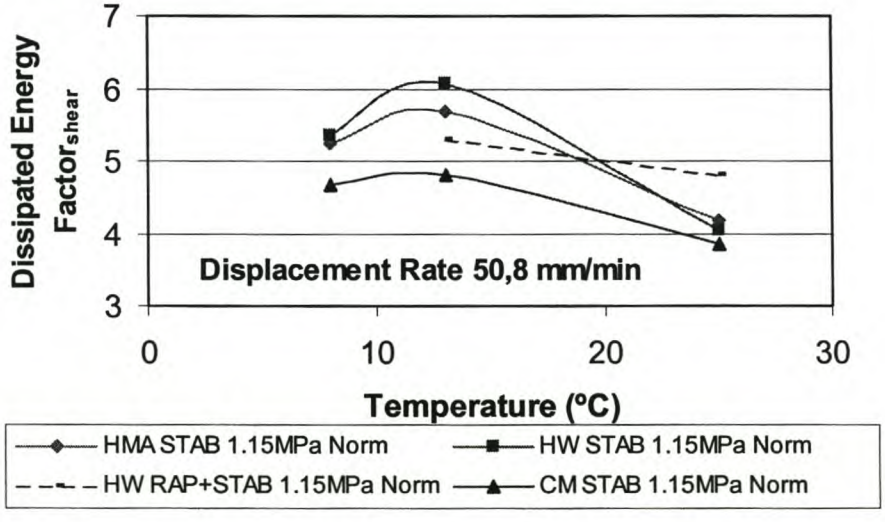

Figure 5 - 21. Dissipated Shear Energy Factor for Equivalent Asphaltic Mixes from Leutner Testing at 1,15 MPa normal pressure

4.3.6 Combination of Compression and Shear Test Results

It is possible to superimpose the results of tests with known stress states within the Mohr-Coloumb space and combine these results in the determination of a composite failure envelope. For visco-elastic materials, only tests that have been performed at the same temperature and strain rate may be combined in this manner. In this section, comparisons are made between the failure envelopes of the four different mixes of equivalent compositions at three different test temperatures, namely 8°C, 13°C and 25°C. Although the displacement rate for the compression and shear tests were the same, due to differences in the geometry of the specimens, the strain rates differ slightly. Cognisance of this fact should be taken for the analysis in this section and results treated as indicative rather than absolute.

The plots of failure envelopes, as provided in Figure 5 - 22 to Figure 5 - 24 reflect the characteristics of the different mixes in terms of their cohesion and friction angle. At low temperatures, very little difference in the friction angle is evident, as the binder is in a stiff condition. Hot mix asphalt with its continuously distributed binder throughout the mix, exhibits highest cohesion at the lowest temperatures.

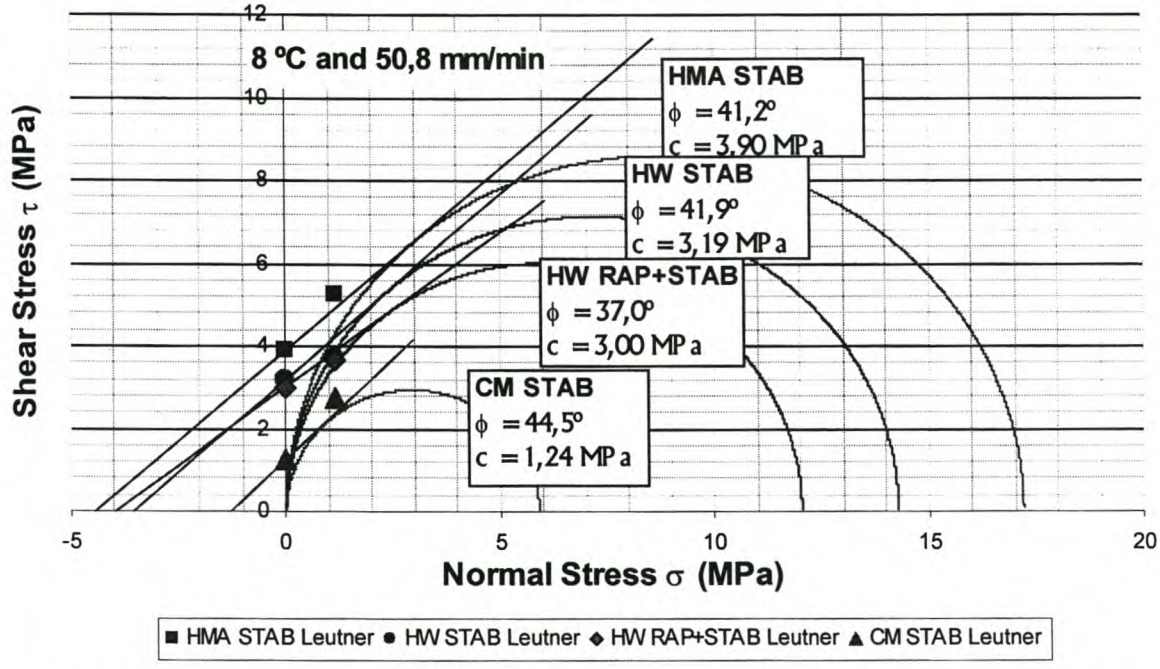

Figure 5 - 22. Failure Envelopes for Combination of UCS and Leutner Tests at 8°C and 50,8 mm/min

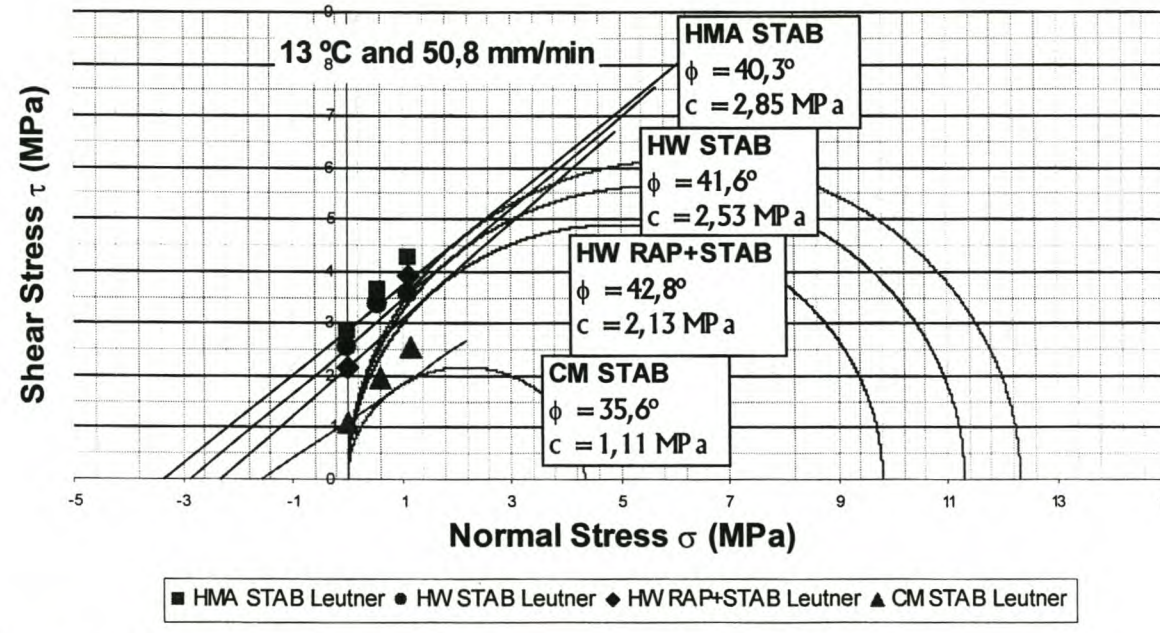

Figure 5 - 23. Failure Envelopes for Combination of UCS and Leutner Tests at 13°C and 50,8 mm/min

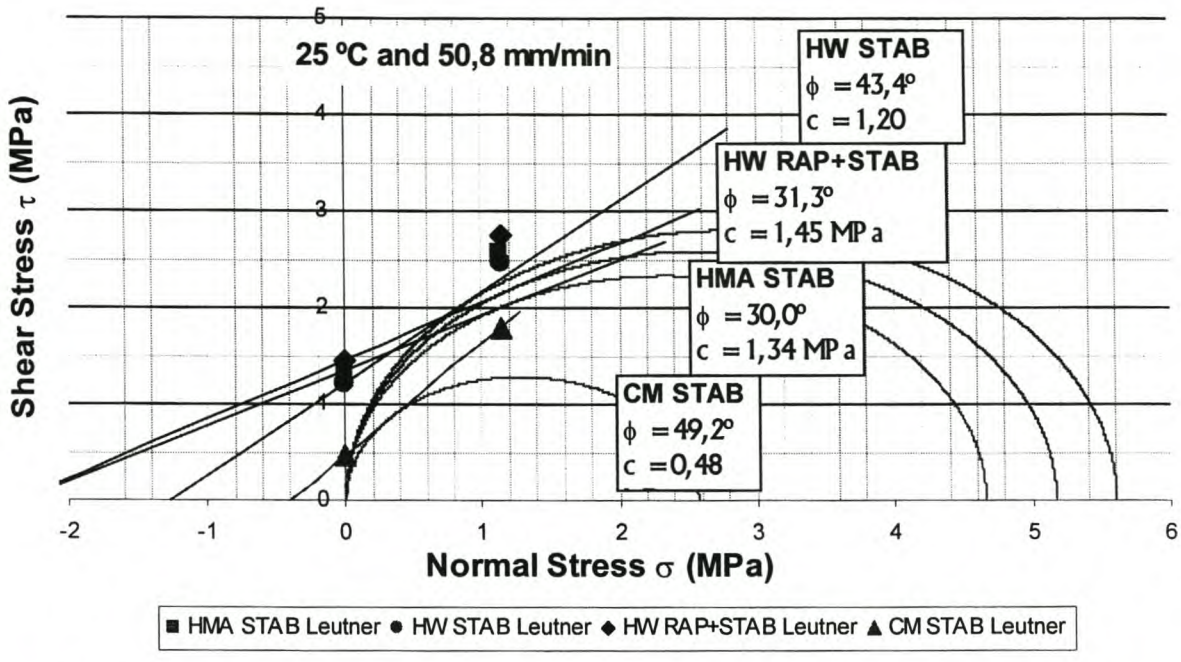

Figure 5 - 24. Failure Envelopes for Combination of UCS and Leutner Tests at 25°C and 50,8 mm/min

With increase in the test temperature, an increase in the relative height of the failure envelope of the half-warm mixes compared to hot mix, is apparent. This is particularly notable at higher normal stresses. Some degree of variability in the failure envelope from the Leutner Tests relative to Compressive Test results is evident, which is predominantly influenced by the non-uniform shear-stress distribution within the specimen during Leutner testing, aggregate size to specimen diameter ratios and differences in displacement rates.

5. DYNAMIC PROPERTIES OF HALF-WARM FOAMED MIX

Static tests such as the uniaxial compression tests and the shear tests conducted provide insight into the peak strength of equivalent hot, half-warm and cold mixes at equivalent temperatures and loading rates. However, vehicular traffic imposes dynamic loads on pavement layers with dynamic displacements that are substantially smaller than those encountered during static tests. The visco-elastic nature of the bitumen that it utilised in half-warm foamed mixes makes it imperative to study these materials using dynamic tests in addition to the aforementioned static tests.

For the purpose of ascertaining dynamic properties of a half-warm foamed mix, an investigation was conducted using the Four Point Beam (4PB) apparatus. For economy of investigation, only one reference mix could be tested under the equivalent dynamic conditions. The hot mix (HMA STAB) was selected for this purpose. The 4PB apparatus was utilised to carry out analyses for master-curve determination for flexural stiffness as well as fatigue testing.

5.1 Manufacture of Beams

Compositional requirements and production of the two mixes selected for dynamic analysis viz. HMA STAB and HW STAB, comply with the details of these mixes produced as cylindrical specimens for static testing, see Section 4. However, in the manufacture of beams for 4PB testing, differences in air void content of the specimens with the equivalent cylindrical specimens are unavoidable and these are detailed in this section.

In order to procure suitable beams for testing, the mixes were initially compacted into slabs of 500 x 500 x 70 mm in a wooden mould using a 7 ton static-mass, smooth-drum roller. This operation was carried out by van Hees en Zonen B.V., contractors in Tilburg, The Netherlands. Compaction was carried out without vibration. A sufficient number of passes were applied to achieve densities in the same order as the specimens compacted in the gyratory compactor. After preparation of four plates of HW STAB and three plates of HMA STAB, beams could be sawed from each plate. In this manner, eight beams of 400 x 50 x 50 mm were sawed from each plate, in the same direction as the roller compaction.

Determination of the bulk relative density of each of the beams provides the distribution of density across each of the asphalt plates. Table 5 - 13 presents the statistics of the air voids in the beams used for 4PB tests, as well as the maximum variation in voids within each plate. The complete volumetric results of all of the beams manufactured, are included in Appendix D. Selection of individual beams with equivalent air voids is required for unbiased testing, which is important considering the higher voids encountered in the HMA STAB beams as recorded in the Appendix. The void contents of the beams for both mixes are slightly more than 2% higher than the laboratory compacted mixes, which is a shift between laboratory and field compaction that is to be expected. The reduction in fatigue life caused by an increase in voids can be approximated using the equations of (Shell, 1978).

Table 5 - 13. Volumteric Properties of Beams selected for 4PB Tests

	Voids in Mix (%)			
Mix Type	**HW STAB**		**HMA STAB**	
4PB Test Type	Fatigue	Master Curves	Fatigue	Master Curves
Average	6.11	6.09	7.43	6.51
Standard Deviation	0.10	0.25	0.43	0.16
Variation (Max- Min)	0.34	0.35	1.18	0.22
Moisture Content (%)	0.39	0.29	0.00	0.00

5.2 Four Point Beam (4PB) Apparatus

If half-warm foamed bitumen mix is applied as a pavement layer, it will be subjected to numerous load repetitions during its service life. The wheel loads imposed by traffic cause deflections that create tensile stresses in layers in the upper reaches of a pavement. The resultant tensile strains experienced by bound materials will cause fatigue of the material with time i.e. cracks will propagate through the layer resulting in a loss in stiffness.

Preliminary assessment of the HW STAB mix shows that it has potential for use in the upper layers of pavement structures and would therefore be exposed to conditions that cause distress related to fatigue. To simulate these conditions in the laboratory, the Beam Fatigue Apparatus ® of IPC can be utilised, see Plate 5 - 1. This test can be carried out at different temperatures and loading frequencies, thus providing information that assists in characterising dynamic material stiffness and fatigue.

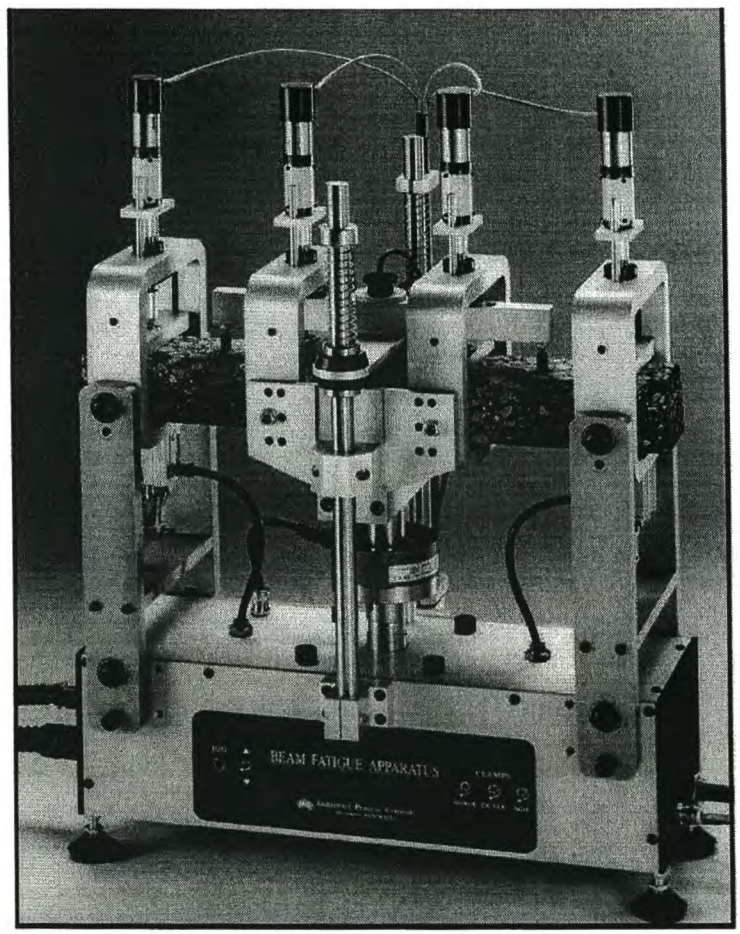

Plate 5 - 1. Beam Fatigue Apparatus ® of IPC

Several input parameters are required for the 4PB Test using the IPC apparatus, the most relevant of which include:

- rise time which defines the wave frequency,
- rest period which defines the time lag between waves,
- specimen cross-sectional dimensions, and
- mode of loading and loading wave.

For the purpose of comparative analysis of HMA STAB and HW STAB a sine wave signal was applied to the beam specimens under displacement controlled conditions, applicable

to thicker layers, on the Beam Fatigue Apparatus. No rest period was included in the loading wave signal.

Some of the input parameters, in conjunction with other parameters measured during the test, provide the necessary data for calculation of relevant test parameters. For the geometry of the Beam Fatigue Apparatus (IPC,1998), these include amongst others:

Maximum Tensile Stress σ_t (kPa)

$$\sigma_t = 3000aP/wh^2 \qquad \textbf{Equation 5 - 6}$$

where,

a = distance between reaction and load clamps (typically 118,5mm)
P = peak force (N)
w = width of beam (mm)
h = height of beam (mm)

Maximum Tensile Strain ε_t (mm/mm)

$$\varepsilon_t = 12\delta h/23a^2 \qquad \textbf{Equation 5 - 7}$$

where,

δ = peak deflection at the centre of the beam

Flexural stiffness S (MPa)

$$S = \sigma_t/1000\varepsilon_t \qquad \textbf{Equation 5 - 8}$$

Phase Angle (degrees)

$$\phi = 360fs \qquad \textbf{Equation 5 - 9}$$

where,

f = load frequency (Hz)
s = time lag between P(min) and δ(min) in seconds

Although the flexural stiffness calculated using the software of the Beam Fatigue Apparatus provides the desired measure of this property for the beam-specimen (IPC, 1998), maximum tensile strain requires redefinition as the "strain amplitude" for sine wave loading cycles.

The vertical force required to provide the desired displacement is measured during pulsing. Variation in the initial readings during a test is substantial and reduces considerably within the first one hundred pulses. For this reason, initial flexural stiffness (S_i) is defined as being measured from a regression relationship of the data at the 100^{th} pulse, see Figure 5 - 25. This parameter is used for the determination of the master-curve stiffness where only 100

pulses were measured, as well as the termination stiffness for fatigue testing where the regression line was fitted over 500 pulses.

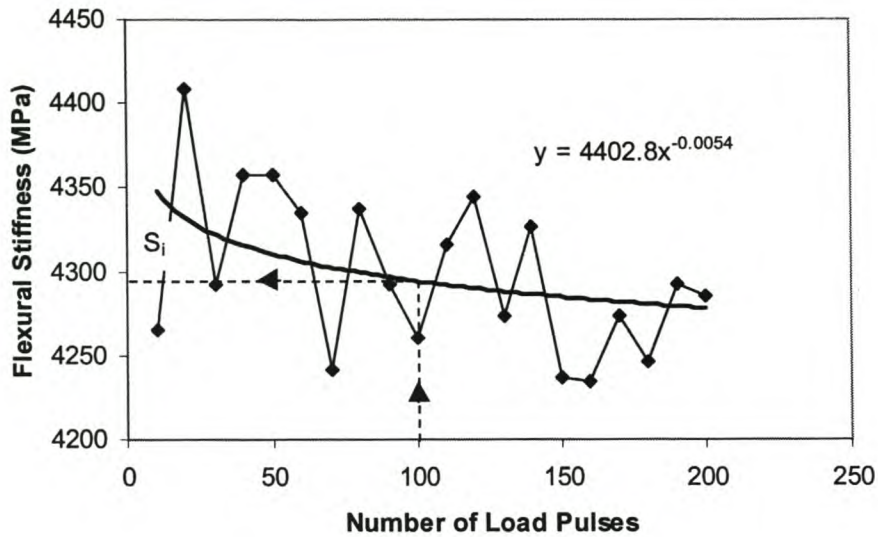

Figure 5 - 25. Example of Flexural Stiffness as a Function of Load Repetitions in a Displacement Controlled 4PB Test at 20°C

5.2.1 Master Curves

Due to the visco-elastic properties of the bituminous binder in asphalt mixes they generally exhibit an increasing flexural stiffness for decreasing temperature and higher frequency of loading cycles. The stiffness can be defined by a unique curve or "master curve" for a given asphaltic material by shifting the stiffness modulus (as the ordinate) horizontally with respect to loading time (as the abscissa) for various temperatures until the curves co-incide. This provides a complete stiffness versus loading time relationship at a selected reference temperature.

For the hot-mix and half-warm STAB mixes investigated, master curve testing was carried out on two representative beam specimens selected for each mix. The range of temperatures selected for testing spanned 5°C to 25°C in intervals of 5°C, inclusive. The loading frequency in these displacement-controlled tests included 0.5Hz, 1Hz, 2Hz, 5Hz and 10Hz. In order to minimise damage of the specimens during measurements, testing commenced at the lower temperatures and higher frequencies. In addition, all testing was carried out at 80 μm/m strain with a sine wave in displacement controlled conditions for the master curve investigation.

The initial flexural stiffness determined from the 4PB tests provides uniform results for the load frequency sweeps at a given temperature, see Figure 5 - 26. Such a plot is

representative of both the HW STAB and the HMA STAB mixes and facilitates the creation of master-curves of desirable uniformity. The complete record of results is provided in Appendix D.

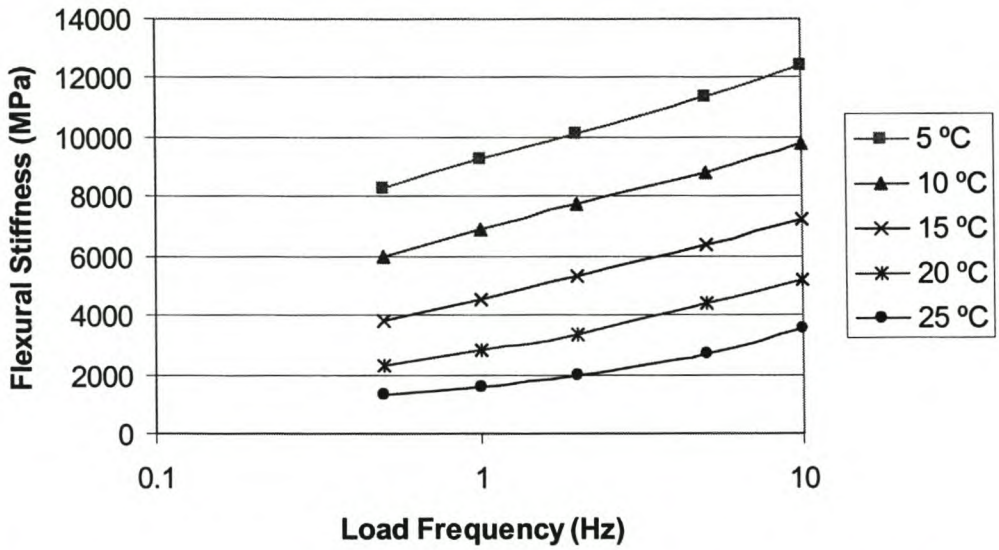

Figure 5 - 26. Flexural Stiffness determined for Load Frequency Sweeps at given Temperature for HW STAB Mix

The principle of time-temperature correspondence or thermo-rheological simplicity, forms the basis of master-curve determination. This technique uses the equivalence between frequency and temperature for stiffness modulus of bituminous mixes as:

$$\log f_{eq} - \log f = \log \alpha_t \qquad \textbf{Equation 5 - 10}$$

where,

f_{eq} = frequency for master curve converting test temperature to reference temperature (Hz)
f = actual frequency of loading of test (Hz)
α_t = shift factor

Three methods exist for determination of the shift factor i.e. graphical shifting of experimental results (Germann and Lytton, 1977), using the Arrhenius type equation (Francken and Clauwaert, 1988; Jacobs, 1995; Lytton, 1993) and using the Williams-Landel-Ferry equation (Williams *et al.,*1955). Provided the Arrhenius approach yields satisfactory results in terms of master curve fit, it is not necessary for the other approaches to be employed in a limited study. The Arrhenius approach uses Equation 5 - 11.

$$\log \alpha_t = C\left(\frac{1}{T} - \frac{1}{T_{ref}}\right) = \log e.\frac{\Delta H}{R}\left(\frac{1}{T} - \frac{1}{T_{ref}}\right) \qquad \textbf{Equation 5 - 11}$$

where,

T = experimental or test temperature (K)

T_{ref} = reference temperature selected (K)
C = constant (K) [Francken C=10920K; Lytton C=13060K; Jacobs C=7680K]
ΔH = activation energy (J/mol)
R = ideal gas constant = 8.314 (J/(mol.K))

Employment of Francken's constant for the Arrhenius equation yields a good fit for the master curve of both the HMA STAB and HW STAB mixes, see Figure 5 - 27 and Figure 5 - 28. Use of other approaches and other constants does not improve the correlation coefficient sufficiently to justify their use. Some variation from the regression line is to be expected, not only from random error influence, but also from the assumption that C and ΔH are independent of temperature. Saygeh (1967) found this assumption thermodynamically inconsistent as the activation energy can reduce by some 60% with an 60K increase in temperature from 253K.

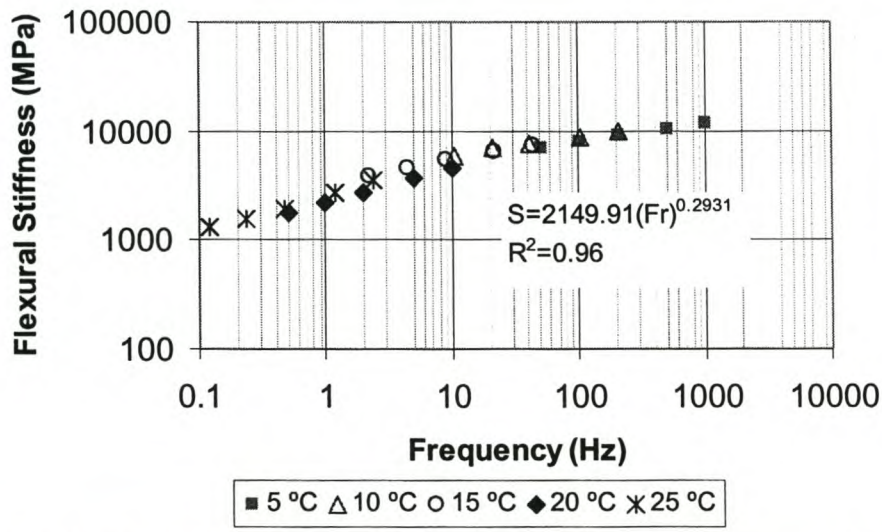

Figure 5 - 27. Master Curve of HMA STAB at 20°C Reference Temperature

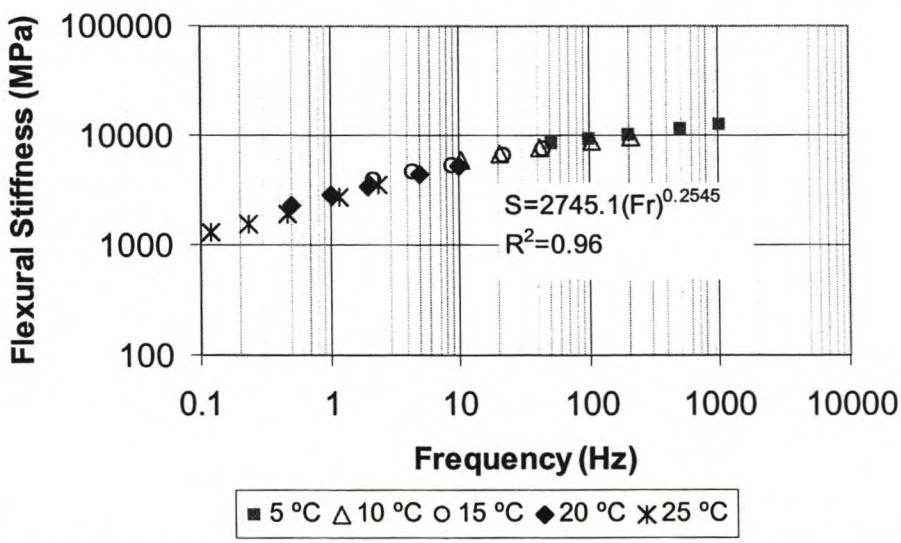

Figure 5 - 28. Master Curve of HW STAB at 20°C Reference Temperature

The superimposition of the master curves of the two mixes in the same graph provides insight into differences in the behaviour of half-warm foamed bitumen mix compared with the equivalent hot mix. A notable shift in the flexural stiffness of the material is evident at lower frequencies of loading, see Figure 5 - 29. This concurs with the findings of Brosseaud *et al.*(1997) who found that cold bituminous mixes with foamed bitumen produce master curves with significantly lower slopes than the equivalent HMA, see Chapter 2 Section 2.9. Half-warm foamed mixes do not provide a shift of the same magnitude as the cold foamed mixes do relative to HMA. This is probably due to improved dispersion of the binder within the mineral aggregate for half-warm mixes i.e. they are more like HMA than the equivalent cold foamed mix.

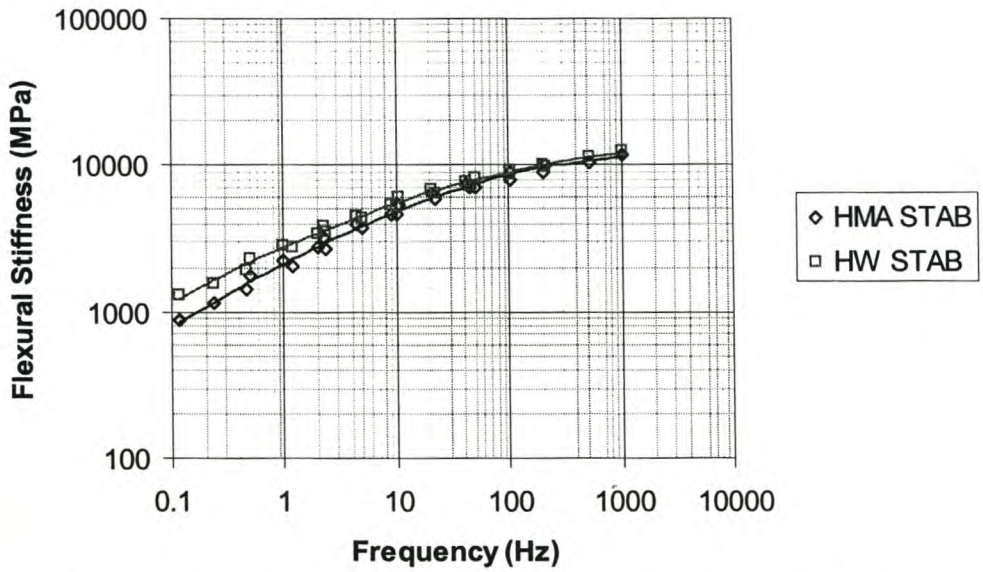

Figure 5 - 29. Master Curves of HMA STAB and HW STAB at 20°C Reference Temperature with respective Mean Air Voids of 6,51% and 6,09%

The relevance of the differences in flexural stiffness shown by the master curves is apparent considering particularly permanent deformation under extended loading times i.e. low frequencies and high pavement temperatures. The higher flexural stiffness of half-warm foamed bitumen mixes will ensure improved resistance to permanent deformation. Whether this property is at the expense of fatigue characteristics, is the objective of the investigation into the fatigue properties of the mixtures outlined below.

5.2.2 Fatigue Behaviour

The test conditions selected for fatigue analysis of the HW STAB and HMA STAB beams include a sine wave signal being applied under displacement controlled conditions. No rest period was included in the loading wave signal. A temperature of 20°C and frequency of 10Hz has been applied during the fatigue tests.

The Wöhler model for fatigue behaviour is applicable to fatigue damage data of asphalt materials amongst others, providing a relationship between number of load cycles to failure and level of tensile strain.

$$N_f = k_1\left(\frac{1}{\varepsilon}\right)^n \qquad \textbf{Equation 5 - 12}$$

or

$$\text{Log}N_f = \log k_1 - n\log\varepsilon \qquad \textbf{Equation 5 - 13}$$

where,

N_f = number of strain applications to failure
ε = flexural strain at the bottom of the asphalt layer
k_1, n = factors dependent on asphalt mix composition and properties

Failure requires definition for fatigue testing in the displacement controlled mode. In accordance with accepted practice N_f is defined as the number of load repetitions to reduce the flexural stiffness to half of its original value. The original flexural stiffness is determined using the procedure illustrated in Figure 5 - 25. In this manner a relationship may be established for each material i.e. HMA and HW STAB, see Figure 5 - 30.

The Wöhler parameters can be determined from linear regressions of the data points. These parameters are provided in Table 5 - 14 for the tests carried out at 20°C and 10Hz. In addition, an equivalent fatigue line using the SPDM (1978) is included for the purpose of comparison.

Table 5 - 14. Fatigue Characteristics for Mixes for Wöhler Equation

Mix Type	Log (k_1) (m/m)	n	R^2
HMA STAB	-10.397	4.1344	0.95
HW STAB	-6.523	3.1144	0.98
SPDM F2*	-12.9	5	-

* Shell Pavement Design Manual Equivalent Mix

The steeper the slope of the fatigue line for HMA STAB on the given axes portrayed in Figure 5 - 30 , represents higher sensitivity of a material to increasing levels of strain. The n value in the fatigue relationship provides a measure of the slope of this function. The relevance of different n values obtained from fatigue testing is apparent when viewed in the context of the law of Paris, see Equation 5 - 14 (Molenaar, 1983 and Sabha *et al.*, 1995). Higher n values represent greater sensitivity to crack extension under given loading conditions.

$$\frac{dc}{dN} = AK^n \qquad \textbf{Equation 5 - 14}$$

Where,

c = crack length

N = number of strain repetitions
A, n = parameters dependent on material and loading conditions (temperature, frequency and waveform)

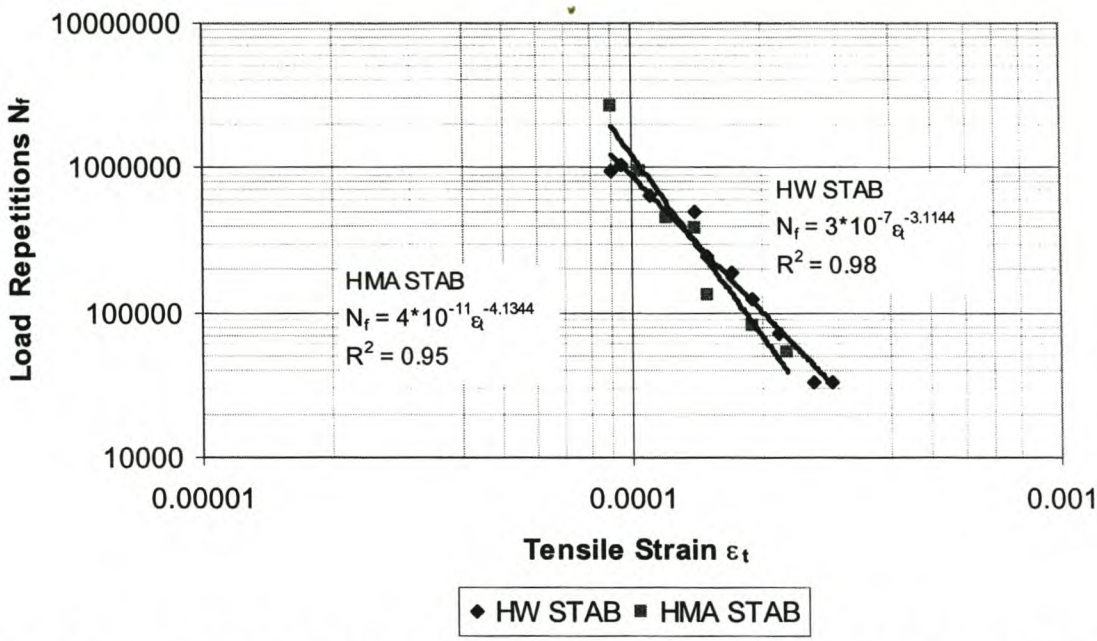

Figure 5 - 30. Fatigue Characteristics of HMA and HW STAB from 4PB Tests at 20°C in Displacement Controlled Mode at 10Hz

Notwithstanding this analysis, only modest differences between the mixes are notable from the 4PB tests and the data points of the two mixes are interspersed when viewed in the absence of the regression lines.

The approach of LCPC (1997) summarised in Section 2.11.2 of Chapter 2 can be utilised to ascertain the relative field performance of HW STAB and HMA STAB in terms of fatigue. LCPC's research showed that the relative shift factors to convert laboratory fatigue to field fatigue for cold foamed mix (CMA) and the equivalent HMA are approximately $k_C^{CMA} = k_C^{HMA} = 1.3$. This can be used to establish the horizontal tensile working strain ratios at 10^6 standard axles in the field (M) relative to the laboratory (L). Using Equation 2 – 3 and Equation 2 - 5 from Chapter 2 for HW mix instead of GM (cold mix), along with the ratios of LCPC, the following relationship for the shift factors is obtained:

$$\frac{k_C^{HW}}{k_C^{HMA}} = \frac{1.3}{1.3} = \frac{\varepsilon_{6M}^{HW}}{\varepsilon_{6M}^{HMA}} \times \frac{\varepsilon_{6L}^{HMA}}{\varepsilon_{6L}^{HW}}$$

Equation 5 - 15

Goacolou *et al.* (1997) concluded that the shift factor for cold foamed mix was equivalent to that of HMA i.e. 1.3 where the mixes have the same volumetrics. Assuming that the shift factor value for half-warm foamed mix is equivalent to that of cold foamed mix and HMA (which is a reasonable assumption considering that HW mix behaves more like HMA than

CMA), then Equation 5 - 15 is valid. Substituting the values obtained from Figure 5 - 30 in this relationship yields:

$$\frac{\varepsilon_{6M}^{HW}}{\varepsilon_{6M}^{HMA}} \times \frac{105}{95} = 1 \qquad \textbf{Equation 5 - 16}$$

This implies that under field loading conditions, HW STAB would require 90% of the working horizontal tensile strain of HMA STAB to yield an equivalent 10^6 standard axle load repetitions to failure for similar loading conditions in terms of temperature and frequency.

5.2.3 Dissipated Energy Approach

An alternative approach for the characterisation of the fatigue results, is the use of dissipated energy. According to van Dijk (1975) the following relationship is applicable to fatigue testing:

$$W_f = B_f N_f^z \qquad \textbf{Equation 5 - 17}$$

or

$$\text{Log } W_f = \log B_f + z \log N_f \qquad \textbf{Equation 5 - 18}$$

where,

W_f = total dissipated energy per volume (J/m^3)
N_f = number of load repetitions to fatigue failure
B_f, z = constants

From regression analysis of the results, a good fit is obtained for both functions. Values of 0.198 to 0.0256 are obtained for B_f , which is slightly higher than those reported by van Dijk and Visser (1977) of 0.012. This is compensated by the lower values obtained for z of between 0.41 and 0.57 compared with the 0.7 reported by these authors. However, the results of the HMA STAB and HW STAB are in line with results reported by Medani (1999) obtained for different asphalt mixes using the same test apparatus (4PB).

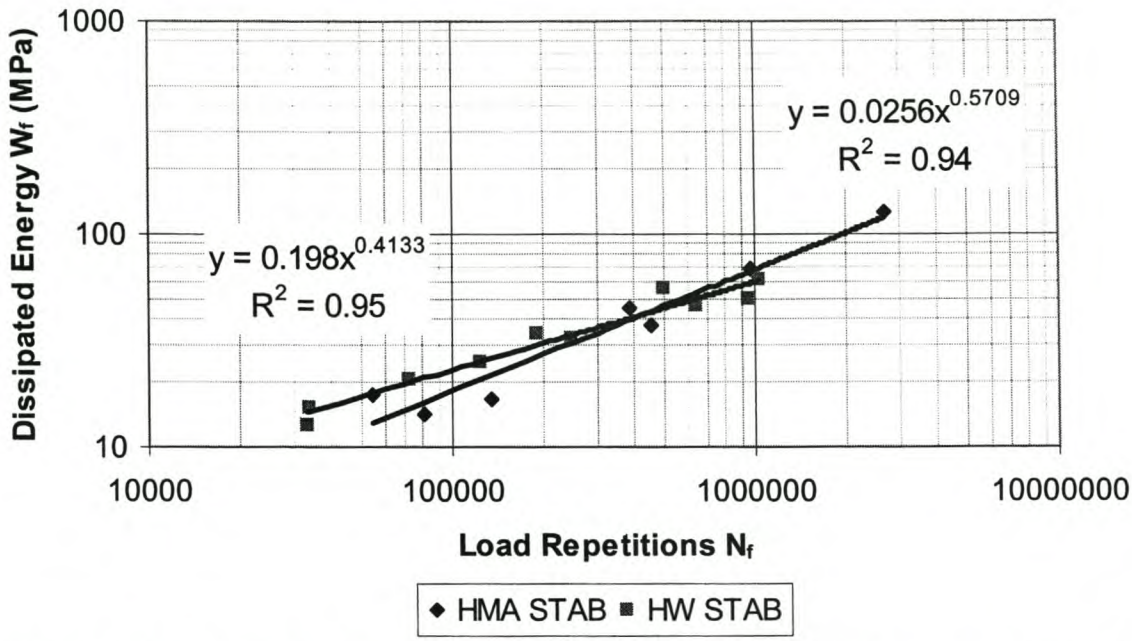

Figure 5 - 31. Relationship between Accumulated Dissipated Energy and Number of Load Repetitions to Failure for 4PB Fatigue Test at 20°C and 10Hz

The dissipated energy approach to comparing the mixes, as with the Wöhler approach, indicates greater sensitivity of the HMA STAB mix to the dependent variable than the HW STAB mix, see Figure 5 - 31. However, it should be noted that for both approaches a moderate difference in the slope of the function is observed.

The initial phase angle, defined as the phase angle measured after 100 load repetitions of the beam fatigue test, has a distinct relationship with the level of tensile strain applied to the material, see Figure 5 - 32. This trend concurs with findings of Brosseaud *et al.*(1997), as discussed in Chapter 2 Section 2.9. Brosseaud *et al.* found a decrease in phase angle for cold foamed mix relative to the equivalent hot mix tested at the same frequency. In ranking of asphalt mixtures for use in road pavements, phase angle assists in gaining insight into rutting potential of a mix amongst other factors, with lower phase angles indicating a lower viscous component and hence more elastic behaviour. In this respect, the half-warm foamed mix exhibits some of the desirable properties that cold foamed mix is known to have i.e. lower phase angles than the equivalent hot mix asphalt. Although, the shift in phase angle for half-warm mixes compared with HMA, is not as significant as the shift between cold foamed mix and HMA, the trend remain non-linear with respect to level of strain.

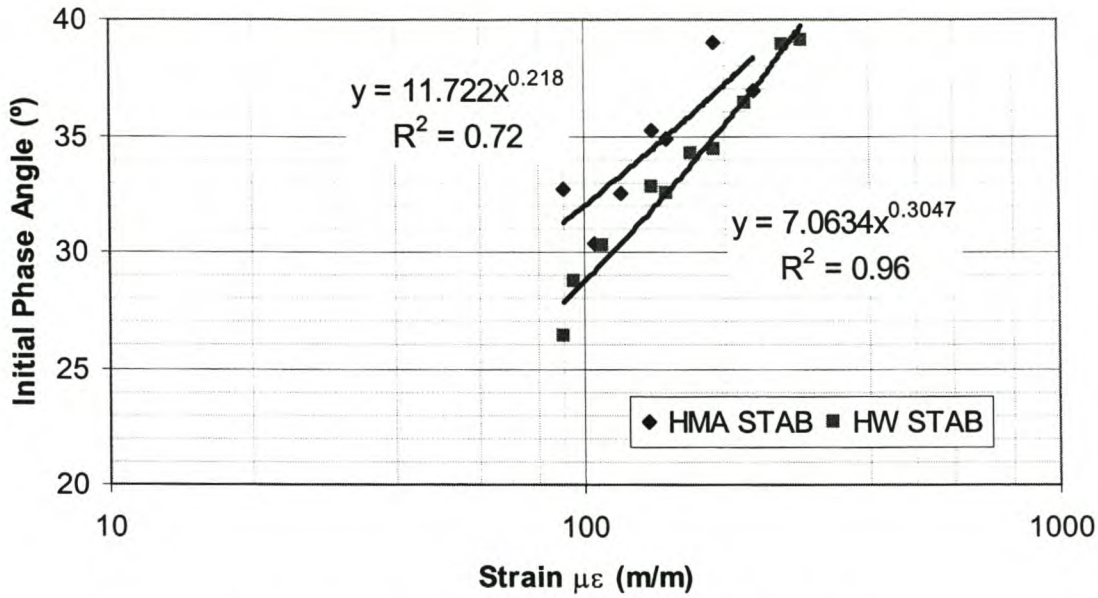

Figure 5 - 32. Relationship between Phase Angle and Strain Level of Loading for 4 Point Beam Fatigue Tests at 20°C and 10Hz

6. CONCLUSIONS

The development of a new process or product requires substantial research and development before a sufficient level of reliability is achieved to enable implementation on a large scale. This holds true for the half-warm foamed bitumen treatment process. This investigation has been limited to laboratory research at this point and not yet to full-scale production. The laboratory investigation, as outlined in this chapter, has however enabled conclusions to be drawn regarding this new process before full-scale trials and appurtenant research commences.

6.1 Energy Considerations

- The half-warm foamed bitumen process facilitates the production of bituminous mixes below the boiling point of water, thus reducing the energy consumption in heating the aggregates compared with that of HMA. This does result in the inclusion of moisture in the half-warm foamed mix, however. The extent of the energy savings is dependent, in particular, on the moisture content of the aggregate before mixing, but can exceed 40%.

6.2 Particle Coating

- The theory of physics that is considered applicable to the mixing of foamed bitumen with aggregate of different temperatures predicts improvement in dispersion of the bitumen binder with increasing aggregate temperature. These predictions were verified through physical mix production with aggregate temperature as a variable.

- The maximum particle size that is completely coated by foamed bitumen can be increased from in the order of 1mm to in excess of 10mm through an increase in aggregate temperature from 35°C to 85°C before mixing.

6.3 Workability and Compactability

- As with the maximum size of particles coated, the cohesion of half-warm foamed mixes increases with increasing aggregate temperature before mixing. This is more apparent with fine-grained material than coarse-grained mineral aggregates.
- Inclusion of moisture in HW foamed mixes is necessary for facilitating shelf-life, if this is a desirable property, otherwise HW mixes experience similar difficulties to HMA in terms of compaction at temperatures below 50°C.
- Notwithstanding the need for moisture in HW foamed mix, increasing compaction temperatures from 45°C to 90°C can reduce the air voids in the mix by up to 30%.
- Procedures for determination of an optimal fluids regime for compaction of cold foamed bitumen mixes are not applicable to half-warm mixes. Instead, moisture losses between production and compaction need to be accounted for in addition to the compaction temperature, and simulated in the laboratory to verify the optimum fluids regime.

6.4 Failure Properties of Half-warm Foamed Mix under Monotonic Loads

- Substantial increase in the compressive strength of foamed mix results from production of the mix at half-warm temperatures compared with production at ambient temperature. Although the HW foamed mix does not provide the same compressive strength as the equivalent HMA at temperatures lower than 25°C, the HW mix has comparable compressive strength at higher temperatures.
- The shear strength of HW foamed mix also increases significantly after production of the mix at half-warm temperatures, as opposed to production at ambient temperature. The sensitivity of shear strength of the HW mix to test temperature exhibits the same trend as compressive strength in comparison with the equivalent HMA.
- Analysis of the fracture energy in both compressive and shear tests indicates the tendency of half-warm mixes to approach hot mix behaviour at higher test temperatures.
- The use of reclaimed asphalt RAP in the HW mix is not necessarily detrimental to the mix properties, and can in fact improve the shear strength parameters compared with HW mix using virgin aggregate. However, a minimum threshold exists for the percentage of foamed bitumen that is added. Below this threshold, which is 2,4% foamed bitumen for mixing in a laboratory pugmill, a poorer quality mix results. The extent of the blending of the new bitumen with the old in such a half-warm mix has not been investigated at this point.

6.5 Dynamic Properties of Half-warm Foamed Mix under Cyclic Loads

- Master-curves of flexural stiffness determined for half-warm foamed STAB and hotmix STAB yields a significant shift in stiffness at lower frequencies of loading. This concurs with research into the master curves of cold foamed mix compared with the equivalent hot mix at similar binder contents. However, the shift occurs to a lesser degree with half-warm mix than with cold mix. The higher flexural stiffness of the half-warm mix at extended loading times will assist in resisting permanent deformation.
- The fatigue relations of half-warm foamed mix from beam fatigue tests are comparable with those of the equivalent hot mix. However, the HW mix fatigue relationship is moderately less sensitive to the level of tensile strain than the HMA.
- The relationship between the initial phase angle and the tensile strain level from the fatigue tests indicates that the HW foamed mix has a lower phase angle by several degrees. This phenomenon can be advantageous in resistance of permanent deformation considering the Burger's Model of Rheological Properties, see Figure 5 - 33. If the elastic components of a binder (or mix), illustrated by springs E_1 and E_2 remain unchanged, but the viscous components illustrated by dashpots λ_2 and λ_3 experience a decrease in phase angle, then the permanent deformation after unloading will reduce. This finding concurs with previous research into cold mixes relative to the equivalent hot mix; however, with the cold mix, the shift is more significant.

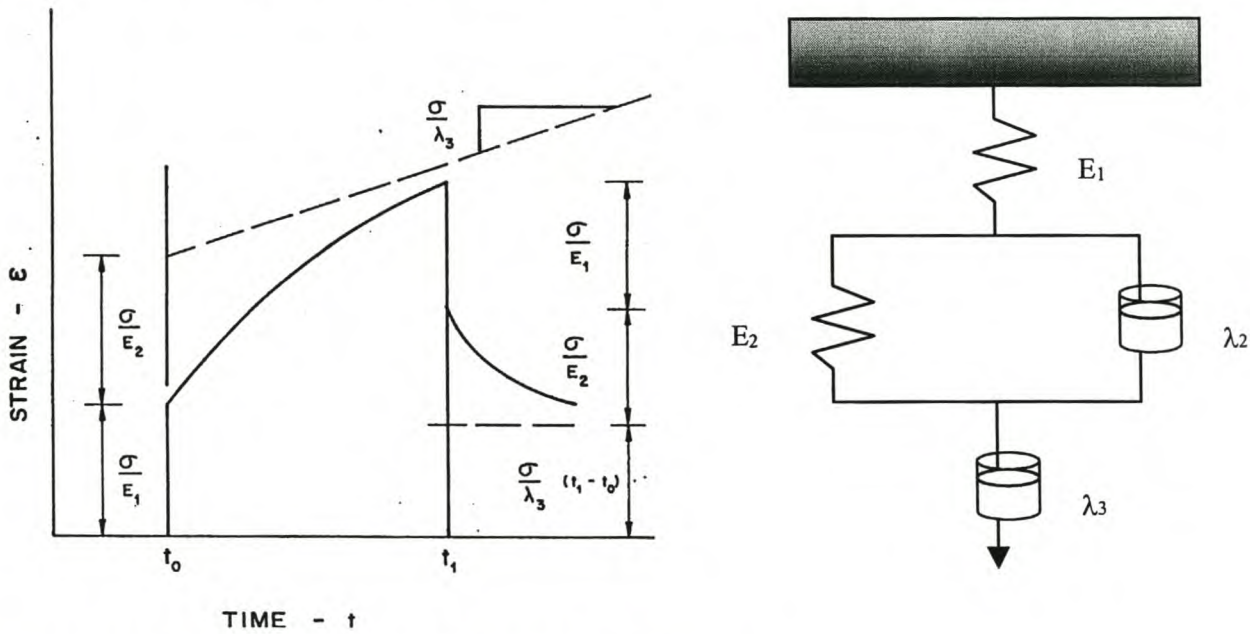

Figure 5 - 33. Burgers Rheological Model for Bitumen

6.6 General

- The investigation into half-warm foamed mixes at temperatures of less than 100°C does not restrict the production of these mixes to this temperature. Figure 5 - 34, which is a summary of the results from Section 4.3.5, shows the trend of shear strength with

increasing aggregate temperature at production. It is evident that scope exists for the production of semi-hot or "Warm foamed mixes" too, depending on the requirements of the mix in the road pavement. The energy savings would naturally diminish with increasing aggregate temperature.

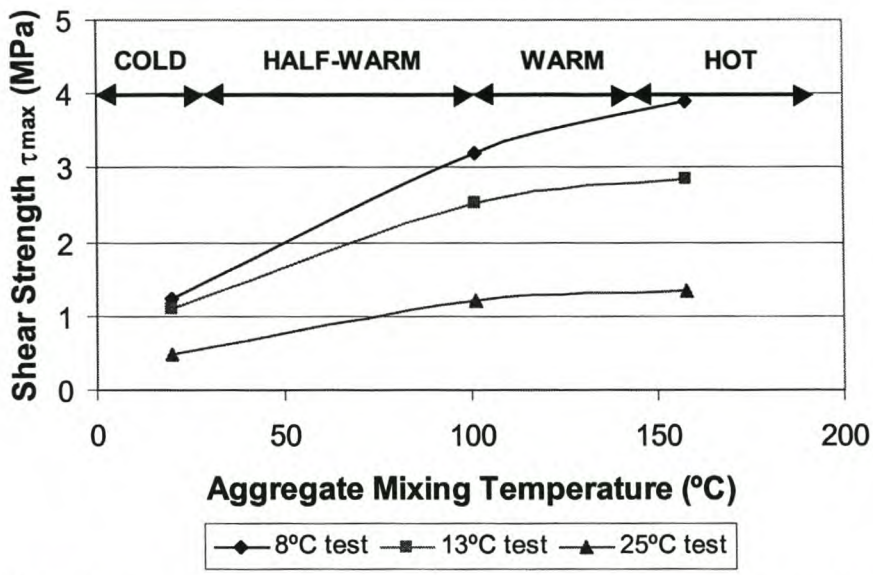

Figure 5 - 34. Summary of Influence of Aggregate Temperature of STAB before Mixing with Foamed Bitumen on Shear Strength from Leutner Test at Displacement Rate of 50,8 mm/min

- "Warm Foamed Bitumen Mixes" do not necessarily imply the exclusion of moisture within the mix considering the aggregate temperatures in excess of 100°C. Besides the aggregate's moisture content in stock-pile, the duration of warming of the aggregate and delay time between production and compaction will influence the moisture content of the mix.
- Ignoring marginal differences in binder content, compaction levels and other random variability between equivalent mixes, the fundamental differences between cold, half-warm and hot mixes lie in the moisture content and aggregate temperature during production. Chapter 4 has shown that the moisture in a foamed mix disperses the bitumen in threads in the mix, rather than as a continuum. This changes the characteristics of the mastic. This chapter has shown that the aggregate mixing temperature influences the binder distribution in terms of particle coating and cohesion. In combination, these phenomena go towards explaining the results of the static and dynamic properties of the three types of mixes that have been observed. At colder aggregate temperatures, the binder is more fragmented and threadlike in the mix providing an increase in flexural stiffness compared with HMA. With increase in aggregate temperature at production, the binder is distributed in more of a continuum within the mix, increasing the cohesion (and hence tensile strength) of the mix but reducing the resistance to permanent deformation at higher temperatures and extended loading times.

- The variability of half-warm mixes is significantly higher than both cold and hot mix, and that the influence of aggregate temperature is the additional factor that requires the attention in terms of quality control, to minimize this variability. This is particularly pertinent for dependent variables such as temperature, moisture content, viscosity and compaction.

7. REFERENCES

Acott S.M.,1980. **The stabilisation of a sand by foamed bitumen – A laboratory and field performance study**. Dissertation for Master of Science in Engineering. University of Natal.

Bowering R.H. and Martin C.L., 1976. **Foamed Bitumen Production and Application of Mixtures : Evaluation and Performance of Pavements**. *Proceedings Association of Asphalt Paving Technologists*. New Orleans, USA. Pp 453-477

Brosseaud Y., Gramsammer J-C., Kerzreho J-P., Goacolou H. and Le Bourlot F., 1997. **Expérimentation (premiére partie) de la Grave-Mousse ® sur le manége de fatigue**. *RGRA No 752 (Revue Généralé des Routes et des Aerodromes),* Juin. Pp 61 - 70

Buschkühl G., Gapski J. and Gründel R., 1990. **Bituminöse Tragschichten aus Müllverbrennungssasche und Schaumbitumen**. Diplomarbeit, Fachbereich Bauingenieurswesen, Fachhochschule Hamburg. Germany.

CROW, 1995. **Standard RAW Bepalingen**. Stichting Centrum voor Regelgeving en Onderzoek in de Grond-, Water- en Wegenbouw en de Verkeerstechniek., Ede, Netherlands

CSIR Transportek, 1998. **Foamed Asphalt, Mix Design**. Website http:\\foamasph.csir.co.za:81/chap4.htm

de Bondt A.H. and Scarpas A., 1993. **Shear Interface Test Set-Ups**. Report 7-93-203-12, Road and Railway Research Laboratory, Delft University of Technology, Netherlands.

de Bondt A.H. and Scarpas A., 1994. **Theoretical Analysis of Shear Interface Test Set-Ups**. Report 7-94-203-15, Road and Railway Research Laboratory, Delft University of Technology, Netherlands.

Eggers C., Holzhausen M. and Bartels J., 1990. **Bituminöse Tragschichten aus Müllverbrennungssasche und Schaumbitumen under besonderer Berücksichtigung von unterschiedlichen Tensiden**. Diplomarbeit, Fachbereich Bauingenieurswesen, Fachhochschule Hamburg. Germany.

Erkens S.M.J.G. and Poot M.R., 1998. **The Uniaxial Compression Test, Asphalt Concrete Response (ACRe)**. Delft University of Technology, Report 7-98-117-4. Netherlands.

Erkens S.M.J.G. and Poot M.R., 2000. **Meten is Weten : Invloed van de h/D Verhouding op Druksterkte**. *Wegbouwkundige Werkdagen 2000.* Doorwerth, Netherlands. Pp 181-185

FHWA Federal Highway Administration, 1994. **Superpave Asphalt Mixture Design and Analysis**. Strategic Highway Research Programme, USA.

Francken L. and Clauwaert C., 1988. **Characterisation and Structural Assessment of Bound Materials for Flexible Road Structures**. *Proceedings of 6th International Conference on the Structural Design of Asphalt Pavements*, Ann Arbor 1987, University of Michigan. Pp 130-144

Germann F.P. and Lytton R.L., 1977. **Methodology for Predicting the Reflection Crack Life of Asphalt Concrete Overlays**. Report No. TTI-2-8-75-207-5, Texas Transportation Institute of the Texas A&M University, College Station.

Goacolou H., Le Bourlot F., Brosseaud Y., Gramsammer J-C., and Kerzreho J-P., 1997. **Expérimentation (premiére partie) de la Grave-Mousse ® sur le manége de fatigue**. *RGRA No 752 (Revue Géneralé des Routes et des Aerodromes)*, Septembre. Pp 61 - 70

IPC (Industrial Process Controls Ltd), 1998. **Beam Fatigue Apparatus**. Reference Manual. Boronia, Australia.

Jacobs M.M.J., 1995. **Crack Growth in Asphaltic Mixes**. PhD Dissertation, Delft University of Technology

Jenkins K.J., de Groot J.L.A., van de Ven M.F.C., and Molenaar A.A.A., 1999. **Half-warm Foamed Bitumen Treatment, A New Process**. *Conference on Asphalt Pavements for Southern Africa, CAPSA 1999*. Victoria Falls, Zimbabwe.

LCPC (Laboratoire Central des Ponts et Chaussée) and SETRA (Service d'Études Techniques des Routes et Autoroutes), 1997. **French Design Manual for Pavement Structures : Guide Technique.** LCPC and SETRA, France.

Leutner R.L., 1979. **Adhesion between Flexible Pavement Layers**. In German, Bitumen 3.

Lytton R.L., Uzan J., Fernando E.M., Roque R., Hiltunen D. and Stoffels S.M., 1993. **Development and Validation of Performance Prediction Models and Specifications for Asphalt Binders and Paving Mixes**. SHRP Report A-357, SHRP/NRC, Washington DC.

Medani T.O., 1999. **A Simplified Approach for Estimation of the Fatigue and Crack Growth Characteristics of Asphalt Mixes**. MSc Thesis. International Institute for Infrastructural, Hydraulic and Environmental Engineering (IHE) and Delft University of Technology, Netherlands.

Molenaar A.A.A., 1983. **Structural Performance and Design of Flexible Road Constructions and Asphalt Concrete Overlays**. PhD Dissertation, Delft University of Technology, Netherlands.

Molenaar A.A.A., Jenkins K.J., van de Ven M.F.C. and de Groot J.L.A., 1999. **Feasibility Report: Half-warm Foamed Bitumen Mixes**. Confidential Report for Zuid Nederlandse Asfalt Centrale (ZNAC) by TU Delft, Stellenbosch University and van Hees en Zonen bv.

Roberts F.L., Engelbrecht J.C. and Kennedy T.W., 1984. **Evaluation of Recycled Mixtures Using Foamed Asphalt**. *Transportation Research Record 968*. Pp 78-85

Ruckel P.J., Acott S.M. and Bowering R.H., 1982. **Foamed-Asphalt Paving Mixtures: Preparation of Design Mixes and Treatment of Test Specimens**. *Transportation Research Record 911*. USA. Pp 88-95

Sabha H., Groenendijk J. and Molenaar A.A.A., 1995. **Estimation of Crack Growth Parameters and Fatigue Characteristics of Asphalt Mixes Using Simple Tests**. Delft University of Technology, Road and Railway Research Laboratory.

Sayegh G., 1967. **Viscoelastic Properties of Bituminous Mixtures**. *Proceeedings of 2nd International Conference on the Structural Design of Asphalt Pavements*, Ann Arbor, University of Michigan. Pp 743-755

Shell International Pertoleum Company Limited, 1978. **Shell Pavement Design Manual; Asphalt Pavements and Overlaysfor Road Traffic**. London.

Van de Ven M.F.C., Smit A.de F. and Lorio R., 1997. **A New Stone Mastic Mix Design Based on a Binary Approach**. *Volume 3A, Transport Infrastructure II, South African Transport Convention*. Pretoria

Van Dijk W., 1975. **Practical Fatigue Characterisation of Bituminous Mixes**. *Proceedings of the Association of Asphalt Paving Technologists AAPT*, Volume 44. Pp 38-74

Van Dijk W. and Visser W., 1977. **The Energy Approach to Fatigue for Pavement Design**. *Proceedings of the Association of Asphalt Paving Technologists AAPT*, Volume 46. Pp 1-40

Van Wijk A. and Wood L.E., 1983. **Use of Foamed Asphalt in Recycling of an Asphalt Pavement**. *Transportation Research Record 911*. Pp 96-103

Williams M.L., Landel R.F. and Ferry J.D., 1955. **The Temperature Dependence of Relaxation Mechanism in Amorphous Polymers and other Glass Forming Liquids**. *Journal of ACS, Volume 77*. Pp 3701

CHAPTER 6

COLD MIX BLOCKS

1. INTRODUCTION

Block pavements, although historically constructed with concrete blocks, are also a form of application of cold bituminous mixes. The first records of block pavements that utilised asphalt properties extend far back in history. The ancient road of Aibur-shabu, the sacred route for procession of the Great Lord Marduk, built by Nebuchadnezzar II in about 600 B.C. was probably one of the first routes using these elements. Weinert (1980) describes this road as being constructed using sun-dried brick as a base layer followed by a natural asphalt tack-coat and dressed limestone and breccia surfacing with asphalt filled joints. Obviously the Babylonians had some innate understanding of the visco-elastic properties of asphalt (possibly more than they are credited for) and how it could be used to the benefit of block pavements.

The reason for exploring the use of cold mix technology in blocks is primarily demand for viable, alternative road-construction techniques that are simple, include a high labour component and use locally available materials. In many developing countries, appropriate techniques are required for the upgrading of roads not yet proclaimed and lacking in maintenance. This, against the backdrop of steadily increasing global unemployment figures, provides a fertile environment for innovation in road construction. In South Africa alone, the employment intensity of the non-agricultural private sector declined to 17% in 1995 and at the percentage labour force in agriculture declined from 17% to 14% from 1980 to 1990 (Roux, 1997).

The ancient techniques of road construction such as block paving, amongst others, included an intrinsically high labour component due to limited availability of plant. This already indicates that blocks provide a "back-to-the-future" technique for employment creation. In addition to this, cold mixes are eminently suited for the manufacture of blocks. Not only are cold bituminous mixes workable at a wide range of temperatures, but they also have shelf-life characteristics and make use of locally available construction materials such as gravels and reclaimed asphalt (RAP). In the latter half of the twentieth century, the technology related to and application of cold bituminous mixes has increased substantially. The combination of these factors makes cold-mix eminently suited for use in employment intensive block manufacture and construction.

This chapter covers the construction of trial sections using bitumen-emulsion and foamed bitumen stabilized blocks. The focus is not on the development of a new construction technique but rather the relevant cold mix design aspects and subsequent performance results obtained.

2. BLOCK MANUFACTURE TECHNIQUES

2.1 Systematic development

Compaction is a critical factor in the performance of cold mix bituminous materials and this aspect is even more important for CAPs (Cold Mix Asphalt Paving-blocks) that are exposed directly to the action of the traffic. Insufficient compaction of these mixes results in a high void content and that leads to premature ageing, deformation, moisture ingress and stripping of binder. In order to achieve adequate compaction, initial trials for block manufacture therefore utilised bolt-up rectangular moulds on a vibrating table with a dead-weight hammer (Jenkins *et al*, 1997). This compaction technique required a hammer of 38 kg based on the findings of an investigation into the density of blocks manufactured using continuously graded ferricrete gravel, compacted with hammers at a variety of weights, see Figure 6 - 1.

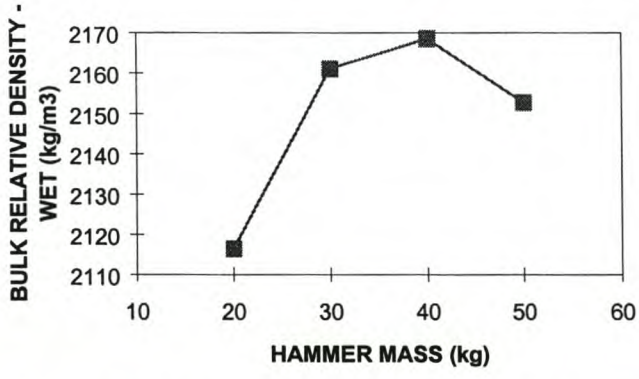

Figure 6 - 1. Influence of Hammer Mass on Block Density Achieved for 120 second Compaction Period on Ferricrete Gravel

Although the blocks manufactured using this technique enabled a limited trial section to be successfully constructed, the method proved cumbersome for full-scale production, not enabling rapid compaction and quick extrusion of blocks for storage and curing. The compaction duration of 100 seconds per block achieved an average of 100,1% of Marshall Density and an average block height of 67,9 mm with a standard deviation of 3,6 mm.

A new technique was designed to address the shortcomings of the initial system. This method uses interlocking plates to create a simple collapsible mould system (Ebels, 1998). The moulds are assembled on a portable wooden compaction board with guides to ensure that the geometry of the grid is accurately maintained, see Plate 6 - 1. This system provides for 20 blocks to be compacted per cycle, with each block 200 x 100 mm in plan i.e. the same surface area as the initial system. The moulds are removed after compaction leaving 20 blocks on the portable wooden board ready to be placed in stockpile. The thickness of blocks able to be manufactured using these moulds, ranges between 50mm and 100mm.

Plate 6 - 1. Compaction of CAPS using Kango Hammer in Collapsible Mould System

The compaction tool identified to efficiently compact the material in the rectangular moulds to a minimum of 95% of Modified AASHTO density was a Kango Hammer 637 ®. This level of compaction is necessary because, contrary to concrete blocks, cold bituminous mixes require a substantial compactive effort to yield a final product that is going to perform well under traffic loading whilst exposed to environmental influences. A Kango Hammer 637 ® with a mass of 7,5kg and a specially designed foot or contra-mould fulfils this function, providing adequate compaction to each block in a vibratory mode within approximately 40 seconds (depending on material type).

The procedure for compaction to achieve relevant densities is dependent on type of compaction foot utilised and duration of compactive effort. Increasing the weight of the compaction foot does not necessarily improve compaction, see Figure 6 - 2. Using this criteria, evolution of the compaction foot to an optimum tool for block manufacture was found possible (Ebels, 1998).

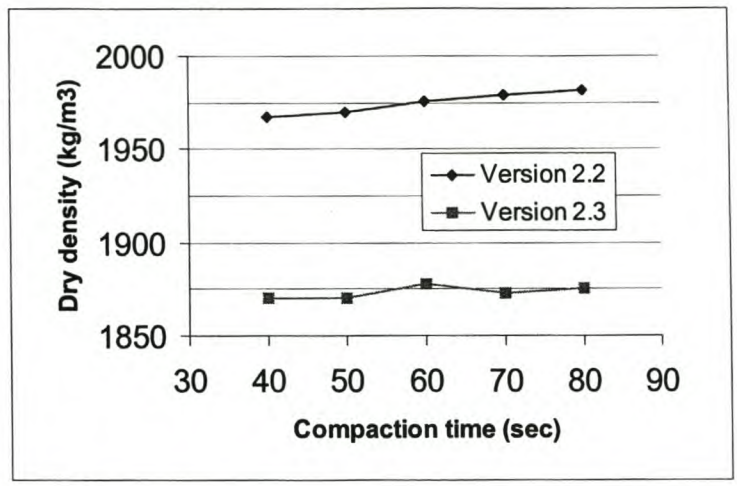

Figure 6 - 2. Compaction of Blocks Manufactured using Emulsion Stabilized Sandy Gravel with Kango Hammer®

Note:
Version 2.2 : Compaction foot excludes lead surcharge and has an overall weight of 19kg
Version 2.3 : Compaction foot includes a lead surcharge providing an overall weight of 25kg.

In order to standardise the compaction of the blocks, relative densities for Modified AASHTO compaction of the granular material and Marshall Density on the bound material were determined for comparative purposes, see Table 6 - 1. This verifies that a density greater than 95% of Modified AASHTO density is achieved using the Version 2.2 compaction foot. Additional tests have proven that the increase of the density during the initial 20 to 35 seconds of compaction is substantial, followed by only nominal increase after 40 seconds. In the interests of optimum productivity, the compaction time should be kept as short as possible. Since compaction times in excess of 40 seconds result in insignificant further increase in the density, this time interval was selected for full scale production of blocks. The residual binder contents utilised in block manufacture, selected primarily for economic reasons, are considered to be low for surfacing materials.

Table 6 - 1. Dry Densities of Sandy Gravel used for Block Manufacture (residual binder content = 3,6% in bound mixes)

	Granular	Foamed Mix	Emulsion Mix
Mod. AASHTO specimens	2050	-	-
Marshall specimens	-	2100	2050

2.2 Philosophy Behind Flexible Blocks

Currently utilised block pavement systems incorporate rigid elements of high stiffness in a segmental structure to provide an overall pavement with some flexibility. The use of visco-elastic elements such as CAPs (with sufficient binder) creates a more flexible structure,

alleviating the need for high crushing and tensile strength values for the blocks. This philosophy can be illustrated by considering the fracture energy (from a tensile test) for a rigid and a flexible element, as shown in Figure 6 - 3.

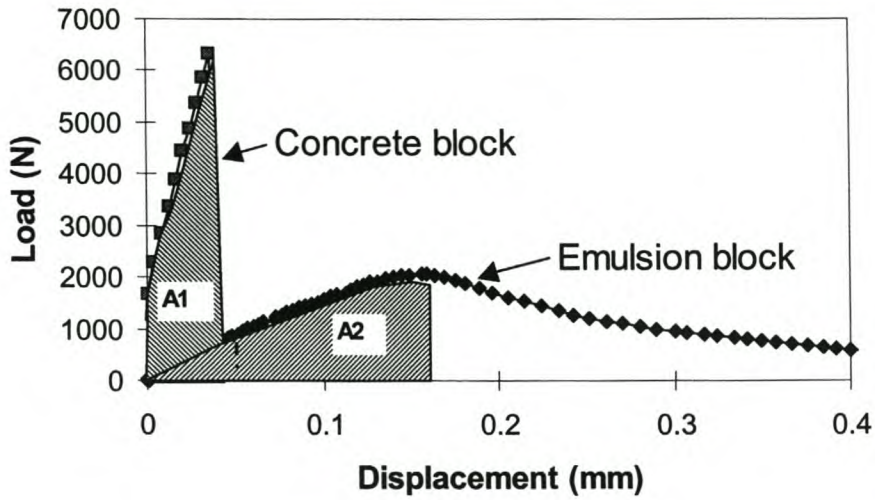

Figure 6 - 3. Typical Static Three Point Load Test Results for Emulsion and Concrete Blocks

Although the ultimate load is considerably higher for the concrete block, the area A2>A1 indicating that the fracture energy of the flexible element is at least equivalent but can be greater. This is the case even if higher deformation energy beyond the yield point is excluded. This phenomenon is applicable to both bitumen emulsion and foamed bitumen treated mixes. This fracture energy provides an indication of the fatigue life of the material under repeated loading and is therefore an important parameter in the consideration of flexible block pavements, particularly where low stiffness block elements are to be utilised.

In addition to energy considerations for the individual elements, the visco-elastic behaviour of the cold mix material influences the composite block matrix. The relatively higher Poisson Ratios for the bituminous material than for concrete blocks allows CAPs to deform laterally with repeated vertically applied wheel loads. This provides a natural "lock-up" of the block matrix with improved load transfer at joints.

A modified mix design procedure is required for the formulation of cold mixes for use in CAPs compared with the approach utilised for mix application in continuous layers, to take account of these aspects. The areas of focus in the mix design include volumetric properties, tensile strength, moisture susceptibility and stiffness. In particular, the spatial composition of the mix and the appurtenant volumetric properties, require consideration.

3. CHARACTERISATION OF THE BLOCK ELEMENTS

The characteristics of the individual block elements require investigation and interpretation before a composite block pavement can be considered. To this end, an apparatus is required for the testing of cold mix paving blocks that will provide measurements of the block properties such as tensile strength and stiffness, for analysis.

3.1 Three-point Block Testing Apparatus

A three point bending apparatus was developed for the static and dynamic testing of cold mix block elements, see Figure 6 - 4. Although the apparatus was designed for a 200x100x70mm block, it can accommodate a variety of sizes through adjustable settings. Loading is provided by means of a vertically applied force on a 20mm wide loading strip over the width of the block at its centre, which is simply supported at 65mm either side of the centreline.

Utilisation of the three-point block testing apparatus in the MTS 1364 press enables vertical displacement measurements to be made using the Linear Variable Displacement Transducer (LVDT) in the ram. For dynamic testing of blocks, an LVDT with a higher sensitivity is required. This transducer is placed vertically underneath the block in a protective cylinder, see Figure 6 - 4.

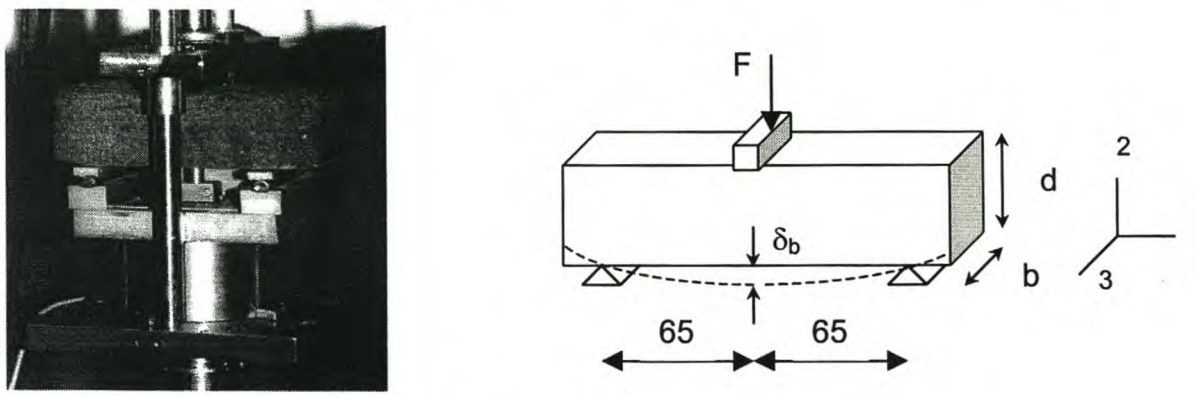

Figure 6 - 4. Block Element Test Configuration

The $^{l}/_{d}$ ratio of the individual block elements of 2,85 renders classical beam theory invalid for such a "deep beam". In addition, the "deep beam theory" equations of Timoshenko and Goodier (1970) are not applicable to the loading apparatus. A finite element analysis is therefore necessary in order to establish the stress-strain distribution within a block test setup. To this end a 3-D Finite Element Model (FEM) was established using ABAQUS Software (Hibbit *et al.*, 1996) to analyse the blocks as tested in the three point bending apparatus. A 2-D model could not be applied as the deep beam theory shows plane stress conditions to be inapplicable. A block of dimensions 200x100x70mm was analysed in the model, with a loading strip of 20mm wide and two support-strips of 20mm free to rotate in Plane 12 and translate along Axis 1. The 3-D FEM included 20-noded isoparametric

elements. Seven hundred and ninety five (795) elements in total were used to model the block, loading head and supports. Symmetry was applied in the FEM in two directions i.e. the test specimen was quartered and, in the absence of alternative material models, linear-elastic properties assumed for the elements.

The Finite Element Analysis (FEA) for the blocks followed similar procedures to those of Lytton *et al.* (1993) and van de Ven *et al.* (1997) for developing stress-strain relationships for the ITS Test and SCB Test respectively. The analysis requires variation of factors such as load and material properties in order to verify the applicability of relationships extracted from the model.

The deformed shape of the block analysed with ABAQUS is shown in Figure 6 - 5. In the FEM, the prismodic object represents the simple support allowing rotation and translation without vertical displacement and the small rectangular solid represents the loading head.

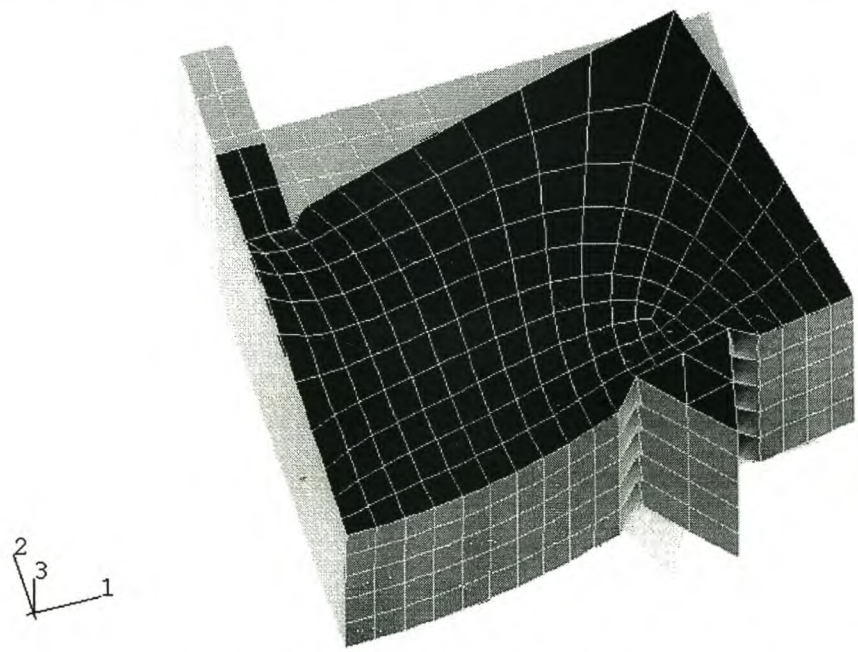

Figure 6 - 5. Finite Element Model of Block Before and After Displacement

The three point bending apparatus results are applicable to the determination of both static and dynamic properties. The models developed for block analysis may be compared with the closest applicable theoretical models for both of these cases.

3.2 Tensile Strength of Blocks

In the establishment of an equation for the tensile strength of a standard block that has been tested in three point bending mode, only the influence of the bending requires consideration. Shear stresses will not contribute to the principal stresses.

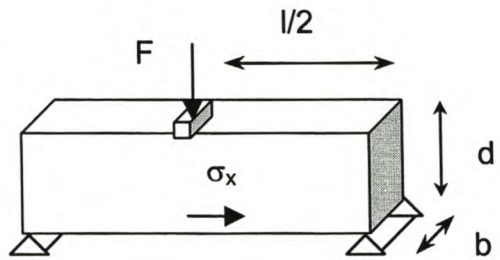

Figure 6 - 6. General Configuration of 3 Point Beam Test with Tensile Stress

The standard equation for the tensile stress in the soffit of a beam takes the form:

$$\sigma_x = \frac{M.y}{I}$$ **Equation 6 - 1**

Where,

M = bending moment at analysis point
y = distance from neutral axis to analysis point
I = moment of inertia = $bd^3/12$ for a rectangular section beam

Using the geometry of the standard block (200x100x70mm) and 130mm between supports, this equation simplifies to:

$$\sigma_x = 0.343 * F$$ **Equation 6 - 2**

Varying the Poisson Ratios(μ) in the FEA between 0,3 to 0,44 for a linear elastic material yields a variation of the maximum tensile stress in the model of only 1%. A value of μ = 0,35 was therefore utilised throughout the detailed analyses. A linear relationship exists between maximum horizontal tensile stress and applied load as shown in Figure 6 - 7. The form of this relationship conforms to that of the SCB model (van de Ven *et al.*, 1997).

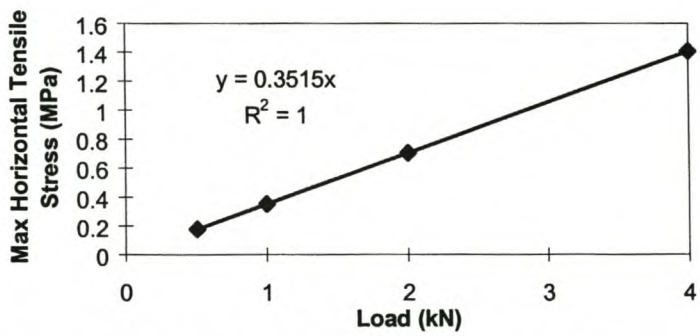

Figure 6 - 7. Relationship between Maximum Horizontal Tensile Stress and Applied Load on a Standard Block in Three-Point Bending Test, from Finite Element Analysis

The linear relationship in Figure 6 - 7 allows the tensile strength of a mix to be calculated from Three-point Static Testing of the blocks (Jenkins *et al.*, 1997) as given in the following equation:

$$\sigma_x = 0.3515 * F \qquad \textbf{Equation 6 - 3}$$

The differences between theory (Equation 6 - 2) and the FEA (Equation 6 - 3) can be partly accounted for due to the imperfections of the finite element model with limited number of elements and nodes etc. Notwithstanding this, the conformity is acceptable and the finite element model may be used to calculate the maximum tensile strength of a block in the three point testing mode. Using these equations, an adjustment may be made for deviations in the block height using the following formula:

$$\sigma_x = 0.3515 * F * \left(\frac{70}{h_a}\right)^2 \qquad \textbf{Equation 6 - 4}$$

3.3 Block Stiffness

The stiffness behaviour of the individual block elements influences the composite stiffness of a block pavement. This is particularly true for cold mix bituminous blocks that have relatively low stiffness and can potentially deform vertically and laterally with time increasing lateral stresses at the joints and enabling increased load transfer. The Resilient Modulus of the block elements can be analysed using the three-point bending beam apparatus. The geometry of individual block elements does not facilitate the use of standard equations derived from beam theory. Finite element analysis is a methodology for the development of relevant equations. However, these equations may be checked using the best available theory, following a similar approach to that of Netherlands Pavement Consultants (1998).

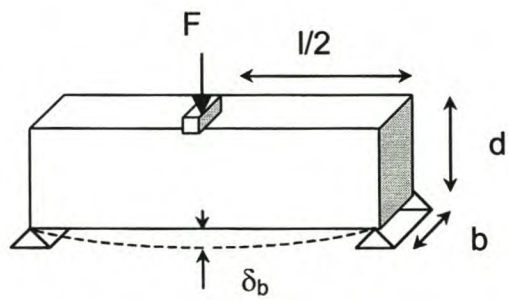

Figure 6 - 8. Three-point Bending System for Elastic Stiffness Measurement

3.3.1 Bending

From conventional beam theory, the deflection in the centre of a beam loaded in a three-point system as shown above, with linear elastic materials is:

$$\delta_b = \frac{F.l^3}{48EI} \qquad \textbf{Equation 6 - 5}$$

$$I = \frac{b.d^3}{12} \quad \text{(Moment of Inertia)} \qquad \textbf{Equation 6 - 6}$$

Substitution of these equations yields:

$$\delta_b = \frac{1}{48}\frac{F}{b.E}\left(\frac{l}{d}\right)^3 \qquad \textbf{Equation 6 - 7}$$

Where,

δ_b = deflection in the beam due to bending (mm)
F = applied load (N)
l = length of beam (mm)
b = breadth of beam (mm)
d = depth of beam (mm)
E = Elastic Modulus (MPa)

Ignoring shear in the beam and using the geometry of a standard block test set-up given below, an inaccurate equation for the block stiffness can be developed, see Equation 6 - 8.

- length between supports = 130mm
- breadth = 100mm
- depth = 70mm

This equation is, however, incomplete without the shear component. The magnitude of the error becomes apparent through comparison of the constant 16,013 with that developed through more detailed analysis, including the use of finite elements.

$$E = \frac{16.013 * F}{\delta} \qquad \textbf{Equation 6 - 8}$$

3.3.2 Shear

In particular, where $^{l}/_{d} < {}^{10}/_{1}$ the contribution of the shear component to the beam deflection needs to be accounted for. This may be done using Equation 6 - 9.

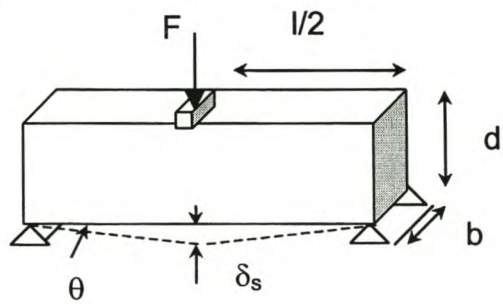

Figure 6 - 9. Shear Components for Three-point Beam Test

$$\delta_s = \gamma\frac{1}{2} \qquad \textbf{Equation 6 - 9}$$

Where,

δ_s = deflection in the beam due to shear (mm)
γ = shear strain = $\tan\theta = \delta_s/(l/2)$ ($=\theta$ where $l/2 >> \delta_s$)
l = length of beam (mm)

In addition, it is known that the Shear Modulus is defined as:

$$G = \frac{\tau}{\gamma}$$ **Equation 6 - 10**

Where,

G = Shear Modulus (MPa)
τ = Shear stress (MPa)
γ = Shear strain

The relationship between the Elastic Modulus (E) and the Shear Modulus (G) for elastic materials, is dependent on Poisson's Ratio (μ) as given below:

$$E = 2(1+\mu)G$$ **Equation 6 - 11**

For a beam that is rectangular in section, the shear stress throughout the beam may be defined as:

$$\tau = \frac{F}{b.d}$$ **Equation 6 - 12**

Substituting Equation 6 - 10 to Equation 6 - 12 in Equation 6 - 9 yields:

$$\delta_s = \frac{\tau}{G}\frac{l}{2} = \frac{F}{b.d}\frac{2(1+\mu)}{E}\frac{l}{2}$$

$$= (1+\mu)\frac{F.l}{E.b.d}$$ **Equation 6 - 13**

The total deflection observed in a beam loaded in three-point bending mode is therefore the sum of the deflection due to bending and shear, as given below:

$$\delta = \delta_b + \delta_s = \frac{1}{48}\frac{F}{b.E}\left(\frac{l}{d}\right)^3 + (1+\mu)\frac{F.l}{E.b.d}$$ **Equation 6 - 14**

Solving Equation 6 - 14 for E yields:

$$E = \frac{F.l}{\delta.b.d}\left[\frac{1}{48}\left(\frac{l}{d}\right)^2 + (1+\mu)\right]$$ **Equation 6 - 15**

For a fixed geometry of beam or block being tested with material of given Poisson Ratio, this equation may be simplified to the form:

$$E = \frac{const * F}{\delta}$$ **Equation 6 - 16**

Utilising Equation 6 - 15 to analyse the bituminous blocks tested, a sensitivity analysis could be carried out for different Poisson Ratios, as given in Table 6 - 2.

Table 6 - 2. Sensitivity analysis of Constant in Beam Stiffness Equation versus Poisson Ratio (analytically determined)

Poisson Ratio μ	0.25	0.3	0.35	0.4	0.45
Const. in Eqn. 6 –16	24.55	25.48	26.41	27.33	28.26

The values for the constant obtained in Table 6 - 2 using a theoretical approach can be compared with the equivalent results from the finite element analyses. A sensitivity analysis for the load and Poisson Ratio in the FEA provides the relationship between the primary measurements of a stiffness test on a standard block of 200x100x70mm, as shown graphically in Figure 6 - 10.

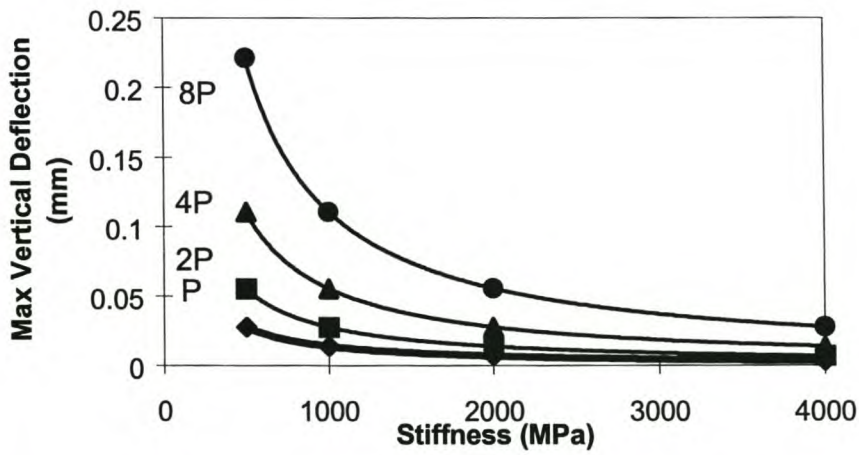

Figure 6 - 10. Relationship between Maximum Vertical Deflection, Applied Load and Stiffness for a Three-Point Bending Test on a Standard Block from Finite Element Analysis

The relationships obtained for the curves in Figure 6 - 10 may be normalised in terms of the magnitude of the load in order to obtain an equivalent constant for Equation 6 - 16. This constant, obtained using finite elements, is recorded in Table 6 - 3. The average value for the constant of 27,18 from FEA compares favourably with the value of 26,41 obtained analytically for the equivalent material with μ = 0,35 in a standard block.

Graphical representation of the relationship shown in Figure 6 - 10 assists in identifying suitable magnitudes of deflections in order to achieve reliable resilient stiffness values. Where the material stiffness exceeds 2500 MPa, a substantial force needs to be applied in

order to obtain reliable stiffness results. Maximum vertical deflections of at least 0,05mm are necessary for utilisation of the curve in Figure 6 - 10 with ample gradient and hence sensitivity to determine reliable M_r values.

Table 6 - 3. Equation Constant Values for Resilient Stiffness based on FEA based on a Poisson Ratio of μ = 0.35

Load	Constant C	Normalised constant (C/P)
P	13.386	26.77
2P	27.222	27.22
4P	54.626	27.31
8P	109.676	27.18
Average		**27.18**

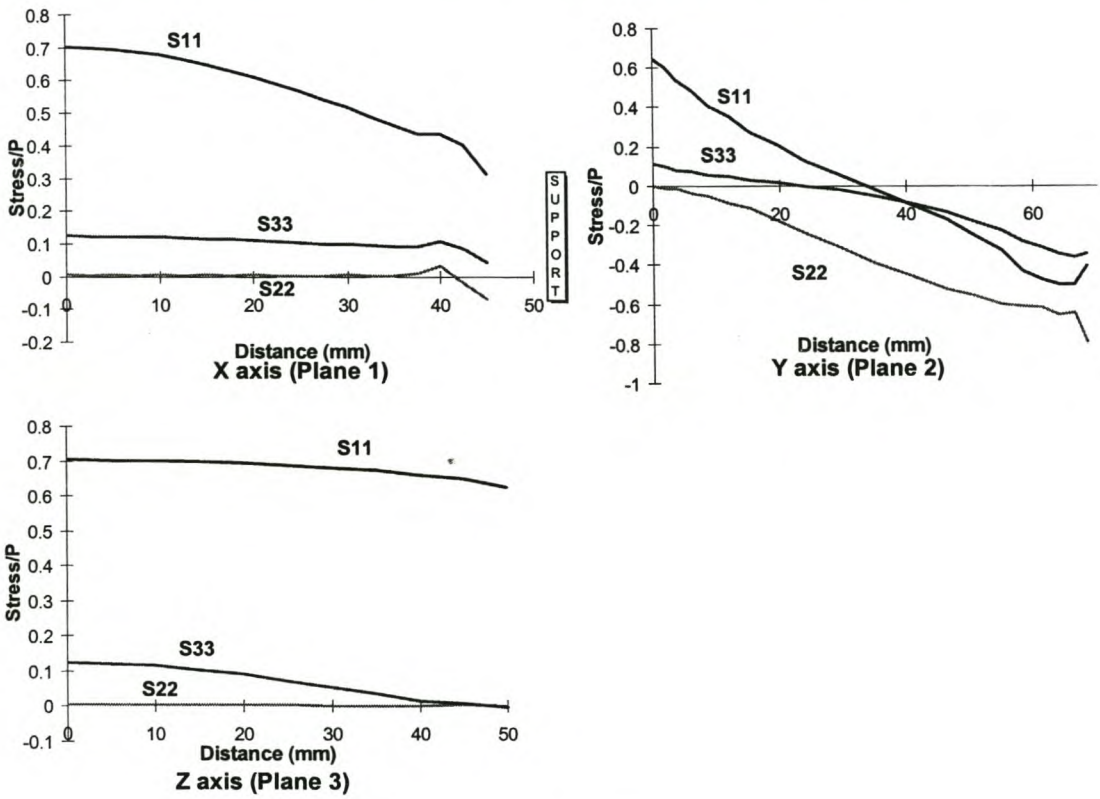

Figure 6 - 11. Distribution of Principal Stresses as a Fraction of Applied Stress, along Principal Axes for a Three-point Bending Test from Finite Element Analysis

The influence of shear stresses in the effectively deep beam that the standard block represents in the Three-point Bending Test is evident from the non-uniform stress distribution in certain planes e.g. over the width of the block i.e. Plane 3. This invalidates conventional beam theory and necessitates the use of finite elements, as applied.

3.4 Comparison of Tests on Cold Mix Blocks

The inclusion of a visco-elastic binder such as bitumen in the block elements makes the stress distribution and rate of loading of bituminous test specimens important considerations. The type of cold mix binder i.e. foamed or emulsified, percentage of binder and characteristics of the aggregate will contribute to the mix behaviour in terms of loading speed. The influence of loading speed is evident from the reduction in ultimate load required for the failure of blocks manufactured with Ferricrete and 3% residual bitumen from emulsion with 1% cement. More than 25% decrease in maximum load is required, as the rate of deformation is increased to one tenth of the original value, see Figure 6 - 12.

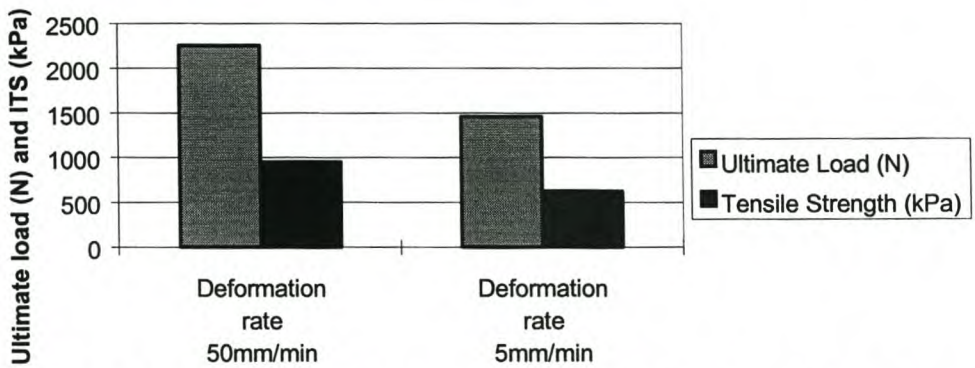

Figure 6 - 12. Three-point Beam Tests at 25°C for Blocks with 3% Residual Bitumen averaged for 4 tests

Due to the geometry of three-point beam test, only a small deflection under static loading is necessary to achieve failure. For this reason, a slower displacement rate is required than the typical rates of 50 mm/minute. A rate of 5 mm/minute provides more accuracy and repeatability for 3 point beam tests. For a valid comparison between the Indirect Tensile Strength (ITS) and the Three-point Beam Tensile Strength of visco-elastic materials, both of the tests need to be carried out at 5mm/minute.

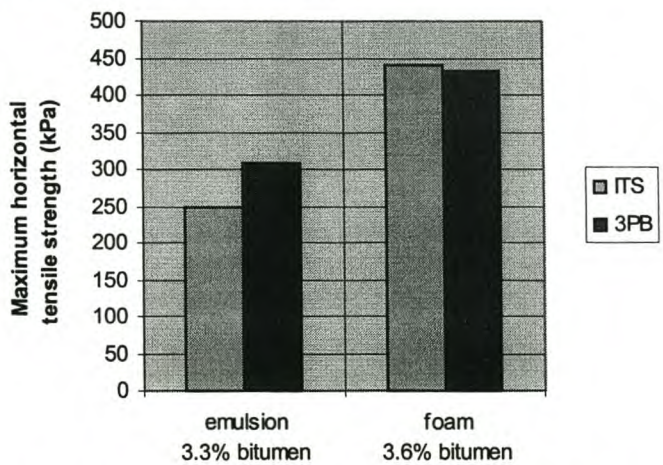

Figure 6 - 13. Comparison between Three-point Beam (3PB) and Indirect Tensile Tests (ITS) Results for Quartzitic Aggregate Stabilized Blocks

Absolute differences between tensile strengths in cold mixes compacted to equivalent densities and tested with different geometric specimens, as seen in Figure 6 - 13 , cannot be justified without insight into the most relevant issue i.e. variability. Analysis of the coefficient of variation for the same series of tests using the Indirect Tensile apparatus and the Three-point Beam, see Figure 6 - 14, shows a significantly higher variability for ITS results. One of the contributory factors to this variability is the compressive stresses that occur in an ITS specimen. Lytton *et al.* (1993) showed that these compressive stresses are three times the magnitude of the tensile stresses at the critical stress point in the specimen, making a combination of compressive and tensile failure possible. The three-point beam test configuration has substantially lower compressive stresses thus eliminating this convoluting factor.

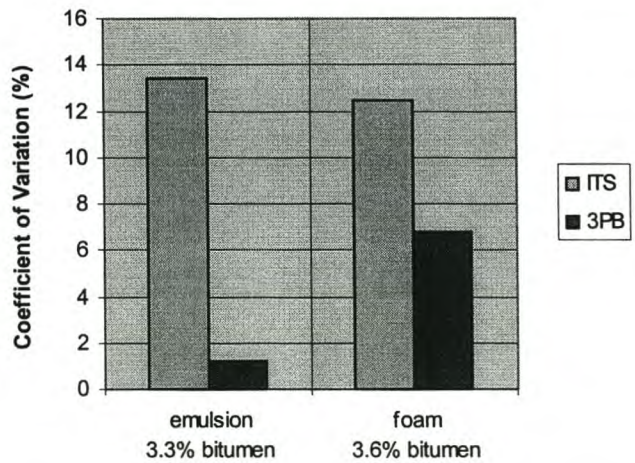

Figure 6 - 14. Variability of Results of Indirect Tensile Strength (ITS) and Three-point Bending (3PB) Tests on Cold Mix Blocks with Different Binders

4. TRIAL SECTIONS

Characterisation of cold bituminous mixes through laboratory testing requires a link to field performance. For this purpose, field trials are usually undertaken with parallel testing between the laboratory and the field. The inclusion of a number of factors such as manufacture and curing procedure for the blocks is facilitated through such trials, thus providing an insight into acceptable limits for material properties and construction procedures.

Two trial sections have been constructed in South Africa using cold mix paving blocks (CAPs). These trials comprised blocks manufactured with locally available materials, namely ferricrete gravel and sandy gravel, which were selected in the interests of investigating the usability and performance of marginal materials.

4.1 Colas South Trial : Ferricrete CAPs

Development of efficient procedures for cold-mix block manufacture requires trials of potential apparatus under laboratory conditions. Initial manufacture of cold mix blocks included the use of a dead mass in excess of 35kgs in a rectangular bolt-up mould. The use of three such moulds on a vibrating table enabled the manufacture of some 500 blocks for a trial section of 10 m^2, refer Jenkins *et al.* (1997b).

Emulsion stabilized ferricrete blocks manufactured solely under laboratory conditions, provided the elements for a trail section at the entrance to an asphalt plant. A binder content of 5% anionic emulsion (60:40) and 1% cement was used to enhance the material properties. Utilising a vibrating table for compaction, an average density of 100,1% of Marshall density was achieved. Variable thickness of block elements is created using this manufacture technique and the average thickness measured 67,9mm with a standard deviation of 3,6mm. Although the method used for block manufacture is effective, its low production rate makes it unsuitable for large-scale production.

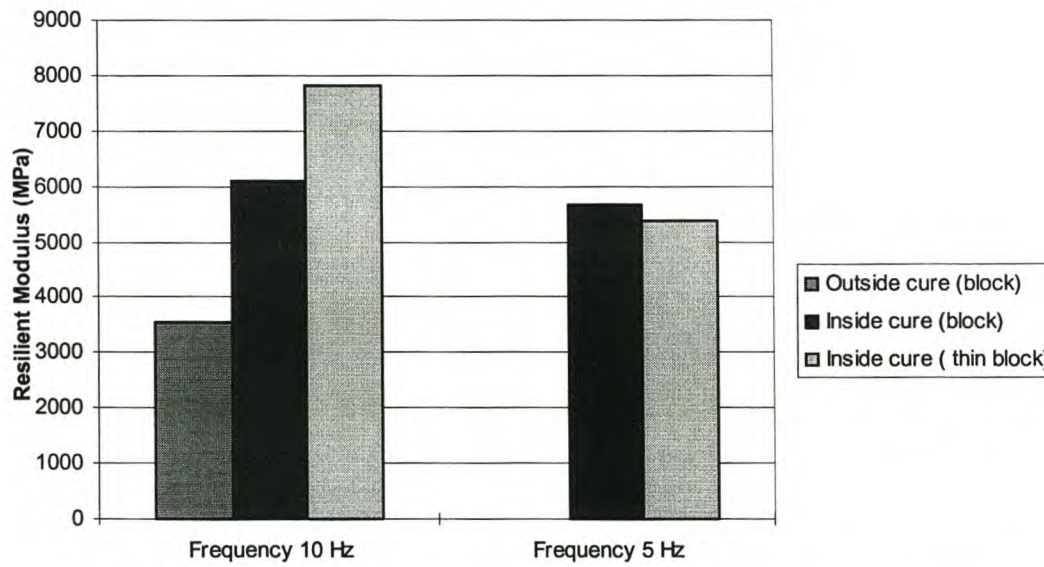

Figure 6 - 15. Influence of Curing and Test Frequency on Block Stiffness for an Average of Four Repeat Tests using 3PB Apparatus

In order to investigate the influences of temperature and moisture on curing, half of the blocks were cured with full exposure to the elements (outside) for four weeks with the other half being cured inside at lower temperatures for the same period. The curing included 5°C differences between average maximum temperatures outside (31°C) and inside (26°C). No protection was provided during curing in terms of covering. After full term curing the average moisture content of the blocks varied between 1,6% (inside curing) and 0,5% (outside curing). The dangers of substantial drying-out blocks during curing, through exposure to the sun and wind becomes apparent, with desiccation resulting in lower stiffness values (outside cure).

Even at a residual binder content of 3% bitumen, visco-elastic behaviour of the mix is evident from the shift in resilient modulus at different frequencies. This visco-elastic behaviour is apparent through the deformation of the individual blocks under traffic loads seen on the trial where moulding and closing of joints became apparent, noted during visual observation.

4.2 Sir Lowry's Pass Village Trial : Sandy gravel CAPs

As part of the infrastructural development of a new residential area, a trial section of 100 m^2 of CAPs was constructed in the access road network (Ebels, 1998). Locally available sandy gravel stabilized either with bitumen emulsion and foamed bitumen as binders formed the content of the blocks. A residual binder content of 3,6% was selected for both cold mixes, including a small percentage of cement for early strength. Due to the cohesionless nature of the parent material, the mix was supplemented with inert filler.

4.2.1 Block production using a Kango Hammer ®

Primary improvements in the manufacturing technique in the second trial include the development of an interlocking grid mould system and use of a Kango Hammer ® for block manufacture. In particular, the new system provides for higher production rates for blocks without prejudicing quality. Details of the block manufacturing system are provided in the work of Ebels (1998).

The trial comprised 3 000 blocks that were manufactured under laboratory conditions in order to verify the suitability of the manufacture system, followed by in excess of 2000 blocks manufactured on site in four days. Unskilled labour, under the guidance of a supervisor, manufactured the blocks on site. Minor modifications to the manufacture apparatus were made during production, including strengthening of the moulds and contra-moulds (the foot of the Kango Hammer that fits into the mould), refer Ebels (1998). The procedure utilised for the production of the blocks is outlined below, refer Jenkins *et al.* (1999)

1. *Preparation of the mix.* The various components of the cold mix are blended in a concrete mixer in the case of the emulsion-stabilized gravel. Foamed bitumen stabilized mix needs to be manufactured and stockpiled on site utilising a static plant mixer.
2. *Setting of the Moulds.* The collapsible mould system is assembled on a firm base in preparation of block manufacture.
3. *Filling of the Moulds.* A measuring cup of selected volume to provide the desired block height is used together with a square funnel to fill the moulds with cold mix.
4. *Precompaction of the Mix.* In order to minimise segregation of material in adjacent panels during compaction, each of the 20 cells on the mould board requires gentle hand-ramming before the Kango Hammer is employed, as shown in Plate 6 - 2. Between 3 and 5 blows is required per cell.
5. *Compaction of the Mix.* The Kango Hammer is applied to each cell for a short period to achieve the required density (40 seconds/cell is sufficient for sandy gravel). Other materials require some experimentation to establish an optimum compaction time.

6. *Release of Moulds and Removal of Blocks.* The compaction boards are so designed to be portable by four people, to the place of curing. For limited production, two people can fulfil this function. Release of the moulds can be carried out efficiently by one person followed by cleaning of the interlocking plates before reuse. Care needs to be exercised to avoid damage to the freshly compacted blocks.
7. *Curing of Blocks.* At least two weeks of curing is recommended before the CAPs are ready for placement on the road, although this should be verified for a particular climate and specific materials. Handling of the blocks requires more attention than with rigid elements such as concrete blocks.
8. *Surface treatment.* Emulsion stabilised CAPs require surface enrichment to prevent excessive ravelling under traffic. A diluted emulsion (50:50 with water) has been used with some degree of success, although alternative procedures could be considered.
9. *Stockpiling of Blocks.* After some 3 to 4 days curing, CAPs have generally achieved sufficient strength to be stockpiled, thus reducing the occupation of space. Due to the visco-elastic nature of the cold mix resulting in creep deformation under lack of support, the blocks should be stored on their side creating a higher moment of inertia and limited to a height of four blocks.
10. *Laying of Blocks.* The procedures for placement of the CAPs adhere to the standard methods of block pavement construction. Conventional filler sand is used in the block joints to encourage frictional load transfer, see Plate 6 - 3.

Plate 6-2: Pre-compaction of cold mix prior to application of Kango Hammer

Plate 6-3 : Laying of CAPs with brooming of filler sand into joints

4.2.2 Performance characteristics of CAPs

The trial section that has been constructed provides data on the behaviour of the block elements themselves rather than the entire pavement structure. In particular, several factors form the focus of the cold-mix block behaviour, namely:

- Type of binder used in the cold-mix i.e. bitumen-emulsion or foamed bitumen,
- influences of active filler,
- effects of curing on the block tensile strength, and
- influence of traffic on the properties of CAPs.

The manner in which the above-mentioned factors were investigated on the trial section is indicated in Table 6 - 4. Monitoring of juxtaposed sections, each with variations of the relevant factors, allows comparative performance properties to be evaluated. The six sections selected all include 3,6% residual bitumen as binder, although the type of cold-mix binder is detailed in the table.

Table 6 - 4. Sub-division of Sir Lowry's Block Trial Section according to Variables

Section Number	Binder Type	Cement (%)	Block surface treated with diluted emulsion	Manufacture Location
1	Emulsion	1	Yes	Laboratory
2	Emulsion	1	Yes	Site
3	Emulsion	0	Yes	Laboratory
4	Foam	1	Yes	Laboratory
5	Foam	1	No	Laboratory
6	Emulsion	1	No	Laboratory

Results from the initial trial section at Colas revealed the importance of curing technique as an influence on the block properties, highlighting the need for the determination of a suitable curing period for cold mix blocks before handling and construction. Considering that tensile strength of the blocks provides a relevant criterion for determining the readiness of a block for paving, the three-point beam testing apparatus provides a suitable measurement tool for determining this property. Data shown in Figure 6 - 16 assisted in the selection of 14 days as the minimum period of curing for the given material and climate, before laying of the blocks could commence. For economic reasons, curing was arranged during storage outside in an uncovered environment.

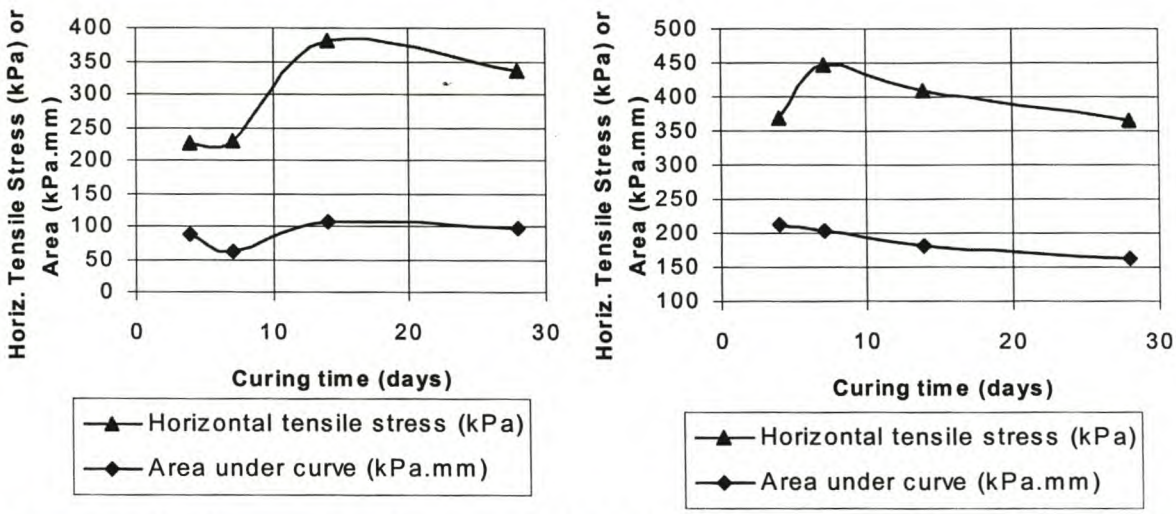

Figure 6 - 16. Strength gain versus time for Bitumen Emulsion (left) and Foamed Bitumen (right) Stabilised Blocks from Bending Beam Test

Due to the relatively low stiffness values of the cold mix blocks as determined during the laboratory mix design stage, decrease in stiffness under repeated traffic loading becomes a relevant mode of deterioration. Utilising a dynamic three point bending test, the stiffness of CAPs can be determined for blocks trafficked under laboratory conditions and field

conditions. Laboratory trafficking was carried out using an accelerated pavement testing device i.e. the Model Mobile Load Simulator (MMLS) with 1,9 kN wheel loads and 570 kPa tyre pressure for four wheels travelling in a continuous loop. Chapter 8 provides additional information on the MMLS device. A total of 48 610 axle repetitions for the (lab) conditions without lateral wander are compared with the same CAPs trafficked under field conditions for six months in the (field) in Figure 6 - 17. The field traffic in the comparative analysis equates to 2244 standard axle repetitions and 20 440 light vehicles which is substantially less than the accelerated traffic.

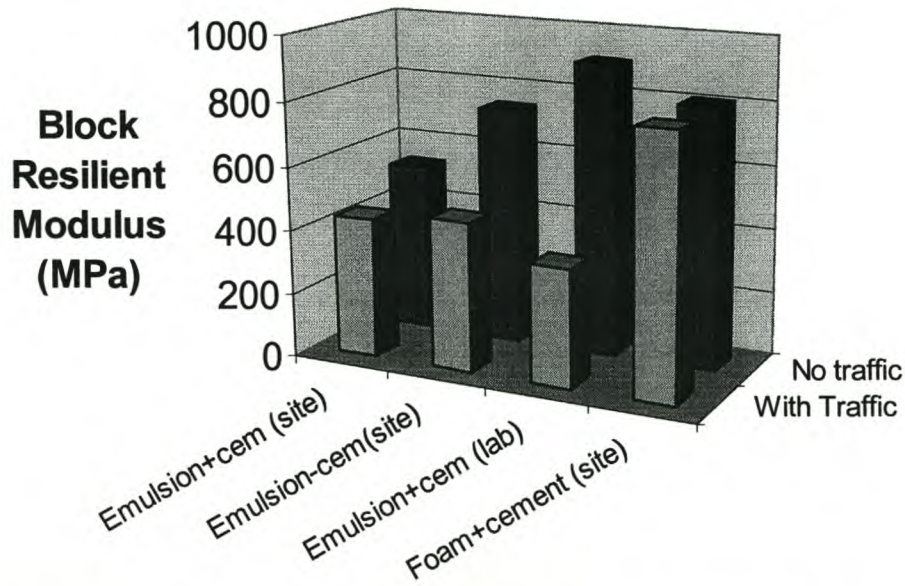

Figure 6 - 17. Decrease in Resilient Modulus as a Function of Traffic for Cold Mix Blocks using 3PB Test at 10Hz and 25°C

The results in the figure, namely the 80% Reliable Lower Limit of stiffness for three tests at each condition, indicate a significant decrease in resilient stiffness, even at relatively low traffic levels. The inclusion of cement is not necessarily detrimental, as its exclusion can provide relatively higher rates of stiffness loss. The type of binder significantly influences the rate of deterioration, with foamed bitumen treated sandy gravel not showing signs of distress under the same conditions that result in substantial degradation of emulsion blocks. Visual observations of the blocks at various stages of trafficking indicate that cracking is not evident at the surface, where the resilient modulus has reduced by 37%, but is evident when the modulus has reduced by 60%. Even at a binder content of 3,6% fatigue of the bituminous material can be observed and this will contribute to failure.

Predictably, ravelling is a dominant mode of degradation of cold mixes used as surfacing layers. In particular, the emulsion-stabilized blocks (even with surface enrichment using diluted emulsion) are prone to ravelling, see Figure 6 - 18. Sections 1 and 6 suffered most material loss, although dynamic loading at the approaches to the trial section with a slightly uneven level transition has exacerbated the degradation. Foamed bitumen binder provides significantly higher resistance to gravel loss at the equivalent residual binder content.

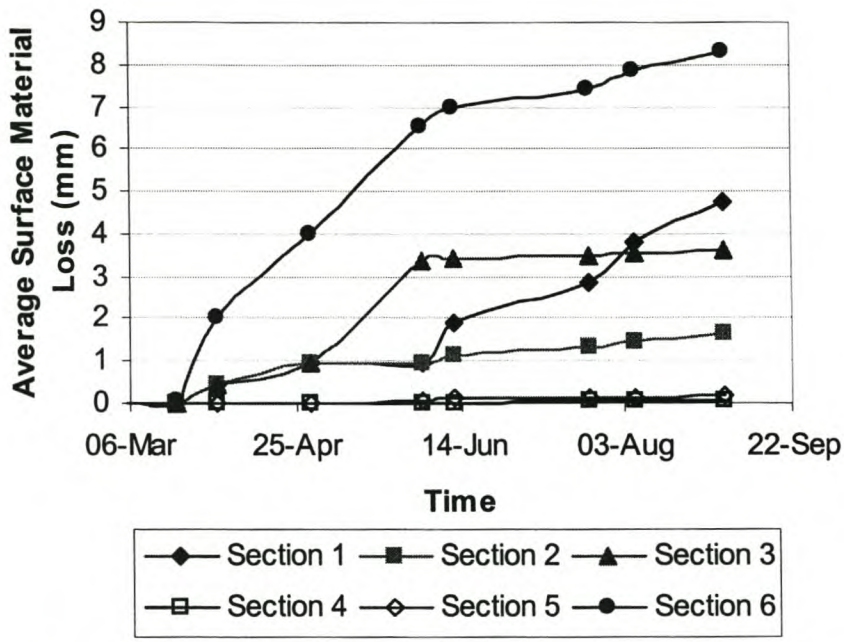

Figure 6 - 18. Ravelling of different sections of Sir Lowry's Pass Trial under Traffic

The contribution of climatic influences is apparent from the reduced ravelling of the same blocks in laboratory conditions with accelerated pavement testing using the MMLS, see Figure 6 - 19. Notwithstanding the concentrated loading utilised for this APT in the laboratory and the higher number of load repetitions, the benefits of surface enrichment are shown to be more promising under laboratory conditions without moisture influences, than in the field. Alternative methods of treatment of the block surface to diluted emulsion are required to prevent ravelling.

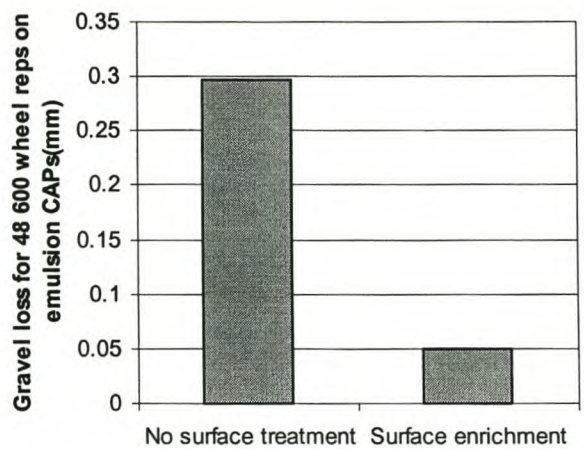

Figure 6 - 19. Ravelling of Emulsion CAPs from Sir Lowry's Trial under MMLS in Laboratory

In addition to the ravelling analyses, investigation of the load transfer at the joints of the blocks requires investigation, following evidence of moulding of these joints under traffic. The spectral analysis of surface waves (SASW) technique provides an effective method to monitor the stiffness change of the individual block elements and the joints with time and

traffic. This includes analysis of surface waves generated by impacts on the blocks using a spectral waveform analyser. The dispersion curves of the phase velocities versus wavelength are plotted for two sections in Figure 6 - 20.

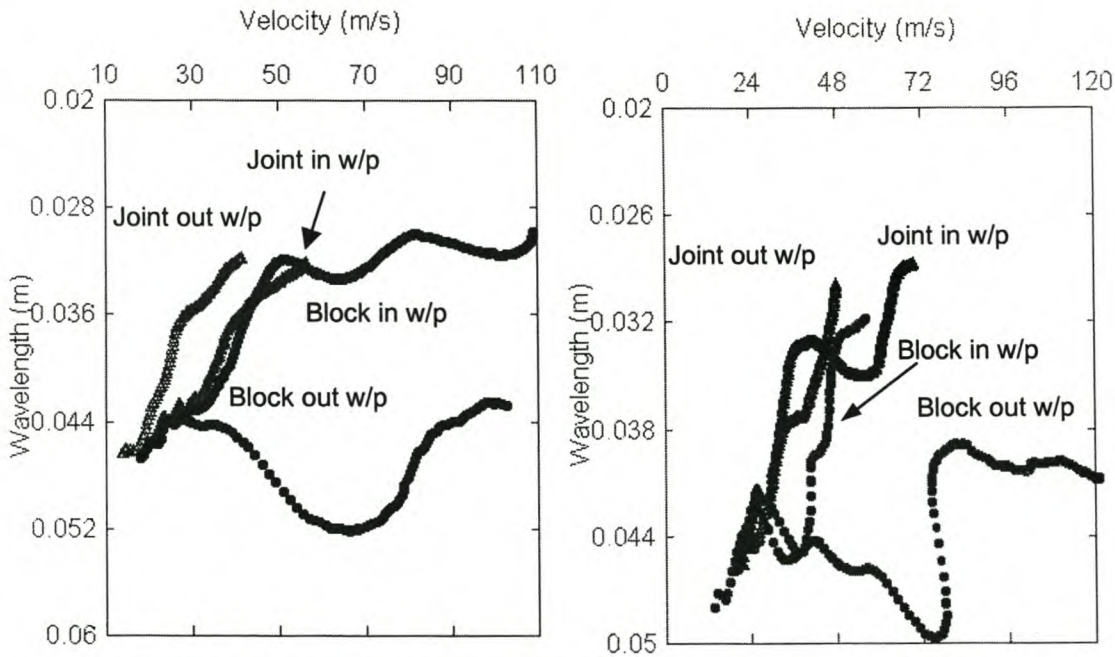

Figure 6 - 20. Dispersion curves from SASW analysis of Section 3 (left) and Section 4 (right) for Cold Mix Blocks

Legend: Joint = measurement across joint,
Block = measurement within block element,
w/p = wheel-path

From the dispersion curves, an indication of the dynamic stiffness modulus can be obtained. Considering the block thickness is 67mm, a wavelength of 0.040m is utilised to compare phase velocities. It is apparent from Figure 6 - 20 that a decrease in stiffness of the block elements has occurred under traffic, considering the decrease in phase velocity moving into the wheel-path from without. This has been verified through 3PB tests on blocks retrieved from the road, see Figure 6 - 17. There is also a notable increase in effective stiffness across the joints of the CAPs under traffic, as measured with SASW, which confirms the observation of blocks moulding in a visco-elastic manner. The moulding is more pronounced in Section 3 (the emulsion CAPs without cement), than in Section 4 of the trial (the foamed CAPs with cement). The inclusion of active filler, most likely through the reduction in Poisson's Ratio of the compacted material, restricts the lateral deformation and moulding of the blocks under repeated loads.

5. ECONOMIC CONSIDERATIONS

5.1 Capital Investment

The capital investment that is required by an emerging contractor to set up a cold-mix block manufacturing enterprise is not onerous. Table 6 - 5 provides a summary of the cost of the main items required. This capital outlay will provide a rudimentary block manufacturing enterprise, but will not necessarily be the most efficient system. An increase in the plant e.g. the number of Kango Hammers, to satisfy critical path criteria and improve productivity, could be considered once an enterprise is established. In addition, purchase of generators and mixers could also be selected as opposed to hire of these items.

Table 6 - 5. Capital cost of main equipment for CAP manufacture (base date= Dec 1997 using South African Rands R)

Description	Quantity	Rate	Amount
Kango Hammer	1	4 400.00	R4 400.00
Compaction mould: • Wooden base plate • Mild steel separation plates • Labour	3	 85.00 180.00 360.00	 R1 875.00
Contra-mould for Kango Hammer:	1	1 030.00	R1 030.00
Mild steel hand compactor	1	100.00	R100.00
Ancillary equipment (funnel, buckets, wheelbarrows etc)	1	Lump sum	R380.00
Concrete mixer (for emulsion)	1	10.00/hr	R10.00/hr
Generator	1	6.50/hr	R 6.50/hr

5.2 Production Rates

Time analyses carried out during the production of CAPs on site at Sir Lowry's Village have facilitated an analysis of productivity during block manufacture. Table 6 - 6 provides the detail of the cycle time for each operation, including a projected achievable cycle time for activities after some further training of labourers and improvements in efficiency.

Table 6 - 6. Cycle time and labour content for individual activities in block production

Production activity	Actual time (minutes)	Labourer symbol	Achievable time (min)	Labourer symbol
Mixing (/40 blocks)	20	A	20	A
Assemble moulds	4	B	3	B
Fill moulds	8	B	6	B
Pre-compaction	3	B	2	B
Compaction (/20 blocks)	20	C	18	C
Release + clean moulds	4	B	4	B
	TOTAL	3	TOTAL	3

These given activities are used to establish a critical path analysis for the block production. Such an analysis takes cognisance of activities that are dependent on the completion of prior activities before they can commence. Variables such as the number of Kango Hammers and mould boards require consideration in the optimisation of the manufacture process. A sensitivity analysis of the different variables allows the productivity per labourer employed and the production rates for the blocks to be established, see Table 6 - 7. The benefits of economies of scale are self-evident, with an increase in the number of Kango Hammers, increasing productivity levels. This does not preclude a small operator from commencing production at the lowest entry level i.e. 1 Kango Hammer.

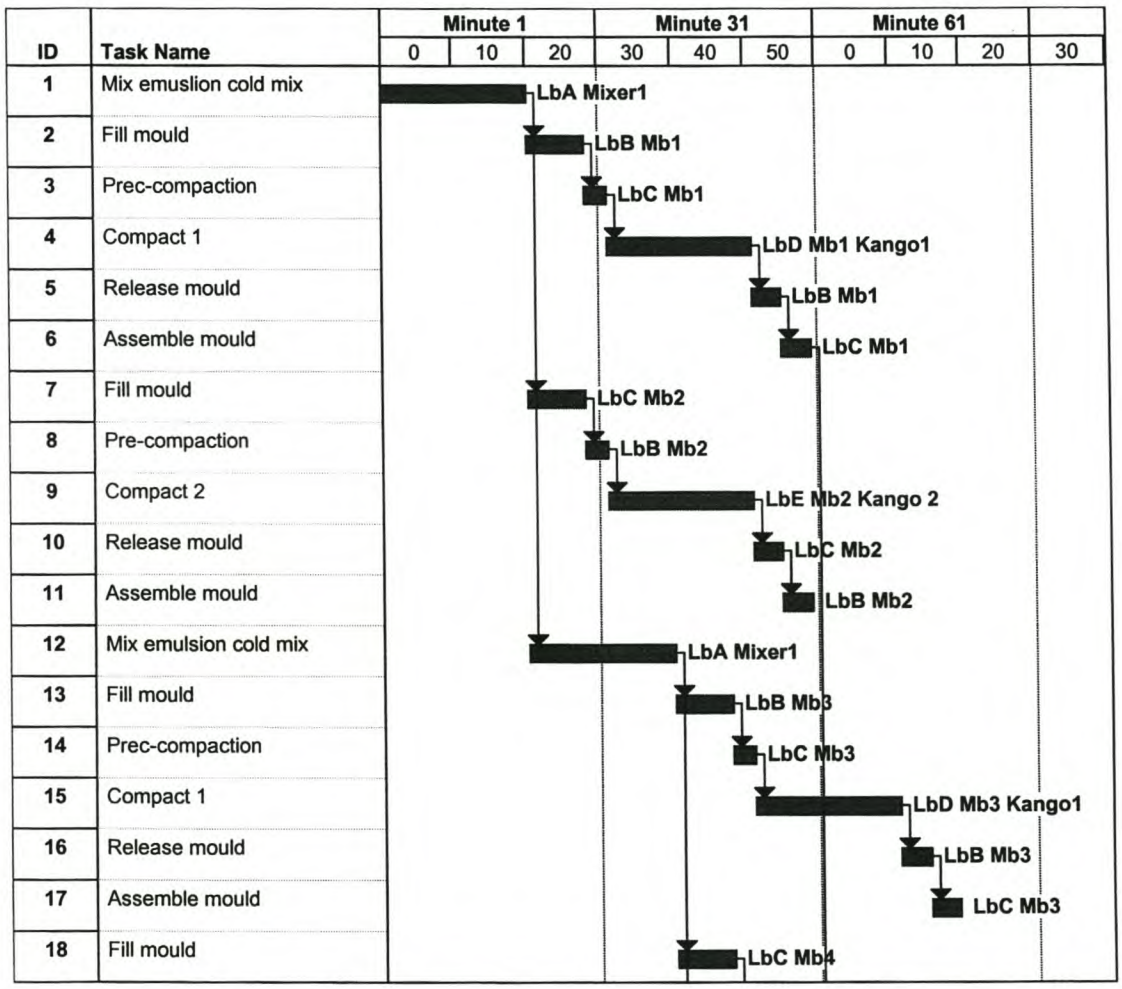

Figure 6 - 21. Ghant chart of activities for Block Production with Two Kango Hammers and Four Mould Boards using Actual Cycle Times .

Legend : Lb = labourer symbol, Mb = Mould board, Kango = Hammer

The benefits of an additional mould board, where efficient labour cannot be relied upon, is illustrated in Figure 6 - 21 and Table 6 - 7 where productivity levels are maintained due to an improved balance of tasks. If operating efficiency is increased, however, the extra

mould board becomes superfluous. Proper tasking and time management is required for efficient manufacture of CAPs.

Table 6 - 7. Employment rates, Productivity and Production Rates for different Block Production Set-ups

Capital emlpoyed	Efficiency level	Labourers (number)	Productivity (blocks/man.hr)	Production rates (blocks/hr)
1 Kango Ham.	Actual	3	20	60
3 Mould Bds	Achievable	3	22.2	66.6
2 Kango Hams	Actual	6	20	120
3 Mould Bds	Achievable	5	24	120
2 Kango Hams	Actual	5	24	120
4 Mould Bds	Achievable	5	24	120

5.3 Pavement Costs

It is not possible to carry out life-cycle costing until the performance of the CAPs has been verified over an extended period. Only then can equivalent pavement structures using other labour intensive methods be compared.

The trial sections have however facilitated a more accurate comparison to be carried out between alternative block paving materials. Table 6 - 8 provides a comparison between the costs per square metre of concrete and emulsion blocks, illustrating the potential benefits of CAPs.

Table 6 - 8. Cost of emulsion treated CAPs versus Concrete Blocks

Item	Cost per m^2 (Rand)		Savings per m^2 (Rand)
	Emulsion	Concrete	
Materials	12,00	23,45	11,45
Manufacture (labour)	14,25	10,50	-3,75
Laying (labour)	6,33	3,80	-2,53
Total	**32,58**	**37,75**	**5,17**

The cost of foamed bitumen CAPs are not included in the analysis because the establishment of a static foaming plant could distort the figures for a small-scale operation. Besides the mixing cost, the various emulsion costs are directly applicable to foamed stabilised CAPs too.

6. CONCLUSIONS

Paving blocks manufactured using bituminous cold-mix materials provide potential as a new road construction technique. Investigation of the material properties of such blocks provides insight into behavioural characteristics of cold bituminous mixes, which falls within the scope of research into cold mix design.

Laboratory analysis and on-site construction of trial sections using bituminous paving blocks has highlighted the following findings pertinent to the mix design of cold bituminous materials and their use in block pavements:

- The process of treating mineral aggregate with bitumen emulsion or foamed bitumen and using the resultant cold-mix for the manufacture of paving blocks provides a viable technique for road construction either using employment intensive or conventional methods. The use of a vibratory hammer with appropriate compaction foot and a suitable mould system for fashioning the blocks provides a labour intensive technique that is efficient for block production.
- A three point beam test apparatus facilitates the measurement of important material properties of blocks viz. tensile strength and stiffness. Measurement of tensile strength with this apparatus provides substantially greater repeatability than tests carried out in the indirect tensile mode, primarily due to the preferable stress-state in the specimen during failure in tension. Resilient stiffness measurements using the three-point beam test require special attention to achieve adequate load levels that induce deflections providing sufficient accuracy for the modulus calculations. The deflections are measured using an LVDT mounted centrally under the block.
- The use of mineral aggregates of marginal quality i.e. lower than the relevant conventional specified standards for base and surfacing layers, can result in a relatively low resilient stiffness of the cold-mix. For this reason, sufficient curing of the blocks is necessary before handling and laying can commence. Using tensile strength criteria, a minimum period of 14 days is deemed adequate for blocks exposed to a warm climate. This period requires verification for each specific application of materials and set of conditions.
- Reduction in resilient modulus under the repeated loading of traffic provides insight into the deterioration of bituminous cold-mix. Although crack propagation is not yet visible at the surface with a stiffness reduction of up to 37%, at 60% reduction micro-cracking does become visible.
- Ravelling of cold-mixes intended for use as a surfacing layer, becomes an important factor for consideration. Although resistance to ravelling can be improved through mix design of the cold-mix material by means of increased cohesion or tensile strength, the higher sensitivity of these mixes to gravel loss does not entirely eliminate the problem. In addition, although the use of diluted emulsion substantially reduces the ravelling of emulsion treated CAPs, it remains a primary mode of deterioration that can result in premature failure. For this reason, cold-mix will not function adequately as a surfacing layer until a suitable ravelling-retarder treatment process has been developed.

However, use of foamed bitumen as a binder, rather than bitumen emulsion, reduces the ravelling potential significantly.

- Unlike rigid paving blocks (made of brick or concrete), the visco-elastic properties and low stiffness of the bituminous blocks result in permanent deformation that has been observed under repeated traffic loading. Relatively high Poisson Ratios for this material result in lateral deformation that creates better load transfer ability at the joints of the blocks and visible moulding of the joints.
- The inclusion of active filler in the cold-mix, such as cement, will have different levels of efficacy in stiffening different materials. Where the stiffening is not profound, moulding of the block joints may still be evident. However, where the inclusion of cement results in substantial stiffening of the cold mix i.e. M_r values in excess of 5000MPa at 10Hz and 25°C, the behaviour of the CAPs in a pavement will closely resemble that of a concrete block pavement.
- Production of cold mix blocks can be cost-effectively undertaken at various entry levels. Small emerging contractors can produce more than 60 blocks per hour with three labourers, one Kango hammer and three sets of moulds, at a competitive rate in comparison with alternative block making procedures. This operation can be gradually scaled up to achieve the requisite level of productivity to suit the particular demands, without exorbitant capital outlay, making the process eminently suited to developing countries intent on creating employment opportunities.

7. REFERENCES

Ebels L.J., 1998. **Bitumen stabilised paving blocks**. MIng thesis. Delft University of Technology, Netherlands

Hibbit, Karlson and Sorenson, Inc., 1996. **ABAQUS Users Manual Version 5.5**, Pawtucket, R.I., USA

Jenkins K.J., Hugo F., van de Ven M.F.C. and O'Connell J., 1997a. **Bitumen Emulsion Stabilised Paving Blocks – Development of Labour Intensive Manufacture and Construction Techniques**. *Second World Congress on Emulsion, Ref 4.1b-257.* Bordeaux, France

Jenkins K.J., Hugo F. and van de Ven M.F.C., 1997b. **Development of Labour Intensive Block Manufacture and Road Construction Techniques using Bitumen Emulsion and Foamed Bitumen Stabilised Paving Blocks**. *South African Transport Conference, Session 4A*. Pretoria, South Africa

Jenkins K.J., van de Ven M.F.C., Ebels L.J. and Bredenhann S.J., 1999. **Possibilities for Cold Mix Bituminous Paving Blocks**. *Conference on Asphalt Pavements for Southern Africa, CAPSA 1999*. Victoria Falls, Zimbabwe.

Lytton R.L., Uzan J., Fernando E.G., Roque R., Hiltunen D. and Stoffels S.M., 1993. **Asphalt Concrete Pavement Distress Prediction : Laboratory Testing, Analysis, Calibration and Validation**, SHRP Project RF 7157-2, National Research Council, Washington DC.

Netherlands Pavement Consultants, 1998. **Evaluatie Veiligheid Driepuntsbuigproef voor Waterbouwasfaltbeton**, Dienst Weg- en Waterbouwkunde, Netherlands

Roux A. 1997. **Socio-political change**. Construction Management Programme, University of Stellenbosch, South Africa

SABITA, 1993. **GEMS – The Design and Use of Granular Emulsion Mixes**, Manual 14, Cape Town

SABITA, 1994. **Methods and Procedures – Labour Enhanced Construction for Bituminous Surfacings**, Manual 12, Cape Town

Shackel, B., 1990. **Design and construction of Interlocking Concrete Block Pavements**. Elsevier Science Publishers Ltd, England

Timoshenko S.P. and Goodier J.N., 1970. **Theory of Elasticity**, McGraw-Hill, New York

van de Ven M.F.C., de Fortier Smit A. and Krans R.L., 1997. **Possibilities of a Semi-Circular Bending Test**, *Eighth International Conference on Asphalt Pavements*, Seattle Washington

Weinert H.H., 1980. **The Natural Road Construction Materials of Southern Africa**. Council for Scientific and Industrial Research. Pretoria.

CHAPTER 7

PERFORMANCE AND MODELLING OF FOAMED BITUMEN MIXTURES

1. INTRODUCTION

Probably the least researched and documented aspect of foamed bitumen mixes is performance. This is evident from the literature summarised in Section 2.11 of Chapter 2. Most publications into performance provide procedures for pavement design that are empirically based and do not take cognisance of nor indeed attempt to account for the mode of failure of the foamed bitumen material. In addition, early publications on pavement design using cold foamed mix ignore some of the fundamental factors that influence the behaviour of the mix, as outlined in previous chapters of this dissertation. This leaves scope for investigation of new methods of appraising the performance of foamed mixes that would assist pavement engineers in designing with these materials.

The quest for development of a methodology for modelling the behaviour of foamed bitumen treated materials and prediction of the performance thereof, is complicated by the diversity of materials that need to be accounted for. As is to be noted in the foregoing chapters, foamed mix can range from lower binder content cold mix that resembles weakly bound granular material, to higher binder content half-warm mix that resembles hot mix asphalt. Development of a unified model that satisfies this range of mixes is ambitious and probably unrealistic. For this reason, performance testing and modelling of foamed mixes has been selected to focus upon mixes particularly pertinent to the developing world i.e. granular type mixes. This type of foamed mix forms the subject of this chapter.

Although highly relevant, performance analysis and modelling of foamed mixes is not the main thrust of this dissertation and receives, therefore, only a moderate portion of the focus. With the selection of lightly bound cold foamed mixes as the material to be modelled, triaxial testing is a highly effective way of simulating loading conditions in a pavement layer. For this reason, triaxial test set-ups at University of Stellenbosch and Delft University of Technology have been used for investigating the performance of the foamed mixes.

In addition to the triaxial tests, limited accelerated testing was also carried out on a foamed bitumen layer that had been constructed as part of a rehabilitation contract of an arterial route called Vanguard Drive in Cape Town, South Africa. A Model Mobile Load Simulator (MMLS) Mk 3 with quarter scale super single wheels was used to traffic the cold foamed mix to some 150 000 axle repetitions before a surfacing layer was applied. The same material was analysed using triaxial testing in the laboratory. The results of this testing are also included in this chapter.

2. SELECTION OF MIXES

2.1 Gradation

The suitability of continuously graded aggregates for cold treatment with foamed bitumen has been verified in previous chapters and previous research. Aggregates with this type of gradation are also commonly used in pavement structures, either as granular, cemented or asphaltic base or sub-base layers. Although crushed materials are blended to achieve such gradations, weathered gravel that conforms to such a particle-size distribution is also commonly encountered. Not surprisingly, such materials form a substantial proportion of the mineral aggregates utilised for foamed bitumen treatment, particularly in countries such as South Africa.

Continuously graded aggregates become therefore a priority choice for a focused investigation into performance of cold foamed mixes. Two graded crushed rock samples used in the road industry as unbound base material, were selected for this purpose G1gau (quartzite) and G1eer (hornfels). In addition, a recycled layer with a blend of crushed hornfels and asphalt (23:77) called G2van was analysed. Finally, a mix granulate of crushed concrete and brick (78:22) called MGtud was analysed. The gradation of these four materials is shown in Figure 7 - 1 relative to the equivalent Fuller gradation with a power of n = 0,45.

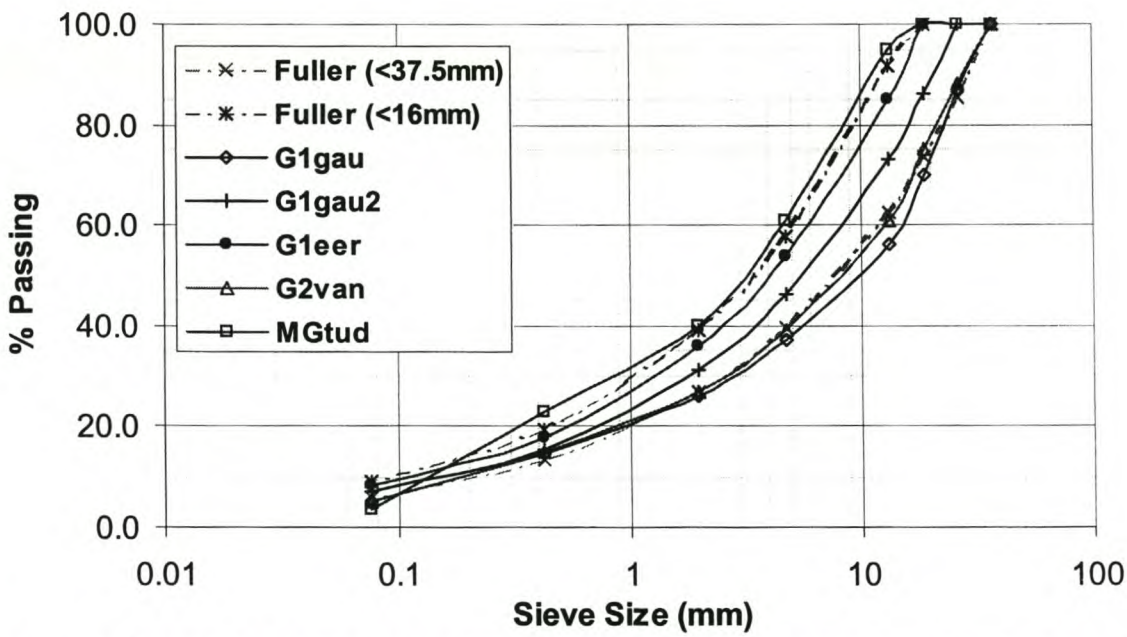

Figure 7 - 1. Gradations of Aggregates Selected for Performance Testing as Foamed Bitumen Mixes

2.2 Material Properties

Characterisation of the natural materials is necessary before treatment with foamed bitumen for purposes of compaction and curing, as outlined in Chapter 4. The properties of the G1gau material is detailed in the report (van de Ven *et al.,* 1997), the G2van material is covered in (Jenkins and van de Ven, 2000) whilst the MGtud is detailed in (Saleh, 2000). Table 7 - 1 provides a summary of the pertinent properties of the materials. The first three materials originate from South Africa and the MGtud material from the Netherlands. The materials were all tested in their country of origin.

Table 7 - 1. Aggregate Properties on Natural Materials

Material	$MDD_{Mod.AASHTO}$ (kg/m^3)	$OMC_{Mod.AASHTO}$ (%)	ARD (t/m^3)	RSD (t/m^3)
G1gau	2159	5.8	2.667	2.625
G1eer	2150	6.8	2.480	2.467
MGtud	1853	12.0	-	2.628
G2van	2160	6.8	2.672	2.625

Note: Applicable tests are detailed in van de Ven *et al.* (1997)
ARD = Apparent Relative Density
RSD = Relative Solid Density

The G1eer aggregate was used to prepare four different foamed mixes for performance testing at different binder contents. The remaining three mineral aggregates were used to prepare only one foamed mix each. The Wirtgen WLB10 ® laboratory foaming plant was used throughout, with untreated bitumen (without foamants) having an Expansion Ratio = 19, Half-life = 35 seconds and Foam Index = 533 for the G1eer mix. The remaining mixes all utilised bitumen with an Expansion Ratio = 15, Half-life = 15 seconds and Foam Index = 199.

Compaction of specimens was carried out in a gyratory compactor with settings of 1,25° angle of gyration and 600kPa vertical pressure. Additional details for the mixes prepared are included in Table 7 - 2. The procedure for manufacture of the mixes and specimens is provided in Appendix E.

Table 7 - 2. Details of Granular and Foamed Mixes for Triaxial Test Specimens

Material	Binder Content (%)	Cement Content (%)	Mixing MC (%)	Compaction MC (%)	No. of Gyrations
$G1gau_2$	2	0	3.5	3.0	147
$G1eer_1$	1	0	4.1	4.0	233
$G1eer_2$	2	0	4.03	3.0	233
$G1eer_{2c}$	2	1	4.0	3.0	233
$G1eer_4$	4	0	4.03	2.0	233
$G2van_{1.5}$	1.5	2	4.8	3.3	200
$MGtud_2$	2	0	10.5	9.5	*

Note: For the first five mixes the name convention includes material classification according to TRH14 (NITRR,1986b) [2 letters], material source [3 letters], and subscript [binder content and c for cement].
The MGtud mix tested at TU Delft was manufactured in accordance with procedures developed by van Niekerk *et al.* (2000). Name convention: MG=mix granulate, tud=TU Delft and subscript = binder content.

Following the manufacture of the foamed mixes, curing was carried out to simulate a medium-term cure for a moderate climate in terms of Chapter 4 at 50°C for 72 hours. The MGtud mix was cured at ambient temperature (20-23°C) for 7 days because an oven large enough to accommodate the specimen could not be procured. The $G2van_{1.5}$ mix was cured at 25°C for 24 hours, simulating an initial cure equivalent to early trafficking conditions that were investigated with accelerated pavement testing. The general curing techniques are detailed in Table 7 - 3.

Table 7 - 3. Curing Procedures for Triaxial Specimens

Foamed Mixes	Simulation	Curing Procedure
$G1gau_2$ $G1eer_1$ $G1eer_2$ $G1eer_{2c}$ $G1eer_4$	Medium Term	50°C for 72 hours
$G2van_{1.5}$	Initial	25°C for 24 hours
$MGtud_2$	Medium Term	20-23°C for 168 hours

Details of the moisture and density of the mixes as tested are summarised in Table 7 - 4. The granular material G1gau was compacted using the vibratory technique under a dead-weight, as detailed by van de Ven *et al.* (1997).

Table 7 - 4. Compaction and Moisture Regime of Triaxial Specimens at Testing, Mean Values and (Standard Deviation)

Material	Testing MC (%)	Percent RSD (%)	% Modified AASHTO	Air Voids (%)	Rice Dens. (kg/m^3)
G1gau	2.1 (0.77)	85.50 (1.60)	103.9 (1.90)	-	-
$G1gau_2$	1.3 (0.50)	86.79 (0.65)	105.5 (0.79)	5.8 (0.23)	2563
$G1eer_1$	3.2 (0.23)	86.21 (0.58)	104.8 (0.71)	7.9 (0.78)	2612
$G1eer_2$	2.7 (0.52)	84.48 (0.78)	102.7 (0.94)	9.0 (0.23)	2588
$G1eer_{2c}$	2.8 (0.22)	83.02 (0.56)	100.9 (0.68)	6.5 (0.47)	2529
$G1eer_4$	2.1 (0.29)	84.10 (1.13)	101.2 (1.35)	9.9	2610
$G2van_{1.5}$	3.3 (0.34)	84.24 (0.93)	97.8 (1.07)	10.8 (0.16)	2454
MGtud	7.2** (0.95)	70.7*	100.3 (0.9)	-	-
$MGtud_2$	5.4 (0.30)	70.5*	100.1 (0.3)	*	2595

* Unrealistic void content due to absorptive nature of brick component, refer rather to % Mod.AASHTO
**Moisture content adjusted before compaction to provide same fluids content as equivalent foamed mix
RSD = Relative Solid Density of the aggregate, refer (NITRR, 1986a)
Rice Density = Maximum Theoretical relative Density, refer (NITRR, 1986a)

The triaxial testing facility at Delft University of Technology (TU) utilises specimens with a diameter of 300mm and a height of 600mm, making it eminently suited for analysis of coarse-grained materials. The University of Stellenbosch (US) triaxial set-up utilises specimens of 150mm diameter and 300mm height, thus limiting its suitability for coarse aggregates considering a desirable maximum particle size to diameter ratio of less than 1:8. This influenced selection of certain gradations in Figure 7 - 1.

3. TRIAXIAL TEST METHODOLOGY AND RESULTS

The triaxial test set-ups at both TU and US utilise hydraulic actuators and a closed feed-back loop control system. Both systems have at least the capacity to apply accurately controlled vertical monotonic or cyclic (haversine wave) loading. The TU system has a load capacity of 150 kN and frequency of 5 Hz whilst the US system is limited to 100 kN and in excess of 10Hz.

The method of creating confining stress on the large specimen for the TU set-up is reliant on internal vacuum within the membrane (van Niekerk *at al.*, 2000a&b). The range of pressures extends from 0 to 90 kPa. The US triaxial set-up uses a cell with pressure capacity of 2,5 MPa with air or fluid as medium (the former was selected). Both set-ups do not have the facility for cyclic confining pressure, a specialist resource that closer approximates granular behaviour in the field.

3.1 Monotonic Failure Shear Behaviour

3.1.1 Monotonic Triaxial Test Methodology

An envelope that is plotted in the Mohr-Coloumb space i.e. normal stress and shear stress conditions describes the failure behaviour of granular materials. From monotonic failure tests, the angle of internal friction ϕ and cohesion C can be obtained using the Mohr-Coloumb model. The ratio of stresses within a granular material to the failure stresses has been shown by Huurman (1997) to relate closely to the response of the material in terms of resilient and permanent strains.

A tangent line between two Mohr circles of stress obtained from two monotonic failure-tests at different confining stresses is used to approximate the failure envelope for granular materials. A third test, conducted at a different confining pressure, creates more reliability in the definition of the envelope shape. A regression line can be fitted through the three data circles. Such an approach for defining the shear parameters is considered applicable to cold foamed mixes with low binder contents (< 4%). This limit requires verification in this research initiative. The multi-stage test approach (van Niekerk *et al.*, 2000b) used for testing granular materials where three failure tests are performed on the same specimen avoiding post peak conditions, however, is not applicable for foamed mixes. Bitumen bonds are broken during the initial failure tests influencing subsequent tests (Saleh *et al.*, 2000). For example, one set of multi-stage tests on MGtud$_2$ foamed mix, starting at higher confining pressures and subsequently testing at lower confinement, resulted in shear parameters of C=139kPa and ϕ=55°. The true values obtained from single-stage tests were C=331kPa and ϕ=36°.

The monotonic triaxial tests are conducted in a displacement-controlled mode. In the case of the TU set-up a displacement rate of 1mm/sec (strain rate of 10% per minute) was used and confining pressures of 12, 36 and 72kPa. Displacements are measured using vertical LVDTs with a range of 20mm over the 20V output. The US set-up utilised a displacement rate of 6.25mm/min (strain rate of 2,1%) and confining pressures of 50, 100 and 200kPa.

Displacements are measured using a vertical LVDT with a sensitivity range of 100mm over 10V. The load cell settings are 100 kN over 10 volt range for the monotonic test.

The major principal stress $\sigma_{1,f}$ in the Mohr-Coloumb failure condition, can be defined geometrically using a relationship between the failure parameters C and ϕ and the minor principal (confining) stress σ_3 according to Equation 7 - 1.

$$\sigma_{1,f} = \frac{(1+\sin\phi).\sigma_3 + 2.C.\cos\phi}{(1-\sin\phi)} \qquad \textbf{Equation 7 - 1}$$

If the relationship between the major principal stress $\sigma_{1,f}$ and the minor principal stress σ_3 is considered linear, it can be represented by Equation 7 - 2.

$$\sigma_{1,f} = m.\ \sigma_3 + b \qquad \textbf{Equation 7 - 2}$$

where,

$$m = \frac{1+\sin\phi}{1-\sin\phi} \qquad \textbf{Equation 7 - 3}$$

and

$$b = 2.C.\frac{\cos\phi}{(1-\sin\phi)} \qquad \textbf{Equation 7 - 4}$$

3.1.2 Results of Monotonic Failure Tests

Displacement-controlled triaxial tests provide relatively uniform relationships between deviator stress and displacement. Figure 7 - 2 provides a typical result of such tests, by including the three phases of a multi-stage test on a granular material. The strain at the ultimate deviator stress remains below 1%, a trend confirmed by van Niekerk *et al.* (2000a&b) for granular materials.

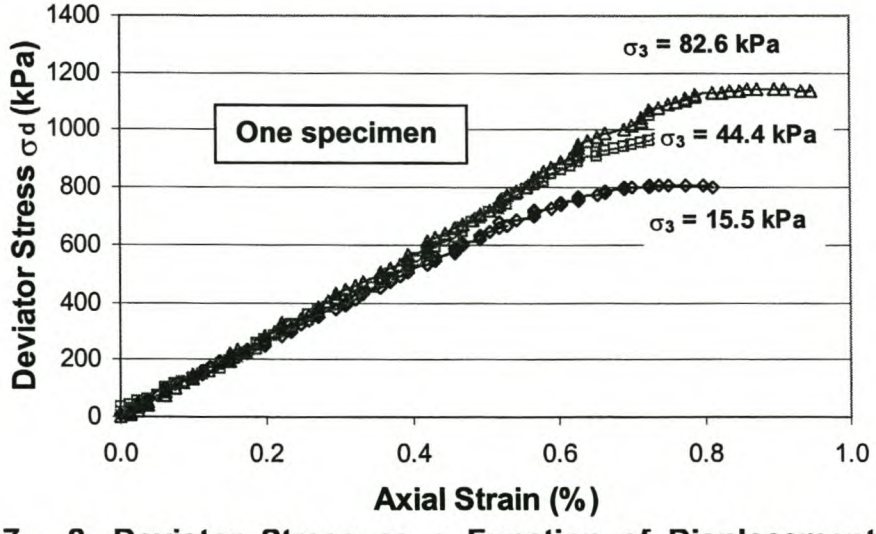

Figure 7 - 2. Deviator Stress as a Function of Displacement during Multi-stage Monotonic Failure Tests on MGtud Granular Material (TU apparatus)

By comparison, a superimposition of three single-stage triaxial failure tests on mixed granulate aggregate using the TU apparatus, see Figure 7 - 3, reveals that the axial strain at failure increases to in excess of 1% for the equivalent foamed mixes stabilized with 2% foamed bitumen. This phenomenon is verified for crushed stone aggregate using the US apparatus, see Figure 7 - 4. Anomalies such as the deviations in the stress path shown for σ_3 = 100kPa in this figure can be a result of localised failure and reorientation of large particles.

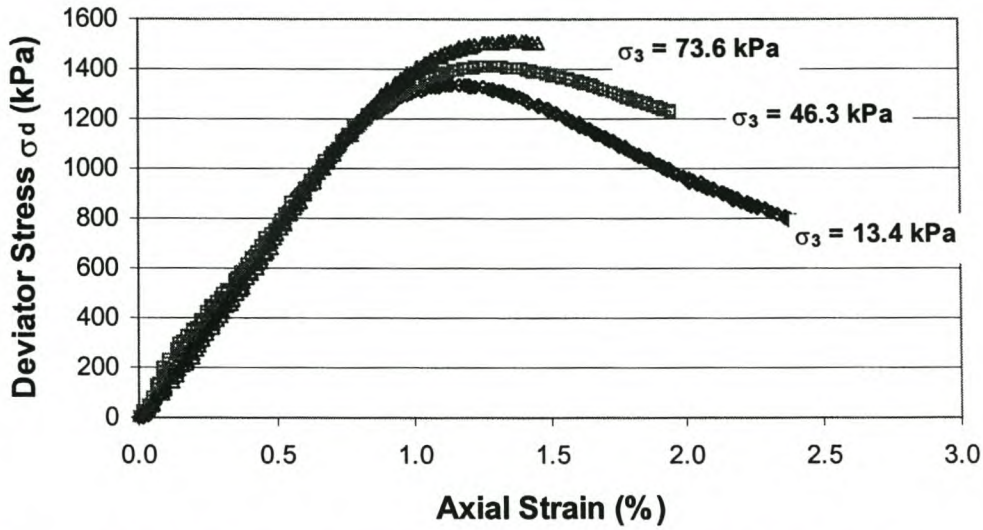

Figure 7 - 3. Deviator Stress as a Function of Vertical Strain during Single-stage Monotonic Failure Tests on MGtud$_2$ Foamed Mix (TU apparatus)

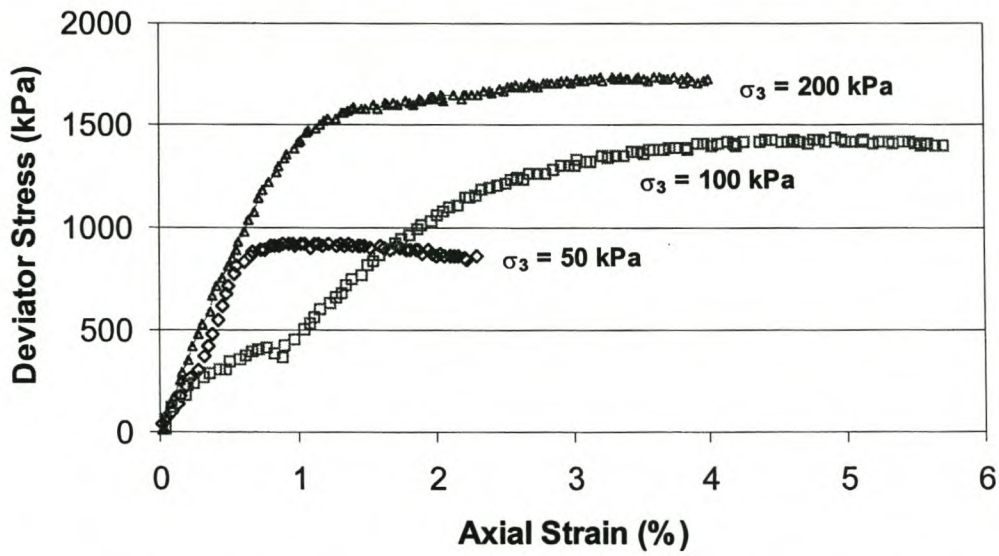

Figure 7 - 4. Deviator Stress as a Function of Vertical Strain during Single-stage Monotonic Failure Tests on G1eer$_2$ Foamed Mix (US apparatus)

Mohr-Coloumb analysis of the results of the monotonic triaxial tests conducted on the granular materials and their equivalent cold foamed bitumen mixes provides a clearer insight into the function of the bitumen binder. According to the summary of the monotonic triaxial test in Table 7 - 5 results and as shown in the Figure 7 - 5, the friction angle ϕ decreases whilst the cohesion of the mix increases with the inclusion of foamed bitumen in a cold mix. This shift in the failure envelope leads to an increase in the maximum principal stress $\sigma_{1,f}$ at low σ_3 through the addition of foamed bitumen. Depending on the confining stress, $\sigma_{1,f}$ can increase by up to 100% relative to the granular material through the incorporation of 2% foamed bitumen. Comprehensive results are included in Appendix E.

Table 7 - 5. Summary of Shear Failure Parameters C and ϕ for Granular and Equivalent Foamed Mixes

Material	Type	C (MPa)	ϕ (°)	R^2	m	b
G1gau	Granular	0.082	53.0	*	8.853	485.5
$G1gau_2$	Foamed	0.166	44.7	0.99	5.756	797.9
$G1eer_1$	Foamed	0.162	45.8	0.95	6.071	793.1
$G1eer_2$	Foamed	0.156	45.9	0.92	6.100	769.5
$G1eer_{2c}$	Foamed	1.137	0.0	*	0.000	2274.0
$G1eer_4$	Foamed	0.280	29.9	0.96	2.991	968.7
$G2van_{1.5}$	Foamed	0.821	0.0	*	0.000	1642.4
MGtud	Granular	0.158	45.3	1.00	5.909	768.1
$MGtud_2$	Foamed	0.331	36.0	0.99	3.844	1298.4

* Only 2 test results (other R^2 values indicate the fit of a linear failure envelope to 3 tests)

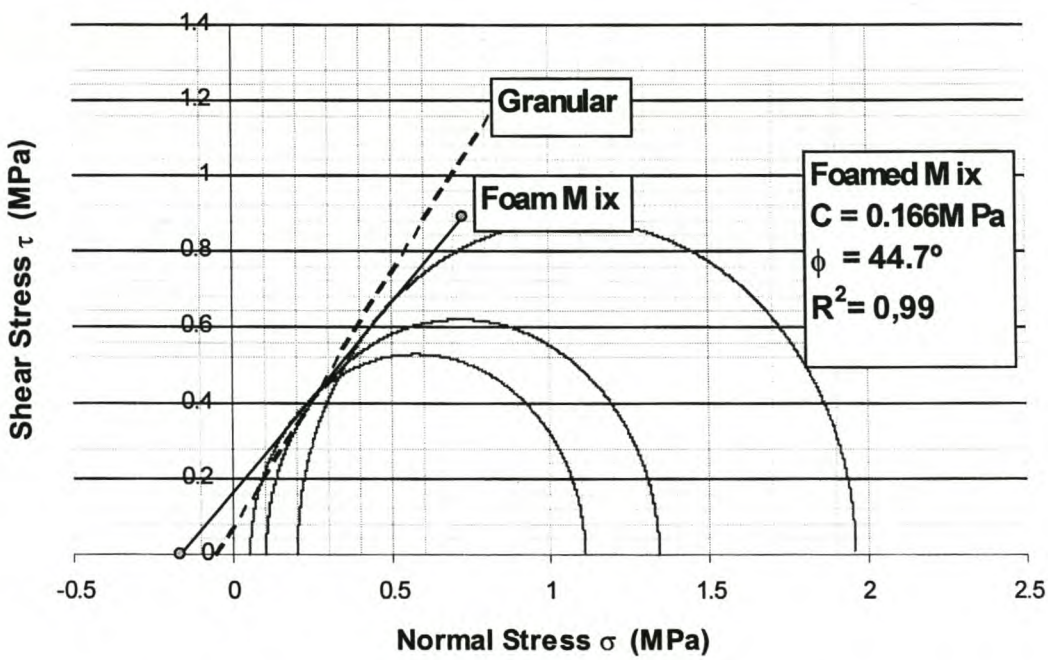

Figure 7 - 5. Mohr-Coloumb Circles for $G1gau_2$ Foamed Mix with Failure Envelopes for G1gau Superimposed

Within the range of 0% to 4% binder, the cohesion value increases with a higher binder content. This trend is valid for all the mixes tested using the triaxial apparatus. With the incorporation of only foamed bitumen into a mix, the shear parameters continue to exhibit granular behaviour of the material. However, for the limited tests carried out with the inclusion of 1% of cement or more i.e. two mixes, the cold foamed mix obtains a marked increase in cohesion with reduction of the value of the internal friction to approximately 0°. This indicates that stress dependent behaviour i.e. non-linear mechanical behaviour is only valid for foamed mixes without the addition of cement.

3.2 Resilient Deformation Behaviour

The resilient behaviour of granular and foamed bitumen treated materials can be tested in the triaxial set-up by applying relatively low stresses creating low strains, so that the elastic range of the particular material is not exceeded. It is assumed that within this elastic range, the stress history does not affect the material response. The selection of a range of stress magnitudes, in terms of a combination of deviator and confining stresses, allows the non-linear resilient deformation behaviour to be analysed on one specimen. A further condition for this test is that the number of load repetitions is limited i.e. permanent deformation is restricted.

3.2.1 Resilient Deformation (M_r-θ) Test Methodology

The procedures for carrying out the resilient deformation (M_r-θ) tests is fundamentally the same for the US and the TU set-up with slight variations in certain details. The US triaxial testing procedure is detailed in Appendix E, with a summary of the stress combinations for the tests provided in Table 7 - 6. All test were performed at 25°C.

Table 7 - 6. Stress Combinations for Resilient Deformation Triaxial Tests at US

σ_3 (kPa)	σ_p (kPa)	σ_d (kPa)				
50	20	50	100	200	300	
100	20	100	200	300	400	500
200	20	200	350	500	600	700

σ_p = seating stress (pre-load)
σ_d = deviator stress

The graphical expression of the stresses applied in the US triaxial set-up shown in Figure 7 - 6. The value of the pre-load setting is selected to include the dead-weight of the apparatus. The US M_r-θ test is carried out at a frequency of 2Hz. The axial deformations are measured using two vertical LVDTs measuring the cell displacement, with the range of 10V spanning 1mm. A load cell with a range of 10V spanning 20kN is used to monitor and record the applied load.

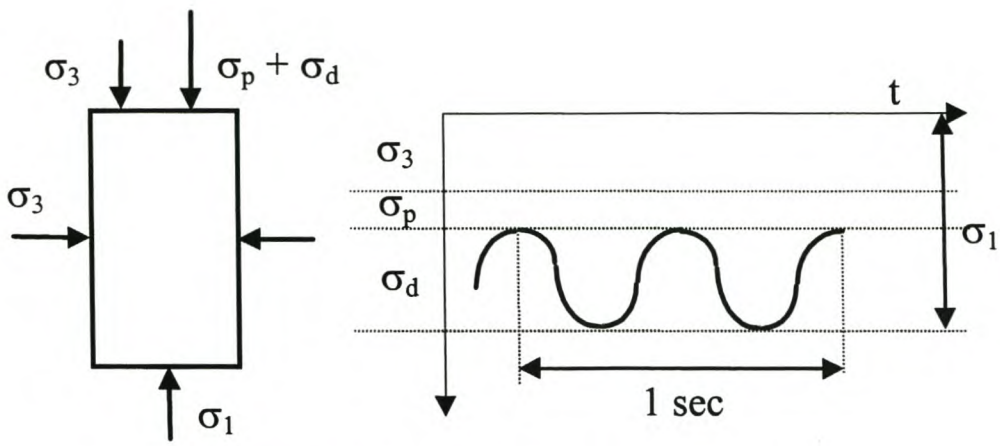

Figure 7 - 6. Stresses Applied in Triaxial Test at US

For the M_r-θ test at US a correction is made to the applied stress for the increase in surface area of the specimen under loading i.e. vertical strain results in horizontal strain of the specimen, according to Poisson, which increases the surface area that the cyclic load is applied to. In the absence of radial deformation data, the equation of Maree (1979) is used, see Equation 7 - 5.

$$\text{Corrected stress } (\sigma_d) = \text{Measured stress} \times (1 - \varepsilon_{ax}) \qquad \textbf{Equation 7 - 5}$$

where ,

ε_{ax} = measured axial strain ($\Delta l / l$)

l = specimen height before test commenced.

The M_r-θ test procedure for resilient deformation triaxial tests at TU is outlined by van Niekerk *et al.* (2000). This test is carried out at a frequency of 1 Hz. The axial and radial deformations resulting from a given stress combination are measured by means of on sample LVDTs. These LVDTs are mounted on rings that are fixed to the specimen at $^1/_3$ and $^2/_3$ of the specimen height respectively. Two self-centring rings provide the basis for the three axial and two sets of three radial LVDTs, see Plate 7 - 1. The range of the LVDTs is 1mm over 20V output.

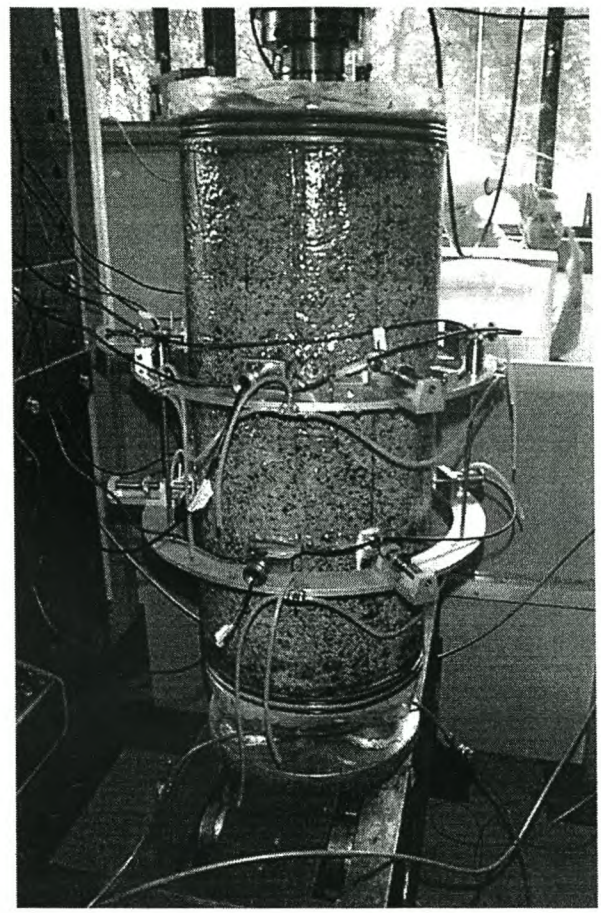

Plate 7 - 1. Instrumented Triaxial Specimen in TU Apparatus

Due to limitations with the capacity of vacuum confinement, the stress combinations for the TU Triaxial set-up are generally lower than those utilised for the US set-up. The stress combinations for M_r-θ tests on the $MGtud_2$ foamed mix is detailed in Table 7 - 7. At each σ_c/σ_3 ratio, where σ_c is the applied cyclic stress, the specimen is subjected to 50 repetitions. At the 50^{th} load pulse the data acquisition system captures and records full load, stress and deformation signals.

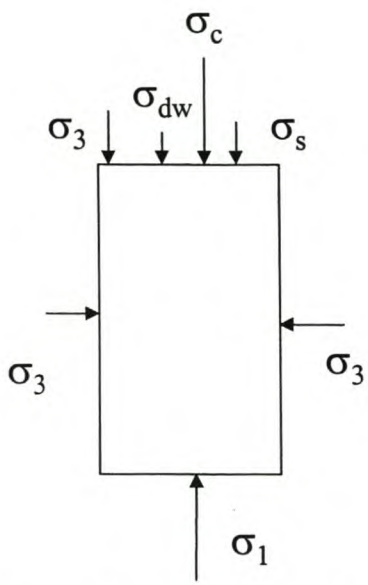

where:

σ_1 = main principal stress [kPa]

σ_3 = minor principal (confining) stress [kPa]

σ_c = cyclic axial stress [kPa]

σ_s = static axial stress [= 12 kPa]

$\sigma_{d.w.}$ = dead weight stress [= 7 kPa]

$\sigma_1 = \sigma_c + \sigma_s + \sigma_3 + \sigma_{dw}$

Figure 7 - 7. Stresses Applied in Triaxial Test at TU (van Niekerk *et al.*, 2000a&b)

The granular M_r-θ tests on the TU set-up use deviator to confining stress ratios of $\sigma_d/\sigma_3 = (\sigma_1-\sigma_3)/\sigma_3 \cong$ 2,3,4 to 8 and levels of σ_3 of 12,24,36, 48, 60 and 72kPa. The layout of the stresses applied to the specimen in the TU triaxial set-up are shown in Figure 7 - 7.

Table 7 - 7. Stress Combinations for Resilient Deformation Triaxial Tests at TU on Foamed Mixes

Confining Stress σ_3 (kPa)	Vertical Stress Ratio σ_c/σ_3				Vertical Stress σ_1 (kPa)				Principal to Failure Stress Ratio $\sigma_1/\sigma_{1,f}$			
12	1	3	6	8	43	67	103	127	0.03	0.05	0.08	0.09
24	1	3	6	8	67	115	187	235	0.05	0.08	0.13	0.17
48	1	3	6	8	115	211	355	451	0.03	0.10	0.19	0.26
72	1	3	6	8	163	307	523	667	0.10	0.19	0.33	0.42

From the measured deformations, the axial (ε_{ax}) strains are calculated from the deformation divided by the measuring length (approximately 300mm for the US set-up and 200mm for the TU set-up). The radial strains (ε_{rad}) are only applicable to the TU set-up and are calculated over the specimen radius (150mm).

From the applied stresses and resultant strains, the resilient modulus (M_r) for both set-ups and Poisson's Ratio (ν) in the case of TU, can be determined according to Equation 7 - 6 and Equation 7 - 7 respectively. For the cyclic stress in the US set-up, $\sigma_d = \sigma_c$.

$$M_r = \frac{\sigma_c}{\varepsilon_{ax}}$$ **Equation 7 - 6**

$$\nu = \frac{\varepsilon_{rad}}{\varepsilon_{ax}}$$ **Equation 7 - 7**

A variety of methods exist for the modelling of the stress dependency of M_r and ν (van Niekerk and Huurman, 1995) and (Huurman, 1997). Several of these models are applicable to the material behaviour demonstrated by the foamed bitumen mixes. Equation 7 - 8 provides the relationship for the **M_r-θ model**.

$$M_r = k_1\left(\frac{\theta}{\theta_o}\right)^{k_2}$$ **Equation 7 - 8**

In exceptional cases a linear relationship may be found between the total stress-state and the resilient modulus as shown in the **Linear Model** below.

$$M_r = k_3\,\theta + k_4$$ **Equation 7 - 9**

In order to account for the decrease in resilient stiffness noticed as the vertical stress ratio $\sigma_1/\sigma_{1,f}$ approaches a critical value, the relationship in Equation 7 - 10 was developed by van Niekerk and Huurman (**M_r- σ_3-$\sigma_1/\sigma_{1,f}$ Model**).

$$M_r = k_5\left(\frac{\sigma_3}{\sigma_{30}}\right)^{k_6}\left(1 - k_7\left(\frac{\sigma_1}{\sigma_{1,f}}\right)^{k_8}\right)$$ **Equation 7 - 10**

In addition, the **M_r- θ-$\sigma_1/\sigma_{1,f}$ Model**, utilises a function of the total stress on a granular (or foamed) material to express the resilient modulus, as shown below.

$$M_r = k_5\left(\frac{\theta}{\theta_0}\right)^{k_6}\left(1 - k_7\left(\frac{\sigma_1}{\sigma_{1,f}}\right)^{k_8}\right)$$ **Equation 7 - 11**

Where,

M_r	= Resilient Modulus (MPa)
θ	= sum of principal stresses (kPa)
	$= \sigma_1 + 2.\,\sigma_3 = \sigma_c + \sigma_s + 3.\sigma_3 + \sigma_{d.w.}$
σ_3	= minor principal stress (kPa)
σ_d	= deviator stress ($\sigma_1 - \sigma_3$) (kPa)
θ_0, $\sigma_{3,0}$,$\sigma_{d,0}$	= reference values (= 1 kPa)
k_1, k_3, k_5	= regression coefficients (MPa)
k_2, k_4, $k_{6\text{-}8}$	= regression coefficients (-)

The **M_r- θ-$\sigma_d/\sigma_{d,f}$ Model** utilises the same format as the M_r- θ-$\sigma_1/\sigma_{1,f}$ Model with the only difference being the use of the term $\sigma_d/\sigma_{d,f}$ to describe the stress ratio rather than $\sigma_1/\sigma_{1,f}$.

Models for the change in Poisson's Ratio with variation in the stress condition have also been established by van Niekerk *et al.*(2000a) for granular materials. The models that were found to be suited for the modelling of the granular and foamed mixes are given below.

$$\nu = a + b.\left(\frac{\sigma_1}{\sigma_3}\right) \qquad \textbf{Equation 7 - 12}$$

$$\nu = c.\left(\frac{\sigma_1}{\sigma_3}\right)^d \left(\frac{\sigma_3}{\sigma_{3,0}}\right)^e \qquad \textbf{Equation 7 - 13}$$

$$\nu = f + g\left(\frac{\sigma_1}{\sigma_{1,f}}\right)^h \qquad \textbf{Equation 7 - 14}$$

Where,

a to e = dimensionless regression coefficients (-)
other symbols = as above

3.2.2 Results of M_r-θ Tests

The granular-type behaviour of foamed mixes without cement is apparent when analysing the resilient response to loading at different stress levels below failure. Typical granular behaviour of unbound mixes in terms of resilient stiffness is shown in Figure 7 - 8. The values of M_r are seen to increase with increasing σ_3. In addition, as σ_1 increases, the resilient modulus increases further until a critical value is reached and thereafter the M_r decreases. Although the latter phenomenon is not evident in the figure, it is usually analysed as a critical vertical stress ratio $\sigma_1/\sigma_{1,f}$. The values for M_r obtained in the US triaxial set-up are lower than the values quoted by Maree (1979) for equivalent materials and test conditions.

Appendix E provides a comprehensive set of figures for the unbound and foamed-bitumen bound materials. The increase in M_r with a higher rate of loading is notable from the results of foamed mix tests plotted in Appendix E. An increase in loading frequency from 0.5Hz to 5Hz results in an increase in excess of 20% for a foamed mix with 2% foamed bitumen.

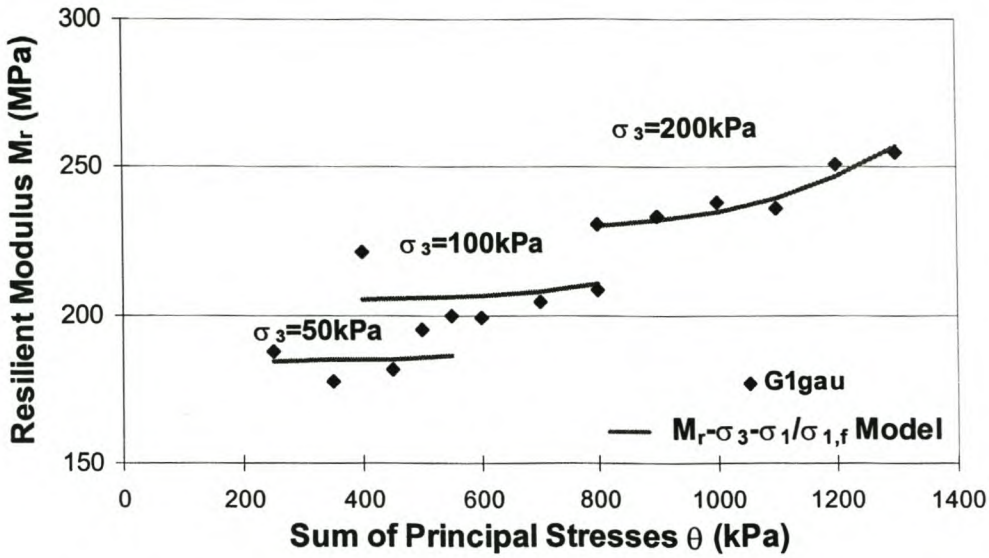

Figure 7 - 8. Resilient Modulus as a Function of Total Stress from Triaxial Tests on G1gau Granular Material

The addition of 2% foamed bitumen to the high quality crushed stone base, does not impede the stress dependent behaviour, as exhibited in Figure 7 - 9. A moderate increase in resilient stiffness is notable with the addition of the foamed bitumen.

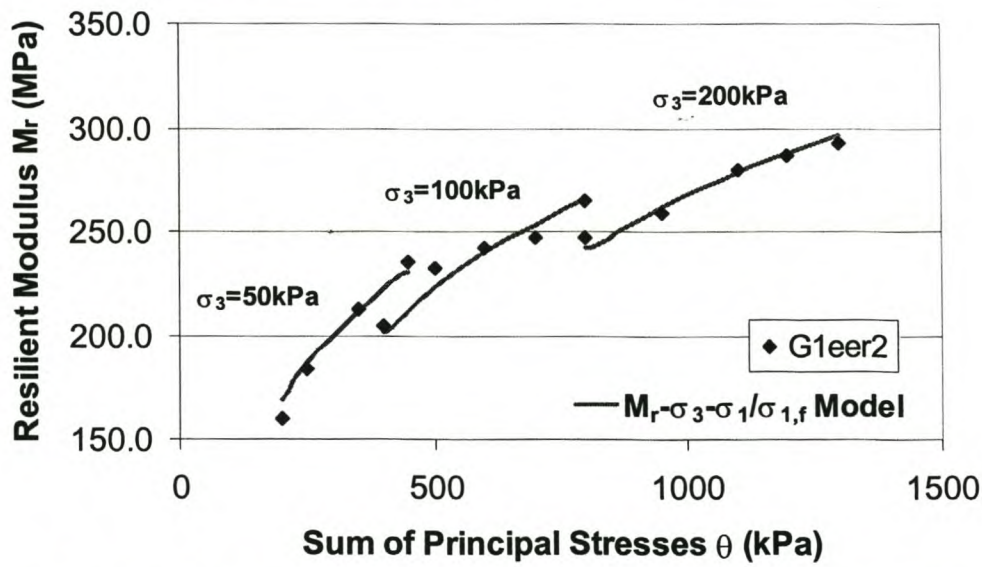

Figure 7 - 9. Resilient Modulus as a Function of Total Stress from Triaxial Tests on G1eer$_2$ Foamed Mix with 2% Binder

Cases where stress dependent behaviour of foamed mixes becomes less evident or insignificant, as seen from Appendix E and Figure 7 - 10, include:

- the inclusion of cement in the foamed mix,
- foamed bitumen contents approaching 4% (and possibly higher), and
- specimens that have not been conditioned with cyclic pulses.

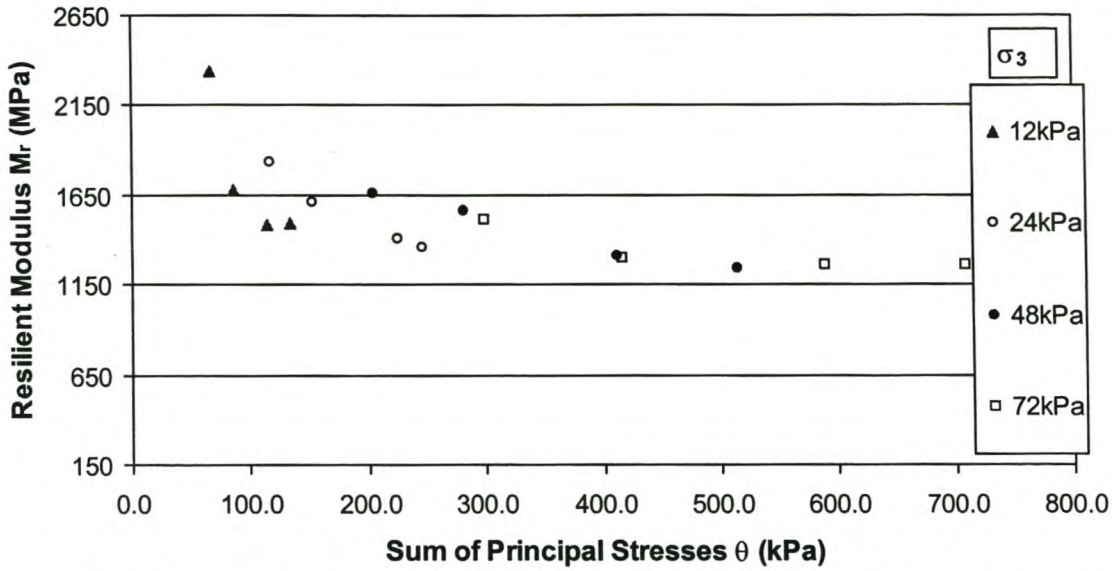

Figure 7 - 10. Resilient Modulus as a Function of Total Stress from Triaxial Tests on MGtud$_2$ Foamed Mix with 2% Binder and Without Conditioning Pulses

Independence of M_r to the sum of the principal stresses indicates behaviour that is associated with more strongly bound materials e.g. cement bound materials. In addition, susceptibility to conditioning loads, as is noted from the change in resilient behaviour from before conditioning to after conditioning, see Appendix E, is typical of lightly cemented materials. Conditioning is therefore necessary to create a representative foamed mix that behaves in a similar manner to a trafficked laver.

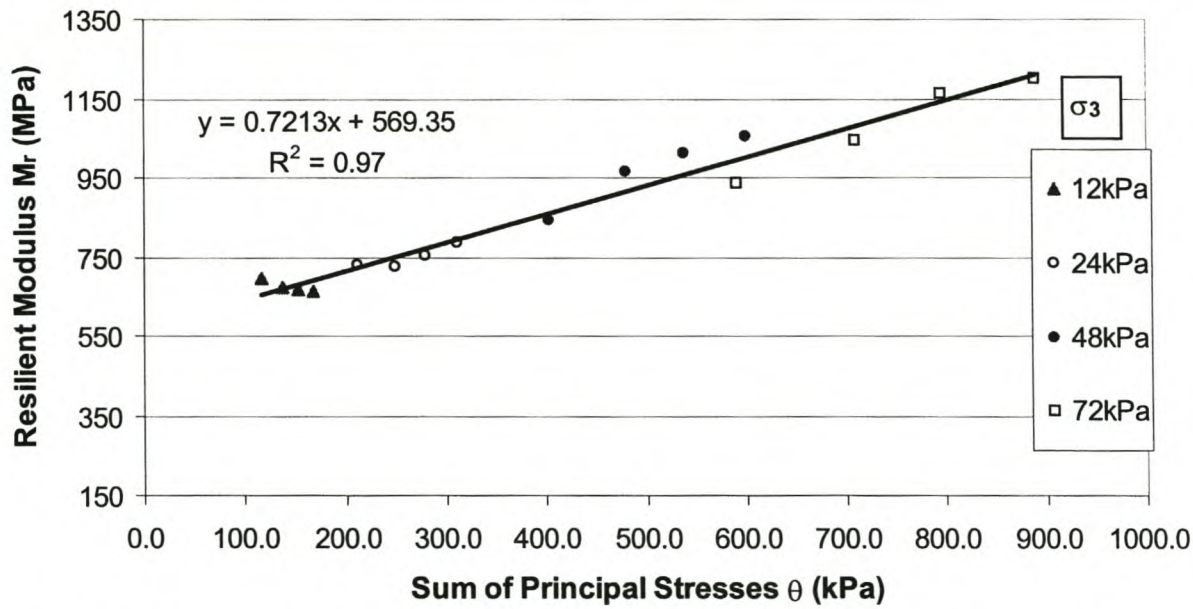

Figure 7 - 11. Resilient Modulus as a Function of Total Stress from Triaxial Tests on MGtud$_2$ Foamed Mix with 2% Binder after Conditioning with 10 000 Load Pulses at $\sigma_d/\sigma_{d,f}$ of 40%

The M_r values obtained from the TU triaxial set-up provide results representative of values obtained from simple stiffness tests detailed in Chapters 4 to 6. The shifts obtained in the US triaxial tests are explained by the findings of van Niekerk *et al.* (2000a) where scaling of the gradations resulted in 25% downward shift of the M_r-θ relations. The difference in gradations shown in Figure 7 - 1 assists in explaining a portion of the lower resilient stiffness achieved.

Models used for application to the M_r-θ data depend on the form of the relationship between stiffness and stress, as exhibited graphically. In the case of the results obtained for the materials outlined in this chapter, the models previously detailed have been utilised. These models and their coefficients are summarised in Table 7 - 8. Although regression analysis can provide negative values for coefficient k_7, this results in increasing M_r with increase in $\sigma_1/\sigma_{1,f}$ at the same confining pressure, which is unrealistic. Manual manipulation is necessary to rectify this phenomenon, or use of an alternative model albeit with lower R^2 correlation value. The implications of such an adjustment is observed in the application of the models in the next section. Relationships with negative coefficients have not been utilised for modelling and second term functions which model the material softening with increasing $\sigma_1/\sigma_{1,f}$ have been applied for the most realistic pavement analysis.

Table 7 - 8. Summary of M_r-θ Model Coefficients for Granular Materials and Equivalent Foamed Bitumen Mixes

Material	Model	K_1	K_2	R^2		
G1gau	M_r–θ	55.6	0.207	0.73		
$G2van_{1.5}$	M_r–θ	48.0	0.330	0.86		
$MGtud_2$	M_r–θ	132.5	0.319	0.94		
Material	**Model**	**K_3**	**K_4**	**R^2**		
$MGtud_2$	Linear	0.721	569.35	0.97		
Material	**Model**	**K_5**	**K_6**	**K_7**	**K_8**	**R^2**
G1gau	M_r-σ_3-$\sigma_1/\sigma_{1,f}$	100.6	0.155	-5.818	3.757	0.92
$G1gau_2$	M_r-σ_3-$\sigma_1/\sigma_{1,f}$	125.4	0.139	-4.391	6.217	0.91
$G1eer_1$	M_r-σ_3-$\sigma_1/\sigma_{1,f}$	82.4	0.140	-1.183	1.230	0.86
$G1eer_2$	M_r-σ_3-$\sigma_1/\sigma_{1,f}$	0.792	0.127	-223.7	0.249	0.97
$G1eer_{2c}$	M_r-σ_3-$\sigma_1/\sigma_{1,f}$	141.6	-0.005	-3.228	0.593	0.98
$G1eer_4$	M_r-σ_3-$\sigma_1/\sigma_{1,f}$	290.1	-0.056	-0.556	2.098	0.79
$G2van_{1.5}$	M_r-σ_3-$\sigma_1/\sigma_{1,f}$	273.2	-0.040	-2.801	0.917	0.99
MGtud	M_r-σ_3-$\sigma_1/\sigma_{1,f}$	350.0	0.300	0.600	0.100	0.69
$MGtud_2$	M_r-θ-$\sigma_1/\sigma_{1,f}$	30.0	0.600	0.700	1.000	0.89
$MGtud_2$	M_r-θ-$\sigma_d/\sigma_{d,f}$	48.0	0.500	0.500	1.200	0.90
$MGtud_2$	M_r-σ_3-$\sigma_1/\sigma_{1,f}$	531.5	0.0362	-2.241	1.108	0.97

Poisson's Ratio could be calculated from the results of the triaxial tests using the TU set-up using the radial and axial resilient deformation readings. As with the resilient stiffness results, the influence of conditioning on the results is significant. Before conditioning low Poisson Ratios are evident see Figure 7 - 12, averaging 0.18 which is commonly associated with cemented materials.

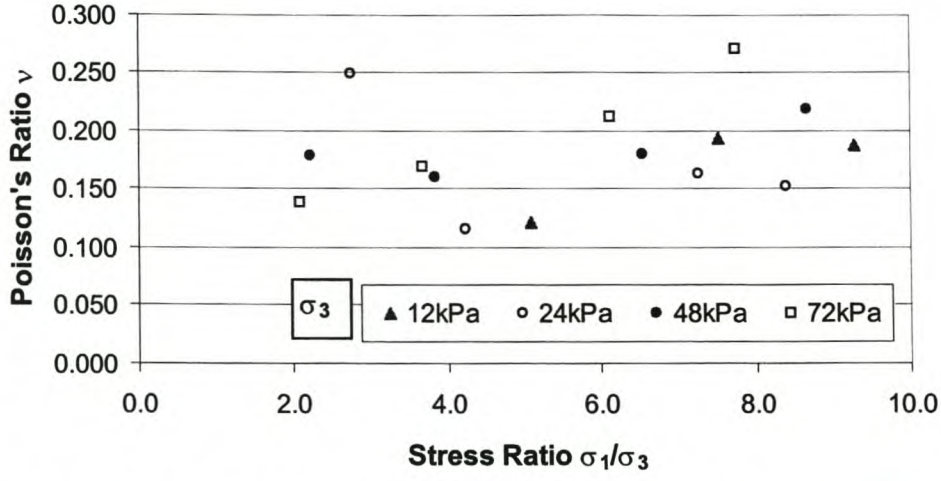

Figure 7 - 12. Poisson's Ratio as a Function of Stress Ratio σ_1/σ_3 from Triaxial Tests on MGtud$_2$ Foamed Mix before Conditioning

After conditioning, the Poisson Ratios develop dependence on the σ_1/σ_3 stress ratio, see Figure 7 - 13. Compliance with this model is also indicative of granular material behaviour, as reported by van Niekerk *et al.* (2000a). As with the M_r after conditioning, the Poisson Ratio relationship indicates disturbance of bonds during conditioning of the specimen. This procedure is therefore necessary for closer representation of field behaviour.

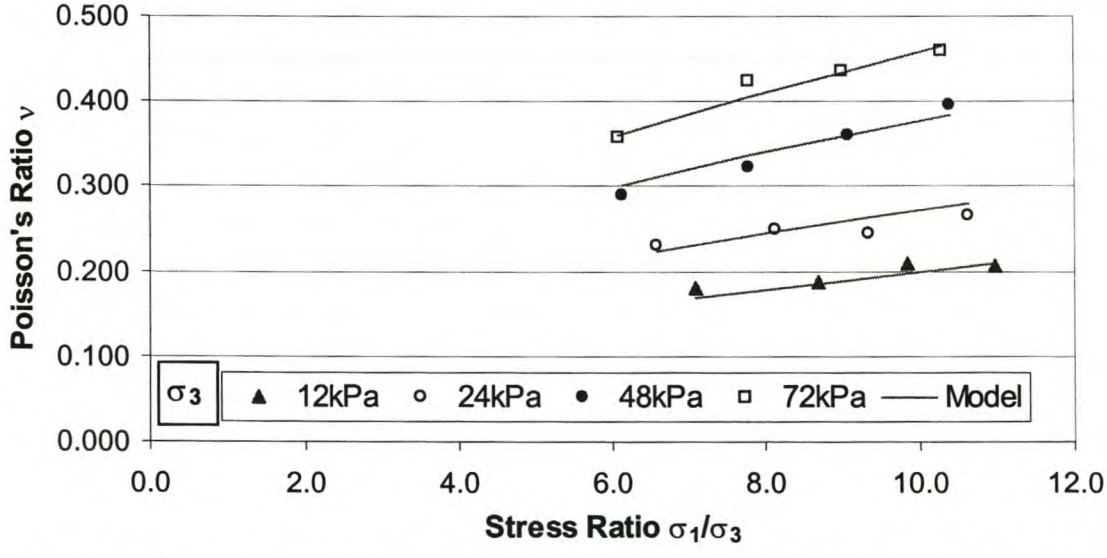

Figure 7 - 13. Poisson's Ratio as a Function of Stress Ratio σ_1/σ_3 from Triaxial Tests on MGtud$_2$ Foamed Mix after 10 000 Conditioning Cycles at $\sigma_d/\sigma_{d,f}$=40%

For the purpose of modelling foamed bitumen material behaviour in a pavement structure, relationships require establishment for the Poisson Ratio as a function of the stress. The results of regression coefficients for the Poisson Ratio relationships are provided in Table 7 - 9 for the granular material and its equivalent foamed mix with 2% binder. With bound mixes, jumps in the Poisson Ratio can occur through damage to a specimen during testing. This can be limited through reduction in the maximum σ_1/σ_3 ratio utilised.

Table 7 - 9. Summary of Coefficients for Poisson Ratio Models

Material	Model	a	b	R^2	
Mgtud	Eqn 7-12	0.06279	0.05057	0.65	
Material	**Model**	**c**	**d**	**e**	**R^2**
$Mgtud_2$	Eqn 7-13	0.01885	0.48607	0.483312	0.99
Material	**Model**	**f**	**g**	**h**	**R^2**
$Mgtud_2$	Eqn 7-14	70.098	-69.549	-0.00214	0.95

3.3 Permanent Deformation Behaviour

3.3.1 Permanent Deformation (ε_p) Test Methodology

Permanent Deformation (ε_p) Tests are performed in the triaxial set-up by means of repeated load applications for a controlled stress ratio. Tests are carried out on virgin specimens at different stress ratios to establish the stress dependency of the permanent deformation behaviour. At least three but preferably four specimens require testing for a particular mix and given test conditions, for a suitable sensitivity analysis and model to be established.

Slight differences in the settings for the ε_p tests are noted for the set-ups at the University of Stellenbosch (US) and Delft University of Technology (TU). The ε_p tests on the US triaxial set-up utilised a haversine wave load signal at a frequency of 2Hz and at one constant σ_3 value of 50kPa. The load during the test was monitored using a load cell with a range of 20kN over the 10V output. Axial deformation, both resilient and permanent, was monitored using a vertical LVDT within the loading ram i.e. measured over the entire height of the specimen. The LVDT has a range of 10mm over the 10V output. Tests were monitored and readings were manually initiated and recorded at intervals necessary to obtain information on changes in deformation behaviour. Generally this included readings at 100, 200, 500, 1000, 2500, 5000, 10 000, 20 000, 50 000, 100 000, ...1 000 000 load repetitions. If excessive deformation, in excess of 4%, occurred before the required number of load repetitions had been reached (at least 100 000), the test was terminated.

The ε_p tests on the TU triaxial set-up utilised a haversine wave load signal at a frequency of 5Hz and at one constant σ_3 value of 12kPa, refer (van Niekerk *et al.*, 2000a) and (Saleh, 2000). Axial and radial deformation, both resilient and permanent, was monitored using three vertical LVDTs over the middle 200mm height of the specimen and six radial LVDTs. The LVDT ranges were the same as for the resilient stiffness tests. Tests were monitored and readings were automatically recorded at intervals necessary to obtain information on changes in deformation behaviour. This included readings at 100, 200, .., 1000, 2000, .., 10 000, 20 000, .., 100 000, 200 000,..,1 000 000 load repetitions. If excessive deformation, in excess of 10% axial strain over 200mm occurred before the required number of load repetitions had been reached (1 000 000), the test was terminated. Both the TU and the US ε_p tests were load controlled and carried out at 25°C.

Relationships utilised for modelling of permanent deformation data, requires account to be taken of the stress level at which the triaxial test is performed. Van Niekerk *et al.* (2000a) utilize the formula provided in Equation 7 - 15 for granular materials. This approach is more applicable to foamed bitumen mixes than that of Wolff (1992) which uses only total stress considerations for granular materials.

$$\varepsilon_p = A \cdot \left(\frac{N}{1000}\right)^B + C \cdot \left(e^{D \cdot \frac{N}{1000}} - 1\right) \qquad \textbf{Equation 7 - 15}$$

Where,

$$A = a_1 \cdot \left(\frac{\sigma_1}{\sigma_{1,f}}\right)^{a_2}; B = b_1 \cdot \left(\frac{\sigma_1}{\sigma_{1,f}}\right)^{b_2} \qquad \textbf{Equation 7 - 16}$$

$$C = c_1 \cdot \left(\frac{\sigma_1}{\sigma_{1,f}}\right)^{c_2}; D = d_1 \cdot \left(\frac{\sigma_1}{\sigma_{1,f}}\right)^{d_2} \qquad \textbf{Equation 7 - 17}$$

The model coefficients and correlation coefficients for this model are determined by means of multivariate non-linear regression analysis in this research. This is carried out for axial as well as radial deformation data. The model provides the sum of two different forms of deformation behaviour. The first term in Equation 7 - 17 determines the linear increase of the ε_p term with load repetitions, in terms of the logarithm of both of these terms. The A term provides the ε_p value at N=1000 whilst B determines the subsequent slope of the function. With both the terms A and B being stress dependent, the equations above utilise the $\sigma_1/\sigma_{1,f}$ term as the stress function. The C and D terms are used to describe accelerated deformation of an exponential form at higher stress ratios, a phenomenon not commonly found in foamed mixes utilising good quality, hard aggregate.

For foamed bitumen materials, a stress ratio term $\sigma_d/\sigma_{d,f}$ has been selected to replace the $\sigma_1/\sigma_{1,f}$ term. In such a case, Equation 7 - 16 and Equation 7 - 17 remain the same, with only the suffix 1 being extended with d making a_1 become a_{1d} etc. The reason for use of the deviator stress rather than major principal stress is explained graphically.

The objective of the stress ratio is as an indicator of a stress state's relation to the failure envelope. For the stress state given as example in Figure 7 - 14, a significant difference is noted between the $\sigma_1/\sigma_{1,f}$ term and the $\sigma_d/\sigma_{d,f}$ term. As ϕ decreases, which is a tendency with foamed mixes relative to their equivalent granular materials, the differences in the two stress ratios becomes more significant. In the extreme (bound) case with $\phi = 0°$, the $\sigma_1/\sigma_{1,f}$ term is unaffected by changes in σ_3 of a stress state, whilst $\sigma_d/\sigma_{d,f}$ is influenced by confinement, thus making the latter a preferable ratio. Where σ_3 is a tensile stress, the disparity between the two stress ratios becomes greater, once again showing the $\sigma_d/\sigma_{d,f}$ to be preferable.

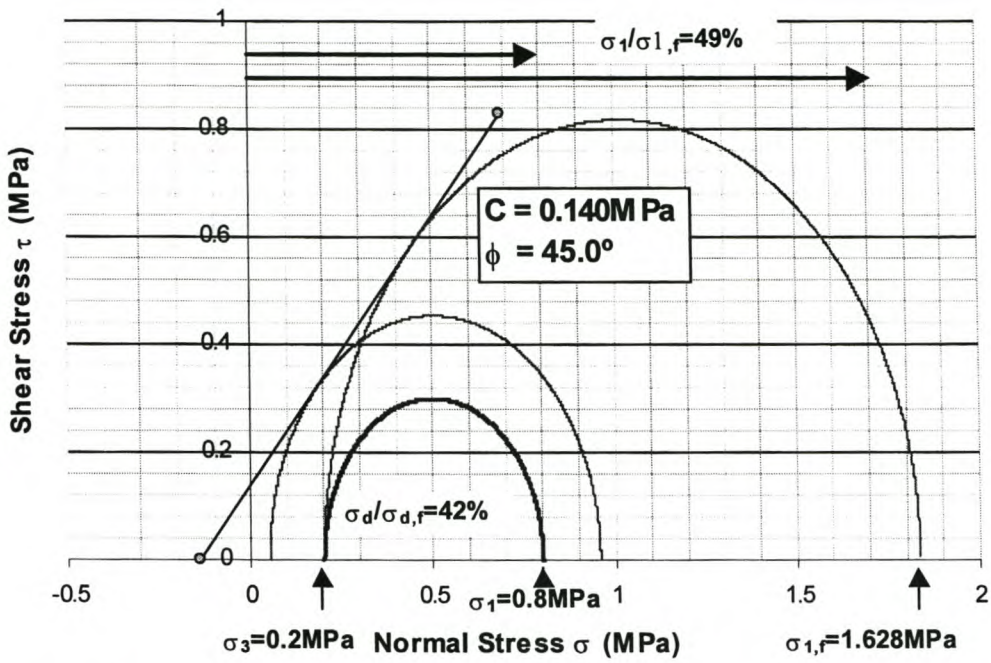

Figure 7 - 14. Graphical Illustration of Stress Ratios in the Mohr-Coloumb Space

Regression analysis of permanent deformation of foamed mixes can be accurately modelled by an additional relationship as detailed in Equation 7 - 18.

$$\varepsilon_P = \left(\frac{\alpha + \beta.\ln(N)}{1000} \right)$$ **Equation 7 - 18**

Where,

$$\alpha = \alpha_1 e^{\alpha_2 \frac{\sigma_d}{\sigma_{d,f}}}$$ **Equation 7 - 19**

$$\beta = \beta_1 e^{\beta_2 \frac{\sigma_d}{\sigma_{d,f}}}$$ **Equation 7 - 20**

For a dimensionless strain value to be calculated, dimensionless coefficients $\alpha_1, \alpha_2, \beta_1$ and β_2 are determined from the permanent deformation triaxial tests on the foamed materials. These coefficients are detailed in the following section.

3.3.2 Results of ε_p Tests

Cumulative axial permanent strain ($\varepsilon_{p,axial}$) analysed as a function of load repetitions (N) provides insight into performance of different foamed bitumen mixes. Variability in the ultimate shear strength and hence failure envelope of triaxial specimens is inherent and therefore forms an intrinsic factor in ε_p analysis. At the same time, repeat tests are not always feasible with complex and time consuming triaxial testing. For this reason, oversight

of collective results is necessary. Specimens utilised for permanent deformation testing in the triaxial set-up were prepared in identical procedures to those utilised for C-ϕ and M_r-θ tests.

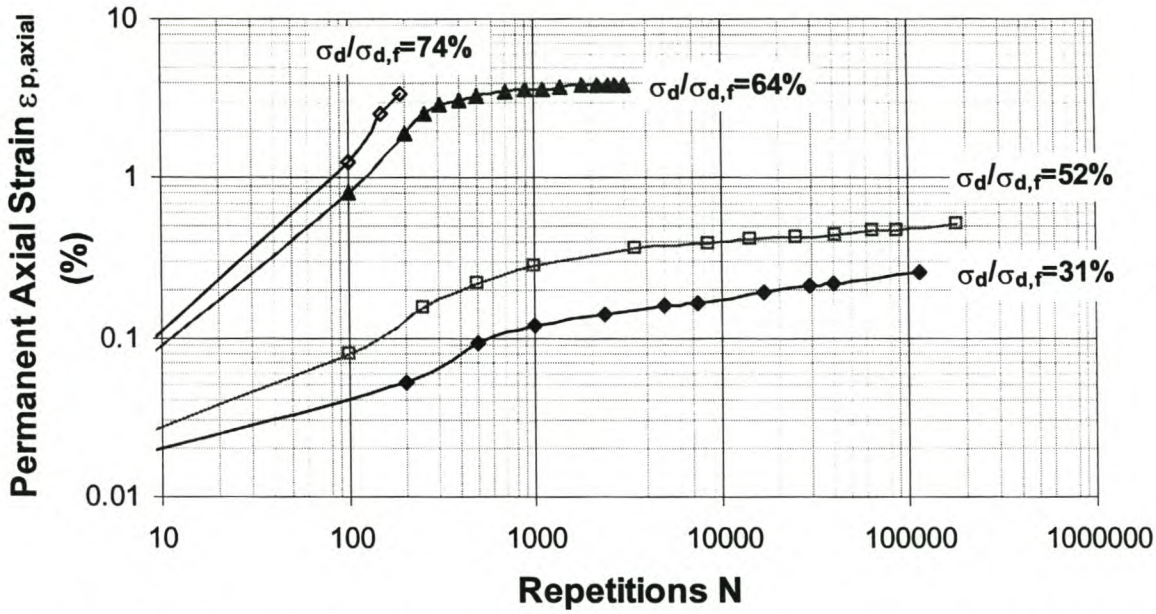

Figure 7 - 15. Permanent Axial Deformation versus Load Repetitions for G1eer$_1$ Foamed Mix with 1% Binder, Tested in US Triaxial with σ_3 = 50kPa

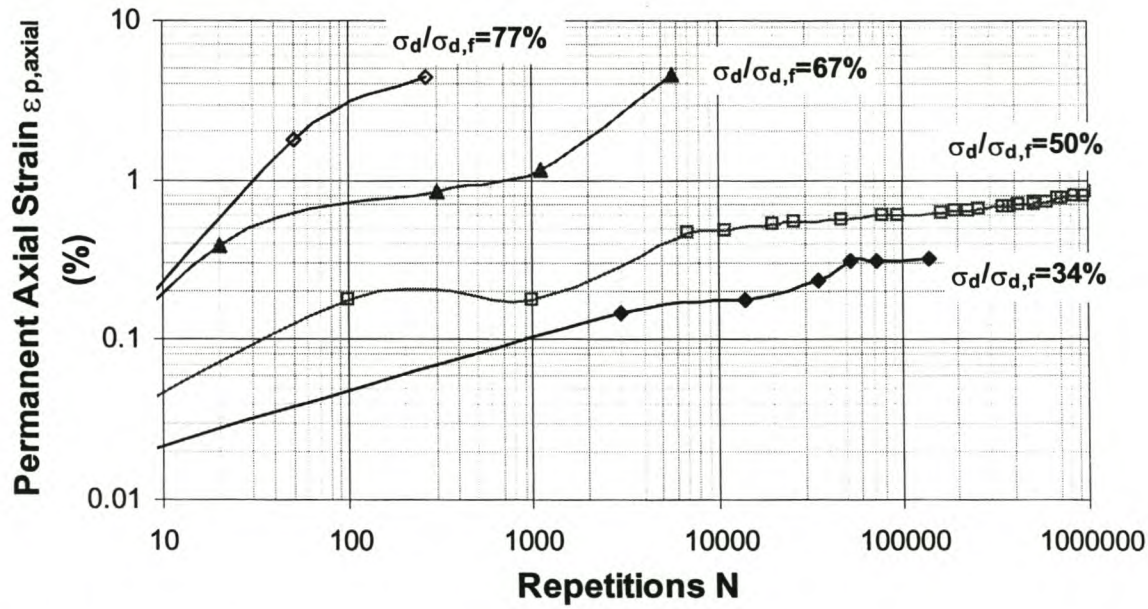

Figure 7 - 16. Permanent Axial Deformation versus Load Repetitions for G1eer$_2$ Foamed Mix with 2% Binder, Tested in US Triaxial with σ_3 = 50kPa

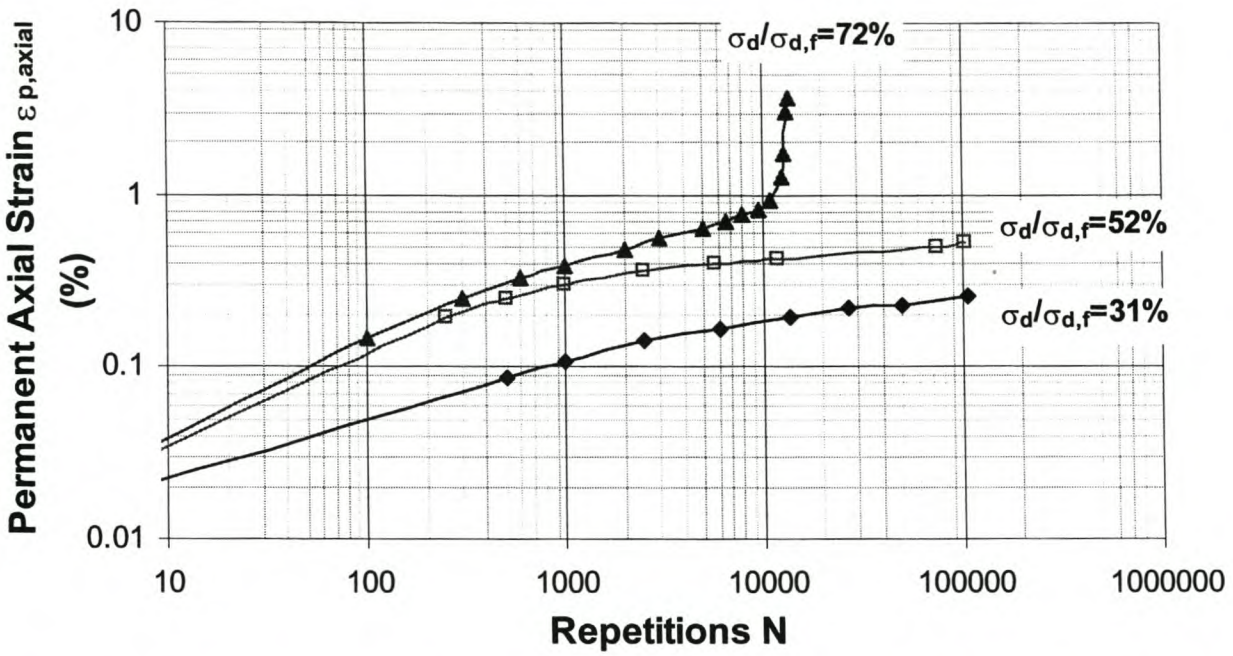

Figure 7 - 17. Permanent Axial Deformation versus Load Repetitions for $G1eer_{2C}$ Foamed Mix with 2% Binder 1% Cement, with σ_3 = 50kPa

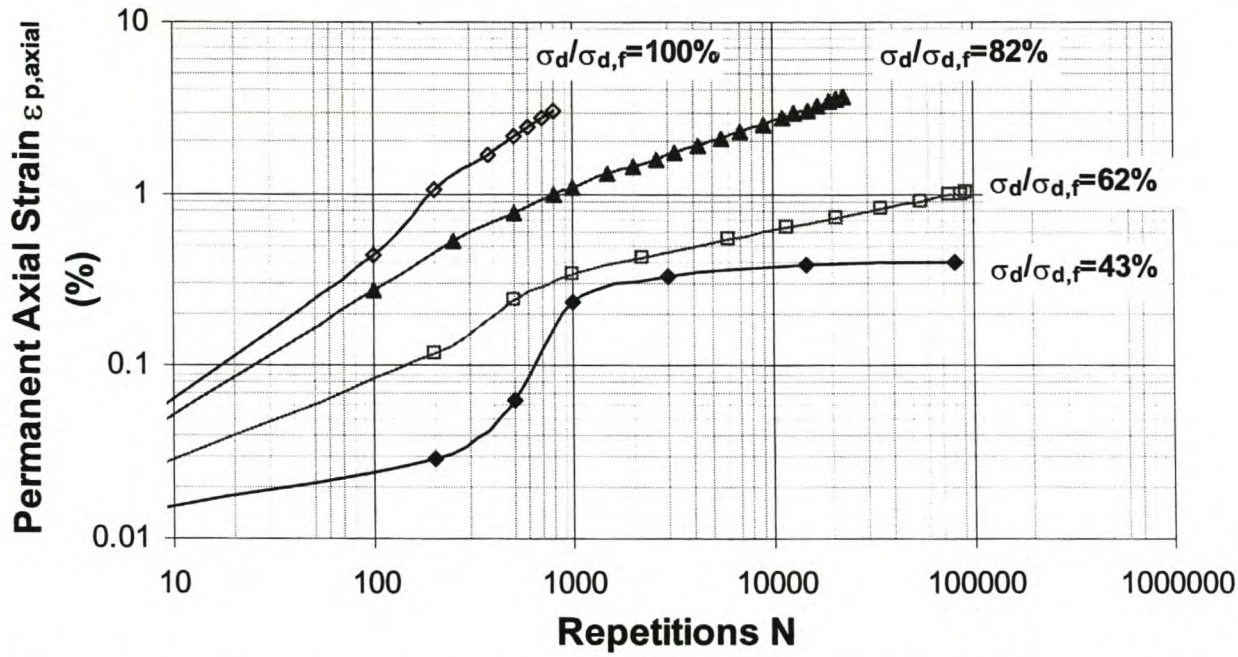

Figure 7 - 18. Permanent Axial Deformation versus Load Repetitions for $G1eer_4$ Foamed Mix with 4% Binder, Tested in US Triaxial with σ_3 = 50kPa

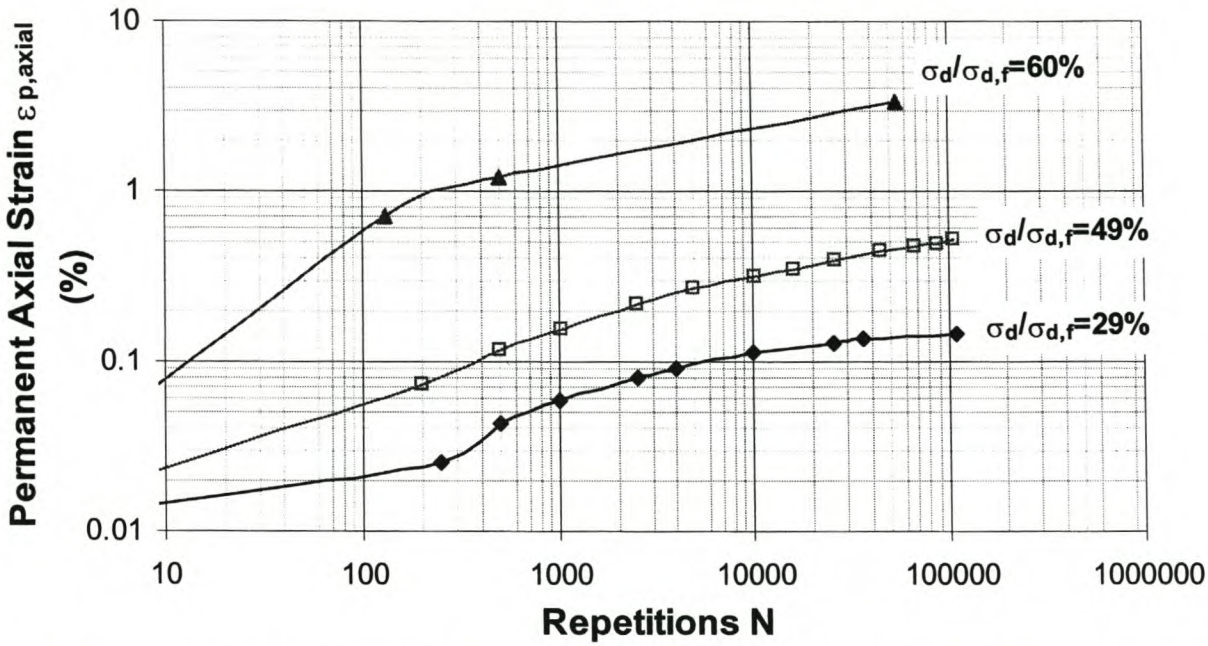

Figure 7 - 19. Permanent Axial Deformation versus Load Repetitions for G2van$_{1.5}$ Foamed Mix with 1.5% Binder and 2% Cement, with σ_3 = 50kPa

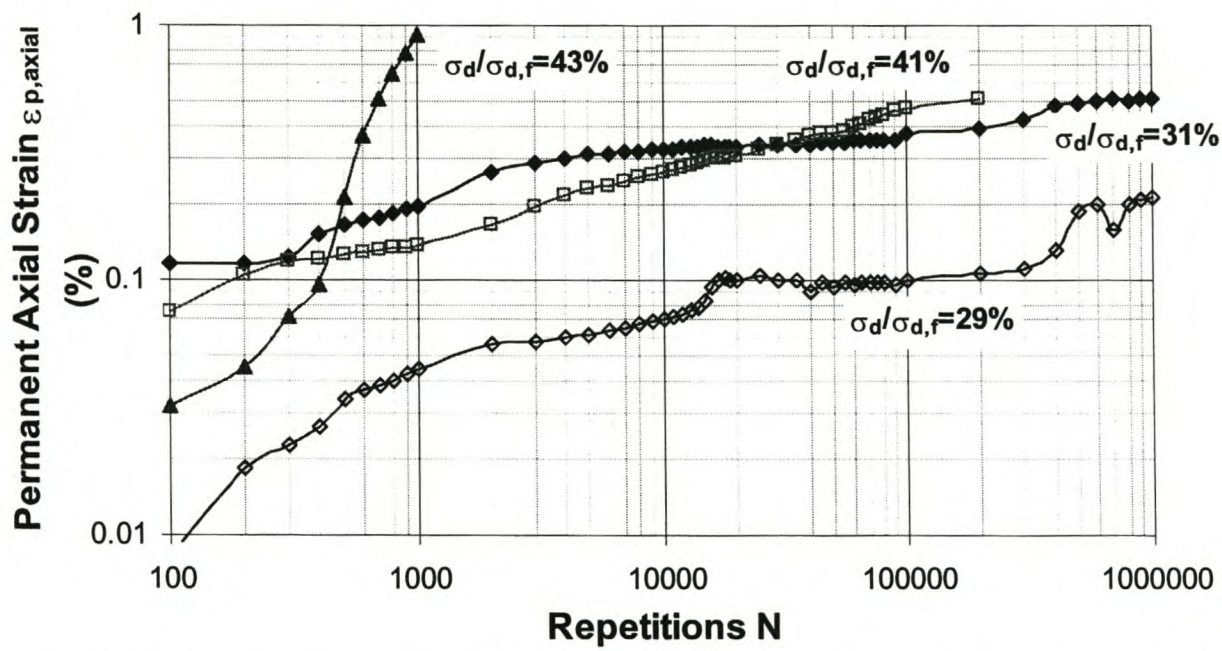

Figure 7 - 20. Permanent Axial Deformation versus Load Repetitions for MGtud Granular Material, Tested in TU Triaxial with σ_3 = 12kPa

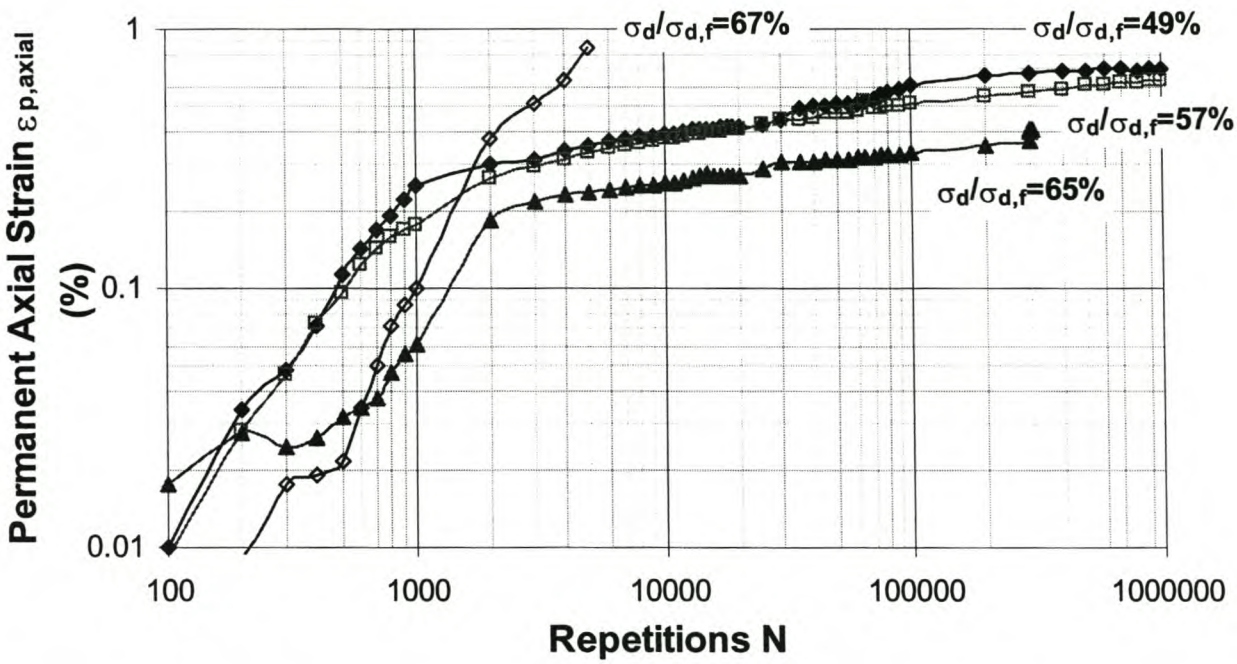

Figure 7 - 21. Permanent Axial Deformation versus Load Repetitions for MGtud$_2$ Foamed Mix with 2% Binder, Tested in TU Triaxial with σ_3 = 12kPa

It is apparent from the results of the permanent deformation tests on foamed treated materials that, as with granular materials, a critical stress ratio defines the boundary between stable ε_p growth and accelerated ε_p growth under repeated loading up to 10^6 cycles. As with the static triaxial tests and resilient deformation tests, a differentiation is necessary between stress dependent behaviour i.e. typical of granular materials, and strongly bound behaviour (including cement). The results of the ε_p tests are divided into foamed materials with and without cement to achieve this distinction and summarised both graphically and using the mathematical models.

A ratio of $\sigma_d/\sigma_{d,f}$ = 55% defines this critical boundary for foamed treated materials with 4% or less binder and without cement. This is evident from the summary of foamed materials without cement, see Figure 7 - 22. The model shown in the figure uses Equation 7 - 15. Below a ratio of $\sigma_d/\sigma_{d,f}$ = 55%, less than 2% axial strain is observed in the foamed treated material after 10^6 load repetitions. The summarised permanent deformation results are also modelled using Equation 7 - 18, see Figure 7 - 23. This provides a better correlation coefficient.

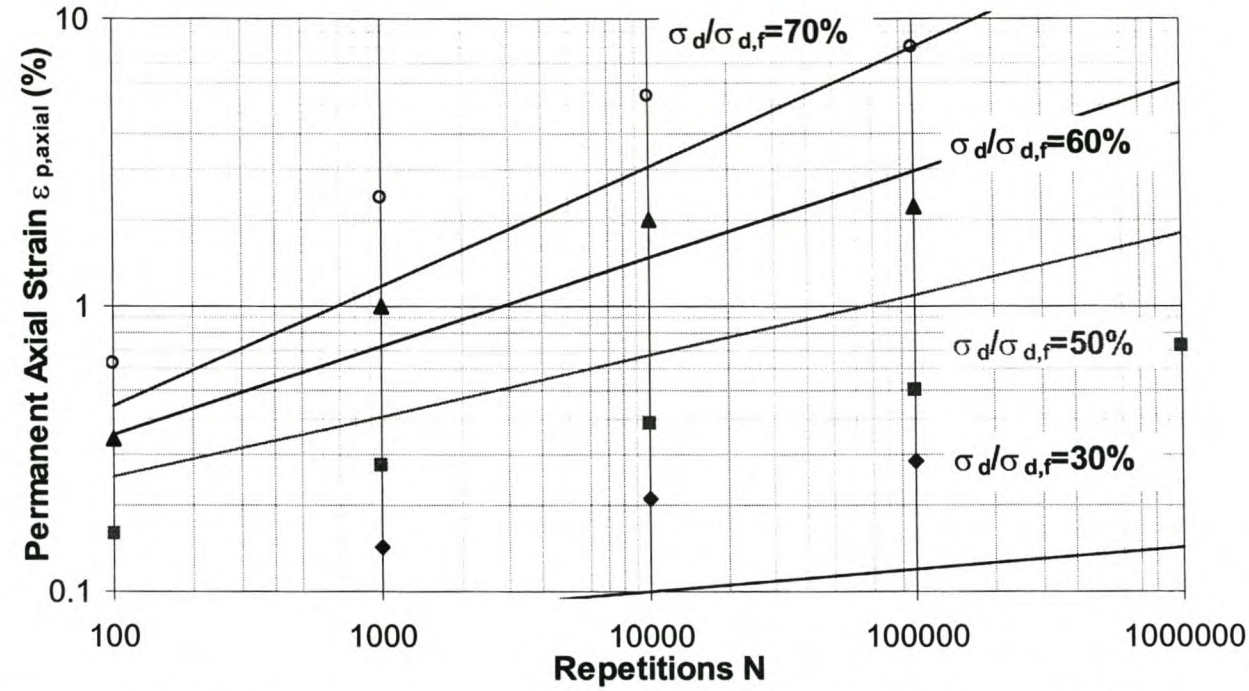

Figure 7 - 22. Template for Permanent Deformation Modelling of Foamed Mixes with <4% Binder and Without Cement based on Equation 7-15 and Averaged Triaxial Results

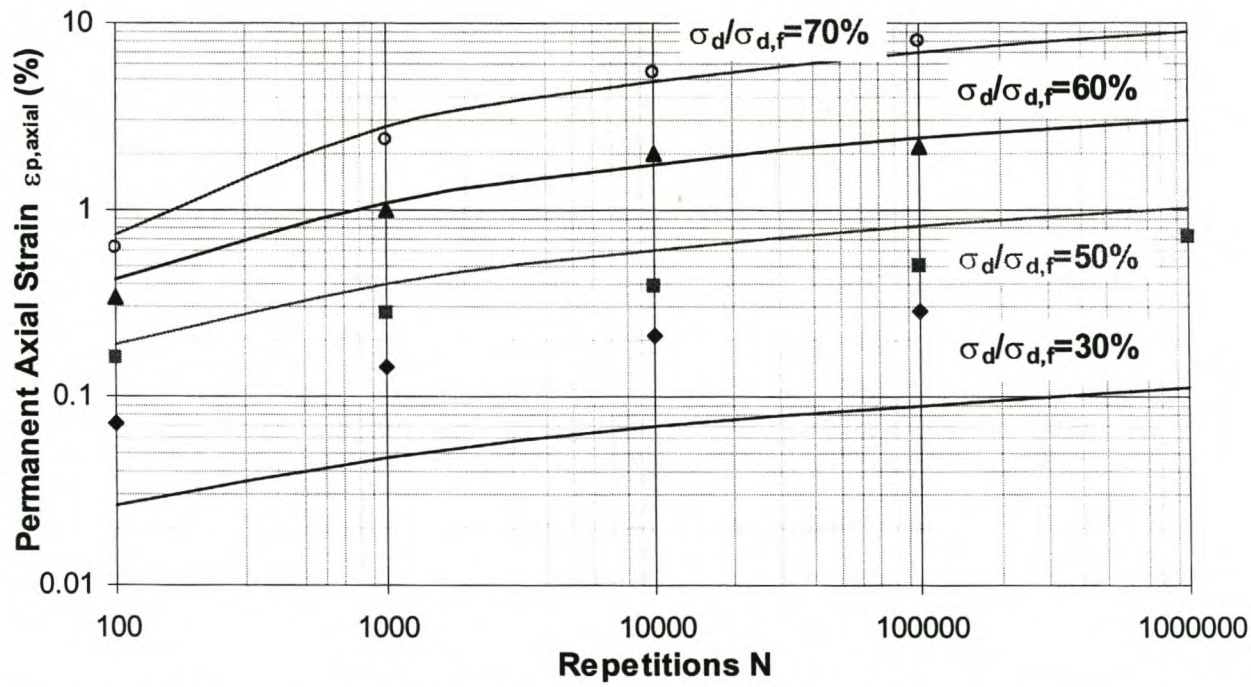

Figure 7 - 23. Template of Permanent Deformation Modelling for Foamed Mixes with <4% Binder and Without Cement, based on Equation 7-18 and Averaged Triaxial Results

The critical boundary for excessive permanent deformation of foamed treated materials with cement is defined by a ratio of $\sigma_d/\sigma_{d,f}$ = 52%, see Figure 7 - 24. Below this ratio, less than 2% axial strain is observed in the foamed treated materials after 10^6 load repetitions. Differences in the deformation behaviour with the inclusion of cement are linked to the change in behaviour under monotonic and cyclic loads noted for foamed mix with cement.

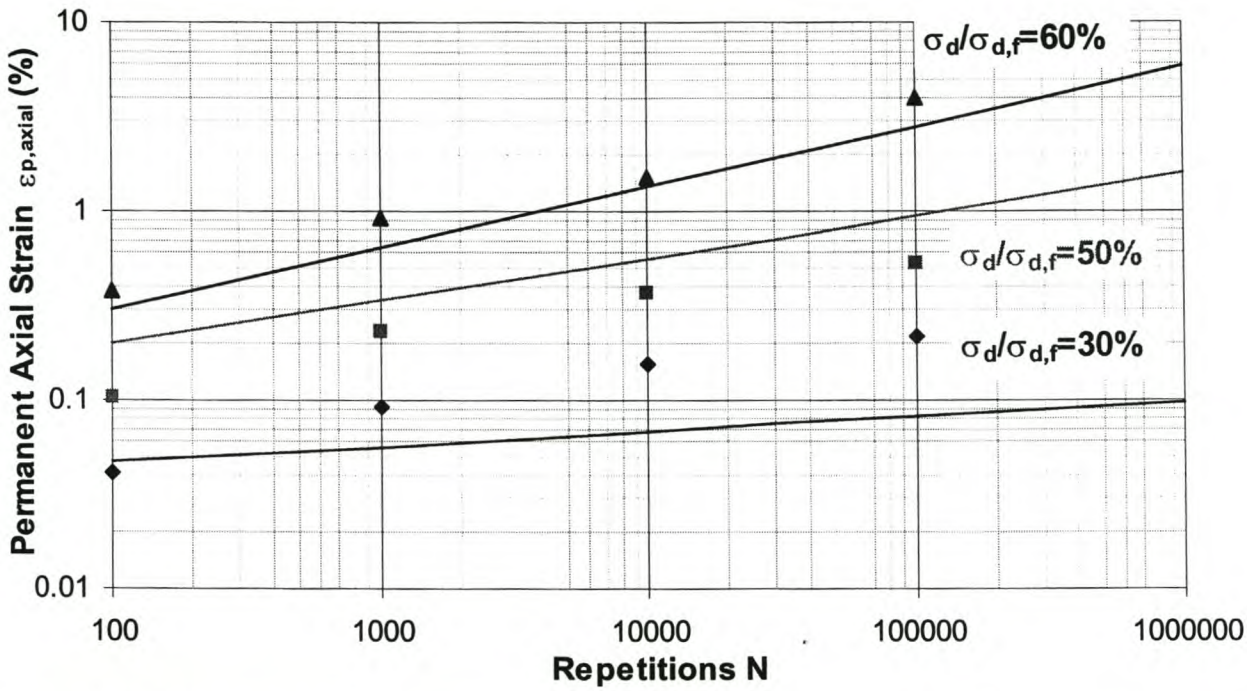

Figure 7 - 24. Template for Permanent Deformation Modelling of Foamed Mixes with Cement, based on Equation 7-15 and Averaged Triaxial Results

The coefficients for the relationships applicable used for ε_p models are detailed in Table 7 - 10. Coefficients of 0 for c_{1d} and d_{1d} indicate an inactive second term in the Equation 7 - 15, which specifies that accelerated deformation will not occur at a high number of load repetitions to the already log-linear functions.

Table 7 - 10. Summary of Coefficients for $\varepsilon_{p,axial}$ Models Applicable to Foamed Bitumen Mixtures

Model	Mix	a_{1d}	a_{2d}	b_{1d}	b_{2d}	c_{1d}	c_{2d}	d_{1d}	d_{2d}	R^2
Eqn 7-15 with $\sigma_d/\sigma_{d,f}$	Foamed Mix No cement	3.5	3.1	0.85	2	0	1	0	1	0.90
	Foamed Mix with cement	3.8	3.5	0.9	2	0	1	0	1	0.88
Model	**Mix**	α_1		α_2		β_1		β_2		R^2
Eqn 7-18	Foamed Mix No cement	-0.00288		13.4008		0.002982		11.45		0.99
	Foamed Mix with cement	-0.00394		13.3808		0.00330		11.45		0.68

In the same manner as the permanent axial deformations are modelled, so the permanent radial deformation data can be modelled too. The facility for measurement of radial deformation was available on the TU Triaxial set-up allowing the model coefficients of the radial deformation for the $MGtud_2$ foamed mix to be established, see Figure 7 - 25 and Table 7 - 11.

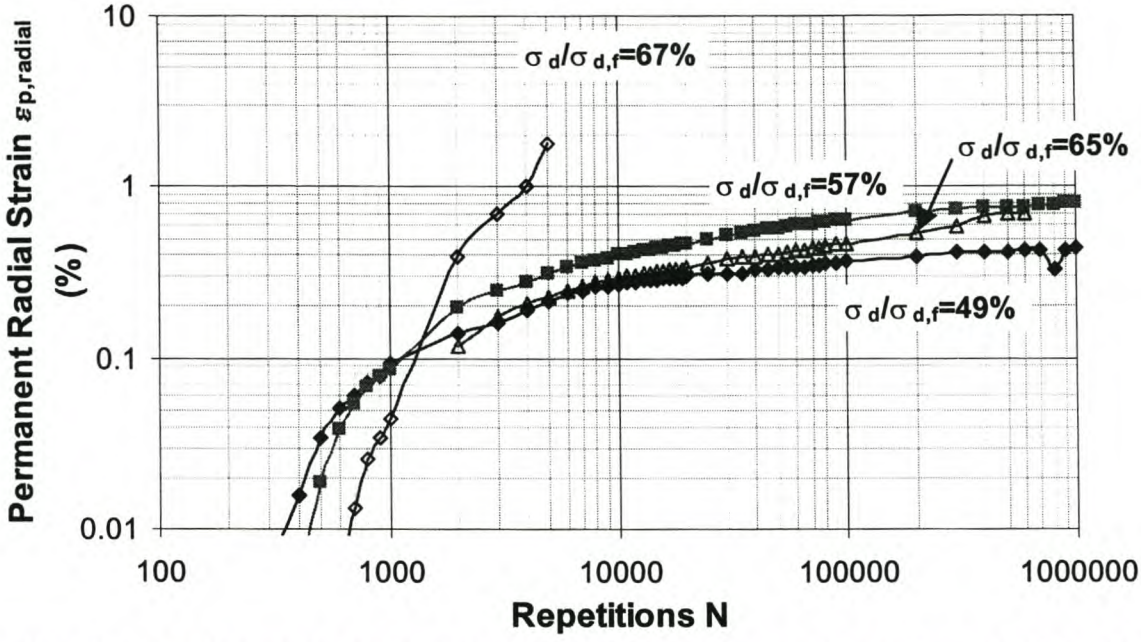

Figure 7 - 25. Permanent Radial Deformation versus Load Repetitions for $MGtud_2$ Foamed Mix with 2% Binder, Tested in TU Triaxial with σ_3 = 12kPa

Table 7 - 11. Coefficients for $\varepsilon_{p,radial}$ Model Applicable to Foamed Mix

Model	Mixture	a_{1d}	a_{2d}	b_{1d}	b_{2d}	c_{1d}	c_{2d}	d_{1d}	d_{2d}	R^2
Eqn 7-15 with $\sigma_d/\sigma_{d,f}$	Foamed Mix $MGtud_2$ No cement	10	7	100	8.5	1	7	0.1	5	<0.1

The permanent radial deformation data is related to the permanent axial deformation to provide values for Poisson's Ratio during repeated loading of foamed mix. The results show that the change in Poisson Ratio is not only a function of the number of load repetitions, but also of the critical stress ratio i.e. $\sigma_d/\sigma_{d,f}$ = 55%, as summarised in Table 7 - 12. The radial deformation trends are consistent with the axial deformation trends.

Table 7 - 12. Change in Poisson Ratio in Foamed Mix (2% Bitumen and No Cement) with Load Repetitions

Stress State	0 to 10 000 cycles	> 10 000 cycles
$\sigma_d/\sigma_{d,f}$ < 55%	0.28 to 0.60	0.60 to 0.70
$\sigma_d/\sigma_{d,f}$ > 55%	0.28 to 1.10	1.10 to 1.30+

Foamed mix with the inclusion of cement exhibits stiffer behaviour and higher sensitivity to over-stressing than if the cement is excluded, which is consistent with the behaviour of lightly cemented materials. A stress ratio approach satisfactorily models the material behaviour at cement contents of up to 2%, but higher active filler contents have not been investigated.

4. CASE STUDY : VANGUARD DRIVE RECYCLED FOAMED MIX LAYER

4.1 Accelerated Pavement Testing

The influences of traffic on a recycled layer comprising G2van$_{1.5}$ foamed bitumen mix have been simulated for analysis using a Model Mobile Load Simulator MMLS Mk3. This investigation was carried out in addition to the triaxial testing on the same material, with the aim of establishing a comparison between field deformation behaviour and laboratory modelling.

The MMLS Mk3 is an accelerated pavement testing tool that includes four pneumatic-tyred wheels that cycle in a closed loop, trafficking a trial section in a single direction. The wheels are 300 mm in diameter and 70 mm wide. A general layout of the MMLS Mk3 is provided in Figure 7 - 26 (van de Ven and Smit, 2000).

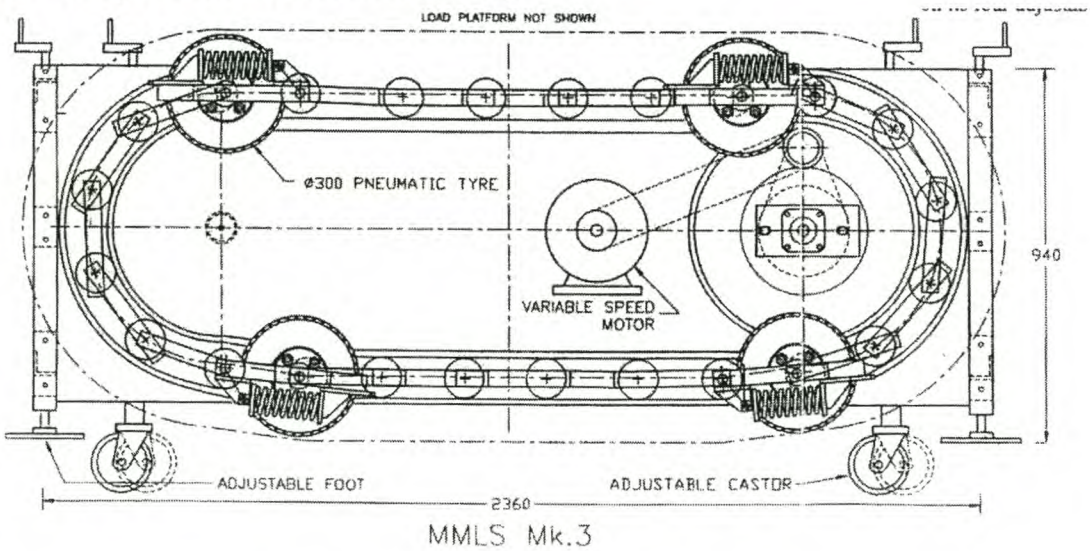

Figure 7 - 26. General Configuration of MMLS Mk3 Accelerated Pavement Testing Apparatus

The most applicable settings of the MMLS Mk3 for the APT test programme for Vanguard Drive were selected as:

- Tyre pressures of 600 kPa,
- Axle loads (= wheel load for single wheel) of 2,1 kN for each of the four wheels,
- Average rotations of approximately 30 rpm or 120 axle loads per minute, and
- Lateral wander of 150 mm total in a triangular distribution about the centre-line.

Each test was terminated at 100 000 to 150 000 axle-repetitions. Testing was carried out at ambient temperature, with air temperature ranging between 17°C and 27°C. Where ravelling was experienced, this was measured through collection of the material loosened during trafficking and weighing of this material. This enabled differentiation to be made between rutting as a result of material loss and permanent deformation.

Measurements of rut-depth i.e. vertical profiles, were made at two points along the wheel tracking axis. These measurements were made perpendicular to the wheel-tracking axis 200 mm either side of the longitudinal midpoint, with profile AB being the upstream profile and CD the downstream profile. The rut measurements were recorded at regular intervals during the trafficking, to enable a rut-depth versus time relationship to be established. A profilometer using arc measurements from a beam that passes over two reference points fixed to the road surface, was used. The readings on a multi-meter were used to calibrate the profilometer depth measurements.

Density and moisture details of the recycled layer analysed using the MMLS Mk3 are provided in Table 7 - 13. The G2van$_{1.5}$ material creates a density profile when compacted in a 300mm layer, as depicted in Figure 7 - 27. The "troxler" stands for nuclear gauge measurements at 50mm depths, compared with a sand-replacement test over 150mm. This profle is important to consider with wheel loading under the MMLS Mk3, as the depth of influence of the 300mm diameter wheels and the average profile is misleading.

Table 7 - 13. Density and Moisture Content of Foamed Bitumen Layer for APT Tests

	Troxler			Sand Replacement	
Section	% Mod. AASHTO	Std. Dev of 6 tests (%)	Moisture (%)	% Mod. AASHTO	Moisture (%)
Foam Trial Section	100.28	0.74	4.5	-	-
Foam MMLS Test	97.2	-	7.1	98.1	4.4

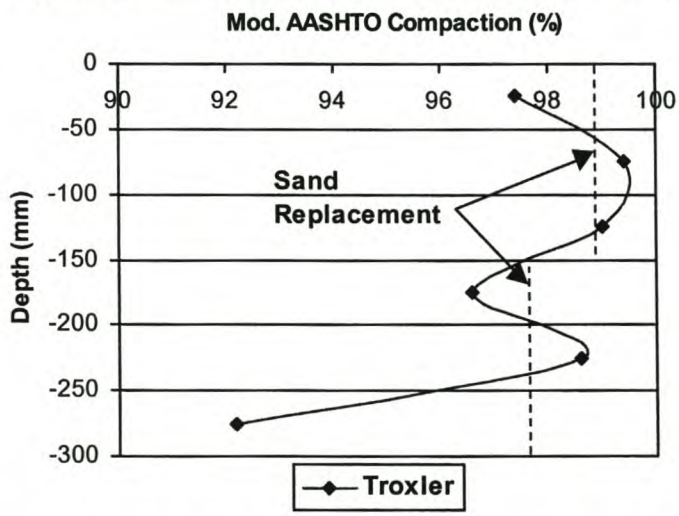

Figure 7 - 27. Compaction Profile for 300mm deep Recycled G2van$_{1.5}$ Layer Treated with Foamed Bitumen

The results of the accelerated tests in terms of rut depth are averaged across the width of the wheel-path that experienced lateral wander. As is to be expected with a triangular lateral wander distribution, the rutting follows a similar triangular profile, see Figure 7 - 28 which shows a typical rutting profile. The wheel-trafficking profile is symmetrical about the centre of the offsets i.e. 150 mm offset lies on the longitudinal axis of symmetry. The rutting profile is calculated for the average rut depth from 75 mm to 225mm offsets. As seen in the figure, some shoving is prevalent at the edges of the wheel path indicating shearing-action in the fresh foamed bitumen mix (less than 24 hours after compaction). This material above the original level of the road surface was not loose otherwise it would have been considered as ravelled material in rutting versus ravelling considerations.

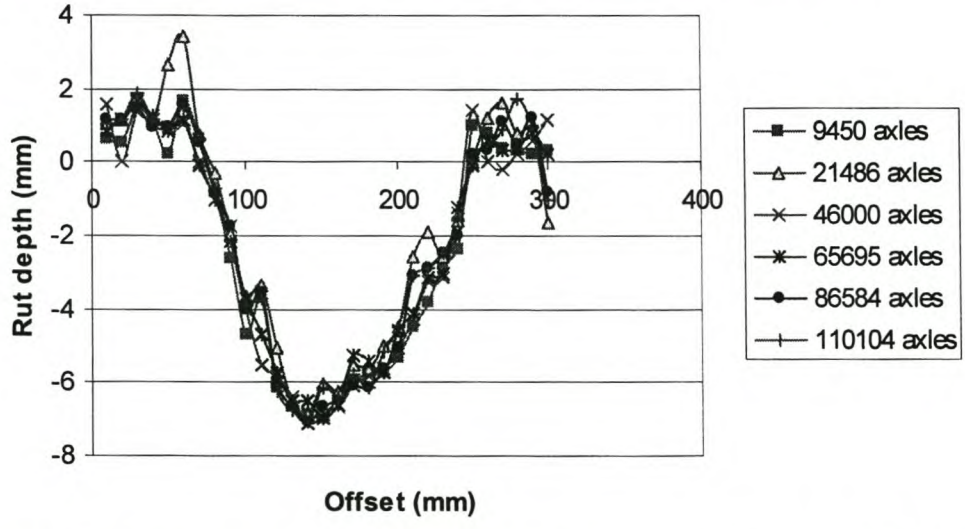

Figure 7 - 28. Cross-sectional Profilometer Readings on Recycled G2van$_{1.5}$ Foamed Material Tested in situ a half-day after Compaction using MMLS Mk3 APT

The proportion of ravelled material obtained from the APT trial was used to differentiate between rutting and ravelling, see Figure 7 - 29. Cold foamed mix can be susceptible to ravelling (Jenkins and van de Ven, 1999) and cognisance of this form of failure requires consideration in APT. In this way, a rutting profile caused solely by permanent deformation behaviour could be established.

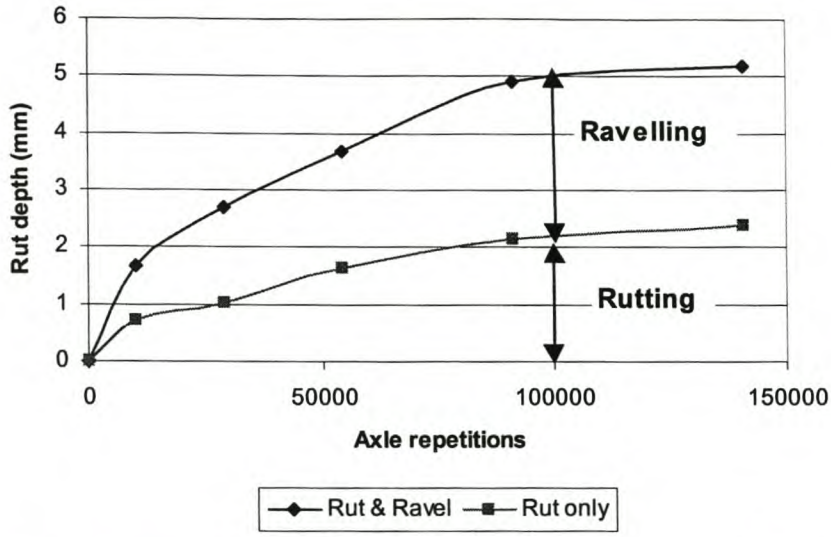

Figure 7 - 29. Deformation Profile for the Foamed Bitumen Section Tested 3 days after Compaction with MMLS Mk3

4.2 Finite Element Analysis using NOLIP

The NOLIP programme is an axial symmetric non-linear finite element model developed by Huurman (1997). Being axial symmetric NOLIP requires fewer elements than a 3-dimensional model. The pavement is divided into vertical layers and radial columns by NOLIP, thus creating a mesh of elements for analysis. The mesh is adapted in size to suit the geometry of the pavement structure being analysed.

NOLIP is suited to modelling of non-linear materials as the programme calculates the resilient modulus together with the stresses for each element in an iterative procedure as well as the displacements at each node, based on the applied wheel load. The resilient modulus and Poisson's Ratio are adjusted after every iteration based on the stresses calculated during the iteration. The iterative procedure continues until convergence is achieved, measured as the maximum difference in successive resilient moduli and Poisson's Ratios complying with a threshold limit.

The output of NOLIP comprises vertical and radial displacements of the nodes and the vertical stress σ_{zz} , the horizontal stress σ_{rz} and the shear stress for each element. The principal stresses σ_1, σ_2 and σ_3 are calculated from these stresses. NOLIP also provides the failure stress ratios $\sigma_1/\ \sigma_{1,f}$ and $\sigma_d/\ \sigma_{d,f} = (\sigma_1 - \sigma_3)/(\sigma_{1,f} - \sigma_3)$ for elements with a specified cohesion and angle of internal friction.

Shear properties for the $G2van_{1.5}$ foamed mix are provided in Table 7 - 5. These values are representative of the material after a 24hour cure at ambient temperature. In addition, the M_r-σ_3-$\sigma_1/\sigma_{1,f}$ model for this material is included in Table 7 - 8. Utilising these material properties for the 300mm recycled, underlain by a 200mm ferricrete sub-base layer (M_r=200MPa and ν=0.35) and soil sub-grade (M_r=200MPa and ν=0.35) in NOLIP, non-linear modelling may be carried out using the MMLS wheel load configuration.

Stress distributions of σ_1 and σ_2 with depth, as provided in Figure 7 - 30 and Figure 7 - 32 show that the depth of influence of the $^1/_3$ scale wheel does not extend beyond a depth of 200mm. In addition, lateral influences of the wheel are also restricted to approximately 100mm of the wheel centre. This is advantageous for analysis of the behaviour of an upper layer, as underlying layers with contribute insignificantly to the overall behaviour.

The non-linear behaviour of the material is evident from the M_r distribution with depth and lateral offset. Due to stress dissipation, the material experiences a significant reduction of resilient modulus with depth i.e from 500MPa to 100MPa under the wheel.

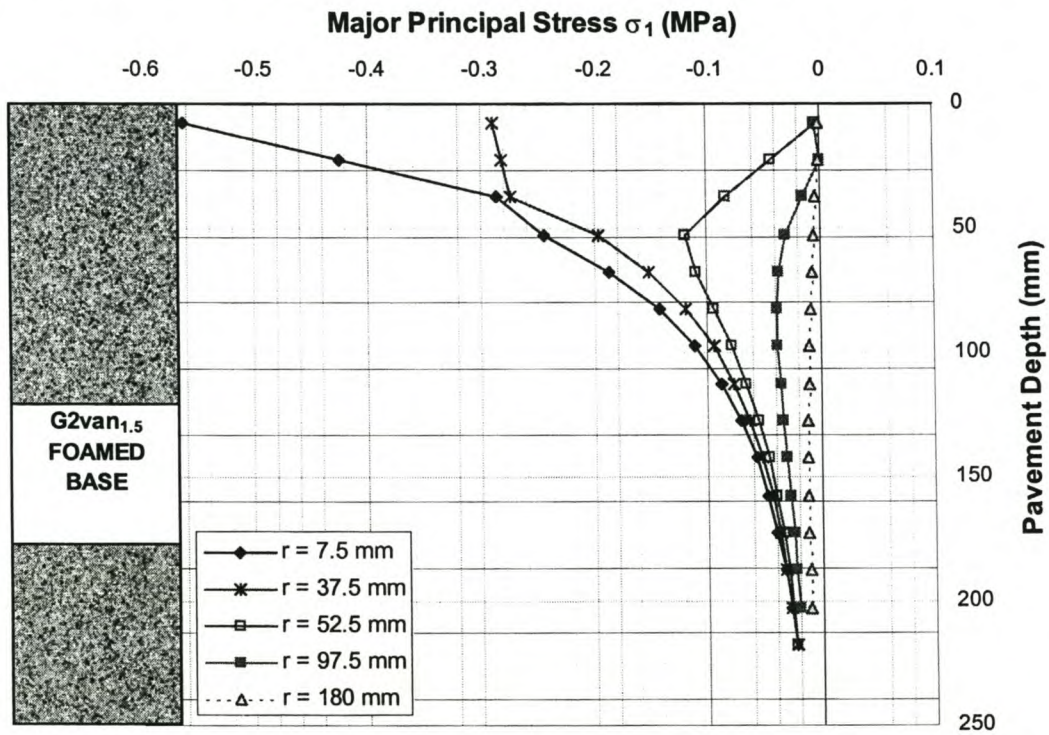

Figure 7 - 30. Major Principal Stress σ_1 with Depth in Recycled Foamed Mix under MMLS Mk3 Wheel Load (r = 33.4mm) [negative is compressive]

Note: Radial distance for stresses is measured from the centre of the wheel

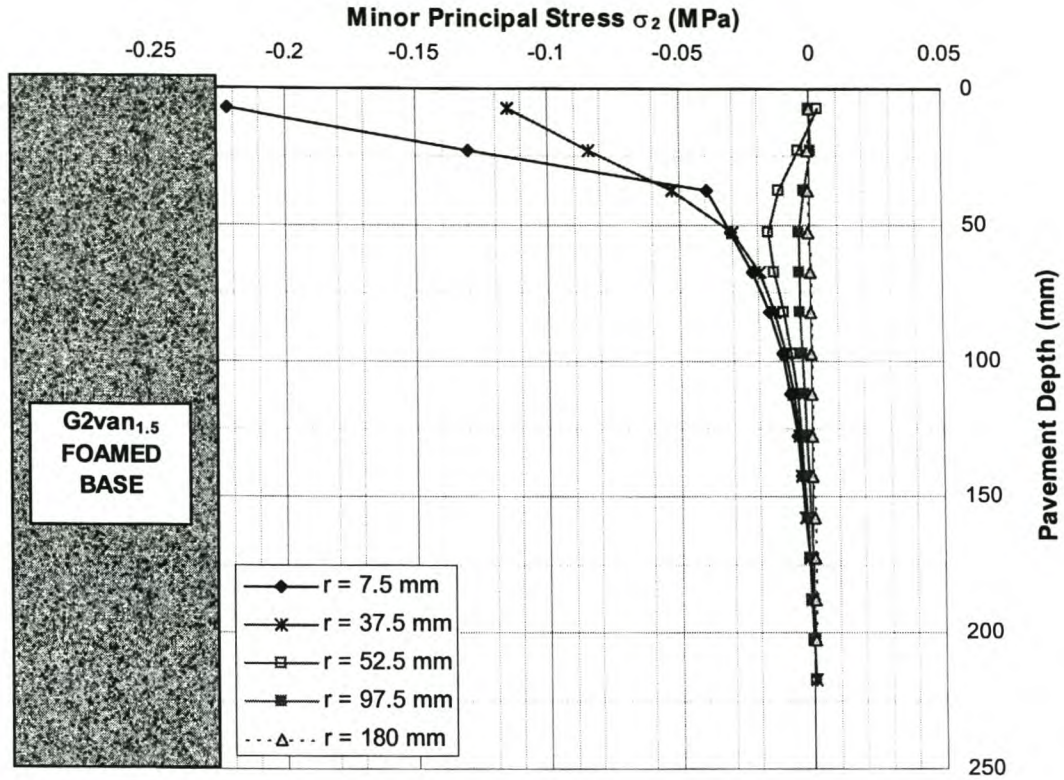

Figure 7 - 31. Minor Principal Stress σ_2 with Depth in Recycled Foamed Mix under MMLS Mk3 Wheel Load (r = 33.4mm) [negative is compressive]

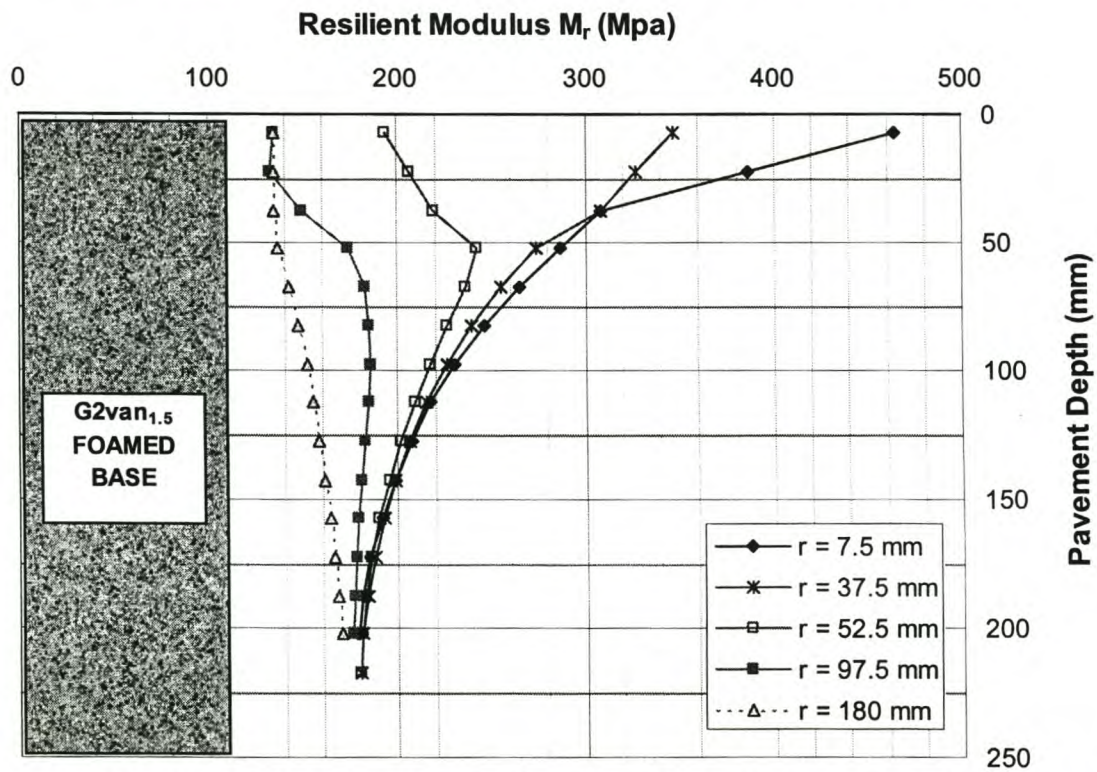

Figure 7 - 32. Resilient Modulus M_r with Depth in Recycled Foamed Mix under MMLS Mk3 Wheel Load (r = 33.4mm) at distances from Wheel Centre

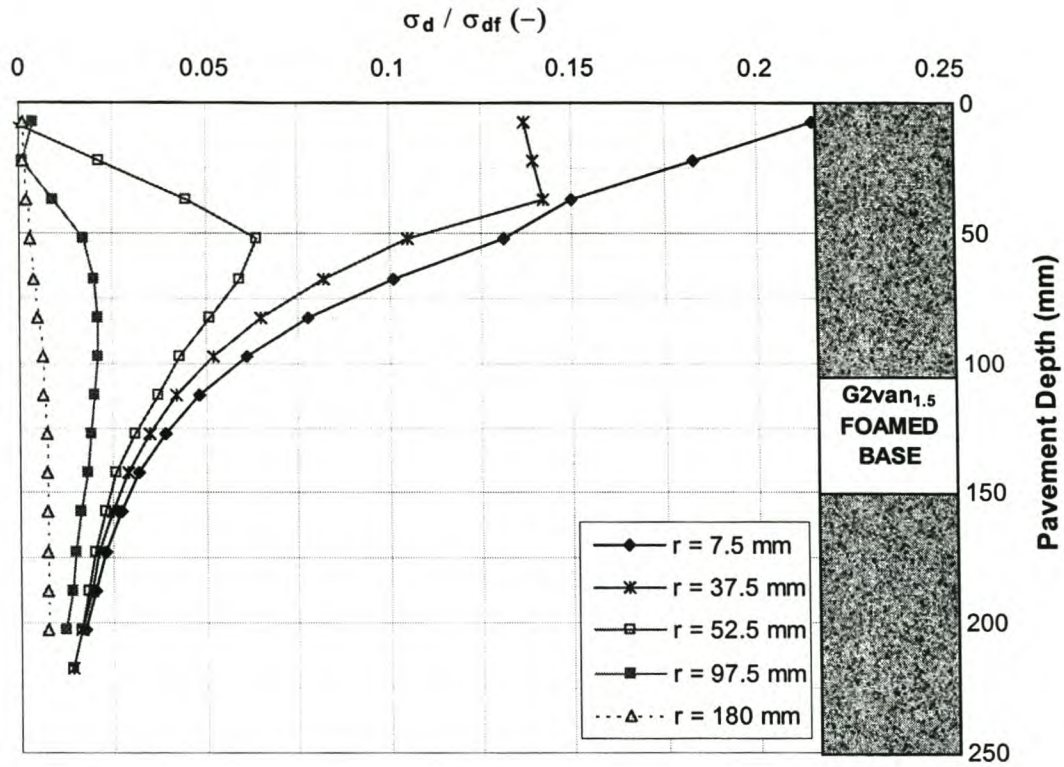

Figure 7 - 33. Deviator Stress Failure Ratio $\sigma_d/\sigma_{d,f}$ for Recycled Foamed Mix under MMLS Mk3 Wheel Load (r = 33.4mm) at Distances from Wheel Centre

The distribution of the deviator stress ratio $\sigma_d/\sigma_{d,f}$ shows that the upper part of the layer is most critical in terms of the layer performance. Nevertheless, the maximum ratio measured of $\sigma_d/\sigma_{d,f}$ = 0.22 results in less than 0,1mm of permanent deformation according to the model expressed in Equation 7 - 18. This, however, does not take cognisance of the slushing of the recycled layer with diluted emulsion during compaction (Jenkins and van de Ven, 1999). This operation, which is carried out to elevate the finer material and create a better-knit surfacing, saturates the upper 60mm of material. The influence of the slushing, in fact, delayed the commencement of accelerated pavement testing due to softening of the upper layer. Account can be taken of the softening through adjustment in the material properties of the upper 60mm and remodelling with NOLIP. To this end, a saturated material of this quality (G2), in accordance with (Theyse *et al.,* 1996), has ϕ = 50° and C = 39kPa. Allowance is made through increase in cohesion in the slushed material, from 50kPa up to 63kPa, due to the inclusion of foamed bitumen and curing of 3 days. These values are determined through back analysis i.e. a sensitivity analyses with identification of the values that provide the best fit. The modulus for the slushed material is accounted for through adjustment of the M_r-θ model coefficients to k_1 = 20 and k_2 = 0.252 , representative of this material.

Modelling of an upper layer that begins in a saturated state and cures with time, results in a substantial increase in the deviator stress ratio $\sigma_d/\sigma_{d,f}$, see Figure 7 - 34. These ratios are representative of the actual stress imparted during accelerated testing with the MMLS Mk3.

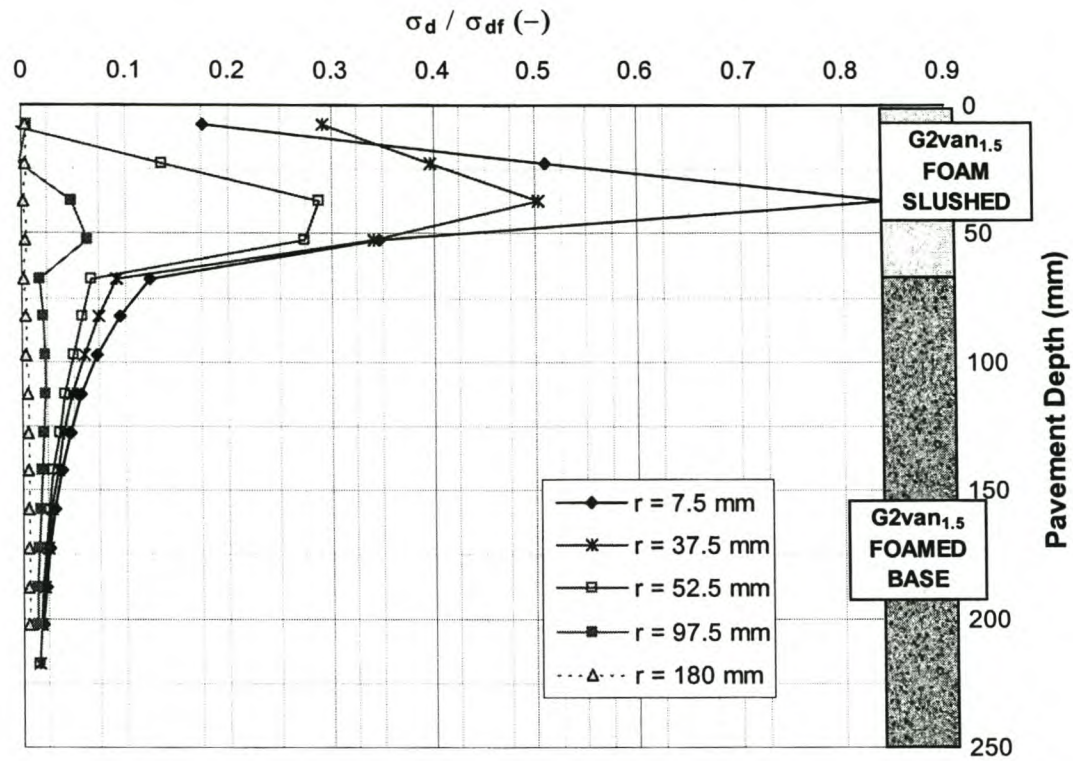

Figure 7 - 34. Deviator Stress Failure Ratio $\sigma_d/\sigma_{d,f}$ for Recycled Foamed Mix with Top 60mm Slushed ϕ=50° and C=50kPa, under MMLS Mk3 Wheel Load (r = 33.4mm) at Different Offsets from Wheel Centre

Utilising the stress ratios provided in Figure 7 - 34 and the models developed for foamed bitumen materials including cement provided in Table 7 - 10, a rutting profile can be determined for the G2van$_{1.5}$ material and compared with the results of the accelerated pavement testing. A sensitivity analysis of material cohesion illustrates the importance of curing and dangers in trafficking layers that have been saturated through slushing during road rehabilitation contracts. Figure 7 - 35 shows that with the upper 60mm of the recycled layer with a cohesion value of 11kPa higher than the equivalent granular material and the remainder of the layer with properties given in Table 7 - 5, a good correlation between field testing and the model is obtained. One cause of disparity between the field results and model output is the lateral wander of the wheels. Although the rutting is determined over a 15cm wheel-path for both cases, the MMLS Mk3 uses a triangular lateral wander distribution and NOLIP uses a normal distribution.

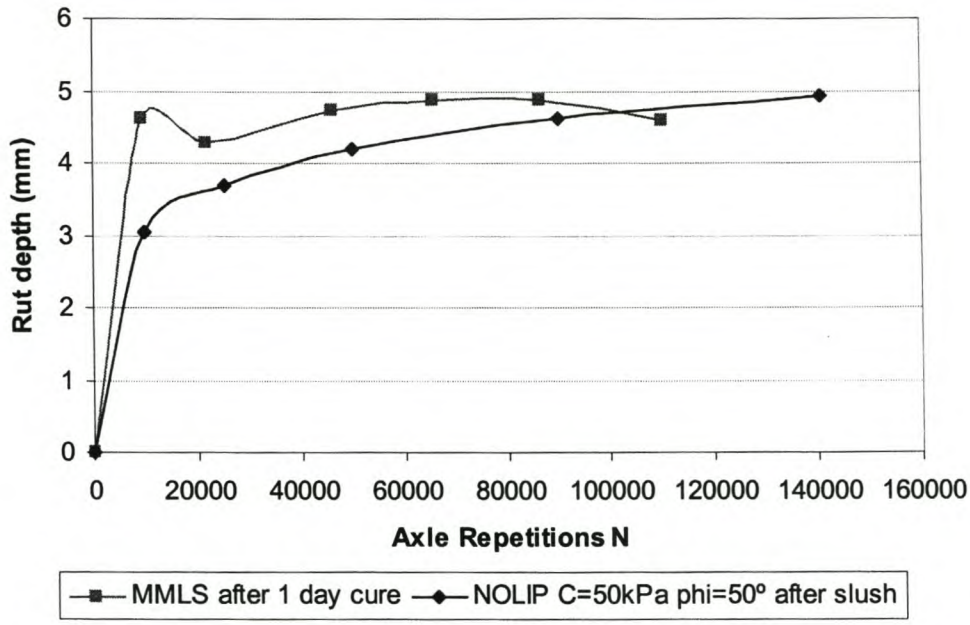

Figure 7 - 35. Rutting of G2van$_{1.5}$ Recycled Foamed Mix Layer from APT with MMLS Mk3 and Modelling using Finite Elements (NOLIP) after 1 day Cure

A further increase of 13kPa in the upper 60mm of the recycled foamed mix during curing of the layer through exposure to the atmosphere provides the rutting results for NOLIP analysis shown in Figure 7 - 36. With an additional 48 hours of curing, a significant reduction in rutting is evident, a phenomenon that is dependent on climate, traffic levels, material composition and slushing procedure. The models applicable with output from NOLIP finite element analysis provide a relevant procedure, therefore, for analysis of road pavements incorporating foamed bitumen layers.

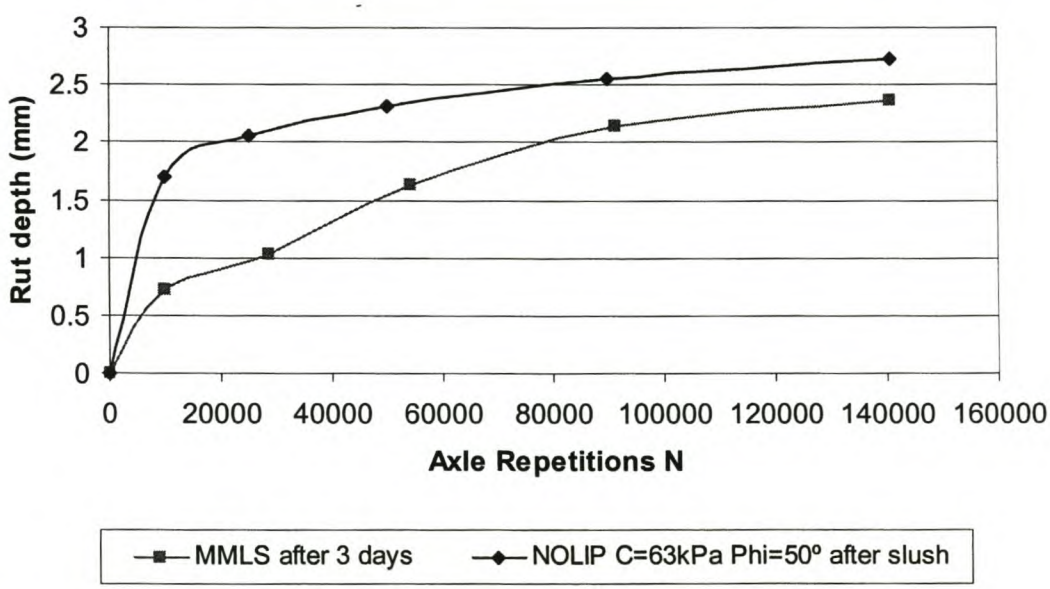

Figure 7 - 36. Rutting of G2van$_{1.5}$ Recycled Foamed Mix Layer from APT with MMLS Mk3 and Modelling using Finite Elements (NOLIP) after 3 days Curing

5. ANALYSIS OF FOAMED BITUMEN TREATED LAYERS IN TYPICAL PAVEMENT STRUCTURES

The influence of foamed bitumen treatment of granular materials is effectively demonstrated through the analysis of virtual pavement structures incorporating such layers. To this end, a granular material is modelled as a base in pavement structures in an unbound state and with 2% foamed bitumen, for comparison purposes. The NOLIP finite element programme provides the tool for non-linear, stress-dependent modelling of the pavement structures with the pertinent materials.

The type of pavement structure selected for analysis is typical of second order roads in developing areas that should have the capacity to accommodate at least 3×10^6 standard axle (80kN) repetitions. In such a pavement, a relatively thin asphalt surfacing of less than 80mm overlies a granular or foam treated base, which in turn is underlain by a good quality sand sub-base. Sub-grade with a CBR value of 5% is utilised as the foundation material in the comparative analyses.

5.1 Material Properties in Pavement Analysis

The material characteristics of the different pavement layers have been obtained through research, in the case of the granular materials, and assumed in the case of the asphalt and foundation layers. Considering that the analysis is focussed on the performance of the granular base and equivalent foam treated material, the asphalt layer is simply modelled as a linear elastic layer, see Table 7 - 14.

Table 7 - 14. Properties for Materials Modelled Elastically using NOLIP

Material	M_r (MPa)	Poisson Ratio ν
Asphalt surfacing	4500	0.35
Subgrade	50	0.35

The granular material utilised in the analysis is MGtud and the equivalent foamed mix $MGtud_2$, both of which are detailed earlier in this chapter. This material is a mixed granulate i.e. crushed building rubble incorporating concrete and brick. The specific properties of these two materials utilised in the NOLIP analysis are provided in the tables that follow. The sand sub-base material is Weiver Sand, researched by Huurman (1997). Details of Weiver Sand are also included in the following tables.

Table 7 - 15. Shear Parameters of Stress-dependent Materials for NOLIP

Material Type	C (kPa)	ϕ (°)
Granular MGtud	154	45.1
Foamed Mix $MGtud_2$	331	36.7
Weiver Sand	6.8	43.0

Table 7 - 16. Resilient Stiffness Model Coefficients of Stress-dependent Materials for NOLIP Analysis

Material	Model	K_5	K_6	K_7	K_8	R^2
MGtud	M_r-σ_3-$\sigma_1/\sigma_{1,f}$	350.0	0.30	0.10	0.10	0.69
$MGtud_2$	M_r-θ-$\sigma_d/\sigma_{d,f}$	48.00	0.50	0.50	1.20	0.90
Weiver Sand	M_r-σ_3-$\sigma_1/\sigma_{1,f}$	38.40	0.60	0.89	5.79	0.98

Table 7 - 17. Poisson Ratio Model Coefficients of Stress-dependent Materials for NOLIP Analysis

Material	Model	a	b	R^2	
MGtud	Eqn 7-12	0.06279	0.05057	0.65	
$MGtud_2$	Poisson Ratio fixed at 0.28 for NOLIP				
Material	**Model**	**f**	**g**	**h**	**R^2**
Weiver Sand	Eqn 7-14	0.165	0.578	4.225	0.91

5.2 Results of NOLIP Finite Element Analysis

Utilising a "super-single" axle type configuration a wheel load of 65kN with a tyre pressure of 920kPa, a finite element analysis of three alternative pavement structures has been carried out using NOLIP. The wheel load of 65kN was selected from a sensitivity analysis of loads carried out initially on a reference pavement with 80mm asphalt surfacing, 350mmm granular (MGtud) base and 500mm sand (Weiver) sub-base. For such a pavement, the given load is a critical case that will result in shear failure of the unbound base (Saleh,2000).

A sensitivity analysis of the pavement structure with adjustment in base thickness, for both the granular and foamed treated materials, as well as reduction in asphalt thickness for the structure with the foamed treated base, provides comparative structures with similar design lives. A criterion of $\log(N) = 33.50 - 7.36\log(S_{mix}) + 0.78.\log^2(S_{mix}) - 5.24\log(\varepsilon_t)$ for the asphalt layer and vertical compressive strain (ε_c) criterion at the top of the subgrade for a permanent deformation $N = 6.15.10^{-7}.\varepsilon_c^{-4}$ is applicable for the analysis. However, these layers do not prove to be the critical pavement layers. The comparative structures are depicted diagrammatically in Figure 7 - 37.

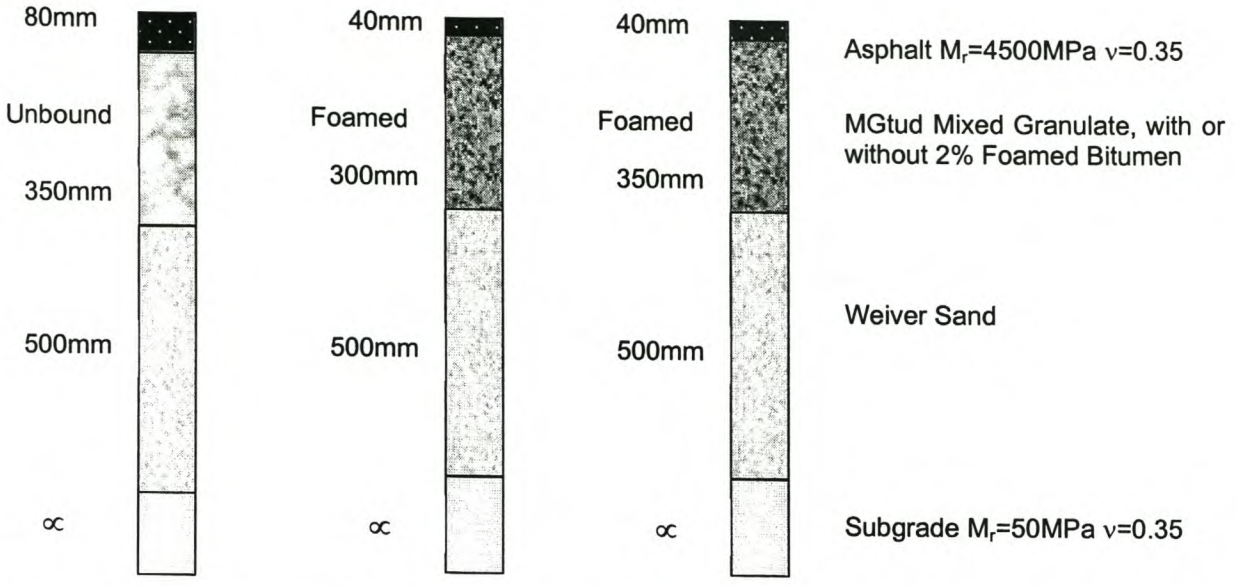

Figure 7 - 37. Comparative Pavement Structures selected for Finite Element Analysis

A typical example of the mesh utilised for the finite element analysis is provided in, for the case of 350mm base. The mesh extends to 17 180mm depth with ever increasing element sizes, and to a width of 5 696mm in accordance with the requirements of NOLIP. More extensive details of mesh design and utilisation are provided by Huurman (1997).

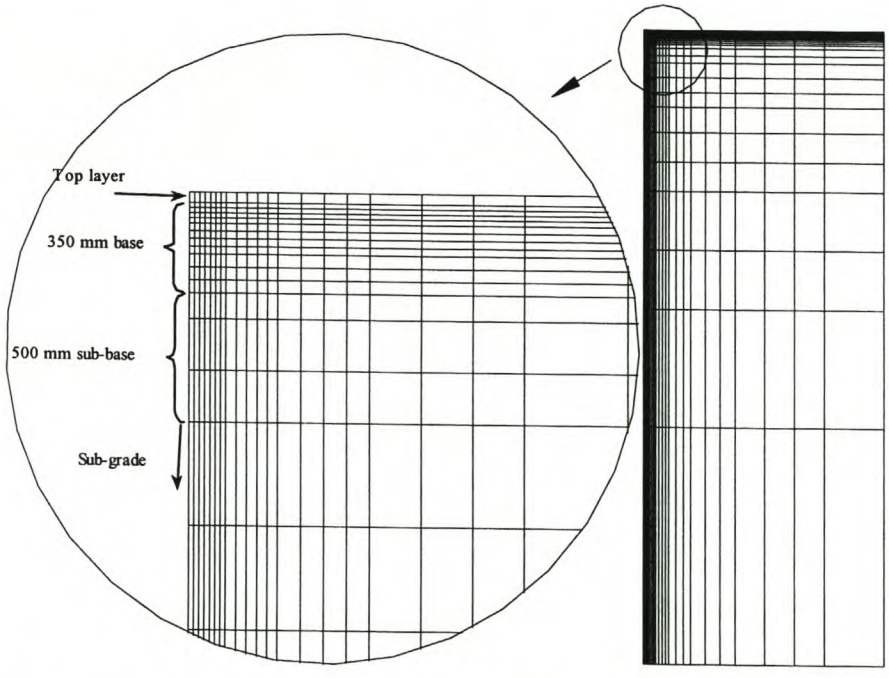

Figure 7 - 38. Mesh utilised for Finite Element Analysis of Pavements incorporating Granular or Foamed Mix Base, utilising NOLIP

The behaviour of the different pavement structures with either granular or foamed mix base layers, is most effectively interpreted through plots of relevant material parameters with depth in the structure. Figure 7 - 39 to Figure 7 - 41 provide the distribution of major and minor principal stress with depth in the three different structures, as well as the resilient modulus and relevant stress ratio $\sigma_1/\sigma_{1,f}$ with respect to depth. These parameters are recorded at given radial distances from the load centre. The stress ratio $\sigma_1/\sigma_{1,f}$ rather than $\sigma_d/\sigma_{d,f}$ has been used in this analysis due to restrictions in the combinations of the models used in the finite element analysis. It is possible for horizontal tensile stresses (σ_2) to occur in such a pavement structure with the cohesion values of the foamed mix.

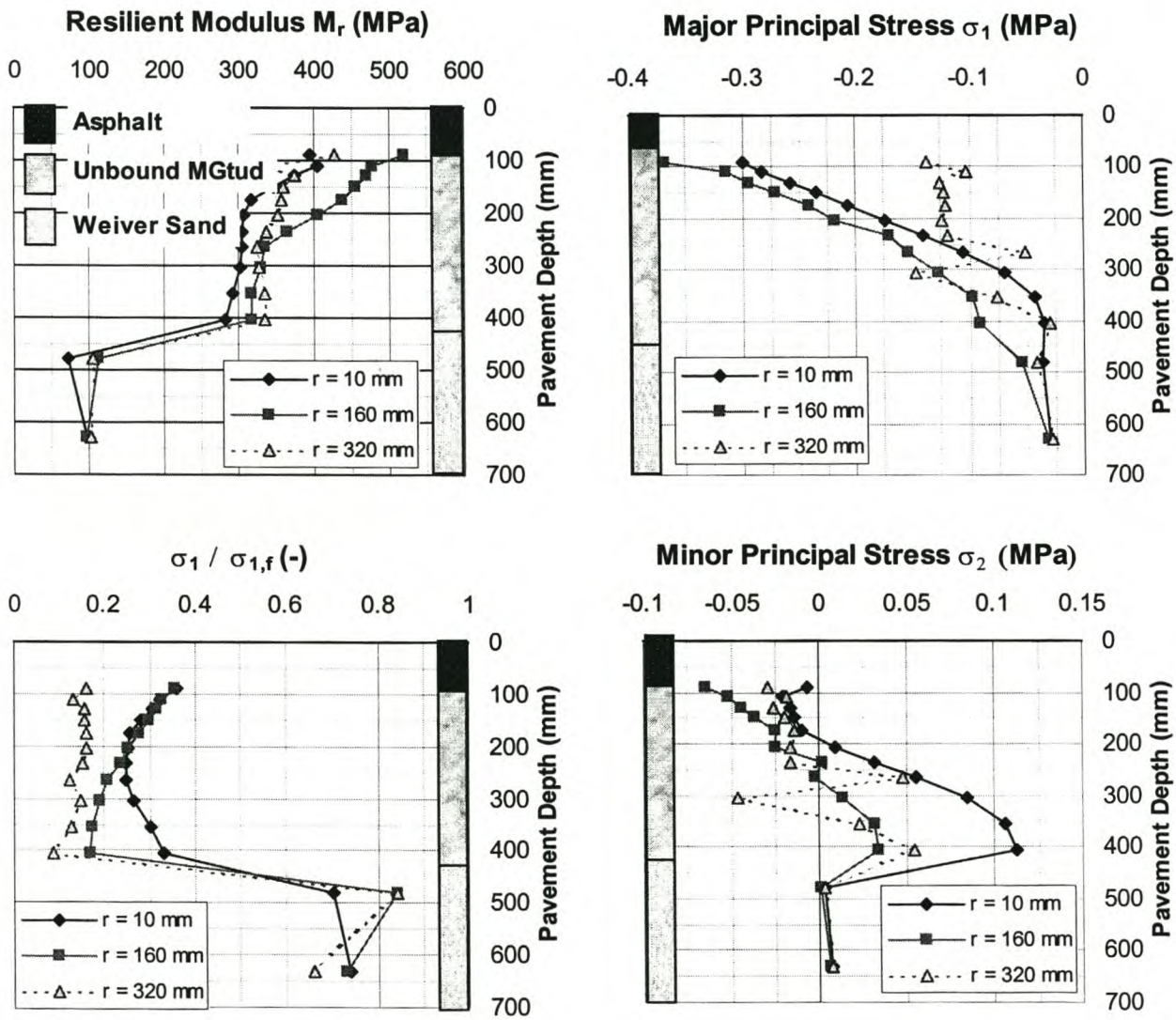

Figure 7 - 39. Finite Element Analysis Results for Pavement with 350mm Unbound MGtud Base and 80mm Asphalt under 65kN Super Single Wheel Load

The capacity for the granular material to develop resilient stiffness under applied stresses, is increased significantly through the inclusion of 2% of foamed bitumen. For the mix granulate material the maximum resilient stiffness generated in the upper base layer is 525MPa, whereas the equivalent foamed mix reaches up to 1000MPa under the wheel load. Differences in the thickness of the asphalt surfacing does contribute to the disparity that is evident between the granular and foamed base M_r values.

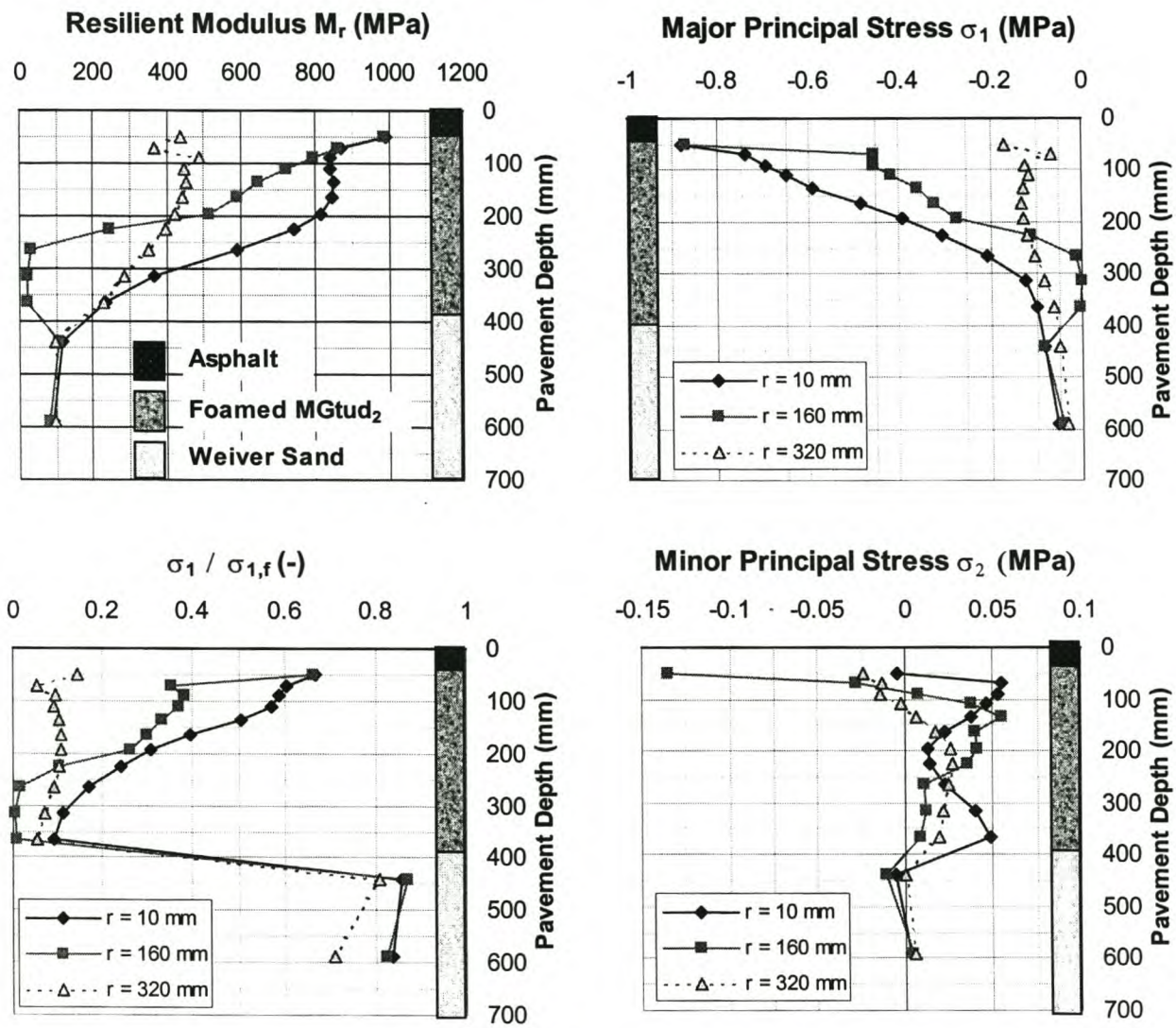

Figure 7 - 40. Finite Element Analysis Results for Pavement with 350mm Foamed $MGtud_2$ Base and 40mm Asphalt under 65kN Super Single Wheel Load

The stress ratios of $\sigma_1/\sigma_{1,f}$ obtained for Weiver Sand sub-base layer, are not increased to detrimental proportions where a foamed base replaces the granular base, and the thickness of the appurtenant layers are reduced. This is a consideration that will determine the contribution of the sand sub-base to the permanent deformation of the entire pavement

structure. The same applies to the change in the stress ratios of $\sigma_1/\sigma_{1,f}$ for the foamed mix base layers after a reduction in thickness. The use of a 300mm foamed mix base layer will not result in substantially higher contribution of this layer to the overall pavement deformation.

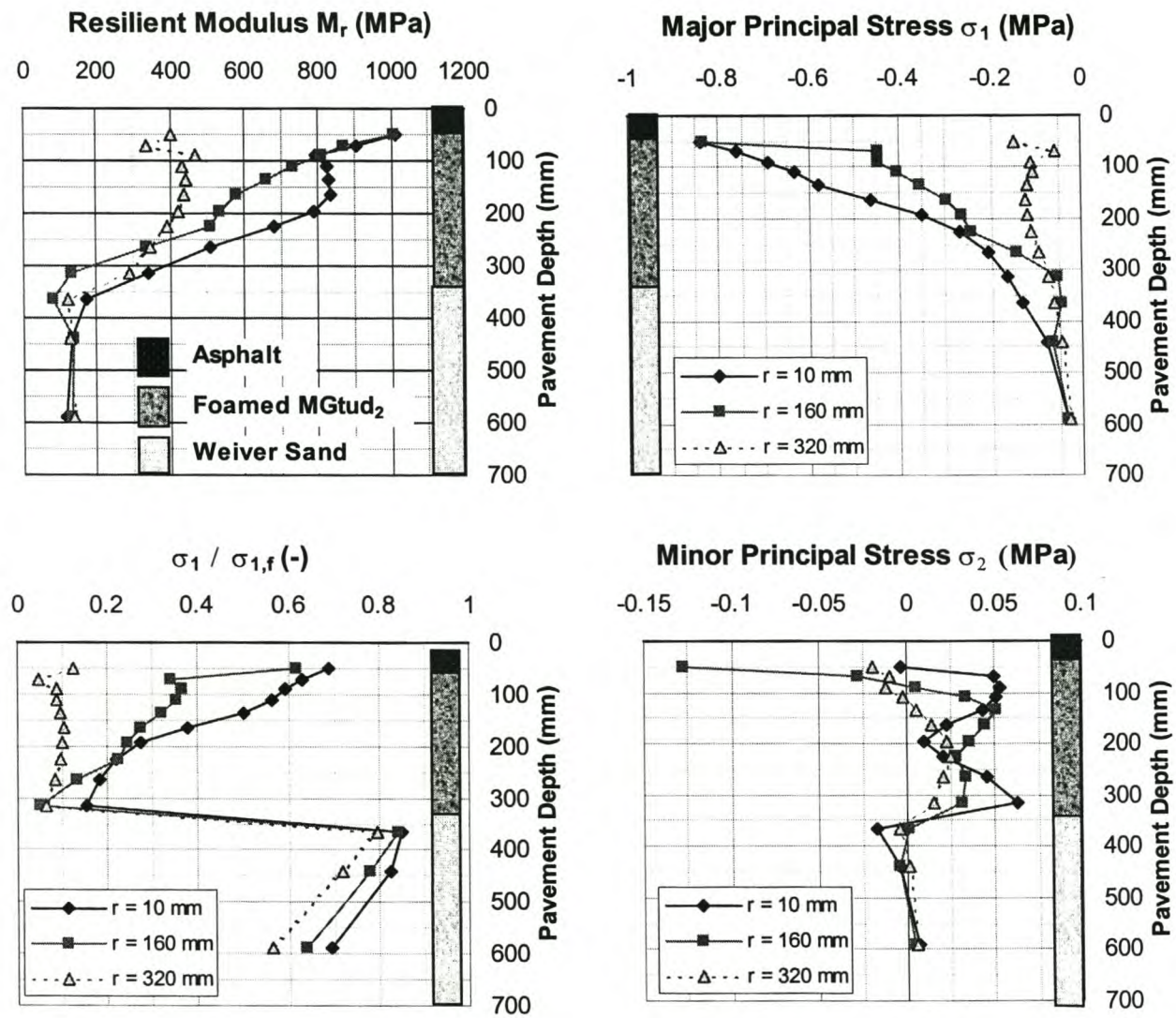

Figure 7 - 41. Finite Element Analysis Results for Pavement with 300mm Foamed MGtud$_2$ Base and 40mm Asphalt under 65kN Super Single Wheel

5.3 Rut depth calculations in Typical Pavements

In order to determine the accumulation of rutting in a pavement during repeated axle loading at the surface, each of the layers requires modelling in terms of permanent deformation. For the purpose of the given analysis, only the stress-dependent layers have

been considered in terms of rut development as the objective is to interpret the behaviour of these layers, thus ignoring permanent deformation in the asphalt layer. The coefficients for the rutting models of the granular base and sand are provided in Table 7 - 18 and Table 7 - 19, whilst those of the foamed mix are provided in Table 7 - 10 and Table 7 - 11.

Table 7 - 18. Permanent Deformation Model Coefficients for $\varepsilon_{p,axial}$ used in NOLIP

Model	Mix	a_1	a_2	b_1	b_2	c_1	c_2	d_1	d_2	R^2
Eqn 7-15 with $\sigma_1/\sigma_{1,f}$	Granular MGtud	-1	1.5	2.82	1.70	1	7	1	5	0.51
	Weiver Sand	-2.72	6.64	0.27	6.05	0	1	0	1	0.99

Table 7 - 19. Permanent Deformation Model Coefficients for $\varepsilon_{p,radial}$ used in NOLIP

Model	Mix	a_1	a_2	b_1	b_2	c_1	c_2	d_1	d_2	R^2
Eqn 7-15 with $\sigma_1/\sigma_{1,f}$	Granular MGtud	6000	11	538	8.15	1	7	1	5	0.64
	Weiver Sand	3.13	9.16	0.32	8.67	0	1	0	1	0.95

Permanent deformation in the subgrade is calculated using the approach of Veverka (1979). Veverka utilises the following equation for soils:

$$\varepsilon_p = \varepsilon_r \times [a + b.\log(N)] \qquad \textbf{Equation 7 - 21}$$

Where,

ε_p, ε_r = permanent strain and resilient strain respectively (-)
a, b = model parameters (-)
N = number of load repetitions (-)

For the purpose of this research a=0 and b=0.7. Parameter "a" could vary from –1.3 to 1.3 depending on this stiffness of the subgrade. However, this parameter does not have a significant influence on the given analysis due to the low subgrade resilient strain values.

The lateral wander of the wheel that is tracking the pavement also requires consideration in the analysis. For this purpose, the findings of Buiter *et al.* (1989) are utilised. Assuming an average lane width of 3.5 metres, a standard deviation of lateral wander of 290mm is utilised. This is considered representative for the type of pavement being analysed and is thus incorporated in the calculation of rut development.

Utilising the distribution of stress ratios with depth in the three different pavement structures, as determined using NOLIP, a rutting profile can be calculated at different offsets from the wheel centre-line with time. The maximum rut development, which occurs under the wheel centre-line, is summarised in Figure 7 - 42. This rutting accounts for all layers except the asphalt surfacing.

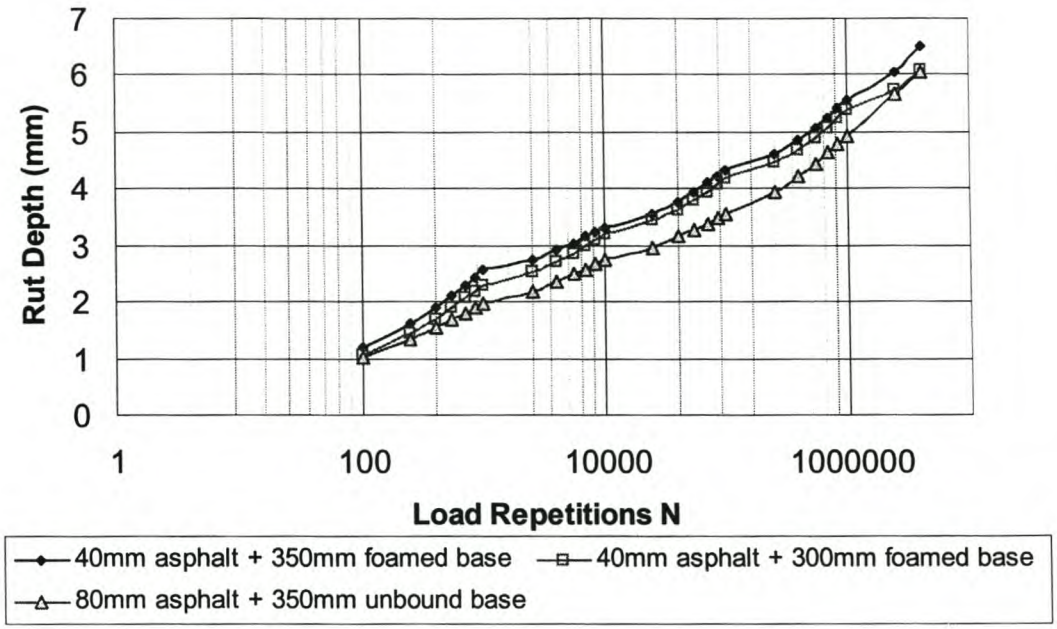

Figure 7 - 42. Permanent Deformation Development under 65kN Super Single Wheel Centreline with Lateral Wander for Three Pavement Structures

The equivalency of such pavement structures in terms of permanent deformation is apparent. The degree of rutting after 2 million axle repetitions is comparable for the three different structures. It should be noted that this analysis utilises models of all of the materials under optimal conditions in the virtual pavement. The effects of moisture ingress during the pavement's life have not been modelled, although this can be adequately performed for given climatic, topographic and other conditions.

6. CONCLUSIONS

Following the testing of granular and cold foamed bitumen mixes with "low" binder contents using the triaxial tests and accelerated pavement tests, insight has been gained into the performance properties of foamed mixes. These foamed mixes, which exhibit "granular type" behaviour, can be analysed by adapting techniques used to model the performance of granular materials. The conclusions of this chapter are provided below.

6.1 Monotonic Failure Shear Behaviour

- Multi-stage testing of cold foamed mixtures is not possible due to disturbance of bonds within the specimen before the maximum applied stress is reached. This is unlike the behaviour of granular materials, which can be loaded to the optimum point and reloaded at a higher confining pressure without damage to the specimen. Use of multi-stage tests with foam can result in a 19° shift in ϕ due to disturbance of the specimen. Instead it is necessary for foamed mixes to be tested using at least three specimens at different confining stresses, to gain an acceptable level of statistical reliability.
- Compared with the equivalent granular material, cold mixing with foamed bitumen results in an increase in cohesion C, to in excess of 100kPa after moderate curing. An

associated moderate reduction in the friction angle ϕ of less than 10° occurs after inclusion of the binder.

- In cases where active filler such as cement is included in the foamed mix, a substantial increase in cohesion occurs, taking C to in excess of 800kPa. The associated friction angle ϕ in such cases approaches 0°.
- The strain at maximum applied axial stress in the monotonic triaxial test, is higher for foamed bitumen mixes than for the equivalent granular material. The strain value increases from 0,6% to 1,3% through the inclusion of foamed bitumen, from the results of test on mix granulate at a displacement rate of 1 mm/sec.

6.2 Resilient Deformation Behaviour

- Conditioning of triaxial specimens before testing for resilient stiffness has a profound effect on the magnitude of M_r and behaviour at different stress levels. Exposure to 10 000 load pulses changes the resilient deformation behaviour from stress-independent to stress-dependent behaviour. Stress history i.e. the use of conditioning pulses, is necessary to simulate field conditions and thus obtain representative results.
- Models used for resilient behaviour of granular materials are applicable to foamed bitumen mixes with less than 4% binder content and no cement. The M_r-θ-$\sigma_d/\sigma_{d,f}$ model and M_r-σ_3-$\sigma_1/\sigma_{1,f}$ models are most applicable. The simple M_r-θ model is inadequate for pavements with high wheel loads imposed at the surface as exclusion of the last term, which provides for the reduction in M_r as σ_d approaches $\sigma_{d,f}$, results in spiralling increase in M_r. Elements exposed to high stresses in finite element modelling with NOLIP develop higher M_r values with the M_r-θ model and in turn attract higher stresses in the following iteration. Although the M_r-θ model mathematically satisfies the data, a softening term is necessary for finite element analysis.
- Foamed materials incorporating cement can be mathematically modelled with the M_r-σ_3-$\sigma_1/\sigma_{1,f}$ equation, but zero or small negative k_6 terms indicate a lack of stress dependency in the material's resilient behaviour. The amount of cement added and degree to which the material becomes linear-elastic will determine whether the triaxial models are applicable to these materials, as determined by separate permanent deformation models.
- Poisson's Ratio, as with Resilient Modulus, requires measurement after conditioning of a foamed mix triaxial specimen. Before conditioning, the measured Poisson's Ratios show independence to stress state, whereas after conditioning granular-type behaviour of the mix is notable. Once again, models developed for granular materials using ν-σ_1/σ_3 are applicable to foamed mixes.

6.3 Permanent Deformation Behaviour

- The permanent deformation behaviour of a range of cold foamed mixes has shown that a critical stress ratio for $\sigma_d/\sigma_{d,f}$ defines the boundary between stable ε_p growth and accelerated ε_p growth under repeated loading up to 10^6 cycles. A differentiation is

necessary between stress dependent behaviour i.e. typical of granular materials, and strongly bound behaviour (including cement) for the foamed mixes.

- Two models have been developed to describe the permanent deformation behaviour of a foamed mix. The first model covers foamed mixes with up to 4% bitumen and no cement. This model has a critical ratio of $\sigma_d/\sigma_{d,f}$ = 55% to define the boundary between rapid and moderate permanent deformation development. The second model covers foamed mixes with up to 1% cement in a medium to long term cured state and a 2% cement in an early cured condition. This model has a critical ratio of $\sigma_d/\sigma_{d,f}$ = 52% to define the boundary. By comparison, an equivalent granular material has been shown to have a critical ratio of $\sigma_d/\sigma_{d,f}$ = 41% above which accelerated deformation takes place. This is the case even though the $\sigma_{d,f}$ for the foamed mix at a confining stress of 12kPa is more than 100% greater than the equivalent value for the unbound material.
- Considering that the $\sigma_d/\sigma_{d,f}$ ratio is dependent on C and ϕ of the material, the effects of moisture on a foamed mix's performance in rutting may be modelled through the measurement of these shear parameters using monotonic failure tests. Such tests can be carried out on the material in the desired state of curing and moisture regime in order to predict the foamed mix's behaviour under repeated loading.
- Applicability of the permanent deformation models has been validated through parallel accelerated pavement testing on site and laboratory investigation for a foamed mix incorporating cement. This modelling also accounts for moisture effects due to slushing.
- Considering that the range of foamed bitumen treated materials that has been investigated is not exhaustive (particularly where cement is included in the mix), application of the models developed for pavement design purposes would be most prudently carried out through the use of the critical stress ratios rather than absolute rut depth calculations.

6.4 General

- This chapter has addressed some of the performance characteristics of foamed bitumen treated materials with relatively low binder contents. These materials exhibit stress dependent behaviour and permanent deformation is one of the predominant modes of failure. Where half-warm foamed mixes or cold foamed mixes with binder contents of 4% and higher are concerned, fatigue behaviour requires consideration

7. REFERENCES

Buiter R., Cortenraad W.M.H., van Eck A.C. and van Rij H., 1989. **Effects of Transversal Distribution of Heavy Vehicles on Thickness Design of Full-Depth Asphalt Pavements.** *Transportation Research Board TRB, Record TRR 1227.* Pp 66-74

Huurman M., 1997. **Permanent Deformation in Concrete Block Pavements**. PhD Dissertation. Delft University of Technology, Netherlands.

Jenkins K.J. and van de Ven M.F.C., 1999. **Investigation of the performance properties of the Vanguard drive road, recycled with foamed bitumen and emulsion respectively and analysed using accelerated pavement testing and triaxial testing,** ITT Report 9-1999 for Stewart Scott Inc., University of Stellenbosch

Maree J.H., 1979. **Die laboratoriumbepaling van die elastiese parameters, die skuifsterkteparameters en die gedrag onder herhaalde belasting van klipslagkroonlaagmateriale: toetsmetodes en apparaatbeskrywing**, Technical Report RP/11/78, NITRR, CSIR.

Maree J.H., 1980. **Die Gedrag en Gebruik van Korrelmateriaalkroonlae in Plaveisels met Dun Bitumineuse Oppervlaklae.** Materials and Design Course, University of Pretoria.

National Institute for Transport and Road Research NITRR, 1986a. **Technical Methods for Highways TMH1**, Pretoria

National Institute for Transport and Road Research NITRR, 1986b. **Guidelines for the Use of Road Building Materials TRH14**, Pretoria

Saleh, A.H., 2000. **The Use of Mix Granulates Stabilized with Foamed Bitumen as Road Building Materials**. Master of Science in Engineering Thesis. IHE University, Delft, Netherands

Theyse H.L., de Beer M. and Rust F.C., 1996. **Overview of the South African Mechanistic Pavement Design Analysis Method**. Paper 961294. Transportation Research Board, Washington

van de Ven M.F.C., Jenkins K.J. and de Fortier Smit A., 1997. **Investigation into the Feasibility of Scaling Granular Materials for Use with the MMLS Trial Tests on G1, Waterbound and ETB.** ITT REPORT 18.1-1997 for Gautrans, University of Stellenbosch.

van de Ven M.F.C., and de Fortier Smit A., 2000. **The Role of the MMLS Devices in APT.** South African Transportation Conference, SATC. CSIR Pretoria.

van Niekerk, A.A. and Huurman, M., 1995. **Establishing Complex Behaviour of Unbound Road Building Materials from Simple Material Testing,** Delft University of Technology, Netherlands.

van Niekerk, A.A. van Scheers J. and Galjaard P.J., 2000a. **Resilient Deformation Behaviour of Coarse Grained Mix Granulate Base Course Materials from Testing Scaled Gradings at Smaller Specimen Sizes**. UNBAR 5 Conference, University of Nottingham.

van Niekerk, A.A. van Scheers J., Muraya P. and Kisimbi A., 2000b. **The Effect of Compaction on the Mechanical Behaviour of Mix Granulate Base Course Materials and on Pavement Performance**. UNBAR 5 Conference, University of Nottingham.

Veverka V., 1979. **Estimation of the Rut Depth for Asphaltic Roads**. (in Dutch and French). *De Wegentechniek / La Technique Routiere, No. 3.* Pp 25-44.

Wolff, H., 1992. **The Elasto-Plastic Behaviour of Granular Pavement Layers in South Africa.** PhD Dissertation. University of Pretoria.

CHAPTER 8

CONCLUSIONS AND RECOMMENDATIONS

1. INTRODUCTION

In this, the final chapter, the salient conclusions of this thesis are summarised. These conclusions are divided into findings with relevance to theoretical, design and practical or construction aspects of the work and implications. In addition, where applicable, recommendations are provided for additional research that is deemed necessary in the light of the findings of this thesis.

The conclusions are summarised with the original primary objective of the study in focus viz. to address the need for a fundamental understanding of foamed bitumen and foamed bitumen mixes as pavement engineering materials. This objective was to be achieved through the development of techniques for adjudicating mixes, optimisation of their composition and rationalisation of their design both as mixes and as layers in road pavements. At the same time the exploration of new applications for foamed bitumen and the possibilities for progressive related technology, was a priority

2. THEORETICAL DEVELOPMENTS AND VALIDATION

In the investigation of mix design considerations for foamed bitumen, not only trends are researched but rather fundamental theory behind the trends. The salient features of these theoretical findings are outlined here:

- The behaviour of foamed bitumen that has been produced in a laboratory may be characterised through analysis of its expansion with time. In such an analysis, cognisance must be given to the measurement procedures and in particular the temperature and duration of foam production, the form of the decay curve with time and the intended application of the foam. A new function called the Foam Index, has been developed to characterise the foam. Where asymptotic decay of foamed bitumen is measured, a mathematical model for the calculation of the Foam Index may be utilised. The Foam Index can also be used to optimise the application of foamant water and foaming agent, whichever is used in the production process. In cases where the foam decay is not asymptotic, other mathematical procedures may be used to optimise the foam's characteristics using the Foam Index.
- The "Percent Bulk Volume" of the filler occupied by bitumen in a particular foamed mix mastic that is in optimal moisture conditions, can be used to model the change in the Softening Point Temperature using the Ring and Ball Test on the mastic. This method, which is a revision of a procedure that has been used to model the behaviour of hot mix mastic using different types of filler, provides a substantially different relationship.

Foamed bitumen mastic stiffens dramatically at a significantly lower percent bulk volume than the equivalent hot mix mastic.

- The theory of physics that is considered applicable to the mixing of foamed bitumen with aggregate of different temperatures, predicts improvement in dispersion of the bitumen binder with increasing aggregate temperature. These predictions have been verified through physical mix production with aggregate temperature as a variable. The maximum particle size that is completely coated by foamed bitumen can be increased from in the order of 1mm to in excess of 10mm through an increase in aggregate temperature from 35°C to 85°C before mixing. This process, developed as part of this research project, is termed "Half-warm foamed mix production".
- A three point beam test apparatus facilitates the measurement of important material properties of blocks manufactured using cold bituminous mix i.e. foamed bitumen and emulsion stabilised aggregate. The properties that may be analysed include tensile strength and stiffness. Measurement of tensile strength with this apparatus provides substantially greater repeatability than tests carried out in the indirect tensile mode, primarily due to the preferable stress-state in the specimen during failure in tension. Resilient stiffness measurements using the three-point beam test require special attention to achieve adequate load levels that induce deflections providing sufficient accuracy for the modulus calculations. Finite element analysis of the test set-up has provided the necessary minimum cyclic load limits for resilient stiffness tests in the three point beam apparatus.
- Theoretical models developed for the analysis and performance prediction of granular materials, including sands, gravel and crushed aggregates, in terms of permanent deformation, have been proven to be generally applicable to cold foamed bitumen mixes. The rutting model for foamed mixes uses a classification of the mixtures by binder content and active filler content. The input parameters for the theoretical models can be obtained from triaxial tests. *Monotonic failure tests* using a triaxial apparatus are required to be carried out on the foamed mixes, as single-stage tests and, unlike granular materials, cannot be performed using multi-stage procedures. *Resilient stiffness tests* performed in different states of stress also provide the relevant input coefficients for stiffness relationships applicable to foamed mix. The M_r-θ-$\sigma_d/\sigma_{d,f}$ model and M_r-σ_3-$\sigma_1/\sigma_{1,f}$ models are most applicable. The simple M_r-θ model is inadequate for pavements with high wheel loads imposed at the surface as, exclusion of the last term, which provides for the reduction in M_r as σ_d approaches $\sigma_{d,f}$, results in spiralling increase in M_r. Elements exposed to high stresses in finite element modelling with NOLIP develop higher M_r values with the M_r-θ model and in turn attract higher stresses in the following iteration. Although the M_r-θ model mathematically satisfies the data, a softening term is necessary for finite element analysis.
- The rutting behaviour of foamed mix has been determined through *Repeated load permanent deformation tests* on various mix compositions. The models utilised for granular materials have been successfully adapted for application to specific foamed mixes that exhibit granular-type behaviour. The investigation of permanent deformation behaviour of foamed mixes in triaxial test set-ups used at least four specimens that were analysed at different $\sigma_d/\sigma_{d,f}$ ratios for a model of suitable reliability to be established.

- The resilient stiffness and permanent deformation models require application using relevant procedures for modelling of foamed mix in pavement structures, to ensure that meaningful output is obtained. The NOLIP finite element analysis programme provides an eminently suited method of application of these models, where a suitably fine mesh of elements can be established and sufficient number of iterations will provide output of acceptable reliability. The output is sensitive to selection of a suitable mesh and relevant type of material behaviour models.

3. DESIGN CONSIDERATIONS

- The relationship of percent bulk volume and softening point of mastic has been utilised for hot mix asphalt mix design, with limits of percent bulk volume being established at between 60% and 55%. These limits are not applicable to foamed mixes, where the percent bulk volume should be restricted to 45% for equivalent behaviour in terms of mastic stiffness. In the cases where the mineral aggregate composition of a foamed mix cannot be altered due to construction constraints, the new model that has been developed, may be used to establish the predicted mix characteristics.
- Design of the mineral skeleton for a cold foamed bitumen mixture requires consideration of the "Voids in Mineral Aggregate" or VMA in the sand fraction as well as the spatial composition of the entire stone, sand and filler components. Minimisation of the VMA in the sand fraction can be effectively carried out using the Engelsmann apparatus, following procedures developed in the research. The suitability of the overall composition of the cold foamed mix may be established through analysis of the ratio of the components of stone, sand and filler in the mix. Division of combinations of these ratios into zones of varying suitability assists in selection of desired gradation of mineral aggregate.
- A procedure for the curing of foamed bitumen specimens for testing in the mix design procedures has been successfully established. This procedure, which takes cognisance of the climatic effects of the region for which the mix is being designed, has been verified for South African conditions. The method utilises an equilibrium moisture content of the foamed mix based on the binder content, material optimum moisture content and climatic region.
- Due to the dispersed nature of the binder in a foamed mix i.e. the bitumen is in a non-continuous state with partial coating of aggregate, compacted mixes can be prone to early distress due to moisture damage. The procedure of conditioning specimens for moisture susceptibility using vacuum saturation (found in literature) is an effective method of simulating moisture damage. For a particular cold foamed mix, the effect of moisture ingress and loss of binder cohesion to the aggregate should be analysed through the shift of the Mohr failure envelope before and after moisture exposure. In the absence of triaxial testing facilities, Semi-circular Bending Tests (SCB) provide a suitable procedure for analysing moisture susceptibility of a foamed mix.
- Substantial increase in the compressive and shear strength results from production of foamed mix at half-warm (HW) temperatures, compared with production at ambient temperature. Although the HW foamed mix does not provide the same compressive strength as the equivalent HMA at temperatures lower than 25°C, the HW mix has comparable compressive and shear strength at higher test temperatures.

- Master curve determination of half-warm foamed mix and hot-mix using continuously graded aggregate, yields a significant shift in flexural stiffness at lower frequencies of loading. This concurs with research into the master curves of cold foamed mix compared with the equivalent hot mix. However, the shift occurs to a lesser degree with half-warm mix than with cold mix. The higher flexural stiffness of the half-warm mix at extended loading times will assist in the resistance of permanent deformation under applicable loading conditions.
- The fatigue relations of half-warm foamed mix as developed from beam fatigue tests, are comparable with those of the equivalent hot mix, provided that the production of the HW foamed mix follows pertinent procedures. The HW mix's fatigue relationship is moderately less sensitive to higher levels of tensile strain than the HMA. In addition, the phase angle of the half-warm mix is several degrees lower than that of the equivalent HMA when tested under repeated loading at a frequency of 10Hz and temperature of 20°C.
- Two separate models have been developed to describe the permanent deformation behaviour of a foamed mix. The first model covers foamed mixes with up to 4% bitumen and no cement. This model has a critical ratio of $\sigma_d/\sigma_{d,f}$ = 55% to define the boundary between rapid and moderate permanent deformation development. The second model covers foamed mixes with up to 1% cement in a medium to long term cured state and a 2% cement in an early cured condition. This model has a critical ratio of $\sigma_d/\sigma_{d,f}$ = 52% to define the boundary. Pavements incorporating foamed mix layers can be designed using the relevant model once the stress and modulus distribution within the pavement structure has been established using finite element analysis and relevant material behaviour models, for example with NOLIP. Such analyses utilise an appropriate design wheel load, pavement structure, layer thicknesses and material properties. Iteration is required to obtain convergence of the stress-dependent materials according to their applicable models. Although both the $\sigma_d/\sigma_{d,f}$ or $\sigma_1/\sigma_{1,f}$ ratios obtained from such analyses in determination of the permanent deformation in foamed mixes under repeated load applications, it is imperative that the former is used where materials have high cohesion, low angle of internal friction or negative minor principal stresses (σ_2 or σ_3). In addition, the use of a critical stress ratio in pavement design with foamed mixes is preferred to calculation of predicted rut depth, considering the variability prevalent in permanent deformation results.

4. CONSTRUCTION CONSIDERATIONS

- Although the models developed for the Foamed Index as a parameter for the characterisation and optimisation of foamed bitumen has not been tested for production of the foam under site conditions, the laboratory model should remain applicable. Foamed bitumen can be discharged into a vessel at the plant and analysed for expansion characteristics according to newly established procedures. From the results of a sensitivity analysis, application rates of foamant water and any foaming additives may be optimised and verified in relation to the laboratory mix design.

- Half-warm foamed bitumen mixes can accommodate high percentages of reclaimed asphalt pavement or RAP. The inclusion of RAP in the HW mix is not necessarily detrimental to the mix properties, and can in fact improve the shear strength parameters compared with HW mix using virgin aggregate. However, a minimum threshold exists for the percentage of foamed bitumen that is added. Below this threshold, which is 2,4% foamed bitumen for mixing in a laboratory pugmill, a poorer quality mix results. The feasibility of recycling RAP using the half-warm foamed bitumen process and the permissible proportions thereof, depends largely, therefore, on the gradation and existing binder content and condition of the RAP.
- The production of suitable quality half-warm foamed mixes is reliant on relevant procedures being followed. The most important procedures for laboratory manufacture of these mixes include fractionation of the mineral aggregate before mixing, application of excess moisture and compaction at the highest residual temperatures. An absolute minimum compaction temperature of 65°C is applicable to HW foamed mix in general; but even this temperature results in a loss of compressive and shear strength of the mix and a recommended minimum of 85°C has been established.
- The use of mineral aggregates of marginal quality i.e. lower than the relevant conventional specified standards for base and surfacing layers, can result in a relatively low resilient stiffness of the cold-mix. Such upgraded marginal materials can be utilised for the manufacture of blocks for road construction. In such cases, sufficient curing of the blocks is necessary before handling and laying can commence. Using tensile strength criteria, a minimum period of 14 days is deemed adequate for blocks exposed to a warm climate. This period requires verification for each specific application of materials and site conditions. Tensile strength testing, using a three point loading apparatus, is suitable for the analysis of this property.
- Production of cold mix blocks can be cost-effectively undertaken at various entry levels. Small emerging contractors can produce more than 60 blocks per hour with three labourers, one Kango hammer and three sets of moulds, at a competitive rate in comparison with alternative block making procedures. This operation can be gradually scaled up to achieve the requisite level of productivity to suit the particular demands, without exorbitant capital outlay, making the process eminently suited to developing countries intent on creating employment opportunities.

5. RECOMMENDATIONS FOR ADDITIONAL RESEARCH

- Moisture susceptibility of foamed bitumen stabilized mixes has been effectively analysed using a vacuum saturation technique and determination of the change in shear properties of the mix before and after saturation. The saturation technique has, as yet, not been related to field conditions. Additional analysis is required to correlate the severity of the specimen conditioning with moisture changes in the road pavement due to adverse weather and climatic influences and its implications on field performance of the material. Accelerated pavement testing could be used as an effective tool in such an investigation.
- This dissertation has shown that the manner in which the bitumen is dispersed in foamed mixes exposes a far higher surface area of the binder to the elements than for HMA's binder. This fact, in conjunction with higher void contents in foamed mixes, makes ageing an important consideration in cases where these materials are utilised high in a pavement structure. Further research into ageing of foamed mixes is therefore recommended.
- In conjunction with further investigation into moisture influences, more extensive research into the performance of foamed mixes under different moisture conditions is recommended using the triaxial laboratory testing technique. Up to this point, the investigation of foam treated materials has been restricted to mixes produced under optimal conditions. Further research, using triaxial testing, into various foamed mixes at different states of curing and moisture exposure, is recommended for this purpose.
- Further Three Dimensional Finite Element Analysis of the Leutner Shear Test is required. Current analysis procedures of this test have been limited to Two-dimensional analysis of specimens with an in-built shear plane. A 3-D finite element analysis of homogeneous specimens in the Leutner Test set-up with and without debonding of end plates (applying normal loads) and plates applying the shear load are recommended. The debonding is achieved using glycerine soap and foil in practise.
- When the half-warm foamed mix process is used for treatment of reclaimed asphalt pavement (RAP) material, relatively low percentages of high penetration bitumen are added to mix. The extent of the blending of the soft, new bitumen to the relatively hard existing bitumen is unknown. The degree of blending of two grades of bitumen will have a significant influence on the behaviour of the mix and is therefore an important phenomenon, which requires more attention. Additional research in this field is recommended.

APPENDIX A

FOAMED BITUMEN CHARACTERISTICS

1. PROCEDURE FOR MEASURING FOAM BITUMEN CHARACTERISTICS IN A LABORATORY

Testing Procedure for the measuring foamed bitumen characteristics.

1. Heat the selected bitumen in an oven to 150°C in a draft oven for four hours before testing.
2. Preheat the laboratory foaming plant e.g. Wirtgen WLB10®, to 150°C before application of the bitumen.
3. Apply bitumen to the kettle of the apparatus and circulate until the required temperature is achieved, usually 160°C to 180°C. Monitor with temperature gauge and infra-red gauge, if available.
4. Measure the discharge rate of the bitumen from the nozzle, for the given pump settings of the apparatus e.g. 100 grams/second. This is carried out by dicharging bitumen into a tared vessel for 2 seconds. Weighing is carried out on a scale with an accuracy of 0,5 grams. This procedure is repeated at least twice *without any foamant water or air being added during discharge.*
5. Calculate the amount of bitumen required for the given measurement vessel in the laboratory. An amount of 500 grams of foamed bitumen is generally required for sufficient foam to allow suitable accuracy of measurement.
6. Calibrate a measurement gauge for the given vessel and amount of bitumen i.e. 500 grams. Such a gauge should preferably have graduations of less than 5 for expansion ratio measurement. Steps of 6 are considered maximum for sufficient accuracy.
7. Calibrate the foamant water flow to achieve the desired application rate e.g. 2% by mass of bitumen. The bitumen flow rate measured in Step 4 is required for the calculation of water flow rate. A conversion of units from litres/hour to grams/second is sometimes required. When the water is discharged from the spray nozzle and the flow rate is adjusted to achieve the desired value, no bitumen is sprayed BUT air pressure should be applied as this can affect the flow rate (and ultimately forms part of the foamed bitumen production process).
8. The bitumen discharge time or *spray time* should then be set on the apparatus to yield 500 grams of bitumen (in the form of foam), following the findings of Step 4. This setting must be made to an accuracy of 0,01 seconds.
9. The vessel in which the foam is to be measured must be heated to 75°C for at least 30 minutes before measurement.
10. Foamed bitumen is discharged into the vessel for the calculated *spray time.* Immediately after spraying of the foam stops, a stopwatch is started.
11. Measurement of the maximum expansion ratio ER_m is the first measurement (made immediately). Thereafter the decaying expansion ratio ER(t) of the given bitumen with time is carried out. This is done in steps which are the lesser of :

- graduations of less than 3 for expansion ratio, and
- time intervals of less than 10 seconds.

12. Discharge and measurement of the foam repeated three times for a given set of conditions.

Note

The spray time is an important consideration in the manufacture of foam as, although an average value of 5 seconds is commonly applicable, in industry a range of values of 1 second to 25 seconds has been noted.

2. TYPICAL EXAMPLES OF DECAY CURVES

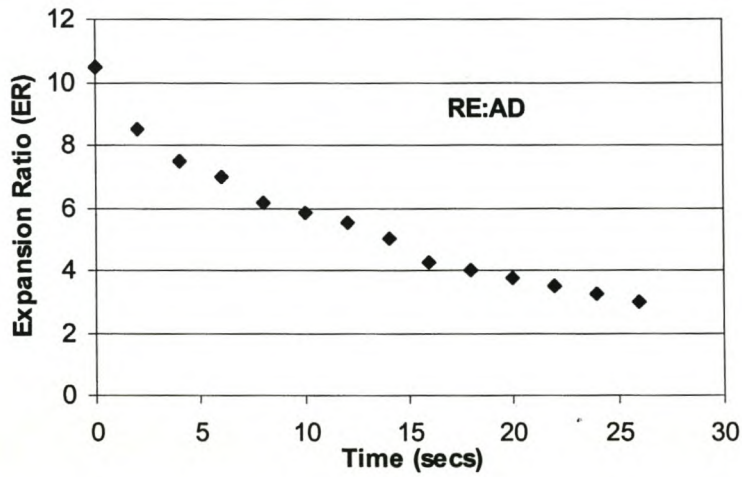

Figure A - 1. Foam Decay Curve for 150/200 Bitumen at 180°C with 2,4% Foamant Water and No Additive (Average of 3 Tests)

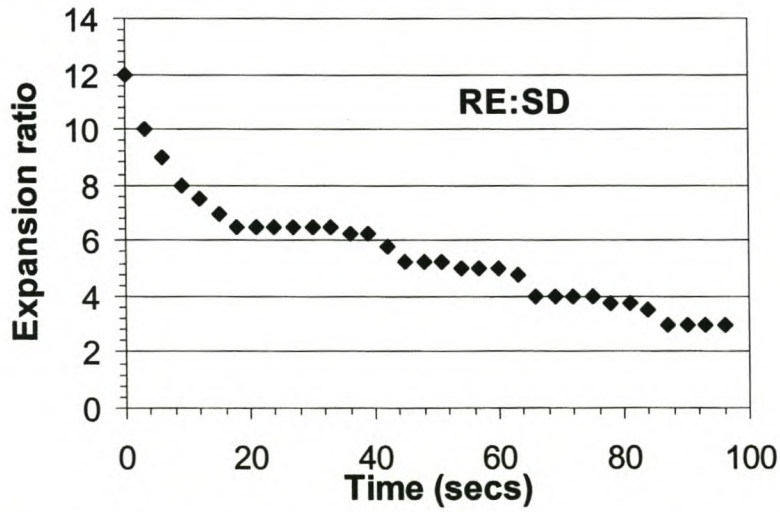

Figure A - 2. Foam Decay Curve for 150/200 Bitumen at 180°C with 2,4% Foamant Water and 0,07% Foamant (Average of 3 tests)

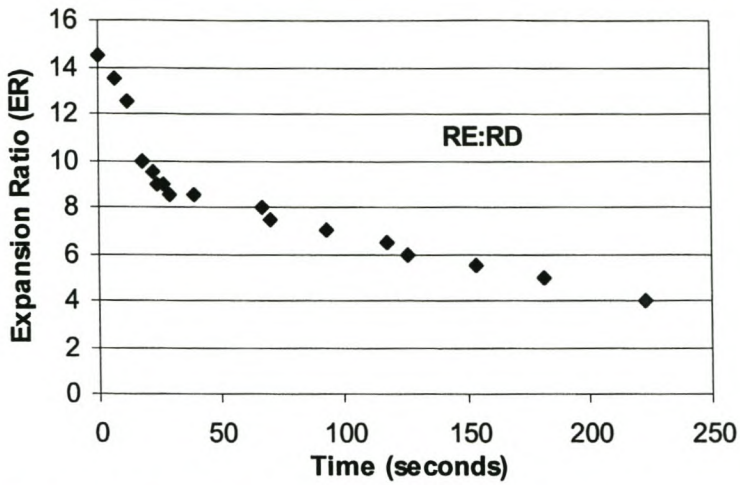

Figure A - 3. Foam Decay Curve for 150/200 Bitumen at 170°C with 2,2% Foamant Water and 0,2% Foamant (Average of 3 tests)

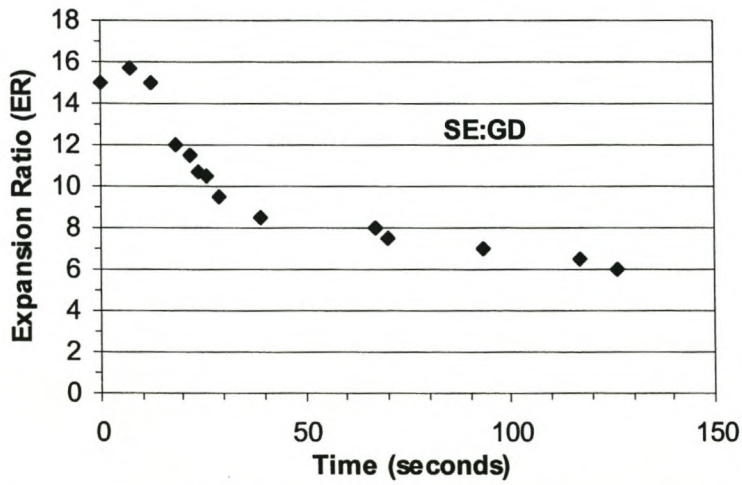

Figure A - 4. Foam Decay Curve for 150 Bitumen at 175°C with 2,2% Foamant Water and 0,2% Foamant (Average of 2 tests)

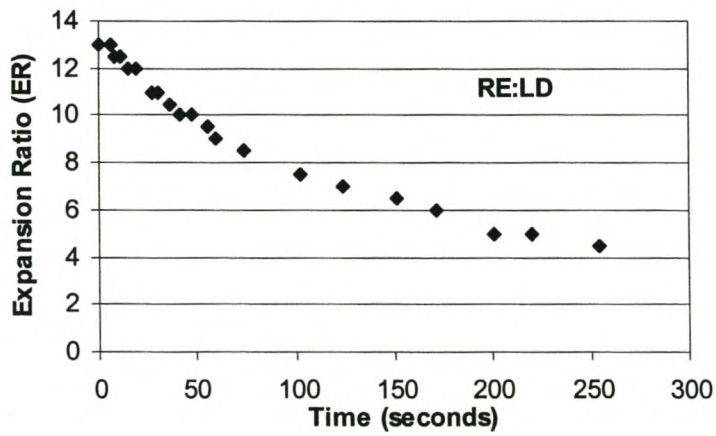

Figure A - 5. Foam Decay Curve for 150/200 Bitumen at 180°C with 2,2% Foamant Water and 0,1% Foamant (with Amine)

APPENDIX B

FILLER AND FOAMED BITUMEN MASTIC

1. PROCEDURE FOR FILLER PLUS FOAMED BITUMEN MASTIC MANUFACTURE

Testing Procedure for the manufacture of filler/foamed bitumen mastic for testing.

1. Sieve out the filler (material passing the 0.075mm sieve) and oven-dry.
2. Select a representative 50g sample of filler and add water equivalent to the "Bitumengetal" and seal to prevent loss of moisture.
3. Calculate the mass of foamed bitumen needed to give the K = f/b ratios selected (generally values of K = 0.7; 0.9; 1.1; 1.3 and 1.5 cover the stiffness range).
4. Prepare a sample of pure foamed bitumen by foaming into a container at optimum expansion ratio and half-life moisture content. Within 20 seconds of foaming, extract sufficient bitumen to mix with the filler (taking account of the water in the bitumen) to attain the desired K value.
5. Add foaming bitumen to the filler on a balance with 2 kg capacity, sensitive to 0,1g until the desired K value is achieved and mix vigorously for 60 seconds with a spatula.
6. Whilst the mastic has a sufficiently low viscosity i.e. directly after mixing, transfer the mastic mix to rings of the Ring and Ball Test apparatus ASTM D36 –76 (ASTM, 1979). Allow for the mastic to extend at least 2 mm above the ring.
7. Carry out curing in the rings at 40°C in a draft oven for 24 hours. This will achieve constant mass of the sample.
8. Remove the sample from the oven and trim the surface of the mastic to be flush with the ring.
9. Allow the sample to cool to ambient temperature and test for Ring and Ball softening point temperature (ASTM D 36 -76). Use glycerin for temperatures in excess of 80°C. At least two replicates should be carried out for each test. If the replicates are not in agreement of 1°C for softening points below 60°C and 2°C for softening points above 60°C. This is a deviation from the standard test to make allowance for the variability introduced by the filler.

2. BACKGROUND TO ENGELSMANN APPARATUS

Although detailed procedures are provided by Goos *at al.* (1996), a brief outline to the Engelsmann apparatus is provided here for the uninformed reader.

- A selected sand fraction (generally up to 4,75mm although any smaller fractions may be tested) is oven dried and a 200 gram sample weighed out.
- This sample of the sand fraction is loosely placed in a calibrated glass pycnometer and a volumetric reading is taken.
- Vibratory compacting is carried out using a cylindrical weight (stamp) placed on top of the sand and a cam-wheel that lifts and drops the calibrated glass pycnometer.
- Periodic readings of the volume of the sand are made after a selected number of cycles.
- A specific gravity determination of a separate sand sample provides the necessary data to calculate the air voids in the sand during compaction.

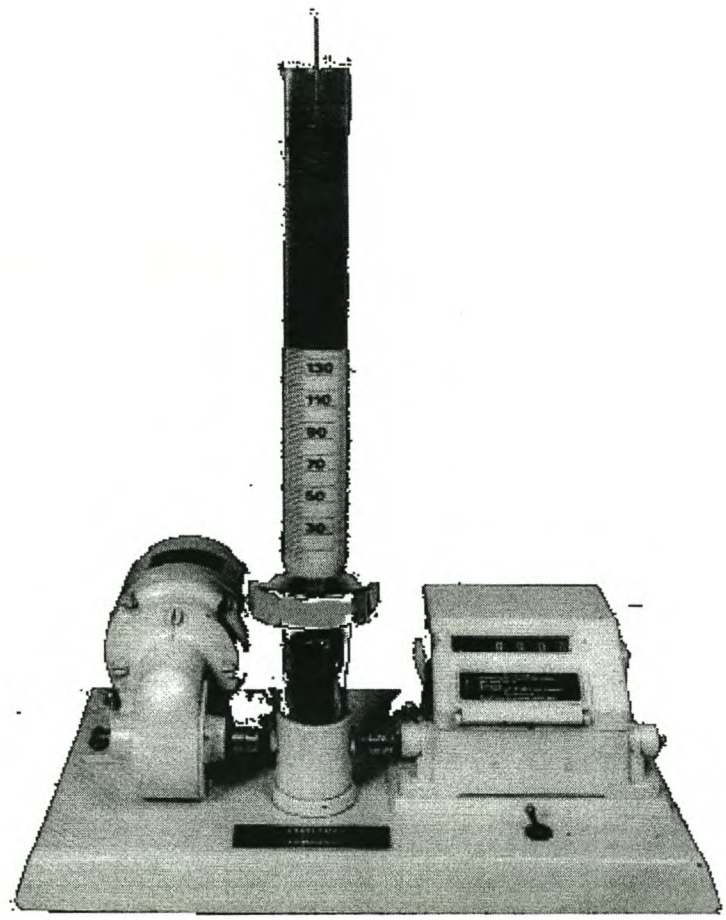

Figure B - 1. Engelsmann Apparatus

APPENDIX C

DETAILS OF HALF-WARM FOAMED BITUMEN MIXES USED IN FEASIBILITY STUDY

1. GRADATIONS, MATERIALS TYPES AND PROPERTIES

Table C - 1. Gradation and Material Type

Material Type	Crushed Hornfels	Crushed Hornfels	Crushed Hornfels	Crushed Hornfels	Crushed Hornfels	Granite Gravel	Quartzitic Gr. Sand
Gradation Type	Contin.	Semi-Gap	SMA	ZOAB	RAP	Contin.	Contin.
Sieve Size (mm)	Percentage Passing (%)						
26.5	100	100	100	100	100	100	100
19.0	90	96	100	100	94.2	100	100
13.2	78	88	100	92	87.7	100	100
9.5	70	80	91.7	60	72.1	100	99
6.7		68	49.7	15			
4.75	51	57	40.7	13	47.5	94	97.2
2.36	39	46	29	11	29.8	75	83
1.18	30	42	22.1	9	17.7	51	61
0.6	22	37	17.5	7	9.8	32	42
0.3	18	29	13.9	5	4.2	19	26
0.15	11	15	10.8	5	1.1	9	10.1
0.075	8	7	8.1	4	0.2	3	5.5

Table C - 2. Targeted Mix Parameters for Half-warm mixes

Gradation	Contin-uous	Semi-Gap	SMA	ZOAB	RAP	Granite Gravel	Gravelly Sand
	Properties for Half-warm mixes						
Mixing Moisture (% m/m)	5	5	6	4	3 (with filler) 0 (without)	6	5.9 to 7.4
Binder Content (% m/m)	4	4.5	6	5.5	2	4	3.6
Compact. Moisture (% m/m)	2	2	2.7	2	2 (with filler) 0 (without)	2.7	4

2. LABORATORY MIXING PROCEDURES FOR HALF-WARM MIXES USING A HOBART ® MIXER

The following is an outline of the laboratory procedures adopted for the manufacture of half-warm foamed mixes using a Hobart ® mixer:

1. Prepare oven dry fractions of 10 kg's of the selected rock-type and grading.
2. Determine the optimum moisture content of the natural material using the Modified AASHTO compaction technique.
3. Divide the mix into two fractions using the Xmm sieve.
4. Heat up the two mix fractions to the required "half-warm" temperature for at least two hours. Measure the aggregate temperature immediately prior to mixing.
5. Mix Fraction A with 30% of the optimum moisture content for the entire mix, and mix for 15 seconds in the Hobart® with mixing bowl preheated to 70°C prior to the addition of 50% of the total mass of foamed bitumen. (Mixing moisture added at ambient temperature is acceptable, but heated water of approximately 90°C is preferred, as it is beneficial to the mix).
6. Mix Fraction B with 70% of the optimum moisture content of hot water, by hand, to obtain an even distribution of moisture.
7. Add the fine slurry to the coarse aggregate and mix for 10 seconds prior to the addition of the foamed bitumen i.e. the remaining 50% of binder.
8. Mix in Hobart for an additional 30 seconds.
9. Remove mix from the mixing bowl and extract a sample for moisture content determination.
10. Carry out an initial drying out routine in order to achieve the desired moisture content for compaction i.e. optimum moisture content. This entails either exposing the mix to the atmosphere or placing the mix in an oven at 50°C for a period of time established from experimentation, until the mix is at the required moisture content (which is checked through sampling and oven drying).
11. Seal the sample and allow cooling to ambient temperature.
12. Extract another moisture sample prior to compaction in the Superpave Gyratory Compactor. The level of compaction should be commensurate with the level of traffic such a mix could be expected to withstand.

3. MOISTURE AND TEMPERATURE RECORDS FOR HALF-WARM MIXES

Table C - 3. Moisture & Temperature Records for Half-warm Continuous and Semi-gap Mixes

Mix Type	Continuous Grade										Semi-gap Grade			
Agg. Temp (°C)	45	67	86	90	97	92	91	89	97	91	45	55	70	85
MC (%)	5	5	5	5	5	5	5	5	5	5	5	5	5	5
Added Moist. Temp	Ambient										Hot			
Mix Temp (°C)	41	55	64	68	-	-	-	-	-	-	41	48	55	60
MC after mix (%)	4.6	3.9	3.8	-	-	-	-	-	-	-	4.4	3.7	2.9	3.2
Comp. Temp (°C)	50	50	44	45	34	39	50	52	68	76	Ambient (23-25°C)			
MC at Comp. (%)	3.2	3.1	3.6	-	0.9	2.1	2.0	1.2	1.4	1.8	2.9	2.9	2.7	2.7

Table C - 4. Moisture and Temperature Records for SMA, ZOAB and RAP Mixes

Mix Type	SMA				ZOAB		RAP				
	As per grading				As per grading		3% Filler			No Filler	
Agg. Temp (°C)	50	68	86	98	68	90	45	60	84	58	87
MC (%)	6	6	6	6	5	5	3	3	3	0	0
Added Moist. Temp	Hot				Hot		Hot			-	
Mix Temp (°C)	48	58	59	44*	60	66	42	54	64	50	82
MC after mix (%)	5.3	4.5	3.9	3.9	4.3	3.4	2.9	2.8	2.8	0.1	0.1
Comp. Temp (°C)	Ambient, 23°C to 25°C				Ambient		Ambient (23°C to 25°C)				
MC at Comp. (%)	2.9	2.8	2.5	2.9	2.8	2.0	2.9	2.8	2.7	0.1	0.1

* Large aggregate allowed to cool to ambient temperature after mixing, then blended with heated fines in slurry form

Table C - 5. Moisture and Temperature Records for Gravel and Gravelly Sand Mixes

Mix Type	Granite Gravel				Gravelly Sand			
Agg. Temp (°C)	45	58	74	88	39	45	74.5	89
MC (%)	4.2	4.2	4.2	4.2	5.9	5.9	7.4	7.4
Added Moist. Temp	Hot				Ambient		Hot	
Mix Temp (°C)	50	53	60	67	52	51	62	60
MC after mix (%)	6.1	4.8	5.0	3.7	5.3	5.4	5.8	5.9
Comp. Temp (°C)	Ambient (23°C to 25°C)				44 38	48 44	56 50	51 46
MC at Comp. (%)	3.1	2.9	3.3	2.7	5.1	5.1	5.1	4.3

4. GYRATORY COMPACTION RECORDS FOR HALF-WARM MIXES

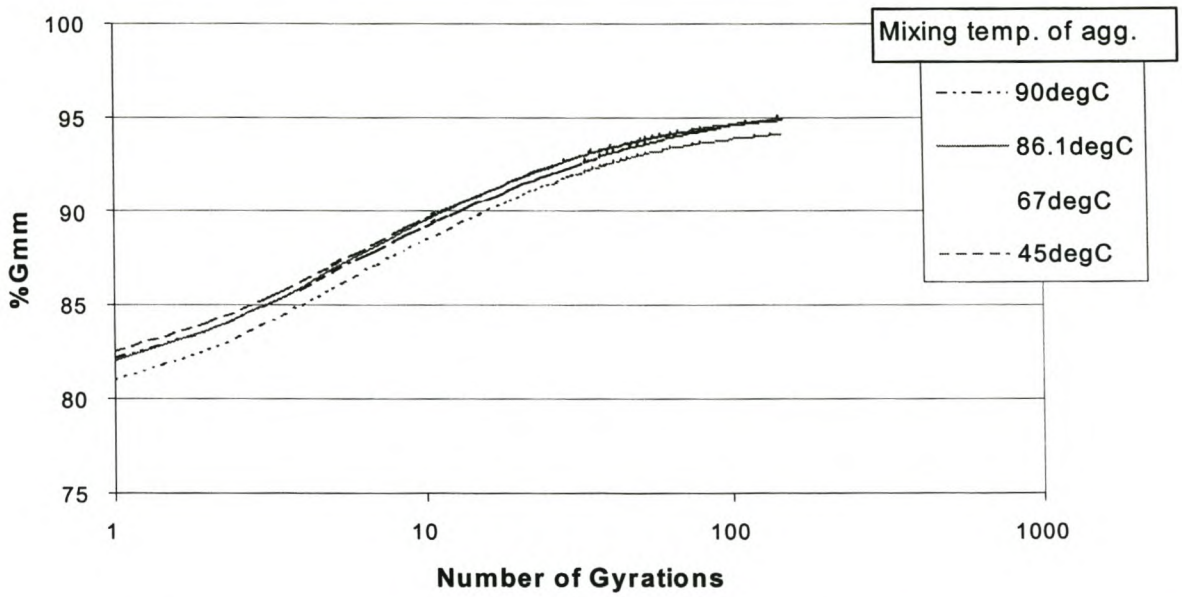

Figure C - 1. Gyratory compaction curves for continuously graded half-warm foamed mix for a variety of aggregate mixing temperatures, compacted at ambient temperature (28°C)

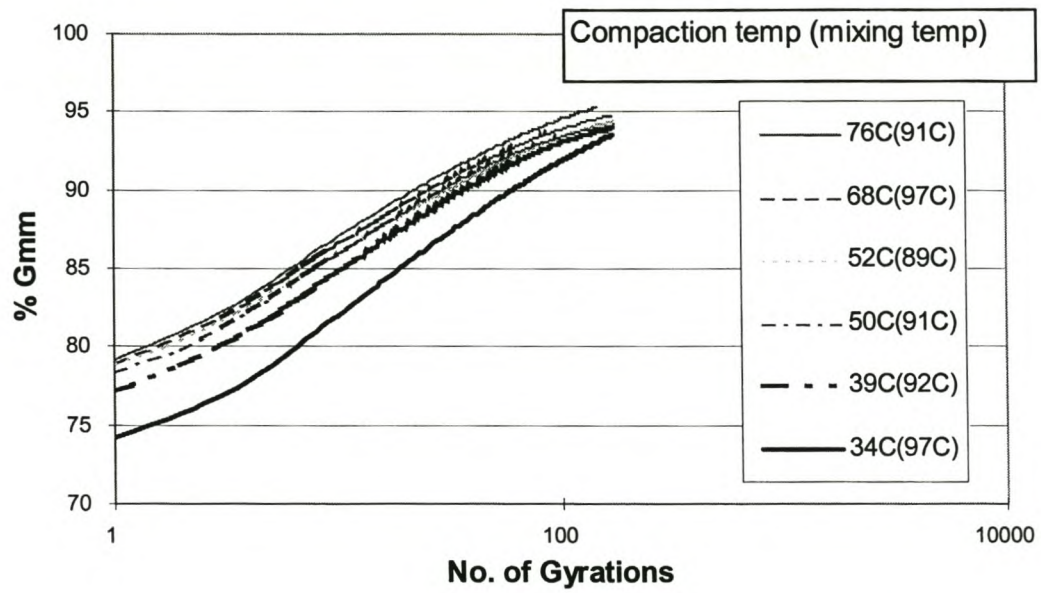

Figure C - 2. Gyratory compaction curves for continuously graded half-warm foamed mix for a variety of aggregate mixing temperatures and compaction temperatures

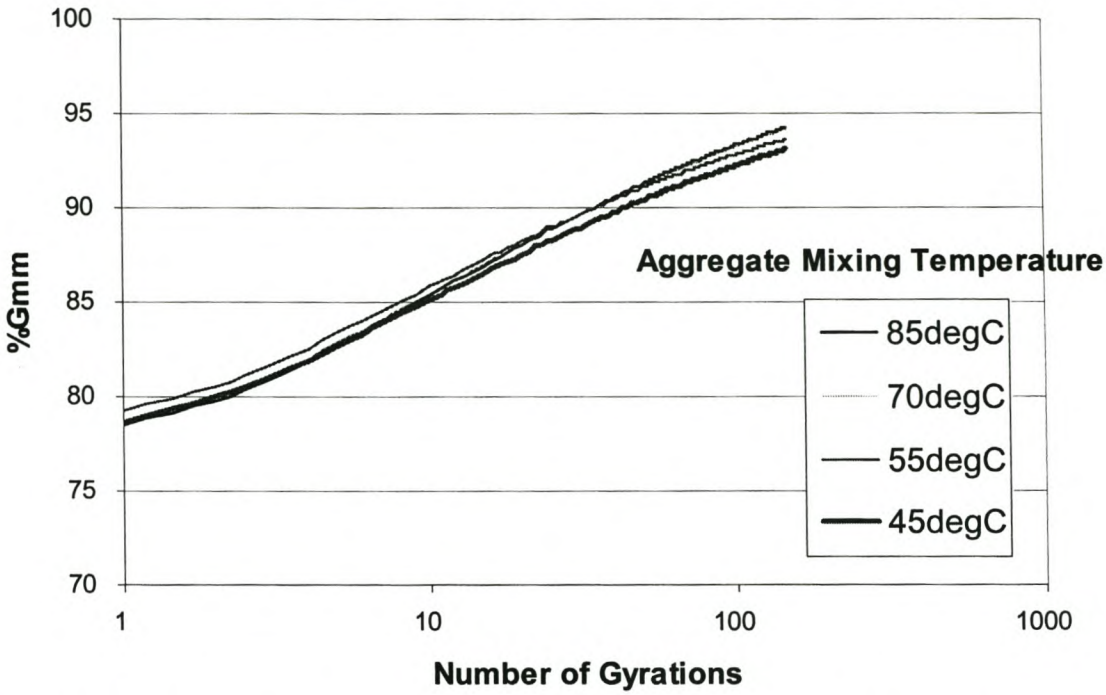

Figure C - 3. Gyratory compaction curves for semi-gap graded half-warm foamed mix for a variety of aggregate mixing temperatures, compacted at ambient temperature (28°C)

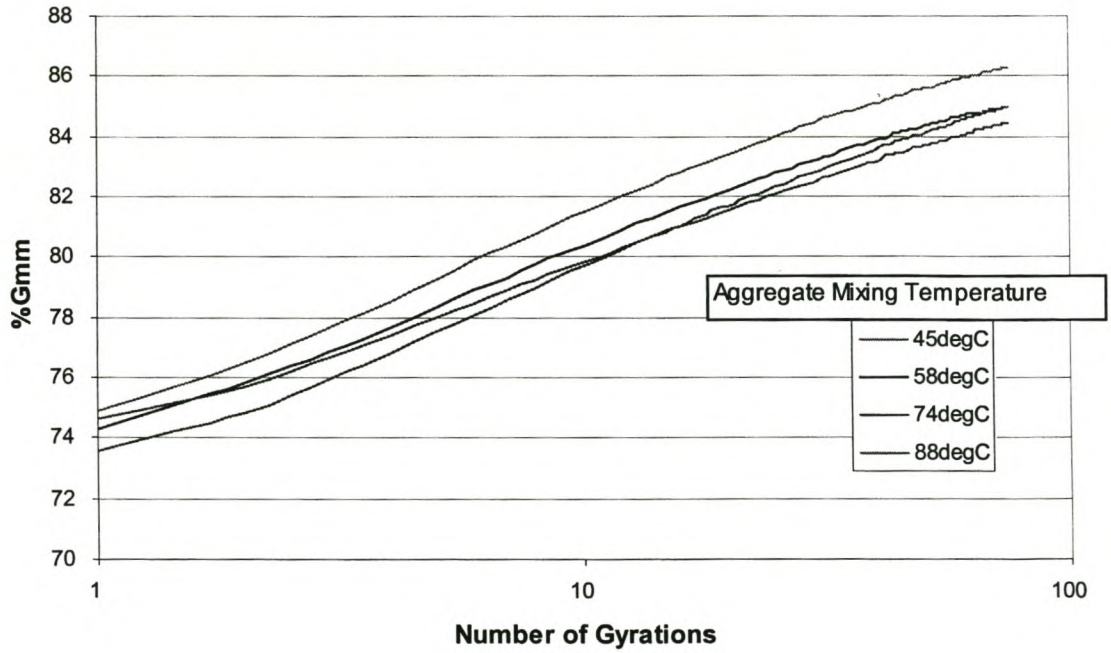

Figure C - 4. Gyratory compaction curves for half-warm gravel foamed mix for a variety of aggregate mixing temperatures, compacted at ambient temperature (28°C)

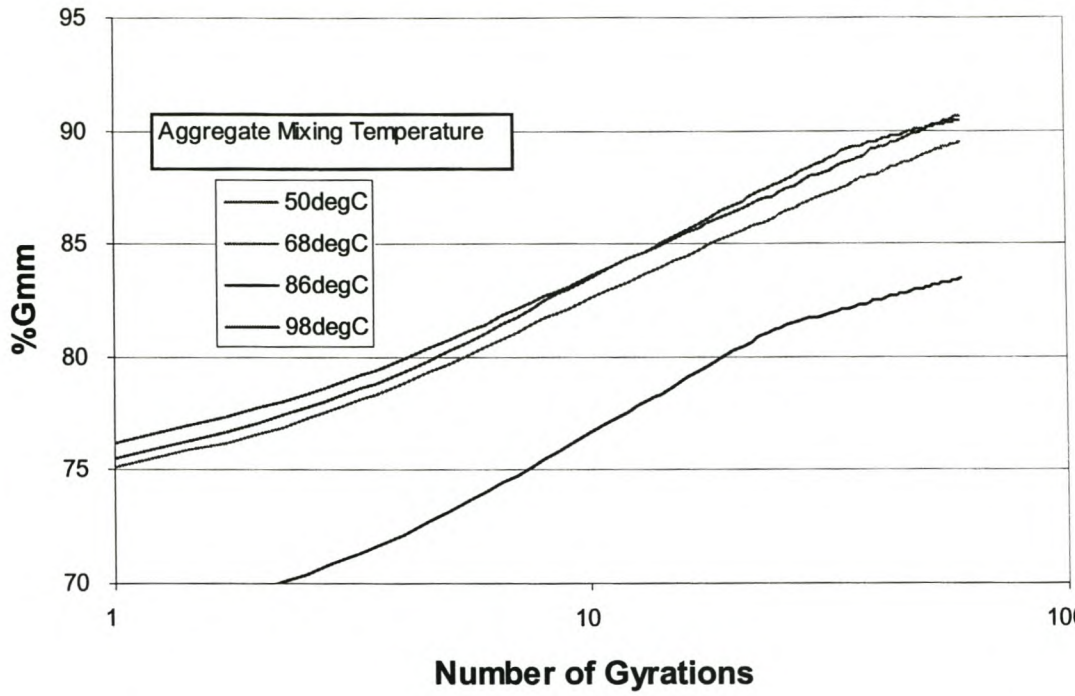

Figure C - 5. Gyratory compaction curves for half-warm SMA foamed mix for a variety of aggregate mixing temperatures, compacted at ambient temperature (28°C)

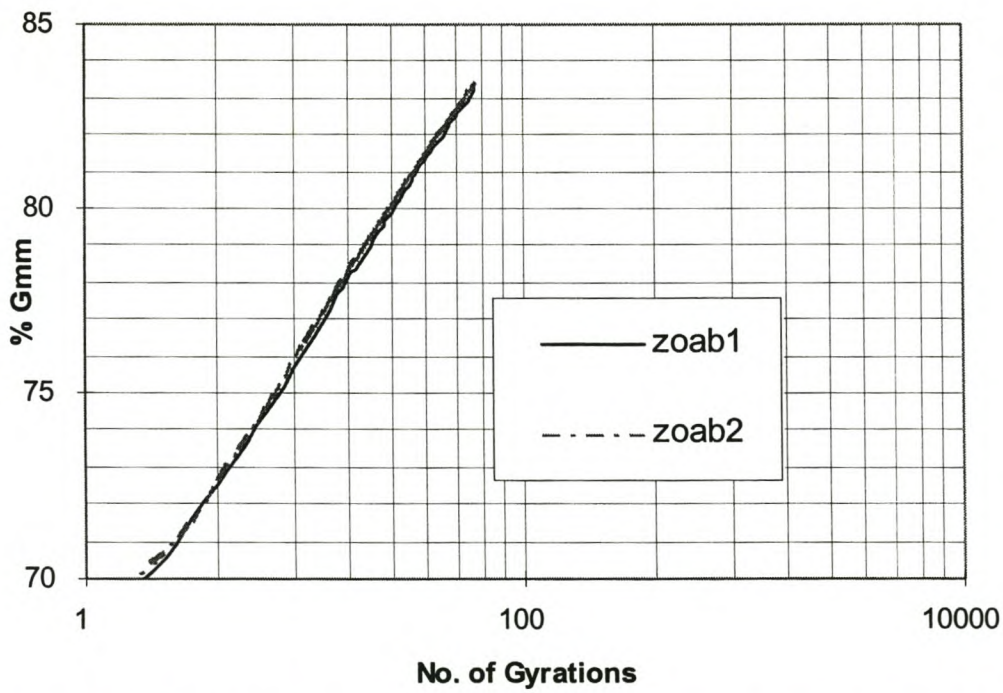

Figure C - 6. Gyratory compaction curves for half-warm ZOAB foamed mix for a variety of aggregate mixing temperatures, compacted at ambient temperature (28°C)

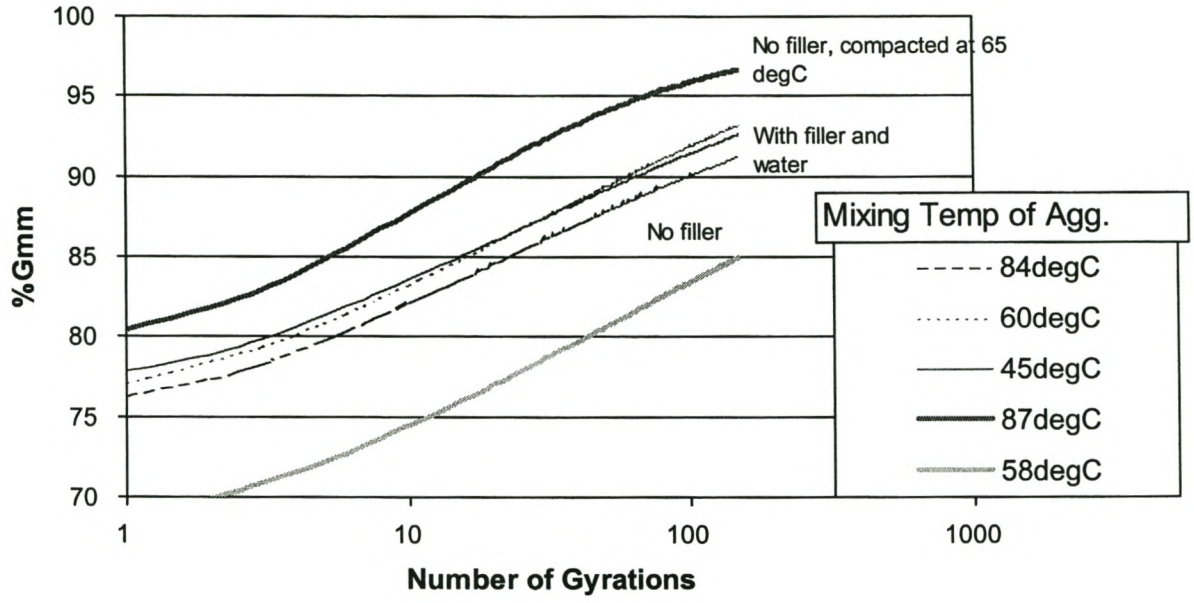

Figure C - 7. Gyratory compaction curves of half-warm foamed RAP at different mixing temperatures, compacted at ambient temperature (28 °C) unless otherwise indicated

5. SELECTED MECHANICAL TESTS ON HALF-WARM FOAMED MIXES

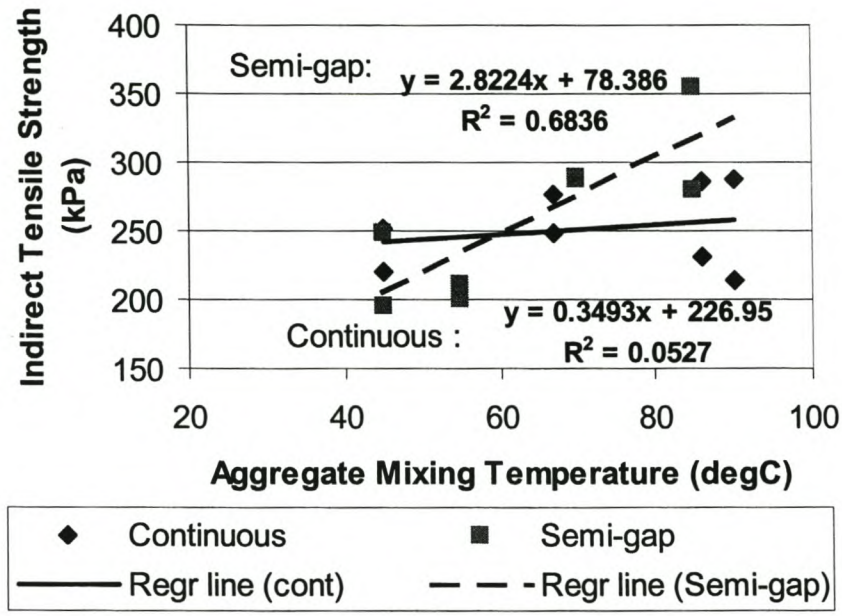

Figure C - 8. Tensile strength versus aggregate temperature for continuous and semi-gap graded foamed mix, cured at 40°C for 72 hours, tested at 25°C

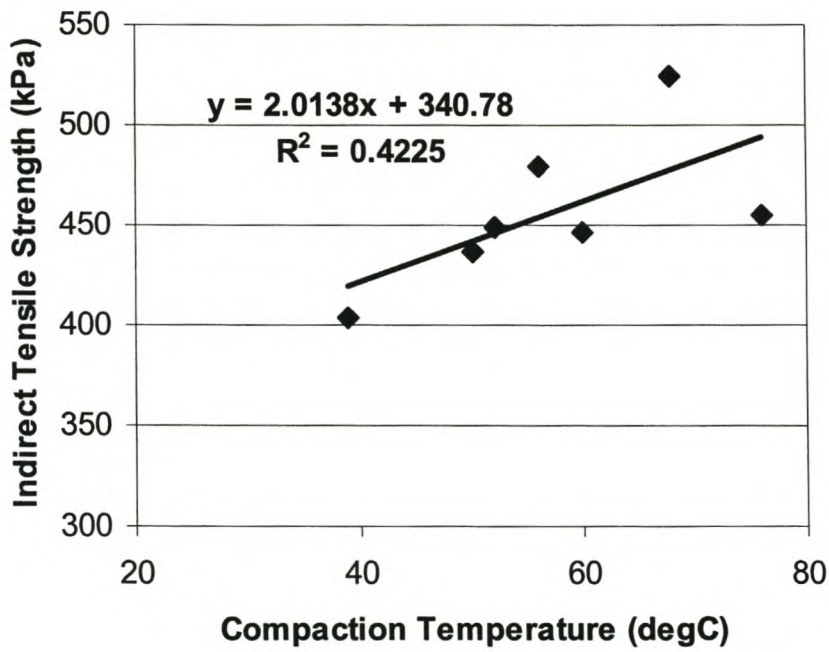

Figure C - 9. Tensile Strength versus compaction temperature for continuous graded crushed rock foamed mix, cured 6 weeks inside at ambient temperature, tested at 25°C

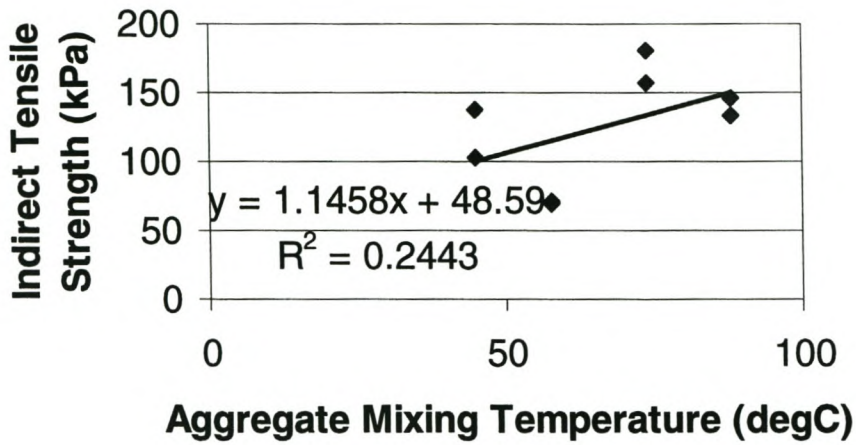

Figure C - 10. Tensile Strength versus aggregate temperature for weathered Granite gravel treated with foamed bitumen, cured for 72 hours at 40°C, tested at 25ºC.

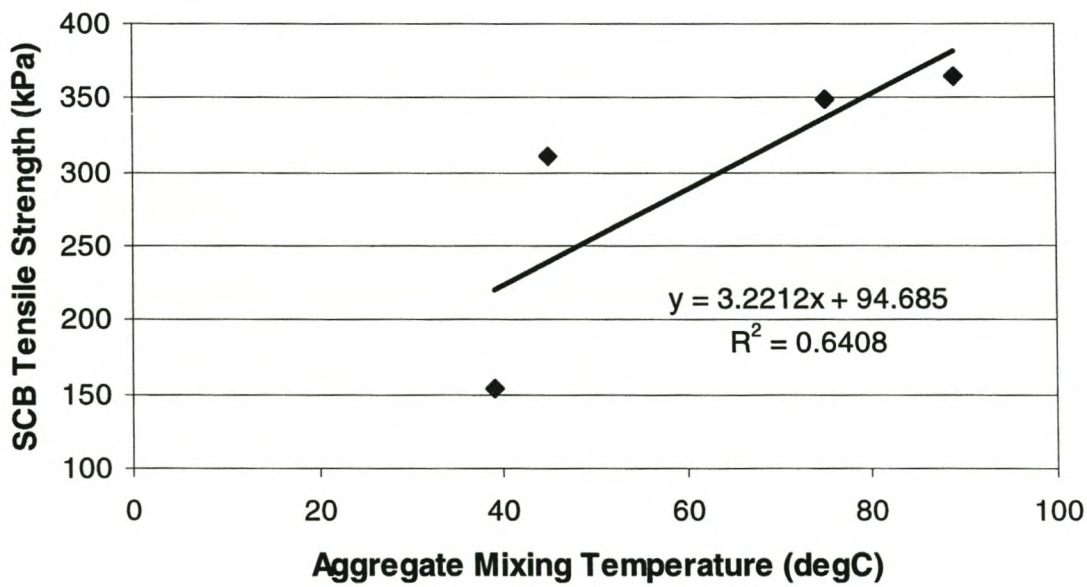

Figure C - 11. Tensile Strength at 25°C (80% Reliability for 4 tests) for a gravelly sand material stabilised with 3,6% foamed bitumen (150/200 penetration)

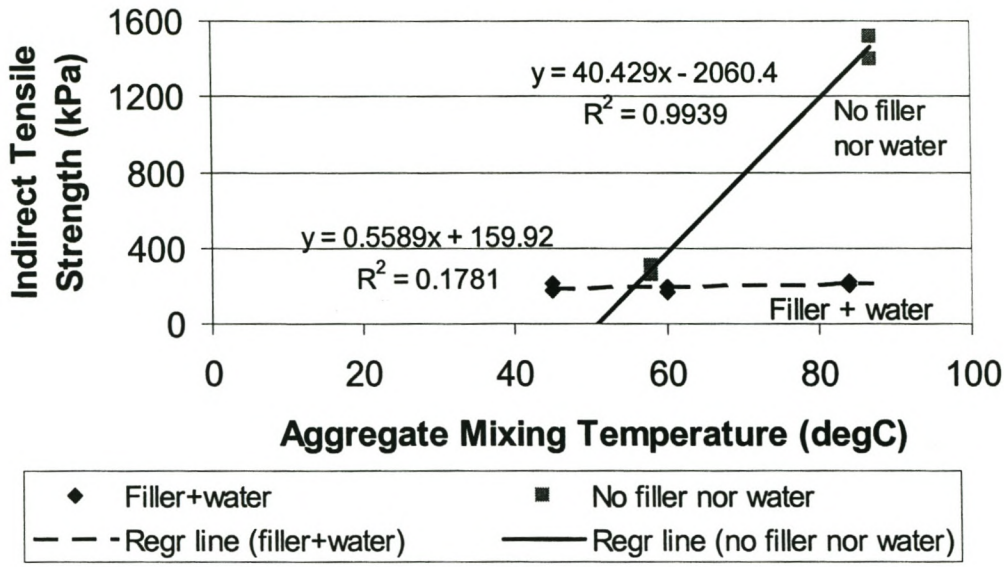

Figure C - 12. Tensile Strength versus aggregates temperature for RAP (4% BC) treated with 2% foamed bitumen (150/200 penetration) for all mixes

APPENDIX D

HALF-WARM FOAMED BITUMEN MIXES DETAILED INVESTIGATION : PRODUCTION & TEST RESULTS

1. HALF-WARM FOAMED MIX PRODUCTION IN A LABORATORY PUGMILL

1. Divide the mineral aggregate to be treated using the half-warm foamed bitumen process into two fractions upon the basis of gradation, Fraction A and B.
2. Dry the mineral aggregate through heating overnight at a temperature of 110°C.
3. For at least 4 hours before mixing, set the oven to achieve the desired aggregate temperature at mixing e.g. 98°C.
4. Prepare the foamed bitumen production apparatus Wirtgen WLB 10 ® with bitumen at the required temperature and test the foam characteristics to ensure that these are suitable.
5. Prepare Gyratory Compactor Moulds by pre-heating to 110°C.
6. Pre-heat the pugmill-mixer's chamber to 150°C.
7. Boil sufficient water for mixing moisture content.
8. Start the pugmill-mixer, add fraction A and measure the temperature with an infra-red gauge.
9. Add a portion of the hot water and mix for 10 seconds.
10. Apply a portion of the foamed bitumen and mix for 10 seconds.
11. Add fraction B and the remainder of the hot water and mix for 10 seconds.
12. Apply the remainder of the foamed bitumen required.
13. Mix for a further 20 seconds and measure the mix temperature.
14. Compact specimens in the gyratory compactor (three from each mix), measuring the temperature of each sample immediately prior to compaction and keeping the mix sealed in the oven at the appropriate compaction temperature.

2. RESULTS OF UNCONFINED COMPRESSIVE STRENGTH TESTS

Table D - 1. Mix A Half-warm Foamed STAB : UCS at Marshall Displacement Rate

Sample no	Test Temp. (°C)	Test speed (mm/s)	Axial stress max $\sigma_{c,max}$ (MPa)	Corrected Axial Stress (MPa)	Vertical strain at $\sigma_{c,max}$ (m/m)	E_{tan} (MPa)	Dissipat. Energy Factor
A4b	8	0.845	13.448	13.498	0.03505	604.8	0.322
A9a	8	0.836	14.444	14.579	0.03050	610.5	0.271
A18c	8	0.836	14.642	14.781	0.03184	622.8	0.295
Average	8	0.839	14.178	14.286	0.03246	612.7	0.297
Std Dev			0.640	0.690		9.2	0.026
A5c	13	0.846	15.508	15.553	0.02711	755.2	0.261
A15br	13	0.845	11.901	11.961	0.02466	697.6	0.192
A10c	13	0.840	10.504	10.612	0.03308	519.0	0.243
A11a	13	0.838	6.923	7.064	0.03060	452.6	0.161
Average	13	0.842	11.209	11.298	0.02886	606.1	0.221
Std Dev			3.551	3.509		143.5	0.046
A16a	25	0.838	5.544	5.606	0.02183	330.5	0.075
A18b	25	0.838	4.244	4.310	0.03079	199.2	0.086
A8c	25	0.836	6.817	6.891	0.02362	367.5	0.098
Average	25	0.837	5.535	5.602	0.02541	299.1	0.090
Std Dev			1.286	1.290		88.5	0.012
A12b	40	0.847	1.353	1.368	0.02817	65.2	0.024
A14a	40	0.847	1.335	1.350	0.02861	65.0	0.025
A3c	40	0.846	1.671	1.695	0.02617	88.6	0.028
A6c	40	0.849	1.468	1.474	0.02621	76.7	0.024
Average	40	0.847	1.457	1.472	0.02729	73.9	0.026
Std Dev			0.155	0.158		11.2	0.002

Table D - 2. Mix A Half-warm Foamed STAB : UCS at Half-Marshall Displacement Rate

Sample no	Test Temp. (°C)	Test speed (mm/s)	Axial stress max $\sigma_{c,max}$ (MPa)	Corrected Max Axial Stress (MPa)	Vertical strain at $\sigma_{c,max}$ (m/m)	E_{tan} (MPa)	Dissipat Energy Factor
A14b	8	0.383	9.788	10.190	0.03272	484.7	0.226
A15c	8	0.383	13.254	13.659	0.03114	644.8	0.281
A10a	8	0.384	7.480	7.872	0.03262	497.0	0.194
Average	8	0.384	10.174	10.574	0.03216	542.2	0.237
Std Dev			2.906	2.913		89.1	0.0
A13a	13	0.256	7.109	9.032	0.02866	598.5	0.191
A16b	13	0.620	10.141	7.919	0.02143	662.6	0.122
A4a	13	0.426	5.871	5.861	0.03548	261.2	0.142
A9c	13	1.097	15.800	8.162	0.03228	690.2	0.215
Average	13	0.600	9.730	7.744	0.02946	553.1	0.174
Std Dev			4.426	1.343		198.4	0.0
A17a	25	0.422	3.519	3.537	0.03673	113.0	0.075
A20b	25	0.422	3.377	3.396	0.03283	135.6	0.069
A7c	25	0.423	3.024	3.034	0.03179	120.8	0.058
Average	25	0.422	3.307	3.322	0.03378	123.1	0.067
Std Dev			0.255	0.259		11.5	0.0

Table D - 3. Mix B Half-warm RAP + STAB (50:50) Representative Binder Content : UCS at Marshall Displacement Rate

Sample no	Test Temp. (°C)	Test speed (mm/s)	Axial stress max $\sigma_{c,max}$ (MPa)	Corrected Axial Stress (MPa)	Vertical strain at $\sigma_{c,max}$ (m/m)	E_{tan} (MPa)	Dissipat Energy Factor
B3b	8	0.853	12.377	12.355	0.02792	637.3	0.225
B2a	8	*0.846*	*10.429*	*10.465*	*0.03274*	*481.9*	*0.229*
B8c	8	0.850	13.262	13.266	0.03094	635.9	0.272
Average	8	0.849	12.023	12.029	0.03053	585.1	0.244
Std Dev			1.449	1.429		89.3	0.026
B1b	25	0.849	5.414	5.420	0.02809	309.7	0.105
B2c	25	0.847	5.678	5.693	0.02858	288.1	0.106
B8b	25	0.843	4.351	4.385	0.03008	257.4	0.095
Average	25	0.846	5.148	5.166	0.02892	285.1	0.103
Std Dev			0.703	0.690		26.3	0.006
B4b	40	0.846	2.312	2.325	0.02570	124.9	0.038
B8a	40	0.846	2.118	2.129	0.02897	102.0	0.039
B3a	40	0.846	2.491	2.504	0.02434	141.4	0.039
Average	40	0.846	2.307	2.319	0.02634	122.8	0.039
Std Dev			0.186	0.187		19.8	0.001

Table D - 4. Mix B Half-warm RAP + STAB (50:50) Binder Content 0,5% Higher : UCS at Marshall Displacement Rate

Sample no	Test Temp. (°C)	Test speed (mm/s)	Axial Stress Max $\sigma_{c,max}$ (MPa)	Corrected Max Axial Stress (MPa)	Vertical Strain at $\sigma_{c,max}$ (m/m)	E_{tan} (MPa)	Dissipat Energy Factor
B19a	8	0.846	7.512	7.541	0.02114	576.8	0.110
B13a	8	0.846	8.526	8.562	0.02307	563.0	0.132
B22a	8	0.848	9.241	9.258	0.02391	607.0	0.151
Average	8	0.847	8.427	8.453	0.02271	582.2	0.131
Std Dev			0.869	0.864		22.5	0.020
B19b	25	0.849	4.016	4.022	0.02473	311.4	0.073
B17b	25	0.851	5.235	5.229	0.02970	283.9	0.107
B21b	25	0.846	3.932	3.950	0.03298	206.4	0.092
Average	25	0.849	4.394	4.400	0.02914	267.3	0.092
Std Dev			0.729	0.718		54.5	0.017
B12b	40	0.842	1.707	1.730	0.02910	81.8	0.032
B17c	40	0.843	2.178	2.198	0.02222	143.4	0.032
B14c	40	0.843	1.892	1.912	0.02664	103.3	0.033
Average	40	0.843	1.926	1.947	0.02599	109.5	0.033
Std Dev			0.237	0.236		31.3	0.001

Table D - 5. Mix C Cold Foamed STAB : UCS at Marshall Displacement Rate

Sample no	Test Temp. (°C)	Test speed (mm/s)	Axial Stress Max $\sigma_{c,max}$ (MPa)	Corrected Axial Stress (MPa)	Vertical Strain at $\sigma_{c,max}$ (m/m)	E_{tan} (MPa)	Dissipat Energy Factor
C3a	8	0.847	6.032	6.035	0.02299	451.0	0.098
C14b	8	0.848	6.481	6.483	0.02763	421.3	0.129
C9c	8	0.849	5.148	5.150	0.02309	410.9	0.087
Average	8	0.848	5.887	5.889	0.02457	427.7	0.104
Std Dev			0.678	0.679		20.8	0.022
C4a	13	0.848	4.481	4.483	0.02396	373.4	0.081
C13b	13	0.850	4.084	4.085	0.02564	314.6	0.078
C8c	13	0.848	4.427	4.429	0.02609	363.8	0.089
Average	13	0.848	4.331	4.332	0.02523	350.6	0.083
Std Dev			0.215	0.216		31.5	0.005
C5a	25	0.852	2.633	2.631	0.02725	171.3	0.051
C12b	25	0.852	2.570	2.568	0.02727	156.4	0.049
C16c	25	0.848	2.507	2.508	0.02797	188.6	0.053
Average	25	0.851	2.570	2.569	0.02750	172.1	0.051
Std Dev			0.063	0.061		16.1	0.002
C6a	40	0.846	1.181	1.182	0.02778	53.6	0.020
C11b	40	0.846	1.082	1.083	0.02312	60.9	0.015
C15c	40	0.844	1.118	1.120	0.02806	61.0	0.021
Average	40	0.845	1.127	1.128	0.02632	58.5	0.019
Std Dev			0.050	0.050		4.3	0.003

Table D - 6. Mix C Cold Foamed STAB : UCS at Half-Marshall Displacement Rate

Sample no	Test Temp. (°C)	Test speed (mm/s)	Axial Stress Max $\sigma_{c,max}$ (MPa)	Corrected Max Axial Stress (MPa)	Vertical Strain at $\sigma_{c,max}$ (m/m)	E_{tan} (MPa)	Dissipat Energy Factor
C7a	8	0.422	5.879	5.881	0.02243	432.3	0.092
C10b	8	0.424	5.220	5.222	0.02216	388.5	0.081
C7c	8	0.425	5.166	5.166	0.02382	399.2	0.090
Average	8	0.424	5.422	5.423	0.02280	406.7	0.087
Std Dev			0.397	0.398		22.8	0.006
C8a	25	0.429	2.236	2.233	0.03036	130.3	0.049
C9b	25	0.425	2.272	2.272	0.02377	153.8	0.037
C14c	25	0.426	2.020	2.019	0.02566	159.0	0.039
Average	25	0.427	2.176	2.174	0.02660	147.7	0.042
Std Dev			0.137	0.136		15.3	0.006
C9a	40	0.424	1.136	1.136	0.02005	74.3	0.014
C8b	40	0.427	1.082	1.081	0.02140	71.5	0.015
C5c	40	0.429	0.839	0.837	0.02014	63.9	0.011
Average	40	0.427	1.019	1.018	0.02053	69.9	0.013
Std Dev			0.158	0.159		5.4	0.002

Table D - 7. Mix D Hot-mix STAB : UCS at Marshall Displacement Rate

Sample no	Test Temp. (°C)	Test speed (mm/s)	Axial Stress Max $\sigma_{c,max}$ (MPa)	Corrected Axial Stress (MPa)	Vertical strain at $\sigma_{c,max}$ (m/m)	E_{tan} (MPa)	Dissipat Energy Factor
D12c	8	0.833	17.966	18.094	0.032621	795.8	0.385
D4b	8	0.878	17.489	17.273	0.032440	746.6	0.361
D9c	8	0.876	16.392	16.192	0.028345	751.5	0.285
Average	8	0.862	17.282	17.186	0.031135	764.6	0.342
Std Dev			0.807	0.954		27.1	0.052
D5b	13	0.836	12.643	12.726	0.028181	603.5	0.224
D8c	13	0.835	11.998	12.086	0.025916	636.0	0.198
D9b	13	0.835	12.025	12.113	0.027042	600.1	0.205
Average	13	0.835	12.222	12.308	0.027047	613.2	0.209
Std Dev			0.365	0.362		19.8	0.014
D5c	25	0.833	4.934	4.941	0.026105	388.8	0.098
D7c	25	1.366	5.057	4.821	0.020295	439.7	0.071
D10a	25	0.835	4.397	4.404	0.019452	447.8	0.064
Average	25	1.011	4.796	4.722	0.021951	425.5	0.077
Std Dev			0.351	0.282		32.0	0.018
D11c	40	0.853	2.405	2.403	0.019035	163.1	0.028
D2b	40	0.849	2.370	2.370	0.017439	172.9	0.025
Average	40	0.851	2.387	2.387	0.018237	168.0	0.027
Std Dev			0.025	0.023		6.9	0.002

Table D - 8. Mix D Hot-mix STAB : UCS at Half-Marshall Displacement Rate

Sample no	Test Temp. (°C)	Test speed (mm/s)	Axial Stress Max $\sigma_{c,max}$ (MPa)	Corrected Max Axial Stress (MPa)	Vertical Strain at $\sigma_{c,max}$ (m/m)	E_{tan} (MPa)	Dissipat Energy Factor
D9a	8	0.427	12.564	12.548	0.028657	600.4	0.228
D8b	8	0.427	13.837	13.822	0.028900	635.2	0.249
D7a	8	0.424	13.979	13.986	0.027949	641.9	0.239
Average	8	0.426	13.460	13.452	0.028502	625.8	0.239
Std Dev			0.779	0.787		22.3	0.010
D4a	13	0.433	9.993	9.946	0.026306	521.0	0.167
D5a	13	0.434	9.788	9.735	0.025688	532.4	0.161
D7b	13	0.430	9.770	9.741	0.023721	536.1	0.143
Average	13	0.432	9.850	9.807	0.025238	529.8	0.157
Std Dev			0.124	0.120		7.9	0.013
D8a	25	0.422	4.262	4.264	0.019123	288.2	0.050
D6a	25	0.432	4.576	4.570	0.018962	314.9	0.053
D6c	25	0.435	4.615	4.607	0.018249	342.7	0.053
Average	25	0.430	4.484	4.480	0.018778	315.3	0.052
Std Dev			0.194	0.188		27.3	0.002

3. RESULTS OF LEUTNER SHEAR TESTS

Table D - 9. Mix A Half-warm Foamed STAB : Shear Test at Marshall Displacement Rate

Sample Number	Test Temp. (°C)	Test speed (mm/s)	Normal Stress (MPa)	Shear Stress Max τ_{max} (MPa)	Displace-ment at τ_{max} (m/m)	Tangent Shear Mod G_{tan} (Mpa)	Dissipat Energy Function
A6b	8	0.85	0.000	3.191	2.004	3.66	2.87
A13c	8	0.85	0.000	3.335	2.199	2.95	3.00
A16cb	8	0.85	0.000	3.044	1.726	3.15	2.03
Average	8	0.85	0.000	3.190	1.977	3.25	2.63
Std Dev				0.146		0.37	0.53
A6b	8	0.85	1.151	3.554	3.490	2.59	5.83
A13c	8	0.85	1.161	3.945	3.350	2.95	6.17
A16c	8	0.85	1.131	3.645	2.448	3.53	4.07
Average	8	0.85	1.148	3.714	3.096	3.02	5.35
Std Dev				0.205		0.48	1.13
A6a	13	0.85	0.000	1.771	2.615	1.89	2.26
A8b	13	0.85	0.000	2.665	1.338	3.96	1.48
A20c	13	0.85	0.000	3.183	3.366	3.62	5.74
Average	13	0.85	0.000	2.540	2.440	3.16	3.16
Std Dev				0.715		1.11	2.27
A6a	13	0.85	0.582	2.344	2.615	2.37	2.93
A8b	13	0.85	0.586	4.022	2.103	4.15	3.69
A20c	13	0.85	0.552	3.758	2.615	2.77	4.00
Average	13	0.85	0.573	3.375	2.445	3.10	3.54
Std Dev				0.902		0.93	0.55
A18a	13	0.85	1.099	3.581	3.961	1.95	6.16
A8a	13	0.85	1.101	3.170	3.460	2.82	5.53
A17c	13	0.85	1.158	3.975	3.691	2.42	6.52
Average	13	0.85	1.120	3.575	3.704	2.40	6.07
Std Dev				0.402		0.44	0.50
A5b	25	0.85	0.000	1.627	2.470	1.38	1.72
A10b	25	0.85	0.000	1.083	4.303	0.52	1.97
A20a	25	0.85	0.000	0.910	5.601	0.35	2.23
Average	25	0.85	0.000	1.207	4.125	0.75	1.97
Std Dev				0.374		0.55	0.25
A5b	25	0.85	1.137	2.957	3.452	1.46	3.81
A10b	25	0.85	1.148	2.250	4.344	0.65	2.62
A20a	25	0.85	1.148	2.212	4.895	1.60	5.69
Average	25	0.85	1.144	2.473	4.230	1.24	4.04
Std Dev				0.420		0.51	1.55

Table D - 10. Mix A Half-warm Foamed STAB : Shear Tests at Slow Displacement

Sample Number	Test Temp. (°C)	Test speed (mm/s)	Normal Stress (MPa)	Shear Stress Max τ_{max}	Displace-ment at τ_{max} (mm)	Tangent Shear Mod G_{tan}	Dissipat Energy Function
A11b	8	0.43	*0.000*	*1.495*	*1.904*	*1.56*	1.18
A14c	8	0.43	0.000	2.967	2.968	2.45	4.07
A19bb	8	0.43	*0.000*	*1.479*	*2.650*	*3.08*	2.26
Average	8	0.43	0.000	1.980	2.507	2.36	2.50
Std Dev				0.855		0.76	1.46
A11b	8	0.43	*1.139*	*2.777*	*3.245*	*2.22*	4.27
A14c	8	0.43	1.114	3.958	3.192	3.29	6.04
A19b	8	0.43	1.142	3.073	4.015	1.91	5.76
Average	8	0.43	1.132	3.269	3.484	2.48	5.36
Std Dev				0.615		0.72	0.95
A7a	13	0.43	0.000	1.399	2.484	1.61	1.71
A9b	13	0.43	0.000	2.757	2.952	2.68	4.01
A5a	13	0.43	0.000	2.826	1.362	4.01	1.57
Average	13	0.43	0.000	2.328	2.266	2.77	2.43
Std Dev				0.805		1.20	1.37
A7a	13	0.43	0.552	1.941	3.171	1.92	3.12
A9b	13	0.43	0.564	3.682	2.952	3.10	5.06
A5a	13	0.43	0.551	3.306	2.290	3.22	3.35
Average	13	0.43	0.556	2.976	2.804	2.75	3.84
Std Dev				0.916		0.72	1.06
A15a	13	0.43	1.121	3.528	3.883	2.37	6.51
A19a	13	0.43	1.132	2.477	5.005	1.50	6.21
A11c	13	0.43	1.145	3.746	3.585	3.10	6.69
Average	13	0.43	1.132	3.250	4.158	2.32	6.47
Std Dev				0.678		0.80	0.24
A7b	25	0.43	0.000	0.666	6.074	0.18	1.50
A12a	25	0.43	0.000	0.676	6.110	0.18	1.46
A17b	25	0.43	0.000	0.825	5.800	0.25	1.81
Average	25	0.43	0.000	0.722	5.995	0.20	1.59
Std Dev				0.089		0.04	0.19
A7b	25	0.43	1.149	1.957	7.592	0.59	6.68
A12a	25	0.43	1.135	1.817	7.009	0.39	4.31
A17b	25	0.43	1.146	2.009	6.697	0.56	5.39
Average	25	0.43	1.143	1.928	7.099	0.52	5.46
Std Dev				0.099		0.11	1.19
A8a	13	0.083	0	1.522	1.690	1.78	1.06
A18a	13	0.083	0	1.543	3.294	1.23	2.42
A17c	13	0.083	0	1.652	2.752	1.57	2.16
Average	13	0.083	0	1.572	2.579	1.53	1.88
Std Dev				0.069		0.27	0.72

Table D - 11. Mix B Half-warm RAP + STAB (50:50) Representative Binder Content: Shear Tests at Marshall Displacement Rate

Sample Number	Test Temp. (°C)	Test speed (mm/s)	Normal Stress (MPa)	Shear Stress Max τ_{max} (MPa)	Displace-ment at τ_{max} (mm)	Tangent Shear Mod G_{tan} (MPa)	Dissipat Energy Function
B1a	13	0.85	0.000	1.456	2.029	1.85	1.40
B4c	13	0.85	0.000	2.367	1.651	2.88	1.63
B9b	13	0.85	0.000	2.590	2.014	2.06	1.85
Average	13	0.85	0.000	2.138	1.898	2.27	1.63
Std Dev				0.601		0.55	0.23
B1a	13	0.85	1.155	3.892	2.909	3.26	5.22
B4c	13	0.85	1.131	4.274	3.350	2.35	5.66
B9b	13	0.85	1.146	3.586	3.157	2.52	4.99
Average	13	0.85	1.144	3.917	3.139	2.71	5.29
Std Dev				0.345		0.48	0.34
B3c	25	0.85	0.000	1.579	3.339	0.97	2.22
B9a	25	0.85	0.000	1.138	3.134	0.82	1.59
B9c	25	0.85	0.000	1.640	3.075	1.16	2.20
Average	25	0.85	0.000	1.452	3.183	0.98	2.00
Std Dev				0.274		0.17	0.36
B3c	25	0.85	1.126	2.812	4.462	1.22	5.13
B9a	25	0.85	1.154	2.579	4.253	1.15	4.43
B9c	25	0.85	1.149	2.858	4.285	1.25	4.89
Average	25	0.85	1.143	2.750	4.334	1.21	4.82
Std Dev				0.150		0.05	0.36

Table D - 12. Mix B Half-warm RAP + STAB (50:50) at 0,5% Higher Binder Content : Shear Tests at Marshall Displacement Rate

Sample Number	Test Temp. (°C)	Test speed (mm/s)	Normal Stress (MPa)	Shear Stress Max τ_{max} (MPa)	Displace-ment at τ_{max} (mm)	Tangent Shear Mod G_{tan} (MPa)	Dissipat Energy Function
B12a	13	0.85	0.000	1.263	1.741	1.88	1.04
B13b	13	0.85	0.000	1.366	1.783	2.01	1.16
B16a	13	0.85	0.000	2.286	2.388	2.14	2.42
Average	13	0.85	0.000	1.639	1.971	2.01	1.10
Std Dev				0.563		0.13	0.76
B12a	13	0.85	1.141	2.694	3.330	1.76	3.92
B13b	13	0.85	1.152	2.801	3.360	1.93	4.24
B16a	13	0.85	1.150	3.226	1.741	2.88	1.94
Average	13	0.85	1.148	2.907	2.811	2.19	3.36
Std Dev				0.281		0.60	1.25
B18b	25	0.85	0.000	1.026	4.498	0.48	1.98
B15b	25	0.85	0.000	0.995	2.072	0.87	0.81
B20c	25	0.85	0.000	1.221	4.115	0.66	2.22
Average	25	0.85	0.000	1.080	3.562	0.67	1.67
Std Dev				0.122		0.20	0.76
B18b	25	0.85	1.117	2.258	4.370	1.69	5.07
B15b	25	0.85	1.118	2.521	3.679	1.32	3.77
B20c	25	0.85	1.148	2.379	4.308	2.05	5.45
Average	25	0.85	1.128	2.386	4.119	1.69	4.77
Std Dev				0.132		0.37	0.88

Table D - 13. Mix B Half-warm RAP + STAB (50:50) at 0,5% Higher Binder Content : Shear Tests at Displacement Rates Slower than Marshall

Sample Number	Test Temp. (°C)	Test speed (mm/s)	Normal Stress (MPa)	Shear Stress Max τ_{max} (MPa)	Displace-ment at τ_{max} (mm)	Tangent Shear Mod G_{tan} (MPa)	Dissipat Energy Function
B12c	13	0.43	0.000	1.372	2.316	1.38	1.44
B20a	13	0.43	0.000	1.445	2.475	1.16	1.48
B16b	13	0.43	0.000	1.553	1.549	1.79	0.93
Average	13	0.43	0.000	1.456	2.113	1.44	1.28
Std Dev				0.091		0.32	0.31
B12c	13	0.43	1.143	2.712	3.561	1.53	4.03
B20a	13	0.43	1.146	2.406	3.501	2.15	4.27
B16b	13	0.43	1.140	3.103	3.077	3.23	4.88
Average	13	0.43	1.143	2.740	3.380	2.30	4.39
Std Dev				0.349		0.86	0.44
B13c	13	0.08	0.000	1.143	2.642	1.21	1.47
B20b	13	0.08	0.000	1.188	3.080	0.83	1.59
B16c	13	0.08	0.000	1.915	3.275	1.32	2.79
Average	13	0.08	0.000	1.416	2.999	1.12	1.95
Std Dev				0.433		0.26	0.73
B13c	13	0.08	1.122	2.632	4.408	1.36	5.18
B20b	13	0.08	1.124	2.131	5.118	0.84	4.56
B16c	13	0.08	1.123	3.138	3.897	2.23	5.95
Average	13	0.08	1.123	2.634	4.474	1.48	5.23
Std Dev				0.503		0.71	0.70

Table D - 14. Mix C Cold Foamed STAB : Shear Tests at Marshall Displacement Rates

Sample Number	Test Temp. (°C)	Test speed (mm/s)	Normal Stress (MPa)	Shear Stress Max τ_{max} (MPa)	Displace-ment at τ_{max} (mm)	Tangent Shear Mod G_{tan} (MPa)	Dissipat Energy Function
C17a	8	0.85	0.000	1.301	2.037	1.22	1.08
C7b	8	0.85	0.000	1.079	1.706	1.35	0.80
C13c	8	0.85	0.000	1.328	2.200	1.50	1.36
Average	8	0.85	0.000	1.236	1.981	1.36	1.08
Std Dev				0.136		0.14	0.28
C17a	8	0.85	1.138	2.774	3.560	2.20	4.84
C7b	8	0.85	1.156	2.605	3.500	2.29	4.60
C13c	8	0.85	1.161	2.808	3.484	2.07	4.61
Average	8	0.85	1.152	2.729	3.515	2.19	4.68
Std Dev				0.109		0.11	0.13
C10a	13	0.85	0.000	1.105	2.261	1.09	1.11
C6b	13	0.85	0.000	1.152	1.965	1.51	1.07
C11c	13	0.85	0.000	1.080	2.800	0.73	1.22
Average	13	0.85	0.000	1.112	2.342	1.11	1.13
Std Dev				0.037		0.39	0.08
C10a	13	0.85	0.592	2.069	3.250	1.40	2.96
C6b	13	0.85	0.595	1.845	3.383	1.57	3.08
C11c	13	0.85	0.588	1.944	3.133	1.88	3.06
Average	13	0.85	0.592	1.953	3.255	1.62	3.03
Std Dev				0.112		0.24	0.06
C5b	13	0.85	1.156	2.506	3.990	1.45	4.50
Cr5b	13	0.85	1.166	2.595	3.595	2.40	4.82
C4c	13	0.85	1.150	2.473	4.050	1.93	5.09
Average	13	0.85	1.157	2.525	3.879	1.93	4.80
Std Dev				0.063		0.48	0.30
C12a	25	0.85	0.000	0.498	4.684	0.20	0.95
C4b	25	0.85	0.000	0.424	5.010	0.13	0.71
C10c	25	0.85	0.000	0.511	4.734	0.19	0.94
Average	25	0.85	0.000	0.478	4.809	0.18	0.87
Std Dev				0.047		0.04	0.13
C12a	25	0.85	1.154	1.862	5.213	0.73	4.09
C4b	25	0.85	1.133	1.828	5.160	0.62	3.61
C10c	25	0.85	1.125	*1.654*	*3.717*	*1.69*	3.29
Average	25	0.85	1.138	1.781	5.187	0.68	3.85
Std Dev				0.111		0.59	0.40

Table D - 15. Mix C Cold Foamed STAB : Shear Tests at Displacement Rates Slower than Marshall

Sample Number	Test Temp. (°C)	Test speed (mm/s)	Normal Stress (MPa)	Shear Stress Max τ_{max} (MPa)	Displace-ment at τ_{max} (mm)	Tangent Shear Mod G_{tan} (MPa)	Dissipat Energy Function
C16a	13	0.43	0.000	1.099	2.300	1.07	1.12
C3b	13	0.43	0.000	0.932	2.121	1.22	0.96
C6c	13	0.43	0.000	0.934	3.231	0.79	1.46
Average	13	0.43	0.000	0.988	2.551	1.03	1.18
Std Dev				0.096		0.22	0.25
C16a	13	0.43	0.586	1.667	3.150	1.33	2.45
C3b	13	0.43	0.590	1.799	2.700	1.50	2.16
C6c	13	0.43	0.589	1.663	3.283	1.33	2.60
Average	13	0.43	0.588	1.710	3.044	1.38	2.40
Std Dev				0.077		0.10	0.23
C14a	13	0.43	1.153	2.474	4.077	1.80	5.03
C15b	13	0.43	1.145	2.405	3.400	2.30	4.20
C3c	13	0.43	1.147	2.179	3.626	1.44	3.62
Average	13	0.43	1.149	2.353	3.701	1.85	4.28
Std Dev				0.155		0.43	0.71
C14a	13	0.08	0.000	0.665	3.396	0.52	1.08
C15b	13	0.08	0.000	0.685	3.583	0.44	1.11
C3c	13	0.08	0.000	0.620	2.424	0.61	0.69
Average	13	0.08	0.000	0.657	3.134	0.52	0.96
Std Dev				0.033		0.08	0.23

Table D - 16. Mix D Hot-mix STAB : Shear Tests at Marshall Displacement Rate

Sample Number	**Test Temp. (°C)**	**Test speed (mm/s)**	**Normal Stress (MPa)**	**Shear Stress Max τ_{max} (MPa)**	**Displace-ment at τ_{max} (mm)**	**Tangent Shear Mod G_{tan} (MPa)**	**Dissipat Energy Function**
Sample Number	Temp (degC)	Test speed (mm/s)	Normal str (MPa)	Shear str max (Mpa)	Displ at S max (mm)	Tang Shear Mod (Mpa)	Diss Energy Function
D17c	8	0.85	0.000	4.399	1.476	4.74	2.29
D16b	8	0.85	0.000	3.637	1.810	4.65	2.97
D13b	8	0.85	0.000	3.664	1.808	4.64	2.97
Average	8	0.85	0.000	3.900	1.698	4.67	2.74
Std Dev				0.433		0.05	0.39
D17c	8	0.85	1.139	5.992	2.354	4.53	5.44
D16b	8	0.85	1.152	4.806	2.332	4.72	5.02
D13b	8	0.85	1.148	4.971	2.442	4.37	5.27
Average	8	0.85	1.146	5.256	2.376	4.54	5.25
Std Dev				0.642		0.17	0.21
D12a	13	0.85	0.000	2.797	1.750	3.04	1.98
D10c	13	0.85	0.000	3.143	0.778	4.19	0.45
D14b	13	0.85	0.000	2.609	2.310	2.64	2.73
Average	13	0.85	0.000	2.850	1.613	3.29	1.72
Std Dev				0.271		0.81	1.16
D14b	13	0.85	0.552	3.796	2.217	3.44	3.52
D10c	13	0.85	0.582	3.611	2.181	4.38	3.76
D12a	13	0.85	0.544	3.556	1.620	3.55	2.06
Average	13	0.85	0.559	3.655	2.006	3.79	3.11
Std Dev				0.126		0.51	0.92
D13c	13	0.85	1.130	4.327	2.562	3.63	4.81
D14a	13	0.85	1.139	4.116	2.976	3.22	5.54
D17a	13	0.85	1.141	4.357	3.304	3.25	6.68
Average	13	0.85	1.137	4.266	2.947	3.37	5.68
Std Dev				0.131		0.23	0.94
D11a	25	0.85	0.000	1.418	2.192	1.30	1.30
D18c	25	0.85	0.000	1.295	2.782	0.85	1.42
D17b	25	0.85	0.000	1.327	2.393	1.01	1.24
Average	25	0.85	0.000	1.347	2.456	1.05	1.32
Std Dev				0.064		0.23	0.09
D11a	25	0.85	1.141	2.356	3.771	1.36	3.89
D18c	25	0.85	1.112	2.699	3.247	1.52	3.44
D17b	25	0.85	1.152	2.674	4.612	1.18	5.19
Average	25	0.85	1.135	2.576	3.877	1.35	4.17
Std Dev				0.191		0.17	0.91

Table D - 17. Mix D Hot-mix STAB : Shear Tests at Half-Marshall Displacement Rate

Sample Number	Test Temp. (°C)	Test speed (mm/s)	Normal Stress (MPa)	Shear Stress Max τ_{max} (MPa)	Displace-ment at τ_{max} (mm)	Tangent Shear Mod G_{tan} (MPa)	Dissipat Energy Function
D19c	8	0.43	0.000	4.159	1.627	5.48	2.93
D13a	8	0.43	0.000	3.288	1.781	5.22	2.87
D15c	8	0.43	0.000	3.654	1.552	5.36	2.54
Average	8	0.43	0.000	3.700	1.653	5.36	2.78
Std Dev				0.437		0.13	0.21
D19c	8	0.43	1.101	5.429	2.246	4.92	5.13
D13a	8	0.43	1.099	4.134	2.695	3.30	4.84
D15c	8	0.43	1.149	4.751	1.969	5.28	4.10
Average	8	0.43	1.116	4.772	2.303	4.50	4.69
Std Dev				0.647		1.05	0.53
D12b	13	0.43	0.000	2.846	1.806	3.95	2.40
D16c	13	0.43	0.000	2.627	1.760	2.91	1.90
D15a	13	0.43	0.000	2.571	1.654	3.27	1.83
Average	13	0.43	0.000	2.681	1.740	3.38	2.04
Std Dev				0.145		0.53	0.31
D12b	13	0.43	0.577	3.332	2.224	3.65	3.42
D16c	13	0.43	0.587	3.310	2.278	3.01	3.21
D15a	13	0.43	0.557	3.325	2.400	2.85	3.38
Average	13	0.43	0.574	3.322	2.301	3.17	3.33
Std Dev				0.011		0.42	0.11
D11b	13	0.43	1.140	3.910	2.576	3.04	4.20
D19a	13	0.43	1.136	4.155	2.572	3.43	4.61
D18b	13	0.43	1.133	3.903	2.631	2.90	4.22
Average	13	0.43	1.136	3.989	2.593	3.12	4.34
Std Dev				0.143		0.28	0.23
D18a	25	0.43	0.000	0.974	2.480	0.76	0.99
D16a	25	0.43	0.000	0.918	3.205	0.52	1.15
D14c	25	0.43	0.000	1.035	3.732	0.77	1.88
Average	25	0.43	0.000	0.976	3.139	0.68	1.34
Std Dev				0.059		0.15	0.48
D18a	25	0.43	1.150	2.362	4.583	0.84	3.88
D16a	25	0.43	1.143	2.230	4.413	0.94	3.91
D14c	25	0.43	1.138	2.404	3.732	1.27	3.71
Average	25	0.43	1.144	2.332	4.242	1.02	3.83
Std Dev				0.091		0.23	0.11

Table D - 18. Mix D Hot-mix STAB : Shear Tests at Slow Displacement Rates

Sample Number	Test Temp. (°C)	Test speed (mm/s)	Normal Stress (MPa)	Shear Stress Max τ_{max} (MPa)	Displace-ment at τ_{max} (mm)	Tangent Shear Mod G_{tan} (MPa)	Dissipat Energy Function
D10b	13	0.08	0.000	1.91	1.642	3.23	1.53
D19b	13	0.08	0.000	2.16	1.845	2.74	1.80
D19br	13	0.08	0.000	1.89	1.718	2.89	1.55
Average	13	0.08	0.000	1.99	1.735	2.95	1.63
Std Dev				0.15		0.25	0.15

4. FOUR POINT BEAM TESTS FOR MASTER CURVES AND FATIGUE

Table D - 19. Volumetrics of Beams for 4PB Tests

	Voids in Mix (%)						
Mix Type	HW STAB				HMA STAB		
Plate	PA-1	PA-2	PA-3	PA-4	PD-5	PD-6	PD-7
Average	5.12	6.03	6.08	5.99	9.52	8.35	7.05
Standard Deviation	0.20	0.29	0.05	0.22	0.29	0.23	0.41
Variation (Max-Min)	0.58	0.71	0.15	0.63	0.74	0.63	1.18
Binder Content (%)	5.35	5.35	5.42	5.39	4.53	5.17	4.55
Moisture Content (%)	0.23	0.23	0.57	0.34	0	0	0

Table D - 20. Master Curve Data for HMA STAB Beam PD-71 at 80 μm/m Tensile Strain

Frequency (Hz)	Temperature (°C)	Tensile Stress (kPa)	Flexural Stiffness (Mpa)	Phase Angle(°)	Dissipated Energy (kPa)
0.5	5	1159.6	7132	4.42	0.0556
1	5	1304	8020.2	7.94	0.065
2	5	1465.4	9034.2	13.94	0.0726
5	5	1695.2	10475.2	15.02	0.081
10	5	1909.2	11810.4	17.3	0.0932
0.5	10	879.4	5434	6.02	0.048
1	10	1030.6	6342.8	9.3	0.0594
2	10	1215.8	7486.4	16.9	0.069
5	10	1456.8	9011.6	16.86	0.0778
10	10	1640.2	10157.8	20.02	0.0858
0.5	15	518.8	3204.6	7.88	0.034
1	15	637.2	3928.4	12.9	0.0436
2	15	752	4616.4	22.48	0.055
5	15	954	5868.2	21.78	0.0684
10	15	1120.2	6962	24.86	0.0764
0.5	20	281.2	1736.4	6.44	0.0212
1	20	363.4	2234.2	17.54	0.027
2	20	448.8	2755	28.92	0.037
5	20	596.6	3692.2	26.62	0.0522
10	20	732.8	4542.2	30.46	0.0624
0.5	25	144.6	886.8	3.58	0.011
1	25	183.2	1134.8	15.12	0.014
2	25	233.4	1435.4	35.12	0.02
5	25	327.6	2034.2	29.96	0.0328
10	25	439	2713.2	35.56	0.0434

Table D - 21. Master Curve Data for HW STAB Beam PA-25 at 80 μm/m Tensile Strain

Frequency (Hz)	Temperature (°C)	Tensile Stress (kPa)	Flexural Stiffness (Mpa)	Phase Angle(°)	Dissipated Energy (kPa)
0.5	5	1345.8	8269	3.02	0.0482
1	5	1501.6	9279.8	5.1	0.055
2	5	1654.4	10140.2	10.8	0.0604
5	5	1850.4	11383.2	11.2	0.0678
10	5	2015.2	12395	14.18	0.083
0.5	10	971.2	5974.8	4.44	0.0436
1	10	1119.8	6888.6	7.24	0.052
2	10	1258.6	7759.4	13.82	0.0592
5	10	1425.6	8809.8	13.94	0.067
10	10	1580.2	9776.2	17.34	0.0742
0.5	15	615.2	3801.6	7.32	0.035
1	15	733.2	4524.8	10.6	0.044
2	15	863.4	5304.4	18.76	0.054
5	15	1030	6351.8	18.84	0.064
10	15	1167.8	7240.4	21.5	0.0712
0.5	20	374.8	2308.8	6.44	0.025
1	20	460.2	2819.8	14.82	0.0318
2	20	552.4	3383.8	24.42	0.0416
5	20	712	4406	22.52	0.055
10	20	843.4	5218.8	25.96	0.0628
0.5	25	211.4	1298	4.64	0.015
1	25	252	1550.4	18.3	0.018
2	25	316.6	1948.8	30.02	0.026
5	25	442	2722.2	27	0.04
10	25	573.4	3559.2	29.6	0.0506

Table D - 22. 4PB Fatigue Test Results for HMA STAB Beams in Displacement Controlled Mode at 20°C

Specimen No.	Total Strain (μm/m)	Load repetitions N_f	Tensile Strain	Voids in Mix (%)
PD6-2	460	54400	0.00023	8.19
PD7-4	380	80820	0.00019	7.04
PD7-5	300	133500	0.00015	7.41
PD7-7	280	385000	0.00014	7.69
PD7-6	240	452000	0.00012	7.44
PD6-1	210	962400	0.000105	8.08
PD7-3	180	2691360	0.00009	7.02
Average				**7.55**
Std Dev				**0.46**

Specimen No.	Initial Stiffness (MPa)	Final Stiffness (MPa)	Initial Phase Angle (deg)	Final Phase Angle (deg)	Dissip. Energy, Initial (kPa)	Accum. Dissip. Energy (MPa)
PD6-2	4297.5	2148.5	36.9	40.6	0.469	17.7
PD7-4	3355	1678	39	38	0.274	14.22
PD7-5	3569.6	1784.8	34.9	35.3	0.18	16.61
PD7-7	3881	1940.5	35.2	45.3	0.167	45.3
PD7-6	3911	1955	32.5	33.1	0.124	37.25
PD6-1	2266.5	1133	30.4	34.3	0.103	69.1
PD7-3	3714	1857	32.7	31.6	0.069	127.71
Average	**3570.66**	**1785.26**				
Std Dev	**646.57**	**323.25**				

Table D - 23. 4PB Fatigue Test Results for HW STAB Beams in Displacement Controlled Mode at 20°C

Specimen No.	Total Strain (μm/m)	Load repetitions N_f	Tensile Strain	Voids in Mix (%)
PA3-6	580	33520	0.00029	6.34
PA4-1	530	33120	0.000265	6.25
PA3-5	440	72460	0.00022	6.34
PA4-4	380	123660	0.00019	6.44
PA3-4	340	188700	0.00017	6.44
PA2-1	300	248000	0.00015	6.05
PA2-6	280	498000	0.00014	6.54
PA3-2a	220	638000	0.00011	6.35
PA3-3b	190	1030430	0.000095	6.38
PA4-2	180	944560	0.00009	6.48
Average				**6.36**
Std Dev				**0.14**

Specimen No.	Initial Stiffness (MPa)	Final Stiffness (MPa)	Initial Phase Angle (deg)	Final Phase Angle (deg)	Dissip. Energy, Initial (kPa)	Accum. Dissip. Energy (MPa)
PA3-6	4048	2024	39.1	38.2	0.708	15.41
PA4-1	3836	1918	38.9	38.5	0.789	12.64
PA3-5	3930	1965	36.4	37.4	0.401	20.61
PA4-4	4104	2052	34.4	36.4	0.31	25.16
PA3-4	4040	2020	34.2	37.7	0.251	34
PA2-1	4254	2127	32.5	35.1	0.197	32.71
PA2-6	3946	1928	32.8	35.7	0.164	56.15
PA3-2a	4090	2045	30.3	32.4	0.101	45.92
PA3-3b	4430	2215	28.7	32.9	0.08	61.16
PA4-2	4570	2285	26.4	31.3	0.073	48.88
Average	**4124.80**	**2057.90**				
Std Dev	**230.00**	**119.67**				

APPENDIX E

TRIAXIAL TESTS ON FOAMED BITUMEN MIXES

1. PROCEDURE FOR MANUFACTURE OF SPECIMENS FOR TRIAXIAL SAMPLES TESTED IN STELLENBOSCH

1. A sample of the desired gradation of aggregate (at 19°C) and percentage of cement (if required) pre-blended in the Hobart Mixer with water to achieve the desired mixing moisture content.
2. The mix is stabilised with foamed bitumen whilst agitating at Speed II in the Hobart Mixer to achieve the desired binder content.
3. A 150/200 penetration bitumen from Calref refinery (or equivalent) is used to produce the foamed bitumen.
4. Mixing continues for 30 seconds.
5. Specimens are compacted in a Troxler Gyratory Compactor at an angle of 1,25° and applied pressure of 600 kPa. Sufficient material is added to produce 100mm high samples after the required number of gyrations.
6. For triaxial testing the G2van samples are cured at ambient temperature for 24 hours to simulate the curing that occurs in a layer that is opened to traffic within a day after compaction.
7. The G1gau and G1eer specimens, after the 24 hour initial cure are dried to the desired moisture content at ambient temperature, sealed and further cured at 50°C in an oven
8. In order to obtain a sample height of 300mm, three specimens were placed on top of one another without any tack coat or adhesion at the interlayers. The friction between specimens was considered as sufficient for stress transfer which was confirmed through the absence of differential deformation between specimens notable after testing.

2. GYRATORY COMPACTION CURVES OF TRIAXIAL SPECIMENS

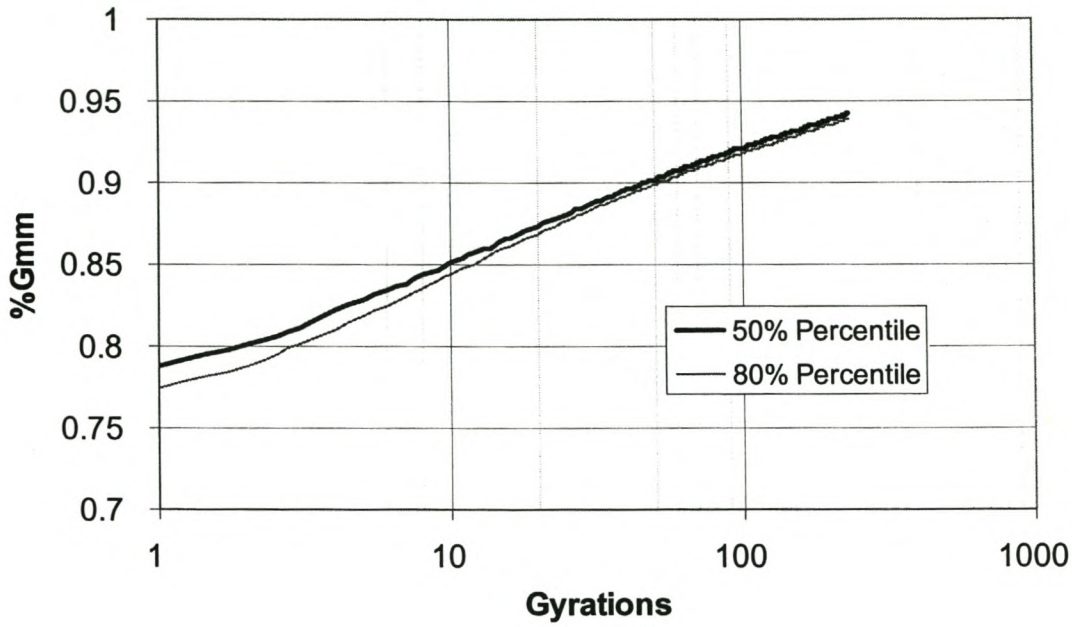

Figure E - 1. Gyratory Compaction Curves for G1eer with 1% Foamed Bitumen and No Cement

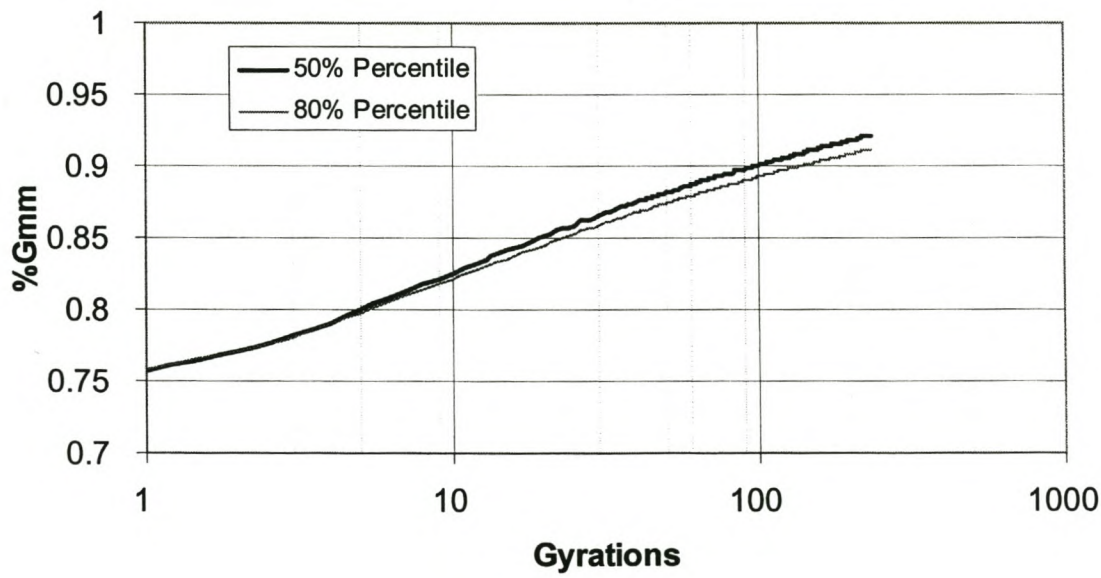

Figure E - 2. Gyratory Compaction Curves for G1eer with 2% Foamed Bitumen and No Cement

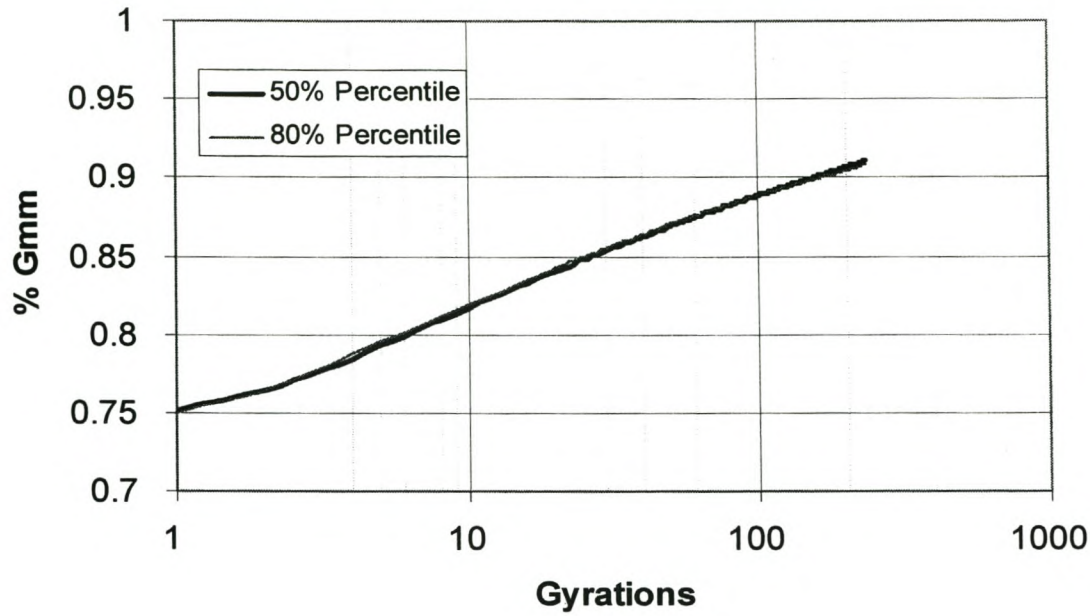

Figure E - 3. Gyratory Compaction Curves for G1eer with 2% Foamed Bitumen and 1% Cement

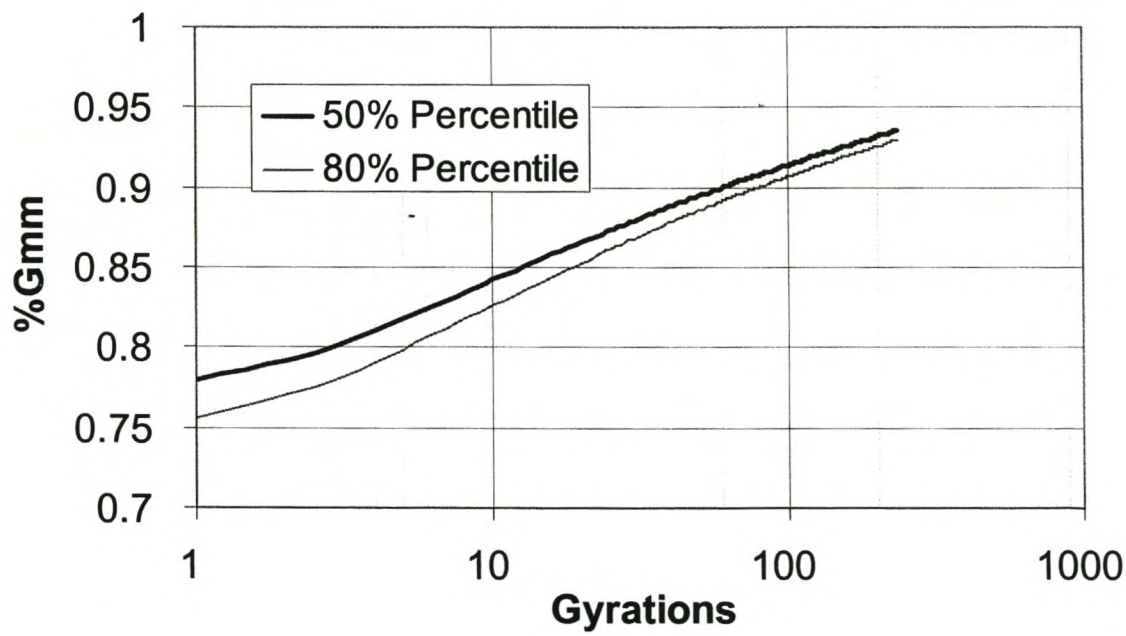

Figure E - 4. Gyratory Compaction Curves for G1eer with 4% Foamed Bitumen and No Cement

3. MOHR-COLOUMB DIAGRAMS FOR TRIAXIAL TESTS ON GRANULAR AND EQUIVALENT COLD FOAMED BITUMEN MIXES

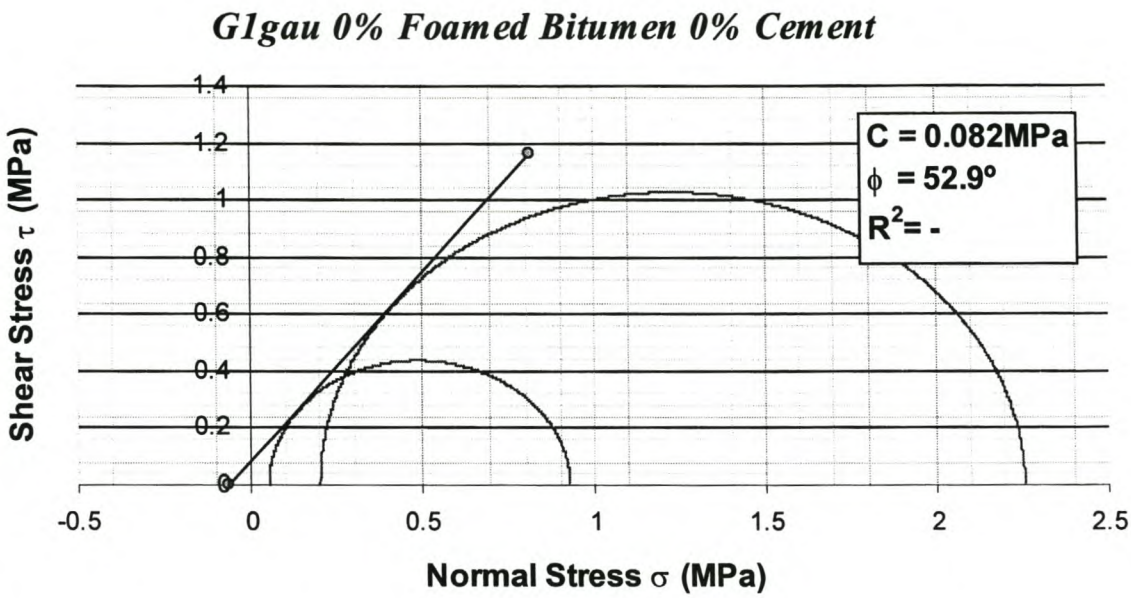

Figure E - 5. Mohr-Coloumb Plot of Monotonic Triaxial Tests on G1gau Granular Material

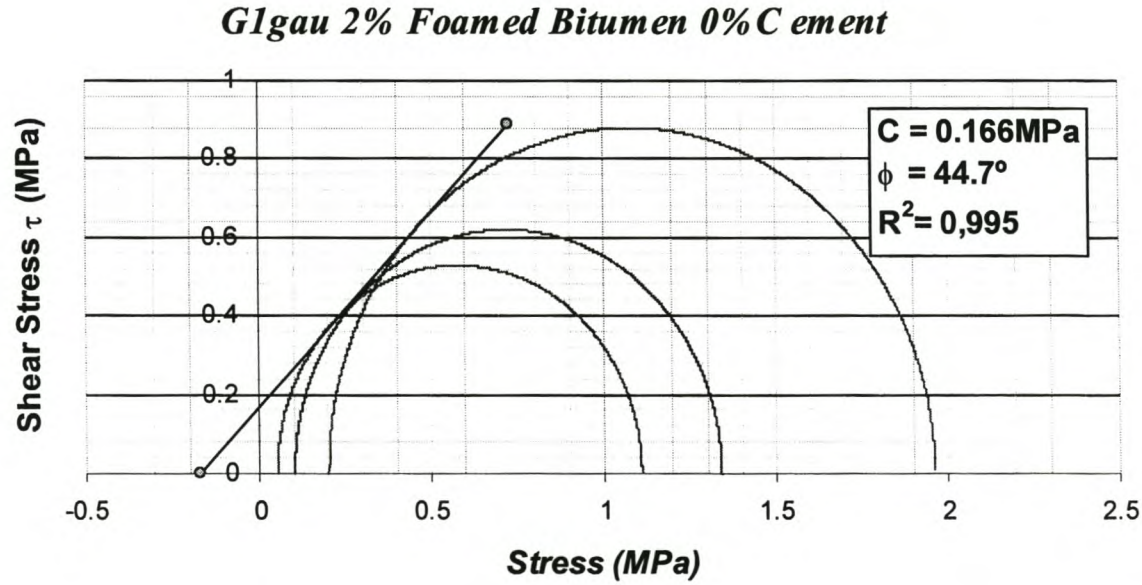

Figure E - 6. Mohr-Coloumb Plot of Monotonic Triaxial Tests on G1gau$_2$ Foamed Mix

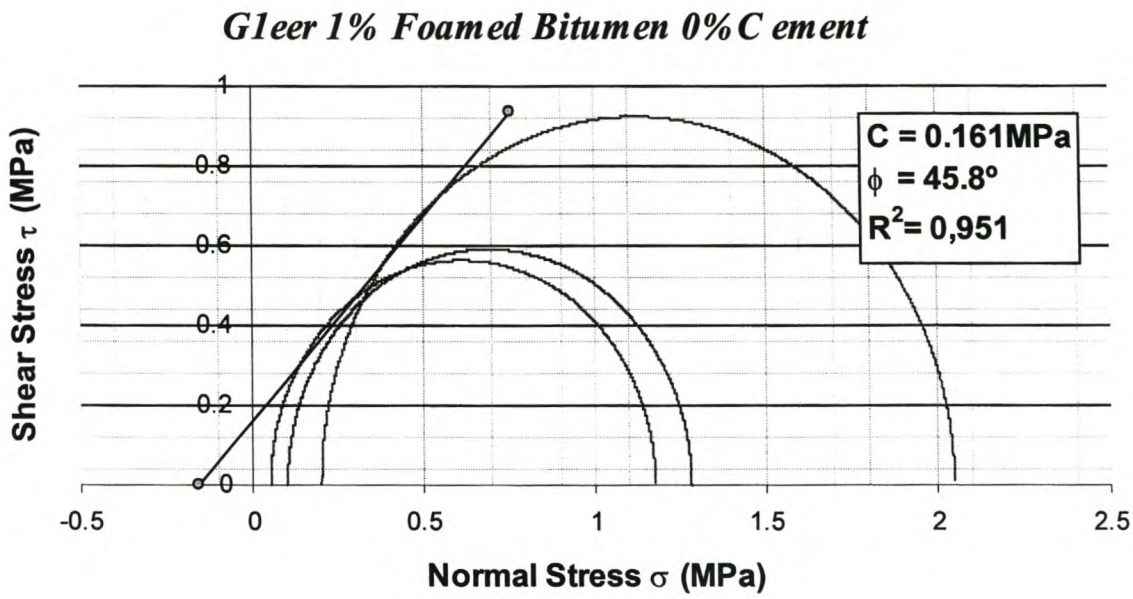

Figure E - 7. Mohr-Coloumb Plot of Monotonic Triaxial Tests on G1eer$_1$ Foamed Mix

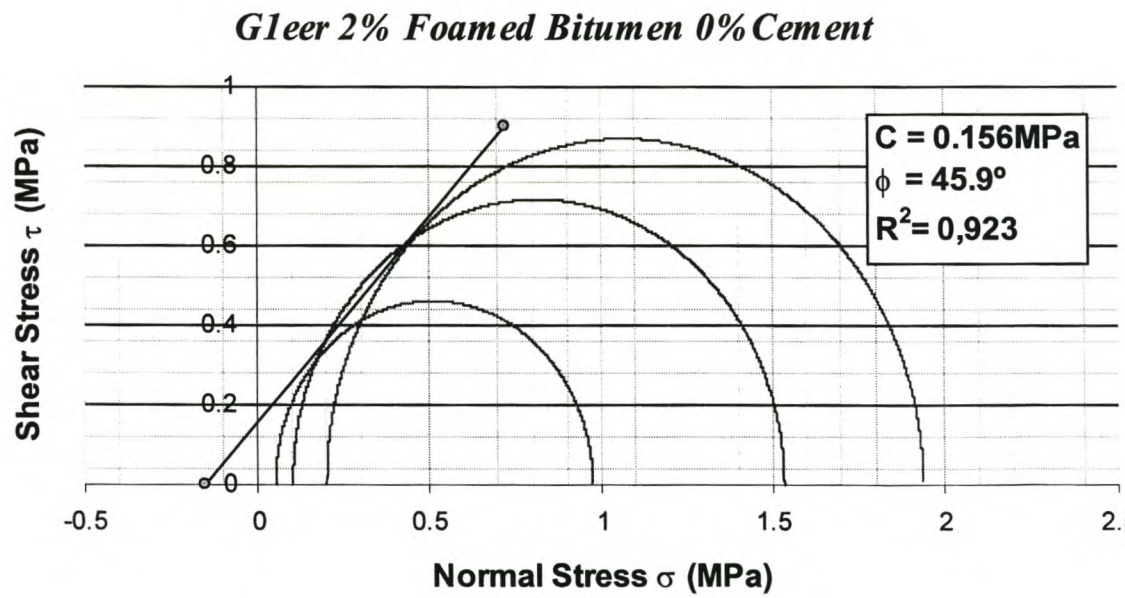

Figure E - 8. Mohr-Coloumb Plot of Monotonic Triaxial Tests on G1eer$_2$ Foamed Mix

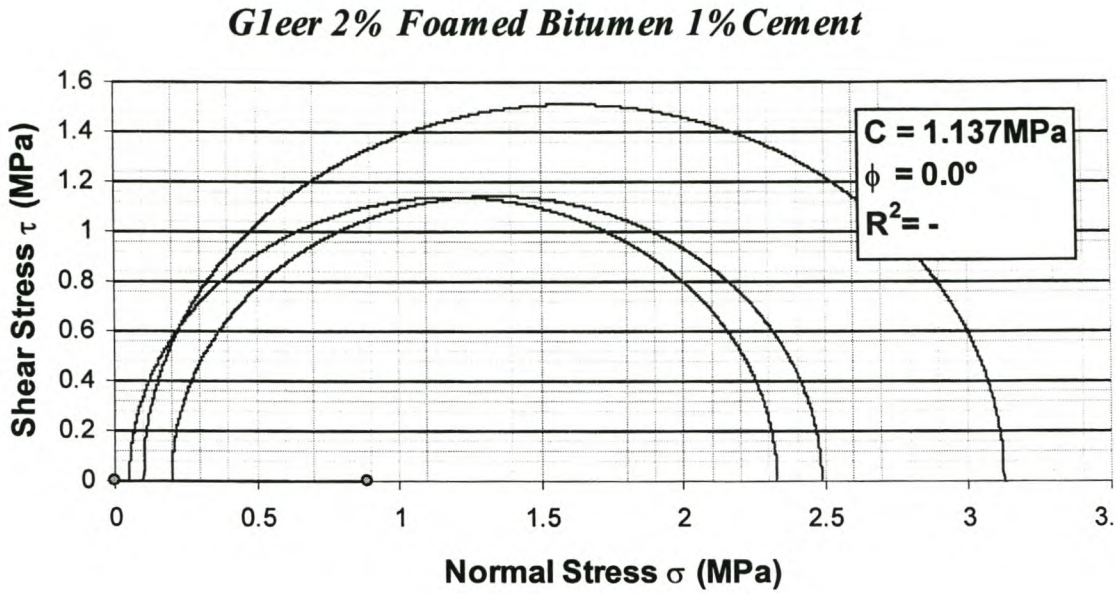

Figure E - 9. Mohr-Coloumb Plot of Monotonic Triaxial Tests on $G1eer_{2c}$ Foamed Mix

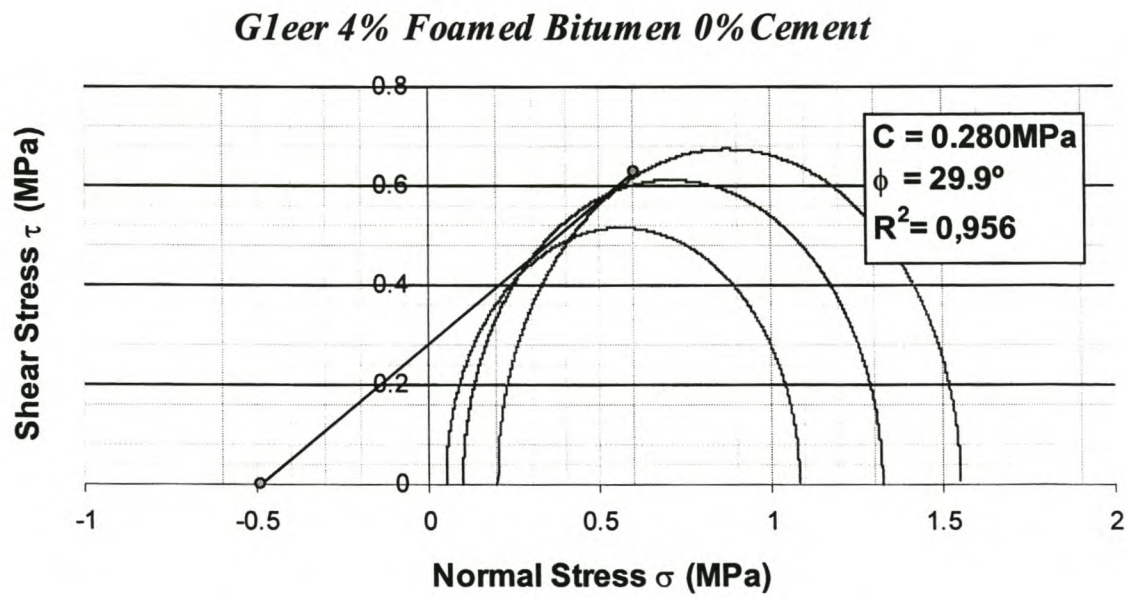

Figure E - 10. Mohr-Coloumb Plot of Monotonic Triaxial Tests on $G1eer_4$ Foamed Mix

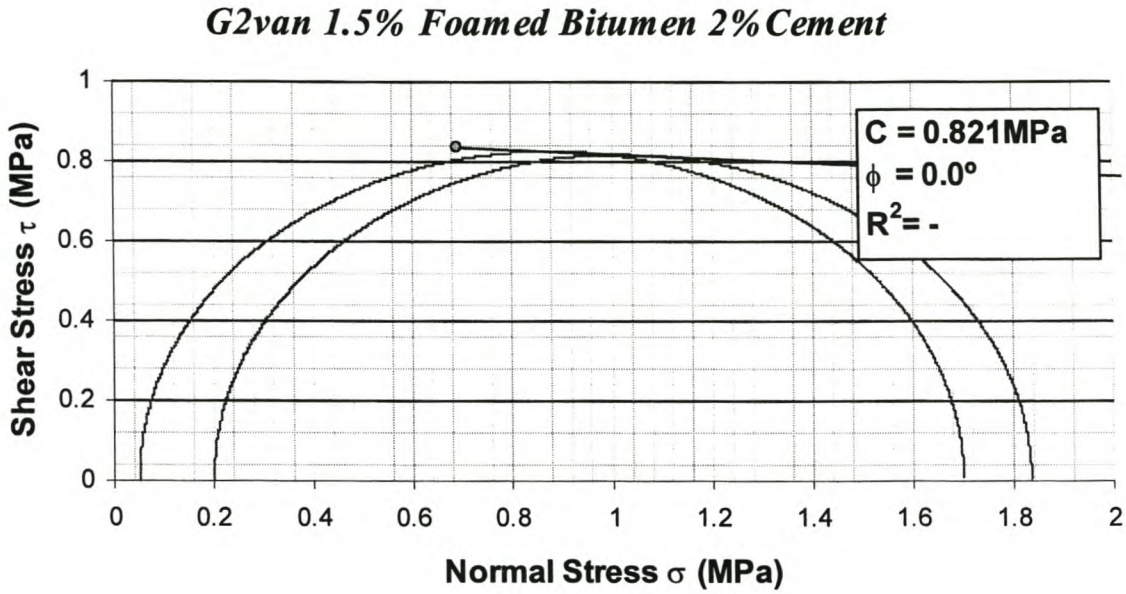

Figure E - 11. Mohr-Coloumb Plot of Monotonic Triaxial Tests on G2van$_{1.5}$ Foamed Mix

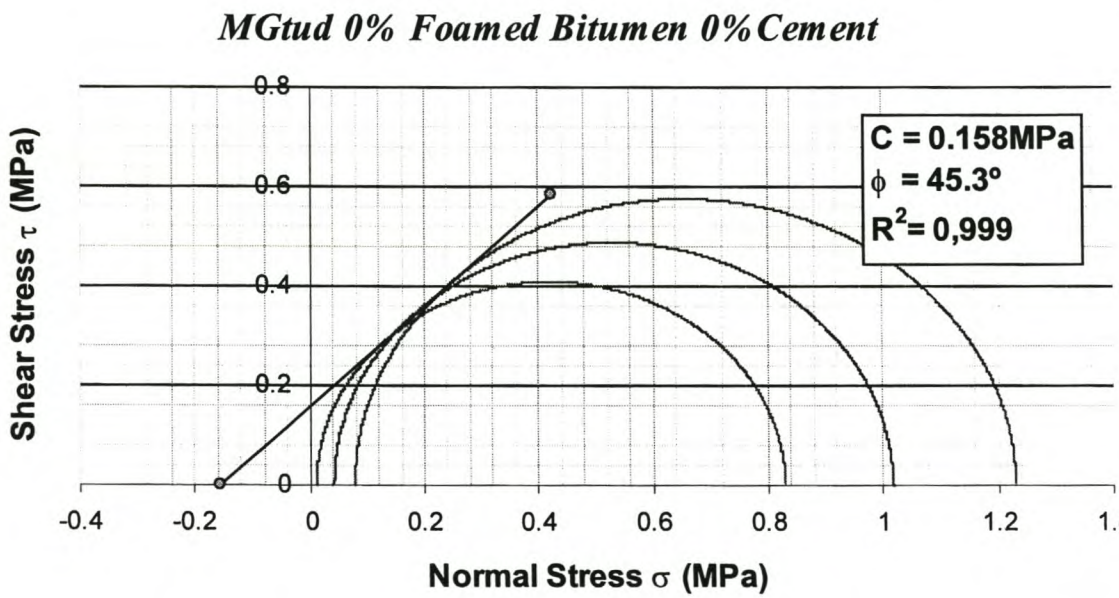

Figure E - 12. Mohr-Coloumb Plot of Monotonic Triaxial Tests on MGtud Granular Material (22:78 Brick:Crushed Concrete)

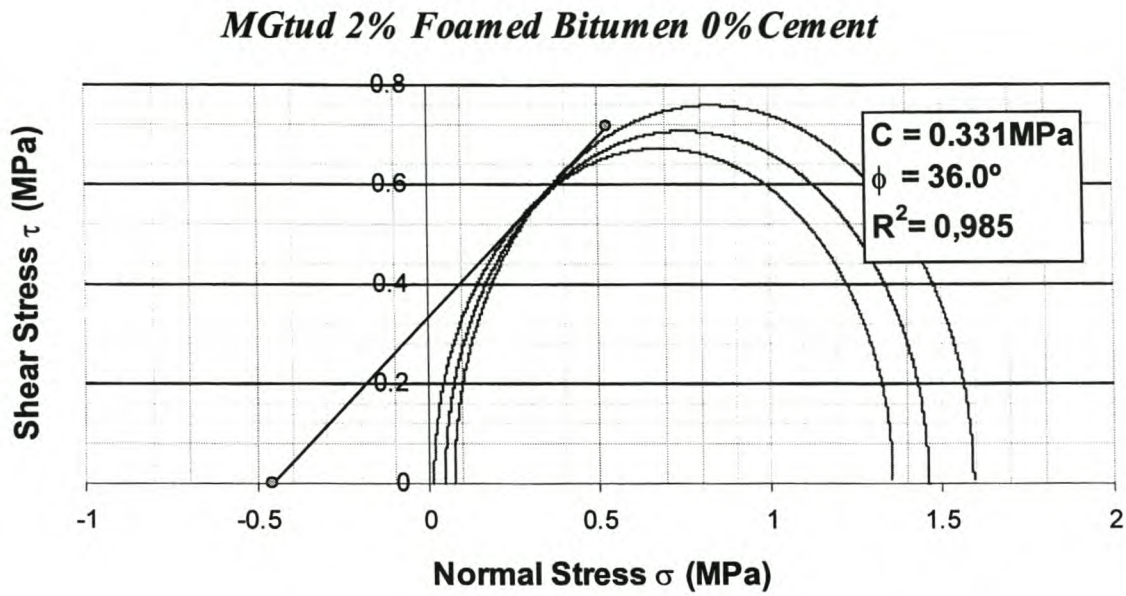

Figure E - 13. Mohr-Coloumb Plot of Monotonic Triaxial Tests on MGtud$_2$ Foamed Bitumen Mix

4. PROCEDURE FOR RESILIENT DEFORMATION TRIAXIAL TESTS (M_r-θ)

1. Specimens are sealed using rubber membranes and set-up within the test cell.
2. A constant cell pressure is applied using pressurised air. Initially a confining pressure of 50 kPa is used.
3. A pre-load of 20 kPa is applied to seat the specimens (including dead-weight).
4. A vertical axial load is applied to the specimen to yield a deviator stress of 100 kPa. This load is pulsed initially for 1200 conditioning cycles using a stress controlled Haversine signal of 2 Hz.
5. The readings for load and displacement are then recorded over a period of 5 seconds. The load is monitored directly from the MTS and the vertical displacements of the specimen using three linear variable displacement transducers (LVDT's), two of which were connected to the triaxial cell.
6. The specimens are allowed to drain during the tests.
7. The deviator stress is then increased to 200 kPa and 120 conditioning cycles are applied. The readings are then recorded as before.
8. Following the same procedure, the deviator is increased in accordance with the stress levels required, repeating the conditioning cycles of 120 pulses for each test.
9. Once all the stress levels for a confining pressure of 50 kPa have been tested, the confining pressure is increased to 100 kPa. A deviator stress of 100 kPa is applied and the specimen conditioned for 1200 cycles.
10. Thereafter the readings for load and displacement are recorded.
11. As before, 120 conditioning cycles are applied between the tests at different deviator stresses but the same confining pressure. Again the deviator stresses are applied in accordance with the required values.

12. The 1200 conditioning cycles are only reapplied when the confining stress (cell pressure) was increased from 100 kPa to 200 kPa.
13. These triaxial tests are in accordance to an amended procedure to the Maree (1979) method. Maree applied 1000 conditioning cycles at a specific axial load before recording the load and vertical displacements for modulus determinations. After a series of tests at increasing axial loads and varying confining pressures the specimens were pulsed for an additional 10 000 cycles and the test series repeated.

5. RESILIENT MODULUS DIAGRAMS FROM TRIAXIAL TESTS ON GRANULAR AND EQUIVALENT FOAMED BITUMEN MIXES

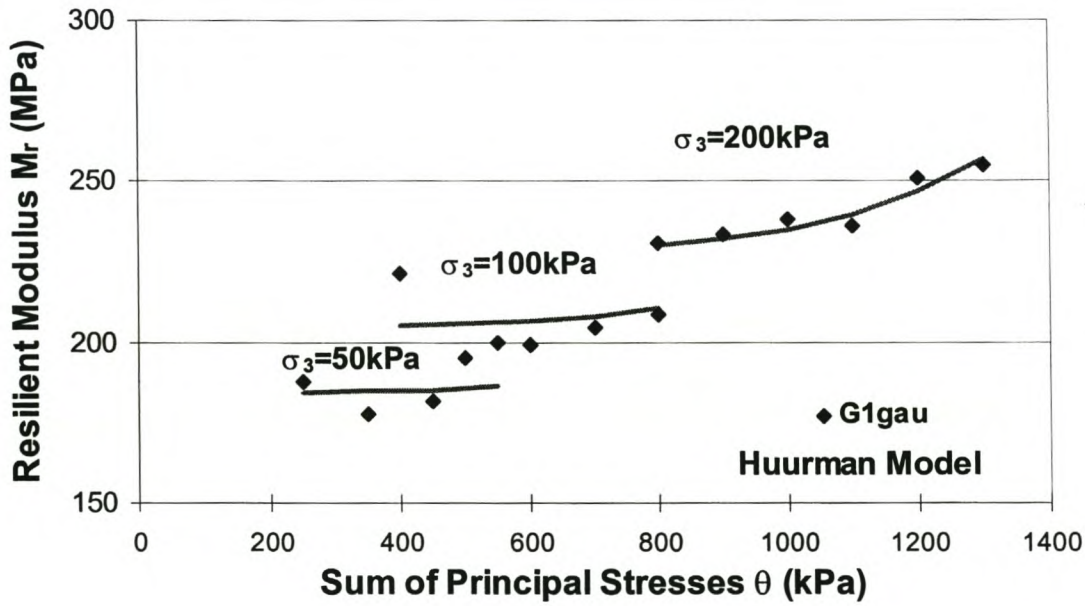

Figure E - 14. Resilient Modulus as a Function of Total Stress from Triaxial Tests for G1gau Granular Material

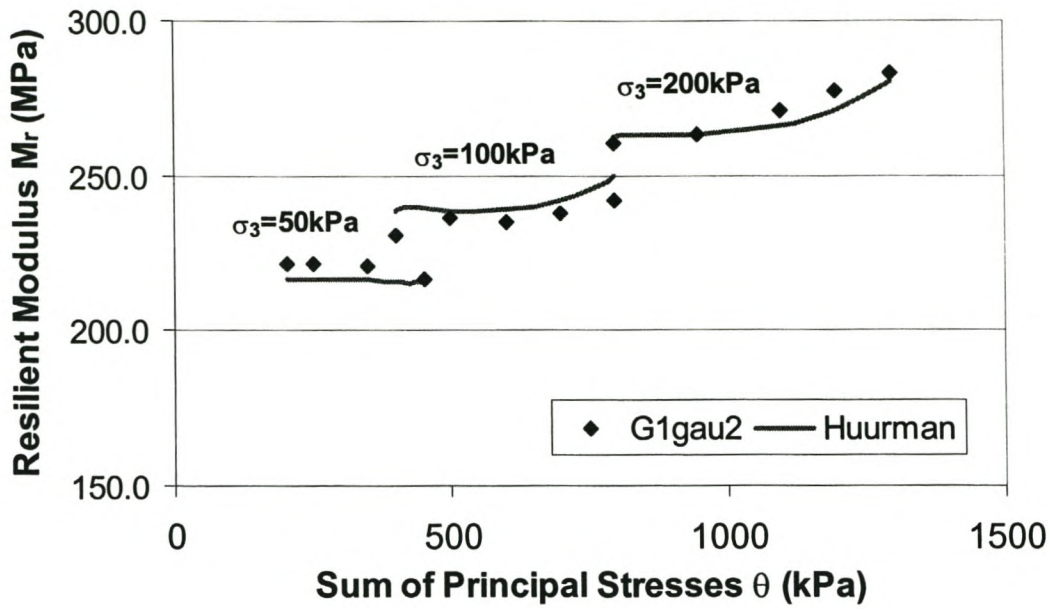

Figure E - 15. Resilient Modulus as a Function of Total Stress from Triaxial Tests on $G1gau_2$ Foamed Bitumen Mix with 2% Binder and 0%Cement

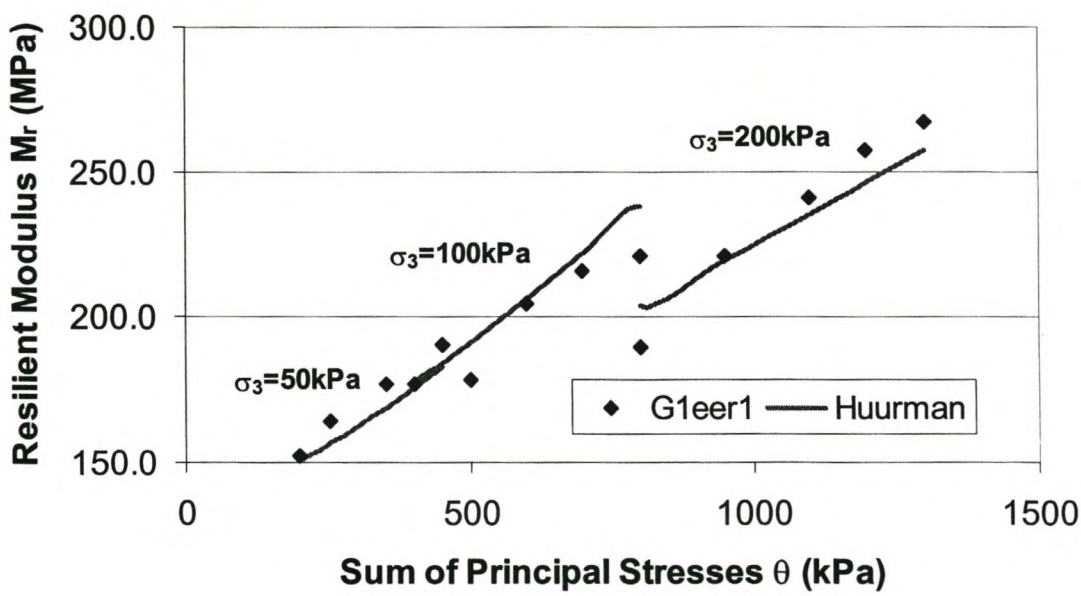

Figure E - 16. Resilient Modulus as a Function of Total Stress from Triaxial Tests on $G1eer_1$ Foamed Bitumen Mix with 1% Binder and 0% Cement

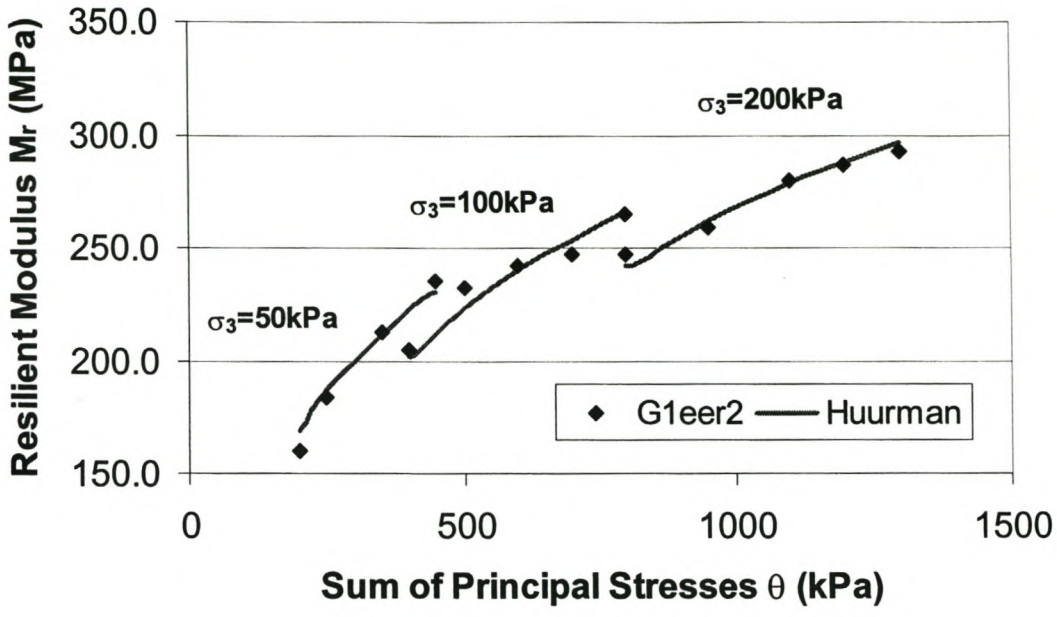

Figure E - 17. Resilient Modulus as a Function of Total Stress from Triaxial Tests on $G1eer_2$ Foamed Bitumen Mix with 2% Binder and 0% Cement

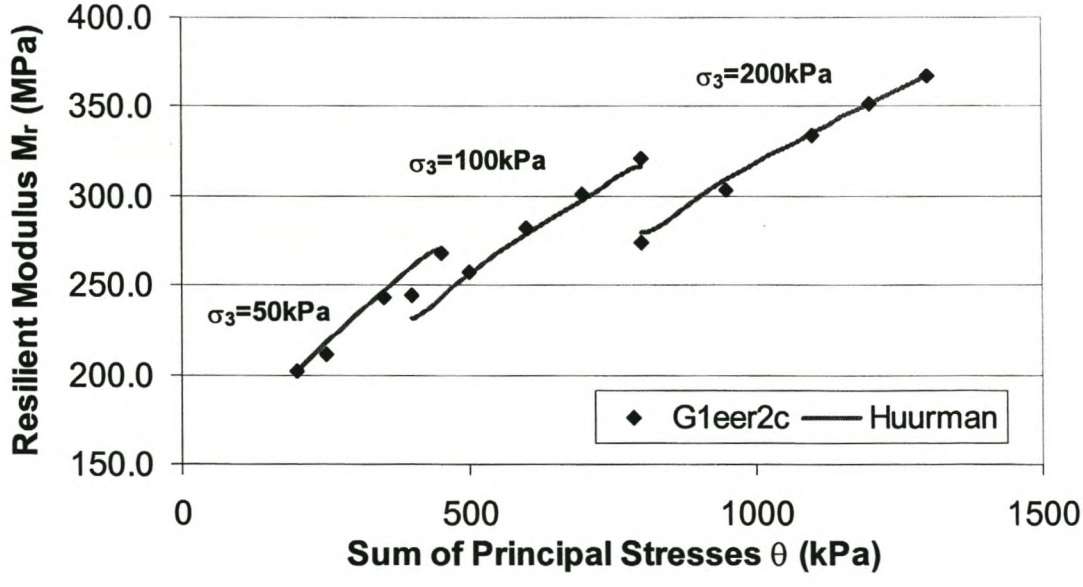

Figure E - 18. Resilient Modulus as a Function of Total Stress from Triaxial Tests on $G1eer_{2c}$ Foamed Mix with 2% Binder and 1% Cement

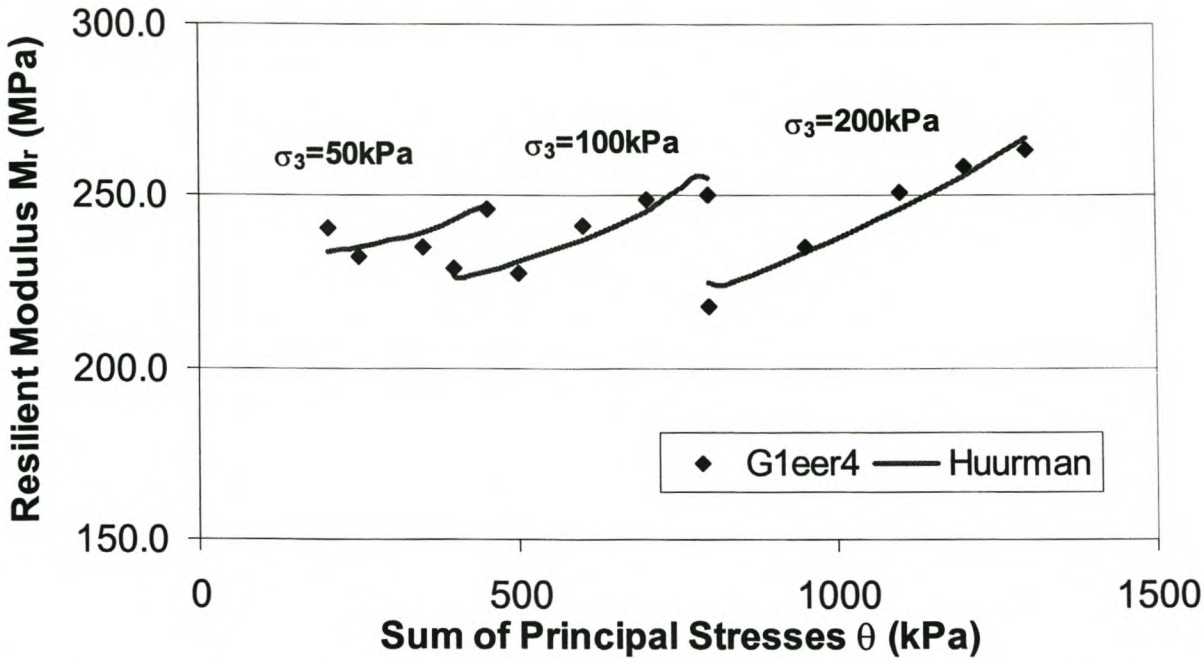

Figure E - 19. Resilient Modulus as a Function of Total Stress from Triaxial Tests on $G1eer_4$ Foamed Mix with 4% Binder and 0% Cement

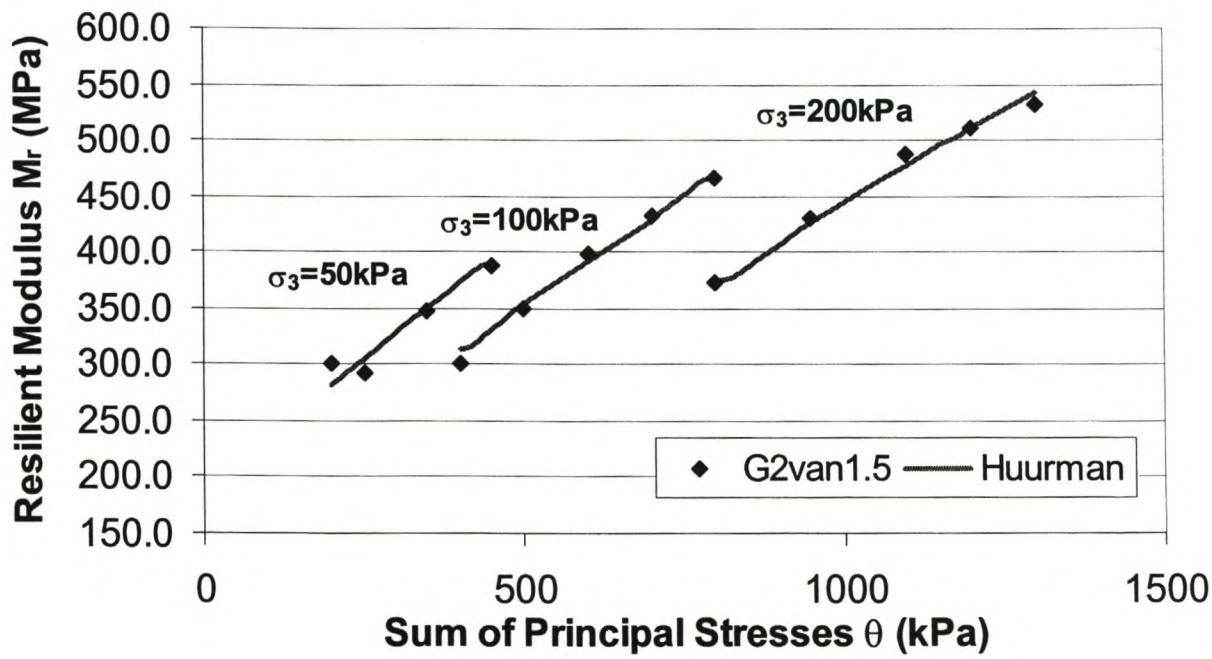

Figure E - 20. Resilient Modulus as a Function of Total Stress from Triaxial Tests on $G2van_{1.5}$ Foamed Mix with 1.5% Binder and 2% Cement

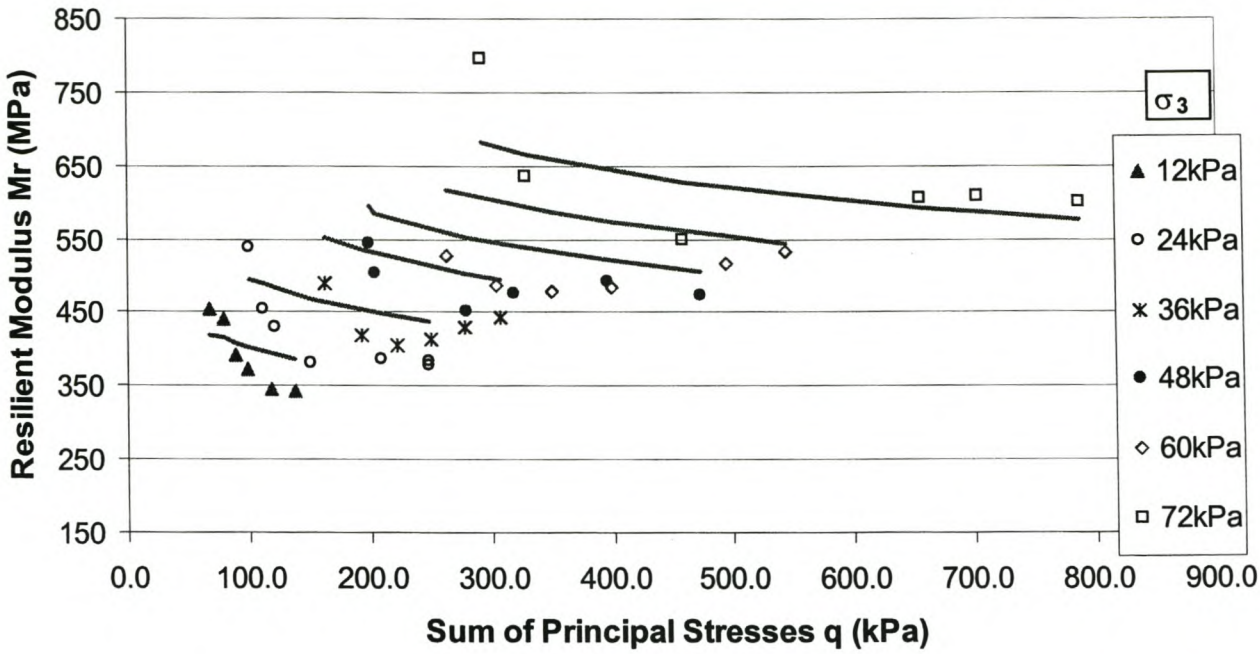

Figure E - 21. Resilient Modulus as a Function of Total Stress from Triaxial Tests on MGtud Granular Material

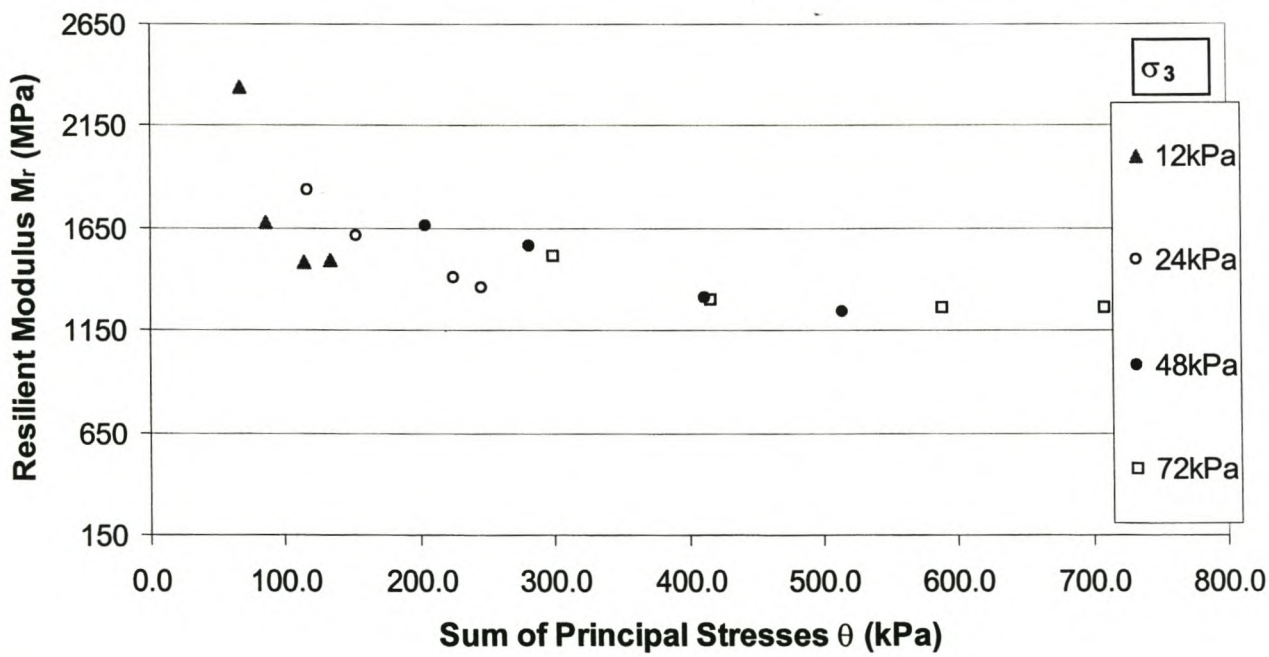

Figure E - 22. Resilient Modulus as a Function of Total Stress from Triaxial Tests on $Mgtud_2$ Foamed Mix with 2% Binder 0% Cement, No Conditioning

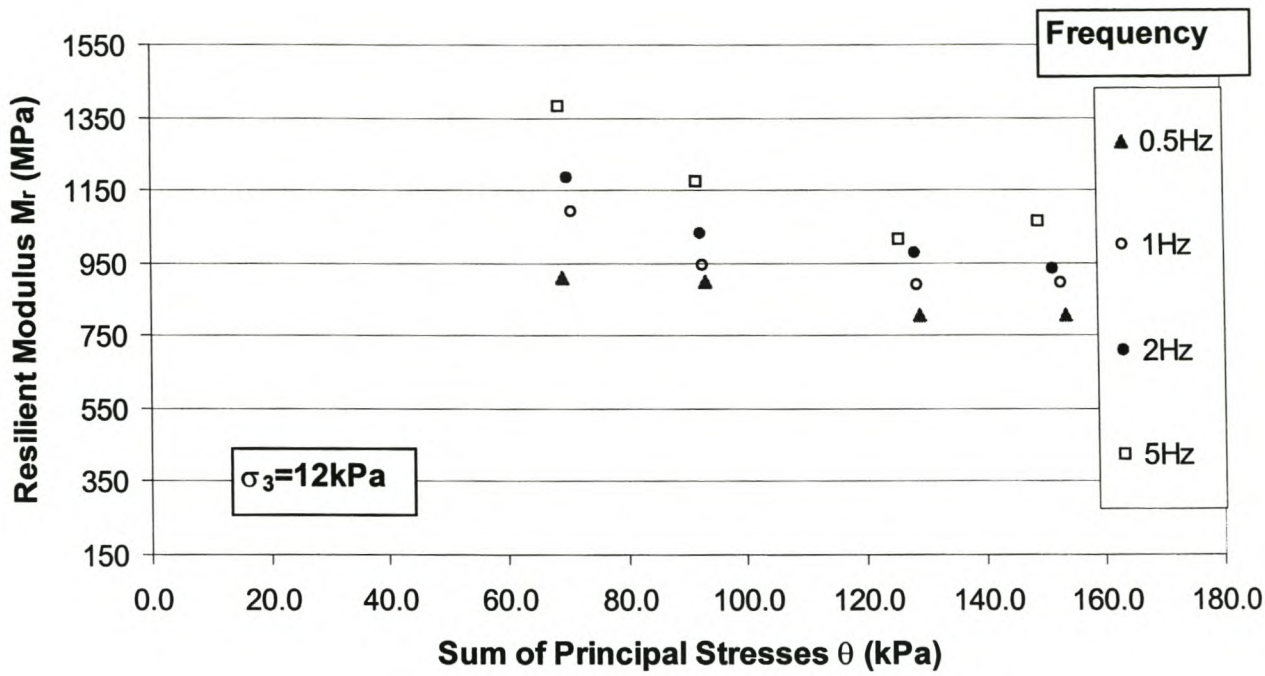

Figure E - 23. Resilient Modulus as a Function of Total Stress from Triaxial Tests on MGtud$_2$ Foamed Mix at Different Loading Frequencies

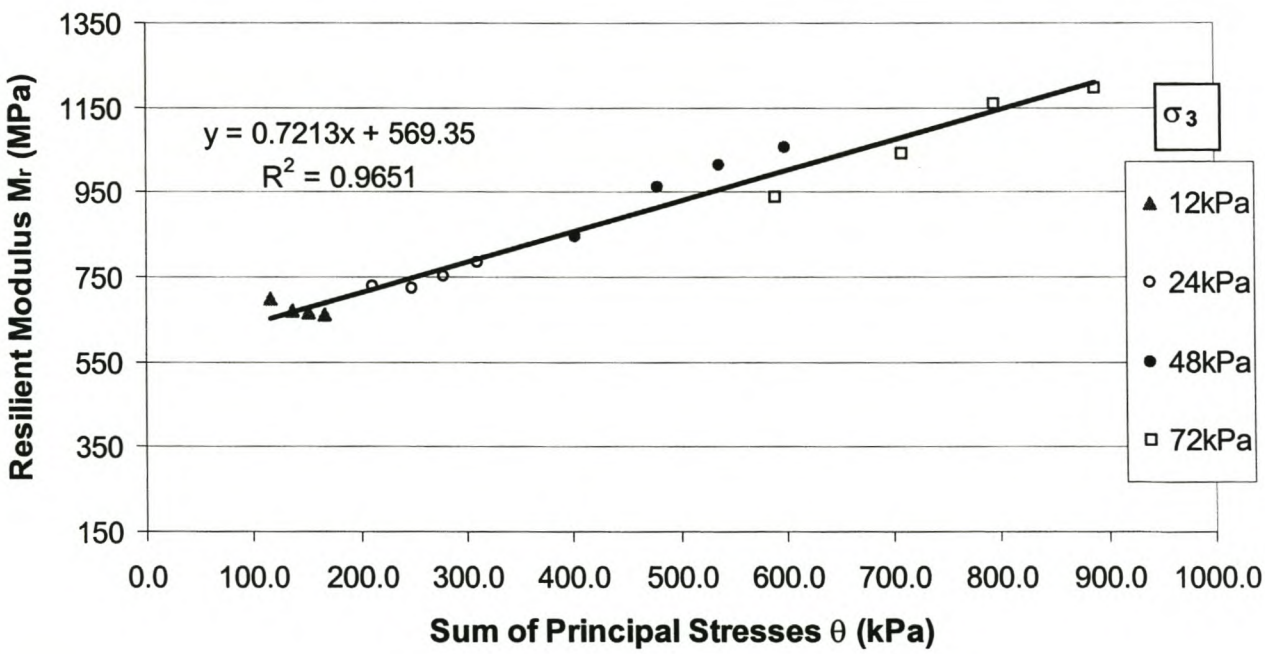

Figure E - 24. Resilient Modulus as a Function of Total Stress from Triaxial Tests on MGtud$_2$ Foamed Mix after 10 000 Conditioning Cycles at $\sigma_d/\sigma_{d,f}$ of 40%

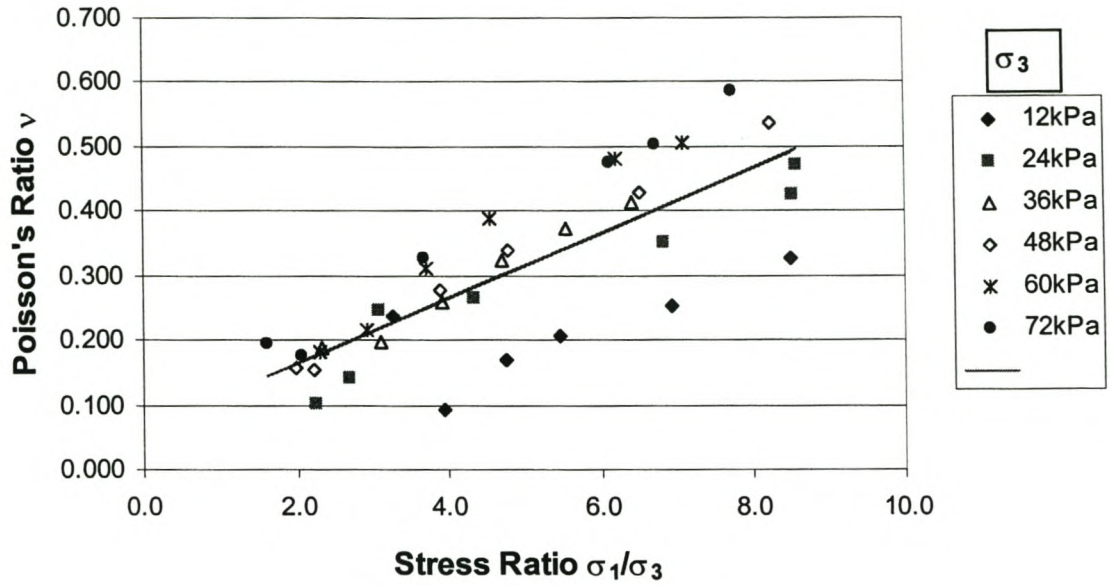

Figure E - 25. Poisson's Ratio as a Function of Stress Ratio σ_1/σ_3 from Triaxial Tests for MGtud Granular Material

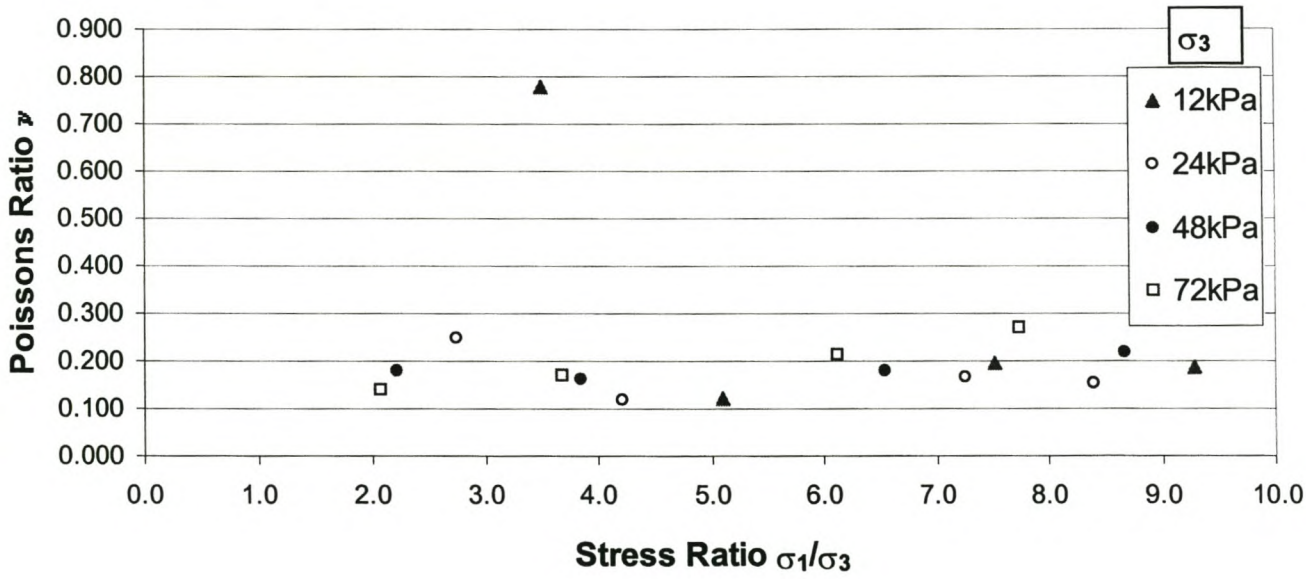

Figure E - 26. Poisson's Ratio as a Function of Stress Ratio σ_1/σ_3 from Triaxial Tests for $MGtud_2$ Foamed Mix before Conditioning

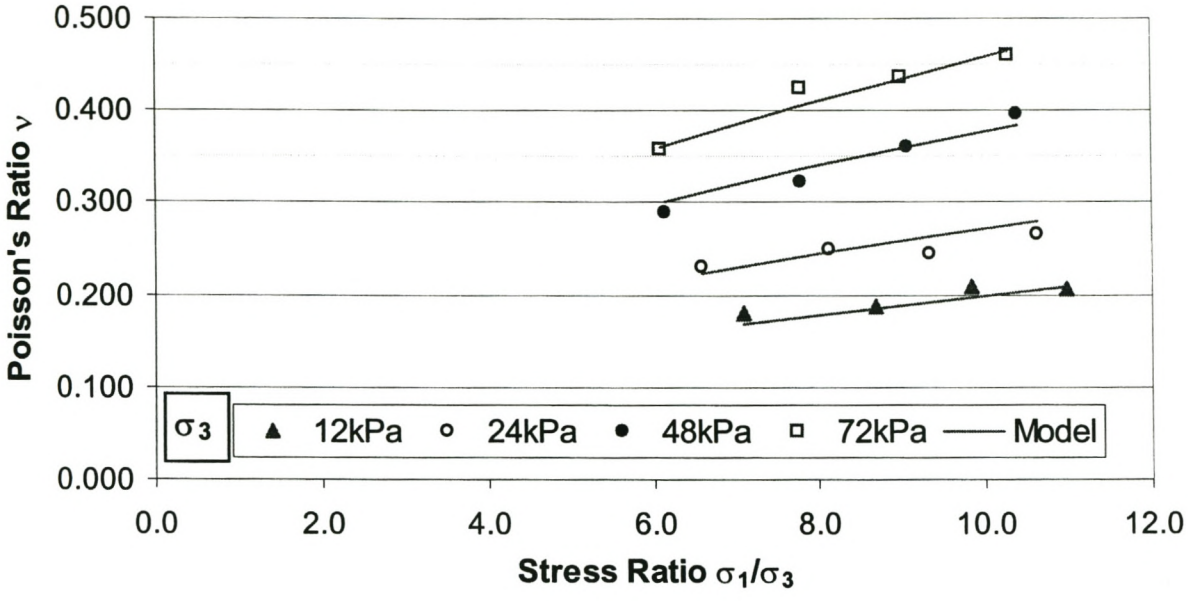

Figure E - 27. Poisson's Ratio as a Function of Stress Ratio σ_1/σ_3 from Triaxial Tests for MGtud$_2$ Foamed Mix after Conditioning with 10 000 Load Pulses

APPENDIX F

PRACTICAL GUIDELINES FOR THE DESIGN AND USE OF COLD AND HALF-WARM FOAMED BITUMEN MIXES

The findings of the research into foamed bitumen mixes detailed in this dissertation that are considered pertinent to practitioners, have been distilled into the sections of this appendix. Each section of Appendix F provides a "map" of a particular method or procedure in order to navigate the reader through the relevant portions of the document without such a person having to wade through its entire contents. Where additional information is required, the reader is referred to the relevant chapter.

1. PROCEDURE FOR OPTIMISATION OF FOAMED BITUMEN PROPERTIES

The suitability of a selected bitumen and its optimal conditions for foam production can be determined in terms of temperature, application rates of foamant water and, where applicable, foamants.

- For a specific type of bitumen at a given temperature, the foam properties should be measured following the testing procedure given in Appendix A. This can be done for a range of foamant water application rates or for additive (foamant) application rates. If the "foamability" of the bitumen is considered sensitive to its temperature, tests should be carried out at a range of bitumen temperatures too. At least three repeat tests are necessary for acceptable statistical reliability.
- The Foam Index is then calculated from the foam properties measured and used to optimise the application rate of either water or additive or both, see Section 4 of Chapter 3.
- The optimal Foam Index should be checked against the allowable lower limits for different types of foamed mixes e.g. surface dressings, cold mix, half-warm mixes etc, see Section 4.3 of Chapter 3.

2. DETERMINATION OF STIFFNESS OF FOAMED BITUMEN: FILLER MASTIC

The stiffening effect of combining filler and binder in a foamed bitumen mix can be determined through the analysis of the voids in the filler and a knowledge of the filler:binder ratio in the mix. This is applicable to cold foamed mixes manufactured in optimal moisture conditions in terms of mixing, with aggregate at 25°C.

- Determine the voids in compacted filler from the specific mix for the fraction smaller than 0,075mm in accordance with the procedure of Anderson (1987), see Chapter 4 Section 2.1.
- Calculate the Percentage Bulk Volume using the voids in the filler and the appropriate filler:binder ratio.
- Determine the change in Softening Point of the binder through the inclusion of the moist filler using Figure 4-5 or Equation 4-2. Compare this change with the equivalent stiffening of HMA mastic using the same figure. The limits of $60\%>V_{db}>55\%$ for HMA are inapplicable to foamed mixes. The V_{db} does however provide an indication of the expected behaviour of a foamed mix i.e. $V_{db}>50\%$ for foamed mastic will create very mixtures of a very stiff nature.

3. OPTIMAL BLENDING OF SAND FRACTIONS IN FOAMED MIXES

Optimal properties of a cold foamed mix may be obtained through the minimisation of voids in the mineral aggregate (VMA) of the sand fraction. The VMA_{sand} can be used as a criterion for establishing the selection of blending ratios of sand fractions.

- Determine the specific gravity of the separate sand samples selected for blending in the mineral aggregate.
- Using a range of blending ratios, determine the composite VMA of the sand fraction for each blend with 10 000 blows of the Engelsmann Apparatus, see Chapter 4 Example 4-2 and Appendix B.
- Select the optimal blend of sand fractions in terms of minimum VMA_{sand}.

4. SUITABILITY OF SAND GRADATION FOR FOAMED MIX

If the gradation of a mineral aggregate includes a gap, this could be detrimental to the mix. This procedure is designed to identify gradations that can cause problems and require modification.

- The mass gradation curve of the mineral aggregate for foamed bitumen treatment is converted to a volumetric gradation using the specific gravity of the different fractions.
- The procedure of Chapter 4 Section 2.2.2 is used to calculate the Gradient Ratio (Equation 4-6) for the gradation. If the Gradient Ratio is greater than or equal to 4, then blending is necessary to modify the gradation, see Example 4-3.
- This procedure is unlikely to be necessary where an optimal blend of sand fractions has been established, see Section 3 above.

5. SUITABILITY OF ENTIRE SKELETAL STRUCTURE FOR FOAMED MIX

The spatial composition of coarse aggregate, sand and filler will determine the suitability of an entire gradation for treatment with foamed bitumen. This may be carried out using the "Magic Triangle" of Francken.

- Figure 4-22 of Chapter 4 provides a Triangle with different zones of suitability i.e.
  - Ideal Foamed Mix Grading
  - Suitable Foamed Mix Grading
  - High Optimum Binder Content Foamed Mix
- Any given skeletal structure can be plotted as a point on this chart and checked for general suitability for foamed mix.

6. LABORATORY FOAMED MIX PREPARATION PROCEDURE

In order to consider the fluids regime throughout the foamed mix production process and to select appropriate mixing and compaction methods, a set procedure is required for laboratory work.

- Figure 4-23 of Chapter 4 provides a flowchart of foamed mix preparation and testing procedures.
- Allowance is made for different types of mixers (blender or pugmill) and compactors (Modified AASHTO and Gyratory).

7. LABORATORY CURING OF FOAMED MIX

The simulation of field curing of foamed mixes is carried out on laboratory prepared specimens using moisture and temperature as the variables. Two different types of curing are outlined, as shown in the table.

Table F - 1. Curing Procedure for Laboratory Specimens of Foamed Mix

Curing Term	Curing Procedure for Specimen
Short term (7 to 14 days in road)	24 hrs in mould then 24 hrs at 40°C sealed in oven
Medium term (6 months in road)	24 hrs in mould, then 72 hrs at selected temperature sealed in oven, then dry out specimen to selected moisture content

- The temperature selected for the medium term cure is a function of the Mean Monthly Air Temperature of the region that the foamed mix layer is being designed for, see Figure 4 – 31 in Chapter 4.
- The Equilibrium Moisture Content to which the specimen should be dried is a function of Optimum Moisture Content, Binder Content and Climatic Area, see Table 4 – 10 of Chapter 4.

8. LABORATORY PRODUCTION OF HALF-WARM FOAMED MIXES

This research has lead to development of the "Half-warm foamed bitumen treatment process" which can be utilised to make asphaltic mixes with similar properties to HMA. At this point only laboratory production of the mixes has been carried out, although full-scale production is likely to follow. Procedures for the laboratory production of these special mixes are outlined below:

- If a Hobart® mixer is used in the laboratory production of the mixes, the mixing procedure provided in Appendix C is to be followed. Section 3.2 of Chapter 5 also provides details of mixing procedures.
- If a pugmill-mixer is used in the laboratory production of the mixes, the mixing procedure provided in Appendix D is to be followed.
- The moisture loss during the mixing process can be estimated using the equation provided in Section 3.3 of Chapter 5.
- The degree of coating of the aggregate that can be anticipated, depending on the temperature of the aggregate, is outlined in Section 3.4 of Chapter 5.

9. PRODUCTION PROCEDURE FOR COLD MIX BLOCKS

A simple procedure is proposed for the manufacture of cold mix asphaltic blocks using a Kango® Hammer.

- Section 4.2 of Chapter 6 provides a step-by-step account of how cold mix asphaltic blocks can be made.
- Details of the equipment required are also included in Chapter 6 and its references.
- A Ghant Chart of activities can be utilised to determine the production rates with varying plant and equipment, see Figure 6 – 21 of Chapter 6.

10. PERFORMANCE PREDICTION OF FOAMED MIXES IN ROAD PAVEMENTS

Models have been established for the prediction of permanent deformation behaviour of foamed bitumen mixes with up to 4% binder, when used in pavement layers. The two models that have been established differentiate between foamed mixes with and without cement. In order to carry out a pavement design for a structure incorporating a foamed mix layer, the following procedure:

- Determine the Mohr-Coloumb failure envelope i.e. C and ϕ for the particular foamed mix that is being considered. This is carried out at representative density and curing conditions. Triaxial testing with monotonic loading should be used with specimens of height : diameter ratio = 2:1 and maximum particle size : diameter ratio < 1:8. In the absence of such apparatus, an Unconfined Compressive Strength (UCS) Test and Semi-Circular Bending (SCB) Test can provide the Mohr Circles for the failure

envelope. These tests should be carried out using suitable procedures e.g. the friction reduction system detailed in Chapter 5 Section 4.3.1 should be used for the UCS, whilst the SCB Test as referred to in Section 4 of Chapter 5 should be utilised. Representative test temperatures e.g. 25 ºC and displacement rates e.g. 50 mm/min should be utilised.

- Determine the Resilient Stiffness (M_r - θ) relationship for the particular foamed mix that is being considered. This is carried out at representative density and curing conditions. Triaxial testing should be used with the same specimen geometry as above, however a conditioning procedure is necessary before testing, see Section 3.2.2 Chapter 7. Suitable stress conditions should be selected so that the $\sigma_d/\sigma_{d,f}$ ratios at a given σ_3 confining pressure result in a decline in M_r. This usually requires $\sigma_d/\sigma_{d,f}$ ratios of up to 60% and possibly higher (without permanent damaging the specimen). Suitable load frequencies should also be selected that is representative of traffic speed and depth of the layer in the pavement structure. The M_r - θ - $\sigma_d/\sigma_{d,f}$ model is most suited for representing resilient deformation of foamed mixes.
- A finite element analysis (FEA) of the pavement structure is required for determination of the stress and strains in the pavement structure under the design wheel load. A FEA programme such as NOLIP is suited for this purpose, see Section 4.2 of Chapter 7. Such an analysis should include representative models for the resilient stiffness of any layers exhibiting "granular type" or stress-dependent behaviour i.e. granular, unbound layers and foamed mix layers. Such layers should be subdivided into elements of 30 mm where possible. An iterative procedure is required to achieve convergence of the resilient stiffness in the elements of the pavement structure with an error of less than 5%. If models for the Poisson Ratio of the foamed mix are available from testing, these should also be incorporated in the analysis otherwise the model of Table 7 - 9 of Chapter 7 may be used as a guide.
- The results of the finite element analysis should be used to analyse the distribution of the $\sigma_d/\sigma_{d,f}$ ratio with depth in the foamed treated layer(s). A foamed mix layer *without* cement should have a limit of $\sigma_d/\sigma_{d,f} < 55\%$ whilst a foamed mix layer *with* cement should have a limit of $\sigma_d/\sigma_{d,f} < 52\%$. If these critical ratios are exceeded, then the pavement structure should be strengthened and the FEA repeated until acceptable ratios are achieved.
- In order to analyse the loss of performance of a foamed mix through exposure to moisture, the moisture exposure procedure outlined in Section 4 of Chapter 4 can be used. The new C and ϕ values of the material after moisture exposure can be determined using the tests recommended, after these parameters have been determined at optimum conditions. These shear properties allow for performance of the foamed mix to be determined with and without moisture exposure and thus a measure of the susceptibility of the material to moisture to be established.

APPENDIX G

STATISTICAL DESIGN OF EXPERIMENTS

1. INTRODUCTION

Research into materials used in pavement engineering forms an experiment that requires evaluation of statistical tendencies in its planning, execution and analysis. Guidelines of such statistical considerations that are pertinent to pavement engineering, are not readily available in literature however. This appendix aims to address this vacuum by providing an appraisal of some statistical tools and techniques that are applicable to experiments with road pavement materials and at the same time to highlight those that are pertinent to this particular study and have been utilised in it.

In order to carry out investigations into areas previously uncharted both efficiently and successfully, a researcher requires two qualities:

- knowledge of the subject matter and a level of intellect, and
- knowledge of strategy.

Albert Einstein's observation "*If we knew what it was we were doing, it would not be research, would it?*" could be perceived as a licence for a researcher to freely explore a specific field in whatever manner comes to mind; but this would be a shallow interpretation. More likely, the observation highlights the need for a sound strategy to navigate the unknown.

According to Box *et al.* (1978), the knowledge of strategy parallels knowledge of statistical methods in scientific investigation. Although it is possible to carry out an experiment with the knowledge of the subject matter but without statistics, the converse is not true; but more importantly, the most unequivocal results will be obtained using both subject-matter knowledge and strategy (or statistics).

Inherent variability is a state of nature and the resulting uncertainty must be taken cognisance of, as it cannot be controlled or reduced. The uncertainty pertaining to prediction or modelling error may be reduced, however, through the use of more accurate models or the acquisition of additional data (Ang and Tang, 1984). Experiments in pavement engineering need to take cognisance of the fact that the variability of road-building materials is notable. In addition, the data acquisition requires optimisation and the prediction models require careful formulation to minimise the two components of errors viz:

- systematic error, and
- random error.

Examples of variability on pavement engineering include AASHTO's (1986) very useful table of low, average and high standard deviations for strength, thickness, compaction and

other properties of pavements. In addition, Hudson *et al.*(1974) report of coefficients of variation of materials within a project in USA ranging between 9% and 24%, depending on the material type. Other coefficients of variation of include 7% and 12% for the ϕ angle of friction of gravel and sand respectively, and 40% for the cohesion parameter. Clearly, performance parameters such as the shear strength will have significant variance given the variability of their components. Notwithstanding this, statistical analysis was only considered in the quality control of road construction in South Africa in the 1970's and even then, it was initially applied to only a limited number of parameters. Statistics in experimentation and research in the road industry has not emerged to the level that could be expected in a field fraught with variation and requiring a tangible level of confidence in the risks that are taken. Instead client bodies in the Civil Engineering industry have historically taken the risk and subsequently adopted conservative philosophies to manage the risk.

Considering that Sir Ronald Fisher, both experimenter and statistician, pioneered the development of experimental design in the 1920's and in 1935 first published his two books *"The Design of Experiments"* (1951) and *"Statistical Methods for Research Workers"* (1958), pavement engineers have had sufficient time to become acquainted with these tools. The application thereof has however been slow and uninspiring. Properties of construction materials have not until recent decades been approached in terms of range of possible outcomes with respective likelihood of occurrence e.g. a probability density function. This probabilistic approach facilitates more realistic, consequential designs of experiments than a deterministic approach, if not the only realistic approach.

Using the background of probabilistic thinking, the design of an experiment involves the planning of the test procedure so that information will be collected which is relevant to the problem under investigation. The purpose of experimental design is to provide the maximum amount of information relevant to the problem under investigation, at the same time keeping the design as simple as possible and conserving time, money, personnel and experimental material. This is achieved by striving for:

- Statistical efficiency
- Resource economy.

Although these two aspects of experimental design appear clearly defined, there is a notable inter-relationship. The dependence becomes apparent as these two factors are considered in more detail.

1.1 Statistical Efficiency

In order to achieve statistical efficiency, the design phase of the experiment must be approached with consideration being given to statistical consequence and stochastic implications. At the outset, it is necessary to consider:

- the nature of the data to be collected,
- what measurements are to be made,
- what is known about the likely variation that is to be encountered, and

- which factors are likely to influence the variation in the measurements.

It is apparent therefore, that a sound knowledge of subject is necessary for statistical efficiency to be achieved. The researcher should assimilate as much pertinent existing information as is possible, before embarking on the design of the experiment i.e. a detailed literature study is of paramount importance. Parameters should be approached probabilistically and not deterministically, and their inference space should be carefully understood.

In attempting to understand the variation in the parameters, it is important to locate the origin of the variability. According to Hudson et al (1974), three sources of difficulty which typically confront the investigator are:

- experimental error (or noise),
- confusion of correlation with causation, and
- complexity of the effects studied.

These three factors, which are discussed in more detail later in this appendix, can be best mitigated through properly designed experiments and the employment of sound statistical methods.

1.2 Resource Economy

Resource economy is the derivation of the maximum benefit from an experiment, within a certain acceptable level of reliability, in terms of trends, models and conclusions drawn. It is achieved through a well contrived and implemented testing strategy.

Resource economy is achieved through a sound understanding of the requirements/needs of the experiment and the level of reliability of the results that is required. Ang and Tang (1975) showed that the accuracy of estimating the statistical parameters of a random variable, such as the mean value and variance, increases with the sample size. Naturally, a larger sample size increases the cost, and the optimal sample size will involve a trade off between accuracy and the cost of sampling. It is economically expedient, therefore, to restrict the scale of an experiment to the minimum that will deliver the desired information.

1.2.1 Optimising Sample Size

Many of the materials in pavement engineering are intrinsically non-homogeneous as they are sourced from nature. It is this heterogeneous character that causes the degree of variability that is prevalent in the mechanical properties measured in these materials. Consequently, conclusive trends with measured reliability can only be obtained from relatively large populations around each control variable. Unfortunately, the cost of material procurement, transport, preparation, treatment and testing with all of the appurtenant apparatus makes large populations of repeat tests prohibitively expensive and impractical. It is imperative, therefore, that the testing strategy be well conceived to derive the maximum benefit, within a certain acceptable level of reliability, in terms of trends and conclusions drawn from the experimentation. This is resource economy and it often

includes the exploration of extremes rather than subtle nuances, in order to cover the range of variability.

The American Association of State Highway and Transportation Officials (AASHTO, 1986) provide a useful method for determining the number of tests required in field data collection i.e. the size of a sample, to achieve the desired confidence level for a specific variable with a given standard deviation σ. The method uses a statistical quantity R called the "limit of accuracy", which represents the probable range of the true mean from the average at a specific level of confidence. The average is calculated from a sample of "n" tests. This is derived directly from the confidence levels for a specific parameter i.e. $100(1-\alpha)$ percent confidence that the (true) mean lies within the limits calculated.

The equation developed for the limit of accuracy is given as:

$$R = K_{\alpha}\left(\frac{\sigma}{\sqrt{n}}\right) \qquad \textbf{Equation G - 1}$$

Where,

K_{α} = standardised normal deviate, which is a function of the desired confidence level, $100(1-\alpha)$

σ = true standard deviation of the random variable (parameter) being considered i.e. of the entire population

n = number of observations

By dividing both sides of the equation by μ the population mean, the equation becomes:

$$\text{Percentage deviation in mean} = R.100/\mu = K_{\alpha}.\ COV/\sqrt{n} \qquad \textbf{Equation G - 2}$$

Where, COV = coefficient of variation (%)

Figure G - 1 provides a graphical representation of Equation G - 2. This is particularly useful where the required reliability is well defined such as in the roads industry in South Africa. The standard guidelines for road pavements (CSRA, 1996) define four discrete categories of road A, B, C and D with approximate design reliabilities of 95%, 90%, 80% and 50% respectively. Figure G - 1 may be used directly to evaluate the number of observations required for a specific parameter. Cognisance needs to be taken, however, of the influence of the specific variable being measured, along with other dependent and independent variables, on the performance function applicable to the particular pavement being analysed. This is investigated further in Section 3.3.

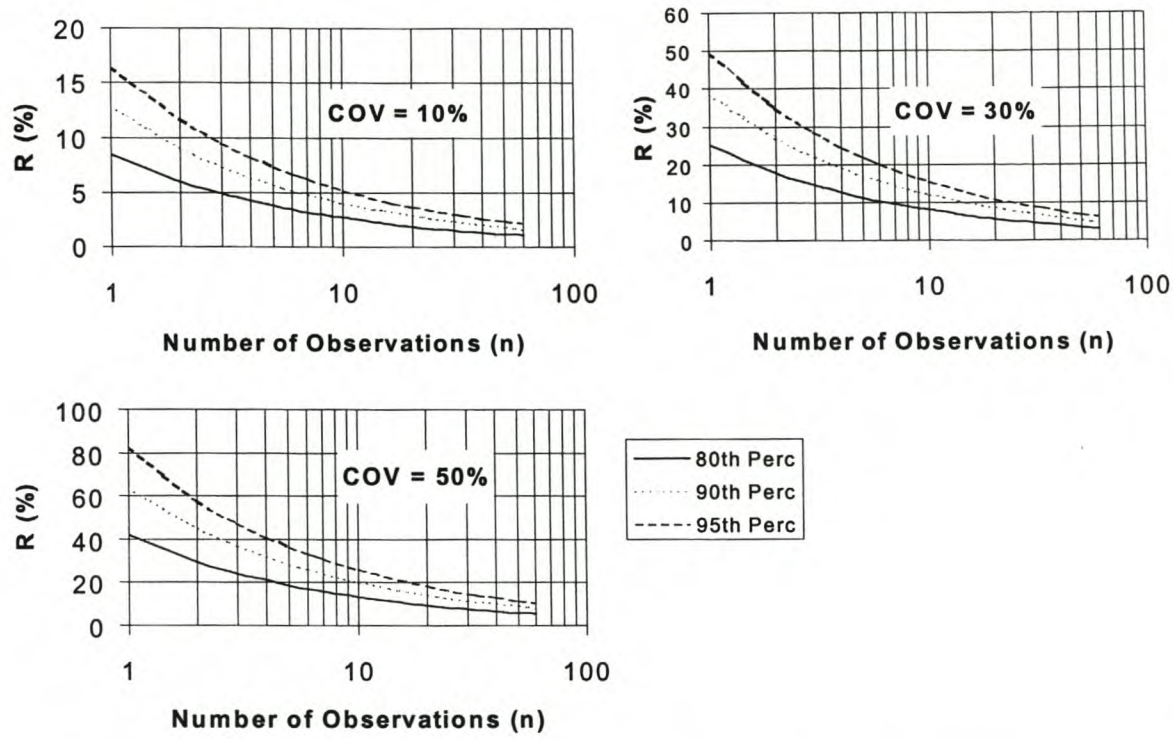

Figure G - 1. Number of tests required for specified level of reliability at a given coefficient of variance (after AASHTO, 1986)

It is apparent from Figure G - 1 that as an experimenter moves to the right on a particular curve i.e. increasing the number of observations, so diminishing returns are experienced in terms of level of reliability per observation (even when illustrated on a logarithmic scale). However, AASHTO emphasises that sufficient observations are necessary to adequately distance the experiment from the steep curve to the left where high variability will be experienced.

1.2.2 Decision Trees for Optimal Experiments

Experiments can be measured in monetary terms, so financial costs become the obvious consideration for optimisation in resource economy. But these often exclude the sometimes "intangible" factors such as the impact of time delays or benefits, use of invaluable resources, safety aspects etc, which should also be brought into consideration.

The following example provides insight into the use of Expected Monetary Value (EMV) as a criterion for the decision of whether it is beneficial to execute an experiment or not.

Example G.1 : Resource Economy

A scenario is created for this example to illustrate the applicability of resource economy in pavement engineering using decision trees. The reader is referred to Ang and Tang (1975) for the background to symbols, conventions and typical practices.

A pavement design engineer is given the brief by a road authority to design the rehabilitation of a rural road. The work is eminently suited to be carried out using "Deep in place recycling" of the in situ layers. Considering the lack of reliable design functions for the materials being treated, as well as the process, the engineer is not able to carry out a conventional design. There are three different options facing the designer regarding the mix design of the recycled layer and the pavement design for the rehabilitation:

1. *Alternative J* : A design based on expert opinion or "engineering judgement", which has no experimental cost. The reliability of the rehabilitation design is dependent on the climatic conditions during the road's 15 year structural design life. Traffic has been predicted to have negligible variability and growth. In particular, the mean annual precipitation (MAP) is considered the determining parameter for the road's integrity as follows:
   - Probability of failure = 20% if the MAP exceeds 1100mm for any year during the 15 year design life.
   - Probability of failure = 10% if the MAP does not exceed 1100mm for any year.

   From rainfall data it has been determined that:
   - P(MAP>1100mm over 15 years) = 25%

2. *Alternative M* : A design based on conventional mix design procedures and standard mechanical tests. The cost of the mechanical testing is estimated at R 30 000-00. As with the previous alternative, the road's integrity during the structural design life is largely dependent on rainfall:
   - Probability of failure = 10% if the MAP exceeds 1100mm for any year during the 15 year design life.
   - Probability of failure = 7% if the MAP does not exceed 1100mm for any year.

3. *Alternative I* : A research programme comprising a laboratory and field testing at a cost of R 150 000-00 that would enable an accurate mix design of the recycled layer and a design of the entire pavement. Once again, the road's integrity is a function of precipitation:
   - Probability of failure = 5% if the MAP exceeds 1100mm for any year during the 15 year design life.
   - Probability of failure = 3% if the MAP does not exceed 1100mm for any year.

Given failure within the structure design period, the premature rehabilitation cost function of the road, as selected for this example, is:

$$R = 20\ D^2 \qquad \textbf{Equation G - 3}$$

Where, D = design life of the road
R = cost of rehabilitation in real terms (Rands * 1000)

Development of cost functions such as Equation G - 3 provides a major challenge in pavement engineering and one of the reasons why risk and reliability is not often considered in this field. Many factors, for example, contribute to rehabilitation cost of a road and a simple function such as the one provided is not often applicable.

The expected cost of the rehabilitation given the alternative selected and the mean annual precipitation, may be expressed by E[RIJ,V_j]. Using this function, the relative costs of the alternatives can be quantified.

$$E(RIJ, V_j) = \sum_{d=0}^{\infty} 20d^2 . P_D[dIV_j]$$

$$= 20.\ E\ [D^2 IV_j]$$

$$= 20.\ [Var(DIV_j) + E^2(DIV_j)]$$

$$= 20\ [(15V_j) + (15V_j)^2]$$

$$= 300V_j + 4500V_j^2$$

$$E[RIJ] = \sum_{j=1}^{2} (300V_j + 4500V_j^n) P[V_j IJ]$$

$$= (300*0{,}25 + 4500*0{,}25^2)(0{,}2) + (300*0{,}75 + 4500*0{,}75^2)(0{,}1)$$

$$= 346{,}88$$

Similarly, $E[RIM] = (300*0{,}25 + 4500*0{,}25^2)(0{,}1) + (300*0{,}75 + 4500*0{,}75^2)(0{,}07)$

$$= 228{,}56$$

and $E[RIM] = (300*0{,}25 + 4500*0{,}25^2)(0{,}05) + (300*0{,}75 + 4500*0{,}75^2)(0{,}03)$

$$= 100{,}50$$

From these results a decision tree may be established to facilitate a graphical solution to be identified. Table G - 1 provides this solution, with rounded off figures.

Table G - 1. Decision tree for Design of Deep in Place Recycling

Design Option	Rainfall in any year	Pavement condition in SDP*	Cost of Experiment	Cost of Rehabilitat'n	Total Cost (Rands)
J	Heavy (0,25)	Failure (0,2)	0	346 000	346 000
		No fail. (0,8)	0	346 000	346 000
	Moder. (0,75)	Failure (0,1)	0	346 000	346 000
		No fail. (0,9)	0	346 000	346 000
M	Heavy (0,25)	Failure (0,1)	30 000	229 000	259 000
		No fail. (0,9)	30 000	229 000	259 000
	Moder. (0,75)	Failure (0,07)	30 000	229 000	259 000
		No fail. (0,93)	30 000	229 000	259 000
I	Heavy (0,25)	Failure (0,05)	150 000	101 000	251 000
		No fail. (0,95)	150 000	101 000	251 000
	Moder. (0,75)	Failure (0,03)	150 000	101 000	251 000
		No fail. (0,97)	150 000	101 000	251 000

*SDP = structural design period

Using the mini-max criterion, based on the Expected Monetary Value (EMV) criterion, which provides for the user minimising the maximum loss, Alternative I would be selected

for the rehabilitation task outlined. A minimum cost of R 251 000-00 in conjunction with a total risk of failure of (0,25*0,05+0,75*0,03) = 0,035 provides the optimal solution.

The benefits of a probabilistic approach to the design of experiments have been highlighted through this example. Although research experimentation is usually adjudicated through budgeting, and is seldom financially motivated, the given benefits of the latter are apparent. In reality, many of the statistics used in the example do not appear readily available to pavement engineers; however, a probabilistic rather than deterministic approach in conjunction with background research, can yield the indices required.

2. TYPES OF EXPERIMENTAL DESIGNS

According to Grivas (1986) there are three basic types of experimental design:

- Factorial design (completely crossed)
- Nested design (or hierarchical)
- Mixed design (combination of crossed and nested designs).

The selection of a particular design type would depend on:

- The scale of the experiment,
- Resources available,
- Expected range of applicability of the results,
- Level of significance of the results,
- Number of factors that require consideration in the experiment, and
- Other influences peculiar to the project or experiment.

It is not the scope of this thesis to describe these types of experiments further, suffice it to report that this subject matter is adequately covered in numerous publications.

3. PRINCIPLES OF EXPERIMENTAL DESIGN

The principles of experimental design, according to Anderson (1984), are:

- replication,
- randomisation, and
- local control.

These principles involve statistical methodology and economic analysis.

3.1.1.1 Replication

Replication implies the repetition of the same basic experiment or a portion of it, under different sets of test conditions. This is different to repeat testing which is two or more test runs for which the factor-level combinations and the test conditions are identical. Repeat tests carried out to determine variability between laboratories is termed *repeatability*. The variability associated with replicates reflects variation between two measurements taken at two different laboratories by two different individuals and is termed *reproducibility*.

The reasons for carrying out replication include the following :

- provision of an estimate of the experimental error which acts as a *"basic unit of measurement"* to assess either the significance of the observed differences or the confidence interval,
- provision of a more accurate estimate of experimental error than would be obtained from assumptions, and
- enabling of a more precise estimate of the mean effect of any factor.

The experimental unit may be defined as the unit to which a single treatment (which may be a combination of many factors) is applied in one replication of the basic experiment. Following on, experimental error is the failure of two identically treated experimental units to yield identical results. This experimental error is discussed in more detail below.

3.1.1.2 Randomisation

A basic assumption which is often applied to experimentation is that the observations (or errors therein) are independently distributed. Randomisation makes a test valid by making it appropriate to analyse data as though the assumption of independent errors is true. Randomisation is therefore introduced as a device to eliminate bias and is usually achieved by assigning factor-level combinations in a random order to the experimental units or test sequence. The opposite of a randomised design is a systematic design.

3.1.1.3 Local control

Local control is the balancing, blocking and grouping of experimental units employed in statistical design. The purpose of local control is to make experimental design more efficient, powerful and sensitive. The three elements of local control may be defined as follows (after Anderson, 1984) :

- Grouping is the placement of a homogenous set of experimental units into a group so that different groups may be subjected to different treatments.
- Blocking is the allocation of experimental units to blocks so that the units within a block are relatively homogenous while the greater part of predictable variation among units has been confounded with the effect of blocks.
- Balancing is obtaining the experimental units, grouping, blocking and assigning treatments to experimental units so that a balanced configuration results.

3.1.2 Experimental error

Experimental error is the variation produced by disturbing effects that are known and unknown to the researcher. Experimental error includes:

- errors of experimentation,
- errors of observation,
- errors of measurement,
- variation of the experimental material i.e. between the experimental units, and
- combined effects of all extraneous factors which could influence the characteristics of the study, but have not been singled out for attention in the current study.

The principles of experimental design require application within the framework of a current hypothesis that is tested against measured data and modified through statistical analysis and iteration. This is illustrated in Figure G - 2 where an experimental design is generated using a current hypothesis from present knowledge. The current knowledge should be considered important to progress, to warrant investigation. A window in the figure represents the design, as the true state of nature is distorted by noise. It is of paramount importance to recognise that the data is generated by a true state of nature. The process requires continual updating of the hypothesis by comparing the deduced state of nature with the actual data to lead to the convergence of the truth.

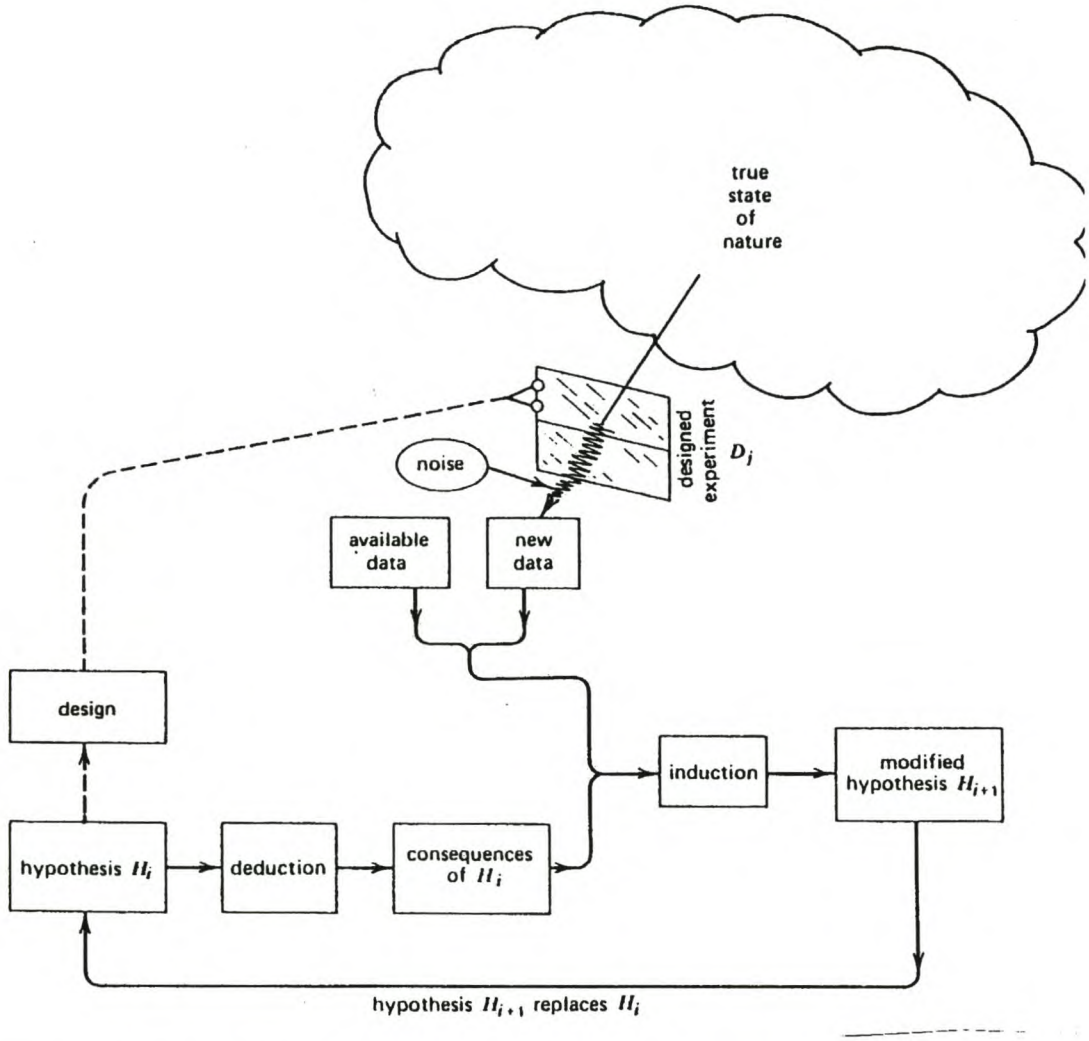

Figure G - 2. Data Generation and Analysis in an Experiment (Box *et al.*, 1978)

3.2 Experimental Design in Pavement Engineering

The framework of statistical experimental design outlined thusfar requires more specific detailing for application in pavement engineering. In particular, the subject matter being

investigated in this field through experimentation requires deeper understanding that stretches beyond the discrete results obtainable from tests, for an efficient experimental design to be fulfilled. Box *et al.* (1978) provide a flow diagram of some of the possible paths to be followed in response surface studies for general experiments, but this requires modification for application in pavement engineering. In particular, the emphasis placed on second-order strategy in the design and performance of an experiment is most often not applicable for road pavement materials due to the variability of first-order effects and irrelevance or insignificance of second order effects. For this reason the flow diagram has been redesigned to be relevant to experimentation in pavement engineering.

The techniques of experimental design provided in Figure G - 3 are not peculiar to pavement engineering; however, the field of investigation dictates the manner in which these tools should be applied. Some of the main features of the flow diagram are further clarified below.

The definition of the objectives of an experiment may seem obvious, recognition of the problem and succinct statement thereof is not always a simple procedure. A clear statement of the problem contributes to improved understanding of the phenomena and a better final solution. During the earlier stages of an experiment the most impact can be made on the efficiency with which an experiment is performed.

In the selection of the independent variables or factors of an experiment, the experimenter should identify the factors as either quantitative or qualitative. Where quantitative factors are identified, the experimenter needs to decide how they are to be controlled at desired values and measured. In addition, the ranges over which the factors are to be varied and the levels at which runs are to be made, require selection.

The response variable or independent variable should be selected and measured so as to provide relevant information with regard to the problem under study. Consideration of the probable accuracy of these measurements is also necessary. Some methods of determining this variance are outlined in Sections 3.2.1 and 3.2.2.

The use of transformations should be highlighted in the flow diagram as this technique can assist in the identification of the correct metric in which analysis should be conducted, even though reporting of results may be done in a more acceptable scale. In addition, the use of reciprocals, squares and logarithms has been found to provide useful transformations for pavement materials.

The flow-chart provides the facility for the improvement of reliability through increased replication of results. This may be carried out with the aid of Figure G - 3 and the applicable coefficient of variation for the subject of the investigation. This would provide due consideration for resource economy in the expansion of the experiment.

In the few cases in the investigation of pavement materials where second-order strategy is required, the flow diagram could be extended to incorporate a second phase. The second-order design can be used to augment the experiment with a more concentrated approach to data collection.

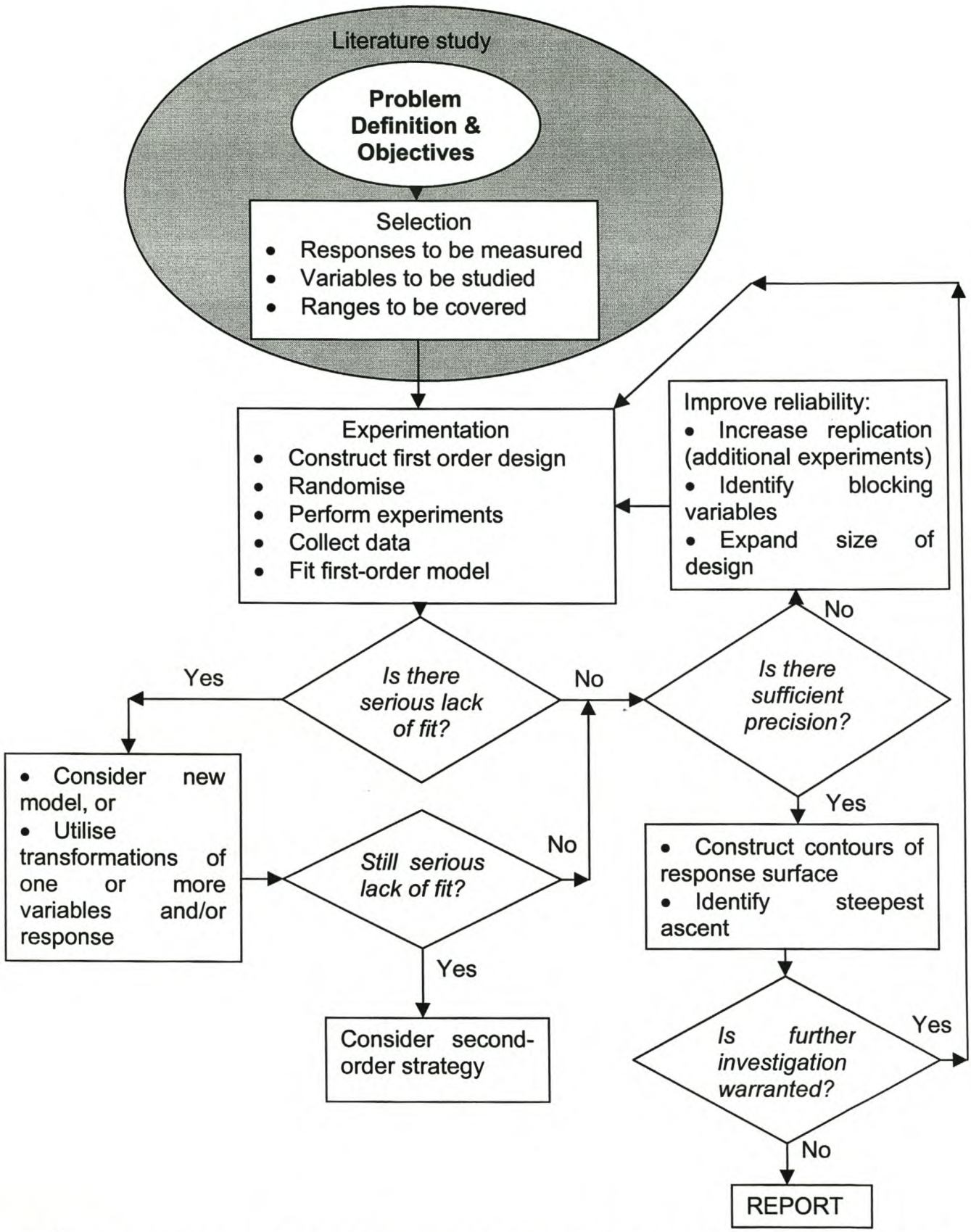

Figure G - 3. Flow diagram for Experimentation in Pavement Engineering (after Box *et al.*, 1978)

In order to enable navigation of the flow diagram in Figure G - 3, it is preferable to place the material properties in perspective with regard to the overall material behaviour. This is carried out with the use of a performance function. Herein lie challenges for the researcher in pavement engineering, as performance functions are generally non-existent or poorly defined. The overall performance functions require identification before the ramifications of the first-order model of the material on the pavement structure can be lucidly understood. This implies that, in order to relate the variability of the property being investigated with the level of reliability of pavement performance where the material is applied, a link is required between the test and reality i.e. in-service conditions. The performance function provides this essential link, and in order to fulfil its function comprehensively, it needs to comply with certain requirements including:

- inclusion of all relevant factors,
- cognisance of dependence and independence between the factors,
- acceptable levels of reliability of the pavement performance,
- understanding of the nature of the distribution of the variables, and
- knowledge or estimation of the type of performance function (linear or non-linear).

Of the given requirements of a performance function, the nature of the distribution of variables in pavement engineering provides some relief from the complexity of the statistical design. This is the case, as the vast majority of pavement materials have been shown through research to be satisfactorily modelled distributed, making the analysis of composite variability a little simpler.

3.2.1 Risk and Reliability in Pavement Engineering

Risk results from the uncertain outcome of an event. In pavement engineering, the event can include for example the exposure of a pavement to traffic, which in turn is dependent on factors such as traffic type and volumes, materials and the environment (climate etc). This is further complicated by the fact that these factors influence different events in any number of combinations and intensities.

There are various definitions of risks, risk events and uncertainty. The approach of Ker-fox (1998&9) which defines risk as the consequence of an event rather than the probability of the event, is selected from these. For example, the probability of high intensity rainfall on a highway route is not a risk. The consequent probability of failure of the road facility is the risk. The rainfall in this example is considered the risk event.

The expected value of risk is given by the following expression:

$$E_{risk} = P_{risk}. f(X) \qquad \textbf{Equation G - 4}$$

which defines the expected value of the risk E_{risk} as the product of the likelihood of exposure to the risk event P_{risk} and a function of modelling the impact of the risk event f(X).

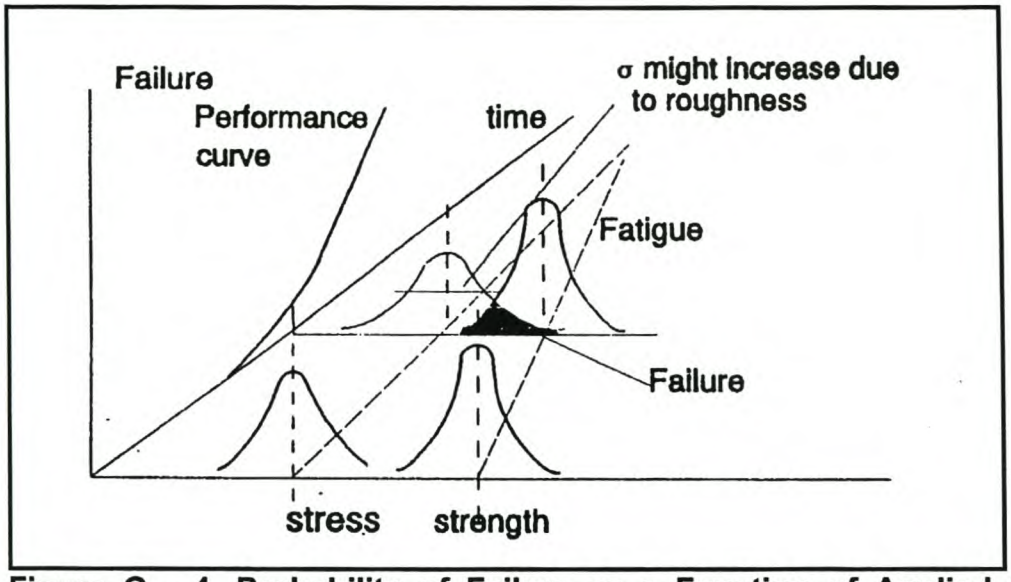

Figure G - 4. Probability of Failure as a Function of Applied Stress and Actual Strength of a Material with Time (Molenaar, 1994)

The performance curve provided in Figure G - 4 provides the P_{risk} value as a function of time, as an example. The impact of the risk event f(x) would, for example, include the wear on vehicles or safety in the case of the probability function applying to roads.

Statistical experimental design has the objective of managing the risks related to the subject under investigation. As such, it needs to take account of all significant variables that influence the subject as well as the distribution of the variability of these factors.

3.2.2 Composite Variance from Partial Derivatives

Benjamin and Cornell (1970) utilise Taylor's expansion to illustrate that the expected value of a function $g(x_1, x_2, \ldots x_n)$ with n random variables x_i can be approximated by the function of the means where the variables are independent and the coefficients of variation of x_i are small. In pavement engineering the variation of at least some of the random variables is significant, so a more complex solution is required. Darter *et al* (1973) and Huang (1993) provide a partial derivative method for the derivation of the variance of the function, which is given in the form of the standard deviation (S) in Equation G - 5.

$$S_g = \left(\frac{\partial g}{\partial x_1}\right)^2 S_{x_1}^2 + \left(\frac{\partial g}{\partial x_2}\right)^2 S_{x_2}^2 + \ldots + \left(\frac{\partial g}{\partial x_n}\right)^2 S_{x_n}^2 \qquad \textbf{Equation G - 5}$$

Where,

$x_1, x_2, \ldots x_n$ are random variables

$S_{x1}, S_{x2} \ldots S_{xn}$ are the standard deviations of the individual variables

Equation G - 5 provides a method of calculating variation in a function where the variables are independent i.e. there is no covariance to be considered, and all of the variables may be described by a normal distribution function.

Example G.2 : Composite Variance in Material Testing

The Indirect Tensile Strength test (ITS), which is commonly applied in cold bituminous mix design procedures, utilises a compressive axial load along the circumference of a cylindrical specimen, to generate horizontal stresses. The equation for the calculation of the tensile strength is given as:

$$ITS = \frac{2P}{\pi dt} \qquad \textbf{Equation G - 6}$$

Where,

ITS = Indirect Tensile Strength (kPa)
P = Maximum Applied Load (kN)
d = Diameter of specimen (m)
t = Thickness or height of specimen (m)

The partial derivative method given in Equation G - 5 provides a procedure for the measurement of the composite systematic errors in the test as a result of the systematic standard deviation of the individual components measured in the test. The systematic coefficients of variation for the individual variables should be established for the apparatus utilised. In the case of this research, the following levels of accuracy have been established.

- *Physical measurements.* The use of ruler measurements at four points along the circumference of a specimen provides an accuracy of 1% for the height or diameter. This may be reduced to 0,5% through the use of callipers. The standard deviation of the radial and axial measurements are taken as 1% of the specimen diameter and height respectively.
- *Linear Variable Displacement Transducers (LVDTs).* These devices are used for the measurement of displacement and deflections during testing. The manufacturer of the LVDTs utilised claim a linearity factor of 0,25% of the full output range of 10V. This translates to 2,5 μm , which has been verified through analysis of output results.
- *Materials Testing System (MTS) Load Cell.* Calibration of the 10ton capacity load cell yielded an accuracy of 3% for the most sensitive setting and 1% for the coarsest setting. One standard deviation is considered to be 2% of the load value.

The relevant information regarding variability may be applied to the partial derivative equation to yield the standard deviation for the ITS test. The average values applicable to the 150mm diameter specimen are:

P = 11,789 kN
d = 0,075m
h = 0,100m

yielding a partial derivative of:

$$S_{ITS}^2 = \left(\frac{\partial ITS}{\partial P}\right)^2 S_P^2 + \left(\frac{\partial ITS}{\partial d}\right)^2 S_d^2 + \left(\frac{\partial ITS}{\partial t}\right)^2 S_t^2$$

$$= \left(\frac{2}{\pi dt}\right)^2 \left(\frac{2}{100} * P\right)^2 + \left(-\frac{2P}{\pi d^2 t}\right)^2 \left(\frac{1}{100} * d\right)^2 + \left(-\frac{2P}{\pi dt^2}\right)^2 \left(\frac{1}{100} * t\right)^2$$

$$= 37{,}5$$

$$S_{ITS} = 6{,}1 kPa$$

Similarly, the testing configuration of the cyclic Indirect Tensile Strength Test or Resilient Modulus Test (ITT) and the Dynamic Creep Test have been analysed and the standard deviations calculated using the partial derivative method. Table G - 2 provides a summary of the results of the error analysis.

Table G - 2. Systematic Standard Deviations for different Mechanical Tests

Test Type	Typical Result	Standard Deviation	COV (%)
ITS (Strength)	250 kPa	6,1 kPa	2,4
ITT (Resilient Modulus)	2000 MPa	40,6 MPa	2,0
Dynamic Creep	20 MPa	0,2 MPa	1,0

3.2.3 Composite Variance from Limit State Analysis

The partial derivative method is useful for determination of the composite variance for linear functions, but it is not ideal for application to non-linear functions. This is so because the variance of a non-linear function (dg/dX_n) will be evaluated at the respective expected values for the individual variables using the partial derivative method, as has been carried out in Section 3.2.1. This can result in error. It would be more appropriate to evaluate the variance at the most probable failure condition, which can be established using the limit state approach.

Limit state analysis uses the most likely combination of variables at the failure point, thus identifying the shortest distance between the origin and the failure surface plotted on standard normalised axes. An infinite number of design points exist on the limit state surface for a performance function. This method identifies the most likely design point to cause failure.

Example G.3 : Limit State Analysis of a Mechanical Test

Extending Example G.2, a limit state analysis is carried out to determine the critical variable as a result of systematic errors in an ITS test. Considering a material that yields a result of 250 kPa in an ITS test where a specification requires a minimum value of 230 kPa. The performance function for the analysis is defined as :

$$g(P,d,t) = 2P/(\pi dt) - T_s = 0$$ **Equation G - 7**

Where,

P,d,t are force and specimen geometry as previously defined

T_s = Minimum tensile strength for a material defined using the Indirect Tensile Mode

Using this performance function, the level of reliability of the tensile strength of the material exceeding the specification can be checked utilising limit state analysis. The distribution of the various input factors is defined in Table G - 3.

Table G - 3. Distribution of Variables for a Specific Material and ITS Specification (T_s)

Variable	Mean (μ)	Standard Dev. (σ)
P (kN)	2.552	0.08
d (mm)	0.1	0.002
t (mm)	0.065	0.001
T_s (kPa)	230	0

As with the partial derivative method, the derivatives of the performance function in terms of the individual variables (dg/dX_i) , are initially determined and calculated using seed values as the expected value i.e. assumed x_i^* . These values are then normalised in terms of the sum of the squares of the derivatives, to give the direction cosine α_i, where

$$\alpha_i = \frac{\frac{\partial g}{\partial X_i}\sigma_{X_i}}{\sqrt{\sum_i^n \left(\frac{\partial g}{\partial X_i}\sigma_{X_i}\right)^2}}$$ **Equation G - 8**

The expression for a component of the failure point x_i^* corresponding to the original variate X_i is given by

$$x_i^* = \mu_{X_i} - \alpha_i \beta \sigma_{X_i}$$ **Equation G - 9**

In this way, a new value for a variable at the failure point is established. This enables repetition of the procedure in an iterative process until convergence is achieved for a certain Reliability Index β i.e. when Equation G - 7 is satisfied. Alternatively, the value of the performance function could be established for a certain level of reliability. In this example, the former approach has been adopted.

The step-by-step procedure for using limit state analysis may therefore be summarised as follows:

1. Establish the performance function for the pertinent analysis.
2. Determine the derivatives of the performance function in terms of the individual variables.

3. Calculate the value of the individual dg/dX_i derivatives utilising seed values i.e. expected values for the variables.
4. Calculate the sum of the squares of the individual derivatives.
5. Calculate the direction cosine α_i of the individual derivatives by normalising the value in Step 3 with the value from Step 4.
6. Calculate a new failure point x_i^* utilising Equation G - 9 and a selected reliability index β.
7. Utilise the new failure point x_i^* as the seed values until convergence of seed value and the calculated failure point is achieved for all variables.

Table G - 4. First Iteration of Limit State Procedure

Iteration	Variable	Assumed x_i^*	dg/dx_i^*	α_i	New x_i^*
1	P (kN)	2.552	7.835	0.779	2.425
	d (mm)	0.1	-4.999	-0.497	0.102
	t (mm)	0.065	-3.845	-0.382	0.0658
	Ts (kPa)	230	0	0	230
		Sum of Sq's	10.058		

The first iteration of the limit state process yields β = 2,042 and the second iteration yields 2,040. This indicates that 95,9% reliability exists that the material tested will satisfy the given specification.

Table G - 5. Second Iteration of Limit State Procedure

Iteration	Variable	Assumed x_i^*	dg/dx_i^*	α_i	New x_i^*
1	P (kN)	2.425	7.588	0.799	2.422
	d (mm)	0.102	-4.509	-0.475	0.102
	t (mm)	0.0658	-3.496	-0.368	0.0658
	Ts (kPa)	230	0	0	230
		SUM	10.058		

What is more important is the distribution of the variability between the variables. The value of $(\alpha_i)^2$ from Table G - 5 provides the ratio of contribution of the variables to the systematic error in the measurement of Indirect Tensile Strength. This indicates that, for the given test configuration, the measurement of the load P will account for 64% of the systematic error, whilst the measurement of diameter d and thickness t will account for 22,5% and 13,5% respectively. These values are calculated using α_i^2 from the table. In this way, the minimisation of systematic errors in testing may be carried out through analysis of the individual components, thus indicating the benefit of the limit state function.

3.2.4 Application of Risk and Reliability

Although statistical quality control was met with resistance in its first implementation in the road engineering industry (Mitchell *et al.*, 1977), it has experienced an increase in application. One of the main advantages of a statistical approach to acceptance criteria for road construction is that it enables the risk of the client and of the contractor to be quantified. The client's risk, denoted by β, represents the probability of accepting a sub-standard or poor quality lot. The contractor's risk, denoted by α, represents the probability

of rejecting an acceptable quality lot, and these two risks can be illustrated on a normal distribution diagram, see Figure G - 5.

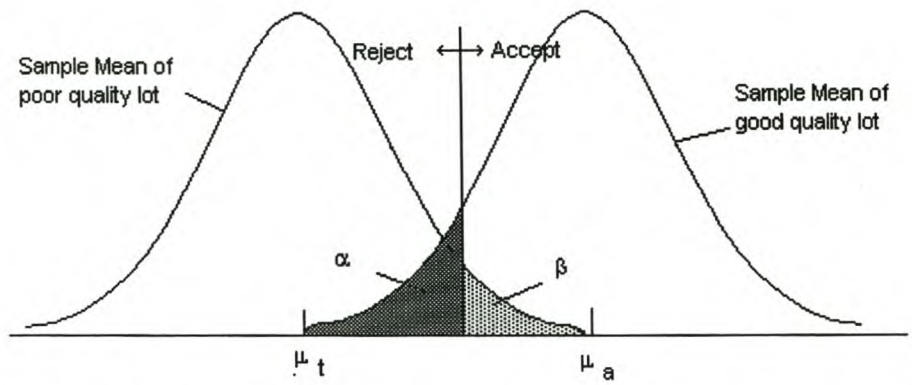

Figure G - 5. Distribution of Sample Mean and corresponding Risk Measures

The statistically based judgement scheme utilised in South Africa (CSRA, 1987) is based on the assumption that product is acceptable in terms of the specifications i.e. the contractor's risk α of having an acceptable product conditionally accepted or rejected is kept at low and fixed levels. However, the client's risk β of erroneously accepting an unacceptable product is variable.

Through statistical analysis of experimental data, however, sufficient information can be obtained to establish both the contractor and client's risk. The following parameters should be established:

- the mean value $\bar{x}_a$ that constitutes good or acceptable quality (from a contractor's standpoint),
- the mean value $\bar{x}_t$ for the lot corresponds to bad or unacceptable quality (from a client's position), and
- the standard deviation S of the variable, which is Gaussian.

Using experimentally derived data or relevant background data, a common acceptance plan may be established to minimise the probability that a good lot (with μ_a) will be rejected, and also minimise the probability that a bad lot (with μ_t) will be accepted. The required sample size n and the standard mean value L can be determined to satisfy **both** these risks. For a sample size n, the sample mean will be Gaussian with standard deviation $\sigma / \sqrt{n}$. Then if a lot is of acceptable quality, the sample mean will be Gaussian with the same standard deviation. If that lot, with the sample mean of less than L, is rejected then to limit the contractor's risk α, the equation is:

Equation G - 10

$$P\left(\bar{X} < L | \mu_a\right) = \Phi\left(\frac{L - \mu_a}{\sigma / \sqrt{n}}\right) = \alpha$$

Similarly, if the lot is of poor quality (with mean value μ_t), to satisfy the client's risk, the following is required:

$$P\left(\overline{X} > L|\mu_t\right) = 1 - \Phi\left(\frac{L-\mu_t}{\sigma/\sqrt{n}}\right) = \beta \qquad \textbf{Equation G - 11}$$

For known values of μ_a, μ_t, α and β (established through experimental design), L and n may be derived through substitution. This provides a specification limit (L) and a sample size (n) that is useful for application in practise. This technique is a useful extension of experimental design and is utilised in this dissertation. Although values of α and β are selected according to the consequence of failure i.e. if a product's failure would result in a life-threatening situation, the β value should approximate zero. In pavement engineering, products are generally considered non-critical and values of 5% and 10% are commonly selected for α and β respectively. An example utilising these principles is given in Section 6 of Chapter 3.

4. SUMMARY

Experiments that are statistically designed should be identifiable by possessing the following attributes:

- Understanding of the level of reliability of the results.
- Optimisation of the range of applicability of the model developed.
- Eradication of systematic errors.
- Simplicity in so far as this is possible.
- Facility for estimation of the magnitude of the experimental error.

The function of statistically designed experiments can best be summarised by their advantages and disadvantages.

4.1 Advantages of statistically designed experiments

The advantages of statistically designed experiments, in general, may be listed as:

- Close teamwork between statistician and researcher results in advantages in the analysis and interpretation stage of the programme.
- Emphasis is placed on anticipating alternatives and systematic pre-planning but allowing logical performance and producing only data useful for analysis in later combinations.
- Attention is focused on inter-relationships and on identifying and measuring sources of variability in the results.
- The required number of tests is determined reliably, which can often result in a reduction in the total number of tests.
- The comparison of the effects of change is more precise because of the grouping of results.
- Correctness of conclusions is known with mathematical preciseness.

4.2 Disadvantages of statistically designed experiments

Cognisance needs to be taken of the disadvantages in order to overcome them:

- Statistical designs and analyses are usually accompanied by statements couched with statistical jargon. A possible solution is the use of graphs.
- Many statistical designs, especially when first formulated, are criticised as being too expensive, complicated and time-consuming.

4.3 Applicable Models for Pavement Engineering

- Decision trees facilitate optimisation of experiments in terms of tangible benefits such as time delay reduction, financial gain or resource economy and as such provide a useful tool for selection of optimal experiments.
- The partial derivative method of analysing composite variance provides a method of calculating variation in a function where no co-variance between variables is considered. It is relatively simple and effective.
- Limit state analysis is a useful technique for the analysis of non-linear functions. This technique analyses the variance at the most possible failure condition, which is not possible using the partial derivative method. As such, the limit state function is especially applicable in pavement engineering where dependent variables are commonplace in performance functions.
- In this thesis, the partial derivative method and the risk and reliability approach are considered highly applicable and therefore utilised. In addition, principles of the limit state function are utilised in terms of repeatability of mechanical test results.

5. REFERENCES

AASHTO® (American Association of State Highway and Transportation Officials), 1986. **AASHTO Guide for the design of pavement structures**. Washington DC, Pp III-42 to III-55.

Anderson R.L. and Bancroft T.A., 1952. **Statistical Theory in Research**. McGraw-Hill Book Company, New York, p. 3-7, 240-241

Anderson T.W., 1984. **An Introduction to Multivariate Statistical Analysis**. Second Edition, Wiley Series in Probability and Mathematical Statistics, John Wiley and Sons, New York.

Ang A.H.S. and Tang W.H., 1975. **Probability Concepts in Engineering Planning and Design : Volume I, Basic Principles**. Wiley Series in Probability and Mathematical Statistics, John Wiley and Sons, New York.

Ang A.H.S. and Tang W.H., 1984. **Probability Concepts in Engineering Planning and Design : Volume II, Decision, Risk and Reliability**. Wiley Series in Probability and Mathematical Statistics, John Wiley and Sons, New York. Pp1-96 and 333-434

Bajpai A.C., Calus I.M. and Fairley J.A., 1978. **Statistical methods for engineers and scientists**. John Wiley and Sons, Great Britain.

Benjamin J.R. and Cornell C.A., 1970. **Probability, Statistics and Decision for Civil Engineers**. McGraw-Hill, New York.

Box G.E.P., Hunter W.G. and Hunter J.S., .1978, **Statistics for Experimenters - An introduction to Design, Data Analysis and Model Building**. Wiley Series in Probability and Mathematical Statistics, John Wiley and Sons, New York.

Cornell J.A., 1990. **Experiments with Mixtures : Designs, Models and the Analysis of Mixture Data**. Second Edition, Wiley Series in Probability and Mathematical Statistics, John Wiley and Sons, New York.

Crow E.L., Davis F.A. and Maxfield M.W., **Statistics Manual**, Research Department of U.S. Naval Ordnance Test Station, Dover Publications, New York. Pp. 109-117

Cheremisinoff N.P., 1980. **Practical Statistics for Engineers and Scientists.** Technomic Publishing Co., Lancaster. Pp. 161-165

CSRA Committee of State Road Authorities, 1987. **Statistical Concepts of Quality Control and their application in Road Construction**. TRH 5. Pretoria.

CSRA Committee of State Road Authorities, 1996. **Structural Design of Flexible Pavements for Interurban and Rural Roads**. Draft TRH 4, Pretoria. Pp 1 – 47.

Darter M.I., Hudson W.R., and Brown J.L., 1973. **Statistical Variations of Flexible Pavement Properties and their Consideration in Design**. *Association of Asphalt Paving Technologists, Volume 42.*

Fisher R.A., 1951. **The Design of Experiments**. 6th Edition, Oliver and Boyd, Edinburgh.

Fisher R.A., 1958. **Statistical Methods for Research Workers**. 13th Edition, Oliver and Boyd, Edinburgh.

Grivas D.A., 1986. **Risk analysis in Civil Engineering**. Course at University of Stellenbosch, South Africa.

Gunst R.F. and Mason R.L., 1986. **How to construct Fractional Factorial Experiments**. *American Society for Quality Control Statistics Division, Volume 14*, ASQC Quality Press, Milwaukee, Wisconsin.

Huang Y.H., 1993. **Pavement analysis and Design**. Prentice-Hall, New Jersey.

Hudson W.R., Brown J.L. and Darter M.I., 1974. **Statistical variation of Pavement Materials**. *Second Conference on Asphalt Pavements for Southern Africa, Volume 1*, August, Durban.

Johnson N.L. and Leone F.C., 1964. **Statistics and Experimental Design in Engineering and the Physical Sciences**. Wiley Series in Probability and Mathematical Statistics, John Wiley and Sons, New York.

Ker-Fox G.M., 1998. **The Limit State Cost Function (LSCF) as a Risk Management Tool for Construction Projects**. Master of Science (Engineering) Thesis, University of Stellenbosch.

Ker-Fox G.M., 1999. **The Limit State Cost Function as a Management Tool for Construction Projects**. Construction Management Programme, Risk Management Source Document, University of Stellenbosch.

Logothetis N. and Wynn H.P., 1989. **Quality through Design - Experimental Design, Off-line Quality Control and Taguchi's Contributions**. Oxford Science Publications, Oxford Series on Advanced Manufacturing, Clarendon Press, Oxford.

Mahoney J.P., 1997. **Statistical methods for Pavements and Material Applications**. Course Notes prepared for the Division of Roads and Transport Technology, CSIR, University of Washington, Seattle.

Mason R.L., Gunst R.F. and Hess J.L., 1989. **Statistical Design and Analysis of Experiments with Applications in Science and Engineering**. Wiley Series in Probability and Mathematical Statistics, Applied probability and Statistics, John Wiley and Sons, New York.

Mitchell M.F., Semmelink C.J. and McQueen A.L., 1977. **Experience in statistical quality control for road construction in South Africa**. National Institute for Transport and Road Research, CSIR Report RR 216, Pretoria.

Molenaar A.A.A., 1994. **Performance Related Quality Management.** *Conference on Asphalt Pavements for Southern Africa, 6th CAPSA*. Cape Town, South Africa. V-54 to 67

Montgomery D.C., 1984. **Design and Analysis of Experiments**. Second Edition, John Wiley and Sons, New York.

Overleg Groep Meettechniek, 1983. **Experimenten in de wegenbouw**. Stichting Studie Centrum Wegenbouw, Arnhem.